Indian and Northern Affairs Canada
Affaires indiennes et du Nord Canada

Exploration and Geological Services Division, Yukon Region

# YUKON
## EXPLORATION & GEOLOGY

## 2001

- Mining & Exploration Overview
- Yukon Geology Program
- Geological Fieldwork
- Property Descriptions

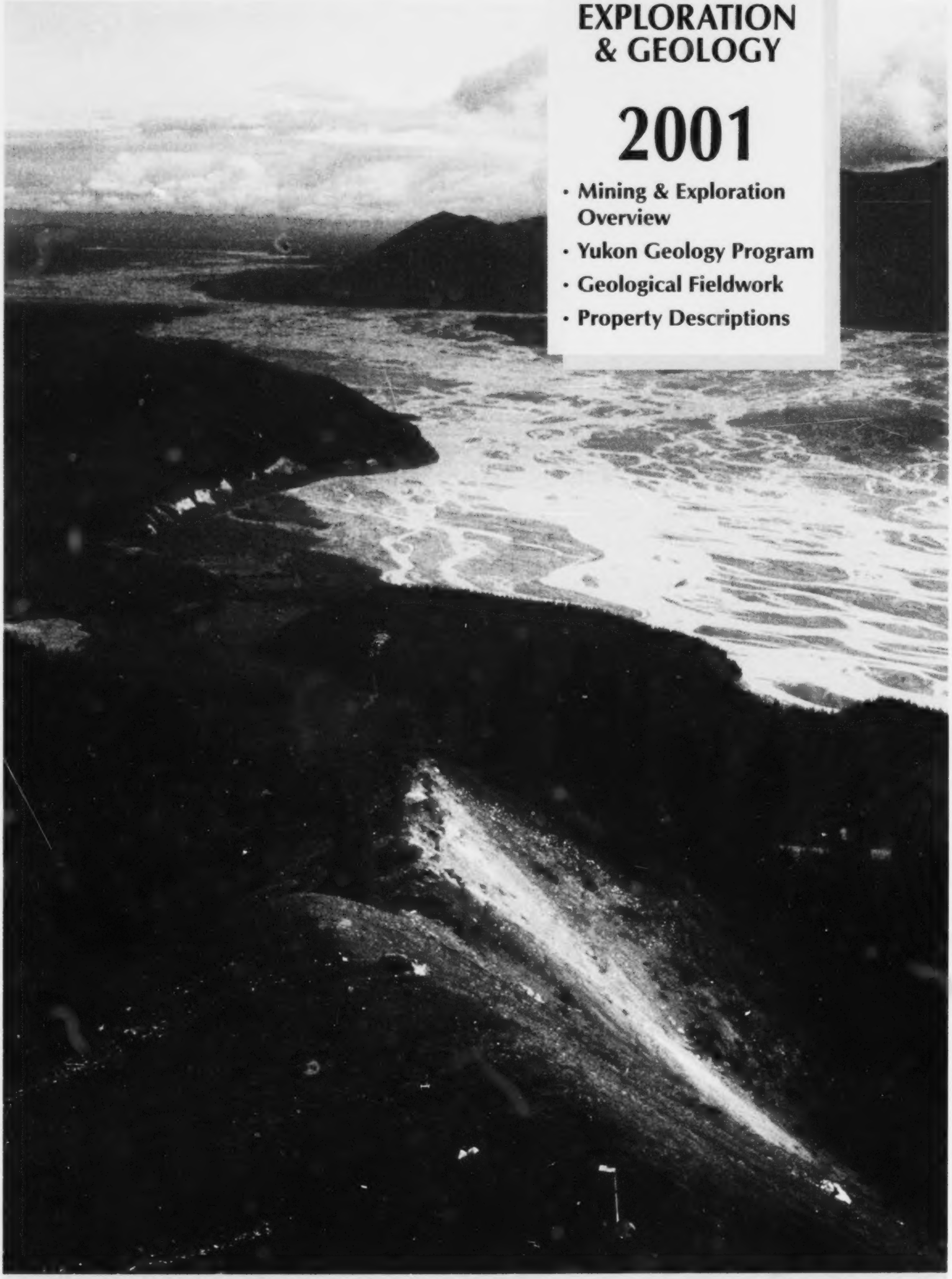

Yukon Government

YUKON GEOLOGY PROGRAM

Canada

103-05167/

# YUKON
# EXPLORATION & GEOLOGY
# 2001

Edited by
D.S. Emond, L.H. Weston and L.L. Lewis

Exploration and Geological Services Division,
Yukon Region
Indian and Northern Affairs Canada

Published under the authority of the Minister of Indian Affairs and Northern Development,
Ottawa, 2002.

http://www.inac.gc.ca

Printed in Whitehorse, Yukon, 2002.

© Minister of Public Works and Government Services Canada

QS-6120-011-EE-A1 Catalogue no. R2-136/2001E ISBN 0-662-29989-2

This, and other Yukon Geology Program publications, may be obtained from:

Geoscience and Information Sales
c/o Whitehorse Mining Recorder
102-302 Main Street
Whitehorse, Yukon, Canada Y1A 2B5
phone (867) 667-3266, fax (867) 667-3267

Visit the Yukon Geology Program web site at www.geology.gov.yk.ca.

In referring to this publication, please use the following citation:

Yukon Exploration and Geology 2001. D.S. Emond, L.H. Weston and L.L. Lewis (eds.), 2002. Exploration and Geological Services Division, Yukon Region, Indian and Northern Affairs Canada, 278 p.

Production by K-L Services, Whitehorse, Yukon.

**Front cover photo**
Quartz-carbonate alteration at the Sax showing defines the footwall contact of the White River intrusive complex, the second largest mafic-ultramafic body located in the Kluane Mafic-Ultramafic Belt. The Sax showing is located on the Canalask-Onion property, one of several properties in the belt being explored for their platinum group elements (PGE) potential. Photo by Mike Burke.

**Back cover photo**
Jim Dodge (right), 2001 Yukon Prospector of the Year, receiving his award from Larry Carlyle of the Yukon Prospectors Association, at the Whitehorse Geoscience Forum, November, 2001.
Photo by, and courtesy of, Whitehorse Star.

# PREFACE

**Yukon Exploration and Geology** (YEG) is the main publication of the Yukon Geology Program (Indian and Northern Affairs Canada and Yukon Government). This is the 24th volume of the YEG series. It contains up-to-date information on mining and mineral exploration activity, studies by industry, and results of recent geological field studies. Information in this volume comes from prospectors, exploration and government geologists, mining companies and students who are willing to collectively benefit the Yukon's mineral industry. Their assistance and patience is sincerely appreciated.

A special mention goes to Maurice Colpron of the Yukon Geology Program for his able assistance in the translation, review and composition of French abstracts. Maurice Colpron, Charlie Roots and Robert Stroshein critically reviewed several manuscripts. Sincere appreciation is extended to co-editors Leyla Weston and Lara Lewis for their diligence, enthusiasm, keen sense of grammar, and for keeping their sense of humour through the process. Wynne Krangle and Peter Long of K-L Services also continue to provide excellent service in putting this production together, including editing suggestions, design of diagrams, volume layout, and working under the pressure of a tight deadline. Max Fraser and Pascale Black of the Queen's Printer ensured that the printing process went smoothly.

The 2001 volume has four parts. The first – **Mineral Industry** – includes overviews of **Mining and Exploration** in the Territory. The second part – **Government** – outlines the activities and organization of the Yukon Geology Program. This section also includes updates on the Mineral Resource Assessments, the Yukon Mining Incentives Program, and announcements of the third Mining Land Use Reclamation Awards, the Robert E. Leckie Awards. The third part – **Geological Fieldwork** – contains reports describing regional mapping, and more detailed geological, geochemical, geophysical, geochronological, paleontological, paleomagnetic and placer deposit studies. The last part – **Property Descriptions** – is a collection of geological reports of mineral occurrences with recent exploration advances or detailed studies, and is authored by industry and government geologists, as well as university students.

We welcome any input or suggestions that you may have to improve future YEG publications. Please contact me at (867) 667-3203 or by email at emondd@inac.gc.ca.

Diane Emond

YUKON
GEOLOGY PROGRAM

# TABLE OF CONTENTS

## MINERAL INDUSTRY

Yukon Mining and Exploration Overview, 2001
  *Mike Burke* .......... 2
  Appendix 1: 2001 exploration projects .......... 24
  Appendix 2: 2001 drilling statistics .......... 25

Placer Mining Overview, 2001
  *William LeBarge* .......... 27

## GOVERNMENT

Yukon Geology Program
  *Grant Abbott and staff* .......... 31
  2001 publications and maps .......... 38

Le Service de géologie du Yukon
  *Maurice Colpron et Grant Abbott* .......... 49

Mineral Resource Assessments Overview, 2001
  *Anna Fonseca* .......... 53

Yukon Mining Incentives Program Overview, 2001
  *Ken Galambos* .......... 57

The Robert E. Leckie Award for Outstanding Reclamation Practices
  *Karen Pelletier* .......... 61

## GEOLOGICAL FIELDWORK

Paleoproterozoic deformation of the Racklan Orogeny, Slats Creek (106D/16) and Fairchild Lake (106C/13) map areas, Wernecke Mountains, Yukon
  *M-A. Brideau, D.J. Thorkelson, L. Godin and J.R. Laughton* .......... 65

Lower to Middle Jurassic stratigraphy, ammonoid fauna and sedimentary history of the Laberge Group in the Fish Lake syncline, northern Whitehorse Trough, Yukon, Canada
  *M.E. Clapham, P.L. Smith and H.W. Tipper* .......... 73

Composition of placer and lode gold as an exploration tool in the Stewart River map area, western Yukon
  *M.R. Dumula and J.K. Mortensen* .......... 87

Geology at the contact between Yukon-Tanana and Cassiar terranes, southeast of Little Salmon Lake (105L/1), south-central Yukon
  *K. Gladwin, M. Colpron, S.T. Johnston and R. Black* .......... 103

No remagnetization in plutonic rocks of the Whitehorse Trough, southern Yukon: An extensive paleomagnetic conglomerate test
  *M.J. Harris, D.T.A. Symons and C.J.R. Hart* .......... 111

*continued*

New mapping around the Slab iron oxide-copper-gold occurrence, Wernecke Mountains (parts of NTS 106C/13, 106D/16, 106E/1 and 106F/4), Yukon
*J.A. Hunt, J.R. Laughton, M-A. Brideau, D.J. Thorkelson, M.L. Brookes and T. Baker* ........ 125

Paleoproterozoic volcanism and plutonism in the Wernecke Mountains, Yukon
*J.R. Laughton, D.J. Thorkelson, M-A. Brideau, J.A. Hunt* ........ 139

White Channel Gravel alteration revisited
*G.W. Lowey* ........ 147

Paleomagnetism and geobarometry of the Granite Mountain batholith, Yukon: Minimal geotectonic motion of the Yukon-Tanana Terrane relative to North America
*P.J.A. McCausland, D.T.A. Symons, C.J.R. Hart and W.H. Blackburn* ........ 163

Lead isotopic constraints on the metallogeny of southern Wolf Lake, southeastern Teslin and northern Jennings River map areas, Yukon and British Columbia: Preliminary results
*J.K. Mortensen and J.E. Gabites* ........ 179

Finlayson Lake Targeted Geoscience Initiative (southeastern Yukon), Part 1: Bedrock geology
*D.C. Murphy, M. Colpron, C.F. Roots, S.P. Gordey and J.G. Abbott* ........ 189

Finlayson Lake Targeted Geoscience Initiative (southeastern Yukon) Part 2: Quaternary geology and till geochemistry
*J.D. Bond and A. Plouffe* ........ 209

Preliminary results of a petrological study of ultramafic rocks of the Northern Cordillera
*J.G. Shellnutt, D. Canil and S.T. Johnston* ........ 229

Resedimentation of the late Holocene White River tephra, Yukon Territory and Alaska
*K.D. West and J.A. Donaldson* ........ 239

## PROPERTY DESCRIPTIONS

Alteration zonation, veining and mineralization associated with the Wernecke Breccias at Slab Creek, Yukon Territory, Canada
*M. Brookes, T. Baker and J. Hunt* ........ 249

Ray Gulch tungsten skarn, Dublin Gulch, central Yukon: Gold-tungsten relationships in intrusion-related ore systems and implications for gold exploration
*V.S. Brown, T. Baker and J.R. Stephens* ........ 259

Geology, mineralization and sampling results from the Kalzas tungsten property, central Yukon
*G.G. Carlson* ........ 269

# YUKON EXPLORATION AND GEOLOGY 2001

## GEOLOGICAL FIELDWORK

| | | |
|---|---|---|
| 1 | **Brideau et al.** | Slats Creek, Fairchild Lake areas |
| 2 | **Clapham et al.** | Northern Whitehorse Trough |
| 3 | **Dumula & Mortensen** | Stewart River area |
| 4 | **Gladwin et al.** | Contact YTT/CTT, Little Salmon Lake area |
| 5 | **Harris et al.** | Paleomagnetism, Whitehorse Trough |
| 6 | **Hunt et al.** | Slab occurrence, Werneckes |
| 7 | **Laughton et al.** | Volcanism, plutonism, Werneckes |
| 8 | **Lowey** | White Channel Gravel |
| 9 | **McCausland et al.** | Paleomagnetism, Granite Mountain batholith |
| 10 | **Mortensen et al.** | Lead isotopes, Wolf Lake, Teslin and Jennings River areas |
| 11 | **Murphy et al.** | Finlayson Lake TGI, Part 1: Bedrock geology |
| 12 | **Bond & Plouffe** | Finlayson Lake TGI, Part 2: Quaternary geology and till geochemistry |
| 13 | **Shellnutt et al.** | Ultramafic rocks, Northern Cordillera |
| 14 | **West & Donaldson** | White River tephra, YT and Alaska |

## PROPERTY DESCRIPTIONS

| | | |
|---|---|---|
| 15 | **Brookes et al.** | Wernecke Breccias, Slab Creek |
| 16 | **Brown et al.** | Gold-tungsten, Ray gulch, Mayo area |
| 17 | **Carlson** | Kalzas Tungsten, Mayo area |

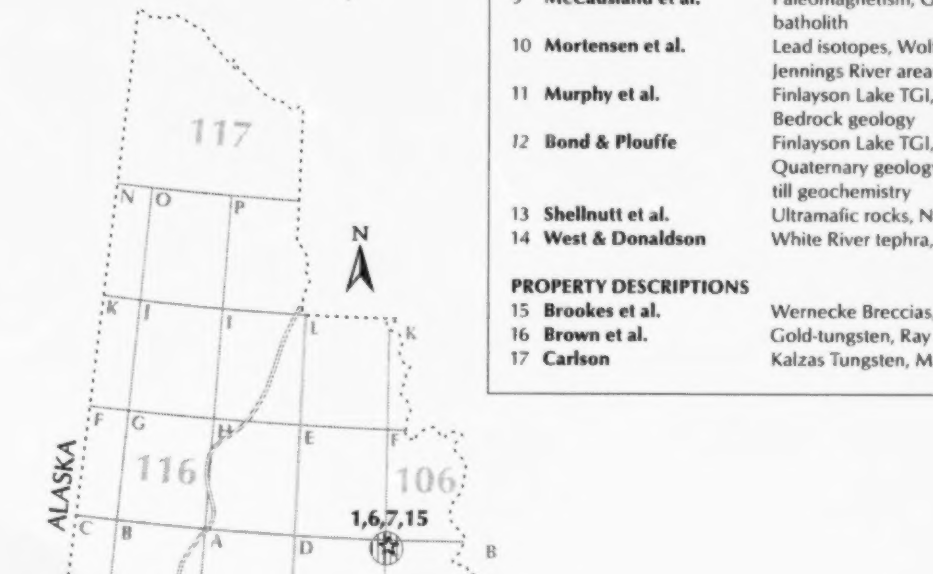
117
116
115
106
105
N
ALASKA
NORTHWEST TERRITORIES
BRITISH COLUMBIA
1,6,7,15
16
17
8
3
9
14
4
11,12
2,5
10
13
Dawson
Mayo
Carmacks
Faro
Whitehorse
Haines Junction
Watson Lake
0
100
km

# MINERAL INDUSTRY

## Yukon Mining and Exploration Overview, 2001

**_Mike Burke_**
*Yukon Geology Program*

Yukon map ........ 2
Résumé ........ 3
Introduction ........ 5
Mining and development ........ 6
Exploration ........ 8
    Base metals ........ 9
    Precious metals ........ 15
    Gemstones ........ 22
Acknowledgments ........ 23
References ........ 23
Appendix 1: 2001 Exploration Projects ........ 24
Appendix 2: 2001 Drilling Statistics ........ 25

## Placer Mining Overview, 2001

**_William LeBarge_**
*Yukon Geology Program*

Summary ........ 27
Aperçu des placers du Yukon, 2001 ........ 28

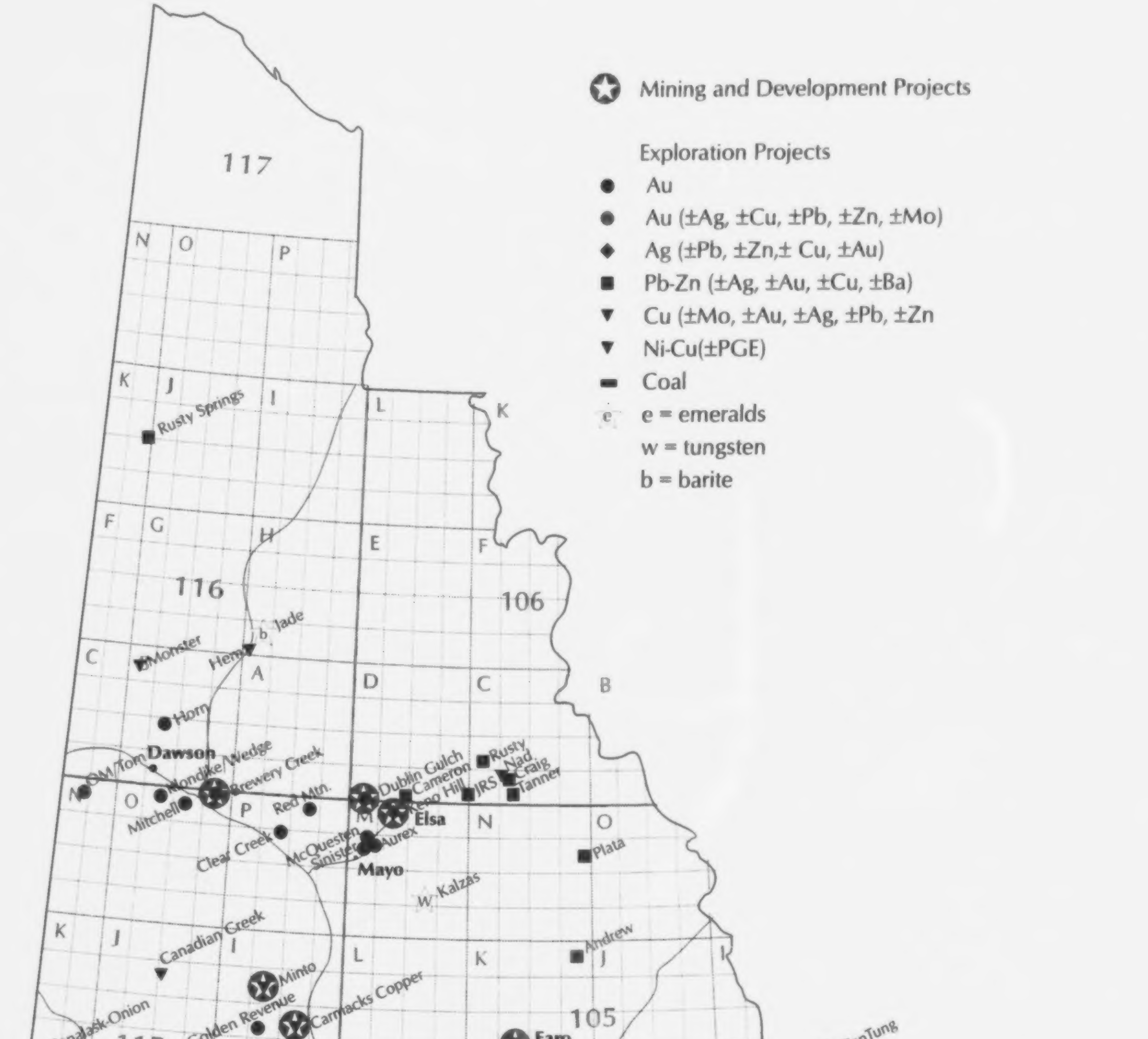
Mining and Development Projects
Exploration Projects
● Au
● Au (±Ag, ±Cu, ±Pb, ±Zn, ±Mo)
◆ Ag (±Pb, ±Zn,± Cu, ±Au)
■ Pb-Zn (±Ag, ±Au, ±Cu, ±Ba)
▼ Cu (±Mo, ±Au, ±Ag, ±Pb, ±Zn
▼ Ni-Cu(±PGE)
▬ Coal
e = emeralds
w = tungsten
b = barite
117
116
106
105
115
0
200
km
Rusty Springs
Monster
Hem
Jade
Horn
Dawson
MOM/Tom
Klondike/Wedge
Brewery Creek
Mitchell
Red Mtn.
Clear Creek
McQuesten
Sinister
Aurex
Dublin Gulch
Cameron
Keno Hill
JRS
Rusty
Nad
Craig
Tanner
Elsa
Mayo
Plata
Kalzas
Canadian Creek
Andrew
Minto
Golden Revenue
Carmacks Copper
Canalask-Onion
Mt. Nansen
Carmacks
Faro
Grew Creek
Ross River
Spice
Fire/Ice
St. Cyr
Tay/LP
Kudz Ze Kayah
Wolverine
Puck
Goal/Net
Regal Ridge
CanTung
Don/Wolv
AR
Wellgreen
Burwash
Mars
Hidden/Obvious
Ultra
Haines Junction
Whitehorse
Hat
Shootamook
Sa Dena Hes
Hyland Gold
Skukum
Mor
Watson Lake

*Figure 1. Location of active Yukon mines, development and exploration projects in 2001. Not all projects are shown on the map. Background of the map shows the National Topographic System (NTS) grid.*

# YUKON MINING AND EXPLORATION OVERVIEW, 2001

**Mike Burke**[1]
*Yukon Geology Program*

Burke, M., 2002. Yukon Mining and Exploration Overview, 2001. *In:* Yukon Exploration and Geology 2001, D.S. Emond, L.H. Weston and L.L. Lewis, (eds.), Exploration and Geological Services Division, Yukon Region, Indian and Northern Affairs Canada, p. 2-25.

## RÉSUMÉ

L'exploration minérale n'a pas repris en 2001; on avait peu investi dans l'exploration en 2000, et cette tendance se poursuit cette saison. On estime les investissements dans l'exploration à 7,2 millions de dollars. La faiblesse des prix des produits, le manque constant de spéculation dans le secteur des petites sociétés minières et les fusions ainsi que les compressions dans les grandes sociétés minières ont entravé toute reprise. L'exploration s'est encore concentrée sur un vaste éventail de modèles de gisements et de produits; les métaux communs ayant reçus autant d'attention que les métaux précieux. Les métaux précieux auxquels on s'est intéressé sont, entre autres, des gisements d'or associés à des intrusions, dans la ceinture aurifère de Tintina, une minéralisation épithermale en or aux environs du gisement Grew Creek, dans la partie centrale du Yukon, une minéralisation en or à contrôle structural, dans le district de la rivière Wheaton près de Whitehorse, et des éléments du groupe platine (ÉGP), dans la ceinture ultramafique de Kluane. Les métaux communs auxquels on s'est intéressé sont, entre autres, des sulfures massifs volcanogènes polymétalliques, dans le district du lac Finlayson, des gisements sédimentaires exhalatifs ainsi que des gisements de substitution de zinc et plomb, dans le bassin de Selwyn, des gisements porphyriques de cuivre et d'or, dans la partie centrale du Yukon et près de Whitehorse, des gisements de cuivre et or associés à de l'oxyde de fer, dans les monts Ogilvie, et des gisements de tungstène, dans le bassin de Selwyn. L'or a été le produit principal visé par la moitié des douze petits programmes de forage exécutés en 2001. Les autres programmes de forage ont portés sur des métaux communs, en particulier le zinc et le cuivre, ainsi que les ÉGP.

La mine d'or Brewery Creek a été la seule mine en roche dure exploitée au Yukon en 2001. Pendant la première partie de l'année, on a poursuivi la lixiviation et extrait 10 811 onces d'or de cette mine, à un coût d'exploitation au comptant de 199 $US l'once. Depuis son ouverture en 1996, on a extrait un total de 263 139 onces d'or de la mine Brewery Creek. L'exploitation saisonnière de la mine Brewery Creek a été interrompue et ne reprendra pas tant que le prix de l'or n'aura pas augmenté.

La mise en valeur du gisement de cuivre Minto de la société Minto Explorations Ltd. et l'aménagement, vers la fin de l'année, de la mine d'argent Keno Hill de la société A.M.T. Canada. Inc. ont exigé des investissements d'environ 500 000 $. En octobre 2001, la société A.M.T Canada a acheté le site historique de la mine d'argent Keno

---

[1] *burkem@inac.gc.ca*

Hill, qui se trouve dans la partie centrale du Yukon. En novembre, elle a conclu une alliance stratégique avec la société cotée en bourse Pacific Cart Services Ltd. du Nevada. Dans les Territoires du Nord-Ouest, la mine CanTung de la société North American Tungsten Corp. Ltd. est appelée à rouvrir en janvier 2002. C'est principalement au Yukon que se trouvent les moyens d'accéder à la mine et le soutien à l'exploitation. Le gouvernement du Yukon a signé une entente selon laquelle il s'engage à entretenir les routes et à appuyer la réouverture de la mine.

Le gouvernement du Yukon continue à favoriser le développement de l'industrie minière et à l'appuyer en augmentant à 850 000 $ le financement accordé pour la saison 2002 dans le cadre de son Programme d'encouragement des activités minières. Ce programme a pour objectif de fournir une partie du capital de risque nécessaire à la localisation de gisements minéraux au Yukon et à leur exploration. Le gouvernement du Yukon soutien également l'industrie, par le biais du crédit d'impôt à l'exploration minérale au Yukon, en remboursant 25 % de l'impôt perçu sur les investissements admissibles reliés à l'exploration. Le gouvernement du Yukon a récemment augmenté la durée de la période d'admissibilité au remboursement d'impôt, qui prendra maintenant fin le 31 mars 2003. D'autres initiatives ont été mises en œuvre pour aider l'industrie minière du Yukon, dont l'entente sur le transfert de responsabilités conclue en septembre 2001 par les négociateurs fédéraux, territoriaux et des Premières nations. Les négociateurs ont recommandé à leurs supérieurs de fixer la date d'entrée en vigueur de l'entente au premier avril 2003. L'entente porte sur le transfert au gouvernement du Yukon des responsabilités actuelles du gouvernement fédéral relatives à la gestion de la majeure partie des ressources naturelles du Yukon. Dès décembre 2001, 8 des 14 Premières nations étaient parvenues à des ententes sur les revendications territoriales et l'autonomie gouvernementale. Les négociations en vue de conclure les six dernières ententes vont bon train et devraient se terminer d'ici le premier avril 2002.

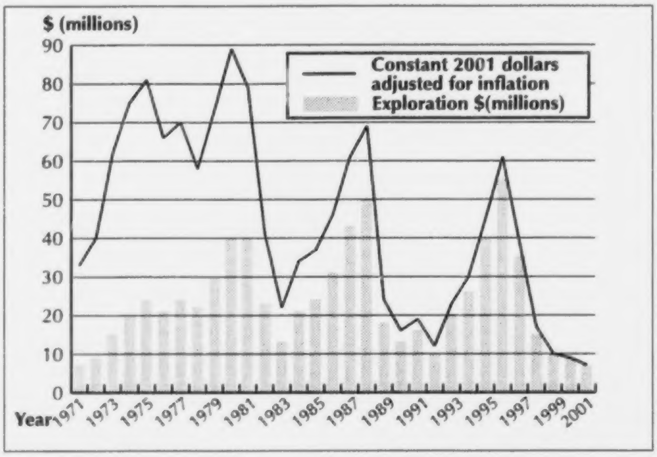

***Figure 2.*** *Yukon exploration expenditures: 1971-2001.*

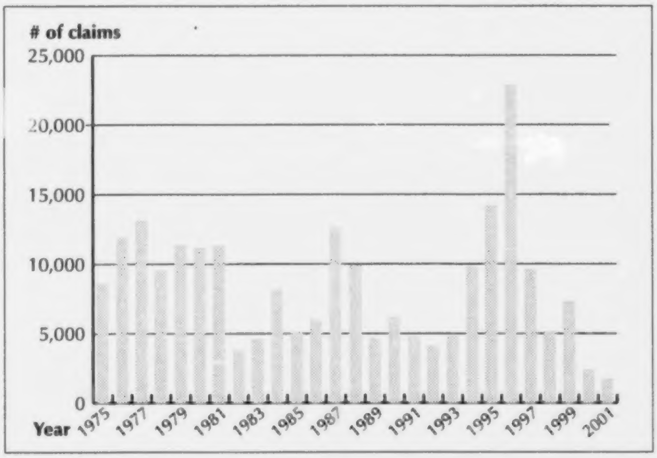

***Figure 3.*** *Quartz claims staked: 1975-2001.*

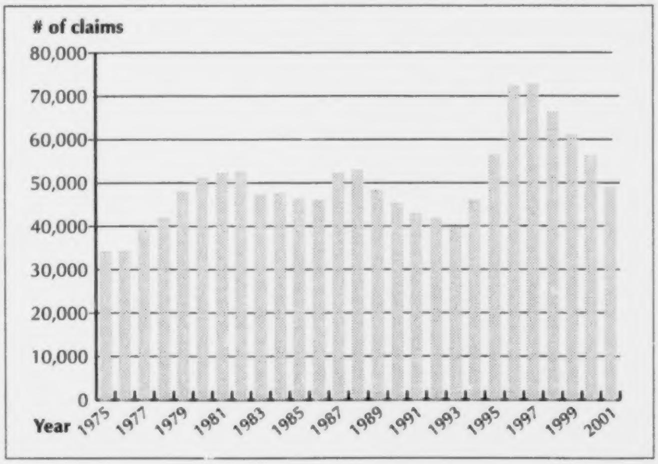

***Figure 4.*** *Quartz claims in good standing: 1975-2001.*

# INTRODUCTION

The map in Figure 1 shows the location of mineral properties active in 2001. Mineral exploration did not recover in 2001, and the low levels of exploration spending experienced in 2000 continued into this season. Exploration expenditures are estimated to be $7.2 million (Fig. 2). Poor commodity prices, the continued lack of speculative investors in the junior mining sector, and mergers and cutbacks in the senior mining industry hampered any recovery. Exploration continued to focus on a wide range of deposit models and commodities (Fig. 1), with approximately 60% of expenditures directed towards base metals and the remainder towards precious metals. Some of the precious metal targets included intrusion-related gold deposits in the Tintina gold belt, epithermal gold mineralization in the vicinity of the Grew Creek deposit in central Yukon, structurally controlled gold mineralization in the Wheaton River district near Whitehorse, and platinum group elements (PGEs) in the Kluane Mafic-Ultramafic Belt. Base metal targets included polymetallic volcanogenic massive sulphides in the Finlayson Lake district, sedimentary-exhalative and replacement zinc-lead deposits in the Selwyn Basin, porphyry copper-gold deposits in central Yukon and near Whitehorse, iron-oxide-associated copper-gold deposits in the Ogilvie Mountains, and tungsten occurrences in the Selwyn Basin. One half of the dozen small drill programs conducted during 2001 were directed at gold as the primary commodity. The remaining drill programs targeted base metals, mainly zinc, copper, and PGEs. The amount of claim staking in Yukon continued to decline with only 1720 claims staked in 2001 (Fig. 3) and a resulting decrease in claims in good standing to 48,982 (Fig. 4).

The Brewery Creek gold mine was Yukon's only operating hard rock mine in 2001. Heap leaching continued at the mine with production of 336 kg (10,811 ounces) of gold in the first half of the year, at a cash operating cost of US$199 per ounce. Total gold production at Brewery Creek has been 8185 kg (263,139 ounces) since the mine opened in 1996. Seasonal mining has been discontinued at Brewery Creek and will not resume unless gold prices increase.

Mine development expenditures of approximately $500,000 were incurred at the Minto copper deposit of Minto Explorations, and late in the year at the Keno Hill silver mine of A.M.T. Canada Inc. A.M.T. Canada purchased the historic Keno Hill silver mine in central Yukon in October of 2001. They subsequently formed a strategic alliance with the publicly traded company Pacific Cart Services Ltd. of Nevada in November. The CanTung mine of North American Tungsten Corp. Ltd., located in the Northwest Territories, is slated for reopening in January, 2002. Access to the mine and support for the operation is dominantly Yukon based. The Yukon government has signed a road maintenance agreement to support the reopening.

The Yukon government continued to support and encourage the mining industry by increasing funding in the Yukon Mining Incentive Program to $850,000 for the 2002 season. The function of the program is to provide a portion of the risk capital required to locate and explore for mineral deposits in Yukon. The Yukon Government also supports the industry through the Yukon Mineral Exploration Tax Credit, which provides a 25% tax refund on eligible exploration expenditures. The Yukon government recently extended the eligibility period of the tax credit to March 31, 2003. Other developments, which will help the Yukon's mining industry, include the initialing of the Devolution Transfer Agreement in September, 2001 by federal, territorial and First Nation negotiators. The negotiators have recommended to their Principals that the effective date of devolution be April 1, 2003. Devolution is the transfer of the federal government's current responsibilities for managing most of the Yukon's natural resources to the Government of Yukon. As of December 2001, 8 of 14 Yukon First Nations had reached land claim and self-government agreements. Negotiations on the remaining six agreements are progressing well, with a target completion date of April 1, 2002.

## MINING AND DEVELOPMENT

The **Brewery Creek gold mine** (Yukon MINFILE, 2001, 116B 160) was Yukon's only operating hard rock mine in 2001. The mine is a bulk tonnage, heap leach operation located 57 km east of Dawson City. Intrusive-related gold mineralization is hosted by intrusions of the mid-Cretaceous Tombstone Plutonic Suite, and Silurian to Carboniferous clastic metasedimentary rocks of the Steel Formation and Earn Group. Heap leaching continued at the mine with production of 336 260 g (10,811 ounces) of gold in the first half of 2001 at a cash operating cost of US$199 per ounce. Production in 2000 was 1494.5 kg (48,048 ounces) at a cash operating cost of US$243 per ounce. Seasonal mining has been discontinued at Brewery Creek and will not resume without the onset of higher gold prices. Measured and indicated resources at Brewery Creek as of December 31, 2000 were 920 000 tonnes grading 1.43 g/t gold. Viceroy Resources continued to demonstrate their environmental stewardship of the mine with their ongoing program of reclamation. A substantial amount of reclamation work was conducted on five of the pit and waste rock areas (Fig. 5).

Mine development expenditures were incurred at the **Minto copper deposit** (Yukon MINFILE, 2001, 115I 021, 022) of Minto Explorations, and late in the year at the **Keno Hill silver mine** (Yukon MINFILE, 2001, 105M 001) of A.M.T. Canada. Work at the Minto site included geotechnical and environmental studies, finishing work in the camp facilities, and site work around the mill, camp and access road.

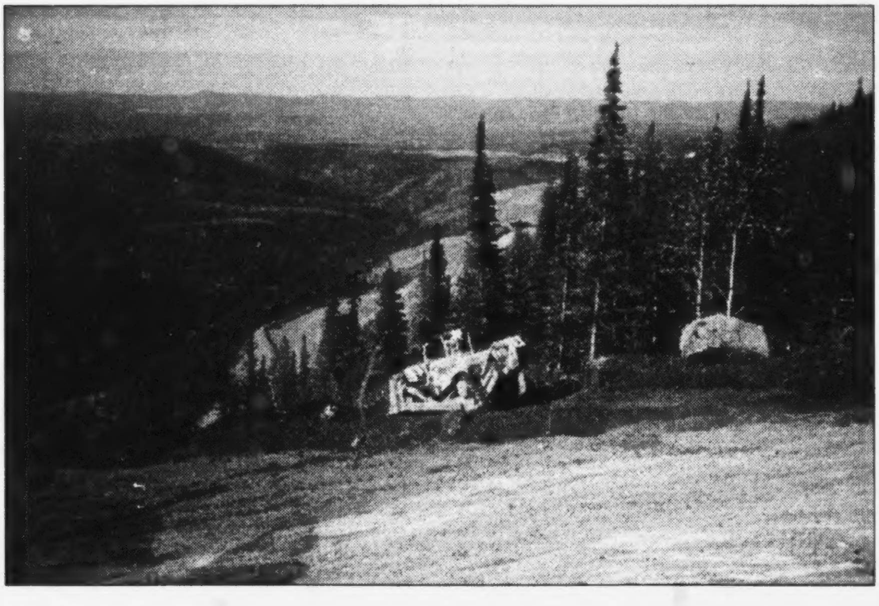

***Figure 5.*** *Resloping of the backfilled Kokanee pit at the Brewery Creek mine.*

The Minto deposit is located 240 km northwest of Whitehorse and is being developed as a conventional open pit mine and milling operation. The deposit has a mineable reserve of 6.51 million tonnes grading 2.13% Cu, 0.62 g/t Au and 9.3 g/t Ag at a 4.9:1 strip ratio. The company has a mining venture agreement with ASARCO Inc. (a subsidiary of Grupo Mexico), under which ASARCO can acquire a 70% interest in the project in consideration for providing up to US$25 million for development of the project. Although the project is fully permitted and could be placed into production within one year, ASARCO did not commit sufficient funds in 2001 to complete development of the project. A 'confirmation' diamond-drilling program was approved by ASARCO Inc./Grupo Mexico for the Minto property in the 2001 season. Five HQ (63.5 mm) diamond-drill holes with a total length of 552 m were drilled (Fig. 6). Core size for the original drilling conducted in the 1970s was BQ (36.4 mm). Hole #2001-12 was drilled to provide a comparison of lower grade intercepts. The hole yielded an increase in the copper content of the main ore zone of 48.6%. A gold grade of 0.10 g/t was recorded for the main ore zone in hole #2001-12; no gold was recorded for this zone in the original 1974 hole #A101. Hole #2001-13 was drilled for comparison with a higher-grade intercept in angle hole #K09-73, a hole drilled by United Keno Hill Mines Ltd. in 1973. A comparison of the mineralized intercepts in these two holes showed an increase in the copper and gold contents of the main ore zone in hole #2001-13 of 17.8% and 45.2%, respectively. Additional holes were drilled to test a lower mineralized horizon located 15 - 24 m below the existing reserves, as well as to aid in detailed mine planning; results from these tests were encouraging. Hole #2001-08 intersected 1.27% Cu and 0.31 g/t Au over 16.9 m in the lower horizon. Hole #2001-14, drilled to test the southwest corner of the Phase 1 open pit, intersected an unexpected 22.3 m of 3.05% Cu, 2.06 g/t Au and 12.93 g/t Ag. These results indicate that the tonnage and grade of the current reserves will increase with the onset of mining.

A.M.T. Canada Inc. purchased the historic Elsa properties of United Keno Hill silver mine in central Yukon in October of 2001. The company formed a strategic alliance with the publicly traded company Pacific Cart Services Ltd. of Nevada in November.

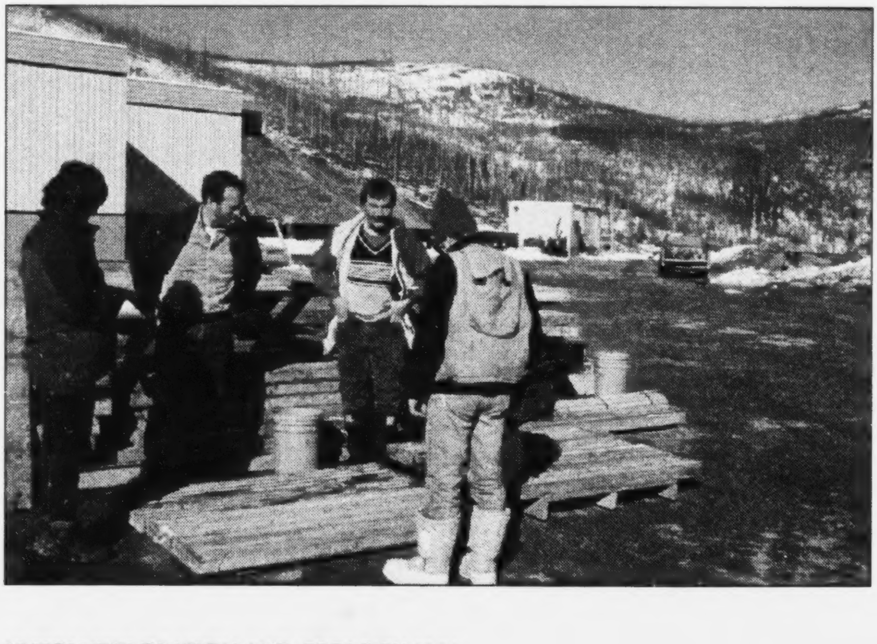

***Figure 6.*** *Jim Proc (second from right) of Minto Exploration reviews core from the confirmation drill program at the Minto project.*

The acquisition of the property and merger are significant steps in returning the historic mining camp to active production. Since the onset of production in 1914, the mines at Elsa have produced over 200 million ounces of silver at a historic camp grade of approximately 1370 g/t Ag (40 oz/ton Ag), from veins within Mississippian Keno Hill Quartzite. Proven and probable underground reserves at the mine currently stand at 415 000 tonnes grading 1145 g/t Ag, 7.5% Pb and 5.6% Zn.

The **CanTung mine** of North American Tungsten Corp. Ltd. is located in the Northwest Territories, 310 km northeast of Watson Lake, Yukon. Access to the mine is through the Yukon, and services and supplies for the operation will be dominantly Yukon based. The Yukon government has signed a road maintenance agreement to support reopening of the mine, which is slated for January of 2002. The Department of Community and Transportation Services will spend approximately $730,000 this year to reopen and upgrade the road to the Yukon/Northwest Territories border located at kilometre 188, and to maintain the road to kilometre 134. In addition, the Yukon government will incur expenditures of approximately $150,000 this year to strengthen the upper Frances River bridge to allow for higher gross vehicle weight crossing capacity. Beginning next year, the government will spend an estimated $450,000 annually to maintain the road year-round up to kilometre 134. North American Tungsten, in turn, will perform year-round maintenance from kilometre 134 to the mine site, a distance of approximately 70 km. The mine has a strategic alliance and supply contract agreement with Sandvik AB of Stockholm, Sweden and Osram Sylvania Products of Pennsylvania, USA to supply 900 000 MTUs (1 MTU = 10 kg) of ore over a three-year period. Cantung was the largest producer of tungsten in the western world with production beginning in 1962 and ending in 1986 when the mine was placed on a program of care and maintenance. Current mineable reserves at Cantung are 630 000 tonnes grading 1.82% $WO_3$.

## EXPLORATION

The focus of exploration shifted slightly towards base metals in 2001 with 60% of the estimated $7.2 million spent on the search for zinc, lead, copper and tungsten. Projects directed towards nickel and copper with associated platinum group elements (PGEs) have been included in the precious metals section. Exploration for gold suffered the greatest downturn, with a reduction of 40% over the amount spent in 2000, however, exploration for PGEs increased substantially in 2001. The reduced expenditures are directly reflected in the amount and size of advanced projects involving diamond drilling that were conducted in 2001. Junior mining companies and/or prospectors spent 70% of the total expenditures in Yukon. Results from all the programs were generally good, but the continuing malaise in the markets denied junior companies the opportunity to expand their programs.

This overview highlights a number of exploration projects conducted in Yukon during the 2001 field season, and it is by no means a comprehensive review of all exploration carried out. Several projects have not been included because of restrictions on disclosure for publicly traded companies, and for competitive reasons, when companies and individuals choose to not openly share exploration results.

The amount of claim staking in Yukon continued to decline with only 1720 claims staked in 2001, and a resulting decrease in claims in good standing to 48,982.

## BASE METALS

Expatriate Resources continued with their program of exploration on their extensive land holdings in the Finlayson Lake volcanogenic massive sulphide (VMS) district in 2001. Expatriate holds a 60% interest in the **Wolverine deposit** (Yukon MINFILE, 2001, 105G 072) with the remainder belonging to Atna Resources. The Wolverine deposit has an indicated resource of 4.941 million tonnes, containing a probable reserve of 3.47 million tonnes (calculated by Hatch and Associates in the 2000 prefeasibility study), grading 12.53% Zn, 1.44% Pb, 1.37% Cu, 336.6 g/t Ag and 1.59 g/t Au. Expatriate conducted drilling on the **Puck** (Yukon MINFILE, 2001, 105G 134) and **Goal Net** (Yukon MINFILE, 2001, 105G 123) properties with one 220-m hole on the Puck and nine holes totalling 1561 m on the Goal Net. Expatriate also conducted geophysical surveys consisting of Horizontal Loop Electromagnetics (HLEM) on the Goal Net and **Redline** (Yukon MINFILE, 2001, 105G 124) properties. Drilling on the Goal Net property (Fig. 7) yielded low-grade stratiform zinc mineralization over a 16-m interval within an argillaceous felsic tuff horizon in hole GN-01-5. The nearest drill hole, located 480 m away, failed to encounter zinc mineralization at a similar stratigraphic horizon. The nine holes completed on the Goal Net property have identified two altered and mineralized horizons over an area of approximately 5 km by 6 km. The predominantly felsic volcanic strata shows considerable similarity to the rocks hosting Teck Cominco's GP4F deposit (1.5 Mt at 6.4% Zn, 3.1% Pb, 0.1% Cu, 90 g/t Ag and 2.0 g/t Au) located 6 km to the north of the Goal Net property.

Expatriate also had a purchase agreement with Cominco to acquire the **Kudz Ze Kayah** (Yukon MINFILE, 2001, 105G 117) and **GP4F** (Yukon MINFILE, 2001, 105I 012) deposits and 2800 surrounding mineral claims. In late August, 2001, Expatriate terminated their acquisition agreement with Teck Cominco.

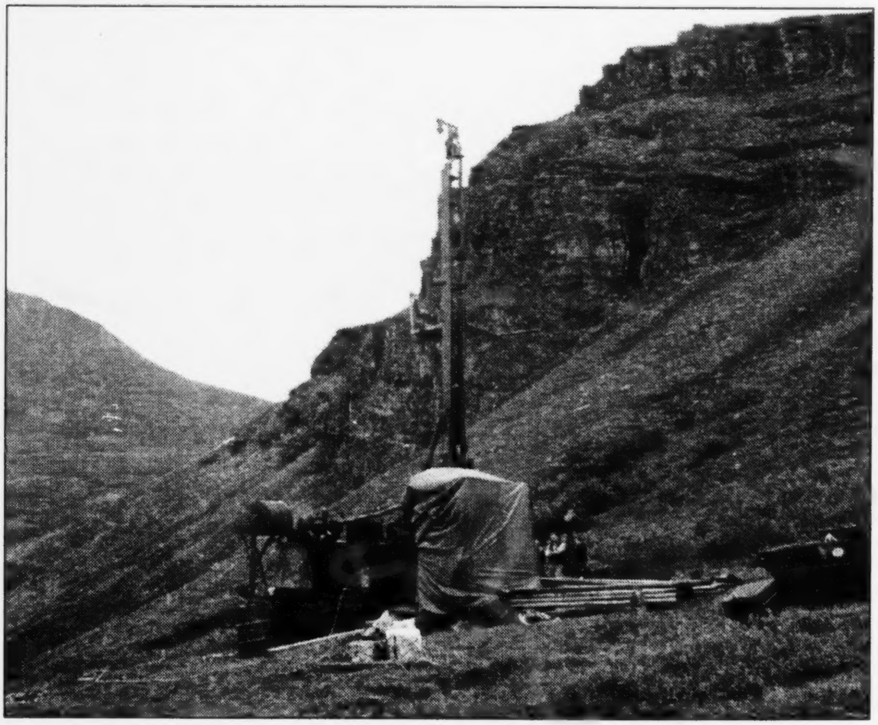

***Figure 7.*** *Drill set-up on the Goal Net VMS property of Expatriate Resources.*

Fairfield Minerals conducted a small program at the **Mor** volcanogenic massive sulphide property near Teslin in southern Yukon (NTS 105C/1). The property is 7 km north of the Alaska Highway and is staked on Category B (surface rights) land of the Teslin Tlingit Council. The claims are underlain by rocks of the Big Salmon Complex in Yukon Tanana Terrane, which have been most recently studied by Mitch Mihalynuk of the British Columbia Geological Survey Branch. Property geology consists of rocks of volcanic origin, including chlorite schist, quartz-sericite schist and ryholite tuff. Slightly higher in the stratigraphy, but not located on the property, is the regionally extensive 'crinkle chert', a manganiferous meta-chert horizon. Field relations, including stratiform magnetite within the 'crinkle chert', as well as geochemical data, indicate a hydrothermal origin of the horizon (Mihalynuk and Peter, 2001). Work by Fairfield Minerals consisted of auger sampling (soil-profile and bedrock at 25 m x 5 m, or 10-m grid spacing), detailed prospecting, and local bedrock geological mapping (Fig. 8). Approximately 200 auger samples (from a maximum depth of 2.4 m) were collected and returned very good results. Bedrock samples returned up to 5.95 g/t Au, 171.4 g/t Ag, 10,665 ppm Pb, 2640 ppm Cu and 1350 ppm Zn. Soil samples within the multi-element geochemical anomaly returned values up to 1492 ppm Cu, 2062 ppm Pb, 2109 ppm Zn, 17.9 ppm Ag and 485 ppb Au, with elevated values of As, Sb and Bi. The program was successful in further defining and enhancing trench and drill targets within the 2 km by 100- to 250-m-wide soil geochemical anomaly.

***Figure 8.*** *Wojtek Jakubowski of Fairfield Minerals poses with a power auger on the Mor VMS property.*

Eagle Plains Resources continued exploring in the Pelly Mountains for volcanogenic massive sulphide deposits on the **Fire** and **Ice** properties (Yukon MINFILE, 2001, 105F 071, 073). These properties are located in the northern portion of the Pelly Mountains volcanic belt, a belt of Mississippian volcanic stratigraphy, which hosts numerous VMS showings including Atna Resources' **Wolf** deposit (Yukon MINFILE, 2001, 105G 008; 4.1 Mt at 6.2% Zn, 1.8% Pb and 84 g/t Ag). Eagle Plains conducted additional staking in the region following exploration success during last season's drilling program. Drilling highlights from the 2000 program on the Fire property included a 15.1-m intersection which assayed 22.4 g/t Ag, 1529 ppm Pb and 6033 ppm Zn, including 3.3 m (approximate true thickness) grading 65.5 g/t Ag, 4930 ppm Pb and 2.15% Zn. A single hole drilled on the Ice property in 2000 intersected a thick-bedded exhalative barite unit containing numerous stratiform sulphide horizons over an approximate true thickness of 48.4 m (158.8 ft). The best mineralized interval within the barite horizon was at 56.7 m to 58.0 m, which contained 5.64% Zn, 0.17% Pb and 12.3 g/t Ag. This season's work included a regional stream sediment geochemical program followed by geological mapping and prospecting (Fig. 9). The program identified five creeks with highly anomalous base and precious metals values, and extended the package of prospective stratigraphy to

***Figure 9.*** *Dr. Charlie Greig conducting 1:10 000-scale geology mapping in less than ideal weather conditions on Eagle Plains Resources' Pelly Mountains VMS project.*

cover an area of 20 km$^2$. Prospecting was successful in discovering one new showing consisting of a lens of massive pyrite with sphalerite, galena and trace chalcopyrite, which assayed 3.0 g/t Ag, 5.48% Zn, 227 ppm Cu, 368 ppm Pb, 414.4 ppm Cd, 152 ppm Hg and 353 ppm W.

Manson Creek Resources has been conducting reconnaissance and property-scale geologic programs on the **Rusty/JRS/Tanner/Nad** claims (NTS 106C/5; 106C/4, D/1; 106D/3; 106C/3) in the Kathleen Lakes area east of Keno Hill. Previous exploration has been directed at high-grade silver-lead veins and Mississippi Valley-type deposits such as the **Val-Vera** (Yukon MINFILE, 2001, 106C 083) and **Craig** (Yukon MINFILE, 2001, 106C 073) deposits. The focus of recent exploration on the properties has shifted towards the potential for sedimentary-exhalative type and volcanogenic massive sulphide (VMS) deposits. Geologic mapping has identified similar stratigraphy to that which hosts the **Marg** VMS deposit (Yukon MINFILE, 2001, 106D 009; 3.48 million tonnes grading 1.8% Cu, 2.7% Pb, 5.0% Zn, 65 g/t Ag and 1.2 g/t Au) located 50 km to the east (Fig. 10). The geological data, combined with anomalies identified in an airborne geophysical survey conducted in the 2001 season, have generated three main areas on the Rusty, JRS and Tanner claim blocks that warrant drill programs. In addition to the VMS targets, two new areas of nickel and gold mineralization have been identified on the claims. Grab sampling of heavily serpentinized ultramafic flows and associated rocks on the Nad property has consistently returned elevated nickel values in the 0.10%

***Figure 10.*** *Water sampling of a rusty seep at the contact of black shale and overlying sericite schist. Mapping at this locality by Manson Creek Resources outlined similar stratigraphy to that hosting the Marg deposit 50 km to the east.*

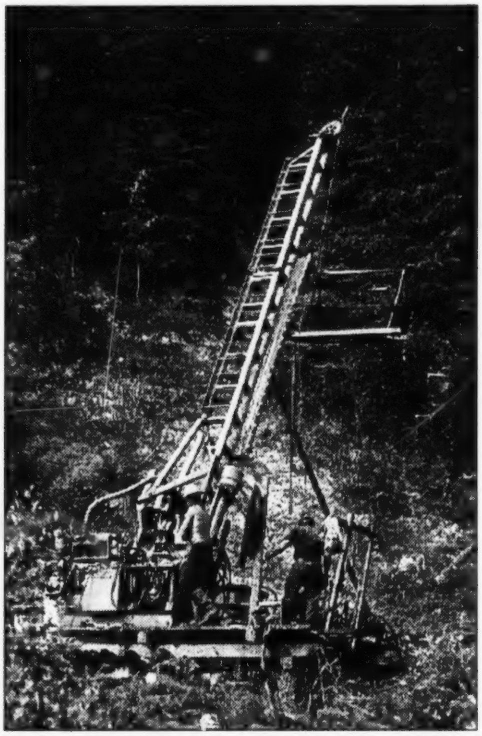

***Figure 11.*** *Noranda Exploration conducted helicopter-supported diamond drilling on the Andrew claims.*

to 0.56% range (29 grab samples). To date, these flows have been identified over a minimum strike length of 8 km. Whole rock geochemistry indicates that the ultramafic rocks are komatiitic; pentlandite has been positively identified under petrographic examination as the nickel-bearing sulphide phase. A new gold showing has also been staked as part of the JRS property. Gold occurs in quartz-carbonate-arsenopyrite veins hosted in black shales. A grab sample of the mineralization in outcrop has returned 4.27 g/t Au, while a 3-m chip sample returned a value of 1.28 g/t Au.

Noranda Exploration optioned the **Andrew** property (Yukon MINFILE, 2001, 105K 089), east of Faro in the Selwyn Basin, from Whitehorse prospector Ron Berdahl. Exploration in the 1970s had identified silver-lead-zinc-copper veins hosted in Earn Group quartzites. Berdahl identified a large (75-m by 150-m) kill zone which returned a surface composite grab sample of 17% Zn. Hand trenching revealed stratabound mineralization at the contact of quartzites and overlying green and maroon shales. In 2001, Noranda conducted a 15-hole, helicopter-supported diamond drill program (Fig. 11) on the kill zone and other targets on the Andrew property. No results from the drilling have been publicly released.

Copper Ridge Exploration conducted a small program on the **Plata** property (Yukon MINFILE, 2001, 105N 003), optioned from Big Blackfoot Resources Ltd. The Plata is air-accessible, located in the eastern portion of the Selwyn Basin, and produced approximately 16 million g (500,000 ounces) of silver from 1983 to 1987 from high-grade silver-lead vein deposits. Copper Ridge examined the property for its potential to host sedimentary-exhalative deposits in Devonian Earn Group stratigraphy which hosts the Tom (9.3 Mt at 6.2% Zn, 7.5% Pb and 69.4 g/t Ag) and Jason (14.1 Mt at 7.1% Pb, 6.6% Zn and 79.9 g/t Ag) deposits located 100 km to the southeast.

Noranda also completed a small three-hole helicopter-supported diamond drilling program on the **Cameron** (Yukon MINFILE, 2001, 106D 012) lead-zinc-silver property east of Keno Hill, which was optioned from Whitehorse-based Tanana Exploration. No results have been released from this program.

Kluane Drilling and Norwest Enterprises continued to explore for skarn and porphyry mineralization on the **Hat** claims (Yukon MINFILE, 2001, 105D 053) in the Whitehorse Copper Belt. From 1900 to 1982, mineral production from several skarn deposits in the Copper Belt produced 123 145 041 kg Cu, 7062.4 kg Au and

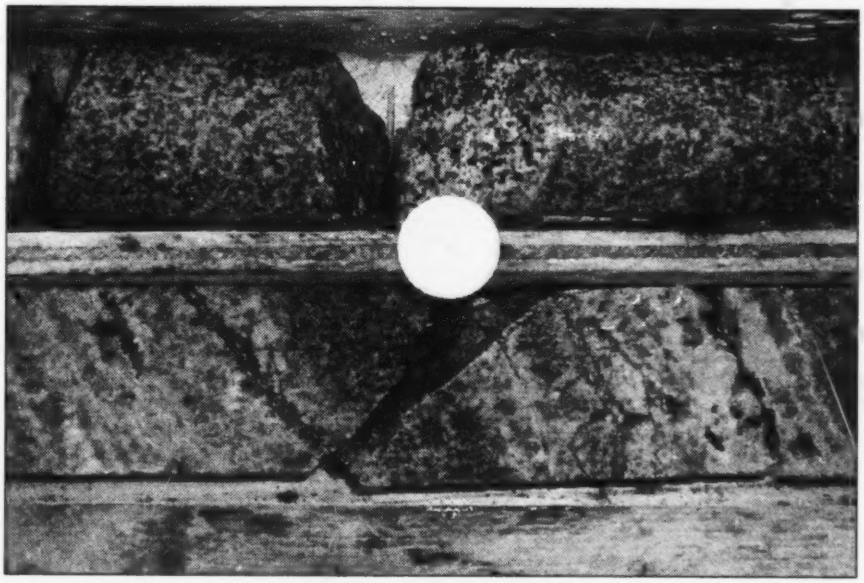

*Figure 12. Sheeted chalcopyrite and quartz-calcite veining hosted in granodiorite. The drill hole targeted an IP chargeability anomaly on the Hat claims in the Whitehorse Copper Belt.*

85 577 kg Ag from 10 247 936 tonnes of ore. Drilling in 2000 revealed a new skarn zone that assayed 4.99% Cu, 1.05 g/t Au and 40.3 g/t Ag over 10.55 m. A single hole, drilled in 2001, 25 m up dip, at a right angle to last year's intersection, hit 2.92 m of skarn mineralization grading 3.12% Cu, 359 ppb Au and 13.8 g/t Ag. Kluane also drilled a single hole to test an Induced Polarization (IP) chargeability anomaly identified in a survey conducted in 2000 by Aurora Geosciences. The drilling intersected granodiorite with fine sheeted quartz-(calcite-) chalcopyrite-(bornite) veinlets with disseminated chalcopyrite halos (Fig. 12). Veining was developed throughout the entire hole with an 80-m section having a density of veinlets of 2 to 10 per metre. The entire section was not sampled, however, the best intersection from selected sampling assayed 1.02% Cu, 560 ppb Au and 11.2 g/t Ag over 1.37 m. The highest gold value was returned from another section, which yielded 1.76 g/t Au, 0.54% Cu and 4.4 g/t Ag over 0.97 m. The IP anomaly remains relatively untested and the new style of mineralization discovered in this recent drilling deserves further attention.

Wildrose Resources conducted a small program of geology and geochemistry on its **Canadian Creek** property (Yukon MINFILE, 2001, 115J 036), located in the Dawson Range in central Yukon. The company has been exploring for porphyry copper-gold-molybdenum and porphyry-gold mineralization adjacent to the Casino deposit.

Sixty miles northeast of Whitehorse, Saturn Ventures Inc. conducted a program of geology, prospecting and soil sampling on the **Mars** property (Yukon MINFILE, 2001, 105E 002). The Mars property covers the Teslin Crossing pluton, an alkalic monzonite stock of Middle Jurassic age. The copper-gold porphyry target was last explored by Placer Dome in 1997. No drilling has ever been conducted on the Mars property although several targets were outlined by Placer Dome.

Monster Copper Resources Inc. has a purchase agreement with Blackstone Ventures for the **Monster** property (Yukon MINFILE, 2001, 116B 103), located approximately 75 km north of Dawson City in the southern Ogilvie Mountains. Exploration on the property is targeting iron-oxide-associated copper-gold deposits similar to the large Olympic Dam copper-uranium-gold-silver deposit in Australia. The area is cored by the Coal Creek Inlier, an oval-shaped east-trending window of Middle and Late Proterozoic clastic rocks that have been penetrated by mineralized 'Wernecke Breccias' and cut by mafic sills and dykes. In 1994, Blackstone Resources conducted a program of geological mapping, prospecting, soil geochemistry and radiometric surveys over the whole claim block. In 2001, Monster Copper Resources conducted a program of ground geophysics, geochemistry, mapping and prospecting (Fig. 13).

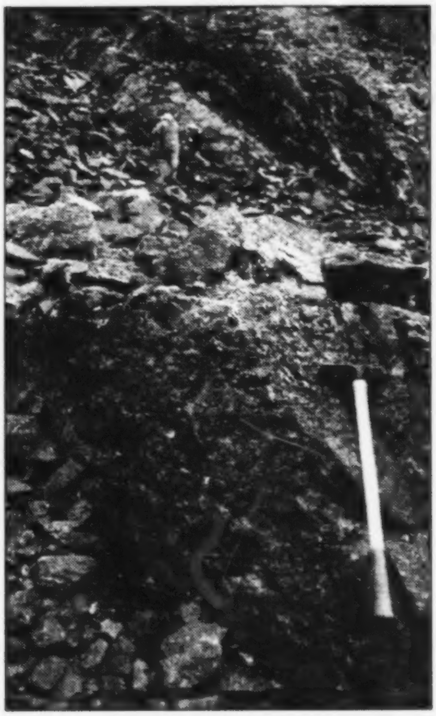

***Figure 13.** Iron-oxide-associated copper-gold deposits are the target on the Monster claims of Monster Copper Resources. Talus and outcrop of hematitic 'Wernecke Breccia' are visible in this photo. Tom Setterfield of Monster Copper and Al Doherty (upper middle) are sampling a copper showing in the background.*

Shawn Ryan of Dawson staked the **Hem** claims (Yukon MINFILE, 2001, 116G 082) located on a pronounced, linear, northeast-trending regional magnetic anomaly. This anomaly connects the Monster, **Olympic** (Yukon MINFILE, 2001, 116B 099) and Hem claims. The Hem claims cover a hematitic 'Wernecke Breccia' (Fig. 14) cut by mafic dykes exposed in a small window of Proterozoic clastic rocks. The Hem claims and the breccia body are bisected by the Dempster Highway, where the road cut provides a nice exposure of the breccia mineralized with disseminated chalcopyrite. The hematitic breccia can be found in a continuous exposure along a creek cut on the east side of the Blackstone River for over 1.5 km.

Copper Ridge Exploration conducted a program of due diligence sampling on the **Kalzas** tungsten-tin-silver property (Yukon MINFILE, 2001, 105M 066) south of Mayo in central Yukon. The property had been previously explored by Union Carbide in the 1980s. Wolframite occurs with minor scheelite, molybdenite, cassiterite, galena and beryl in a 1000-m by 800-m quartz stockwork cutting gritty quartzite and phyllite of the Neoproterozoic to Early Cambrian Hyland Group. The property has an extensive infrastructure of roads and is accessed via a winter road and airstrip. Copper Ridge conducted extensive sampling along road cuts, trenches and from historic drill core. Sampling within an area of 500 m by 300 m returned values from trenches of 66 m grading 0.493% $WO_3$, 70 m grading 0.427% $WO_3$, 66 m grading 0.427% $WO_3$, 16 m grading 0.306% $WO_3$, 8 m grading 0.705% $WO_3$, and 20 m grading 0.268% $WO_3$ (Fig. 15). The sampling highlights the potential of the property to host not only a large tonnage deposit, but has also revealed areas where higher grade material may be exploited. Copper Ridge is extremely encouraged by these results and is planning on further exploration, including drilling, for 2002 (see also Carlson, this volume).

***Figure 14.** Ken Galambos (left), Mineral Development Geologist with the Yukon Government, examines hematitic 'Wernecke Breccia' exposed in a creek cut on Shawn Ryan's (right) Hem claims.*

Strategic Metals (formerly Nordac Resources) also conducted exploration for tungsten in Yukon, and staked and

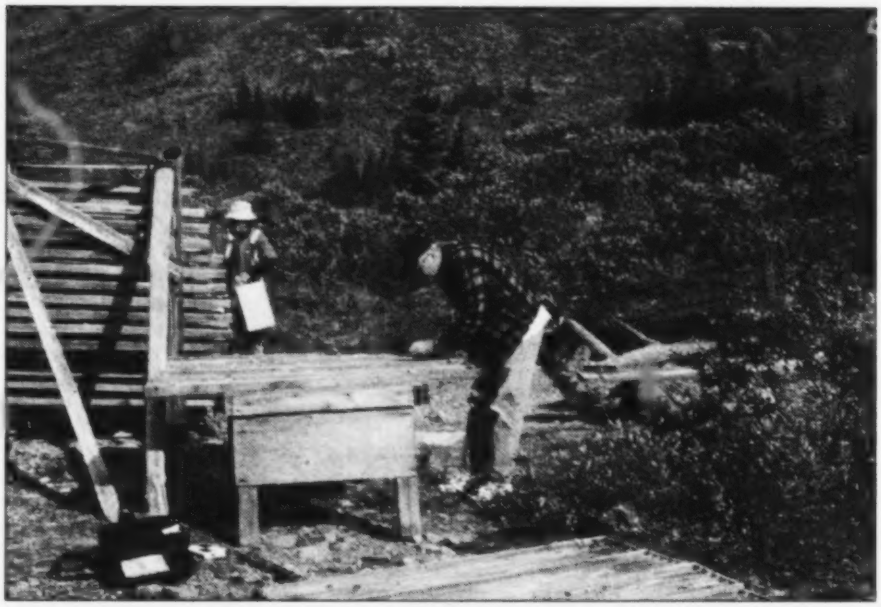

***Figure 15.*** *Gerry Carlson (right), President of Copper Ridge Exploration, examines core drilled in 1983 by Union Carbide on the Kalzas tungsten property.*

performed small geological programs on the **Hidden** (Yukon MINFILE, 2001, 105F 092) and **Obvious** (Yukon MINFILE, 2001, 105F 094) claims. These cover areas of tungsten skarn mineralization associated with Cretaceous plutons in south-central Yukon.

## PRECIOUS METALS

Canadian United Minerals, a private Yukon-based exploration company, conducted a 26-hole, 1100-m diamond drilling program on the **Horn** property (NTS 116B/7) within the boundary of the proposed Tombstone Park. The claims cover part of a roof pendant of sedimentary rocks of Devonian to Jurassic age enclosed by quartz monzonite of the Cretaceous Tombstone pluton. Pyroxene and pyrrhotite skarns containing gold, silver, copper, lead, zinc, arsenic and bismuth are developed in Permian Takhandit Formation limestone. Drilling in 2000 was directed at defining a high-grade resource in a small skarn lens that was exposed by surface trenching. The lens was drilled at 15-m centres, and the drilling outlined a resource of 6000 tonnes grading 67.2 g/t Au. The lens is open to depth. Drilling in 2001 was directed at several geophysical (magnetic) anomalies (Fig. 16) in the immediate area of the resource outlined by last years work. Several holes intersected additional skarn mineralization, but no assays have been released from this year's drilling. The company intends on applying for a winter road permit to access the claims, as well as a water license and mine production permit for the skarn deposit.

Regent Ventures completed a 5-hole, 1280-m diamond drilling program (Fig. 17) on the **Red Mountain** property

***Figure 16.*** *Shawn Ryan conducting a magnetic survey on the Horn claims of Canadian United Minerals.*

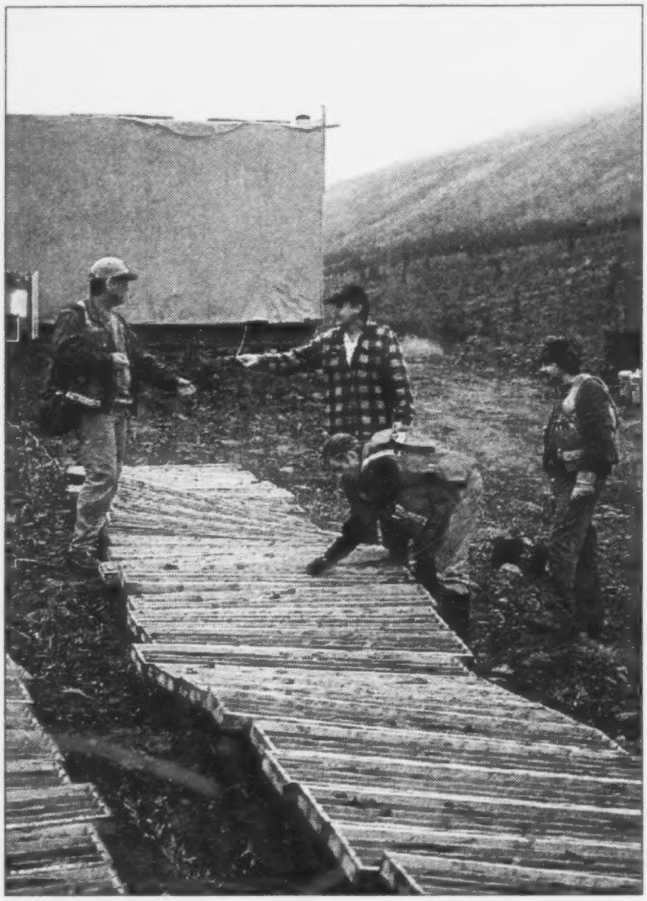

*Figure 17. Cory Coe (upper centre) with Regent Ventures viewing core on the Red Mountain property.*

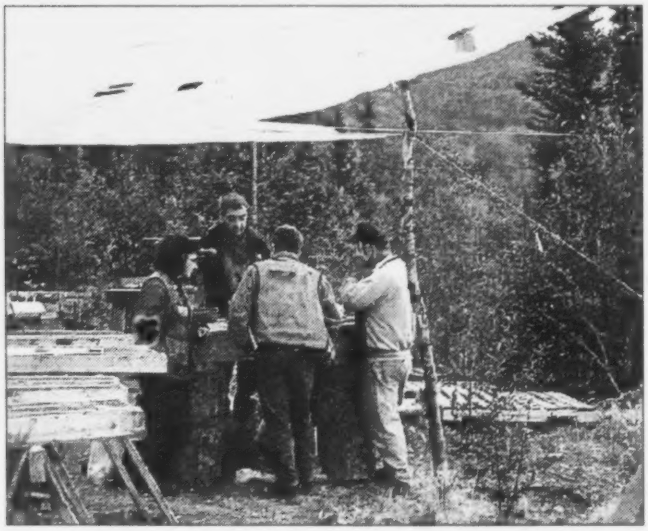

(Yukon MINFILE, 2001, 115P 006), near Mayo. Intrusive-related gold mineralization on the property is hosted in Neoproterozoic to Early Cambrian Hyland Group quartzites and hornfels proximal to small plugs of Cretaceous intrusive rocks. Drill holes intersected large zones of tourmaline breccias, tourmaline-quartz breccias and quartz-feldspar porphyry dykes. Minor quartz and quartz-sulphide mineral veins within the breccias were also intersected. One hole, DDH-01-28, intersected significant gold mineralization and returned three intersections: 9.8 m grading 1.0 g/t Au; 3.3 m grading 19.8 g/t Au (including 1 m grading 46.07 g/t Au, and 0.8 m grading 33.45 g/t Au); and 9.4 m grading 0.7 g/t Au. The onset of winter conditions forced an early closure of the program, and the drill and camp were fully winterized and remain in place for continuation of the program next year.

Atac Resouces Ltd. conducted a program of geophysics, excavator trenching, geological mapping and diamond drilling on the **Golden Revenue** property (Yukon MINFILE, 2001, 115I 042, 107) in central Yukon. The property is road accessible in a historical placer mining area within the Tintina gold belt (British Columbia and Yukon Chamber of Mines, 2000). Previous exploration on the property has identified numerous showings ranging from high-grade gold veins to larger stockwork breccia zones. The property is underlain by Paleozoic or older metamorphic rocks belonging to the Yukon-Tanana Terrane, which are extensively intruded by Mesozoic igneous rocks of the Coast Plutonic Complex. The metamorphic rocks consist of schist, gneiss, amphibole, quartzite and minor limestone. The intrusive rocks are Jurassic syenite and a Cretaceous suite comprising a granodiorite to monzonite stock cut by microgranite plugs, porphyritic dykes and a large breccia complex. Atac completed 6 diamond drill holes totaling 1201 m, 10 line-km of Induced Polarization surveys, and excavator trenching during the program. The drilling was designed to test for mineralization beneath the oxidized cap in the Nucleus zone. Drilling was successful in intersecting significant mineralization in all holes, and the deeper drilling resulted in a much better understanding of the controls on mineralization (Fig. 18).

***Figure 18.** (bottom) Drilling through the oxidized cap on the Golden Revenue property of Atac Resources revealed new insights into the controls on mineralization. Company President Doug Eaton (right) disscusses findings with other geologists examining drill core.*

Mineralization appears to be associated with a series of en-echelon, moderately east-dipping quartz-feldspar porphyry dykes. The following selected results were obtained from drilling:

| Hole # | From (metres) | To (metres) | Width (metres) | Gold (g/t) |
|---|---|---|---|---|
| DN01-01 | 3.05 | 30.70 | 27.65 | 0.84 |
| | 65.00 | 68.28 | 3.28 | 1.71 |
| DN01-02 | 35.66 | 71.65 | 35.99 | 1.32 |
| | 130.76 | 142.95 | 12.19 | 1.82 |
| DN01-03 | 58.38 | 75.90 | 17.52 | 1.36 |
| | 88.09 | 145.85 | 57.76 | 1.32 |
| Including | 121.50 | 138.09 | 16.59 | 2.10 |
| DN01-04 | 68.07 | 72.85 | 4.78 | 3.30 |
| | 185.26 | 188.52 | 3.26 | 2.33 |
| DN01-05 | 61.57 | 71.02 | 9.45 | 1.03 |
| | 147.70 | 153.13 | 5.43 | 1.24 |
| DN01-06 | 120.55 | 128.48 | 7.93 | 1.90 |

The trenching program on the property was successful in discovering a new zone of vein mineralization. A quartz vein was exposed in two trenches located 120 m apart. Channel samples returned 8.89 g/t Au over 3.3 m in one trench, and 3.63 g/t Au over 9.5 m in the other.

Klondike Source Limited, a private Australian exploration company, continued to work on their **Klondike/Wedge** block of claims (NTS 115NO/14,15) optioned from Barramundi Gold. Klondike Source continued a regional-scale geochemical survey of the large claim block, using the mobile-metal-ion (MMI) geochemical analytical method of sampling. The geochemical traverses are based on a structural analysis of the property from satellite imagery and airphoto interpretation. Anomalies generated from the program correlate well with the structural interpretation and also with conventional soil anomalies for gold and arsenic, while providing a much more coherent anomalous signature. Klondike Source has based their exploration program on the Thermal Aureole Gold (TAG) model (Wall, 1999), and has generated several drill targets with the current program.

Tagish Lake Gold Corporation conducted a program of geological mapping, prospecting and diamond drilling (Fig. 19) on the **Skukum** gold/silver property, located 80 km south, by road, from Whitehorse, Yukon. The Skukum property encompasses three known gold/silver mineral deposits, **Skukum Creek** (Yukon MINFILE, 2001, 105D 022), **Mt. Skukum mine** (Yukon MINFILE, 2001, 105D 158) and **Goddell** gully (Yukon MINFILE, 2001, 105D 025), as well as numerous exploration targets. Skukum Creek is a polymetallic, shear-hosted gold-silver vein within mid-Cretaceous granodiorite of the Coast Plutonic Complex, and is the main exploration target of Tagish Lake Gold. Mt. Skukum mine consists of epithermal gold-silver veins and breccias hosted in the Eocene Mt. Skukum Volcanic Complex. The Mt. Skukum mine was in production from 1986 to 1988 and produced 2419 kg (77,790 troy ounces) of gold from 233 400 tonnes of ore. Goddell gully consists of polymetallic gold veins hosted in the Goddell shear zone within mid-Cretaceous granite of the Coast Plutonic Complex. In all, the three gold/silver mineral deposits on the Skukum property have estimated geological resources of 1.072 million tonnes grading 9.63 g/t Au and 175.21 g/t Ag, or 10.3 million g (332,000 ounces) of gold and 187.8 million g (6,039,000 ounces) of silver. Tagish Lake Gold acquired the properties by amalgamating Omni Resources and Trumpeter Yukon Gold, resulting, for the first time, in the consolidation of the three deposits under a single company.

In 2001, Tagish Lake Gold conducted drilling of four holes totaling 1502 m at targets in the Ridge Zone on the Skukum Creek property. The Ridge Zone is located along strike approximately 500 m west of the Skukum Creek deposit, and consists of two main areas of mineralization termed Zone 2 and the Ridge Zone. Previous drilling in the area intersected values up to 7.82 g/t Au and 234.3 g/t Ag over 13.0 m. The current holes cut quartz-sulphide mineral veins and breccias in Zone 2 that yielded 9.9 m grading 1.77 g/t Au and 19.2 g/t Ag, including 0.42 m grading 40.37 g/t Au and 243.3 g/t Ag. Zone 2 remains open in both directions along strike, and most significantly, down dip. Ridge Zone drilling intersected a fault zone approximately 20 m wide (true thickness), which consists of highly sheared to brecciated granodiorite, rhyolite and andesite dykes with quartz-sulphide mineral breccias and veins. Multiple intersections at a high angle to the fault zone returned assays up to 3.0 m grading 2.15 g/t Au and 160.2 g/t Ag, 1.99 m grading 1.17 g/t Au and 44.3 g/t Ag, and 2.05 m grading 3.84 g/t Au and 251.1 g/t Ag from Hole SC01-01. The Ridge Zone also remains open along strike and to depth. Long sections of the Skukum Creek deposit and Ridge Zone show an increase in thickness and grade with depth. Tagish Lake Gold plans on testing the zones at depth in 2002 by re-entering the existing underground workings and developing a proposed lower adit.

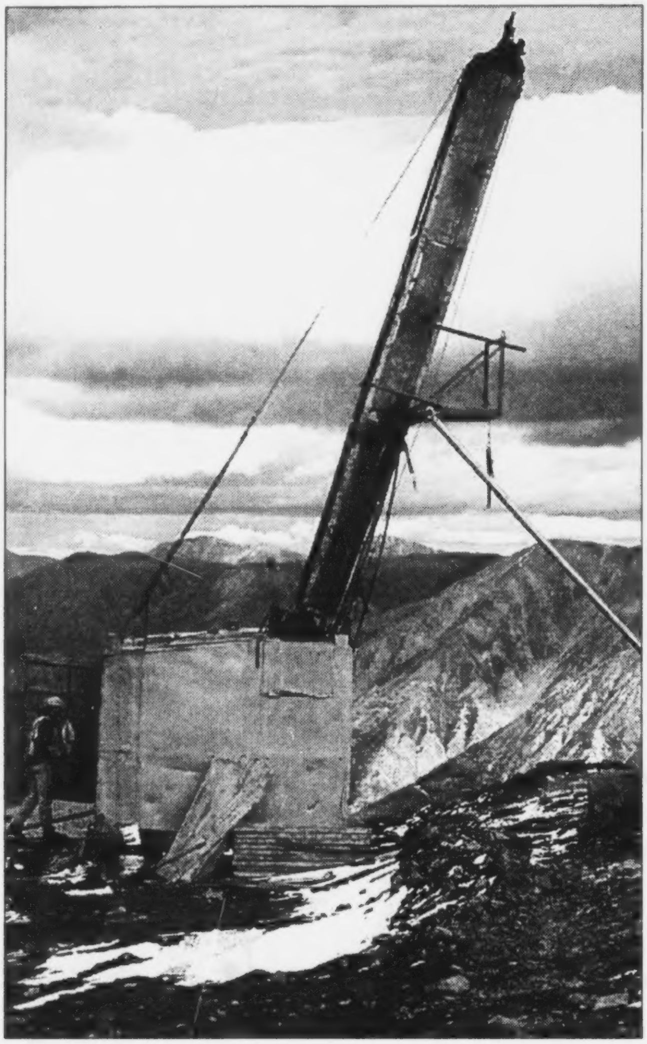

***Figure 19.*** *Diamond drill rig on the Skukum Creek property of Tagish Lake Gold Corporation.*

Numerous other exploration targets exist on the claims, with the main target outside the known Skukum Creek deposits being the Charleston vein. Relatively continuous chip sampling, carried out by Total Erickson Resources in 1987 along the outcropping Charleston structure, produced uncut results averaging 7.44 g/t Au and 91.6 g/t Ag over an average width of 1.36 m and a strike length of 250 m. Check sampling and geological mapping by Tagish Lake Gold confirmed previous results from the vein. The Charleston vein has never been diamond drilled and is a high priority drill target for the 2002 program.

Al Carlos of Whitehorse drilled five holes totaling 262 m on his **Grew Creek** property (Yukon MINFILE, 2001, 105K 009), an Eocene epithermal gold-silver deposit near Faro. The deposit hosts a drill-indicated geological resource of 773 012 tonnes grading 8.9 g/t Au and 33.6 g/t Ag (Christie, 1992). Al has been conducting extensive compilation work on the property, and in 2000 conducted a geochemical survey using the Enzyme Leach Process on targets outside of the main Grew Creek

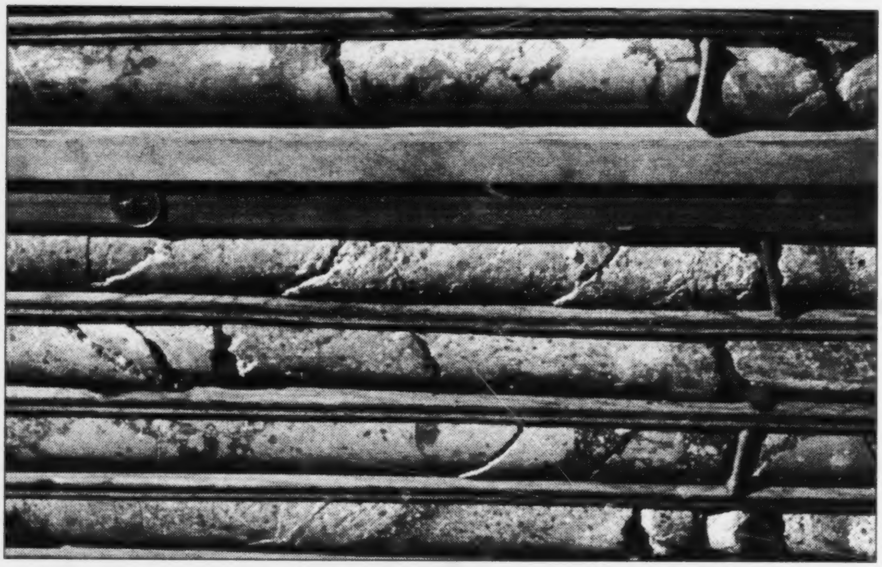

*Figure 20.* Hydrothermal breccia intersected in drilling on the Grew Creek property of Whitehorse prospector, Al Carlos. Quarter for scale.

deposit. Several anomalies were outlined with the survey that were supported by historical airborne geophysical data, conventional geochemistry and prospecting. Drilling was successful in intersecting an intriguing siliceous hydrothermal breccia (Fig. 20). Assays on the core returned low values for gold, however, additional work to locate mineralized phases of the breccia will be conducted in 2002.

Tanana Exploration Inc. followed up on a highly anomalous till geochemical sample (Fig. 21) released by Jeff Bond (Bond, 2001) of the Yukon Geology Program in 2000. Bond's sample JB00-155 contained 28.9 ppb Au, 484.5 ppm As, 151.4 ppm Sb, 21,020 ppm Hg, 1 ppm Tl and 1374 ppm Ag. The sample was taken from a mudflow-like deposit on a small peninsula next to a lake. The soil at the site was highly oxidized. Tanana staked the area as the **Spice** claims (NTS 105G/13) in early 2001 and performed soil sampling, prospecting and hand trenching. The claims are covered by a thin continuous blanket of Quaternary cover, which limits outcrop exposure in the area. Recent mapping by Don Murphy of the Yukon Geology Program indicates that the claims are underlain by Permian-aged quartzite and conglomerate of the Yukon Tanana Terrane. High-level quartz porphyritic felsic dykes were also noted by Murphy on the claims (D. Murphy, pers. comm., 2001). Soil sampling by Tanana Exploration indicated a linear soil geochemical anomaly with values up to 316 ppb Au, 959 ppm As, 256 ppm Sb and 37,551 ppb Hg. Follow-up work by Bond in 2001 included more detailed till sampling on the Spice claims. Results included a gold value of 13,891 ppb with coincident anomalous silver, arsenic, antimony and mercury. Detailed results are presented in Bond, 2002 (this volume).

Northern Platinum Ltd. conducted a program of geology, geochemistry, geophysics, underground rehabilitation, trenching and diamond drilling on their **Wellgreen** property (Yukon

*Figure 21.* Geochemical till sampling on the Spice claims.

MINFILE, 2001, 115G 024) in the Kluane Mafic-Ultramafic Belt (Hulbert, 1997), in western Yukon. The Wellgreen nickel-copper mine was operated by Hudson Bay Mining and Smelting from 1972 to 1973. Hudson Bay's early drilling outlined 669 150 tonnes grading 2.04% Ni, 1.42% Cu, 0.07% Co, 1.3 g/t Pt, 0.93 g/t Pd and 0.17 g/t Au, contained in massive sulphide lenses along the footwall contact of the Quill Creek Complex. Drilling in 1987 and 1988 by Kluane Joint Venture expanded the resource to include disseminated sulphides in the basal gabbro and overlying peridotite. Current resources are estimated at 49.9 million tonnes grading 0.36% Ni, 0.35% Cu, 0.51 g/t Pt and 0.34 g/t Pd. In the current program, six holes were drilled in the vicinity of the Wellgreen deposit. Drill hole WGS 01-144 intersected 37.0 m grading 0.19% Cu, 0.32% Ni, 0.014% Co, 0.31 g/t Pt, 0.43 g/t Pd and 0.03 g/t Au near surface, and an additional 17.1 m grading 0.15% Cu, 0.17% Ni, 0.01% Co, 0.22 g/t Pt, 0.32 g/t Pd and 0.05 g/t Au deeper in the hole. Hole WGS 01-145 was collared in mineralization and intersected 13.9 m grading 0.37% Cu, 0.25% Ni, 0.013% Co, 0.56 g/t Pt, 0.71 g/t Pd and 0.09 g/t Au, and deeper in the hole, an additional 10.2 m grading 0.23% Cu, 0.36% Ni, 0.02% Co, 0.44 g/t Pt, 0.70 g/t Pd and 0.06 g/t Au. Soil sampling, prospecting and self-potential geophysical surveys by Dave Javorsky (Fig. 22) on the Arch claims 3 km west of the Wellgreen deposit exposed significant new mineralization. Chip sampling across the new SP showing yielded 10.3 m grading 1.24% Cu, 1.34% Ni, 0.065% Co, 0.9 g/t Pt and 1.2 g/t Pd, including 3.5 m grading 2.08% Cu, 3.18% Ni, 0.15% Co, 2.71 g/t Pt, 3.46 g/t Pd and 0.37 g/t Au. One hole was drilled under the showing which intersected similar grading material returning 14.5 m of 0.45% Cu, 0.43% Ni, 0.019% Co, 0.38 g/t Pt and 0.55 g/t Pd, including a higher grade intersection of 1.6 m grading 2.92% Cu, 1.54% Ni, 0.058% Co, 1.31 g/t Pt, 1.89 g/t Pd and 0.14 g/t Au. The discovery of the SP showing on the Arch claims highlights the potential of the entire Kluane Mafic-Ultramafic Belt considering that a significant new showing can be found on the most advanced property in the belt.

Uravan Minerals completed a program of geophysics (max-min, induced polarization), prospecting, mapping, hand-trenching and sampling on the **Canalask-**

***Figure 22.*** *David Javorsky, prospector, indicates the size potential of his newly discovered SP showing on the Arch claims of Northern Platinum Resources.*

**Onion** property (Yukon MINFILE, 2001, 115K 077), optioned from Expatriate Resources. The property covers the White River intrusive complex, the second largest mafic-ultramafic body located in the Kluane Mafic-Ultramafic Belt. Uravan concentrated its work along a 5-km length of the most northwestern section of the complex. Previous work had identified areas of Ni-Cu-PGE mineralization in marginal gabbros in the basal section of the ultramafic body in the Discovery-Onion and Sax-Cessna areas. Hand trenching in the footwall of the White River intrusive complex exposed the base of the sill in several areas. Assays up to 4.69% Ni, 0.79% Cu, 0.17% Co and 6.83 g/t PGEs, including >4 g/t Os, Re, Rh, Ir, were obtained. In the areas of the Discovery-Onion Southeast (Fig. 23) and Sax-Cessna surface mineral occurrences, two exceptionally strong max-min conductors with coincident strong Induced Polarization (IP) chargeability-resistivity anomalies were delineated within the footwall of the complex and along strike from the known outcropping mineralization. These geophysical anomalies have strike lengths of over 800 m and 1100 m, respectively. Uravan interprets these strong geophysical responses as semi-massive to massive sulphide. The strong coincident max-min/IP geophysical anomalies occur at or near the base of the steeply dipping ultramafic sill and coincide with a pronounced thickening or embayment of the sill. Hulbert (1997) identified basal embayments within the White River intrusive complex as high priority areas for exploration. High-grade Ni-Au values occurring at the Onion SE showing, assaying 27.4% Ni and 30.6 g/t Au, are related to a later hydrothermal episode that overprinted the main Ni-Cu-Co-PGE magmatic ultramafic-hosted mineralization. Uravan intends on drilling the property in 2002.

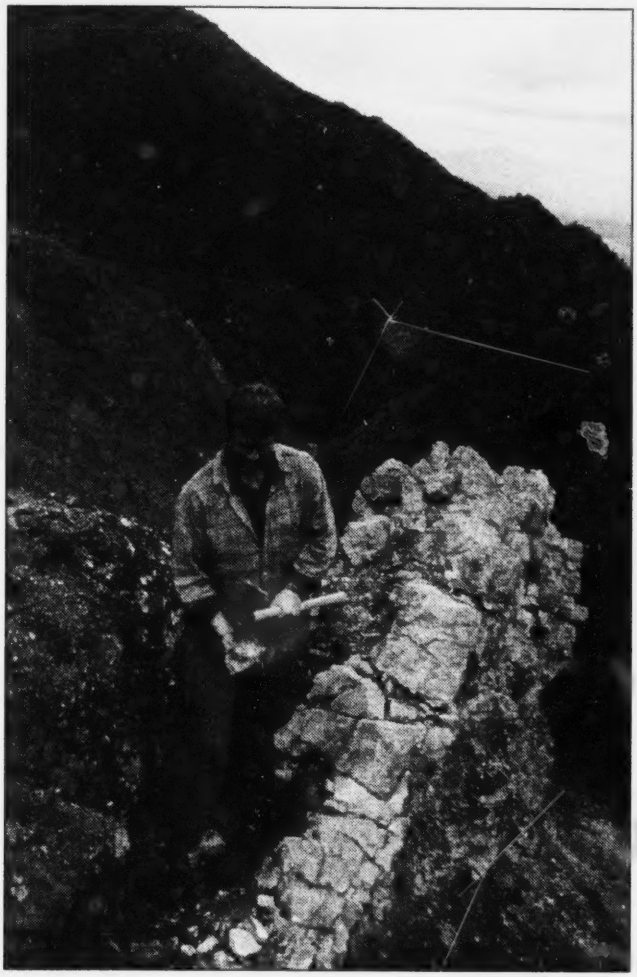

***Figure 23.*** *Uravan Minerals conducted a program of geology, geochemistry and geophysics on the Canalask-Onion property optioned from Expatriate Resources. Jim Barr with Aurora Geosciences examines Ni-Cu-PGE mineralization exposed in hand trenching on the Discovery showing.*

In the southern portion of the Kluane belt, Yukon prospector Tom Morgan restaked the **Ultra** showing (Yukon MINFILE, 2001, 115B 008). Tom conducted prospecting, mapping, sampling and magnetic surveys on the claims. Two types of mineralization are evident on the property: magmatic Ni-Cu-PGE associated with gabbro dykes, and enigmatic massive sulphide boulders exposed on a terminal moraine. The property is underlain by volcanic and sedimentary rocks of the Permian Station Creek Formation. Gabbro dykes are 2-4 m wide, and chip sampling returned values up to 1.66% Cu, 6420 ppm Ni, 1970 ppb Pd, 203 ppb Pt and 240 ppb Au over 1 m. A cluster of seven massive sulphide boulders over a 50-m area returned a composite assay of 2.7% Cu, 4.1% Zn, 69 ppb Au and 43.2 ppm Ag. The boulders consist of banded fine-grained pyrite with lesser sphalerite, chalcopyrite, quartz, carbonate and minor galena. Previous workers proposed a source for the mineralization to be a massive sulphide lens in andesite exposed in a cliff face 5 km away.

## GEMSTONES

True North Gems optioned the **Regal Ridge** emerald property (NTS 105G/7) from Expatriate Resources in 2001. True North obtained a Mining Land Use Permit to walk an excavator to the property. The excavator was walked from the end of the Kudz Ze Kayah access road to the emerald showings, a distance of approximately 15 km. The excavator was used to develop access trails, conduct stripping, trench, and facilitate sampling and mapping of the emerald showings (Fig. 24). Property geology consists of Mississippian meta-gabbro and chlorite schist of the Fire Lake mafic metavolcanic unit intruded by ultramafic rocks, Cretaceous granite and Tertiary feldspar porphyry dykes. Emeralds occur in stacked or near horizontal bands of 'golden schist' containing sub-parallel quartz-tourmaline veins or pods. The golden schists are brownish-weathering chlorite-sericite schists, which host coarse mica and emerald near the selvages of quartz veins. Trenching revealed vertical joints intersecting the golden schist horizons and hosting emerald mineralization. True North interprets the joints as conduits for the mineralizing fluids. Soil geochemistry was utilized to direct trenching and was successful in identifying three new areas of mineralization. Emeralds collected from trenches during the 2001 program were larger and of excellent colour, indicating that the effects of near-surface weathering has been responsible for degradation and fracturing of many previously recovered crystals. True North is very encouraged with this year's results and is planning on an expanded program for 2002.

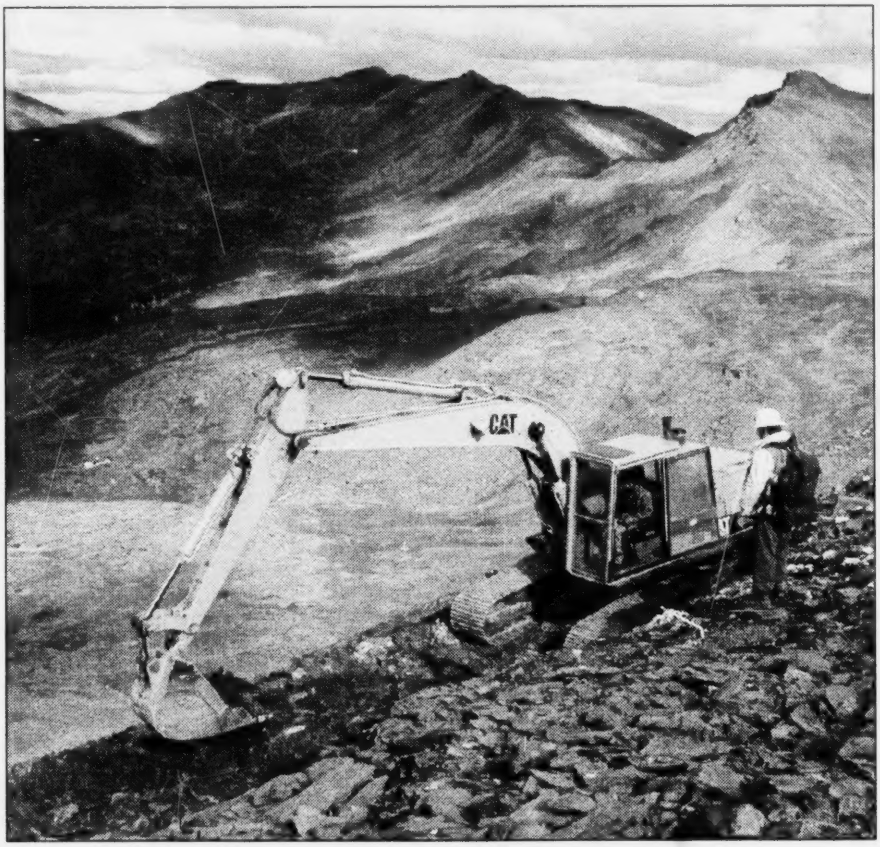

***Figure 24.*** *Bernie Gaboury of True North Gems directs excavator trenching on the Regal Ridge emerald property. Photo by Brad Wilson, True North Gems.*

## ACKNOWLEDGEMENTS

This report is based on public information gathered from a variety of sources. It also includes information provided by companies through press releases, property summaries provided to the department, and from property visits conducted in the 2001 field season. The cooperation of companies in providing information, as well as their hospitality and access to the property during field tours are gratefully acknowledged. Editing by Leyla Weston and Diane Emond is greatly appreciated.

## REFERENCES

Bond, J.D., 2001. Surficial geology and till geochemistry of Weasel Lake map area (105G/13), east-central Yukon. *In:* Yukon Exploration and Geology 2000, D.S. Emond and L.H. Weston (eds.), Exploration and Geological Services Division, Yukon Region, Indian and Northern Affairs Canada, p. 73-96.

Bond, J.D. and Plouffe, A., 2002 (this volume). Finlayson Lake Targeted Geoscience Initiative (southeastern Yukon), Part 2: Quaternary geology and till geochemistry. *In:* Yukon Exploration and Geology 2001, D.S. Emond, L.H. Weston and L.L. Lewis (eds.), Exploration and Geological Services Division, Yukon Region, Indian and Northern Affairs Canada, p. 209-228 plus 10 fold-out maps.

British Columbia and Yukon Chamber of Mines, 2000. The Tintina Gold Belt: Concepts, Exploration, and Discoveries. Cordilleran Roundup, January, 2000, T.L. Tucker and M.T. Smith (session chairs), Special Volume 2, 225 p.

Christie, A.R., 1992. Grew Creek epithermal gold-silver deposit, Tintina Trench, Yukon. *In:* Yukon Geology, Volume 3, T.J. Bremner (ed.), Exploration and Geological Services Division, Yukon Region, Indian and Northern Affairs Canada, p. 223-359.

Hulbert, L., 1997. Geology and Metallogeny of the Kluane Mafic-Ultramafic Belt, Yukon Territory, Canada: Eastern Wrangellia – A New Ni-Cu-PGE Metallogenic Terrane. Geological Survey of Canada, Bulletin 506, 265 p.

Mihalynuk, M.G. and Peter, J.M., 2001. A hydrothermal origin for "crinkle chert" of the Big Salmon Complex. *In:* Geological Fieldwork 2000, B.C. Ministry of Energy and Mines, Paper 2001-1, p. 83-84.

Wall, V.J., 1999. Pluton-related (thermal aureole) gold. Short course for Yukon Geoscience Forum 1999. Taylor Wall and Associates, Brisbane, Australia.

Yukon MINFILE, 2001. Exploration and Geological Services Division, Yukon Region, Indian and Northern Affairs Canada.

# APPENDIX 1: 2001 EXPLORATION PROJECTS

BS - Bulk Sample
D - Development
DD - Diamond Drilling
ES - Environmental Studies
F - Feasibility
G - Geology
GC - Geochemistry
GP - Geophysics
M - Mining
P - Prospecting
PD - Percussion Drilling
PF - Prefeasibility
R - Reconnaissance
T - Trenching
U/GD - Underground Development

| PROPERTY | COMPANY/OWNER | MINING DISTRICT | MINFILE # or (1:50 000 NTS) | WORK TYPE | COMMODITY |
|---|---|---|---|---|---|
| **Andrew** | Noranda Exploration | Whitehorse | 105K 089 | G,GC,DD | Zn-Pb-Ag |
| **AR** | Auterra Ventures Inc | Whitehorse | 115G 026 | G,GC,T | PGE,Cu,Ni |
| **Brewery Creek** | Viceroy Resources | Dawson | 116B 160 | M | Au |
| **Cameron** | Noranda/Tanana Exploration | Mayo | 106D 012 | G,DD | Zn-Pb-Ag |
| **Canadian Creek** | Wildrose Resources | Whitehorse | 115J 036 | G,GC | Cu-Au |
| **Canalask-Onion** | Uravan/Expatriate Resources | Whitehorse | 115K 077 | G,GC,GP,T | Ni-Cu-PGE |
| **Clear Creek** | Redstar/Newmont Exploration | Mayo | 115P 012,013 | G,GC | Au |
| **Fire/Ice** | Eagle Plains Resources | Watson Lake | 105F 071,073 | G,GC | Pb-Zn-Ag |
| **Goal Net** | Expatriate Resources | Watson Lake | 105G 123 | G,GC,DD | Pb-Zn-Cu-Ag-Au |
| **Golden Revenue** | ATAC/YKR International | Whitehorse | 115I 042,107 | G | Cu-Au-Ag-$WO_3$-$MoS_2$ |
| **Grew Creek** | Al Carlos | Whitehorse | 105K 009 | DD | Au-Ag |
| **Hat (Whitehorse Copper)** | Kluane Drilling/Norwest Enterprises | Whitehorse | 105D 053 | G,DD | Cu-Au-Ag |
| **Hem** | Shawn Ryan | Dawson | 116G 082 | G,GC | Cu-Au |
| **Hidden/Obvious** | Strategic Metals | Watson Lake | 105F 092,094 | G,GC | $WO_3$ |
| **Horn** | Canadian United Minerals | Dawson | (116B/7) | G,DD | Au-Cu |
| **Hyland Gold** | Cash Resources | Watson Lake | 95D 011 | G,GC | Au |
| **Jade** | Cash Resources | Dawson | 116G 062 | G,GC | Barite |
| **Kalzas** | Copper Ridge | Mayo | 105M 066 | G,GC | $WO_3$ |
| **Keno Hill** | A.M.T. Canada | Mayo | 105M 001 | D | Ag-Pb-Zn |
| **Klondike/Wedge** | KSL Limited/Barramundi Resources | Dawson | (115NO/14,15) | G,GC | Au |
| **Mars** | Saturn Ventures Inc. | Whitehorse | 105E 002 | G,GC | Cu-Au |
| **Minto** | Minto Exploration | Whitehorse | 115I 021,022 | DD,D | Cu-Ag-Au |
| **Mitchell** | JAE Resources | Dawson | 115O 068 | T | Au |
| **Monster** | Monster Copper Resources | Dawson | 116B 003 | G,GC,P,GP | Cu-Au |
| **Mor** | Fairfield Minerals | Watson Lake | (105C/1) | G,GC | Pb-Zn-Ag-Cu |
| **OM/Tom** | Carta Resources | Dawson | 115N 042 | G,GC | Cu-Pb-Zn-Ag-Au |
| **Plata** | Copper Ridge Exploration | Watson Lake | 105N 003 | G,GC | Pb-Zn-Ag |
| **Puck (Wolverine)** | Expatriate/Atna Resources | Watson Lake | 105G 073 | G,GC,DD | Pb-Zn-Cu-Ag-Au |
| **Red Mountain** | Regent Ventures | Mayo | 115P 006 | G,DD | Au |
| **Regal Ridge** | True North Gems/Expatriate | Watson Lake | (105G/07) | G,GC,T | Emeralds |
| **Rusty/JRS/ Tanner/Nad** | Manson Creek Resources | Mayo | (106C/5; C/4; D/3) | G,GC,GP | Zn-Pb-Ag |
| **Rusty Springs** | Eagle Plains Resources | Dawson | 116K 003 | G,GC | Ag-Cu-Zn-Pb |
| **Skukum** | Tagish Lake Gold | Whitehorse | 105D 022,025,158 | G,GC,DD | Au-Ag |
| **Spice** | Tanana Exploration | Watson Lake | (105G/13) | G,GC,T | Au |
| **Ultra** | Tom Morgan | Whitehorse | 115B 008 | G,GC | Ni-Cu-PGE; Cu-Zn-Au-Ag |
| **Wellgreen** | Northern Platinum | Whitehorse | 115G 024 | G,GC,GP,DD | Ni-Cu-PGE |
| **Regional reconnaissance** | Hudson Bay | Watson Lake | Selwyn Basin | G,GC | Zn-Pb-Ag |

# APPENDIX 2: 2001 DRILLING STATISTICS

| PROPERTY | COMPANY | DIAMOND DRILL | |
|---|---|---|---|
| | | METRES | # HOLES |
| **Andrew** | Noranda Exploration | 2789 | 15 |
| **Cameron** | Noranda/Tanana Exploration | (included in total for Andrew) | 3 |
| **Goal Net** | Expatriate Resources | 1560.6 | 9 |
| **Grew Creek** | Al Carlos | 262 | 5 |
| **Golden Revenue** | ATAC Resources | 1201 | 6 |
| **Hat (Whitehorse Copper)** | Kluane Drilling/Norwest Enterprises | 611 | 3 |
| **Horn** | Canadian United Minerals | 1100 | 26 |
| **Minto** | Minto Exploration | 552 | 5 |
| **Puck (Wolverine)** | Expatriate/Atna Resources | 220 | 1 |
| **Red Mountain** | Regent Ventures | 1280 | 5 |
| **Skukum Creek** | Tagish Lake Gold | 1502 | 4 |
| **Tay-LP** | Newmont/Ross River Gold | 1213 | 11 |
| **Wellgreen** | Northern Platinum Ltd. | 593.4 | 7 |
| **TOTAL** | | **12 884** | **100** |

# YUKON PLACER MINING OVERVIEW, 2001

***William LeBarge***[1]
*Yukon Geology Program*

LeBarge, W., 2002. Yukon Placer Mining Overview, 2001. *In:* Yukon Exploration and Geology 2001, D.S. Emond, L.H. Weston and L.L. Lewis (eds.), Exploration and Geological Services Division, Yukon Region, Indian and Northern Affairs Canada, p. 27-28.

## SUMMARY

Placer mining in the Yukon continued to be an important industry in 2001 despite low precious metal prices and steadily declining mineral exploration activity. A total of 124 mines were operating in 2001, with approximately 400 people directly employed in the industry. This represents a 12% decrease in the number of operating mines from the 2000 mining season. There are, however, many jobs generated annually in the service and hospitality industries due to seasonal placer mining activity, especially in and near the communities of Dawson and Mayo. As usual, the majority of active mining operations were in the Dawson Mining District (78) followed by the Whitehorse Mining District (33) and the Mayo Mining District (13).

For 2001, over 85% of the Yukon's placer gold was produced in the Dawson Mining District, which includes the unglaciated drainages of Klondike River, Indian River, west Yukon River (Fortymile, Sixtymile, Moosehorn) and lower Stewart River. The remaining gold came from glaciated regions, including Clear Creek, Mayo, Dawson Range, Kluane and Livingstone. Increases in placer gold production were seen in the Klondike (Hunker and Last Chance creeks), lower Stewart (Black Hills and Thistle creeks) and Kluane (Gladstone and Fourth of July creeks) areas, while decreases in production were noted in all other regions.

Placer gold production in 2001 totalled 70,813 crude ounces (2202.5 kg), compared to 76,507 crude ounces (2379.6 kg) in 2000, which represents a 15% decrease (Fig. 1). In the last two years, placer gold production has dropped 26% to its lowest level since 1979. The total dollar value of Yukon placer gold also dropped in 2001, down to $23.7 million from the $25.3 million generated in 2000. The continuing low price of gold and high fuel prices once again made for difficult economic conditions for the Yukon's placer mining industry.

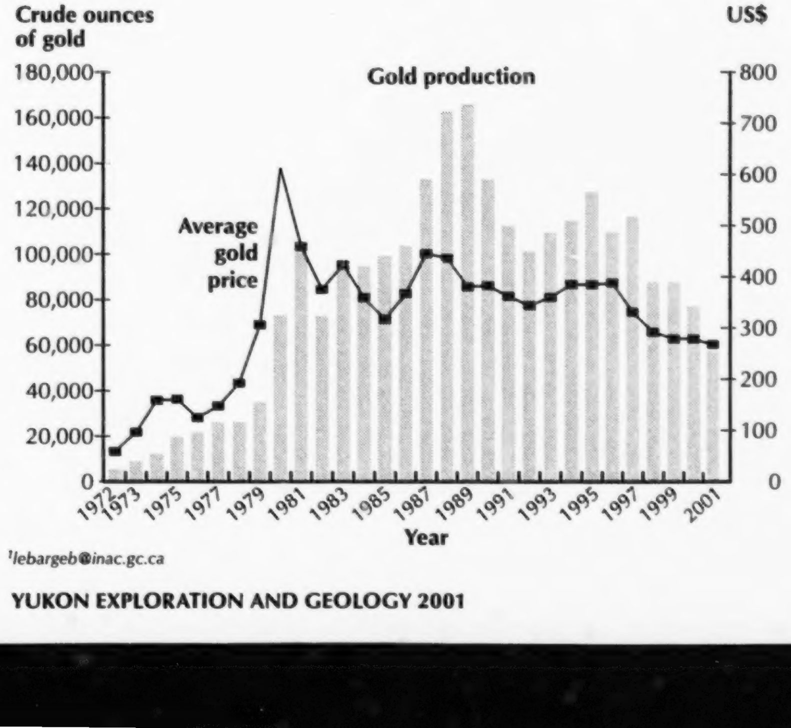

***Figure 1.*** *Yearly gold production figures and average US gold price, 1972-2001, for the Yukon.*

---

[1] *lebargeb@inac.gc.ca*

## APERÇU DES PLACERS DU YUKON, 2001

En 2001, l'exploitation de placers constitue toujours une importante industrie au Yukon et ce, même si les prix des métaux précieux sont bas et l'exploration minérale décline régulièrement. En 2001, 124 mines au total étaient en exploitation, et environ 400 personnes occupaient des emplois directement liés à l'industrie minière; cela représente une chute de 12 % du nombre de mines exploitées par rapport à la saison minière 2000. Cependant, l'exploitation saisonnière de placers créé un grand nombre d'emplois chaque année dans les industries des services et du tourisme, en particulier dans les communautés de Dawson et de Mayo ainsi que dans leurs environs. Comme d'habitude, la majeure partie des activités minières se sont concentrées dans les districts miniers de Dawson (78), de Whitehorse (33) et de Mayo (13).

En 2001, plus de 85 % de l'or placérien du Yukon a été extrait dans le district minier de Dawson, où l'on trouve les bassins versants non glaciés de la rivière Klondike, de la rivière Indian, de l'ouest du Yukon (Fortymile, Sixtymile et Moosehorn) et de la basse Stewart. Les 15 % restants provenaient de régions glaciaires, dont celles du ruisseau Clear, de la rivière Mayo, de la chaîne Dawson, de la rivière Kluane et du ruisseau Livingstone. La production d'or placérien s'est accrue dans les régions de la rivière Klondike (ruisseaux Hunker et Last Chance), de la basse Stewart (ruisseaux Black Hills et Thistle) et de la rivière Kluane (ruisseaux Gladstone et Fourth of July), alors qu'elle a chuté dans toutes les autres régions.

En 2001, un total 70 813 onces troy (2202.5 kg) d'or placérien ont été extraites, comparativement à 76 507 onces troy (2379.6 kg) en 2000, ce qui représente une chute de 15 %. Au cours des deux dernières années, l'exploitation de placers aurifères a chuté de 26 % et atteint sont plus bas niveau de production depuis 1979. La valeur total de l'or placérien du Yukon a également diminué, en passant de 25,3 millions de dollars générés en 2000 à 23,7 millions de dollars en 2001. Le prix de l'or est toujours bas et celui du carburant est encore élevé, ce qui constitue une fois de plus des conditions économiques défavorables pour l'industrie de l'exploitation de placers du Yukon.

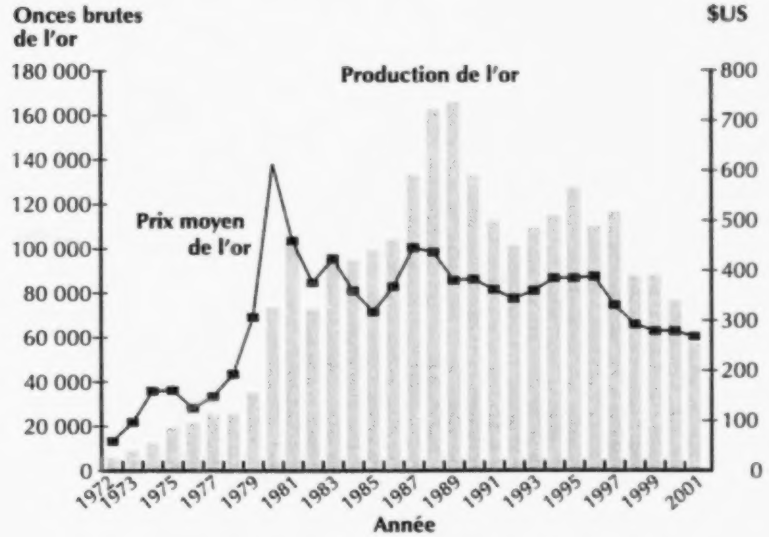

***Figure 1.*** *Production annuelle d'or et prix moyen de l'or en $US au Yukon, entre 1972 et 2001.*

# GOVERNMENT

## Yukon Geology Program

***Grant Abbott and staff***
*Yukon Geology Program*

Overview ........ 31
Program highlights for 2001 ........ 33
2001 publications and maps ........ 38

## Le Service de géologie du Yukon

***Maurice Colpron et Grant Abbott***
*Le Service de géologie du Yukon*

Aperçu ........ 49

## Mineral Resource Assessments Overview, 2001

***Anna Fonseca***
*Mineral Resources Branch, Yukon Government*

Summary ........ 53

## Yukon Mining Incentives Program Overview, 2001

***Ken Galambos***
*Mineral Resources Branch, Yukon Government*

Summary ........ 57

## The Robert E. Leckie Awards for Outstanding Reclamation Practices

***Karen Pelletier***
*Yukon Geology Program*

Awards ........ 61

# Yukon Geology Program

***Grant Abbott[1] and staff***
*Yukon Geology Program*

Abbott, J.G., 2002. Yukon Geology Program. *In:* Yukon Exploration and Geology 2001, D.S. Emond, L.H. Weston and L.L. Lewis (eds.), Exploration and Geological Services Division, Yukon Region, Indian and Northern Affairs Canada, p. 31-47.

## OVERVIEW

Now in its sixth year, the Yukon Geology Program (YGP; Fig. 1) is a de facto Yukon Geological Survey, consisting of two integrated and jointly managed offices with different administrative structures (Fig. 2). Federal funding is provided through the Exploration and Geological Services Division (EGSD), Yukon Region of the Department of Indian Affairs and Northern Development (DIAND), while Yukon Territorial Government (YTG) and cost-shared (YTG/DIAND) funding comes through the Mineral Resources Branch of the Department of Economic Development (YTG). YTG independently manages and funds the Mineral Assessment Group and the Yukon Mining Incentives Program (YMIP). These are described separately. The Geological Survey of Canada (GSC) also maintains an office with the program.

***Figure 1.*** *Yukon Geology Program staff, from left to right, Grant Abbott, Karen Pelletier, Diane Emond, Don Murphy, Bill LeBarge, Ken Galambos, Grant Lowey, Rod Hill, Mike Burke, Lee Pigage, Maurice Colpron, Lara Lewis, Leyla Weston, Panya Lipovsky, Jeffrey Bond, Anna Fonseca, Patrick Sack, Charlie Roots, Jo-Anne vanRanden, Julie Hunt, Monique Raitchey, Steve Traynor, Ali Wagner, Robert Deklerk, Craig Hart and Rick Zuran. Missing: Roger Hulstein, Gary Stronghill, Robert Stroshein.*

---

[1] *abbottg@inac.gc.ca*

The Yukon Geology Program is an informal and temporary organization that will be transformed into a Yukon Geological Survey when the responsibilities of the Northern Affairs Program of DIAND are devolved to YTG. A Devolution Transfer Agreement is now signed and the transfer date firmly set for April 1, 2003.

During the past year, the Program saw several staff changes (Fig. 2). On the Northern Affairs side, Karen Pelletier joined the Geology Division after the Mining Land Use Division was amalgamated with the Mineral Rights Divisions. Karen will continue her role as an environmental geologist, and will take on additional duties including land use issues. Steve Traynor and Rick Zuran have joined the Division for a short period to assist with bringing the Yukon MINFILE database up to date. On the YTG side, Rod Hill has returned to his substantive position as manager of the Mineral Resources Branch, in place of Shirley Abercrombie; Tammy Allen has taken a short-term secondment to the Oil and Gas Division, replacing Riona Freeman; and Gord Nevin has taken a one-year leave of absence. Roger Hulstein and Robert Stroshein have joined the Mineral Assessment Group on term positions.

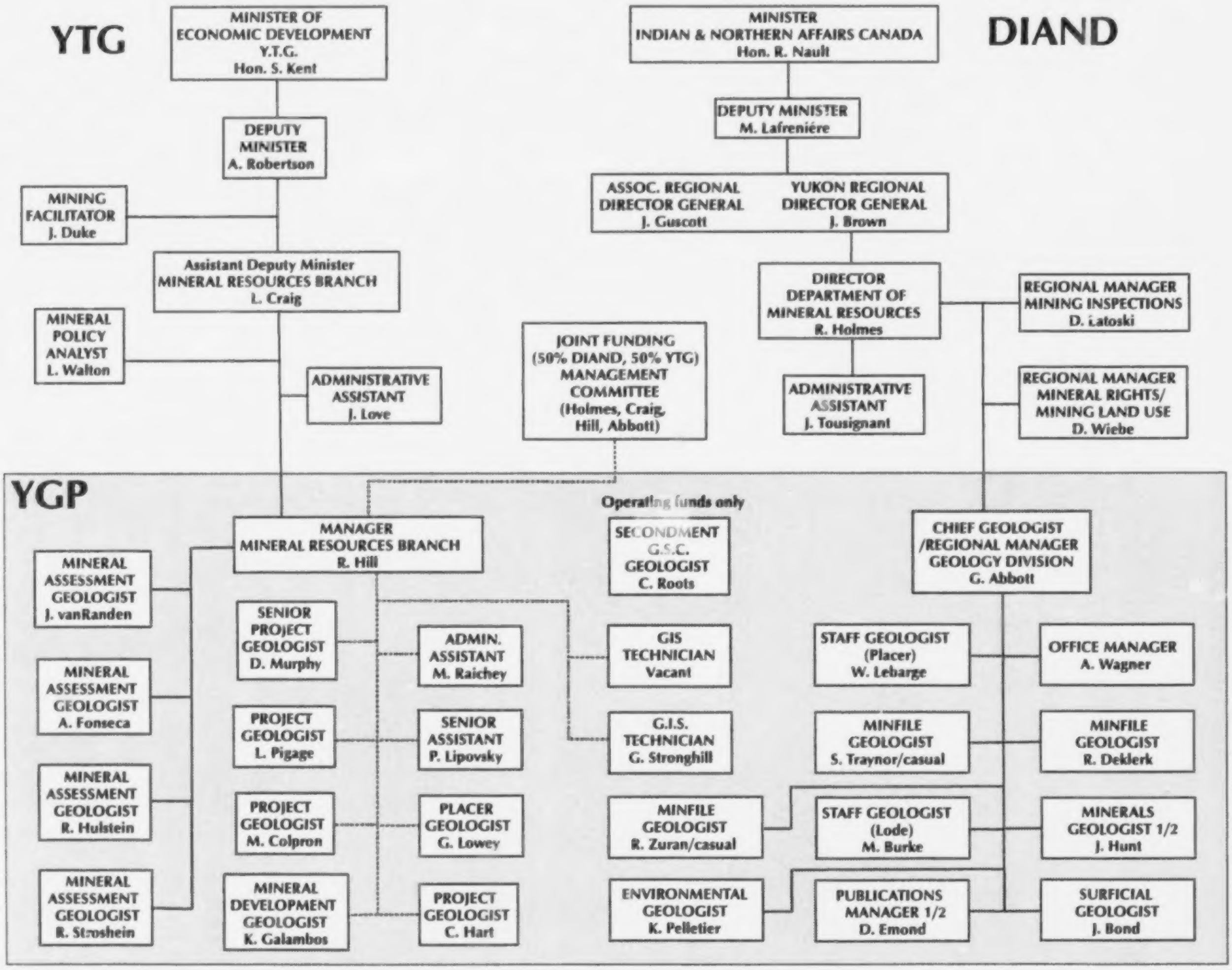
YTG
MINISTER OF ECONOMIC DEVELOPMENT Y.T.G. Hon. S. Kent
MINISTER INDIAN & NORTHERN AFFAIRS CANADA Hon. R. Nault
DIAND
DEPUTY MINISTER A. Robertson
DEPUTY MINISTER M. Lafrenière
MINING FACILITATOR J. Duke
ASSOC. REGIONAL DIRECTOR GENERAL J. Guscott
YUKON REGIONAL DIRECTOR GENERAL J. Brown
Assistant Deputy Minister MINERAL RESOURCES BRANCH L. Craig
DIRECTOR DEPARTMENT OF MINERAL RESOURCES R. Holmes
REGIONAL MANAGER MINING INSPECTIONS D. Latoski
MINERAL POLICY ANALYST L. Walton
JOINT FUNDING (50% DIAND, 50% YTG) MANAGEMENT COMMITTEE (Holmes, Craig, Hill, Abbott)
ADMINISTRATIVE ASSISTANT J. Love
ADMINISTRATIVE ASSISTANT J. Tousignant
REGIONAL MANAGER MINERAL RIGHTS/ MINING LAND USE D. Wiebe
YGP
Operating funds only
MANAGER MINERAL RESOURCES BRANCH R. Hill
SECONDMENT G.S.C. GEOLOGIST C. Roots
CHIEF GEOLOGIST /REGIONAL MANAGER GEOLOGY DIVISION G. Abbott
MINERAL ASSESSMENT GEOLOGIST J. vanRanden
SENIOR PROJECT GEOLOGIST D. Murphy
ADMIN. ASSISTANT M. Raichey
GIS TECHNICIAN Vacant
STAFF GEOLOGIST (Placer) W. Lebarge
OFFICE MANAGER A. Wagner
MINERAL ASSESSMENT GEOLOGIST A. Fonseca
PROJECT GEOLOGIST L. Pigage
SENIOR ASSISTANT P. Lipovsky
G.I.S. TECHNICIAN G. Stronghill
MINFILE GEOLOGIST S. Traynor/casual
MINFILE GEOLOGIST R. Deklerk
MINERAL ASSESSMENT GEOLOGIST R. Hulstein
PROJECT GEOLOGIST M. Colpron
PLACER GEOLOGIST G. Lowey
MINFILE GEOLOGIST R. Zuran/casual
STAFF GEOLOGIST (Lode) M. Burke
MINERALS GEOLOGIST 1/2 J. Hunt
MINERAL ASSESSMENT GEOLOGIST R. Stroshein
MINERAL DEVELOPMENT GEOLOGIST K. Galambos
PROJECT GEOLOGIST C. Hart
ENVIRONMENTAL GEOLOGIST K. Pelletier
PUBLICATIONS MANAGER 1/2 D. Emond
SURFICIAL GEOLOGIST J. Bond

***Figure 2.*** *Yukon Mineral Resources organization chart.*

# PROGRAM HIGHLIGHTS FOR 2001

## FIELDWORK

The Yukon Geology Program is committed to providing a balanced complement of field projects that not only quickly stimulate the mining and exploration industry, but also take the longer-term view towards developing an understanding of the Yukon regional geological framework, and building the Yukon Geoscience Database. Field projects carried out in 2001 are shown in Figure 3, and the present state and location of geological, geochemical and geophysical surveys are shown in Figure 4.

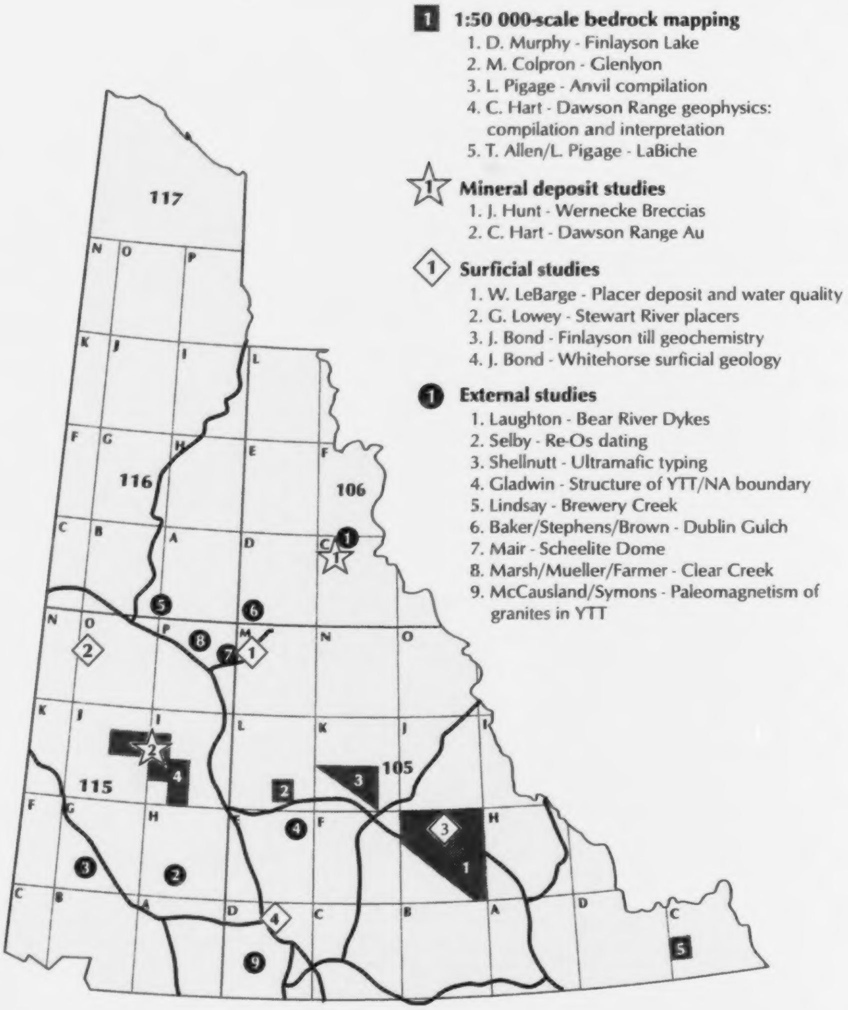
1:50 000-scale bedrock mapping
1. D. Murphy - Finlayson Lake
2. M. Colpron - Glenlyon
3. L. Pigage - Anvil compilation
4. C. Hart - Dawson Range geophysics: compilation and interpretation
5. T. Allen/L. Pigage - LaBiche
Mineral deposit studies
1. J. Hunt - Wernecke Breccias
2. C. Hart - Dawson Range Au
Surficial studies
1. W. LeBarge - Placer deposit and water quality
2. G. Lowey - Stewart River placers
3. J. Bond - Finlayson till geochemistry
4. J. Bond - Whitehorse surficial geology
External studies
1. Laughton - Bear River Dykes
2. Selby - Re-Os dating
3. Shellnutt - Ultramafic typing
4. Gladwin - Structure of YTT/NA boundary
5. Lindsay - Brewery Creek
6. Baker/Stephens/Brown - Dublin Gulch
7. Mair - Scheelite Dome
8. Marsh/Mueller/Farmer - Clear Creek
9. McCausland/Symons - Paleomagnetism of granites in YTT
117
116
106
105
115

*Figure 3. Field projects carried out or sponsored by the Yukon Geology Program in 2001.*

The Yukon Geology Program continued to commit substantial resources to a joint Geological Survey of Canada-British Columbia Geological Survey Branch - Yukon Geology Program initiative, the Ancient Pacific Margin NATMAP (National Mapping Program) project. This project is a multidisciplinary effort to better understand Yukon-Tanana and Kootenay terranes, arguably the least understood parts of the North American Cordillera. Yukon mapping projects are underway in Finlayson Lake map area (Don Murphy), Glenlyon (Maurice Colpron), Stewart River (Steve Gordey, Jim Ryan/GSC), and Wolf Lake (Charlie Roots/GSC). In southern B.C., the project also includes regional mapping by Bob Thompson of the GSC, and in east-central Alaska, mapping by David Szumigala of the Alaska State Geological Survey, and mineral deposit studies by Cynthia Dusel-Bacon of the U.S. Geological Survey. Participation by numerous university researchers, graduate students and other specialists has greatly added to the depth and complexity of the project. In Yukon, these include lithogeochemical studies in the Finlayson Lake area by Steve Piercey (now at Laurentian University) and Jim Mortensen of the University of British Columbia, and mineral deposit studies by Suzanne Paradis of the GSC. Regular workshops and field trips are one of the main benefits of such a large and diverse project. This summer Charlie Roots led a field trip along the Alaska Highway, from Teslin to Rancheria.

In 2001, the Yukon portion of the project received a substantial boost from funds obtained through NRCan's Targeted Geoscience Initiative. In the Finlayson Lake map area (105G) the extra funding enabled a program of accelerated regional bedrock mapping and till geochemistry. By using a contract helicopter for five weeks, four

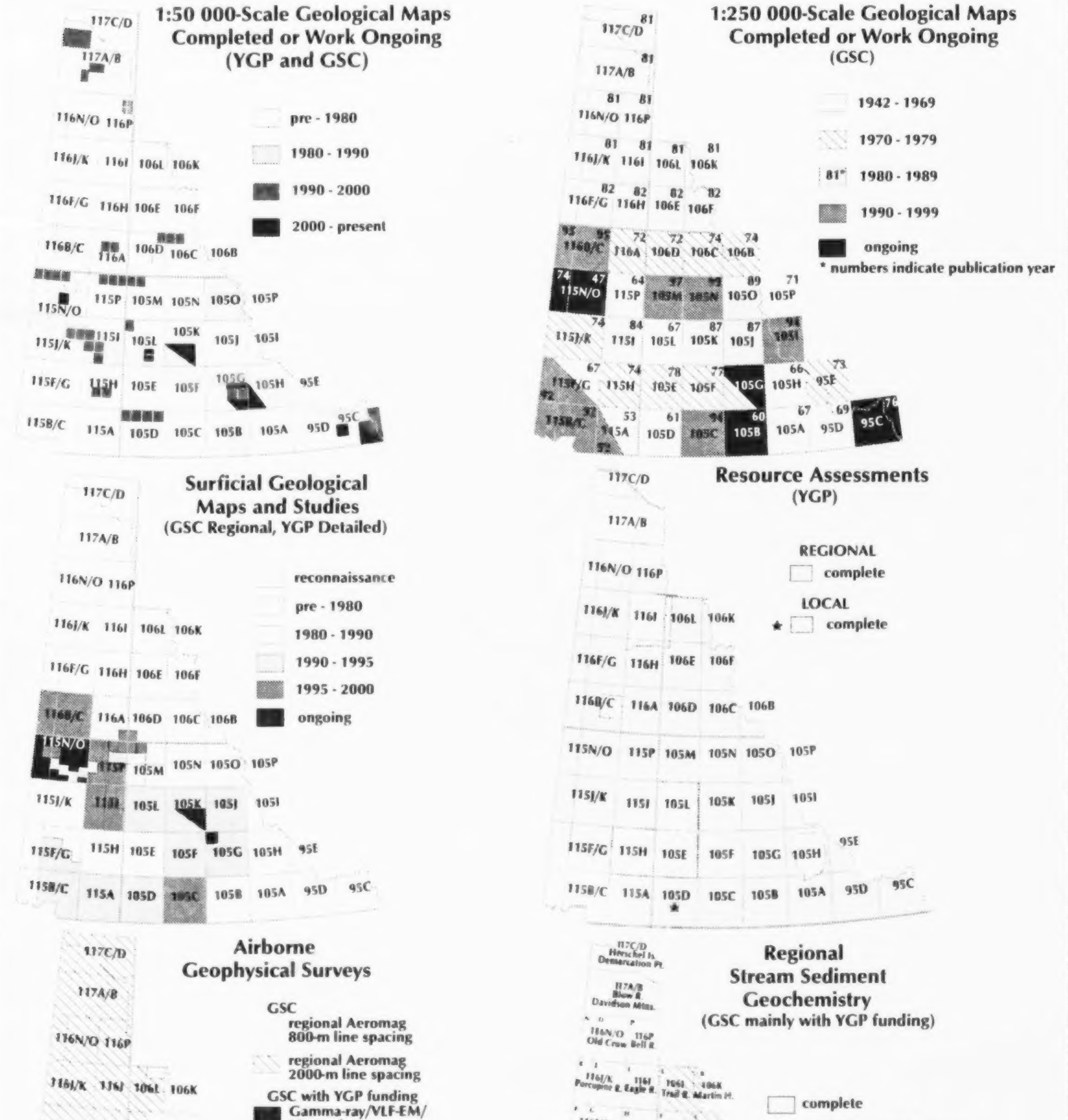
1:50 000-Scale Geological Maps
Completed or Work Ongoing
(YGP and GSC)
pre - 1980
1980 - 1990
1990 - 2000
2000 - present
1:250 000-Scale Geological Maps
Completed or Work Ongoing
(GSC)
1942 - 1969
1970 - 1979
81* 1980 - 1989
1990 - 1999
ongoing
* numbers indicate publication year
Surficial Geological
Maps and Studies
(GSC Regional, YGP Detailed)
reconnaissance
pre - 1980
1980 - 1990
1990 - 1995
1995 - 2000
ongoing
Resource Assessments
(YGP)
REGIONAL
complete
LOCAL
★ complete
Airborne
Geophysical Surveys
GSC
regional Aeromag 800-m line spacing
regional Aeromag 2000-m line spacing
GSC with YGP funding
Gamma-ray/VLF-EM/Magnetic
YGP
EM/Magnetic
Regional
Stream Sediment
Geochemistry
(GSC mainly with YGP funding)
complete
ongoing (available 2002)
117C/D
117A/B
116N/O
116P
116J/K
116I
106L
106K
116F/G
116H
106E
106F
116B/C
116A
106D
106C
106B
115N/O
115P
105M
105N
105O
105P
115J/K
115I
105L
105K
105J
105I
115F/G
115H
105E
105F
105G
105H
95E
115B/C
115A
105D
105C
105B
105A
95D
95C

*Figure 4.* Summary of available of geological maps, and regional geochemical and geophysical surveys in the Yukon.

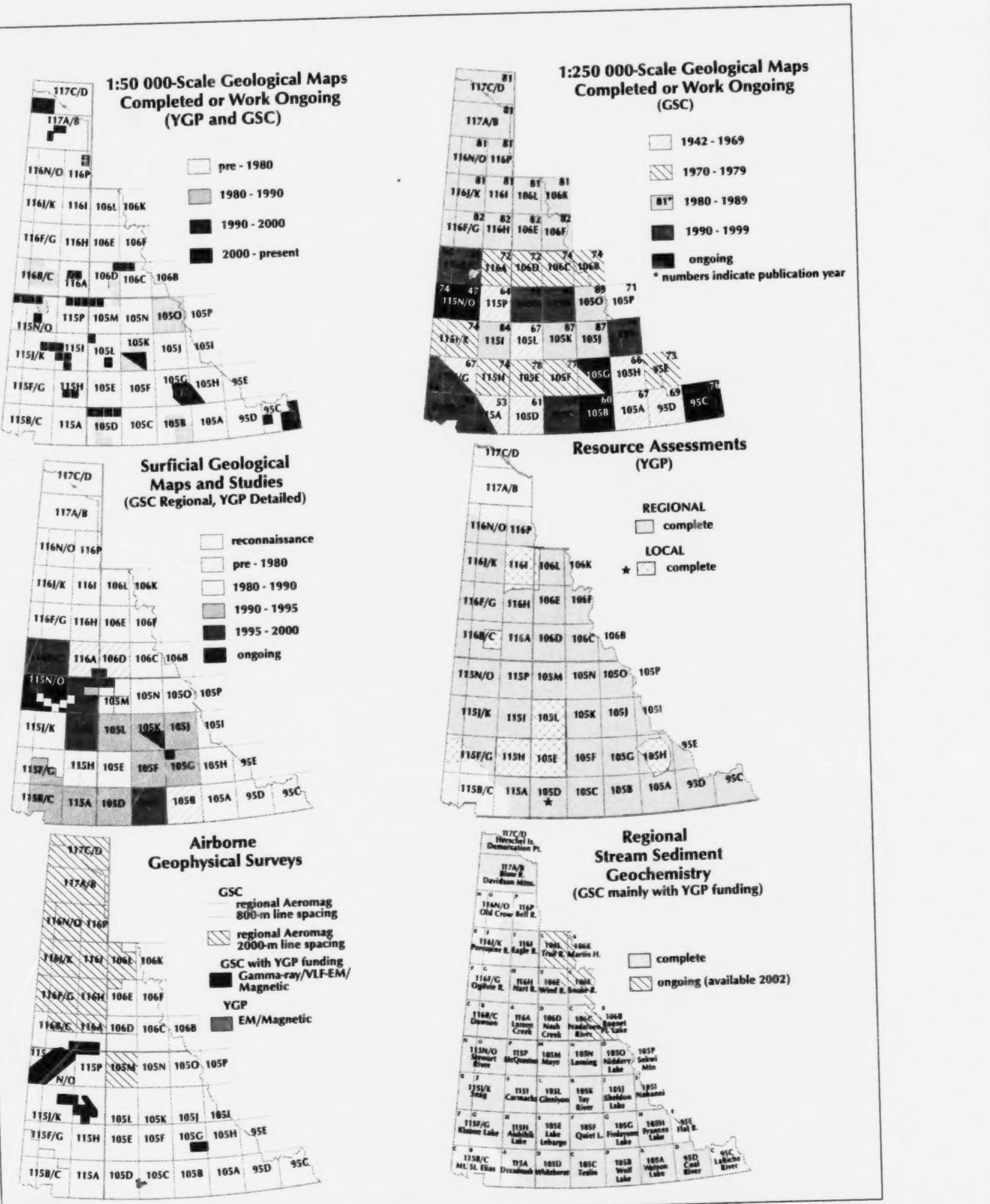
1:50 000-Scale Geological Maps Completed or Work Ongoing (YGP and GSC)
pre - 1980
1980 - 1990
1990 - 2000
2000 - present
1:250 000-Scale Geological Maps Completed or Work Ongoing (GSC)
1942 - 1969
1970 - 1979
81* 1980 - 1989
1990 - 1999
ongoing
* numbers indicate publication year
Surficial Geological Maps and Studies (GSC Regional, YGP Detailed)
reconnaissance
pre - 1980
1980 - 1990
1990 - 1995
1995 - 2000
ongoing
Resource Assessments (YGP)
REGIONAL
complete
LOCAL
★ complete
Airborne Geophysical Surveys
GSC
regional Aeromag 800-m line spacing
regional Aeromag 2000-m line spacing
GSC with YGP funding
Gamma-ray/VLF-EM/Magnetic
YGP
EM/Magnetic
Regional Stream Sediment Geochemistry (GSC mainly with YGP funding)
complete
ongoing (available 2002)

***Figure 4.*** *Summary of available of geological maps, and regional geochemical and geophysical surveys in the Yukon.*

expert NATMAP participants (D. Murphy, S. Gordey, M. Colpron, and C. Roots) were able to map the northern half of the map sheet at 1:100 000 scale. As well, J. Bond, A. Plouffe and two assistants successfully carried out a regional till geochemical sampling program across the extensive overburden-covered parts of the area. Promising geological and geochemical targets were defined as a result.

Elsewhere, Maurice Colpron continued mapping in Glenlyon map area (105L). Charlie Roots continued mapping in the western half of Wolf Lake map area (105B) and in the adjoining northern half of Jennings River map area (104O). In the Stewart River area (105N, O), work included GSC bedrock mapping by Gordey and Ryan, surficial mapping by Lionel Jackson for the GSC, and placer deposit studies by Grant Lowey. The second and final year of airborne multispectral geophysical surveys, funded under the Targeted Geoscience Initiative, resulted in total coverage of about 2/3 of the map sheet. Data released from the first survey has already resulted in staking and prospecting of promising targets.

The success of previous multispectral geophysical surveys prompted the territorial government to fund the GSC to administer a survey over prospective ground near the Minto and Williams Creek copper deposits northwest of Carmacks.

The Yukon Geology Program is also a partner with GSC Calgary staff and university researchers in the Central Forelands NATMAP Project. The Central Forelands Project is primarily focused on hydrocarbon-related geoscience, and includes regional mapping and topical studies in two separate areas: Trutch (94G) and Toad River (94N) in northern British Columbia, and Fort Liard (95B) and La Biche (95C) in Yukon and Northwest Territories. Tammy Allen and Lee Pigage joined the project in La Biche map area in southeast Yukon. Now in the second of three years, the project will better define the geologic framework of the area with the highest hydrocarbon potential in all of Yukon. Mapping in the eastern part of the La Biche area has resulted in new structural interpretations that are key to hydrocarbon exploration. Work by Lee and Tammy in the western part of the map area has resulted in significant reinterpretation of both structure and stratigraphy.

Another major effort by the Yukon Geology Program is to synthesize and enhance the geological database of the Anvil district. The Faro mine remains closed for the foreseeable future, but the possibility remains for renewed exploration and mining at some point. Lee Pigage has completed bedrock mapping, and has released a complete set of 11 geological maps of the district at 1:25 000 scale, and a compilation at 1:100 000 scale. A final report will be prepared in 2002. Jeff Bond has completed surficial mapping and a till geochemical survey, and released 11 final maps and a bulletin in the spring of 2001.

Craig Hart has begun a year's leave to undertake a PhD Program at the University of Western Australia. Most of the requirements for the degree will entail writing papers on his previous field studies of the Tintina gold belt and other Yukon gold occurrences. Craig also assisted many of the students who received support from the YGP to study various aspects of Yukon gold deposits. These included Mark Lindsay and Julian Stephens, under the supervision of Tim Baker at James Cook University (JCU) and John Mair at the University of Western Australia; and Erin Marsh and Seth Mueller under the supervision of Rich Goldfarb at the U.S. Geological Survey.

Bill LeBarge and Mark Nowasad continued their studies of the relationship between sedimentology, grain size distribution, and water quality of effluent from placer deposits. Fieldwork is now complete and the technique will be evaluated for possible long-term applications and further research. Data gathered from this study will be used in the review of the Yukon Placer Authorization, which is currently underway. The bulletin for the Mayo Placer project is scheduled for release in the spring of 2002.

Julie Hunt has returned to University to undertake a PhD program at James Cook University in Australia. YGP is funding fieldwork. Julie will carry out research on the Wernecke Breccias and take advantage of the Australian connection by comparing the Yukon breccias with similar Australian rocks which host giant copper, uranium, gold deposits.

## EXTERNAL SUPPORT

The YGP is providing financial and logistical support to, or is a partner with, graduate students and university researchers in the following projects.

John Laughton is working on an MSc thesis on the Slab volcanics in the Wernecke Breccias under the supervision of Derek Thorkelson at Simon Fraser University. Derek also continued his research on Proterozoic rocks and mineral deposits in the Wernecke Mountains, with a small study of the Bear River dykes.

Gregory Shellnutt carried out detailed mapping and study of ultramafic rocks in the Yukon as part of a PhD program at the University of Victoria under the supervision of Dante Canil. The aim of the project is to use petrologic and geochemical studies to determine the mode of origin of ultramafic bodies in a variety of terranes and tectonic settings. The results should help identify those rocks with the most potential to host deposits of platinum group elements.

Kaesy Gladwin began mapping and structural studies to characterize the boundary between the Yukon-Tanana and Cassiar terranes in southeast Glenlyon map area. This is an MSc project under the direction of Stephen Johnston at the University of Victoria.

Tim Baker at James Cook University has completed work on understanding the fluid compositions of the Eagle Zone gold veins at Dublin Gulch. This is a step towards characterizing fluids in intrusion-related gold systems.

Julian Stephens, under the direction of Tim Baker at JCU, has been working on the nature of the brittle structural controls of intrusion-related gold systems in central Yukon with a focus on Dublin Gulch and Clear Creek. This will be used to develop a structural exploration model.

Mark Lindsay, under the direction of Tim Baker at JCU, has been developing a structural history and mineral paragenesis for the Brewery Creek gold deposit. He will direct future efforts towards determining what the critical factors were that resulted in gold deposition.

Similarly, Veronica Brown at JCU has completed her Honours BSc thesis on the Ray Gulch tungsten deposit at Dublin Gulch. She has determined that the lack of a retrograde alteration event on the tungsten skarn is the reason for the lack of gold enrichment in that deposit.

John Mair, under the direction of David Groves at the University of Western Australia, has been examining the metallogenic relationships between gold, tungsten and silver-lead-antimony mineralization in intrusion-related systems, with an emphasis on the Scheelite Dome area. In particular, John has found some very high gold grades in tungsten skarns, and this study will aid in the understanding of those metallogenic controls.

Erin Marsh has recently completed her MSc thesis at the University of Colorado on the "Geology and geochemistry of the Clear Creek intrusion-related gold occurrences." Erin has found, among other things, that Au ± Bi ± W related veins are up to 100°C hotter than Ag-Pb veins.

Seth Mueller and Lang Farmer, also at the University of Colorado, have used isotopes to indicate the sources for magmas associated with intrusion-related gold deposits in the Clear Creek area.

David Selby and Rob Creaser at the University of Alberta have been applying a new technique for dating mineral deposits to Yukon rocks. The Rhenium-Osmium method allows the dating of sulphide minerals, in particular molybdenum, and they have been using it to understand the timing of intrusion-related sulphide deposition throughout the Yukon.

Phil McCausland and David Symons at the University of Windsor in Ontario are wrapping up paleomagnetic studies on Mesozoic and Early Tertiary granites in Yukon-Tanana Terrane. Progress so far indicates differences in the timing and amount of motion between Yukon-Tanana Terrane and Stikine Terrane rocks. Rocks as young as Eocene have endured up to 40° of post-emplacement, tectonic rotations.

In addition to providing geochronological support to the GSC's Steward River project, Mike Villenueve has been using argon geochronology to: 1) determine the cooling and uplift history of the Klondike region to aid in determining mineralizing and tectonic processes in that region; 2) define the timing of recent volcanism in the Yukon, particularly the Fort Selkirk region; and 3) provide timing constraints on intrusion-related gold mineralization in the Tintina gold belt.

In order to make Regional Stream Geochemical data from the National Geochemical Reconnaissance Program more accessible, Peter Friske, with the Geological Survey of Canada in Ottawa, was funded to reformat existing open file data in Portable Document Format (PDF). The first four open files were released in December.

## INDUSTRY LIAISON AND SUPPORT

Mike Burke and Bill LeBarge, YGP's main links to the exploration industry, continued to monitor Yukon hard-rock and placer mining, and mineral exploration activity. They continued to visit active properties, review reports for assessment credit, and maintain the assessment report library.

### Yukon MINFILE

Robert Deklerk maintains the Yukon MINFILE, the Yukon's mineral occurrence database, which is another mainstay of the Yukon Geology Program. The upgrade from

Microsoft Access Version 2 to Access 97 has been completed, with major revision and simplification of the database structure. The updated digital version, with data revised to 1998, was released on CD-ROM in the spring of 2001. New mineral occurrence location maps produced in Arcview accompany the release. The text version of MINFILE is available on our website and in hard copy through Exploration and Geological Services Division.

## Yukon GEOPROCESS File

The Yukon GEOPROCESS File, under the direction of Diane Emond, is an inventory of information on geological process and terrain hazards, including 1:250 000-scale maps showing permafrost, landslides, recent volcanic rocks, structural geology and seismic events, and also includes references and summaries of bedrock and surficial geology. The GEOPROCESS File is intended as a planning tool for development activities and is available for most areas south of 66° latitude. The maps have recently been standardized in colour, and will soon be released on a single compact disk.

## H.S. Bostock Core Library

Mike Burke and Ken Galambos maintain the H.S. Bostock Core Library. The facility contains about 128 000 m of diamond drill core from about 200 Yukon mineral occurrences. Confidentiality of material is determined on the same basis as mineral assessment reports. Confidential core can be viewed with a letter of release from the owner. Rocks saws and other rock preparation equipment are available to the public.

## Information Management and Publications

The Yukon Geology Program is now converted to digital publishing. All new geological maps and publications are produced on-demand from a digital format, and most of our recent products are available free of charge in PDF format from our website (http://www.geology.gov.yk.ca). The Yukon Geology Program is also pleased to make spatial data available through the interactive map server. The Map Gallery can be accessed through the YGP website and the YTG Department of Economic Development website. It currently allows viewing of regional geology, MINFILE locations, topography, roads and communities. The intent is to continually improve the site. Enhancements will include allowing downloading of vector data, and adding additional information, such as Regional Stream Geochemistry, geophysics, geochronology and paleontology. The Map Gallery is the prototype for the Yukon Government's Data Access Window. Eventually, coverages, such as mineral claims from other agencies, will be available. Users are encouraged to provide feedback and suggest improvements.

Exploration and Geological Services Division, DIAND, publishes Yukon Geology Program publications. Hard copies are available at the address below.

Geoscience Information and Sales
c/o Whitehorse Mining Recorder
102-300 Main Street
Whitehorse. Yukon Y1A 2B5
Ph. (867) 667-3266
Fax. (867) 667-3267
E-mail: geosales @inac.gc.ca

To learn more about the Yukon Geology Program, visit our website at http://www.geology.gov.yk.ca or contact us directly:

Grant Abbott, Chief Geologist
Exploration and Geological Services Division
Indian and Northern Affairs Canada
345-300 Main Street
Whitehorse, Yukon Y1A 2B5
Ph. (867) 667-3200
E-mail: abbottg@inac.gc.ca

Rod Hill, Manager
Mineral Resources Branch
Department of Economic Development
Government of Yukon
P.O. Box 2703
Whitehorse, Yukon Y1A 2C6
Ph. (867) 667-5384
E-mail: Rod.Hill@gov.yk.ca

# 2001 PUBLICATIONS AND MAPS

## BULLETINS

Bond, J., 2001. Quaternary geology and till geochemistry of the Anvil district (parts of 105K/2, 3, 5, 6 and 7), central Yukon Territory. Exploration and Geological Services Division, Yukon Region, Indian and Northern Affairs Canada, Bulletin 11, 38 p., 11 surficial geology maps at 1:25 000 scale, and 1 glacial ice-flow patterns map at 1:250 000 scale, paper and CD-ROM.
http://www.geology.gov.yk.ca/pdf/YGPBulletin11.pdf

## OPEN FILES

Allen, T.L. and Weston, L.H., 2001. Preliminary geological map of Division Mountain area (105E/5 west-half and 115H/8 east-half), central Yukon (1:50 000 scale). Exploration and Geological Services Division, Yukon Region, Indian and Northern Affairs Canada, Open File 2001-3.
http://www.geology.gov.yk.ca/publications/pdf/OF2001-03.pdf

Gordey, S.P. and Makepeace, A.J. (comps.), 2001. Bedrock Geology, Yukon Territory. Geological Survey of Canada, Ottawa, Ontario; Exploration and Geological Services Division, Yukon Region, Indian and Northern Affairs Canada; GSC Open File 3754 and EGSD Open File 2001-1, one colour map, 1:1 000 000 scale.

Friske, P.W.B., Day, S.J.A. and McCurdy, M.W., 2001. Regional Stream Sediment and Water Geochemical Data, Eastern Yukon and Western Northwest Territories. Geological Survey of Canada, Ottawa, Ontario; Exploration and Geological Services Division, Yukon Region, Indian and Northern Affairs Canada; GSC Open File 4016 and EGSD Open File 2001-12(D), CD-ROM.

Friske, P.W.B., Day, S.J.A. and McCurdy, M.W., 2001. Regional Stream Sediment and Water Geochemical Data, Southwestern Yukon (Parts of NTS 115A and 115B). Geological Survey of Canada, Ottawa, Ontario; Exploration and Geological Services Division, Yukon Region, Indian and Northern Affairs Canada; GSC Open File 2859 and EGSD Open File 2001-11(D), CD-ROM.

Friske, P.W.B., Day, S.J.A. and McCurdy, M.W., 2001. Regional Stream Sediment and Water Geochemical Data, Western Yukon. Geological Survey of Canada, Ottawa, Ontario; Exploration and Geological Services Division, Yukon Region, Indian and Northern Affairs Canada; GSC Open File 1364 and EGSD Open File 2001-13(D), CD-ROM.

Hart, C.J.R., Burke, M. and Stronghill, G., 2001. Yukon Platinum Occurrences and Potential. Exploration and Geological Services Division, Yukon Region, Indian and Northern Affairs Canada, Open File 2001-2, 1:1 000 000 scale.
http://www.geology.gov.yk.ca/publications/pdf/OF2001-02.pdf

Lipovsky, P., Bond, J. and LeBarge. W., 2001. Mayo area placer activity map, portions of NTS sheets 105M, 106D, 115P and 116A. Exploration and Geological Services Division, Yukon Region, Indian and Northern Affairs Canada, Open File 2001-35, 1:250 000 scale.
http://www.geology.gov.yk.ca/publications/pdf/mayo_42x26.pdf

Lipovsky, P., LeBarge, W., Bond, J. and Lowey, G., 2001. Yukon Placer Activity Map. Exploration and Geological Services Division, Yukon Region, Indian and Northern Affairs Canada, Open File 2001-34, 1:1 000 000 scale.
http://www.geology.gov.yk.ca/publications/pdf/yukon_42x52.pdf

Lipovsky, P., Lowey, G. and LeBarge. W., 2001. Dawson area placer activity map, portions of NTS sheets 116B and C and 115N and O. Exploration and Geological Services Division, Yukon Region, Indian and Northern Affairs Canada, Open File 2001-36, 1:250 000 scale.
http://www.geology.gov.yk.ca/publications/pdf/dawson_30x36.pdf

Murphy, D.C., Colpron, M., Gordey, S.P., Roots, C.F., Abbott, G. and Lipovsky, P.S., 2001. Preliminary bedrock geological map of northern Finlayson Lake area (NTS 105G), Yukon Territory (1:100 000 scale). Exploration and Geological Services Division, Yukon Region, Indian and Northern Affairs Canada, Open File 2001-33.
http://www.geology.gov.yk.ca/publications/pdf/finlayson_map.pdf

Pigage, L.C., 2001. Geological map of Anvil District (NTS 105K/2, 3, 5, 6, 7, 11), central Yukon (1:100 000 scale). Exploration and Geological Services Division, Yukon Region, Indian and Northern Affairs Canada, Open File 2001-31.
http://www.geology.gov.yk.ca/publications/pdf/OF2001_31.pdf

Pigage, L.C., 2001. Geological map of Faro (NTS 105K/3 NE) and Mount Mye (105K/6 SE), central Yukon (1:25 000 scale). Exploration and Geological Services Division, Yukon Region, Indian and Northern Affairs Canada, Open File 2001-27. http://www.geology.gov.yk.ca/publications/pdf/OF2001_27.pdf

Pigage, L.C., 2001. Geological map of Faro (NTS 105K/3 NW) and Mount Mye (105K/6 SW), central Yukon (1:25 000 scale). Exploration and Geological Services Division, Yukon Region, Indian and Northern Affairs Canada, Open File 2001-26. http://www.geology.gov.yk.ca/publications/pdf/OF2001_26.pdf

Pigage, L.C., 2001. Geological map of Mount Mye (NTS 105K/6 W), central Yukon (1:25 000 scale). Exploration and Geological Services Division, Yukon Region, Indian and Northern Affairs Canada, Open File 2001-28. http://www.geology.gov.yk.ca/publications/pdf/OF2001_28.pdf

Pigage, L.C., 2001. Geological map of Rose Mountain (105K/5 SE), central Yukon (1:25 000 scale). Exploration and Geological Services Division, Yukon Region, Indian and Northern Affairs Canada, Open File 2001-4. http://www.geology.gov.yk.ca/publications/pdf/OF2001-04.pdf

Pigage, L.C. and Allen, T.L., 2001. Geological map of Pool Creek (NTS95C/5), southeastern Yukon (1:50 000 scale). Exploration and Geological Services Division, Yukon Region, Indian and Northern Affairs Canada, Open File 2001-32. http://www.geology.gov.yk.ca/publications/pdf/OF2001_32.pdf

Shives, R.B.K., Carson, J.M., Ford, K.L., Holman, P.B., Gordey, S. and Abbott, G., 2001. Multisensor Airborne Geophysical Survey, Stewart River and Dawson areas (115O/16, 116B/1). Geological Survey of Canada, Ottawa, Ontario; Exploration and Geological Services Division, Yukon Region, Indian and Northern Affairs Canada; GSC Open File 3993 and EGSD Open File 2001-9, ten 1:50 000-scale maps.

Shives, R.B.K., Carson, J.M., Ford, K.L., Holman, P.B., Gordey, S. and Abbott, G., 2001. Multisensor Airborne Geophysical Survey, Stewart River and Dawson areas (115O&N and 116B). Geological Survey of Canada, Ottawa, Ontario; Exploration and Geological Services Division, Yukon Region, Indian and Northern Affairs Canada; GSC Open File 3994 and EGSD Open File 2001-10, ten 1:50 000-scale maps, paper and CD-ROM.

Shives, R.B.K., Carson, J.M., Ford, K.L., Holman, P.B, Gordey, S. and Abbott, G., 2001. Multisensor Airborne Geophysical Survey, Stewart River and Dawson areas (115O&N and 116B). Geological Survey of Canada, Ottawa, Ontario; Exploration and Geological Services Division, Yukon Region, Indian and Northern Affairs Canada; GSC Open File D4009 and EGSD Open File 2001-30(D), sixty 1:250 000-scale and 1:50 000-scale maps, CD-ROM.

Shives, R.B.K., Carson, J.M., Ford, K.L., Holman, P.B., Gordey, S. and Abbott, G., 2001. Multisensor Airborne Geophysical Survey, Stewart River area (parts of 115N/1,2,7,8). Geological Survey of Canada, Ottawa, Ontario; Exploration and Geological Services Division, Yukon Region, Indian and Northern Affairs Canada; GSC Open File 3989 and EGSD Open File 2001-5, ten 1:50 000-scale maps.

Shives, R.B.K., Carson, J.M., Ford, K.L., Holman, P.B., Gordey, S. and Abbott, G., 2001. Multisensor Airborne Geophysical Survey, Stewart River area (parts of 115N/8,9, 115O/5,6). Geological Survey of Canada, Ottawa, Ontario; Exploration and Geological Services Division, Yukon Region, Indian and Northern Affairs Canada; GSC Open File 3990 and EGSD Open File 2001-6, ten 1:50 000-scale maps.

Shives, R.B.K., Carson, J.M., Ford, K.L., Holman, P.B., Gordey, S. and Abbott, G., 2001. Multisensor Airborne Geophysical Survey, Stewart River area (parts of 115O/11,12,13,14). Geological Survey of Canada, Ottawa, Ontario; Exploration and Geological Services Division, Yukon Region, Indian and Northern Affairs Canada; GSC Open File 3991 and EGSD Open File 2001-7, ten 1:50 000-scale maps.

Shives, R.B.K., Carson, J.M., Ford, K.L., Holman, P.B., Gordey, S. and Abbott, G., 2001. Multisensor Airborne Geophysical Survey, Stewart River area (115O/14,15). Geological Survey of Canada, Ottawa, Ontario; Exploration and Geological Services Division, Yukon Region, Indian and Northern Affairs Canada; GSC Open File 3992 and EGSD Open File 2001-8. Ten 1:50 000-scale maps.

Yukon Geology Bibliography, 2001. Exploration and Geological Services Division, Yukon Region, Indian and Northern Affairs Canada, Open File 2001-29, CD-ROM. http://www.geology.gov.yk.ca/publications/bibliography/bibliography_database.pdt

Yukon MINFILE, 2001. Exploration and Geological Services Division, Yukon Region, Indian and Northern Affairs Canada, text and 33 1:250 000-scale mineral occurrence location maps, paper and CD-ROM.

## YUKON GEOLOGY PROGRAM OUTSIDE ARTICLES

Piercey, S.J., **Murphy, D.C.**, Mortensen, J.K. and Paradis, S., 2001. Boninitic magmatism in a continental margin setting, Yukon-Tanana Terrane, southeastern Yukon, Canada. Geology, vol. 29, p. 731-734.

Froese, D.G., Duk-Rodkin, A. and **Bond J.D.** (eds.), 2001. Field Guide to Quaternary Research in Central and Western Yukon Territory. Heritage Branch, Yukon Government, Occasional Papers in Earth Sciences No. 2, 104 p.

Thorkelson, D.J., Mortensen, J.K., Creaser, R.A., Davidson, G.J. and **Abbott, J.G.**, 2001. Early Proterozoic magmatism in Yukon, Canada: Constraints on the evolution of northwestern Laurentia. Canadian Journal of Earth Sciences, vol. 38, p. 1479-1494.

## YUKON GEOLOGY PROGRAM ABSTRACTS/ EXTENDED ABSTRACTS/LITHOPROBE CONTRIBUTIONS

**Bond, J.D., LeBarge, W.P.** and **Weston, L.H.**, 2001. Placer deposit exploration in glaciated terrain: Understanding climate impacts on drainages in the Mayo Mining District, central Yukon, Canada. *In:* Canadian Quaternary Association Meetings, 2001, Whitehorse, Yukon, Program and Abstracts. Heritage Branch, Government of the Yukon, Occasional Papers in Earth Sciences No. 1, p. 29.
http://cgrg.geog.uvic.ca//abstracts/BondPlacerUnderstanding.html

**Hart, C.J.R.**, Selby, D. and Creaser, R.A., 2001. Timing relationships between plutonism and gold mineralization in the Tintina gold belt (Yukon and Alaska) using Re-Os molybdenite dating. *In:* 2001: A Hydrothermal Odyssey, Extended Conference Abstracts, P.J. Williams (ed.), EGRU Contribution 59, p. 72-73.

Johnston, S.T., Enkin, R., Baker, J., Francis, D., **Colpron, M.** and Larson, K., 2001. Solitary Mountain, Yukon: Preliminary paleomagnetic results strengthen the correlation with the Carmacks Formation. *In:* Lithoprobe SNORCLE – Cordilleran Tectonics Workshop, Victoria, BC, F. Cook and P. Erdmer (eds.), vol. 79, p. 85.

**LeBarge, W.P.**, 2001. Economics and geology of Yukon placer deposits. *In:* Canadian Quaternary Association Meetings, 2001, Whitehorse, Yukon, Program and Abstracts. Heritage Branch, Government of the Yukon, Occasional Papers in Earth Sciences No. 1, p. 47.
http://cgrg.geog.uvic.ca//abstracts LeBargeEconomicsThe.html

**LeBarge, W.P.**, 2001. Geology and environmental regime of technogenous Yukon placer deposits. *In:* Abstracts, International Scientific-Practical Conference on Technogenous Placers, Simferopol-Sudak, Ukraine, September 24-29, 2001.

Lindsay, M.J., Baker, T., **Hart, C.J.R.** and Oliver, N.H.S., 2001. The structural history and mineral paragenesis of the Brewery Creek gold deposit, Yukon Territory, Canada. *In:* 2001: A Hydrothermal Odyssey, Extended Conference Abstracts, P.J. Williams (ed.), EGRU Contribution 59, p. 118-119.

Long, D.G.F. and **Lowey, G.W.**, 2001. Wandering gravel-bed rivers and high-constructive stable channel sandy fluvial systems in the Ross River area, Yukon Territory, Canada. *In:* Fluvial Sedimentology 2001, 7th International Conference on Fluvial Sedimentology, Program and Abstracts, University of Nebraska, Lincoln, Nebraska (USA), August 6-10, 2001, p. 177.

**Lowey, G.W.**, 2001. White Channel alteration: Paradise Hill. *In:* Field Guide to Quaternary Research in Central and Western Yukon Territory, D.G. Froese, A. Duk-Rodkin and J.D. Bond (eds.), Heritage Branch, Government of the Yukon, Occasional Papers in Earth Sciences No. 2, p. 63-64.

**Lowey, G.W.**, 2001. The role of forcing mechanisms, base level change and accommodation space in the formation of the Klondike goldfields, Yukon, Canada (abstract). *In:* Fluvial Sedimentology 2001, 7th International Conference on Fluvial Sedimentology, Program and Abstracts, University of Nebraska, Lincoln, Nebraska (USA), August 6-10, 2001, p. 178.

**Lowey, G.W.**, 2001. The role of forcing mechanisms, base level change and accommodation space in the formation of the Klondike Goldfields, Yukon, Canada. *In:* Canadian Quaternary Association Meetings, 2001, Whitehorse, Yukon, Program and Abstracts. Heritage Branch, Government of the Yukon, Occasional Papers in Earth Sciences No. 1, p. 50.
http://cgrg.geog.uvic.ca//abstracts/LoweyTheThe.html

MacNaughton, R.B., **Allen, T.L.** and **Pigage, L.C.**, 2001. Enigmatic strata of possible Neoproterozoic age, Pool Creek map area (NTS 95C/5), Yukon Territory. *In:* Lithoprobe SNORCLE – Cordilleran Tectonics Workshop, Victoria, BC, F. Cook and P. Erdmer (eds.), vol. 79, p. 259-260.

Marsh, E., Goldfarb, R., **Hart, C.** and Farmer, G.L., 2001. The Clear Creek intrusion-related gold deposit, Tintina gold belt, Yukon, Canada. Geological Society of America, Program with Abstracts, Boston, Massachusetts.

McCausland, P.J.A., Symons, D.T.A., **Hart, C.J.R.** and Blackburn, W.H., 2001. Preliminary paleomagnetism and geothermobarometry of the Granite Mountain batholith, Yukon: Minimal geotectonic motion of the Yukon-Tanana Terrane relative to North America. *In:* Lithoprobe SNORCLE – Cordilleran Tectonics Workshop, Victoria, BC, F. Cook and P. Erdmer (eds.), vol. 79, p. 86-93.

McCausland, P.J.A., Symons, D.T.A., **Hart, C.J.R.** and Blackburn, W.H., 2001. Preliminary paleomagnetism and geothermobarometry of the Granite Mountain batholith, Yukon: Uplift remanence implies minimal tectonic motion for the Yukon-Tanana Terrane. Geological Association of Canada, Program with Abstracts, St. John's, Newfoundland.

Mortensen, J.K., Emon, K., Johnston, S.T. and **Hart, C.J.R.**, 2000. Age geochemistry, paleotectonic setting and metallogeny of Late Triassic – Early Jurassic intrusions in Yukon and eastern Alaska: A preliminary report. *In:* Lithoprobe SNORCLE - Cordilleran Tectonics Workshop, Calgary, AB, F. Cook and P. Erdmer (eds.).

Paradis, S., Bailey, S.L., Bradshaw, G.D., Daughtry, K., Hoy, T., **Murphy, D.C.**, Mortensen, J.K., Nelson, J.L., Peter, J. and Piercey, S.J., 2001. Devonian-Mississippian VMS deposits of western Canada as an expression of continent margin tectonics. *In:* Lithoprobe SNORCLE – Cordilleran Tectonics Workshop, Victoria, BC, F. Cook and P. Erdmer (eds.), vol. 79, p. 185.

Piercey, S.J. and **Murphy, D.C.**, 2001. Contrasting arc and non-arc mafic volcanic rocks in the Fyre Lake unit, Yukon-Tanana Terrane, Finlayson Lake region, Yukon, Canada. *In:* Lithoprobe SNORCLE – Cordilleran Tectonics Workshop, Victoria, BC, F. Cook and P. Erdmer (eds.), vol. 79, p. 261-266.

**Roots, C.F.** and Heaman, L., 2001. Mississippian U-Pb dates from Dorsey Terrane assemblages in the upper Swift River area, southern Yukon Territory. Current Research 2001-A1, Geological Survey of Canada. http://www.nrcan.gc.ca/gsc/bookstore/free/cr_2001/A01.pdf

Schwab, D.L., Thorkelson, D.J., Mortensen, J.K. and **Abbott, J.G.**, 2001. The Bear River dykes: A westward extension of the Mackenzie dyke swarm? *In:* Lithoprobe SNORCLE – Cordilleran Tectonics Workshop, Victoria, BC, F. Cook and P. Erdmer (eds.), vol. 79, p. 82-84.

Selby, D., Creaser, R.A. and **Hart, C.J.R.**, 2001. Timing relationship between plutonism and gold mineralization: Re-Os molybdenite study of the reduced intrusion-related gold deposits of the Tombstone Plutonic Suite, Yukon and Alaska. GAC MAC Annual Meeting, St. John's, Newfoundland, 2001, p. 134.

Simard, R-L, **Roots, C.F.** and Dostal, J., 2001. Tectonic implications of the geologic setting if the Klinkit assemblage (Yukon-Tanana Terrane), northern British Columbia. *In:* Geological Association of Canada - Mineralogical Association of Canada, Abstracts vol. 26, p. 138.

Stephens, J.R., Mair, J.L., Oliver, N.H.S., Baker, T. and **Hart, C.J.R.**, 2001. Structural control on intrusion-related gold deposits in the central Yukon Territory, Tintina gold belt, Canada: Implications for exploration. *In:* 2001: A Hydrothermal Odyssey, Extended Conference Abstracts, P.J. Williams (ed.), EGRU Contribution 59, p. 191-192.

Symons, D.T.A., **Hart, C.J.R.**, McCausland, P.J.A. and Harris, M.J., 2001. Eocene rotation of the northern intermontane terranes: Paleomagnetic results from the Flat Creek pluton in the Yukon. Geological Association of Canada, Program with Abstracts, St. John's, Newfoundland.

Symons, D.T.A., **Hart, C.J.R.**, Harris, M.J. and McCausland, P.J.A., 2001. A preliminary location for the Stikine Terrane at 53.6 Ma: Paleomagnetism of the Flat Creek pluton in the Yukon. *In:* F. Cook and P. Erdmer (eds.), Lithoprobe SNORCLE – Cordilleran Tectonics Workshop, Victoria, BC, vol. 79, p. 94-98.

Villeneuve, M.E., **Hart, C.J.R.,** Edwards, B.R. and Russell, J.K., 2001. $^{40}$Ar/$^{39}$Ar Geochronology of Northern Cordilleran volcanism: Apparent or real spatial-temporal correlations? Abstracts of the contributions of the 26th General Assembly of the European Geophysical Society, Nice, France, Geophysical Research, vol. 3.

## YUKON THESES

Brown, V., 2001. The Geology and Genesis of the Ray Gulch Tungsten Skarn, Yukon Territory, Canada. Unpublished BSc Honours Thesis, James Cook University, Townsville, Australia.

Craig, L.M., 2000. Sustainable development, hardrock mining and instruments of governance in Yukon. Unpublished MSc Thesis, University of Waterloo, Waterloo, Ontario, 179 p.

De Keijzer, M., 2000. Tectonic evolution of the Teslin Suture Zone and the western Cassiar Terrane Northern Canadian Cordillera. Unpublished PhD Thesis, University of New Brunswick, Fredericton, New Brunswick, 391 p.

Howes, J.E., 2000. Regolithic fine-fraction weathering patterns in the northwest Ruby Range of the Yukon Territory, Canada. Unpublished PhD Thesis, Carleton University, Ottawa, Ontario, 205 p.

Madsen, J.K., 2001. The Quaternary History and Placer Deposits of Gladstone Creek, Southwest Yukon. Unpublished BSc Honours Thesis, University of Victoria, Victoria, BC, 131 p.

Piercey, S.J., 2001. Petrology and Tectonic Setting of Felsic and Mafic Volcanic and Intrusive Rocks in the Finlayson Lake Volcanic-hosted Massive Sulphide (VHMS) District, Yukon, Canada: A Record of Mid-paleozoic Arc and Back-arc Magmatism and Metallogeny. Unpublished PhD Thesis, University of British Columbia, Vancouver, BC, 304 p.

Pisaric, M.F.J., 2001. Holocene Environmental Change at the Subarctic Alpine Treeline in Northern British Columbia and the Southern Yukon Territory, Canada. Unpublished PhD Thesis, Queen's University, Kingston, Ontario, 206 p.

## YUKON GEOLOGICAL PUBLICATIONS OF INTEREST

Abbott, M., Anderson, L., Tsukernik, M., Finney, B. and Edwards, M., 2001. Holocene paleohydrology and glacial history of Alaska and the Yukon Territory from lake sediment studies. *In:* Canadian Quaternary Association Meetings, 2001, Whitehorse, Yukon, Program and Abstracts. Heritage Branch, Government of the Yukon, Occasional Papers in Earth Sciences No. 1, p. 20.
http://cgrg.geog.uvic.ca//abstracts/AbbottHoloceneThe.html

Abraham, A.C., Francis, D. and Polve, M., 2001. Recent alkaline basalts as probes of the lithospheric mantle roots of the northern Canadian Cordillera. Chemical Geology, vol. 175, p. 361-386.

Baker, T. and Lang, J.R., 2001. Fluid inclusion characteristics of intrusion-related gold mineralization, Tombstone-Tungsten magmatic belt, Yukon Territory, Canada. Mineralium Deposita, vol. 36, p. 563-582.

Beierle, B., 2001. Holocene climatic changes in the central Yukon Territory, Canada. *In:* Canadian Quaternary Association Meetings, 2001, Whitehorse, Yukon, Program and Abstracts. Heritage Branch, Government of the Yukon, Occasional Papers in Earth Sciences No. 1, p. 24.
http://cgrg.geog.uvic.ca//abstracts/BeierleHoloceneSediment.html

Bradshaw, G.D., Tucker, T.L., Peter, J.M., Paradis, S. and Rowins, S.M., 2001. Geology of the Wolverine polymetallic volcanic-hosted massive sulphide deposit, Finlayson Lake District, Yukon Territory, Canada. Geological Association of Canada, Program with Abstracts, St. John's, Newfoundland.

Cook, F.A., Clowes, R.M., Snyder, D.B., van der Velden, A.J., Hall, K.W., Erdmer, P. and Evenchick, C.A., 2001. LITHOPROBE seismic reflection profiling of the northern Canadian Cordillera: First results of SNORCLE Profiles 2 and 3. *In:* Lithoprobe SNORCLE – Cordilleran Tectonics Workshop, Victoria, BC, F. Cook and P. Erdmer (eds.), vol. 79, p. 36-49.

Coulson, I.M., Dipple, G.M. and Raudsepp, M., 2001. Evolution of HF and HCl activity in magmatic volatiles of the gold-mineralized Emerald Lake pluton, Yukon Territory, Canada. Mineralium Deposita, vol. 36, p. 594-606.

de Keijzer, M., Mihalynuk, M.G. and Johnston, S.T., 2000. Structural investigation of an exposure of the Teslin Fault, northwestern British Columbia. Geological Survey of Canada, Current Research 2000-A5, 10 p.

Elias, S.A., 2000. Climatic tolerances and zoogeography of the late Pleistocene beetle fauna of Beringia. Geographie Physique et Quaternaire, vol. 54, p. 143-155.

Erdmer, P., Cook, F., Clowes, R., Snyder, D., Evenchick, C., van der Velden, A. and Hall, K., 2001. Some geological constraints on Cordilleran structure imposed by line 3 reflections - MacMillan Pass to White Pass. *In:* Lithoprobe SNORCLE - Cordilleran Tectonics Workshop, Victoria, BC, F. Cook and P. Erdmer (eds.), vol. 79, p. 54-55.

Evers, K. and Johnston, S.T., 2000. An alpine peridotite in the Dawson Range, Yukon-Tanana Terrane: Preliminary results and interpretations. Ancient Pacific Margin, National Mapping Meeting, Sidney, BC, December, 2000.

Fallis, K.M. and Lane, L.S., 2001. Geology of the Mount Martin, Fisherman Lake and Mount Flett map areas, Yukon Territory and Northwest Territories. Current Research 2001-A5, Geological Survey of Canada. http://www.nrcan.gc.ca/gsc/bookstore/free/cr_2001/cord_e.pdf

Fraser, R.C. and Spratt, D.A., 2001. Deflection of the La Biche anticline, Yukon and Northwest Territories. *In:* Lithoprobe SNORCLE - Cordilleran Tectonics Workshop, Victoria, BC, F. Cook and P. Erdmer (eds.), vol. 79, p. 243-246.

Friele, P.A., Froese, D., Smith, D.G., Miskovic, A., Jackson, Jr., L.E. and Clague, J.J. 2001. Paraglacial sediment supply and eolian accumulation along the Yukon River during the Pleistocene-Holocene transition. *In:* Canadian Quaternary Association Meetings, 2001, Whitehorse, Yukon, Program and Abstracts. Heritage Branch, Government of the Yukon, Occasional Papers in Earth Sciences No. 1, p. 37. http://cgrg.geog.uvic.ca//abstracts/FrieleParaglacialStratigraphic.html

Froese, D., Westgate, J., Preece, S. and Sandhu, A., 2001. Mid-Pliocene permafrost and the first Cordilleran ice sheet in Yukon Territory. *In:* Canadian Quaternary Association Meetings, 2001, Whitehorse, Yukon, Program and Abstracts, Heritage Branch, Government of the Yukon, Occasional Papers in Earth Sciences No. 1, p. 38. http://cgrg.geog.uvic.ca//abstracts/FroeseMid-PlioceneArctic.html

Huscroft, C.A., Barendregt, R.W. and Jackson, L.E. (Jr.). Late Cenozoic geology: Ancient Pacific Margin NATMAP Project, Report 3: Paleomagnetic and geomorphic evidence for Brunhnes age volcanism, Fort Selkirk and Rosebud Creek area, Yukon Territory. Current Research 2001-A4, Geological Survey of Canada. http://www.nrcan.gc.ca/gsc/bookstore/free/cr_2001/A04.pdf

Huscroft, C.A., Jackson, Jr., L.E., Barendregt, R.W. and Villeneuve, M. 2001. Constraints on ages of Pre-McConnell glaciations based on new Paleomagnetic investigations and Ar-Ar dating of basalt in west central Yukon, Canada. *In:* Canadian Quaternary Association Meetings, 2001, Whitehorse, Yukon, Program and Abstracts, Heritage Branch, Government of the Yukon, Occasional Papers in Earth Sciences No. 1, p. 41. http://cgrg.geog.uvic.ca/abstracts HuscroftConstraintsNew.html

Huscroft, C.A., Ward, B.C., Tarnocai, C. and Jackson, Jr., L.E., 2001. Soil development and the age of river terraces along the Yukon River, Fort Selkirk to White River, west-central Yukon, Canada. *In:* Canadian Quaternary Association Meetings, 2001, Whitehorse, Yukon, Program and Abstracts. Heritage Branch, Government of the Yukon, Occasional Papers in Earth Sciences No. 1, p. 42. http://cgrg.geog.uvic.ca//abstracts/HuscroftSoilThe.html

Jackson, D.E. and Lenz, A.C., 2001. The sequence of Tremadocian graptolites in Yukon, Canada. Geological Association of Canada, Program with Abstracts, St. John's, Newfoundland.

Jackson, L.E. (Jr.), Shimamura, K. and Huscroft, C.A., 2001. Late Cenozoic geology: Ancient Pacific Margin NATMAP Project, Report 3: A re-evaluation of glacial limits in the Stewart River basin of Stewart River map area, Yukon Territory. Current Research 2001-A1, Geological Survey of Canada. http://www.nrcan.gc.ca/gsc/bookstore/free/cr_2001/A03.pdf

Johnston, S.T., 1999. Large scale, orogen-parallel displacement in the Cordillera: A granitic resolution to a paleomagnetic dilemma. Journal of Structural Geology, vol. 21, p. 1103-1108.

Johnston, S.T., 2001. The Great Alaskan Terrane Wreck: Oroclinal Orogeny and reconciliation of paleomagnetic and geological data in the northern Cordillera. Earth & Planetary Science Letters, vol. 193, p. 259-272.

Lane, L.S., Fallas, K.M. and Miles, W.F., 2001. Geology of the Fort Liard region, Yukon and Northwest Territories: Initial results of new mapping by the Central Foreland NATMAP Project. *In:* Lithoprobe SNORCLE - Cordilleran Tectonics Workshop, Victoria, BC, F. Cook and P. Erdmer (eds.), vol. 79, p. 256-257.

Layton-Matthews, D., Peter, J.M., Scott, S.D., Paradis, S., Tucker, T.L. and Bradshaw, G.D., 2001. Distribution of Se and other trace elements in massive sulphides of the Wolverine Zn-Pb-Cu-Ag-Au volcanic-hosted massive sulphide deposit, Finlayson Lake District, Yukon, Canada. Geological Association of Canada, Program with Abstracts, St. John's, Newfoundland.

Ledo, J., Jones, A.G., Ferguson, I.J. and Wennberg, G., 2001. Electromagnetic images of the Tintina Fault. *In:* Lithoprobe SNORCLE - Cordilleran Tectonics Workshop, Victoria, BC, F. Cook and P. Erdmer (eds.), vol. 79, p. 67-73.

Ledo, J., Jones, A.G., Ferguson, I.J. and Wennberg, G., 2001. Regional electrical conductivity of the northern Cordillera: Corridors 2 and 3. *In:* Lithoprobe SNORCLE - Cordilleran Tectonics Workshop, Victoria, BC, F. Cook and P. Erdmer (eds.), vol. 79, p. 258.

Liverton, T. and Botelho, N.F., 2001. Fractionated alkaline rare-metal granites: Two examples. Journal of Asian Earth Sciences, vol. 19, p. 399-412.

Livingston, J.M., Smith, D.G., Froese, D.G., Parkstrom, G.J. and Parker, M.K., 2001. Reconstructing the late Holocene (last 3000 years) ice-jam flood history of the middle Yukon River. *In:* Canadian Quaternary Association Meetings, 2001, Whitehorse, Yukon, Program and Abstracts. Heritage Branch, Government of the Yukon, Occasional Papers in Earth Sciences No. 1, p. 50.
http://cgrg.geog.uvic.ca/abstracts/LivingstonReconstructingA.html

Maloof, T.L., Baker, T. and Thompson, J.F.H., 2001. The Dublin Gulch intrusion-hosted gold deposit, Tombstone plutonic suite, Yukon Territory, Canada. Mineralium Deposita, vol. 36, p. 583-593.

Mezger, J., Creaser, R., Erdmer, P. and Johnston, S.T., 2001. Cretaceous backarc basin along the Coast Belt of the northern Canadian Cordillera: Evidence from geochemical and Neodymium isotope signatures of the Kluane metamorphic assemblage, SW Yukon. Canadian Journal of Earth Sciences, vol. 38, p. 91-103.

Mihalynuk, M.G., Erdmer, P., Ghent, E.D., Archibald, D., Friedman, R.M., Cordey, F. and Johannson, G.G., 2001. Age constraints for emplacement of the northern Cache Creek oceanic crust and implications of youngest blueschist metamorphism. *In:* Lithoprobe SNORCLE - Cordilleran Tectonics Workshop, Victoria, BC, F. Cook and P. Erdmer (eds.), vol. 79, p. 80-81.

Moore, K., Alverson, K. and Holdsworth, G., 2001. On the secular trend in snow accumulation from the Mount Logan ice core, Yukon. Eos Transactions, American Geophysical Union Fall Meeting Abstracts, vol. 82, p. 47.

Mougeot, C.M. and Roots, C.F., 2001. Geoscape Whitehorse: Geology for the community. Geological Association of Canada, Program with Abstracts, St. John's, Newfoundland.

Murphy, J.B., Hynes, A., Johnston, S.T. and Oppliger, G.L., 2001. Flat slab subduction in the geological record: Consideration of modern analogues. Geological Society of America, Annual Meeting 2001, Program with Abstracts, vol. 32.

Pienitz, R., Smol, J.P., Last, W.M., Leavitt, P.R. and Cumming, B.F., 2001. Multi-proxy Holocene paleolimnologic record from a saline lake in the Yukon, Canadian Subarctic. *In:* Canadian Quaternary Association Meetings, 2001, Whitehorse, Yukon, Program and Abstracts. Heritage Branch, Government of the Yukon, Occasional Papers in Earth Sciences No. 1, p. 59.
http://cgrg.geog.uvic.ca/abstracts/PienitzMulti-proxyMulti-proxy.html

Piercey, S.J., Peter, J.M., Bradshaw, G.D., Tucker, T. and Paradis, S., 2001. Geological characteristics of high-level subvolcanic intrusions in the Wolverine volcanic-hosted massive sulphide deposit, Finlayson Lake district, Yukon. (POSTER) Geological Association of Canada, Program with Abstracts, St. John's, Newfoundland.

Reyes, A. and Smith, D.J., 2001. Tree-ring dates for Neoglacial Lake Alsek, Yukon Territory, Canada. *In:* Canadian Quaternary Association Meetings, 2001, Whitehorse, Yukon, Program and Abstracts, Heritage Branch, Government of the Yukon, Occasional Papers in Earth Sciences No. 1, p. 60. http://cgrg.geog.uvic.ca//abstracts/ReyesTree-ringLake.html

Ryan, J.J. and Gordey, S.P., 2001. New Geological mapping in Yukon-Tanana Terrane near Thistle Creek, Stewart River map area, Yukon Territory. Current Research 2001-A2, Geological Survey of Canada. http://www.nrcan.gc.ca/gsc/bookstore/free/cr_2001/A02.pdf

Ryan, J.J. and Gordey, S.P., 2001. Protolith and tectonic significance of amphibolite facies gneisses of the Yukon-Tanana Terrane in the Thistle Creek area (Stewart River map sheet), Yukon Territory. *In:* Lithoprobe SNORCLE - Cordilleran Tectonics Workshop, Victoria, BC, F. Cook and P. Erdmer (eds.), vol. 79, p. 274-277.

Schweger, C., 2001. Glacial, interstadial and interglacial environments of the Yukon - contrasting the extremes. *In:* Canadian Quaternary Association Meetings, 2001, Whitehorse, Yukon, Program and Abstracts, Heritage Branch, Government of the Yukon, Occasional Papers in Earth Sciences No. 1, p. 62.

Snyder, D. and Roberts, B., 2001. Seismic characterization of two major tectonic zones in the Canadian Cordillera: The Teslin and Tintina zones along SNORCLE line 3. *In:* Lithoprobe SNORCLE - Cordilleran Tectonics Workshop, Victoria, BC, F. Cook and P. Erdmer (eds.), vol. 79, p. 50-53.

Storer, J. (ed.), 2001. Canadian Quaternary Association Meetings, 2001. Program and Abstracts, Whitehorse, Yukon, August 2001, Occasional Papers in Earth Sciences No. 1, Heritage Branch, Yukon Government, 73 p.

Thompson, J.F.H. and Newberry, R.J., 2000. Gold deposits related to reduced granitic intrusions. *In:* Gold in 2000, S.G. Hagemann and P.E. Brown (eds.), Reviews in Economic Geology, vol. 13, Society of Economic Geologists, p. 377-400.

Wennberg, G., Ferguson, I.J., Ledo J. and Jones, A.G., 2001. Preliminary results from SNORCLE magnetotelluric data: Johnson's Crossing to Upper Liard. *In:* Lithoprobe SNORCLE - Cordilleran Tectonics Workshop, Victoria, BC, F. Cook and P. Erdmer (eds.), vol. 79, p. 284.

West, K.D. and Donaldson, J.A., 2001. Eruptive timing of White River Ash deposit (Yukon, Northwest Territories, and Alaska). *In:* Canadian Quaternary Association Meetings, 2001, Whitehorse, Yukon, Program and Abstracts. Heritage Branch, Government of the Yukon, Occasional Papers in Earth Sciences No. 1, p. 67. http://cgrg.geog.uvic.ca//abstracts/WestEruptiveOf.html

Westgate, J., Preece, S., Sandhu, A., Froese, D. and Schweger, C., 2001. Age of the Reid Glaciation in central Yukon. *In:* Canadian Quaternary Association Meetings, 2001, Whitehorse, Yukon, Program and Abstracts. Heritage Branch, Government of the Yukon, Occasional Papers in Earth Sciences No. 1, p. 67. http://cgrg.geog.uvic.ca/abstracts/WestgateAgeTephra.html

Westgate, J.A., Preece, S.J., Froese, D.G., Walter, R.C. and Schweger, C.A., 2001. Tephrochronology dates two extensive glaciations in Yukon Territory. Quaternary Research, vol. 56, p. 1-18.

## GEOLOGICAL SURVEY OF CANADA

Duk-Rodkin, A., 2001. Glacial limits, Bonnet Plume Lake, Yukon Territory (NTS 106B). Geological Survey of Canada, Open File 3800, one colour map, 1:250 000 scale.

Duk-Rodkin, A., 2001. Glacial limits, Carmacks, Yukon Territory (NTS 115I). Geological Survey of Canada, Open File 3805, one colour map, 1:250 000 scale.

Duk-Rodkin, A., 2001. Glacial limits, Coal River, Yukon Territory (NTS 95D). Geological Survey of Canada, Open File 3813, one colour map, 1:250 000 scale.

Duk-Rodkin, A., 2001. Glacial limits, Dezadeash, Yukon Territory (NTS 115A). Geological Survey of Canada, Open File 3809, one colour map, 1:250 000 scale.

Duk-Rodkin, A., 2001. Glacial limits, Flat River, Yukon Territory (NTS 95E). Geological Survey of Canada, Open File 3808, one colour map, 1:250 000 scale.

Duk-Rodkin, A., 2001. Glacial limits, Kluane Lake, Yukon Territory (NTS 115G,F). Geological Survey of Canada, Open File 3806, one colour map, 1:250 000 scale.

Duk-Rodkin, A., 2001. Glacial limits, Lake Laberge, Yukon Territory (NTS 105E). Geological Survey of Canada, Open File 3807, one colour map, 1:250 000 scale.

Duk-Rodkin, A., 2001. Glacial limits, Lansing Range, Yukon Territory (NTS 105N). Geological Survey of Canada, Open File 3802, one colour map, 1:250 000 scale.

Duk-Rodkin, A., 2001. Glacial limits, Nadaleen River, Yukon Territory (NTS 106C). Geological Survey of Canada, Open File 3799, one colour map, 1:250 000 scale.

Duk-Rodkin, A., 2001. Glacial limits, Niddery Lake-Sekwi Mountain, Yukon Territory (NTS 105O, P). Geological Survey of Canada, Open File 3803, one colour map, 1:250 000 scale.

Duk-Rodkin, A., 2001. Glacial limits, Ogilvie River, Yukon Territory (NTS 116G, F). Geological Survey of Canada, Open File 3793, one colour map, 1:250 000 scale.

Duk-Rodkin, A., 2001. Glacial limits, Stevenson Ridge, Yukon Territory (NTS 115J, K). Geological Survey of Canada, Open File 3804, one colour map, 1:250 000 scale.

Duk-Rodkin, A., 2001. Glacial limits, Stewart River, Yukon Territory (NTS 115O, N). Geological Survey of Canada, Open File 3801, one colour map, 1:250 000 scale.

Duk-Rodkin, A., 2001. Glacial limits, Watson Lake, Yukon Territory (NTS 105A). Geological Survey of Canada, Open File 3812, one colour map, 1:250 000 scale.

Duk-Rodkin, A., 2001. Glacial limits, Whitehorse, Yukon Territory (NTS 105D). Geological Survey of Canada, Open File 3810, one colour map, 1:250 000 scale.

Duk-Rodkin, A., 2001. Glacial limits, Wolf Lake, Yukon Territory (NTS 105B). Geological Survey of Canada, Open File 3811, one colour map, 1:250 000 scale.

Duk-Rodkin, A., 2001. Glacial limits, Hart River, Yukon Territory (NTS 116H). Geological Survey of Canada, Open File 3794, one colour map, 1:250 000 scale.

Duk-Rodkin, A., 2001. Glacial limits, Larsen Creek, Yukon Territory (NTS 116A). Geological Survey of Canada, Open File 3797, one colour map, 1:250 000 scale.

Duk-Rodkin, A., 2001. Glacial limits, Nash Creek, Yukon Territory (NTS 106D). Geological Survey of Canada, Open File 3798, one colour map, 1:250 000 scale.

Duk-Rodkin, A., 2001. Glacial limits, Snake River, Yukon Territory (NTS 106F). Geological Survey of Canada, Open File 3796, one colour map, 1:250 000 scale.

Duk-Rodkin, A., 2001. Glacial limits, Wind River, Yukon Territory (NTS 106E). Geological Survey of Canada, Open File 3795, one colour map, 1:250 000 scale.

Fallas, K.M., 2001. Preliminary geology, Mount Martin, Yukon Territory-British Columbia-Northwest Territories (NTS 95C/1). Geological Survey of Canada, Open File 3402, one colour map, 1:50 000 scale.

Fallas, K.M., 2001. GIS dataset: Preliminary geology, Mount Martin (95C/1), Yukon Territory, British Columbia, and Northwest Territories. Geological Survey of Canada, Open File D4015, CD-ROM.

Friske, P.W.B., Day, S.J.A. and McCurdy, M.W., 2001. Regional Stream Sediment and Water Geochemical Data, Eastern Yukon and Western Northwest Territories. Geological Survey of Canada, Ottawa, Ontario; Exploration and Geological Services Division, Yukon Region, Indian and Northern Affairs Canada; GSC Open File 4016 and EGSD Open File 2001-12(D), CD-ROM.

Friske, P.W.B., Day, S.J.A. and McCurdy, M.W., 2001. Regional Stream Sediment and Water Geochemical Data, Southwestern Yukon (Parts of NTS 115A and 115B). Geological Survey of Canada, Ottawa, Ontario; Exploration and Geological Services Division, Yukon Region, Indian and Northern Affairs Canada; GSC Open File 2859 and EGSD Open File 2001-11(D), CD-ROM.

Friske, P.W.B., Day, S.J.A. and McCurdy, M.W., 2001. Regional Stream Sediment and Water Geochemical Data, Western Yukon, 2001. Geological Survey of Canada, Ottawa, Ontario; Exploration and Geological Services Division, Yukon Region, Indian and Northern Affairs Canada; GSC Open File 1364 and EGSD Open File 2001-13(D), CD-ROM.

Gordey, S.P. and Makepeace, A.J. (comps.), 2001. Bedrock Geology, Yukon Territory. Geological Survey of Canada, Ottawa, Ontario; Exploration and Geological Services Division, Yukon Region, Indian and Northern Affairs Canada; GSC Open File 3754 and EGSD Open File 2001-1, one colour map, 1:1 000 000 scale.

Ryan, J.J. and Gordey, S.P., 2001. Geology, Thistle Creek area, Yukon Territory (NTS 115O/3). Geological Survey of Canada, Open File 3690, one colour map, 1:50 000 scale.

Shimamura, K., Wagner, C.L. and Cocking, R., 2001. Composite relief map, Stewart River, Yukon Territory (NTS 115N, O). Geological Survey of Canada, Open File 4156, one colour map, 1:250 000 scale.

Shives, R.B.K., Carson, J.M., Ford, K.L., Holman, P.B., Gordey, S. and Abbott, G., 2001. Multisensor Airborne Geophysical Survey, Stewart River and Dawson areas (115O/16, 116B/1). Geological Survey of Canada, Ottawa, Ontario; Exploration and Geological Services Division, Yukon Region, Indian and Northern Affairs Canada; GSC Open File 3993 and EGSD Open File 2001-9, ten 1:50 000-scale maps.

Shives, R.B.K., Carson, J.M., Ford, K.L., Holman, P.B., Gordey, S. and Abbott, G., 2001. Multisensor Airborne Geophysical Survey, Stewart River and Dawson areas (115Oand N and 116B). Geological Survey of Canada, Ottawa, Ontario; Exploration and Geological Services Division, Yukon Region, Indian and Northern Affairs Canada; GSC Open File 3994 and EGSD Open File 2001-10, ten 1:50 000-scale maps, paper and CD-ROM.

Shives, R.B.K., Carson, J.M., Ford, K.L., Holman, P.B., Gordey, S. and Abbott, G., 2001. Multisensor Airborne Geophysical Survey, Stewart River and Dawson areas (115O and N and 116B). Geological Survey of Canada, Ottawa, Ontario; Exploration and Geological Services Division, Yukon Region, Indian and Northern Affairs Canada; GSC Open File D4009 and EGSD Open File 2001-30(D), sixty 1:250 000-scale and 1:50 000-scale maps, CD-ROM.

Shives, R.B.K., Carson, J.M., Ford, K.L., Holman, P.B., Gordey, S. and Abbott, G., 2001. Multisensor Airborne Geophysical Survey, Stewart River area (parts of 115N/1,2,7,8). Geological Survey of Canada, Ottawa, Ontario; Exploration and Geological Services Division, Yukon Region, Indian and Northern Affairs Canada; GSC Open File 3989 and EGSD Open File 2001-5, ten 1:50 000-scale maps.

Shives, R.B.K., Carson, J.M., Ford, K.L., Holman, P.B., Gordey, S. and Abbott, G., 2001. Multisensor Airborne Geophysical Survey, Stewart River area (parts of 115N/8,9, 115O/5,6). Geological Survey of Canada, Ottawa, Ontario; Exploration and Geological Services Division, Yukon Region, Indian and Northern Affairs Canada; GSC Open File 3990 and EGSD Open File 2001-6, ten 1:50 000-scale maps.

Shives, R.B.K., Carson, J.M., Ford, K.L., Holman, P.B., Gordey, S. and Abbott, G., 2001. Multisensor Airborne Geophysical Survey, Stewart River area (parts of 115O/11,12,13,14). Geological Survey of Canada, Ottawa, Ontario; Exploration and Geological Services Division, Yukon Region, Indian and Northern Affairs Canada; GSC Open File 3991 and EGSD Open File 2001-7, ten 1:50 000-scale maps.

Shives, R.B.K., Carson, J.M., Ford, K.L., Holman, P.B., Gordey, S. and Abbott, G., 2001. Multisensor Airborne Geophysical Survey, Stewart River area (115O/14,15). Geological Survey of Canada, Ottawa, Ontario; Exploration and Geological Services Division, Yukon Region, Indian and Northern Affairs Canada; GSC Open File 3992 and EGSD Open File 2001-8, ten 1:50 000-scale maps.

Wolfe, S.A., Kotler, E. and Dallimore, S.R., 2001. Surficial characteristics and the distribution of thaw landforms (1970 to 1999), Shingle Point to Kay Point, Yukon Territory. Geological Survey of Canada, Open File 4115, CD-ROM.

## MINING ENVIRONMENT RESEARCH GROUP (MERG) REPORTS

EBA Engineering Consultants Ltd., 2001. Research of low permeability cover performance at the Arctic Gold and Silver mine site, Carcross, Yukon. Economic Development, Yukon Government, MERG Report 2001-1, 34 p.

Laberge Environmental Services, 2001. Cyanide – the facts. Economic Development, Yukon Government, MERG Report 2001-2, 11 p.

# Le Service de géologie du Yukon

***Maurice Colpron*[1] *et Grant Abbott*[2]**
*Le Service de géologie du Yukon*

Colpron, M. and Abbott, J.G., 2002. Le service de géologie du Yukon. *In:* Yukon Exploration and Geology 2001, D.S. Emond, L.H. Weston and L.L. Lewis (eds.), Exploration and Geological Services Division, Yukon Region, Indian and Northern Affairs Canada, p. 49-51.

## APERÇU

Le Service de géologie du Yukon (fig. 1), qui en est maintenant à sa sixième année d'existence, est dans les faits la commission géologique du Yukon et consiste en deux bureaux intégrés présentant des structures administratives différentes mais qui sont gérés conjointement (fig. 2). Le financement par le fédéral est fourni par l'entremise de la Division des Services d'exploration et de géologie du ministère des Affaires indiennes et du Nord canadien (MAIN), alors que le financement par le territoire et à coûts partagés (GTY/MAIN) est obtenu par l'entremise de la Direction des ressources minérales du ministère de l'Expansion économique (gouvernement du territoire du Yukon (GTY)). Le GTY gère et finance indépendemment le Groupe d'évaluation du potentiel minéral et le Programme d'encouragement pour l'exploitation minérale du Yukon ; ceux-ci sont décrit brièvement ci-dessous. La Commission géologique du Canada (CGC) maintient également un bureau auprès du Service.

Le Service de géologie du Yukon est une organisation informelle et temporaire qui sera transformée en commission géologique du Yukon lorsque les responsabilités du Programme des affaires du Nord seront dévoluées au GTY. Une entente de principe concernant la dévolution a maintenant été signée et la date du transfert des responsabilités est fermement établie au premier avril 2003.

Le programme de géologie du Yukon compte de nombreuses fonctions dont les principales sont les suivantes : assurer la liaison entre l'industrie minérale et le gouvernement; tenir des bases de données géologiques telles que Yukon MINFILE (gîtes minéraux), Yukon GEOPROCESS FILE (processus géologiques et dangers du terrain) et Yukon Placer MINFILE (gisements placériens) ; tenir un point de vente de cartes et de publications et une carothèque (H.S. Bostock Core Library) ; et enfin, promouvoir et exécuter de nouvelles recherches géologiques, et en publier les résultats.

La plupart des travaux de recherche géologique continuent d'être exécutés de concert avec des initiatives d'autres agences gouvernementales. Le Service géologique du Yukon contribue toujours d'importantes ressources au projet CARTNAT (Programme national de cartographie géoscientifique du Canada) de l'ancienne marge du Pacifique, une initiative conjointe des commissions géologiques du Canada, de la Colombie-Britannique et du Service de géologie du Yukon. Ce projet est une étude multidisciplinaire visant à mieux comprendre les terranes de Yukon-Tanana et de Kootenay, soit les parties considérées comme les moins bien connues de la cordillère nord-américaine. Au Yukon, des travaux de cartographie géologique sont en cours dans les régions de Finlayson Lake, de Glenlyon, de Stewart River, et de Wolf Lake. Ce projet inclut aussi des travaux de cartographie géologique dans le sud de la Colombie-Britannique et dans le centre-est de l'Alaska, de même que des études de gîtes minéraux en Alaska. La participation de nombreux chercheurs universitaires, d'étudiants de deuxième et de troisième cycle, et d'autres spécialistes ont grandement contribué à la valeur scientifique du projet. En outre, on a complété une étude lithogéochimique dans la région

---

[1] *maurice.colpron@gov.yk.ca*

[2] *abbottg@inac.gc.ca*

de Finlayson Lake et l'on poursuit des études de gîtes minéraux à plusieurs endroits au sein du terrane de Yukon-Tanana.

En 2001, la partie yukonnaise du projet CARTNAT a reçu du financement additionnel par l'entremise de l'Initiative géoscientifique ciblée du ministère de ressources naturelles du Canada. Ces fonds additionnels ont permis de compléter un levé géochimique du till et la cartographie géologique de la partie septentrionale de la carte de Finlayson Lake. Des cibles géologiques et géochimiques d'interêt furent identifiées lors de ce programme.

L'Initiative géoscientifique ciblée a aussi permis de compléter la deuxième et dernière partie d'un levé géophysique aéroporté multispectral de la région de Stewart River ; celà amène la couverture géophysique de la région à environ deux-tiers du feuillet cartographique. Les résultats du premier levé (publiés plus tôt en 2001) ont déjà engendré le jalonnement de concessions minières et la prospection de cibles promettrices. Le succès des levés géophysiques aéroportés précédents a amené le GTY à financer (par l'entremise de la CGC) un levé multispectral des terrains prometteurs entourant les gisements de cuivre de Minto et Williams Creek, au nord-ouest de Carmacks.

Le Service de géologie du Yukon est aussi un partenaire, avec le bureau de Calgary de la CGC et des chercheurs universitaires, du projet CARTNAT de l'avant-pays central. Ce projet, qui recouvre en partie le nord de la Colombie-Britannique, le sud-ouest des territoires du Nord-Ouest, et le sud-est du Yukon, a pour principal objectif d'augmenter les connaissances géoscientifiques des régions présentant un potentiel d'hydrocarbures. Les travaux de cartographie géologique menés par le Service de géologie du Yukon dans la région de La Biche River en sont maintenant dans leur deuxième année ; ils ont permis de reviser les interprétations stratigraphiques et structurales de cette région.

Au nombre des autres objectifs majeurs visés par le Service de géologie du Yukon, mentionnons celui consistant à synthétiser et à améliorer la base de données géologiques du district d'Anvil, initiative qui comprend la cartographie géologique du socle rocheux et des dépôts superficiels, et des levés géochimiques de till, en plus de l'étude des gites minéraux. Un rapport couvrant la cartographie des dépôts superficiels et la géochimie du till, de même qu'une carte de compilation géologique régionale à l'échelle de 1 : 100,000 sont maintenant disponibles.

Outre les travaux de cartographie géologique et les levés géophysiques, la région de Stewart River est aussi le sujet d'un programme de cartographie des dépôts superficiels par la CGC et d'une étude des placers par le Service de géologie du Yukon. Un autre projet est l'étude de la relation entre la sédimentologie, la répartition granulométrique et la qualité de l'eau des effluents provenant des dépôts placériens. Les travaux de terrain sont maintenant complétés et la technique sera évaluée pour d'éventuelles applications à long termes. De plus, les résultat de ce projet seront considérés lors de la révision (en cours) du processus d'authorisation des placers du Yukon.

L'étude des indices aurifères du Yukon se poursuit. Une série d'articles portant sur la ceinture aurifère de Tintina et d'autres indices du Yukon est maintenant en préparation. Une étude des brèches de Wernecke a aussi été entamée au cours de 2001.

## EVALUATION DU POTENTIEL MINÉRAL

La direction des ressources minérales du Yukon fournit de l'information concernant la géologie et le potentiel minier de régions faisant l'objet d'une planification de l'utilisation des terres. Au printemps de 2001, le gouvernement du Yukon s'est engagé à identifier et à annoter sur des cartes des régions d'intérêt pouvant représenter treize écorégions. L'identification des régions d'intérêt fait intervenir les cartes régionales du potentiel minier produites conformément à la méthodologie élaborée par le Geological Survey des États-Unis et améliorée par la commission géologique de la Colombie-Britannique (voir article à ce sujet dans ce volume).

## PROGRAMME D'ENCOURAGEMENT POUR L'EXPLOITATION MINÉRALE DU YUKON

Cette année, 77 demandes relatives au programme ont été reçues avant la date limite. Au total, 917 400 $ ont été accordés à 59 demandeurs. Vingt demandes ont été approuvées dans le cadre du volet 'Grassroots' et du volet 'Grubstake,' tandis que les trente-neuf autres l'ont été dans le cadre du volet Évaluation de cibles. Un peu moins d'explorateurs commandités dans le cadre de ce programme ont recherché des métaux précieux : environ 61 % des candidats ont recherché de l'or, 11 % des éléments du groupe du platine et 28 % des métaux communs. Des programmes d'exploration ont été proposés dans les quatre districts miniers et presque partout sur le territoire du Yukon (voir article à ce sujet dans ce volume).

## PRIX ROBERT E. LECKIE

Pour une troisième année consécutive, on a décerné à l'industrie minière les prix Robert E. Leckie pour la restauration de sites miniers. Le prix pour les pratiques exceptionnelles de restauration de mines a été décerné aux sociétés Viceroy Resource Corporation, Nova Gold Resources Inc. et Newmont Exploration of Canada Ltd., pour les travaux qu'elles ont effectués en collaboration sur la propriété McQuesten. On a remis le prix pour les pratiques exceptionnelles de restauration de placers à Doug Busat de la société T.D. Oilfield Services, pour les travaux de restauration qui ont été exécutés à l'embouchure du ruisseau Hunker, dans la région du Klondike. Un prix particulier de distinction honorifique pour la restauration à long terme de sites miniers a été remporté par Norm Ross de la société Ross Mining, pour ses pratiques de restaurations mises en œuvres au ruisseau Dominion (voir article à ce sujet dans ce volume).

## DIFFUSION DE L'INFORMATION

Le Service de géologie du Yukon produit maintenant une gamme complète de publications numériques. Toutes nouvelles cartes et rapports géologiques sont disponibles sur demande en format numérique, et toutes publications récentes sont aussi disponibles (sous format PDF) sans frais sur notre site internet (http://www.geology.gov.yk.ca). De plus, nous sommes fier d'annoncer l'inauguration de notre service de carte interactive ('Map Gallery'). Ce service est disponible par l'entremise de notre site internet et permet la visualisation de la géologie régionale, des sites MINFILE, de la topographie, des routes et des communautés du Yukon. Ce service fera l'objet d'améliorations fréquentes.

Les publications du Service de géologie du Yukon sont diffusées par la Division des services géologiques et d'exploration (MAIN). Elles sont disponible à l'addresse suivante :

Bureau d'information et des ventes en géosciences
a/s Conservateur des registres miniers
Affaires indiennes et du Nord canadien
300 rue Main-bur.102
Whitehorse (Yukon) Y1A 2B5
Téléphone : (867) 667-3266
Courriel : geosales@inac.gc.ca

Pour en savoir plus long sur le Programme d'études géologiques du Yukon, visitez site internet à http://www.geology.gov.yk.ca ou communiquez directement avec :

Grant Abbott, Géologue principal intérimaire
Division de l'exploration et des services géologiques
Affaires indiennes et du Nord canadien
300 rue Main-bur.345
Whitehorse (Yukon) Y1A 2B5
Téléphone : (867) 667-3200
Courriel : gabbott@gov.yk.ca

Rod Hill, Gestionnaire intérimaire
Division des ressources minérales
Ministère de l'Expansion économique
C.P. 2703
Whitehorse (Yukon) Y1A 2C6
Téléphone : (867) 667-5384
Courriel : rod.hill@gov.yk.ca

# Mineral Resource Assessments Overview, 2001

**Anna Fonseca**
*Mineral Resources Branch[1], Yukon Government*

Fonseca, A., 2002. Mineral Resource Assessments Overview, 2001. *In:* Yukon Exploration and Geology 2001, D.S. Emond, L.H. Weston and L.L. Lewis (eds.), Exploration and Geological Services Division, Yukon Region, Indian and Northern Affairs Canada, p. 53-56.

## INTRODUCTION

The Yukon Mineral Resources Branch provides information on geology and mineral potential of areas undergoing land use planning. During the spring, 2001, Yukon government committed to identifying and making map notations of areas of interest for representation of 13 ecoregions. The identification of areas of interest makes use of regional mineral potential maps that are produced according to the methodology devised by the United States Geological Survey and refined by the British Columbia Geological Survey.

## REGIONAL MINERAL POTENTIAL MAP OF YUKON

### PHASE III: SELWYN BASIN

In December 2000, the Mineral Resources Branch hosted a six-day assessment workshop for Selwyn Basin. Selwyn Basin was examined in order to complete the third phase of a Yukon-wide mineral potential map. Selwyn Basin covers a 127 700-km$^2$ area bounded by Tintina Fault and allochthonous Yukon-Tanana Terrane rocks to the southwest, Dawson Thrust to the north, Yukon-British Columbia border to the south, and Yukon-Northwest Territories (NWT) border to the east (Fig. 1). The

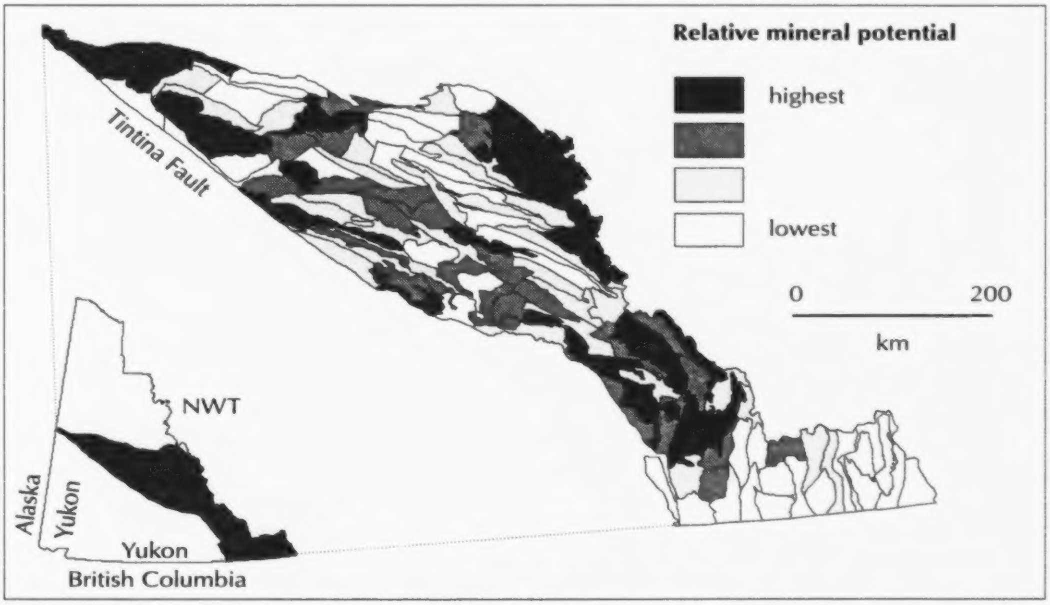

***Figure 1.*** *Mineral potential map of Selwyn Basin.*

---

[1] *Mineral Resources Branch, Yukon Government, 2099-2nd Avenue, Whitehorse, Yukon Canada Y1A 2C6*

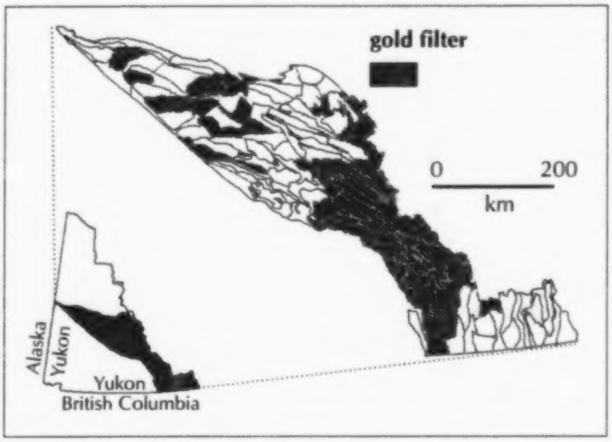

***Figure 2.** Gold filter applied to mineral potential rank, Selwyn Basin.*

assessment area was separated into 127 tracts, which are defined by coherent geology, geochemistry, and/or mineral showings. Five geologists, considered to have outstanding field experience and knowledge of the geology and mineral deposit models applicable to Selwyn Basin, participated in the assessment workshop as expert estimators. The estimators examined all the data for a tract, and agreed upon which metallic mineral deposit models to apply to that tract. They evaluated the likelihood of finding new deposits of each type, while estimating the median tonnage of these deposits within the tract. Each geologist also evaluated the knowledge and experience of the other four estimators. The presence of known non-metallic deposits was recorded in the tract descriptions, however, the estimators did not evaluate potential for new non-metallic deposits. The evaluations were processed in the Mark3b Mineral Deposit Simulator software developed by the United States Geological Survey (USGS), and the 127 tracts were ranked on a relative scale from highest to lowest mineral potential. The resulting mineral potential map of Selwyn Basin (Fig. 1) shows four categories of potential for metallic mineral deposits.

Metallogenically speaking, Selwyn Basin constitutes a base metal anomaly that hosts some of the world's largest sedex deposits. The anomalously large tonnages and grades of sedex deposits in Selwyn Basin yielded a very high median tonnage (14.5 million tonnes, which is the size of the Tom deposit). The median tonnage for sedex deposits was discussed during the assessment workshop, and considered adequate, given that most deposits from which the median was calculated are in Selwyn Basin.

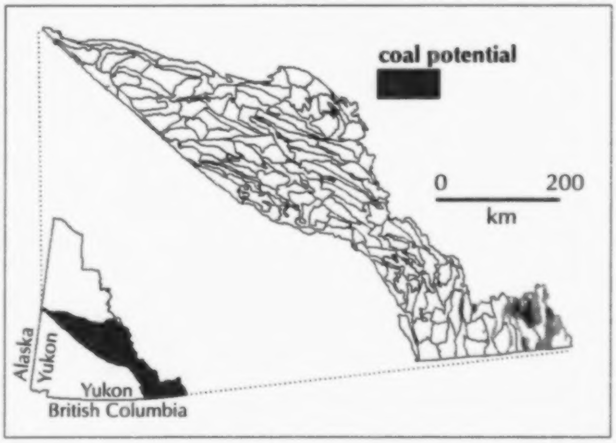

***Figure 3.** Map of Selwyn Basin displaying tracts that contain coal potential, showings, or deposits.*

This high median tonnage resulted in the potential for sedex deposits overpowering potential for most other deposit types. Potential for gold deposits was particularly overpowered by potential for base metals. This is largely due to the fact that gold exploration is more strongly driven by economic factors such as access roads and high net smelter returns. To compensate for this discrepancy, an economic gold filter was applied to the mineral potential map (Fig. 2). The economic gold filter represents the upper half rank of potential for Carlin-type and plutonic-related gold, and is overlain on the mineral potential map to help identify areas of important gold potential.

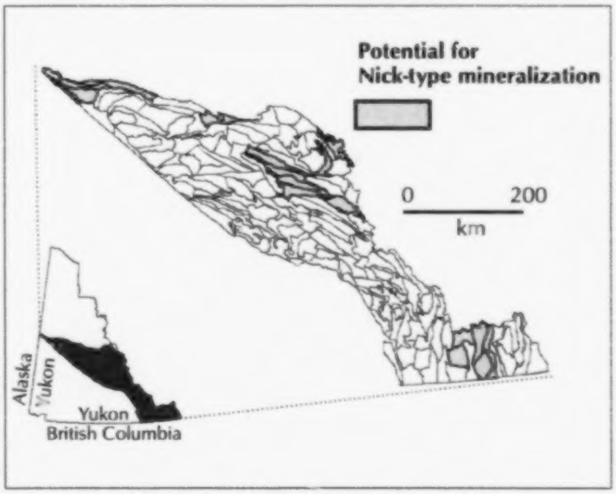

***Figure 4.** Map of Selwyn Basin displaying tracts that have potential for sedimentary-hosted nickel (Nick-type) mineralization.*

No estimates were made for non-metallic minerals such as coal, jade, asbestos, emeralds and rhodonite. Likewise, potential for placer deposits was not evaluated. Coal potential and lithologies containing resources are represented in a separate map (Fig. 3). Potential for sedimentary-hosted nickel (Nick-type) mineralization is also represented on a separate map (Fig. 4), because it was agreed during the assessment workshop that the anomalous geochemical signature observed in the lower Earn Group is not likely to form a mineable deposit.

### PHASE IV: SOUTHWEST YUKON (ONGOING)

A mineral assessment workshop for the 107 262-km$^2$ area between Tintina Fault and D'Abbadie Fault to the north and east, Denali Fault to the southwest, Yukon-Alaska border to the west, and Yukon-British Columbia border to the south is scheduled to take place in December, 2001. This is the final phase of a Yukon-wide mineral potential map, which is scheduled to be completed by January, 2002.

## DETAILED MINERAL ASSESSMENTS

The Yukon Mineral Resources Branch conducts geological fieldwork and detailed mineral assessments to assist in land management guidelines for special management areas established under First Nation final agreements, and in areas of historical conservation interest.

### DDHAW GHRO SPECIAL MANAGEMENT AREA

Ddhaw Ghro Habitat Protection Area Special Management Area (SMA) consists of 1610 km$^2$ in central Yukon (Fig. 5). The SMA occupies the southeastern portion of Mayo map sheet (105M), southwestern corner of McQuesten map sheet (115P), and northwestern corner of Glenlyon map sheet (105L). The northwestern corner of Dhaw Ghro SMA is a densely vegetated area adjacent to the Klondike Highway, and approximately 25 km south of Stewart Crossing. Access is by helicopter from Mayo (approximately 75 km; Fig. 5).

A map notation designating McArthur Wildlife Preserve (#10-21) in what is now Ddhaw Ghro Habitat Protection Area Special Management Area (SMA) discouraged extensive exploration programs in the area since 1972. In 1974, the same area was proposed as an International Biological Program (IBP) site. The area was selected as a Special management area for the Selkirk and Na'Cho N'Y'Ak Dun First Nations and given a Habitat Protection Area designation. Both Selkirk and Na'Cho N'Y'Ak Dun First Nation Final Agreements state that the objective of Ddhaw Ghro Habitat Protection Area is "to conserve and protect important fish and wildlife habitat for the benefit of all Yukon people." The Special Management Area has been interim protected since 1997 for a period of three years. The area contained no active quartz or placer claims, or crown grants at the time of withdrawal. The land withdrawal was recently renewed through

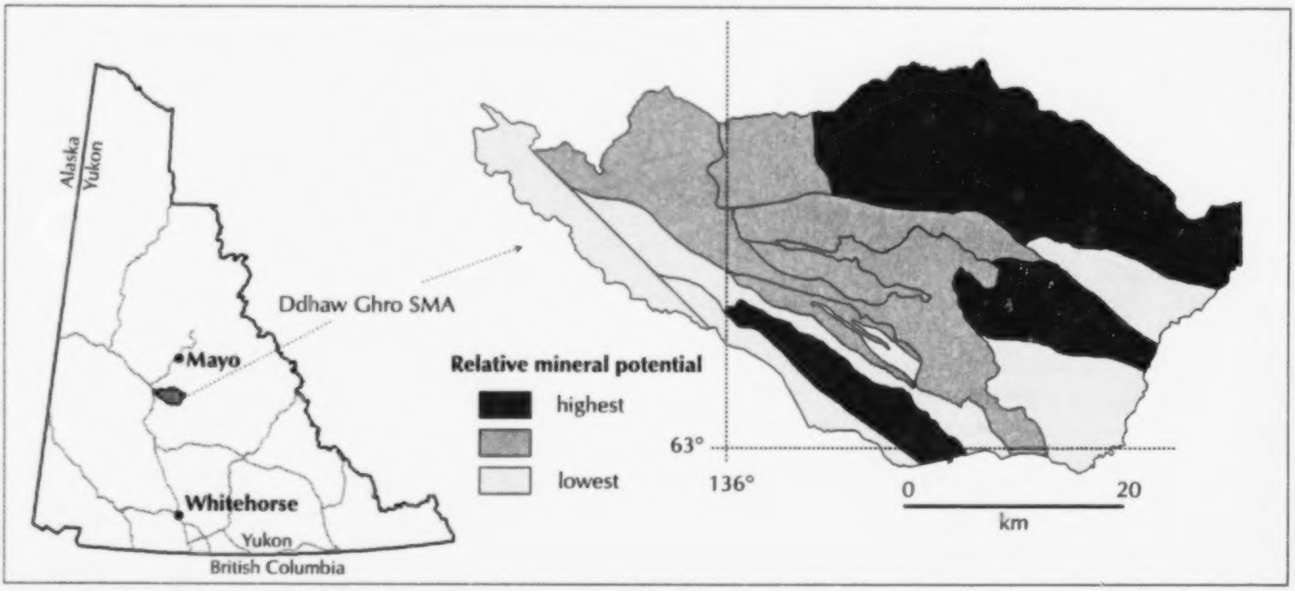

*Figure 5. Mineral potential map of Ddhaw Ghro Special Management Area.*

August, 2005, or until the completion of a management plan. The management plan may make recommendations regarding permanent land withdrawals.

Yukon government mineral assessment geologists carried out 1:20 000- and 1:50 000-scale geological mapping in Ddhaw Ghro SMA in the summers of 2000 and 2001, and hosted a mineral assessment workshop for the SMA in September, 2001. The SMA area was separated into 16 tracts of coherent geology in order to examine the geochemical, geophysical, or metallogenic character of each tract. Four geologists, considered to have outstanding field experience and knowledge of the area, participated in the two-day workshop. The experts examined all the data for each tract, and evaluated potential for discoveries of each plausible metallic mineral deposit type in each tract. At the end of the second day, the experts ranked the tracts by consensus, from highest to lowest mineral potential. The resulting mineral potential map (Fig. 5) displays three mineral potential categories. The experts recommended that further fieldwork be carried out to follow-up on a pronounced tungsten anomaly in the southern part of the SMA, and to map phases within the intrusive rocks.

### FRANCES LAKE AREA

Yukon Territorial Resource base maps show several map notations of areas of conservation interest. Frances Lake map sheet (105H) contains a map notation of a proposed Territorial Park Reserve dated as of December, 1972. The map notation in an ecoregion, which is currently unrepresented by a Yukon Protected Area Strategy (YPAS) Goal 1 protected area, warranted performing a mineral resource assessment of central Frances Lake map sheet.

Yukon government mineral assessment geologists carried out fieldwork in central Frances Lake map area during the summers of 2000 and 2001, and hosted a mineral assessment workshop for central Frances Lake map sheet in November, 2001. The area between Robert Campbell Highway and Nahanni Range Road was divided into 21 tracts. Four geologists, considered to have outstanding field experience and knowledge of the area, participated in three two-day workshops. The experts examined all the data for each tract, and evaluated potential for discoveries of each plausible metallic mineral deposit type in each tract. At the end of the workshop, the experts ranked the tracts by consensus, from highest to lowest mineral potential. The resulting mineral potential map (Fig. 6) shows four mineral potential categories. The experts recommended that further fieldwork be carried out to follow-up on a coincident multi-element geochemical anomaly and geophysical high feature in the low lands east of Robert Campbell Highway and south of Simpson Tower. Mapping phases within intrusive rocks in the northern part of Frances Lake map sheet has also been proposed.

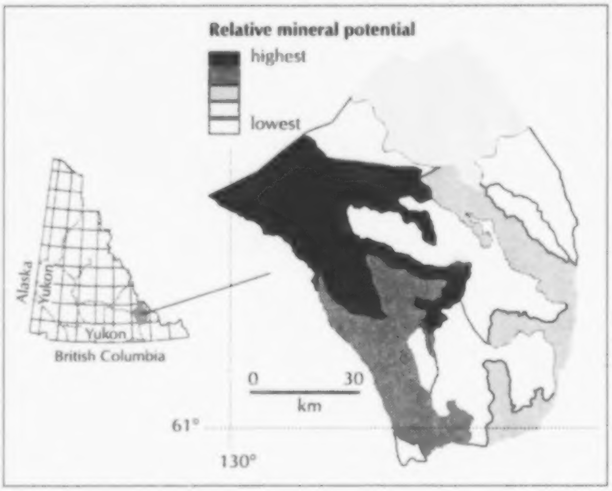

***Figure 6.*** *Detailed mineral potential map of central Frances Lake map area.*

## EAGLE PLAINS ECOREGION

Fieldwork was carried out to follow-up on results from a regional geochemical survey carried out by the Geological Survey of Canada in the Eagle Plains area. Geochemical analyses yielded three multi-element anomalies immediately outside the Eagle Plains Ecoregion. No detailed mineral potential map of Eagle Plains Ecoregion is planned.

# Yukon Mining Incentives Program, 2001

**Ken Galambos**[1]
*Mineral Resources Branch, Yukon Government*

Galambos, K., 2002. Yukon Mining Incentives Program, 2001. *In:* Yukon Exploration and Geology 2001, D.S. Emond, L.H. Weston and L.L. Lewis (eds.), Exploration and Geological Services Division, Yukon Region, Indian and Northern Affairs Canada, p. 57-59.

Seventy-seven applications were received this year by the program deadline. A total of $917,400 was offered to 59 successful applicants. Twenty of these programs were approved under the Grassroots and Grubstake modules while the remaining thirty-nine proposals were part of the Target Evaluation module. Precious metal exploration under the Yukon Mining Incentives Program was down slightly with approximately 61% of applicants searching for gold and 11% for platinum group elements. The remaining 28% of applicants explored for base metals. Exploration programs were proposed for all four mining districts (Watson Lake, Whitehorse, Dawson and Mayo) and were fairly evenly dispersed over the entire Yukon Territory.

Highlights for the year include the discovery of significant gold and pathfinder anomalies in both soils and rock, the extension of known showings through prospecting and geophysics, and the drill discovery of an epithermal system beneath an Enzyme Leach soil anomaly.

Tanana Exploration Inc. (Fig. 1) investigated an anomalous till sample site, which was located by Jeff Bond of the Yukon Geology Program and reported in Yukon Exploration and Geology 2000. The company sampled a small grid on their claims this summer and discovered an open-ended, linear, multi-element soil anomaly in excess of 300 m in length. Tanana's sampling program returned values of up to 316.3 ppb gold, 959.2 ppm arsenic, 256.13 ppm antimony and 37,551 ppb mercury. An orientation survey conducted by Bond, analysing the -230 mesh soil fraction, returned values as high as 13,890.8 ppb gold, 951.6 ppm arsenic, 123.89 ppm antimony and 25,957 ppb mercury. Pebbles collected from this soil pit also assayed up to 1.05 g/t gold. Reanalysis of both the soil and the pebble pulps confirmed these values.

Corwin Coe conducted an infill soil and rock-sampling program on his Ice and JC claims near Red Mountain, located 55 km west of Mayo (Fig. 2). This sampling helped to define an area roughly 400 m x 1100 m and numerous smaller zones with soils averaging greater than 100 ppb and up to 2232 ppb gold. Geochemical patterns suggest a strong east

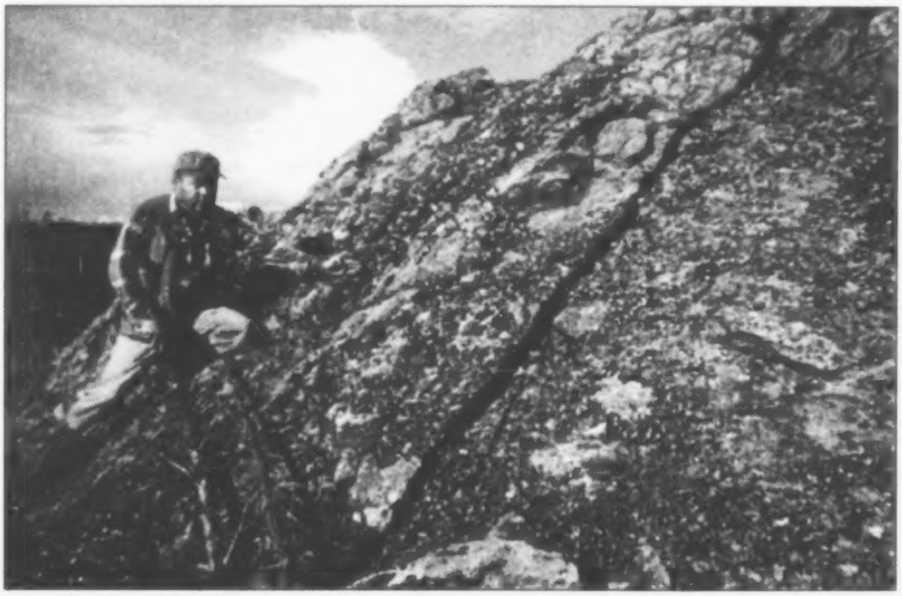

***Figure 1.*** *Wade Carrell examines an outcrop of silicified conglomerate with interbedded sandstone layers on Tanana Exploration Inc.'s Spice property, located 28 km east of Ross River. Photo by Steve Traynor.*

---

[1] ken.galambos@gov.yk.ca

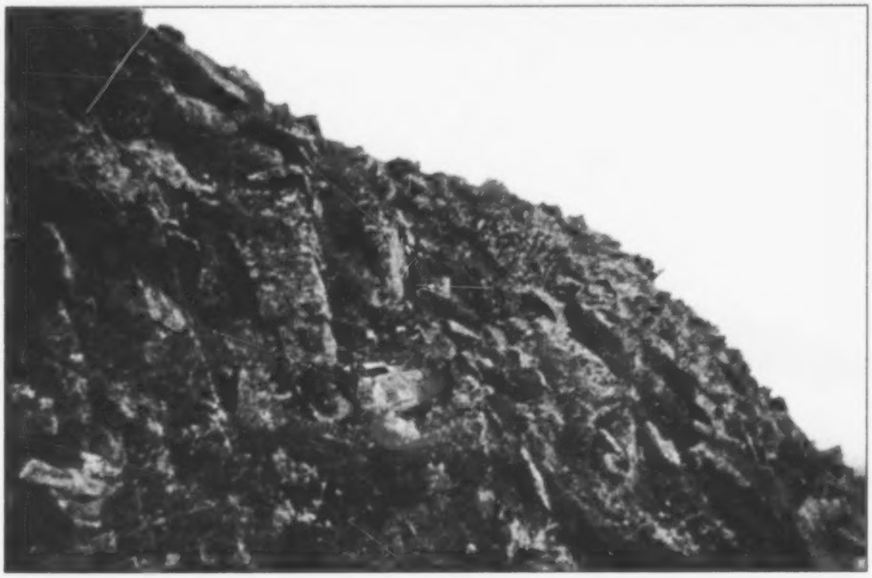

*Figure 2. An outcrop of fresh granodiorite from Corwin Coe's JC and Ice property near Red Mountain, 55 km west of Mayo. This 31-m section contains only minor quartz veining, yet averages 845 ppb gold. Individual 2-m chip samples assay up to 2288 ppb gold. Photo by Corwin Coe.*

and southeast structural control to mineralization. Intermittent chip sampling across a 31-m section of fresh granodiorite with only minor quartz veining averaged 844.9 ppb gold with individual 2-m chip samples assaying as high as 2288 ppb gold. Grab samples of sulphide veins in the vicinity of a collapsed adit returned gold values as high as 9383 ppb.

Shawn Ryan had another successful year exploring in the Dawson City area (Fig. 3). He expanded the hematite breccia target previously covered by his Hem 1-6 claims on the Dempster Highway and subsequently increased his holdings to 94 claims. This expanded claim block now covers most of the large positive magnetic and gravity low anomalies which lead Shawn to infer that there could be an Olympic Dam style copper deposit present in the area. Previous sampling from mineralized showings returned values up to 0.9% copper.

***Figure 3.** Shawn Ryan of Dawson City examines copper mineralization on his Hem claims. The property is bisected by the Dempster Highway. Shawn has staked 94 claims to cover coincident magnetic high and gravity low geophysical anomalies near Windy Pass. Photo by Ken Galambos.*

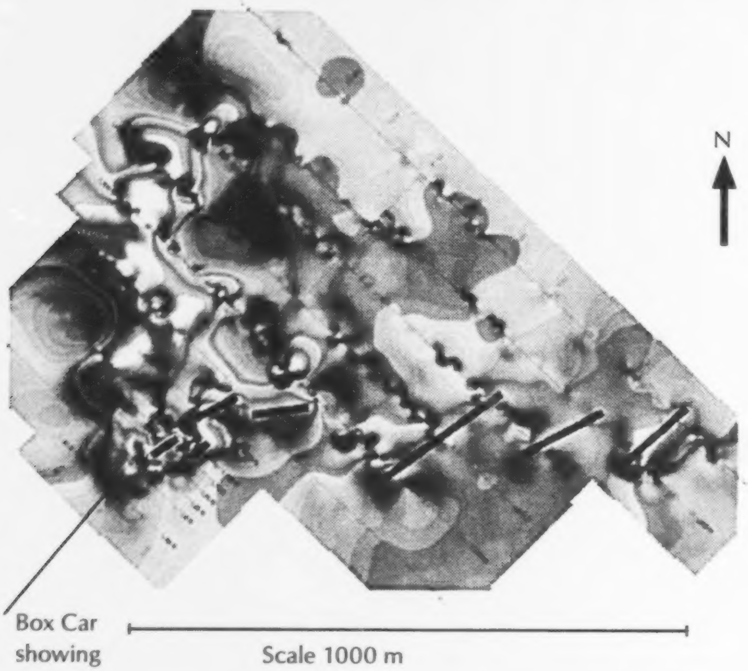

***Figure 4.*** *A geophysical plot of Total Magnetic Field data from a survey completed over the historic Box Car showing. Note the highly magnetic rocks (denoted by black lines) that can be traced for over 1000 m to the east of the main showing. Geophysical plot by Aurora Geosciences Ltd.*

Shawn also collected total magnetic field and vertical gradient data in a geophysical survey around the recently acquired Box Car showing in the Klondike area (Yukon MINFILE, 1997, 115O 071; Fig 4). Chip sampling of the showing in 1991 returned values of 271.5 g/t silver, 3.76% copper, 14.4% lead and 0.24% zinc over 1.0 m.

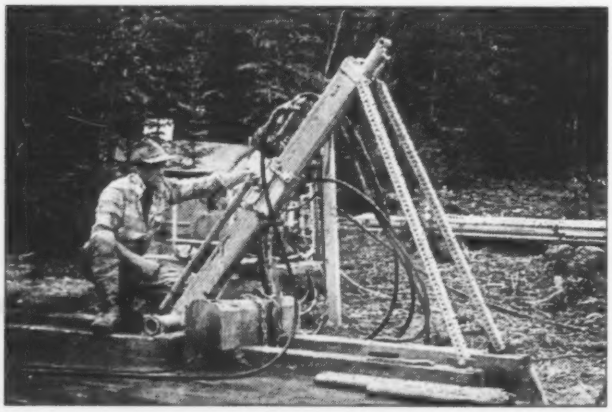

***Figure 5.*** *Al Carlos drilling on anomaly E near the Grew Creek deposit. Al and his two sons spent this past summer drilling 263 m in five holes on two properties. Photo by Ken Galambos.*

Interpretation of the geophysical data suggests that magnetic rocks associated with the showing can be traced for approximately 1000 m to the east with numerous offsets. The anomaly is open along strike and may be related to numerous large lead anomalies, which lie another 1000-4000 m to the northeast.

Al Carlos followed up last year's soil surveys at Grew Creek and several nearby properties, which successfully identified at least seven Enzyme Leach anomalies. This season, he core-drilled two of these anomalies with 263 m in five holes (Fig. 5). Drilling intersected Tertiary felsic to intermediate altered pyroclastic rocks and flows with banded epithermal quartz veining and vein fragments near the Grew Creek deposit. At Al's Km410 target, breccia and quartz crush-zones, as well as dark grey vein quartz in what might be highly silicified and/or clay-altered volcanic sedimentary rocks were intersected. Eighty-four samples totaling 122 m were sent for analysis and results are pending.

## REFERENCE

Yukon MINFILE, 1997. Exploration and Geological Services Division, Yukon Region, Indian and Northern Affairs Canada.

# Robert E. Leckie Awards for Outstanding Reclamation Practices

***Karen Pelletier*[1]**
*Yukon Geology Program*

Pelletier, K., 2002. Robert E. Leckie Awards for Outstanding Reclamation Practices. *In:* Yukon Exploration and Geology 2001, D.S. Emond, L.H. Weston and L.L. Lewis (eds.), Exploration and Geological Services Division, Yukon Region, Indian and Northern Affairs Canada, p. 61-64.

The third annual Robert E. Leckie Awards for outstanding reclamation practices were presented in Whitehorse, November 2001. In addition to the annual awards for the quartz and placer categories, the selection committee presented the first award for Long Time Achievement in Mining Reclamation to Norm Ross of Ross Mining Ltd. This award was created to recognize individuals or companies who have consistently shown long-term commitment and outstanding efforts toward achieving excellence in mining and or exploration reclamation practices. This award is not intended to be presented on an annual basis, but rather, presented occasionally when there is distinct merit.

## QUARTZ MINING RECLAMATION

The Robert E. Leckie Award for Outstanding Quartz Mining Reclamation Practices was awarded to NovaGold Resources Inc., Viceroy Resource Corporation, and Newmont Exploration of Canada Ltd. for the joint reclamation program in 2000 on the McQuesten property (formerly the Wayne), located on the Elsa airstrip (Fig. 1). The history of this property includes cumulative bulldozer trenching activities between 1962 and 1971 and the shipment of 5.9 million tonnes of material to

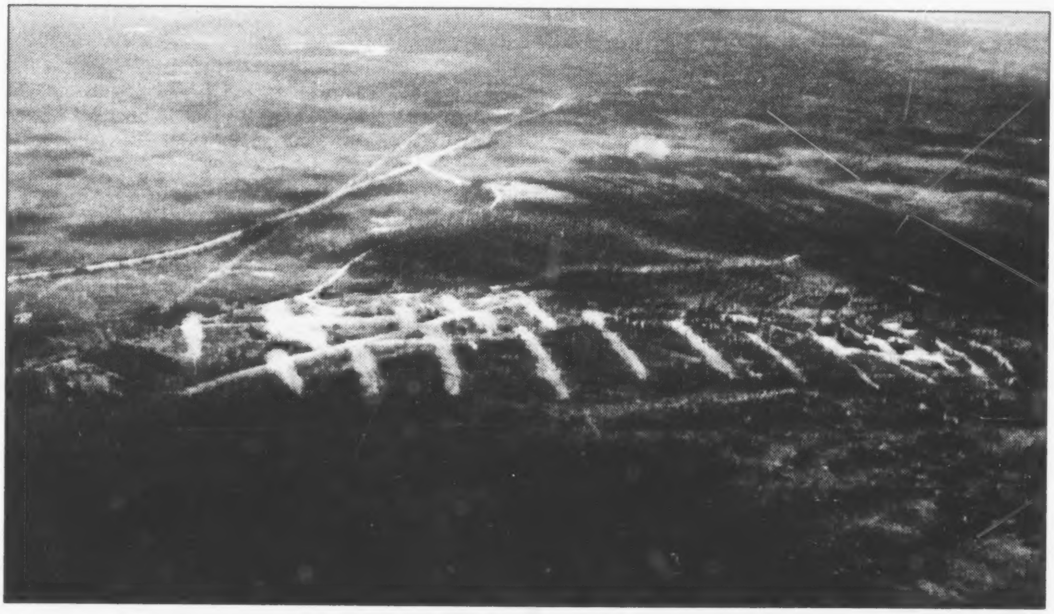

***Figure 1.*** *McQuesten property in the summer of 2001 showing all of the historic and modern trenches buried and contoured.*

---

[1] pelletierk@inac.gc.ca

the Trail Smelter in British Columbia in 1968. Additional trenching was carried out in 1998 by Viceroy Exploration (Canada) Ltd. (Fig. 2), prior to the implementation of new Mining Land Use Regulations in June, 1999. Although Viceroy had transferred its option interest in the property to NovaGold before reclamation work was undertaken in 2000, it participated as a financial partner with NovaGold for its reclamation work. Additionally, Newmont Exploration of Canada optioned some of the claims on this property in 2000 and conducted a concurrent drilling program and reclamation of a portion of the historic trenches.

Approximately 200 000 cubic metres of earth has been backfilled and contoured to the original topography on the McQuesten property, and the airstrip has been restored to a state where re-vegetation of the trenches can occur quickly and effectively. The three companies who supported this accomplishment are commended for their outstanding reclamation efforts which have enhanced both the safety and aesthetic values in the Elsa area.

## PLACER MINING RECLAMATION

Doug Busat of T.D. Oilfield Services Ltd. received the Robert E. Leckie Award for Outstanding Placer Mining Reclamation Practices in recognition of the exceptional restorative work done on his placer mine near the mouth of Hunker Creek. Methodical and progressive reclamation practices have taken place at this site since mining began in 1997. Overburden has been placed over old dredge piles and previously mined areas; old mine cuts and settling ponds have been backfilled by coarse tailings, and topped with finer-grained material in order to encourage natural revegetation.

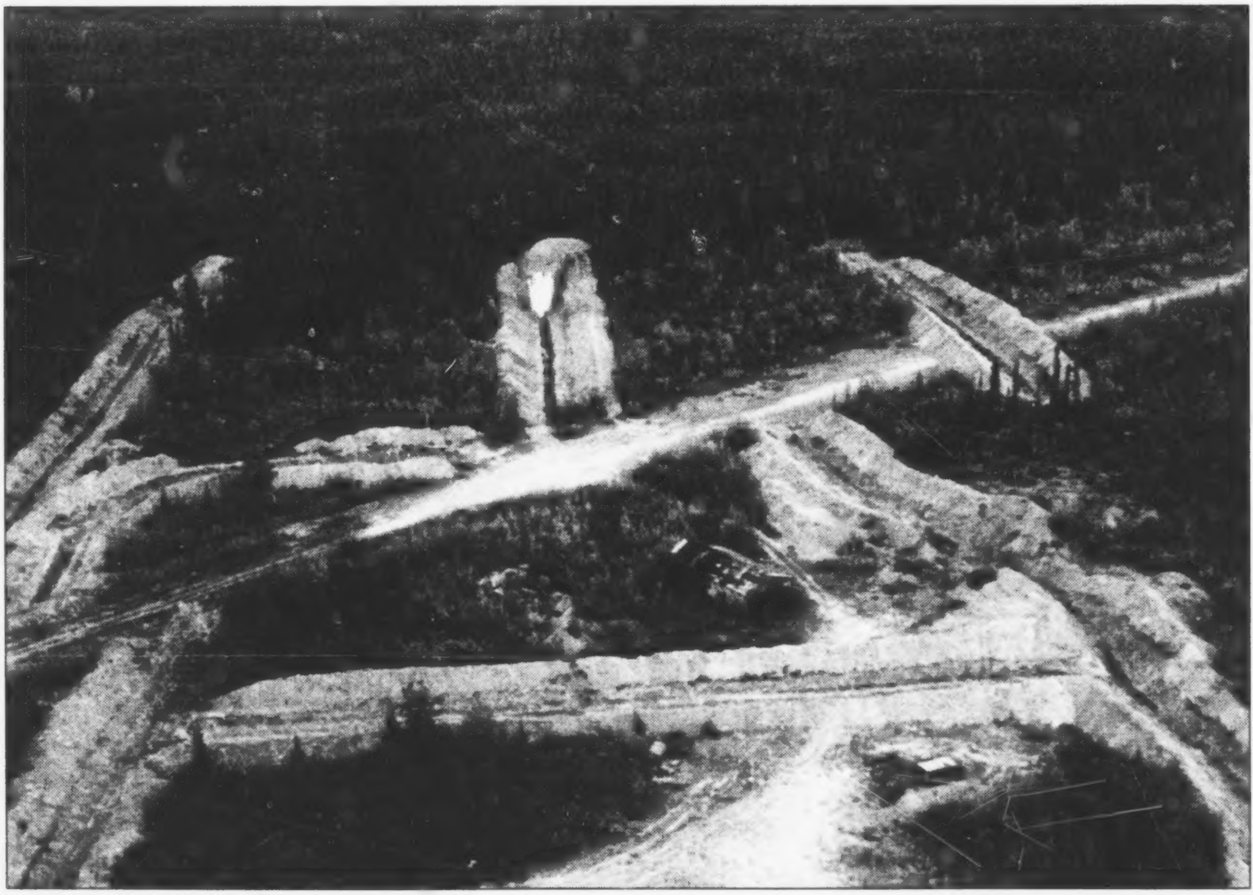

***Figure 2.*** *McQuesten Property in 1999, prior to reclamation.*

The post-mining landscape at the minesite, which incorporates wetlands and grasslands, is a much-improved terrain compared to the historic dredge piles and un-reclaimed tailings ponds and tailing piles left by previous operators (Fig. 3). The reclaimed ponds are aesthetically pleasing and provide habitat for waterfowl and wildlife, as well as a recreational area for people. For the many tourists and local people that drive the Klondike Placer Loop road, the property is an excellent example of responsible and thoughtful placer mining practices.

## LONG TIME ACHIEVEMENT IN MINING RECLAMATION

This year, special recognition was given to Norm Ross of Ross Mining Ltd. for his long time achievement in mining reclamation. The reclamation practices at Ross Mining consistently exceed what is required by legislation, and have included noteworthy land-based reclamation activities long before required to do so by the Mining Land Use Regulations.

Annual land-based reclamation has been a part of the company's operation since it began placer mining on Dominion Creek in the early 1980s. Mined-out areas have been reclaimed methodically, resulting in a landscape with vegetated rolling hills, small lakes and stable and productive stream reaches (Fig. 4). The wetlands are favoured by migratory wildlife, and several moose return annually to calve in the willow-rich reclaimed areas.

Over the last two decades Mr. Ross has dedicated much of his time as a spokesperson for the mining industry. In the 1980s he gave frequent presentations to gold miners on ways to plan for and minimize the costs of land reclamation and stream restoration. He has accommodated many local and foreign government

*__Figure 3.__ T.D Oilfield Services Ltd. located near the mouth of Hunker Creek. This aesthetically pleasing landscape can be easily viewed from the much travelled Hunker road.*

officials and investors on tours of his operation and has shared his knowledge of good mining practices in the Yukon. Mr. Ross has volunteered over many years as Director and President of the Klondike Placer Miners Association and has participated on various committees to help ensure the development of balanced legislation. He is currently the Vice-President of the Association and is a member of the Yukon Placer Committee which is working on the 2001 Review process of the Yukon Placer Authorization.

Congratulations is extended to all the worthy recipients of the 2001 Robert E. Leckie Reclamation Awards.

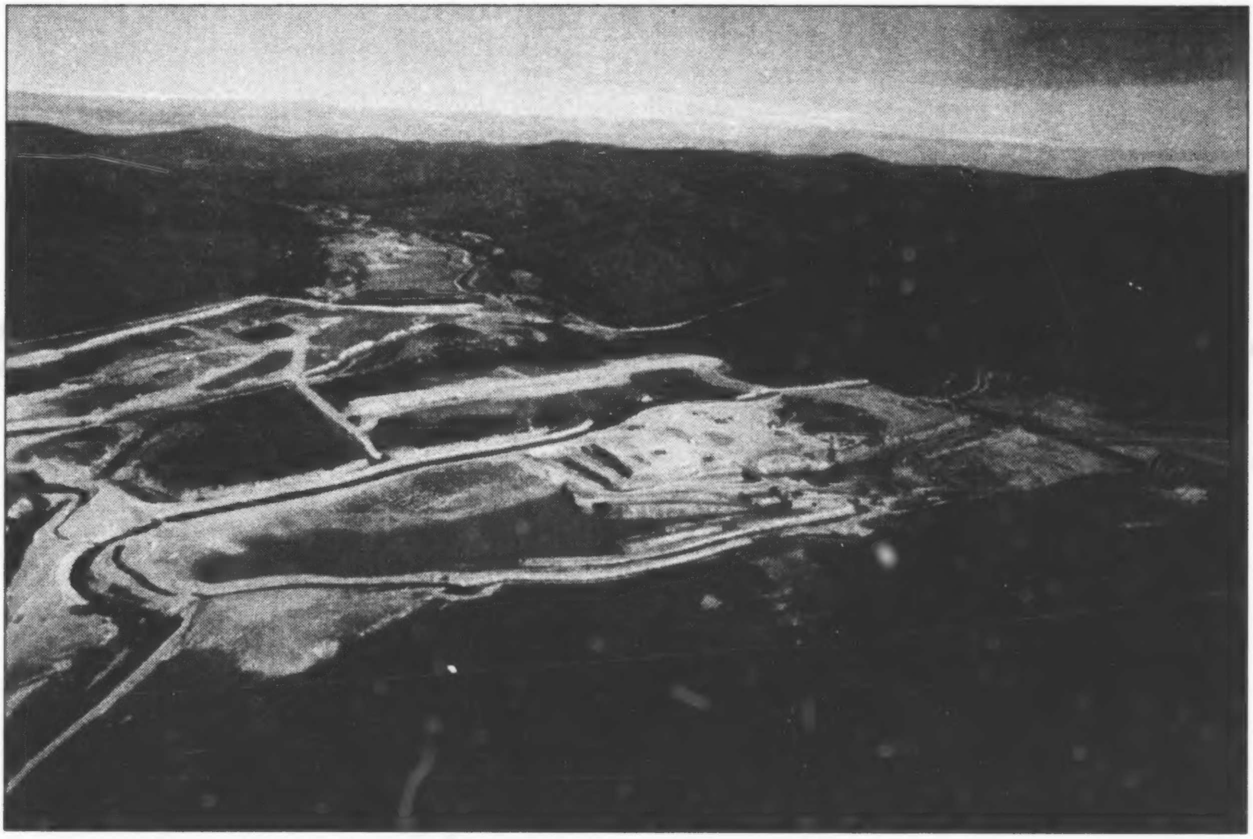

***Figure 4.*** *Ross Mining Ltd. on Dominion Creek with currently mined areas in the foreground and reclaimed ground in the background.*

# GEOLOGICAL FIELDWORK

Paleoproterozoic deformation of the Racklan Orogeny, Slats Creek (106D/16) and Fairchild Lake (106C/13) map areas, Wernecke Mountains, Yukon
*M-A. Brideau, D.J. Thorkelson, L. Godin and J.R. Laughton* ........ 65

Lower to Middle Jurassic stratigraphy, ammonoid fauna and sedimentary history of the Laberge Group in the Fish Lake syncline, northern Whitehorse Trough, Yukon, Canada
*M.E. Clapham, P.L. Smith and H.W. Tipper* ........ 73

Composition of placer and lode gold as an exploration tool in the Stewart River map area, western Yukon
*M.R. Dumula and J.K. Mortensen* ........ 87

Geology at the contact between Yukon-Tanana and Cassiar terranes, southeast of Little Salmon Lake (105L/1), south-central Yukon
*K. Gladwin, M. Colpron, S.T. Johnston and R. Black* ........ 103

No remagnetization in plutonic rocks of the Whitehorse Trough, southern Yukon: An extensive paleomagnetic conglomerate test
*M.J. Harris, D.T.A. Symons and C.J.R. Hart* ........ 111

New mapping around the Slab iron oxide-copper-gold occurrence, Wernecke Mountains (parts of NTS 106C/13, 106D/16, 106E/1 and 106F/4), Yukon
*J.A. Hunt, J.R. Laughton, M-A. Brideau, D.J. Thorkelson, M.L. Brookes and T. Baker* ........ 125

Paleoproterozoic volcanism and plutonism in the Wernecke Mountains, Yukon
*J.R. Laughton, D.J. Thorkelson, M-A. Brideau, J.A. Hunt* ........ 139

White Channel Gravel alteration revisited
*G.W. Lowey* ........ 147

Paleomagnetism and geobarometry of the Granite Mountain batholith, Yukon: Minimal geotectonic motion of the Yukon-Tanana Terrane relative to North America
*P.J.A. McCausland, D.T.A. Symons, C.J.R. Hart and W.H. Blackburn* ........ 163

Lead isotopic constraints on the metallogeny of southern Wolf Lake, southeastern Teslin and northern Jennings River map areas, Yukon and British Columbia: Preliminary results
*J.K. Mortensen and J.E. Gabites* ........ 179

Finlayson Lake Targeted Geoscience Initiative (southeastern Yukon), Part 1: Bedrock geology
*D.C. Murphy, M. Colpron, C.F. Roots, S.P. Gordey and J.G. Abbott* ........ 189

Finlayson Lake Targeted Geoscience Initiative (southeastern Yukon), Part 2: Quaternary geology and till geochemistry
*J.D. Bond and A. Plouffe* ........ 209

Preliminary results of a petrological study of ultramafic rocks of the Northern Cordillera
*J.G. Shellnutt, D. Canil and S.T. Johnston* ........ 229

Resedimentation of the late Holocene White River tephra, Yukon Territory and Alaska
*K.D. West and J.A. Donaldson* ........ 239

# Paleoproterozoic deformation of the Racklan Orogeny, Slats Creek (106D/16) and Fairchild Lake (106C/13) map areas, Wernecke Mountains, Yukon

***Marc-André Brideau, Derek J. Thorkelson[1], Laurent Godin and John R. Laughton***
*Simon Fraser University[2]*

Brideau, M-A., Thorkelson, D.J., Godin, L. and Laughton, J.R., 2002. Paleoproterozoic deformation of the Racklan Orogeny, Slats Creek (106D/16) and Fairchild Lake (106C/13) map areas, Wernecke Mountains, Yukon. *In:* Yukon Exploration and Geology 2001, D.S. Emond, L.H. Weston and L.L. Lewis (eds.), Exploration and Geological Services Division, Yukon Region, Indian and Northern Affairs Canada, p. 65-72.

## ABSTRACT

Three events of Paleoproterozoic deformation are recognized in schist of the Fairchild Lake Group (Wernecke Supergroup) in the Wernecke Mountains. The first event produced a chloritoid ± garnet and opaque porphyroblastic, chloritoid-chlorite-muscovite-quartz schist. Pressure-temperature conditions have been estimated to lie between 3-6 kbar and 450-550°C. The second event produced a crenulation, and the third generated kink bands. All of these features are crosscut by 1.60 Ga Wernecke Breccia. These events are regarded as products of the Racklan Orogeny, a Paleoproterozoic interval of orogenesis, which favourably correlates with the Fifteenmile Orogeny in the Ogilvie Mountains of western Yukon and the Forward Orogeny in the Northwest Territories.

## RÉSUMÉ

On reconnaît trois événements de déformation paléoprotérozoïque du schiste du Groupe de Fairchild Lake (Supergroupe de Wernecke), dans les monts Wernecke. Le premier événement a produit du schiste à quartz-muscovite-chlorite chloritoïde contenant des porphyroblastes de chloritoïde ± de grenat et d'un minéral opaque. On estime que les conditions de pression et température s'établissaient entre 3 et 6 kbar et entre 450 et 550°C. Le second événement a engendré une crénulation et le troisième des zones de plis en chevrons. Toutes ces déformations sont recoupées par la brèche de Wernecke datant de 1,6 milliard d'années. On estime que ces événements résultent de l'orogenèse du Racklan, qui est un intervalle paléoprotérozoïque d'orogenèse, présentant des corrélations favorables avec l'orogenèse de Fifteenmile, dans les monts Ogilvie, et avec l'orogenèse de Forward, dans les Territoires du Nord-Ouest.

---

[1] *dthorkel@sfu.ca*

[2] *Earth Sciences, Simon Fraser University, Burnaby, British Columbia, Canada V5A 1S6*

## INTRODUCTION

Proterozoic unconformities and deformational structures in pericratonic strata along the northwestern margin of ancestral North America have been recorded by several authors (Wheeler, 1954; Gabrielse, 1967; Eisbacher, 1978; Yeo et al., 1978; Kerans et al., 1981; Thompson and Roots, 1982; Mercier, 1989; Cook, 1992; Cook and MacLean, 1995; Thorkelson, 2000). In Yukon, four main periods of Paleoproterozoic to Neoproterozoic age deformation have been recognized (Eisbacher, 1978; Young et al., 1979; Abbott, 1997; Thorkelson, 2000). This paper concentrates on the oldest set of deformation features, specifically those which affected the Paleoproterozoic Wernecke Supergroup before emplacement of Wernecke Breccia at 1.60 Ga (Thorkelson et al., 2001a). These events are recorded by mesoscopic and microscopic structures in the Wernecke Supergroup and are particularly well developed in the 'Slab Mountain' area of the Wernecke Mountains, herein called the study area (Fig. 1). Thorkelson (2000) applied the name Racklan Orogeny to these events, using the term in a more specific sense than originally applied by Gabrielse (1967). The nature of Racklan Orogeny, as applied to pre-1.60 Ga events, is characterized and evaluated in this report.

## SUMMARY OF FIELD RELATIONS

The study area is located in the vicinity of 'Slab Mountain' and 'Slab Ridge' (informal names), northeast of the Bonnet Plume River, at approximately Latitude 65°N and Longitude 134°W. Geologic units in the study area consist of the Fairchild Lake Group of the Wernecke Supergroup (Delaney, 1981), the Slab volcanics (Laughton et al., this volume), the 1.71 Ga Bonnet Plume River Intrusions (Thorkelson et al., 2001b), and 1.60 Ga Wernecke Breccia (Bell and Delaney, 1977; Thorkelson et al., 2001a; Hunt et al., this volume). The structures described in this report

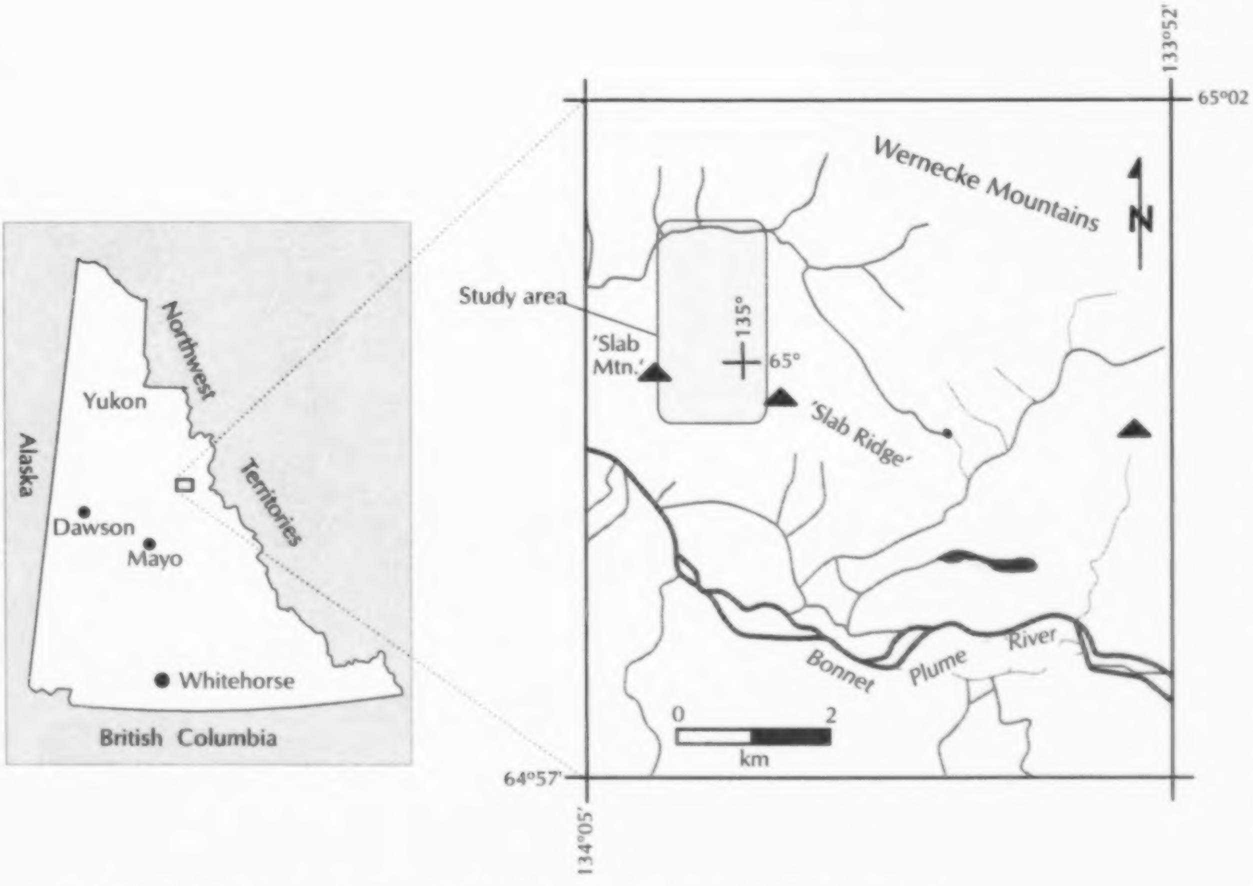

***Figure 1.*** *Regional map displaying the location of the study area in the Wernecke Mountains.*

are best displayed in the area between Slab Mountain and Slab Ridge, where siltstone of the Fairchild Lake Group (Delaney, 1981; Thorkelson, 2000) is deformed into a northwest-striking belt of schist (Fig. 2). Original sedimentary features such as bedding and cross-laminations are commonly preserved in the sedimentary rocks that flank the schist belt. The transition from mudrock to pelitic schist typically occurs over a width of 10-30 m. Zones of Wernecke Breccia, and dykes and small stocks of the dioritic Bonnet Plume River Intrusions crosscut the schist and the sedimentary rocks (Bell and Delaney, 1977; Thorkelson et al., 2001b). The breccia zones consist mainly of clasts of siltstone, subordinate schist and diorite set in a hydrothermally precipitated matrix. The Slab volcanics occur as a megaclast in a large zone of Wernecke Breccia to the southwest of the schist belt (Laughton et al., this volume). Sedimentary bedding is moderately to steeply dipping, and the ridge is situated on the northern limb of an upright to overturned anticlinorium that closes to the south (Thorkelson, 2000). The schist belt appears to represent a region of relatively high strain, possibly developed in a region of tight parasitic folding in the anticlinorium (Thorkelson, 2000). The connection between deformational fabrics and the anticlinorium, however, has not been rigorously demonstrated.

## THREE EVENTS OF PALEOPROTEROZOIC DEFORMATION

Three distinct fabrics in the schist represent three discrete phases of deformation. The first deformational ($D_1$) event produced a penetrative schistosity, the second ($D_2$) produced crenulations, and the third ($D_3$) generated kink bands. All three events are interpreted to have occurred prior to 1.60 Ga, as evidenced by randomly oriented clasts of kinked schist present in the Wernecke Breccia

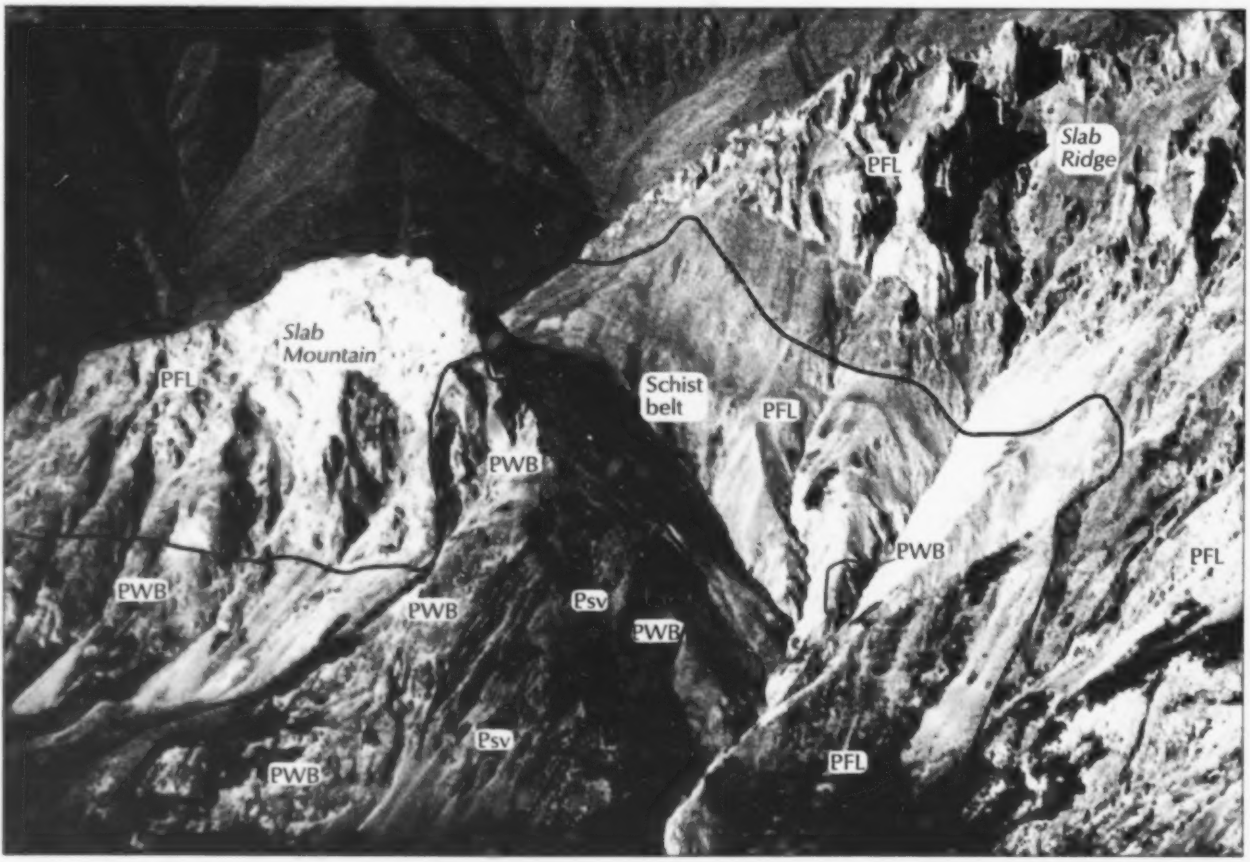

***Figure 2.** Study area on Slab Mountain and Slab Ridge. View to the northwest. PWB = Wernecke Breccia, PFL = Fairchild Lake Group, PSv = Slab volcanics.*

(Thorkelson, 2000). Clasts of tightly folded siltstone are also present in the breccia of the study area. The folds are decimetre- to metre-scale and are truncated at the margins of the clasts, indicating that they formed prior to breccia development. The folding probably occurred during either the first or second events of deformation recorded in the schist. Younger events of folding and faulting (Mesoproterozoic to Tertiary) have been identified in the Wernecke Mountains (Green, 1972; Eisbacher, 1978; Thorkelson, 2000) and some are likely to have affected the study area. Although younger structural features have not been directly identified, the authors expect the Paleoproterozoic fabrics to be affected by younger events and stereonet analysis to be complicated by the resulting faults and folds.

## $D_1$ STRUCTURES

In the study area, the oldest structural feature is a fine-grained schistosity in metapelitic rocks of the Fairchild Lake Group. The schist is typically greenish grey and consists of chloritoid porphyroblasts (0.5-3 mm; Fig. 3) set in a penetrative continuous schistosity ($S_1$), outlined by fine-grained chlorite, muscovite, quartz and opaques. The stereogram in Figure 4 illustrates the distribution of poles to schistosity in the study area. The poles define a broad great circle, interpreted as a consequence of folding about a hinge line plunging gently (~10°) to the northwest. Rotated opaques (1-2 mm), probably magnetite, were observed in hand sample. In thin section, well developed sigma and phi pressure shadows were found around porphyroblasts of chloritoid and opaques (Fig. 3).

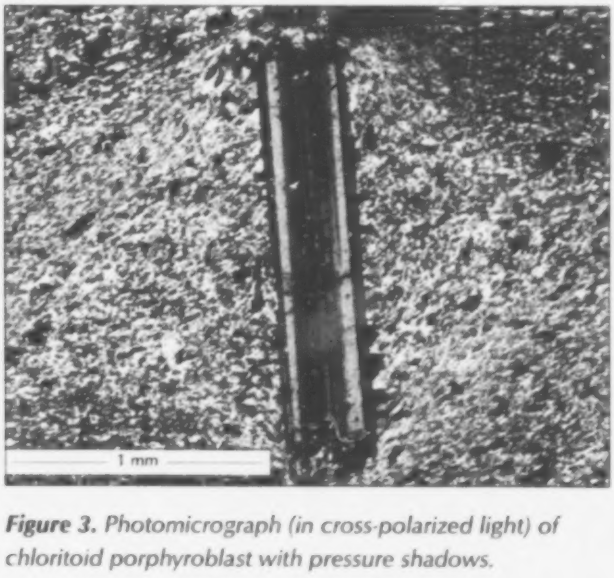

*Figure 3. Photomicrograph (in cross-polarized light) of chloritoid porphyroblast with pressure shadows.*

Compositional layering is highlighted by alternating light coloured (muscovite and quartz-rich) and dark coloured (chlorite and chloritoid-rich) bands, 1-10 cm wide. These layers are commonly oriented at a high angle to the schistosity and appear to represent deformed and possibly transposed sedimentary beds and laminae. Garnet porphyroblasts occur along with chloritoid porphyroblasts in another belt of schist approximately 3 km east of the study area.

## $D_2$ STRUCTURES

In many localities within the study area, the $S_1$ schistosity has been deformed ($D_2$) into tight asymmetric crenulations ($L_2$). The crenulations, which have a typical wavelength of 1-2 mm and an amplitude of < 1 mm, are principally defined by deformed quartz, muscovite, chlorite and opaque grains. No new minerals grew during the crenulation-forming event. The limbs of the crenulations are locally highly attenuated, resulting in a crenulation cleavage ($S_2$). The distribution of crenulation lineations in Figure 5 indicates a dominant northwest- to southeast-trending, shallowly plunging orientation. This orientation is similar to that of the fold axis calculated from the poles to $S_1$ schistosity (Fig. 4) suggesting that

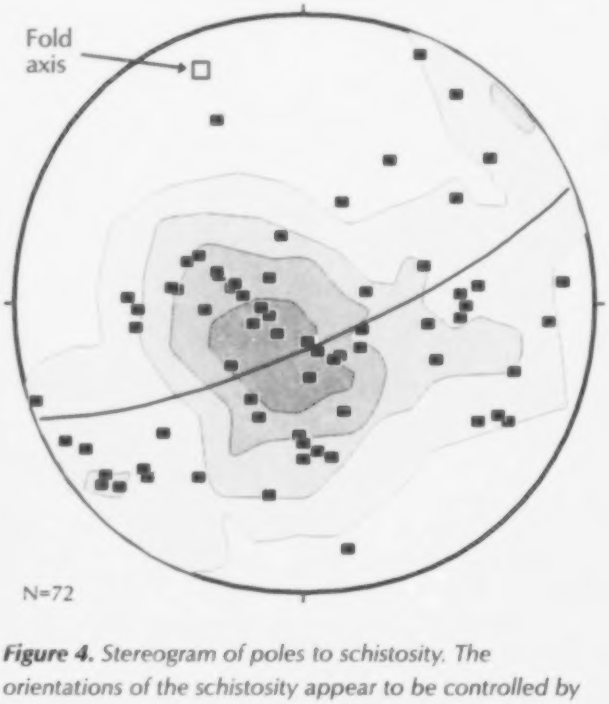

*Figure 4. Stereogram of poles to schistosity. The orientations of the schistosity appear to be controlled by folding about an axis plunging 12° toward 336°. Great circle and fold axis represent a computer-generated best fit.*

crenulation development and folding $S_1$ belong to the same phase of deformation ($D_2$).

### $D_3$ STRUCTURES

Kink bands are abundant in the schist, either as groups of parallel bands or in conjugate, intersecting sets. The kinks affect the orientation of both the main schistosity and the crenulations, and are therefore assigned to a third phase of deformation. The width of most of the bands ranges from 2 to 20 mm. Although the kink bands are mainly restricted to the schist, a small proportion also occurs in sedimentary rock beyond the boundaries of the schist belt. As with the crenulations, the kinks are not associated with new mineral growth. Preliminary stereonet analysis of the kink bands did not reveal any dominant trend in distribution.

## METAMORPHIC CONDITIONS

Metamorphism during schist development ($D_1$) is characterized as lower- to middle-greenschist grade, based on an equilibrium mineral assemblage of chlorite, muscovite, chloritoid and quartz.

This assemblage indicates a maximum temperature of 550°C, according to mineral stabilities in the KFMASH ($K_2O$-FeO-MgO-$Al_2O_3$-$SiO_2$-$H_2O$) system shown on AFM ($Al_2O_3$-FeO-MgO) projections from Bucher and Frey (1994) for metapelites (Fig. 6). The presence of garnet as well as chloritoid porphyroblasts approximately 3 km east of the study area was used to constrain the minimum temperature of metamorphism. Garnet has a high variability in temperature of first appearance in metapelites (Bucher and Frey, 1994). This temperature is controlled by the presence of manganese and calcium. In the presence of these elements, the temperature of first appearance is approximately 450°C (Bucher and Frey, 1994; Fig. 6). Pressure of formation is poorly constrained by the mineral assemblage. Pressure was estimated to be 3-6 kbar by assuming geothermal gradients range from 25-30°C/km, which are typical of continental environments (Hall, 1996; Raymond, 1995). This pressure corresponds to depths ranging from 15-22 km, based on pelitic rock densities of 2250-2700 kg/m$^3$. This depth estimate is somewhat greater than the expected minimum 7.4 km to 12.9 km depth range of the Fairchild Lake Group that would have existed if the Fairchild Lake Group were overlain only by the younger strata of the Wernecke Supergroup (i.e., the 3.4-km-thick Quartet Group and the >4-km-thick Gillespie Lake Group; Delaney, 1981; Thorkelson, 2000). The absence of new mineral growth during $D_2$ (asymmetric crenulation of the schistosity), and $D_3$ (kink-band formation), suggests that metamorphic conditions did not change appreciably from the end of $D_1$

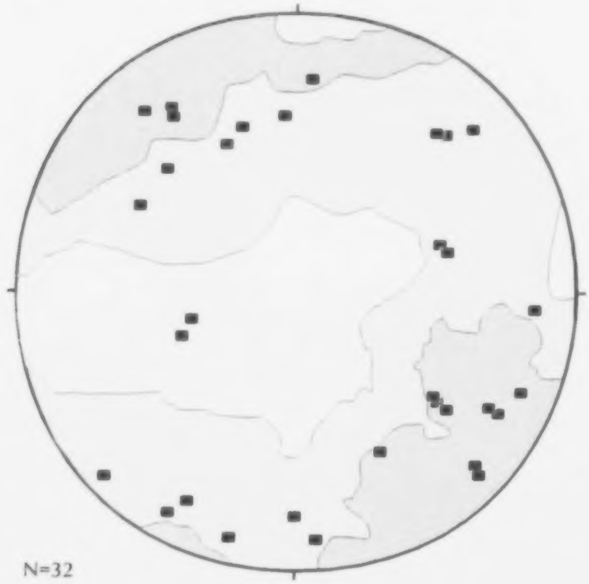

*Figure 5. Stereogram of the crenulation lineation measurements. The lineations preferentially trend northwest and southeast.*

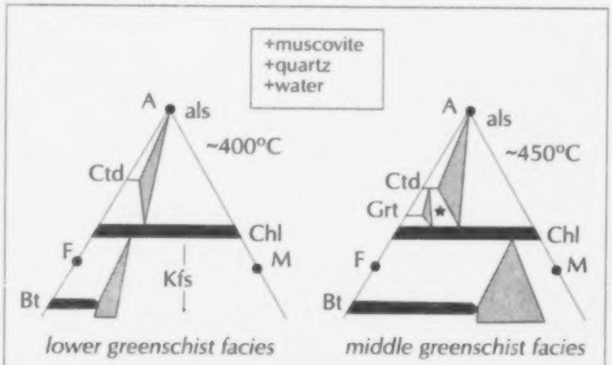

*Figure 6. Mineral assemblages in the KFMASH ($K_2O$-FeO-MgO-$Al_2O_3$-$SiO_2$-$H_2O$) system shown on AFM projections. At 400°C chloritoid is stable and at 450°C chloritoid and garnet are stable. Star represents inferred composition of schist in study area. A = $Al_2O_3$, F = FeO, M = MgO, als = aluminium silicates, Bt = biotite, Chl = chlorite, Ctd = chloritoid, Grt = garnet, Kfs = K-feldspar (modified from Bucher and Frey, 1994).*

(schistosity formation) to the end of $D_3$ (kink-band formation).

## RACKLAN OROGENY: DEFINITION AND RECOMMENDED USAGE

The three events of Paleoproterozoic deformation recorded in the study area are herein regarded as products of the Racklan Orogeny. However, the term Racklan Orogeny has been used to describe more than one unconformity in the Yukon and in the subsurface of the Northwest Territories, and therefore requires clarification. The term Racklan Orogeny was originally applied by Gabrielse (1967) to describe an angular unconformity between 'Purcell-like' strata and the Rapitan Group in the North Rackla River area of Yukon, approximately 60 km south of the study area. The foundation for this description was an angular unconformity between rocks of uncertain affinity previously recorded by Wheeler (1954), and other rocks of uncertain affinity. Subsequently, Eisbacher (1978), Young et al. (1979) and Wheeler and McFeely (1991) recognized that the unconformity noted by Wheeler (1954) actually separated the Wernecke Supergroup from the Pinguicula Group and that the unconformity was well exposed throughout much of the Wernecke Mountains. The lower part of the Pinguicula Group hosts the 1.38 Ga Hart River sills (Blusson, 1974; Abbott et al., 1997; Thorkelson, 2000), constraining the age of the Racklan Orogeny to >1.38 Ga.

Thorkelson (2000) provided evidence that the Racklan Orogeny occurred prior to 1.60 Ga. The evidence lies in the abundance of deformational features in the Wernecke Supergroup (described herein) that are crosscut by Wernecke Breccia (1.60 Ga), and the paucity of deformational features younger than the breccia (and older than the Pinguicula Group). Furthermore, the earliest phase of pre-1.60 Ga deformation, which produced schistosity in the Wernecke Supergroup, has been tentatively linked to large-scale folding (Thorkelson, 2000), and is therefore a plausible cause of the angular unconformity beneath the Pinguicula Group. Similarly, the second and third pre-breccia events that yielded crenulations and kink bands in the study area may have been concurrent with the formation of larger structures that could have deformed the Wernecke strata into folds or tilted panels. These relations infer that the three deformation events described in this report appropriately account for the Racklan discordance, and that Racklan Orogeny is favourably restricted to pre-1.60 Ga.

## REGIONAL CORRELATION

The Racklan orogenic events in the Wernecke Mountains appear to correlate with two other intervals of Paleoproterozoic deformation: the Forward Orogeny in the Northwest Territories (a correlation proposed by Cook and MacLean, 1995), and the Fifteenmile Orogeny in the Ogilvie Mountains of western Yukon (Mercier, 1989). The Forward Orogeny records deformation concurrent with eruption of the Narakay volcanics at ca. 1.66 Ga (Bowring and Ross, 1985; Cook and MacLean, 1995), and is consistent with a pre-1.60 Ga age for the Racklan Orogeny in the Wernecke Mountains (Thorkelson et al., 1998). The Fifteenmile Orogeny is inferred from unconformable relations between the Wernecke Supergroup and the Fifteenmile Group, which has been correlated, in part, with the Pinguicula Group (Abbott, 1997). Taken together, these orogenic events appear to belong to an interval of widespread regional tectonism, which occurred prior to deposition of the Pinguicula Group and correlative strata. Regional thin-skinned deformation extending from Yukon to the Northwest Territories, largely recognized in seismic reflection profiles, was referred to as Racklan Orogeny by Cook (1992). However, some of the deformation considered by Cook (1992) occurred after deposition of the Pinguicula Group and cannot be part of the Racklan Orogeny as used by Thorkelson (2000) and in this report. Additional work is required to clarify the timing, nature and correlation of the unconformities observed in the subsurface.

## CONCLUSIONS

1. Three discrete events of pre-1.60 Ga deformation are recorded in the schist of the Fairchild Lake Group of the Wernecke Supergroup. The first event ($D_1$) produced a schistosity at lower- to middle-greenschist grades. The $D_2$ and $D_3$ events produced crenulations and kink bands, respectively. The $D_1$ schistosity appears to have been folded about a northwest-trending axis, possibly during $D_2$ or $D_3$.
2. The metamorphic conditions present during $D_1$ are estimated to be between 450-550°C and 3-6 kbar, corresponding to a depth of ~15-22 km. Following $D_1$, the mineral assemblage remained unchanged, implying that peak metamorphic conditions developed during $D_1$.

3. The deformation and metamorphism observed in the study area are regarded as products of Racklan Orogeny. This interval of orogenesis, as originally recognized, occurred between deposition of the Wernecke Supergroup and the Pinguicula Group. Relations described in this report suggest that most, if not all, of the Racklan orogenic activity occurred prior to 1.60 Ga, the age of Wernecke Breccia emplacement. The Racklan Orogeny, as used in this report, is considered equivalent to the Fifteenmile Orogeny of western Yukon, and the Forward Orogeny of the Northwest Territories.

## ACKNOWLEDGEMENTS

This research was supported by an NSERC undergraduate student research awarded to Marc-André Brideau, a Lithoprobe grant to Derek Thoskelson, a Northern Studies Training Program grant to John Laughton, and the Yukon Geology Program. Newmont Mines Limited permitted access to unpublished maps and reports. Dan Marshall provided information on metamorphic rocks. Florine Lawrance provided helpful comments on earlier drafts of the manuscript.

## REFERENCES

Abbott, G., 1997. Geology of the Upper Hart River Area, Eastern Ogilvie Mountains, Yukon Territory (116A/10, 116 A/11). Exploration and Geological Services Division, Yukon Region, Indian and Northern Affairs Canada, Bulletin 9, 92 p.

Abbott, G., Thorkelson, D., Creaser, R., Bevier, M.L. and Mortensen, J., 1997. New correlations among Proterozoic successions and intrusive breccias in the Ogilvie and Wernecke mountains, Yukon. *In:* Lithoprobe Report No. 56, p. 188-197.

Bell, R.T. and Delaney, G.D., 1977. Geology of some uranium occurrences in Yukon Territory. *In:* Report on Activities, Part A, Geological Survey of Canada, Paper 77-1A, p. 33-37.

Blusson, S.L., 1974. Geology of the Nadaleen River, Lansing, Niddery Lake, Bonnet Plume Lake, and Mount Eduni map areas, Yukon Territory. Geological Survey of Canada, Open File 205, 1:250 000 scale.

Bowring, S.A. and Ross, G.M., 1985. Geochronology of the Narakay Volcanic Complex: Implications for the age of the Coppermine Homocline and Mackenzie igneous events. Canadian Journal of Earth Sciences, vol. 22, p. 774-781.

Bucher, K. and Frey, M., 1994. Petrogenesis of Metamorphic Rocks, 6th Edition. Complete Revision of Winkler's Textbook. Springer-Verlag, New York, 434 p.

Cook, D.G. and MacLean, B.C., 1995. The intracratonic Paleoproterozoic Forward Orogeny, and implication for regional correlation, Northwest Territories, Canada. Canadian Journal of Earth Sciences, vol. 32, p. 1991-2008.

Cook, F.A., 1992. Racklan Orogen. Canadian Journal of Earth Sciences, vol. 29, p. 2490-2496.

Delaney, G.D., 1981. The mid-Proterozoic Wernecke Supergroup, Wernecke Mountains, Yukon Territory. *In:* Proterozoic Basins of Canada, F.H.A. Campbell (ed.), Geological Survey of Canada, Paper 81-10, 23 p.

Eisbacher, G.H., 1978. Two major Proterozoic unconformities, northern Cordillera. *In:* Current Research, Part A, Geological Survey of Canada, Paper 78-1A, p. 53-58.

Gabrielse, H., 1967. Tectonic evolution of the northern Canadian Cordillera. Canadian Journal of Earth Sciences, vol. 4, p. 271-298.

Green, L.H., 1972. Geology of Nash Creek, Larsen Creek, and Dawson Creek map-areas, Yukon Territory. Geological Survey of Canada, Memoir 364, 157 p.

Hall, A., 1996. Igneous Petrology, Second Edition. Longman Group Limited, New York, 568 p.

Hunt, J.A., Laughton, J.R., Brideau, M-A., Thorkelson, D.J., Baker T. and Brookes M., 2002 (this volume). New mapping around the Slab iron oxide-copper-gold occurrence, Wernecke Mountains (parts of NTS 106C/13, 106D/16, 106E/1 and 106F/4), Yukon. *In:* Yukon Exploration and Geology 2001, D.S. Emond, L.H. Weston and L.L. Lewis (eds.), Exploration and Geological Services Division, Yukon Region, Indian and Northern Affairs Canada, p. 125-138.

Kerans, C., Ross, G.M., Donaldson, J.A. and Geldsetzer, H.J., 1981. Tectonism and depositional history of the Helikian Hornby Bay and Dismal Lakes Groups, District of Mackenzie. *In:* Proterozoic Basins of Canada, F.H.A. Campbell (ed.), Geological Survey of Canada, Paper 81-10, p. 157-182.

Laughton, J.R., Thorkelson, D.T., Brideau, M-A. and Hunt, J.A., 2002 (this volume). Paleoproterozoic volcanism and plutonism in the Wernecke Mountains, Yukon. *In:* Yukon Exploration and Geology 2001, D.S. Emond, L.H. Weston and L.L. Lewis (eds.), Exploration and Geological Services Division, Yukon Region, Indian and Northern Affairs Canada, p. 139-145.

Mercier, E., 1989. Evénements tectoniques d'origine compressive dans le Proterozoique du nord de la Cordillère canadienne (montagnes Ogilvie, Yukon). Canadian Journal of Earth Sciences, vol. 26, p. 199-205.

Raymond, L.A., 1995. Petrology: The Study of Igneous, Metamorphic and Sedimentary Rocks. McGraw-Hill Higher Education, New York, 742 p.

Thompson, R.I. and Roots, C.F., 1982. Ogilvie Mountains Projects, Yukon: Part A: A new regional mapping program. Scientific and Technical Notes. *In:* Current Research, Part A, Geological Survey of Canada, Paper 82-1A, p. 403-414.

Thorkelson, D.J., 2000. Geology and mineral occurrences of the Slats Creek, Fairchild Lake and "Dolores Creek" areas, Wernecke Mountains, Yukon Territory (106D/16, 106C/13, 106C/14). Exploration and Geological Division, Yukon Region, Indian and Northern Affairs Canada, Bulletin 10, 73 p.

Thorkelson, D.J., Abbott, J.G., Mortensen, J.K., Creaser, R.A. and Villeneuve, M.E., 1998. Proterozoic sedimentation, magmatism, metasomatism and deformation in the Wernecke and Ogilvie Mountains, Yukon. *In:* Slave-Northern Cordillera Lithospheric Evolution (SNORCLE) Transect and Cordilleran Tectonics Workshop Meeting (March 6-8), Simon Fraser University, F. Cook and P. Erdmer (comps.), 1998, Lithoprobe Report No. 64, p. 110-119.

Thorkelson, D.J., Mortensen, J.K., Davidson, G.J., Creaser, R.A., Perez, W.A. and Abbott, J.G., 2001a. Early Mesoproterozoic intrusive breccias in Yukon, Canada: The role of hydrothermal systems in reconstructions of North America and Australia. Precambrian Research, vol. 111, p. 31-55.

Thorkelson, D.J., Mortensen, J.K., Creaser, R.A., Davidson, G.J. and Abbott, J.G., 2001b. Early Proterozoic magmatism in Yukon, Canada: Constraints on the evolution of northwestern Laurentia. Canadian Journal of Earth Sciences, vol. 38, p. 1479-1494.

Yeo, G.M., Delaney, G.D. and Jefferson, C.W., 1978. Two major Proterozoic unconformities, Northern Cordillera: Discussion. *In:* Current Research, Part B, Geological Survey of Canada, Paper 18-1B, p. 225-230.

Young, G.M., Jefferson, C.W., Delaney, G.D. and Yeo, G.M., 1979. Middle and late Proterozoic evolution of the northern Canadian Cordillera and Shield. Geology, vol. 7, p. 125-128.

Wheeler, J.O., 1954. A geological reconnaissance of the Northern Selwyn Mountains region, Yukon and Northwest Territories. Geological Survey of Canada, Paper 53-7, 42 p.

Wheeler, J.O. and McFeely, P. (comps.), 1991. Tectonic assemblage map of the Canadian Cordillera and adjacent parts of the United States of America. Geological Survey of Canada, Map 1712A, 1:2 000 000 scale.

# Lower to Middle Jurassic stratigraphy, ammonoid fauna and sedimentary history of the Laberge Group in the Fish Lake syncline, northern Whitehorse Trough, Yukon, Canada

**Matthew E. Clapham[1] and Paul L. Smith**
*University of British Columbia[2]*

**Howard W. Tipper**
*Geological Survey of Canada[3]*

Clapham, M.E., Smith, P.L. and Tipper, H.W., 2002. Lower to Middle Jurassic stratigraphy, ammonoid fauna and sedimentary history of the Laberge Group in the Fish Lake syncline, northern Whitehorse Trough, Yukon, Canada. *In:* Yukon Exploration and Geology 2001, D.S. Emond, L.H. Weston and L.L. Lewis (eds.), Exploration and Geological Services Division, Yukon Region, Indian and Northern Affairs Canada, p. 73-85.

## ABSTRACT

The Upper Triassic to Middle Jurassic Whitehorse Trough is a 500-km-long forearc basin developed on the eastern margin of the Stikine Terrane. Basin fill in the Fish Lake syncline consists of Early to Middle Jurassic strata of the Laberge Group. Re-examined fossil collections record all ammonite zones from the Upper Pliensbachian to lowest Bajocian (except for the recessive or volcanic Aalenian Stage), suggesting that the Laberge Group is a conformable sequence. Biostratigraphic dating of oldest conglomerates indicates that source area uplift occurred first in the north in the Early Pliensbachian, progressing southwards through the Late Pliensbachian. Periodic, basin-wide anoxia was prevalent during the Middle and Late Toarcian, indicated by abundant *Bositra*, a low-oxygen-tolerant bivalve. The final stage of basin-fill, Early Bajocian chert-pebble conglomerates, provides a maximum age constraint on the amalgamation of the Cache Creek and Stikine terranes.

## RÉSUMÉ

La bassin de Whitehorse, qui date du Trias supérieur au Jurassique moyen, est un bassin d'avant-arc de 500 km de longueur qui s'est formé sur la marge est du terrane de Stikine. Le synclinal de Fish Lake contient des strates du Groupe de Laberge datant du Jurassique précoce à moyen. Les collections de fossiles que l'on a réexaminées indiquent la présence de toutes les zones à ammonites du Pliensbachien supérieur au Bajocien basal (à l'exception de l'étage récessif ou volcanique aalénien), ce qui suggère que le Groupe de Laberge est une séquence conforme. La datation biostratigraphique des plus anciens conglomérats indique que le soulèvement régional a commencé au nord, pendant le Pliensbachien précoce, et qu'il a progressé vers le sud au cours du Pliensbachien tardif. Il y a eu anoxie périodique sur tout le bassin pendant le Toarcien moyen et le Toarcien tardif, comme l'indique l'abondance de Bositra, lamellibranches qui vivaient dans des eaux pauvres en oxygène. Des conglomérats à cailloux de chert, qui se sont déposés lors de la dernière étape de remplissage du bassin au Bajocien précoce, fournissent une limite d'âge maximale pour le fusionnement des terranes de Cache Creek et de Stikine.

---

[1] *clapham@geoladm.geol.queensu.ca*

[2] *Earth and Ocean Sciences Department, The University of British Columbia, 6339 Stores Road, Vancouver, British Columbia, Canada V6T 1Z4*

[3] *Geological Survey of Canada, #101-605 Robson Street, Vancouver, British Columbia, Canada V6B 5J3*

# INTRODUCTION

The Whitehorse Trough is a 500-km-long forearc basin on the eastern margin of the Stikine Terrane (Fig. 1) that was an active depocentre from the Late Triassic through Middle Jurassic (Hart, 1997). The Jurassic basin fill of the Laberge Group records a critical time in the evolution of the Whitehorse Trough and can be used to examine tectonic and environmental events affecting both the basin and the Stikine Terrane.

Previous sedimentological work (e.g., Wheeler, 1961) was conducted before the development of a precise North American ammonite biozonation. Hart and Radloff (1990) produced a refined geological study of the region in the context of modern plate tectonics, but did not update ammonite identifications. The biostratigraphy of the Laberge Group was investigated by Pálfy and Hart (1995) based on new fossil collections, but most previously collected specimens were not re-examined.

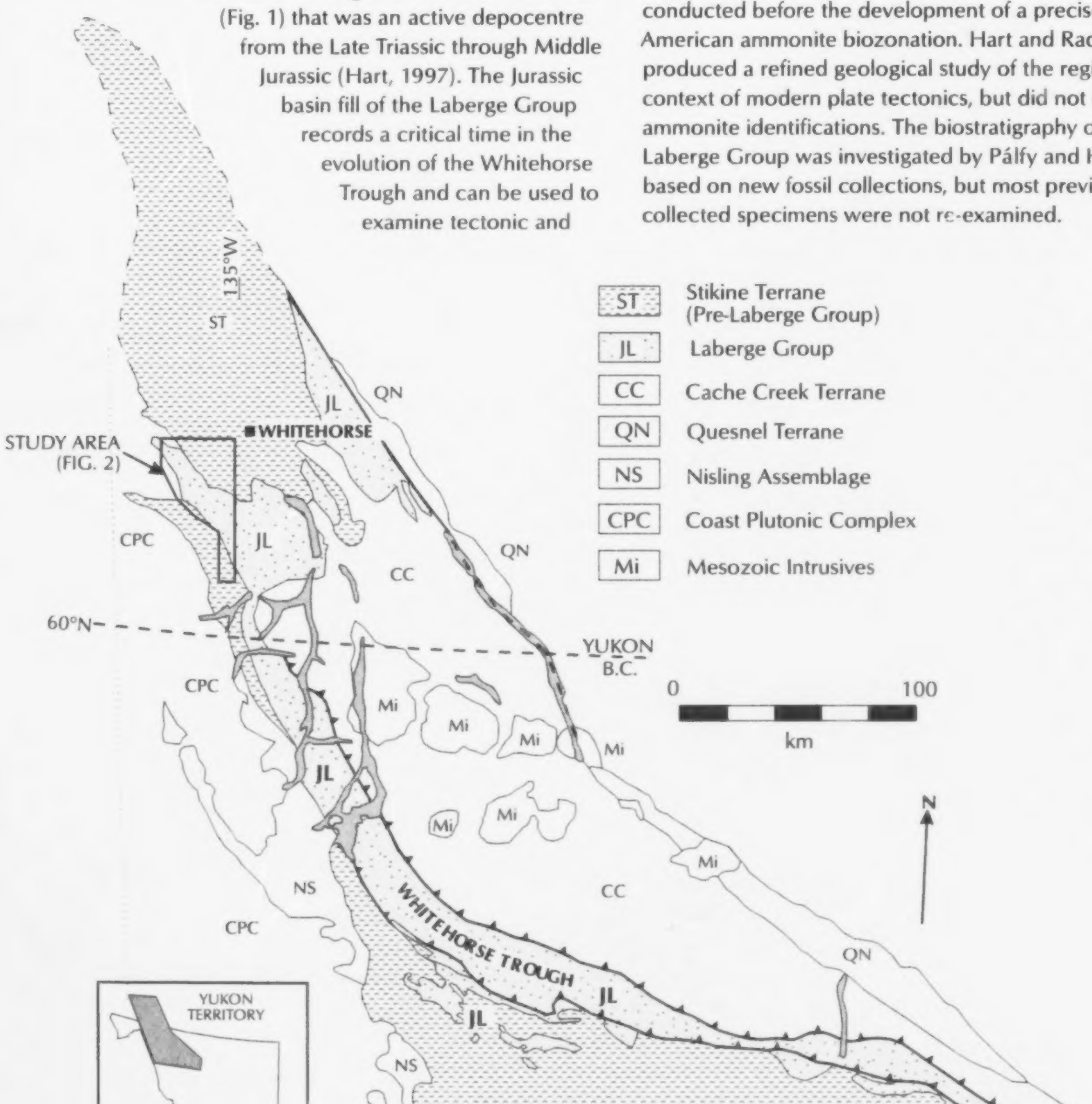
135°W
ST
JL
QN
■ WHITEHORSE
STUDY AREA (FIG. 2)
CPC
JL
QN
CC
60°N
YUKON
B.C.
CPC
Mi
Mi
Mi
Mi
JL
Mi
Mi
Mi
NS
CC
CPC
WHITEHORSE TROUGH
JL
JL
QN
NS
ST
CPC
ST Stikine Terrane (Pre-Laberge Group)
JL Laberge Group
CC Cache Creek Terrane
QN Quesnel Terrane
NS Nisling Assemblage
CPC Coast Plutonic Complex
Mi Mesozoic Intrusives
0
100
km
N
YUKON TERRITORY
BRITISH COLUMBIA
200 km

*Figure 1. Regional map of the northern Stikine Terrane, showing the location of the study area in respect to the preserved extent of the Whitehorse Trough (modified after Johannson et al., 1997).*

The major contribution of this study is a re-examination of all fossil collections from the Fish Lake syncline (Fig. 2). Complete fossil locality information and systematic paleontology is provided in Clapham (2000). Ammonite identifications permit precise biochronological dating of Fish Lake syncline strata. Most specimens were collected from isolated localities that were placed in approximate stratigraphic position based on regional geologic maps. Fossils from Goat Mountain were collected from five levels over 100 m of stratigraphic thickness by Pálfy and Hart (1995), and these collections were compiled to produce an approximate stratigraphic sequence.

Most fossil collections were made by W.E. Cockfield in 1946 and H.W. Tipper in 1985, with several localities visited by other researchers. Fossil localities are shown in Figure 2. All fossil material is currently housed at the Geological Survey of Canada (Vancouver and Calgary). Most stratigraphic information in this study is based on a review of primary literature, predominantly the work published by Hart and Radloff (1990) and Wheeler (1961). Additional information was gathered on a brief trip to the Fish Lake syncline by Smith and Tipper in 1985.

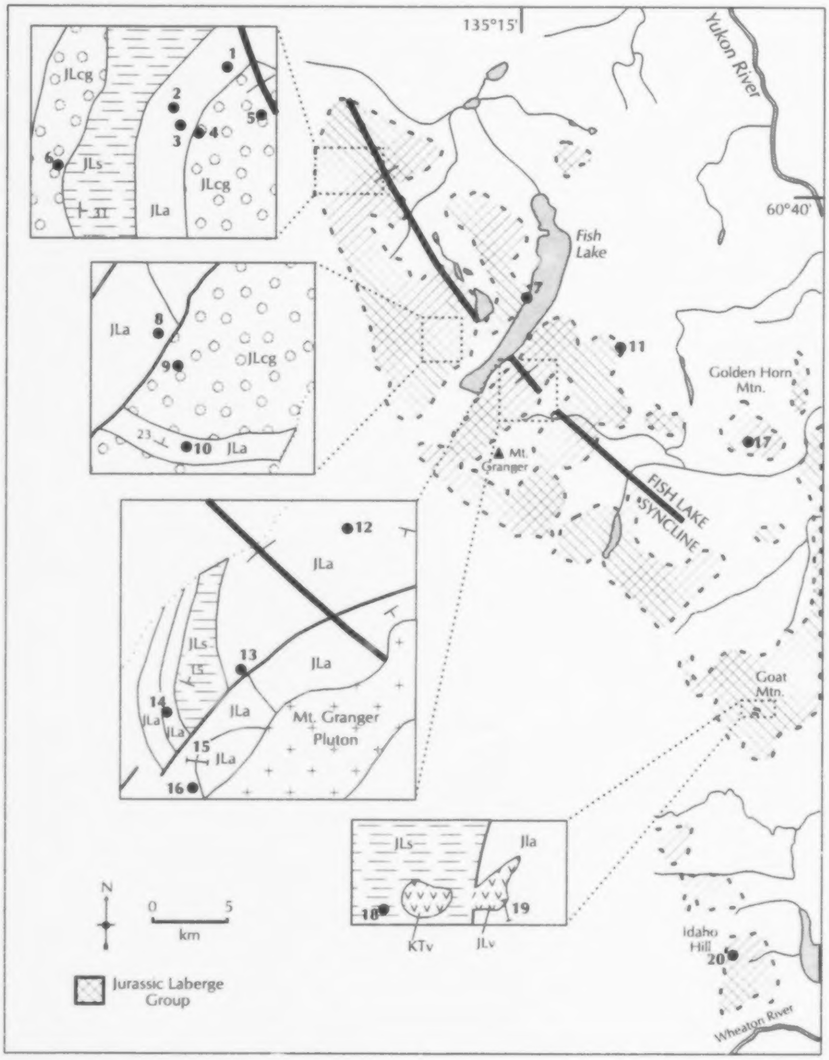

*Figure 2. Location map showing distribution of the Laberge Group within the study area and fossil localities mentioned in the text (base map after Wheeler, 1961; inset maps after Hart and Radloff, 1990). Strata in the inset maps are as follows: Laberge Group conglomerate (JLcg), sandstone (JLs), argillite (JLa), volcanic rocks (JLv) and Hutshi volcanics (KTv).*

Stratigraphic and sedimentological information from regional studies was integrated with the precise ammonite biochronology from this work to investigate the depositional and tectonic history of the Whitehorse Trough. The sedimentology and faunal composition of Fish Lake syncline strata can reveal information about environmental changes within the Whitehorse Trough. In addition, ammonite biochronology can be used to date major influxes of distinctive coarse detritus that can be used to constrain terrane interactions. These interpretations will be discussed after presenting the sedimentological background, based on literature review, and the current biostratigraphic framework developed for the Laberge Group.

## WHITEHORSE TROUGH SEDIMENTOLOGY

The Whitehorse Trough formed on the eastern margin of the Stikine Terrane (or Stikinia), one of many tectonostratigraphic terranes accreted to the western margin of North America during the Mesozoic (Monger et al., 1991). It is a 500-km-long marine basin that was an active depocentre from the Late Triassic to

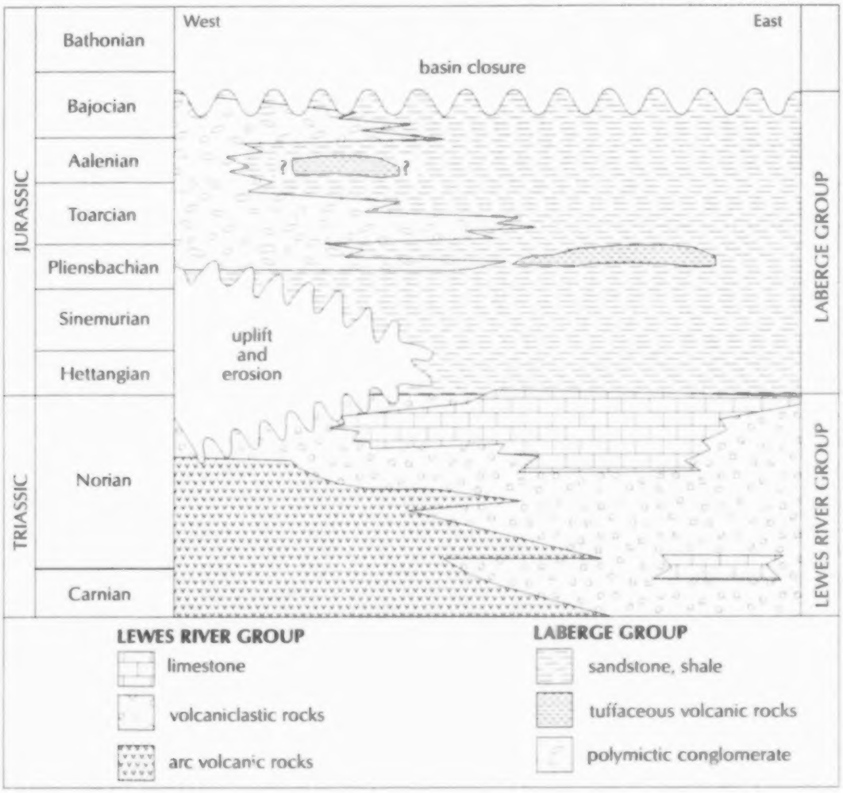

***Figure 3.*** *Generalized stratigraphy of the Whitehorse Trough in the Whitehorse map area (modified after Hart and Radloff, 1990).*

the Middle Jurassic (Hart and Radloff, 1990). Strata of the Laberge Group were deposited in a forearc environment adjacent to the east-facing Lewes River arc (Hart, 1997). In western areas, Laberge Group strata are dominantly coarse-grained and overlie Lewes River arc rocks (Fig. 3). In eastern areas, closer to the basin axis, the basement is not known although an oceanic basement, possibly of Cache Creek Terrane rocks, has been postulated (Hart, 1997).

Jurassic sedimentary rocks of the Whitehorse Trough comprise the Laberge Group (Wheeler, 1961; Hart and Radloff, 1990). Wheeler (1961) estimated a minimum thickness of 2400 m for the group. He did not create formal stratigraphic divisions for the Laberge Group because rapid facies variations, caused by tectonically active source areas, made the recognition of time-stratigraphic formations difficult. In the Carmacks map area (southern Yukon), Tempelman-Kluit (1984) divided Laberge Group strata into four informal formations: the Richthofen, Conglomerate, Nordenskiold, and Tanglefoot, using fossil constraints. Souther (1971) identified two formations in the Tulsequah area (northern British Columbia), namely the Takwahoni Formation consisting of coarse-grained, proximal conglomerates and sandstones, and the Inklin Formation consisting of more distal, finer-grained deposits.

The Triassic and older arc portion of Stikinia has been proposed as the source for Laberge Group sedimentary rocks, based in part on westerly paleocurrent indicators and similarities between volcanic clasts and subjacent Lewes River Group volcanic rocks (Hart et al., 1995). In addition, plutonic clasts with primitive Rb-Sr ratios, Triassic U-Pb radiometric dates, and a lack of inherited zircons suggest that a number of small Late Triassic plutons, which intrude the Lewes River arc, are the likely source for granitic detritus (Hart et al., 1995). Metamorphic clasts in conglomerate near Fish Lake were thought to support a potential Early Jurassic linkage with the Nisling Assemblage (Hart and Pelletier, 1989), which was supported by similar observations in older strata by Jackson et al. (1991); however, a source from Palaeozoic metasedimentary rocks of Stikinia (the Takhini Assemblage of Hart (1997)) is also possible (Hart et al., 1995). Increasing erosional dissection of the arc is suggested by increased granitic clast abundances in younger conglomerates, whereas oldest conglomerates contain only volcanic clasts (Hart and Radloff, 1990).

In the Fish Lake syncline, the Laberge Group is primarily composed of thick, polymictic conglomerate units with thinner greywacke and argillite layers (Wheeler, 1961; Hart and Radloff, 1990). Conglomerates grade laterally into fine greywacke and argillite that dominate more distal deposits of the eastern study area (Wheeler, 1961; Hart and Radloff, 1990). Thin tuff beds and volcanic flows are also present locally (Hart and Radloff, 1990). Detailed descriptions of Laberge Group lithologies in the study area are provided in Wheeler (1961), and Hart and Radloff (1990).

# BIOCHRONOLOGY

Ammonites are one of the most important index fossils for biochronological dating because of their rapid evolution and pelagic habit, which led to a near-worldwide distribution of many species. However, ammonite occurrences are facies-controlled to a minor extent and endemism can be marked, especially in the Early Jurassic Pliensbachian Stage when many European taxa are absent or rare in North America (Smith and Tipper, 1986), making correlation difficult. Biochronozones, regarded as standard zones by Callomon (1984) such that the temporal range of a given fossil or assemblage is constant at all localities, are intended to create a standard reference for temporal correlation within a given region (Smith et al., 1988). Collection of the zonal index species is not required to indicate the presence of the zone; instead, it can be recognized by a specific assemblage of temporally restricted species (Smith et al., 1988).

Biogeographic differences, and the commonly large number of endemic species, have made the standard northwest European zonal scheme of Dean et al. (1961) difficult to apply in western North America. As a result, North American standard zonations for the Pliensbachian (Smith et al., 1988) and the Toarcian (Jakobs et al., 1994; Jakobs, 1997) have been erected. A standard zonation for the Aalenian of North America has not yet been synthesized; in this paper, the regional zonation for Western Canada erected by Poulton and Tipper (1991) is used. Several regional zonations for the Bajocian have been proposed (Hall and Westermann, 1980; Taylor, 1988), but again, no standard North American zonation exists; the Bajocian zonation developed in eastern Oregon for the conterminous United States, proposed by Taylor (1988), is adopted in this paper.

# BIOSTRATIGRAPHY

## PLIENSBACHIAN STAGE

Pliensbachian sedimentary rocks are recorded by fossil collections made northwest of Fish Lake (Localities 1-7; Fig. 2) and near Idaho Hill (Locality 20; Fig. 2). Three ammonite zones are recorded: Whiteavesi Zone (Lower Pliensbachian), Kunae Zone (Upper Pliensbachian), and Carlottense Zone (Upper Pliensbachian). Compiled fossil ranges are illustrated in Figure 4.

### WHITEAVESI ZONE

The oldest Laberge Group rocks preserved are Whiteavesi Zone (Lower Pliensbachian), indicated by a single specimen of *Acanthopleuroceras* cf. *thomsoni*, collected at Locality 7 (Fig. 2). Associated fauna from the same locality include an external mould of a *Pentacrinus* sp. ossicle and moulds of the bivalves *Plagiostoma* sp., *Oxytoma* sp., *Agerchlamys* sp., *Chlamys (Chlamys)* cf. *textoria*, and *Modiolus*? sp., commonly preserved as dense aggregations of fragmented specimens covering bedding surfaces. The presence of relatively large and abundant bivalves, including *Modiolus*, and rarity of ammonites, is consistent with invertebrate depth zone B of Taylor (1982), suggesting relatively shallow water deposition (less than 50-100 m).

### FREBOLDI ZONE

Ammonites from the Lower Pliensbachian Freboldi Zone have not been collected from the study area. Sedimentary rocks of this age are well preserved in the southern Whitehorse Trough, spanning a stratigraphic interval of over 110 m near Atlin (Johannson, 1994). In addition, ammonites collected from localities north of Whitehorse may indicate the presence of Freboldi Zone-aged strata (Hart, 1997).

### KUNAE ZONE

Near Fish Lake, the oldest widespread Laberge Group rocks are Kunae Zone (Late Pliensbachian) in age and unconformably overlie the Triassic Lewes River Group (Wheeler, 1961; Hart and Radloff, 1990) and locally Whiteavesi Zone strata. Kunae Zone strata are present in two main outcrop areas within the Fish Lake syncline: north of Fish Lake and in the south of the study area near Idaho Hill.

The ammonite fauna collected from north of Fish Lake (Localities 2, 3, 6; Fig. 2) is low diversity, composed entirely of hildoceratid ammonites. Specimens include *Leptaleoceras accuratum, Fuciniceras cf. intumescens, Fuciniceras*? sp., and *Protogrammoceras (Protogrammoceras)* sp. Four aptychi were also collected from Kunae Zone strata north of Fish Lake. Amaltheids, typical of the early Kunae Zone, were not collected from Fish Lake, suggesting that only late Kunae Zone strata are present.

Kunae Zone strata are also present near Idaho Hill (Locality 20; Fig. 2), represented by 8 fossil collections and almost

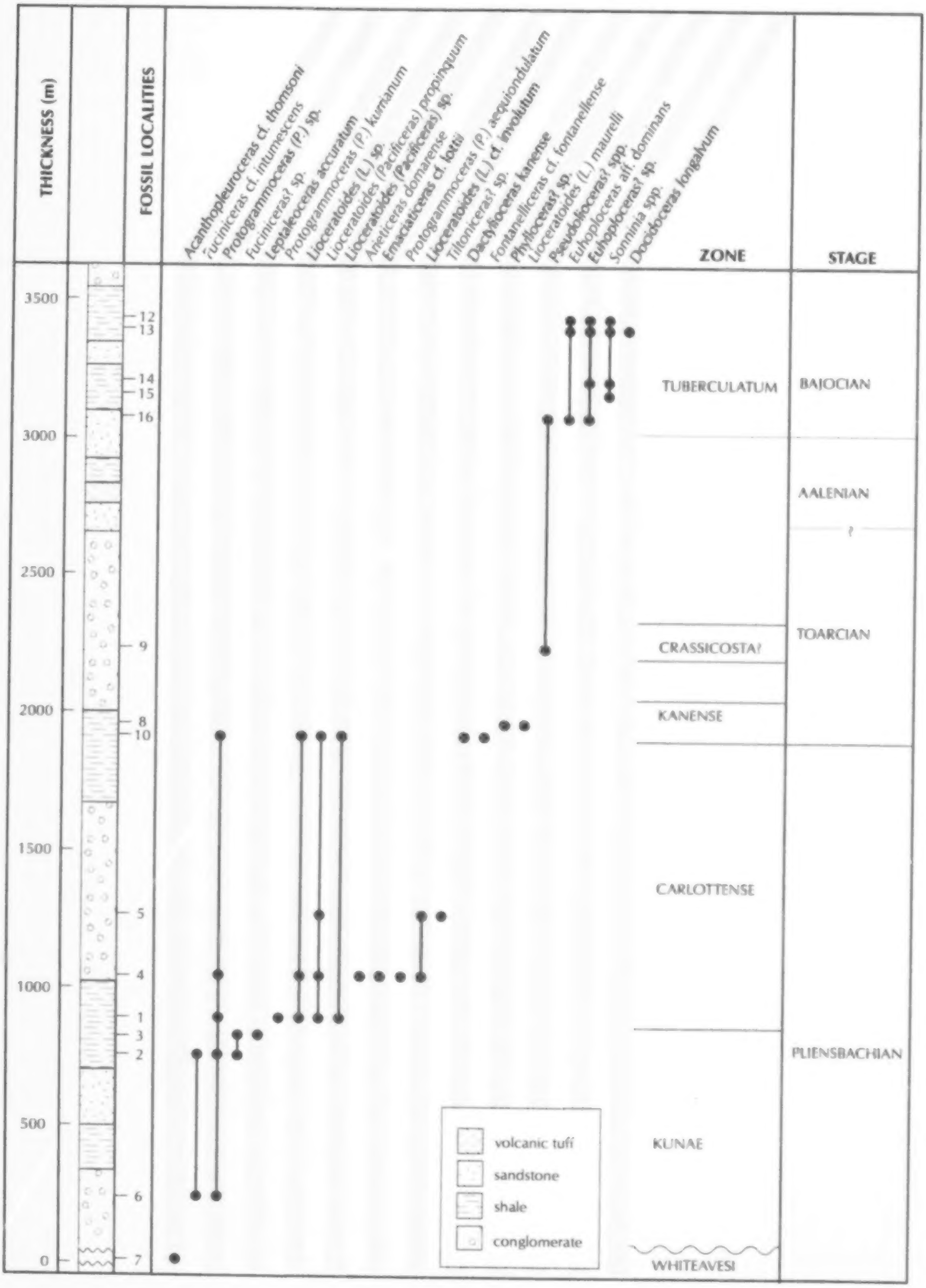

*Figure 4.* Composite stratigraphic column and fossil range chart for the Laberge Group in the Fish Lake section of the study area.

100 ammonite specimens. This fauna is characterized by a higher diversity and a slight dominance of amaltheids (54 specimens) over hildoceratids (43 specimens). Amaltheids are almost entirely *Amaltheus stokesi*; only a single specimen of *A. margaritatus* is present. *Amaltheus margaritatus* is rarely found in the Cordillera and has only been collected from elsewhere in the Whitehorse Trough (Cry Lake (104I) and Tulsequah (104K and L) map areas). Hildoceratids from Idaho Hill are predominantly *Leptaleoceras accuratum* and *Arieticeras algovianum* but also include four specimens of *Fuciniceras* cf. *targionii* and single specimens of *Arieticeras domarense*, *Fuciniceras* cf. *intumescens*, and *Fontanelliceras* cf. *fontanellense*. In addition, a single dactylioceratid, *Reynesoceras italicum*, is present. Two specimens of *Chlamys*? sp. and several indeterminate internal moulds of other bivalves were also collected from Idaho Hill.

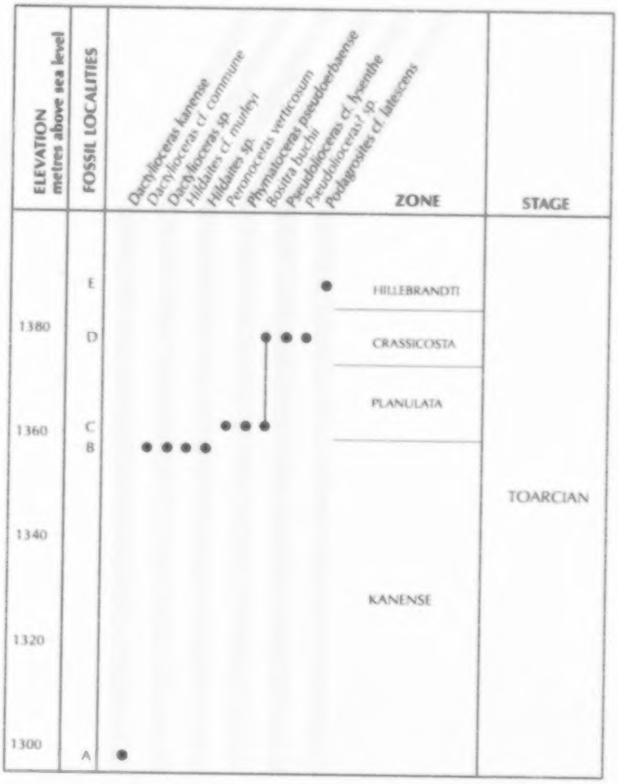

***Figure 5.*** *Fossil ranges from a measured section of Laberge Group argillites, Goat Mountain (Locality 19, Fig. 2). Letters refer to collections from different elevations within the locality.*

## CARLOTTENSE ZONE

The Carlottense Zone in the Whitehorse Trough is indicated by an ammonite fauna, which shows high diversity within the Family Hildoceratidae but lacks representatives of other families (e.g., the East Pacific genus *Fanninoceras*). Specimens characteristic of the Carlottense Zone were collected from Localities 1, 4 and 5 (Fig. 2), and include *Lioceratoides (Lioceratoides)* cf. *involutum*, *Lioceratoides (Pacificeras) propinquum*, and *Tiltoniceras*? sp. Other ammonites present include *Arieticeras domarense*, *Protogrammoceras (Protogrammoceras) kurrianum*, and *P. (P.) aequiondulatum*. In addition, three specimens assigned to *Emaciaticeras* cf. *lottii* have been collected north of Fish Lake (Locality 4, Fig. 2). This genus has previously been described only from northern and central Italy, Sicily, and southern Spain (Braga, 1983).

## TOARCIAN STAGE

Toarcian rocks are found throughout the study area: northwest of Fish Lake (Localities 8-10; Fig. 2), southwest of Fish Lake (Localities 11, 17; Fig. 2), and a series of collections at Goat Mountain (Locality 19; Fig. 2), detailed in Figure 5. Most fossil collections are Lower or lower Middle Toarcian (Kanense or Planulata Zone). The upper Middle and Upper Toarcian (Crassicosta and Hillebrandti Zones) are only recorded from the upper collections at Locality 19 (Fig. 5).

## KANENSE ZONE

The base of the Toarcian stage in the study area is marked by the appearance of *Dactylioceras kanense* occurring with holdovers from the Upper Pliensbachian, such as *Fontanelliceras* cf. *fontanellense*, *Lioceratoides (Pacificeras) propinquum*, and *Protogrammoceras (Protogrammoceras)* sp., all of which extend into the lowermost Toarcian. Basal Kanense Zone strata are present at locality 10 west of Fish Lake (Fig. 2) and at 1298 m elevation on Goat Mountain (Locality 19; Fig. 2). Three fragments of *Phylloceras*? sp. are present, associated with *Lioceratoides (Lioceratoides)* cf. *maurelli* in lower Kanense Zone strata west of Fish Lake (Locality 8; Fig. 2). Upper parts of the Kanense Zone are indicated in the Goat Mountain section by specimens of *Dactylioceras* cf. *commune* and *Hildaites* cf. *murleyi* at 1356 m elevation (Fig. 5).

### PLANULATA ZONE

Presence of the Planulata Zone at Goat Mountain (Locality 19; Fig. 2) is shown by specimens of *Peronoceras verticosum* and *Phymatoceras pseudoerbaense* at 1362 m elevation (Fig. 5). *Peronoceras verticosum* indicates a Planulata Zone age for argillite east of Fish Lake (Locality 11; Fig. 2) and *Peronoceras* sp., present at Golden Horn Mountain (Locality 17; Fig. 2), suggests a Middle Toarcian (likely Planulata Zone) age for that locality. Shell pavements of the bivalve *Bositra buchii* are widespread in the Goat Mountain section younger than mid-Planulata Zone and occur elsewhere in the study area in Middle and Upper Toarcian strata, as well as from Whitehorse Trough strata in the Carmacks, Tulsequah, Telegraph Creek, and Cry Lake areas (Aberhan, 1998). Elsewhere, *Bositra* also forms shell pavements in rocks as old as Middle Toarcian (Damborenea, 1987; Etter, 1996; Hallam, 1995).

### CRASSICOSTA ZONE

The presence of this zone is indicated in the Goat Mountain section (Locality 19; Fig. 2) by specimens of *Pseudolioceras* cf. *lysenthe* and *Pseudolioceras*? sp. collected from 1378 m elevation (Fig. 5). In addition, *Pseudolioceras* cf. *lysenthe* and *Peronoceras* cf. *crassicostatum* are present in talus collections from the same locality. A single specimen of *Pseudolioceras*? sp. from Locality 9, west of Fish Lake (Fig. 2), may suggest a Crassicosta Zone age for that site.

### HILLEBRANDTI ZONE

A single specimen of *Podagrosites* cf. *latescens* from 1388 m of the Goat Mountain section (Locality 19; Fig. 2) is the only Hillebrandti Zone ammonite collected from the study area.

### YAKOUNENSIS ZONE

Presence of the Yakounensis Zone is indicated by a specimen resembling either *Dumortiera* sp. or *Troitsaia* sp. associated with the trigoniid bivalve *Myophorella* sp., reported from the southeastern Fish Lake syncline by Poulton and Tipper (1991) but not re-examined in this study. Abundant *Bositra buchii* shell pavements are also present at the locality (Aberhan, 1998). The ammonite specimens indicate either a Late Toarcian or Early Aalenian age; however, *Bositra* is found in Toarcian deposits elsewhere in the study area and likely confirms a Yakounensis Zone age for this site.

## AALENIAN

Diagnostic Aalenian fossils have not been collected from the study area. A sandy limestone unit on Goat Mountain (Locality 18; Fig. 2) contains a single specimen of *Ceratomya*? sp. and three samples of densely packed bivalve coquina containing the trigoniid *Myophorella lupheri*. The lithology and fossil content are suggestive of shallow water deposition but the stratigraphic position is poorly constrained. *Ceratomya*? sp. ranges from at least the Aalenian through Bajocian, and *Myophorella lupheri* ranges from the Lower or Middle Aalenian to the Middle Bajocian, reaching greatest abundance during the Aalenian (Poulton, 1980). The anomalous lithology of the site compared with Bajocian strata elsewhere in the study area, combined with the maximum abundance of *M. lupheri* in the Aalenian, suggests that the locality may represent Aalenian deposits.

## BAJOCIAN

Only the lowermost zone of the Lower Bajocian, the *Euhoploceras tuberculatum* zone of Taylor (1988), is present in the study area, restricted to outcrops south of Fish Lake (Localities 12-16; Fig. 2). This zone is characterized by the first appearance of sonniniid ammonites. No representatives of the Family Stephanoceratidae are present, suggesting that only the lowest faunal zone of the Lower Bajocian is represented.

### EUHOPLOCERAS TUBERCULATUM ZONE

The ammonite fauna is dominated by sonniniids, although one specimen of *Pseudolioceras*? sp. and three of *Docidoceras longalvum*, previously identified as *Stephanoceras* in Wheeler (1961), are also present at localities 16 and 13 (Fig. 2), respectively. Sonniniid classification is problematic, but at least two species of *Sonninia* and two of *Euhoploceras* are present. Only one, *Euhoploceras* aff. *dominans*, is referrable to a previously described taxon. Numerous aptychi, presumably derived from sonniniid ammonites, are preserved at several localities and four specimens of the bivalve *Camptonectes* (*Costicamptonectes*?) sp. are also found in the uppermost site (Locality 12; Fig. 2).

## DEPOSITIONAL AND TECTONIC HISTORY

The generalized stratigraphic section (Fig. 4) is constructed from regional geological maps (e.g., Hart and Radloff, 1990), using precise ammonite biostratigraphy to place localities in their stratigraphic context. Because no sections were measured during this research, thicknesses are based on published regional geology maps and are only approximate. In addition, deposition in submarine fans from an active source area results in extremely rapid lateral facies variations (Dickie and Hein, 1995), further complicating the construction of a generalized stratigraphic section for the Fish Lake syncline. Nevertheless, it is still possible to recognize major events in the Pliensbachian to Bajocian depositional history of the basin.

### PLIENSBACHIAN

Early Pliensbachian (Whiteavesi Zone) rocks are only found in a single area near Fish Lake. Freboldi Zone (Late Pliensbachian) strata are apparently absent and the oldest widespread deposition is Late Pliensbachian Kunae Zone in age. The Pliensbachian strata near Fish Lake are dominated by thick conglomerate wedges with finer-grained, fossiliferous interbeds, suggesting that the Freboldi Zone should be thick and would likely yield ammonite fossils if it is present. This implies that Freboldi Zone sediments near the basin margins were not deposited, or were eroded during sea-level fall. Deposition of Whiteavesi Zone sediments likely occurred during a small-scale transgression, possibly related to early source area uplift and basin subsidence. These strata were deposited in shallow water, in contrast to the dominantly deep-water facies found in much of the younger basin fill. The strata were partly removed during a later relative sea level drop, but small pockets of Whiteavesi Zone sediments were preserved locally in paleotopographic depressions.

The lowest conglomerate horizon is Early Pliensbachian age in the Carmacks map area (Tempelman-Kluit, 1984) and northern Whitehorse (105D) map area (Hart, 1997). However, the base of the conglomeratic Takwahoni Formation in the Tulsequah area is Late Pliensbachian (Kunae Zone) in age (Souther, 1971). This indicates that rapid uplift and erosion of the Lewes River arc likely began by the Early Pliensbachian in the north and progressed southward during the Late Pliensbachian in Tulsequah. The presence of isolated Whiteavesi Zone strata near Fish Lake may indicate an intermediate stage since the shallow marine sandstones are preserved only in isolated localities, representing initial stages of uplift prior to the major influx of arc-derived material in the Late Pliensbachian (Kunae Zone).

During the late Kunae and Carlottense zones, two major conglomerate wedges, approaching 600 m in thickness, were deposited in the Fish Lake area. They are separated by 800 m of argillite and greywacke. Each wedge contains thinner intercalated beds of finer material. Conglomerates, however, are subordinate or absent in central and eastern areas of the Whitehorse Trough during the Late Pliensbachian (Wheeler, 1961; Hart and Radloff, 1990). For example, Late Pliensbachian (early Kunae Zone) strata near Idaho Hill are dominated by a thick section of fine- to medium-grained greywacke (Hart and Radloff, 1990).

Based on a detailed facies analysis of Laberge Group strata, Dickie and Hein (1995) suggested that conglomerate wedges were deposited in a submarine fan in a base-of-slope setting. Conglomerate fan deposition was triggered by rapid uplift of the Stikinian arc source area (Pálfy and Hart, 1995). Thicker greywacke and argillite units may represent finer turbidite deposits at the margin of fan lobes, possibly generated as a result of lobe switching or migration (Dickie and Hein, 1995). Alternatively, finer-grained sediments may have been deposited during times of relative quiescence, with coarse-grained sedimentation linked to pulses of uplift and denudation (Ineson, 1989).

Whitehorse Trough sedimentation was diachronous: the age of deposition ranges from as old as Sinemurian or possibly Hettangian near the basin axis (Lees, 1934; Frebold and Poulton, 1977) to no older than Late Pliensbachian near the western margin (Souther, 1971). Marginward younging of basal strata is also observed in the Fish Lake syncline. Lowermost strata near Idaho Hill are at least as old as early Kunae Zone, whereas basal strata near Fish Lake, closer to the basin margin, are late Kunae Zone in age.

### TOARCIAN

Toarcian deposits are also typified by rapid facies changes: the transition from conglomerate submarine fan deposits near Fish Lake to argillitic facies near Golden Horn Mountain occurs over only 15 km. Although biostratigraphic control near Fish Lake is minimal, the conglomerate pulse appears to be confined to the Lower and possibly Middle Toarcian near the western basin margin. A single specimen of *Pseudolioceras*? sp. from Locality 9 (Fig. 2) may indicate a Crassicosta Zone youngest age. An excellent Lower to basal Upper Toarcian section near Goat Mountain (Locality 19; Fig. 2) records dominantly argillite deposition in more distal areas. Upper Toarcian deposits, if present, are likely recessive-weathering black shales throughout the entire area (C. Hart, pers. comm., 2000), suggesting a rapid cessation of coarse sediment supply.

Presence of shell pavements consisting of closely packed, articulated *Bositra buchii* specimens in Planulata to Yakounensis Zone strata suggests that the Whitehorse Trough became anoxic during those times. The life mode of *Bositra* has been controversial, although a benthic habit is now preferred based on regular (i.e., non-random) specimen distribution and taphonomic evidence indicative of in situ preservation (Etter, 1996). Distribution of *Bositra* shell pavements along a paleo-oxygenation gradient supports the hypothesis that it was highly tolerant to low oxygen levels and used opportunistic dispersal strategies to rapidly colonize severely dysoxic environments (Etter, 1996). *Bositra* shell pavements are present in Middle Toarcian rocks from the Cry Lake (Aberhan, 1998), Tulsequah, and the Carmacks areas. The spatially widespread, but temporally limited distribution of *Bositra* suggests that anoxia affected the entire basin, at least sporadically, throughout the Middle and Late Toarcian. *Bositra* shell pavements occur after the youngest conglomeratic pulse, suggesting that anoxia and decreased sediment supply may be linked, possibly to a rapid transgression.

### AALENIAN

Aalenian deposits are thought to be widespread, but thin, throughout the Whitehorse Trough (Poulton and Tipper, 1991). In the Fish Lake syncline, the Aalenian is likely represented by a thick argillite unit, which underlies the first distinctive Bajocian fossils. Volcanic rocks may also be more abundant in the Aalenian, although there are minimal stratigraphic and radiometric controls. Rhyolitic tuff, possibly of Aalenian age, is present near the Bonneville Lakes (Hart and Radloff, 1990). In addition, a 15-m-thick andesitic flow or sill overlies the Lower to basal Upper Toarcian section on Goat Mountain (Pálfy and Hart, 1995).

### BAJOCIAN

Early Bajocian strata in the study area are composed of organic-rich argillite to fine-grained greywacke interbedded with cm-scale resedimented tuffaceous turbidite deposits. This unit was informally referred to as 'pyjama beds' in equivalent strata in the Spatsizi (Thomson, 1985) and Iskut (Nadaraju, 1993) areas. The abundance of fine-grained sediment indicates that deposition occurred in a distal setting, possibly beneath a vigorous upwelling zone as suggested by the organic-rich sediments (Calvert et al., 1992; Ganeshram et al., 1999; Pedersen et al., 1992). Probable volcanic spherulites within the argillite layers and abundant tuffaceous turbidites suggest that sediments were deposited near a long-lived volcanic arc, and that volcanism occurred throughout the Early Bajocian.

Upper beds in the Fish Lake syncline are composed of chert-pebble conglomerate (Wheeler, 1961), likely correlative with the Tantalus formation of Tempelman-Kluit (1984). An oldest age of early *Euhoploceras tuberculatum* zone is indicated by a rich sonniniid ammonite fauna in the immediately underlying strata. Early Bajocian strata from the northern Whitehorse (Hart, 1997) and Tulsequah (Souther, 1971) map areas also contain chert-pebble conglomerates. The widespread influx of chert in Early Bajocian times is consistent with the obduction of the Cache Creek Terrane, the most plausible source for large volumes of chert (Hart, 1997). Thus, the final stages of basin-fill record obduction of the Cache Creek Terrane in the Early Bajocian.

## CONCLUSIONS

Fossil identifications and ammonite biochronology indicate that Laberge Group strata in the study area form a conformable sequence from Upper Pliensbachian (Kunae Zone) to Lower Bajocian *(Euhoploceras tuberculatum* zone). Investigation of Fish Lake syncline stratigraphy reveals information about the tectonic and environmental history of the Whitehorse Trough. Dating of the lowest coarse detritus in the Fish Lake syncline indicates that tectonic uplift of the source area was diachronous across the Whitehorse Trough. Early Pliensbachian uplift in the north progressed southward, occurring primarily in the Late Pliensbachian, but with a minor pulse in the Early Pliensbachian. Influx of coarse detritus is restricted to the Late Pliensbachian in southern areas.

It is also possible to correlate environmental events between the Fish Lake syncline and other areas of the Whitehorse Trough. For example, basin-wide anoxia during the Middle and Late Toarcian is suggested by the widespread occurrence of *Bositra buchii* shell pavements.

Biochronological dating of major influxes of lithologically distinctive coarse detritus in the Fish Lake syncline places constraints on terrane interactions. Chert-pebble conglomerate deposited in the Early Bajocian yields a minimum age constraint on the obduction of the Cache Creek Terrane.

## ACKNOWLEDGMENTS

The BSc thesis on which this paper is based was supervised by Paul L. Smith, University of British Columbia, who acknowledges the support of NSERC. Fossil collections were made available by the Geological Survey of Canada. Discussions with Craig Hart regarding the Whitehorse Trough in the southern Yukon were of great benefit and his editorial comments helped focus the manuscript considerably. József Pálfy provided locality information about the Goat Mountain section. This paper is also known as Geological Survey of Canada Contribution No. 2000187.

## REFERENCES

Aberhan, M., 1998. Early Jurassic Bivalvia of western Canada. Part I. Subclasses Palaeotaxodonta, Pteriomorphia, and Isofilibranchia. Beringeria, vol. 21, p. 57-150.

Braga, J.C., 1983. Ammonites del Domerense de la Zona Subbetica (Cordilleras Beticas, sur de España). PhD thesis, Univ. de Granada, 410 p.

Callomon, J.H., 1984. Biostratigraphy, chronostratigraphy and all that - again! *In:* International Symposium on Jurassic Stratigraphy, Erlangen, O. Michelsen and A. Zeiss (eds.), vol. 3, p. 611-624.

Calvert, S.E., Bustin, R.M. and Pedersen, T.F., 1992. Lack of evidence for enhanced preservation of sedimentary organic matter in the oxygen minimum of the Gulf of California. Geology, vol. 20, p. 757-760.

Clapham, M.E., 2000. Lower to Middle Jurassic Stratigraphy and Ammonite Fauna of the Northern Whitehorse Trough, Yukon, Canada. Unpublished BSc thesis, University of British Columbia, 90 p.

Damborenea, S.E., 1987. Early Jurassic Bivalvia of Argentina, Part 2: Superfamilies Pteriacea, Buchiacea, and part of Pectinacea. Palaeontographica Abt. A, vol. 199, p. 113-216.

Dean, W.T., Donovan, D.T. and Howarth, M.K., 1961. The Liassic ammonite zones and subzones of the northwest European province. Bulletin of the British Museum (Natural History), Series A, Geology, vol. 4, p. 438-505.

Dickie, J.R. and Hein, F.J., 1995. Conglomeratic fan deltas and submarine fans of the Jurassic Laberge Group, Whitehorse Trough, Yukon Territory, Canada: Fore-arc sedimentation and unroofing of a volcanic island arc complex. Sedimentary Geology, vol. 98, p. 263-292.

Etter, W., 1996. Pseudoplanktonic and benthic invertebrates in the Middle Jurassic Opalinum Clay, northern Switzerland. Palaeogeography, Palaeoclimatology, Palaeoecology, vol. 126, p. 325-341.

Frebold, H. and Poulton, T.P., 1977. Hettangian (Lower Jurassic) rocks and faunas, northern Yukon Territory. Canadian Journal of Earth Sciences, vol. 14, p. 89-101.

Ganeshram, R.S., Calvert, S.E., Pedersen, T.F. and Cowie, G.L., 1999. Factors controlling the burial of organic carbon in laminated and bioturbated sediments off NW Mexico: Implications for hydrocarbon preservation. Geochimica et Cosmochimica Acta, vol. 63, p. 1723-1734.

Hall, R.L. and Westermann, G.E.G., 1980. Lower Bajocian (Jurassic) cephalopod faunas from Western Canada and proposed assemblage zones for the Lower Bajocian of North America. Palaeontolographica Americana, vol. 9, 93 p.

Hallam, A., 1995. Estimates of the amount and rate of sea-level change across the Rhaetian-Hettangian and Pliensbachian-Toarcian boundaries (latest Triassic to Early Jurassic). Journal of the Geological Society, London, vol. 154, p. 773-779.

Hart, C.J.R., 1997. A transect across northern Stikinia: Geology of the northern Whitehorse map area, southern Yukon Territory (105D/13-16). Exploration and Geological Services Division, Yukon Region, Indian and Northern Affairs Canada, Bulletin 8, 103 p.

Hart, C.J.R. and Pelletier, K.S., 1989. Geology of the Whitehorse (105D/11) map area. Exploration and Geological Services Division, Yukon Region, Indian and Northern Affairs Canada, Open File 1989-2, 51 p.

Hart, C.J.R. and Radloff, J.K., 1990. Geology of Whitehorse, Alligator Lake, Fenwick Creek, Carcross and part of Robinson map areas (105D/11, 6, 3, 2, & 7). Exploration and Geological Services Division, Yukon Region, Indian and Northern Affairs Canada, Open File 1990-4, 113 p.

Hart, C.J.R., Dickie, J.R., Ghosh, D.K. and Armstrong, R.L., 1995. Provenance constraints for Whitehorse Trough conglomerate: U-Pb zircon dates and initial Sr ratios of granitic clasts in Jurassic Laberge Group, Yukon Territory. *In:* Jurassic Magmatism and Tectonics of the North American Cordillera, D.M. Miller and C. Busby (eds.), p. 47-63.

Ineson, J.R., 1989. Coarse-grained submarine fan and slope apron deposits in a Cretaceous back-arc basin, Antarctica. Sedimentology, vol. 36, p. 793-819.

Jackson, J.L., Gehrels, G.E., Patchett, P.L. and Mihalynuk, M.G., 1991. Stratigraphic and isotopic link between the northern Stikinia and an ancient continental margin assemblage, Canadian Cordillera. Geology, vol. 19, p. 1177-1180.

Jakobs, G.K., 1997. Toarcian (Early Jurassic) ammonoids from Western North America. Geological Survey of Canada, Bulletin 428, 137 p.

Jakobs, G.K., Smith, P.L. and Tipper, H.W., 1994. An ammonite zonation for the Toarcian (Lower Jurassic) of the North American Cordillera. Canadian Journal of Earth Sciences, vol. 31, p. 919-942.

Johannson, G.G., 1994. Biochronology and sedimentology of the Laberge Group: Provenance constraints on Early Jurassic evolution of the northern Stikinian arc, Atlin Lake, northwestern British Columbia. Unpublished MSc thesis, University of British Columbia, 271 p.

Johannson, G.G., Smith, P.L. and Tipper, H.W., 1997. Early Jurassic evolution of the northern Stikinian arc: Evidence from the Laberge Group, northwestern British Columbia. Canadian Journal of Earth Sciences, vol. 34, p. 1030-1057.

Lees, E.J., 1934. Geology of the Laberge area, Yukon. Transactions of the Royal Institute of Canada, vol. 20, p. 1-48.

Monger, J.W.H., Wheeler, J.O., Tipper, H.W., Gabrielse, H., Harms, T., Struik, L.C., Campbell, R.B., Dodds, C.J., Gehrels, G.E. and O'Brien, J., 1991. Part B, Cordilleran terranes. *In:* Geology of the Cordilleran Orogen in Canada No. 4, H. Gabrielse and C.J. Yorath (eds.), p. 281-327.

Nadaraju, G.T., 1993. Triassic-Jurassic biochronology of the eastern Iskut River map area, northwestern British Columbia. Unpublished MSc thesis, University of British Columbia, 223 p.

Pálfy, J. and Hart, C.J.R., 1995. Biostratigraphy of the Lower to Middle Jurassic Laberge Group, Whitehorse map area (105D), southern Yukon. Yukon Exploration and Geology 1994, p. 73-86.

Pedersen, T.F., Shimmield, G.B. and Price, N.B., 1992. Lack of enhanced preservation of organic matter in sediments under the oxygen minimum on the Oman Margin. Geochimica et Cosmochimica Acta, vol. 56, p. 545-551.

Poulton, T.P., 1980. Trigoniid bivalves from the Bajocian (Middle Jurassic) rocks of central Oregon. Current Research, Part A, Geological Survey of Canada, Paper 80-1A, p. 187-196.

Poulton, T.P. and Tipper, H.W., 1991. Aalenian ammonites and strata of Western Canada. Geological Survey of Canada, Bulletin 411, 71 p.

Smith, P.L. and Tipper, H.W., 1986. Plate tectonics and paleobiogeography: Early Jurassic (Pliensbachian) endemism and diversity. Palaios, vol. 1, p. 399-412.

Smith, P.L., Tipper, H.W., Taylor D.G. and Guex, J., 1988. An ammonite zonation for the Lower Jurassic of Canada and the United States: The Pliensbachian. Canadian Journal of Earth Sciences, vol. 25, p. 1503-1523.

Souther, J.G., 1971. Geology and mineral deposits of the Tulsequah map area, British Columbia. Geological Survey of Canada, Memoir 362, 84 p.

Taylor, D.G., 1982. Jurassic shallow marine invertebrate depth zones, with exemplification from the Snowshoe Formation, Oregon. Oregon Geology, vol. 44, p. 51-56.

Taylor, D.G., 1988. Middle Jurassic (late Aalenian and early Bajocian) ammonite biochronology of the Snowshoe Formation, Oregon. Oregon Geology, vol. 50, p. 123-138.

Tempelman-Kluit, D.J., 1984. Laberge (105E) and Carmacks (115I) map areas. Geological Survey of Canada, Open File 1101, two 1:250 000 scale maps.

Thomson, R.C., 1985. Lower to Middle Jurassic (Pliensbachian to Bajocian) stratigraphy and Pliensbachian ammonite fauna of the northern Spatsizi area, north central British Columbia. Unpublished MSc thesis, University of British Columbia, 188 p.

Wheeler, J.O., 1961. Whitehorse map-area, Yukon Territory (105D). Geological Survey of Canada, Memoir 312, 156 p.

# Composition of placer and lode gold as an exploration tool in the Stewart River map area, western Yukon

***Matthew R. Dumula and James K. Mortensen[1]***
*University of British Columbia[2]*

Dumula, M.R. and Mortensen, J.K., 2002. Composition of placer and lode gold as an exploration tool in the Stewart River map area, western Yukon. *In:* Yukon Exploration and Geology 2001, D.S. Emond, L.H. Weston and L.L. Lewis (eds.), Exploration and Geological Services Division, Yukon Region, Indian and Northern Affairs Canada, p. 87-102.

## ABSTRACT

A reconnaissance study of the composition of gold from several placer streams in the Stewart River map area was carried out to characterize the likely style(s) of lode mineralization from which the placer gold in each stream was derived. Results of the study indicate that placer gold from Eureka and Black Hills creeks, as well as gold grains from colluvium in exploration pits at the head of Eureka Creek, have relatively low fineness, low copper contents and high mercury contents. These compositions are consistent with both the gold in colluvium and most of the placer gold having been derived from epithermal sources in the Eureka Dome or Henderson Dome area. Gold in placers in the Moosehorn Range is likely derived from intrusion-related, gold-bearing quartz veins exposed in the headwaters of the placer creeks, and is characterized by relatively high fineness, high copper contents and low mercury contents. Placer gold in Thistle, Kirkman and Blueberry creeks is very similar to that from streams in the Moosehorn Range, suggesting that an undiscovered intrusion-related gold deposit is present within the Thistle/Kirkman drainage basin.

## RÉSUMÉ

Une étude de reconnaissance de la composition de l'or placérien de plusieurs des cours d'eau de la région de la carte Stewart River a été effectuée afin de déterminer de quel type de minéralisation filonienne provient l'or placérien de chaque cours d'eau. Les résultats de l'analyse ont révélé que l'or placérien des ruisseaux Eureka et Black Hills, ainsi que les grains d'or colluviaux relativement grossiers extraits de fosses d'exploration situées sur le cours supérieur du ruisseau Eureka, renferment relativement peu de cuivre et beaucoup de mercure. Cette composition suggère que l'or colluvial et la majeure partie de l'or placérien proviennent de sources épithermales localisées dans la région du dôme d'Eureka ou du dôme d'Henderson. L'or placérien de la chaîne Moosehorn provient vraisemblablement de veines de quartz aurifère associées à des intrusions, qui affleurent sur le cours supérieur des ruisseaux placériens; il est caractérisé par des grains relativement grossiers ainsi que par des teneurs en cuivre élevées et des teneurs en mercure faibles. L'or placérien des ruisseaux Thistle, Kirkman et Blueberry est très similaire à celui des cours d'eau de la chaîne Moosehorn, ce qui suggère qu'un gisement d'or non découvert associé à une intrusion serait présent dans le bassin versant des ruisseaux Thistle/Kirkman.

---

[1] *jmortens@eos.ubc.ca*

[2] *Department of Earth and Ocean Sciences, University of British Columbia, 6339 Stores Road, Vancouver, British Columbia, Canada V6T 1Z4*

## INTRODUCTION

Exploration for lode gold in the unglaciated parts of western Yukon is complicated by poor exposure and an incomplete understanding of the bedrock geology of the area. Soil, silt, and heavy mineral geochemistry are the main exploration tools employed. Advanced stages of exploration involving trenching and/or drilling, however, can be expensive, and harmful to the environment. A technique applicable to gold anomalies in soil, silt or heavy mineral samples is the classifcation of mineralization style using geochemical 'fingerprinting'. Development of such a technique is the main goal of this study and it should allow companies to target their exploration efforts and expenditures more efficiently.

Placer gold occurrences, including several major placer gold-producing streams, are widespread in western Yukon; however the source(s) from which the gold in these deposits was derived is in most cases unknown. A study of the composition of placer and lode gold in the Klondike District in west-central Yukon by Knight et al. (1999a) showed that placer gold in that area displays a distinctive geochemical signature that allows it to be related directly to local bedrock occurrences. In this study, we have taken a similar approach to that of Knight et al. (1999a), but have applied the geochemical fingerprinting of gold on a reconnaissance scale in several localities throughout the Stewart River map area in western Yukon. Placer gold samples from Eureka Creek, Kirkman Creek, Black Hills Creek, Thistle Creek, Blueberry Creek, Swamp Creek, Mine Creek and Roo Pup have been investigated in this study, along with gold from lode occurrences near the head of Eureka Creek.

## PREVIOUS WORK ON GOLD COMPOSITION

Workers such as Knight (1985), Morrison et al. (1991), Knight et al. (1991, 1994, 1999a), Palacios et al. (1999a,b,c,d), Chapman et al. (2000), among others, have investigated the geochemical compositions of gold particles in various placer and lode occurrences. Results of these studies indicate that it is possible to characterize the geochemical composition of a gold particle and relate that composition with a specific style of mineralization.

Palacios et al. (1999a,b,c,d) studied concentrations of As, Ag, Au, Cu, Hg and Bi in native gold from epithermal and porphyry deposits. They determined that copper contents of natural gold in such occurrences vary with vertical position within certain deposit types, and that epithermal deposits are depleted in Cu and relatively rich in Ag. Gold-rich copper porphyry deposits, in contrast, were determined to have a relatively high Cu content and variable Ag concentrations. Chapman et al. (2000) investigated the compositions of alluvial gold in the Irish and Scottish Caledonides. They grouped gold samples into ten different compositional populations on the basis of Au, Ag, Cu, Hg and Pd contents, and correlated each population with a specific host rock or probable source rock assemblage.

Morrison et al. (1991) examined the fineness values for gold from different deposit classes. They determined that fineness values were in the range of (and average) 780-1000 (940) for Achaean lode gold deposits, 800-1000 (920) for mesothermal 'Slate Belt'-type deposits, 650-970 (825) for 'plutonic' deposits, 650-1000 (700-1000) for porphyry deposits, 520-870 (650-850) for volcanogenic deposits, and 0-1000 (440-1000) for epithermal deposits.

Knight (1985) studied placer gold from the Fraser River drainage and concluded that it was possible to characterize lode gold deposits and to recognize gold from these lodes in nearby placers using variations in Ag, Cu and Hg contents in the gold. High Cu and high Hg contents were found in gold that appeared to be associated with ultrabasic rocks, and high Hg contents in gold was found to be typical of lode gold associated with major faults.

Knight et al. (1994, 1999a, b) studied the variation in composition and shape of placer gold found in the Klondike District of western Yukon. Concentrations of Ag, Au, Cu and Hg were determined for a large number of samples of placer and lode gold from the area. Results of this study showed that Klondike gold has a considerable compositional range, but much of it is characterized by low fineness, low Cu content and relatively high Hg content. This study showed that by geochemically characterizing gold from specific lode sources, placer deposits can be related to individual types of lode sources, and that the point of entry from each new lode source into a placer stream can be determined. Knight et al. (1999b) also found that the shape and other physical properties of placer gold in the Klondike can be used to estimate the distance the gold has been transported from its source.

## GEOLOGICAL SETTING

The Stewart River map area is underlain mainly by rocks of Yukon-Tanana Terrane, comprising polydeformed metasedimentary, metavolcanic and metaplutonic rocks. These rocks are intruded and overlain by a variety of Early Jurassic to Early Tertiary plutons, and are locally overlain by mid-Cretaceous to Early Tertiary volcanic and sedimentary rocks. The study area is located within the 'Tintina Gold Belt', which hosts a wide range of mainly intrusion-related gold deposits (British Columbia and Yukon Chamber of Mines, 2000). Most gold deposits within the Tintina Gold Belt are thought to be genetically related to mid- and Late Cretaceous intrusive rocks (e.g., Mortensen et al., 2000).

A wide variety of gold-bearing lode occurrences is known or inferred to exist in the Stewart River map area. These include mesothermal ('metamorphogenic') quartz veins such as those in the Klondike District (Fig. 1; Rushton et al., 1998), intrusion-hosted veins such as the Longline occurrence in the Moosehorn Range (southwest corner of Fig. 1; MacDonald, 2001), epithermal vein systems (Glasmacher and Friedrich, 1992), gold-bearing skarns, gold in carbonate-altered ultramafic rocks such as those found in the Sixtymile District (west of the Yukon River on Fig. 1; R. Hulstein, pers. comm., 1999), and precious-metal enriched volcanogenic massive sulphide deposits. Known and inferred ages for intrusion-related gold mineralization in the study area range from Early Jurassic to Late Cretaceous or Early Tertiary.

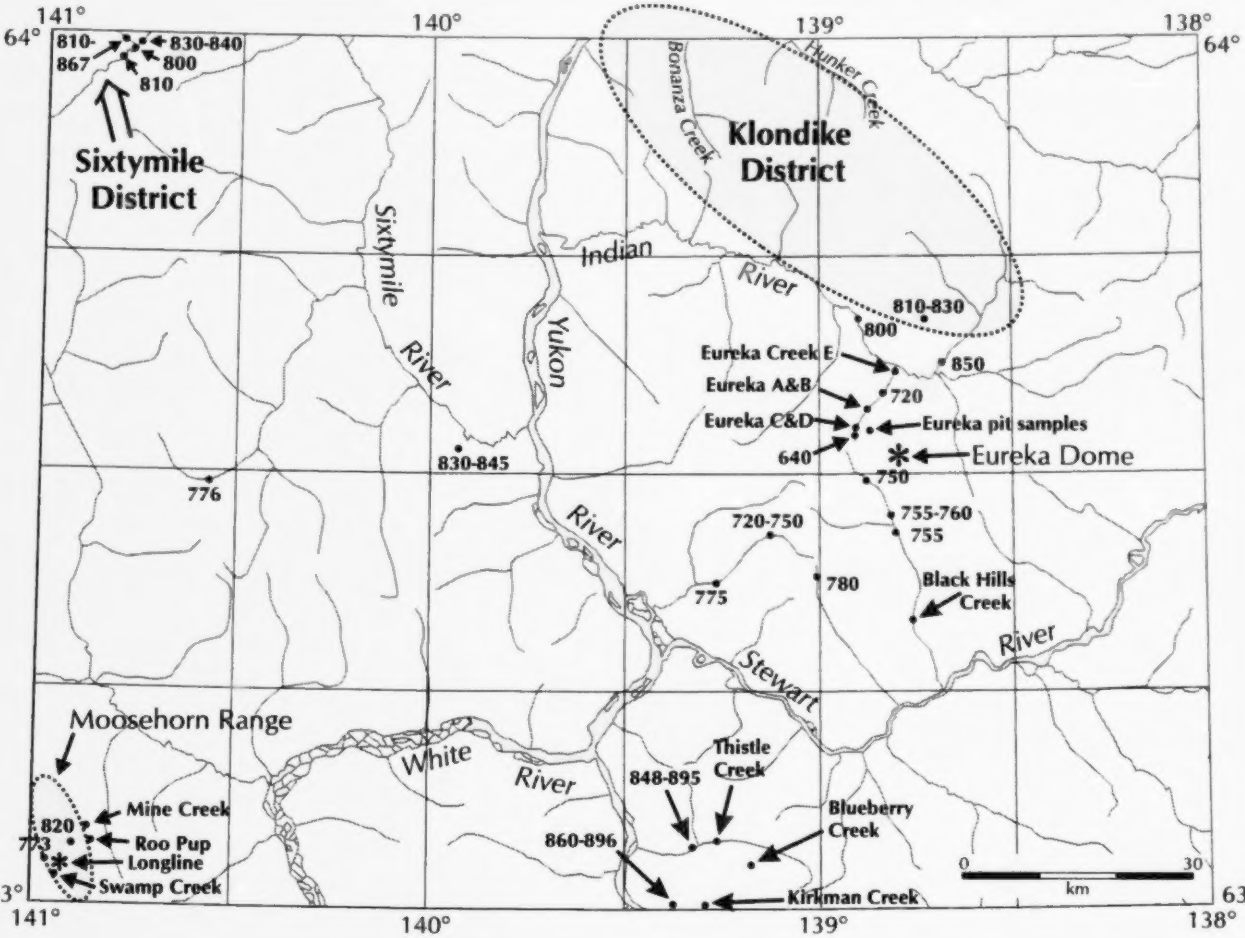
141°
140°
139°
138°
64°
64°
810-867
830-840
800
810
Sixtymile District
Bonanza Creek
Hunker Creek
Klondike District
Sixtymile River
Yukon River
Indian River
810-830
800
Eureka Creek E
850
Eureka A&B
720
Eureka C&D
Eureka pit samples
640
Eureka Dome
750
830-845
776
755-760
755
720-750
775
780
Black Hills Creek
Stewart River
Moosehorn Range
White River
Thistle Creek
848-895
Mine Creek
820
773
Roo Pup
Longline
Swamp Creek
860-896
Blueberry Creek
Kirkman Creek
0
30
km
63°
63°
141°
140°
139°
138°

*Figure 1. Map of the Stewart River area displaying locations of the samples investigated in this study, as well as reported bullion fineness values from some of the major placer streams in the area (data from Debicki, 1982, 1983; Debicki and Gilbert, 1986; Lebarge and Morison, 1990).*

Placer gold is present in streams throughout the Stewart River map area. Major placer deposits occur in the Klondike and Sixtymile districts, as well as the Indian River, tributaries of the lower Stewart River (including Black Hills and Scroggie creeks), and Thistle and Kirkman creeks (Fig. 1). Minor placer gold producers include Eureka Creek as well as Mine Creek and Swamp Creek in the Moosehorn Range (Fig. 1).

## PLACER GOLD FEATURE DEVELOPMENT

Both chemical and physical processes affect a gold grain between the time it is liberated from its lode source and the time it is recovered from a placer deposit. At the source, a gold particle is still attached to the host rock and the composition of the gold at the source is essentially unchanged from its composition at the time of formation. During transport downstream, silver is leached from the rim of the placer gold grain, leading to an increased bulk or 'bullion' gold fineness in the placer gold with increasing distance from the source. (Gold fineness refers to the relative amounts of silver and gold present; it is given as a number out of 1000 and is defined by Au/(Ag+Au)x1000, where Au and Ag are the weight percentages of Au and Ag present.) This leaching only occurs along exposed surfaces of the grain; therefore, a leached rim with a high fineness forms along the outer surfaces of the sample, leaving an unaltered core (Knight et al., 1994, 1999a). The thickness of the leached rim is a function of the distance (or length of time) the particle has traveled from the source. Gold located at or close to its original source can be expected to have at most, a very thin leached rim, and bulk or 'bullion' fineness of placer gold from such a region closely reflects that of the source.

Many physical processes also affect a gold particle during its transport downstream. As the particle travels downstream it is beaten by stream action, causing flattening, rounding, abrasion, and in some cases, folding of the grain. The surface appearance of the particles is thus affected by the time the grain has spent in transport (Knight et al., 1994). At the source, gold grains typically have an angular or hackly appearance. As stream processes work on the grain, the edges of the particle become more rounded, and, overall, the grain becomes more rounded in appearance. The particle will also be hammered as it travels down the stream, causing it to flatten and in some instances even fold over. Roundness and flatness increase dramatically within the first 5 km from the source, after which the roundness remains relatively unchanged (Knight et al. 1994, 1999b). Flattening of a gold particle requires a relatively large amount of transport, whereas rounding of a particle requires less transport and is commonly noticeable before much flattening is observed. Knight et al. (1994, 1999b) argued that grain roundness is a more sensitive measure for distances under 5 km, but grain flatness is a more reliable indicator of transport distances greater than 5 km. The original shape of the grain is also a factor in how the particle will be altered by the transport. A small flat grain will respond differently to these processes than a larger more equant grain.

The thickness of the leached rim on a placer gold grain is not an entirely effective method for gauging the distance from the source, since the abrasive action of the stream is also at work, and some of the rim will be removed. The leached rim can, however, provide a rough estimate of the minimum time since it has been liberated from its source, and an approximate distance from the source.

## METHODOLOGY

Most impurities in pan concentrates were removed using a Franz magnetic separator. The gold grains were then separated from other non-metallic minerals by hand. Samples were examined, and the habits of representative grains were documented.

Plexiglass disks 1 in. (2.5 cm) in diameter, each with three 3/8 in. (9.5 mm) diameter holes, were used as mounts for the gold grains. Double-sided tape was placed on a glass plate and the plexiglass disk placed on top of the tape. Representative grains from each of the sample sites were carefully placed into the mount with the aid of a binocular microscope. Each mount contained grains of equal size such that grains requiring similar amounts of grinding and polishing in order to expose the core were grouped together. Flat and elongated grains were placed on end so that when the mount was ground down and polished, the grain was not plucked out or ground away.

After the grains were carefully placed, each hole was carefully filled in with epoxy. Buehler epoxy resin was used in this study. A toothpick was used to drop in the epoxy. Care was taken to avoid disturbing the grains and to exclude air bubbles in the epoxy. A fine piece of wire was used to gently ease out any major bubbles.

Once the epoxy hardened, 600-grit wet-dry sandpaper was used to grind the mounts down to the desired level. One-micron diamond paste was then used to remove the major scratches from the surface of the mount and a final polish was done using a 0.05-micron alumina powder. An ultrasonic scrubber was used to clean each sample mount between each of the polishing stages. Once the mounts were polished and cleaned using an ultrasonic scrubber, they were carbon coated for examination with the scanning electron microscope (SEM) and electron microprobe (EMP). The SEM was used in backscatter mode to examine each particle to identify weathered zones, leached rims, internal structure, and other important features. Photographs were taken using the SEM to help select specific sample sites for EMP analysis.

Concentrations of Au, Ag, Cu and Hg in the gold were determined using the EMP. A spot size of 1 micron was used. Count time for Au was 20 000 ms, and count time for the remaining elements was 150 000 ms each. A minimum of two points were selected on each grain, taking care to avoid pores, weathered surfaces, scratches, and other deformities that could affect the results. In total, 228 points were analysed from 77 different grains. Three measurements of a standard were made, at the beginning, midpoint, and end of the analytical run. From these 228 sample points, 195 had a total weight percent of 95 or higher, and were considered to be within the acceptable limits. Points totaling less than 95% were likely situated over a piece of gangue, or a pore, and are not included in the following discussion.

The standard consisted of 80% Au and 20% Ag. It was analysed three times and determined to have 20.1445, 20.1159 and 20.0959 wt% Ag, and 79.2806, 78.8039 and 79.3642 wt% Au, respectively, for the three analyses. Copper and mercury were measured at 0.0001 and 0.0002, respectively for each analysis, which is well below the detection limit and well below the standard deviation. Although the standard was not considered to be in the best condition, all of these analyses fall within two standard deviations of the accepted value. For all of the analyses of unknown gold, average detection limits were as follows: Cu=0.02 wt%, Ag=0.04 wt%, Au=0.2 wt%, Hg=0.08 wt%. The average overall standard deviation for each element was as follows: Cu=0.018 wt%, Ag=0.208 wt%, Au=0.991 wt%, and Hg=0.052 wt%.

## RESULTS

Gold grains from eight different creeks from the study area, Eureka Creek, Black Hills Creek, Thistle Creek, Blueberry Creek (tributary to Thistle Creek), Kirkman Creek, Swamp Creek, Mine Creek, and Roo Pup (tributary to Mine Creek; Fig. 1) were analysed. Individual grains analysed varied in size between 0.5 mm and 5 mm.

In general, leached rims on gold particles closer to the headwater of streams (closer to the source) are thin or absent in backscatter images. Leached rims were not visible in the majority of the grains examined in this study. A large number of grains, however, show very high porosity. It is uncertain whether this was primary porosity or was caused by the plucking of inclusions during the polishing process. Gold from all of the sample locations, except for the pit samples on Eureka Dome, showed some porosity, and some grains also showed a rim of very low porosity with a highly porous core. A backscatter image of a grain of placer gold from lower Eureka Creek with a well-developed leached rim and high porosity is shown in Figure 2.

### EUREKA CREEK PLACER AND COLLUVIAL GOLD

Eureka Creek placer gold samples were collected from three different locations along the creek (Eureka A & B, Eureka C & D, and Eureka E; Fig. 1). Gold grain samples closer to the headwaters, and at a midpoint in the creek, were thick, with uneven surfaces and minor evidence of hammering. Bits of wallrock were attached to some of these particles. There was some variation in surface colour among these samples, varying between a silvery to a golden colour. Grains further down Eureka Creek were flattened with well-rounded edges and a pitted surface. Gold grains from hand trenches in colluvium on Eureka Dome (considered to be representative of underlying lode sources) were very angular with rough edges. Some surfaces were very smooth. One particular sample was an extremely thin flake with no evidence of hammering.

Grain mounts of placer gold from Eureka Creek show significant variations in gold composition within the grain in back-scatter images. This internal variation is interpreted to be a primary feature within the grain, and not related to alteration of the grain during or after transport. Deformation of the grain is quite evident. Some particles from Eureka C also show an apparent silver enrichment along fractures. Some samples from Eureka Creek had a 'granular' appearance with gold-rich zones present throughout the entire grain. The processes that formed the silver-enriched zones and granular texture are not completely understood, but are thought to be late- or post-mineralization due to their association with fractures and grain boundaries. Grains from the Eureka Creek placer gold samples show well-developed leached rims (Fig. 2).

A total of 123 points were analysed from the Eureka Creek samples, including Eureka A (12 grains, 30 points), Eureka B (9 grains, 22 points), Eureka C (11 grains, 54 points), Eureka E (6 grains, 11 points) and Eureka Pit samples (5 grains, 6 points). A few of the grains from Eureka C were analysed using seven to nine points, compared to the average of two for all other samples. This caused the data to be more heavily weighted towards the trends of those few grains rather than an average of all the grains. These grains were analysed more extensively as an attempt to determine the nature of unusual internal grain structure found only in grains from Eureka C.

Grains from Eureka Creek (including those from the hand pit) have fineness values less than 800, with a significant number less than 700 (Appendix 1). Many of the points from the Eureka C grains, which were re-analysed several times, had fineness values below 500, and should therefore be termed electrum. For all but two points, Cu values were below the detection limit (Appendix 1). A large number of measured Hg values in the Eureka Creek gold are relatively high (greater than 1.7 wt%), although the average value of 0.04 wt% is actually below the detection limit (Appendix 1).

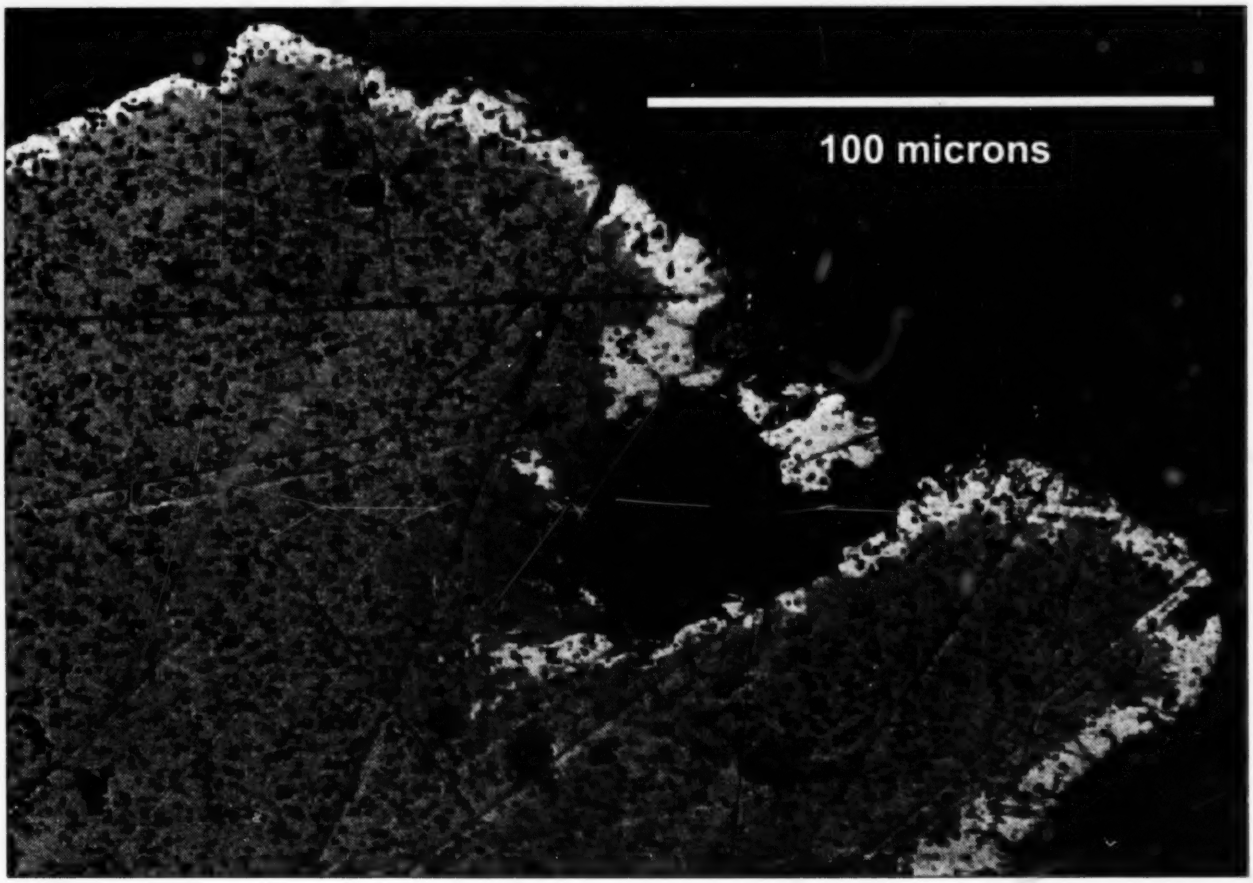

*Figure 2. Back-scatter image of part of a placer gold grain from lower Eureka Creek, showing a well-developed leached rim (pale grey) surrounding an unleached core (darker grey). Note the irregular nature of the contact between the rim and core, and the high degree of porosity in the grain.*

### *Black Hills Creek*

Grains collected from Black Hills Creek were very fine with rounded edges. All of these grains showed signs of hammering. The grain shape was commonly thin and flaky, or pebbly in appearance, although a few grains were very long and slender.

Five grains from Black Hills Creek were analysed for a total of six points. The fineness values from these points ranged from 666-753. None of the points had Cu contents over the detection limit. Two of the points had Hg levels below the detection limit, two points had values around 0.28 wt% and another two had values of 0.63 wt% and 0.89 wt%.

### *Mine Creek, Swamp Creek and Roo Pup*

Mine Creek and Roo Pup in the Moosehorn Range (Fig. 1) produced grains with well-rounded edges and grains in many different shapes, ranging from long and slender to very thin. Some inclusions of wallrock were present, and most grains were thick. Only minor colour variations were observed. Swamp Creek placer gold forms very angular grains with uneven surfaces, attached wallrock, and little evidence of hammering. Gold from Swamp Creek varies in colour from pale brassy colour to a more golden colour.

Eighteen points from eight different grains were analysed from Swamp Creek. All of the fineness values were above 800, except for two at 687 and 739. All but one of the Cu values were below the detection limit. The Hg values were all lower than the detection limit, except for three points. Eleven points from five different grains were analysed from Mine Creek; these yielded fineness values between 750 and 900. Six points yielded Cu values below the detection limit, whereas the remaining averaged around 0.032 wt% Cu. The Hg values were all below the detection limit, except for three points, which had values between 0.21 and 0.27 wt% Hg. Eight points from four different grains from Roo Pup were analysed, and yielded fineness values between 790 and 900. All but two of the Cu values were below the detection limit. Most of the Hg values were around 0.10 wt%, with two below the detection limit, and two around 1.5 wt%.

### *Thistle, Blueberry and Kirkman creeks*

Placer gold grains from Thistle Creek were mostly flattened with rounded edges, and minor inclusions of wallrock. Some grains appeared to be folded flakes. Blueberry Creek produced flat grains with angular to rounded edges. Only small amounts of wallrock inclusions were present, and almost all of the grains show signs of hammering. Grains from Kirkman Creek were flattened with rounded edges and minor inclusions of wallrock. Some grains from Kirkman Creek were elongated, and some showed signs of folding. All grains showed signs of hammering. Grains from Kirkman Creek showed particularly well-developed leached rims.

Four grains from Kirkman Creek were analysed with eleven points. All of these points had fineness values greater than 730. Three points had Cu values above the detection limit, ranging from 0.025-0.032 wt%. Mercury levels were all below 0.75 wt%, with an average around 0.23 wt%. Four grains from Blueberry Creek were analysed with eight points. All of the fineness values were between 735 and 910. Four of the copper values were below the detection limit, and three were around 0.044 wt%. One point had a Cu value around 0.031 wt%. Mercury levels were all below 0.044 wt%, with four points below the detection limit. Four grains from Thistle Creek were analysed with ten different points. Fineness values were between 825 and 925. Four of the Cu levels were below the detection limit, while six fell between 0.02 and 0.03 wt%. Mercury levels averaged around 0.4 wt%, with three values around 0.6 wt%, and two values below the detection limit.

## DISCUSSION

Compositions of placer and colluvial gold analysed in this study, together with the main fields of data previously published from the Klondike District (Knight et al., 1999a) are shown on fineness vs. Cu and fineness vs. Hg in Figures 3 and 4. Compositions of gold from Eureka Creek are distinct from most other samples analysed in the study. Copper concentrations in this gold are low with almost all analyses below the detection limit of 0.02%. Mercury values, on the other hand, are relatively high with a wide range of values, averaging about 0.45%. Fineness values are low, mainly below 800. In terms of physical characteristics, samples collected near the headwaters of these streams showed relatively minor physical alteration, whereas samples from further downstream showed considerable alteration and development of leached rims. There was no noticeable change in the composition of the core of the gold relative to the sample location. Gold grains found in exploration pits dug in colluvium near

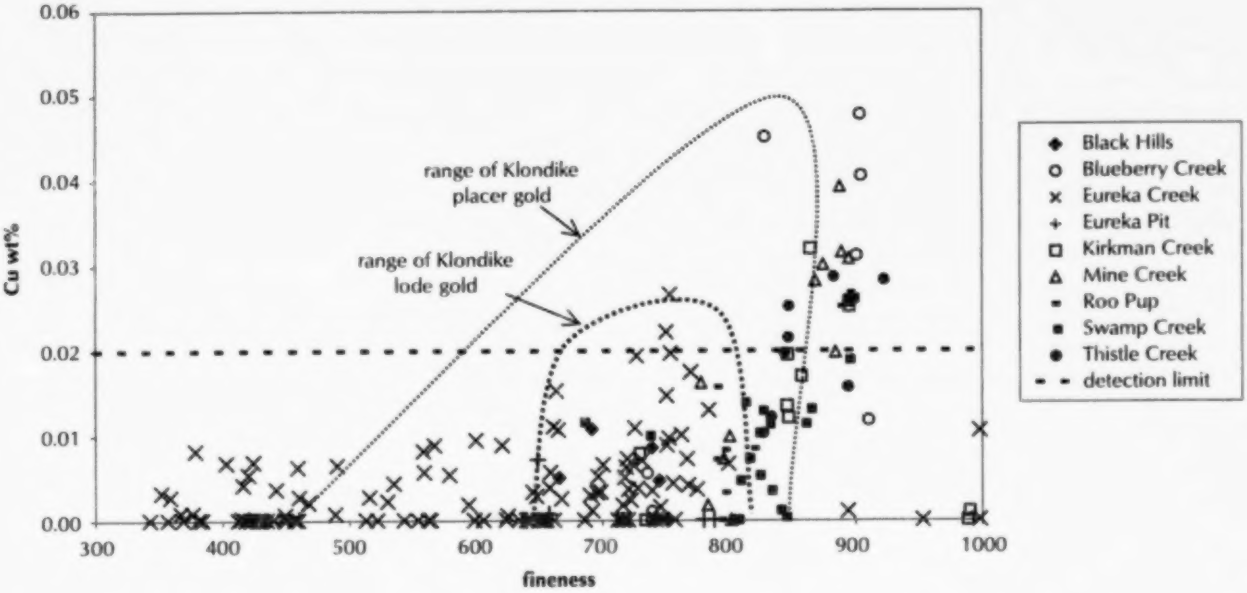

***Figure 3.*** *Plot of measured Cu wt.% against fineness for gold analysed in this study. Also shown are the compositional fields for Klondike District lode and placer gold from Knight et al. (1999a). Detection limit is shown by the dashed line. Copper contents shown for analyses that plot below the detection limit are based on total counts obtained during each analysis.*

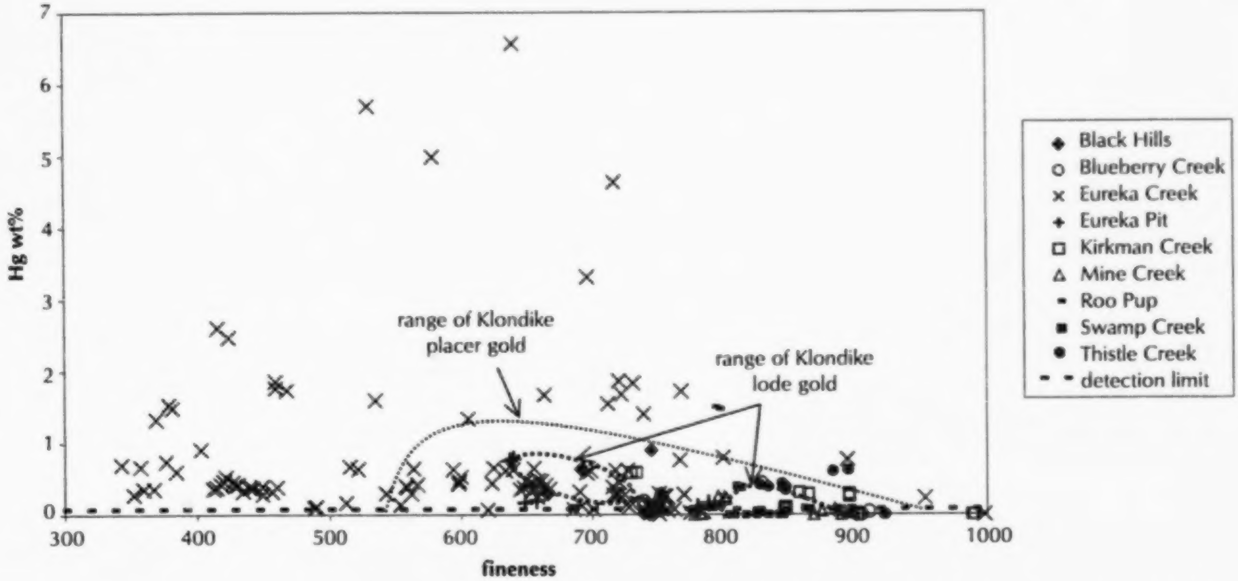

***Figure 4.*** *Plot of measured Hg wt.% against fineness for gold analysed in this study. Also shown are the compositional fields for Klondike District lode and placer gold from Knight et al. (1999a). Detection limit is shown by the dashed line. Mercury contents shown for analyses that plot below the detection limit are based on total counts obtained during each analysis.*

Eureka Dome are thought to be close to the lode source due to the fact that they are located near a topographic high point, are very rough and angular, and apparently have not been transported. Eureka Dome is located near the headwaters of Eureka Creek, and it is likely that the pit samples are representative of the source of at least some of the placer gold in these creeks. Analyses of these colluvial gold samples showed them to be compositionally similar to the placer gold from Eureka Creek, supporting this interpretation. Placer gold in Black Hills Creek is similar to that in Eureka Creek (see later discussion).

Although no definite lode gold occurrences have been identified thus far in the Eureka Dome area, there are abundant Late Cretaceous volcanic rocks with associated high level porphyry dykes in the area, and the composition of the pit and placer gold are typical of samples from epithermal vein sources (e.g., Morrison et al., 1991). It is therefore suggested that significant epithermal vein system(s) exist in the area and supplied gold to the placer deposits.

In contrast, gold from streams draining the Moosehorn Range (Swamp Creek, Mine Creek and Roo Pup) has a compositional range that is quite distinct from placers in the Eureka Dome area. Swamp Creek drains the southwestern side of the Moosehorn Range, whereas Roo Pup and Mine Creek drain the northeast side of the Moosehorn Range. All of the placer samples were taken from near the headwaters of the creeks. The grains were mainly angular in shape, showed little hammering, and were commonly still attached to pieces of wallrock. The source of gold for all three creeks is believed to come from a similar source(s) along the upper part of Moosehorn Range. Gold compositions for all of these creeks are generally similar, as expected for gold coming from the same source. Measured fineness for Moosehorn Range placer gold is high, mostly above 750. Copper values from these creeks are noticeably higher than values from the Eureka Dome area, although a very small proportion of grains from Eureka Creek also had copper contents well above the detection limit. Mercury values in the Moosehorn Range placer gold are generally distinctly lower than those from the Eureka Dome area.

Placer gold in streams draining the Moosehorn Range is thought to come from lode sources at the top of this range. The Longline occurrence comprises intrusion-related, mesothermal, gold-bearing quartz vein systems that occur along the crest and on the western side of the Moosehorn Range (MacDonald, 2001). Although compositions of lode gold from the Longline occurrence were not determined, it is reasonable to conclude that the placer gold in this area was derived from Longline-type veins, and measured compositions are therefore representative of the gold in the veins themselves. The relatively high fineness, moderate to high Cu contents, and low Hg contents in the gold is consistent with derivation from an intrusion-related source.

Placer gold in Thistle, Blueberry and Kirkman creeks shows generally similar compositions to that from the Moosehorn Range, suggesting derivation from a similar type of lode mineralization.

Results of this study, together with previous published results from the Klondike District (Knight et al., 1999a), therefore provide distinct compositional ranges for gold from each drainage area. These compositional ranges are consistent with gold derivation in each drainage from epithermal veins, intrusion-related mesothermal veins, or metamorphic gold-bearing veins.

Fineness values determined in this study are similar to bulk fineness values found by previous workers. Figure 1 shows the locations of placer gold samples investigated in this study and previously reported bulk fineness values for some of the placer creeks in the study area. Bulk fineness values reflect a combination of high fineness leached rims and unleached cores; thus bulk fineness values represent a maximum fineness for the core compositions and therefore the lode source(s) from which the gold was derived. Most placer gold grains examined in this study had relatively thin leached rims, and fineness values determined for cores of grains are therefore similar to reported bulk fineness values in the same area.

## APPLICATION OF THE GOLD COMPOSITION MODEL TO EXPLORATION

Although our study was somewhat limited both in scope and in the total number of analyses carried out, several significant first-order implications for gold exploration in the area can be derived from the data.

1. Gold from Black Hills Creek shows low Cu concentrations, high Hg, and fineness values below 800, and is very similar to gold from Eureka Creek. Black Hills Creek drains the southeast side of Eureka Dome, and the gold compositional data can be interpreted to suggest that the source of the gold in Eureka Creek and

Black Hills Creek consists of epithermal vein occurrences in the Eureka Dome area.

2. Measured fineness values for gold from Blueberry Creek were all above 700, with a large number of analyses around 900. Similarly, gold from Thistle Creek yields fineness values between 825 and 925. Gold from both streams also shows relatively high Cu values, and gold from Thistle Creek has somewhat higher Hg contents than that from Blueberry Creek. Compositions of placer gold from these two streams is similar to that from creeks in the Moosehorn Range, suggesting that the lode source for gold in Thistle Creek and its tributaries is similar to that in the Moosehorn Range. The higher Hg levels in Thistle Creek may indicate that there is more than one lode source contributing gold to Thistle Creek and its tributaries. Gold from Blueberry Creek and Thistle Creek both appeared to have traveled some distance based on grain shape, although that from Blueberry Creek is less-traveled than that from Thistle Creek. This helps constrain the location of the lode source(s) to near the headwaters of these creeks.
3. Kirkman Creek gold all has a fineness greater than 700. Mercury values were moderate, and most measured copper contents were below the detection limit, except for some significantly high points. The presence of scattered high Cu concentrations and high fineness values are similar to what is observed in Moosehorn Range samples. Gold samples from Kirkman Creek were flat and showed a significant leached rim development, suggesting that the gold has traveled a considerable distance. Kirkman Creek and Thistle Creek are approximately 8 km apart, and are located on either side of a drainage divide. Blueberry Creek also drains this same divide. The gold compositional data from these three creeks is consistent with all the gold having been derived from a similar source, and perhaps from a single lode occurrence. The data further suggests that the lode source(s) is likely to be similar to the intrusion-related gold-quartz veins in the Moosehorn Range.
4. Distinct, although partly overlapping, compositional fields can be derived for placer gold from each creek studied in the Stewart River area, using a combination of fineness, Cu wt% and Hg wt%. Plots of Cu wt% and Hg wt% vs. fineness (Figs. 3 and 4), when superimposed on compositional ranges for gold from the Klondike District (from Knight et al., 1999a), also show considerable overlap. The Klondike study demonstrated that Klondike placer gold was derived largely, if not entirely, from mesothermal gold-quartz veins of 'metamorphogenic' origin (Rushton et al., 1998; Knight et al., 1999a). It appears that gold sources for such veins cannot be conclusively distinguished from gold from epithermal or intrusion-related sources using only elements that are detectable by EMP methods.

Western Yukon contains many placer gold deposits; however the ultimate lode source(s) for this placer gold has not yet been identified for most placer streams. Gold exploration in the region over the past decade has also identified a very large number of gold anomalies in soil, silt and heavy mineral surveys. Many different styles of lode gold are known to exist in the region, but only a small number of these are likely to have economic potential. In view of the poor exposure in the region and the still relatively poor understanding of the geology and mineral deposits of the area, it would therefore be very useful to be able to classify gold anomalies (and sources of placer gold) in terms of the likely style of lode gold in the source. This would allow follow-up exploration work to be focused on anomalies that were related to potentially economic sources, and would thus make exploration programs considerably more time- and cost-effective. The results of our study suggest that gold compositional data can provide such a geochemical 'fingerprint' for constraining the likely lode source(s) of placer and colluvial gold, and thus evaluating anomalies.

## FUTURE WORK

This study comprised a relatively small number of analyses from a limited sample suite. However, the data clearly demonstrate that a relationship exists between the composition of placer gold and the style of lode mineralization from which the placer gold was derived. A larger data set for the deposits used in this study would be needed before this relationship can be widely applied to gold exploration in the region. A larger data set would create a more defined statistical range of compositions for each deposit type, and create a more specific geochemical fingerprint for these deposits. Work should also be done to characterize gold from other styles of lode mineralization over a larger study area.

This and previous studies in the region have used electron microprobe (EMP) methods to determine gold compositions. EMP analytical capability is widely available and the method is relatively inexpensive; however, it is limited to elements that are present at a level of at least a fraction of a percent. Application of more sensitive analytical methods such as laser ablation, high resolution

ICP-MS would make it possible to determine the concentrations of a much wider range of elements (including Bi, As, Te, etc.) down to extremely low concentrations (sub-ppb). This would allow a much more complete and specific geochemical signature to be established for different lode and placer deposits and therefore a more efficient geochemical 'filter' to be applied for gold anomaly evaluation purposes.

## ACKNOWLEDGMENTS

This study forms the bulk of a senior thesis in Geological Engineering by the first author at the University of British Columbia (UBC). The authors thank Lionel Jackson from the Geological Survey of Canada and Bill Wengynowski of Expatriate Resources for providing the samples used in the study and for their on-going interest in the project. Mati Raudsepp was invaluable in helping set up the EMP analyses at UBC.

## REFERENCES

British Columbia and Yukon Chamber of Mines, 2000. The Tintina Gold Belt: Concepts, Exploration, and Discoveries. Cordilleran Roundup, January, 2000, T.L. Tucker and M.T. Smith (session chairs), Special Volume 2, 225 p.

Chapman, R.J., Leake, R.C., Moles, N.R., Earls, G., Cooper, C., Harrington, K. and Berzins, R., 2000. The application of microchemical analysis of alluvial gold grains to the understanding of complex local and regional gold mineralization: A case study in the Irish and Scottish Caledonides. Economic Geology, vol. 95, no. 8, p. 1753-1773.

Glasmacher, U. and Friedrich, G., 1992. Volcanic-hosted epithermal gold-sulphide mineralization and associated enrichment processes, Sixtymile River area, Yukon Territory, Canada. *In:* Yukon Geology Volume 3, Exploration and Geological Services Division, Yukon Region, Indian and Northern Affairs Canada, p. 271-291.

Knight, J.B., 1985. A microprobe study of placer gold and its origin in the lower Fraser River drainage basin, B.C. Unpublished M.Sc. thesis, University of British Columbia, 197 p.

Knight, J.B., Mortensen, J.K., and Morison, S.R., 1994. Shape and composition of lode and placer gold from the Klondike District, Yukon, Canada. Exploration and Geological Services Division, Yukon Region, Indian and Northern Affairs Canada, Bulletin 3, 142 p.

Knight, J.B., Mortensen, J.K. and Morison, S.R., 1999a. Lode and placer gold composition in the Klondike District, Yukon Territory, Canada: Implications for the nature and genesis of Klondike placer and lode gold deposits. Economic Geology, vol. 94, p. 649-664.

Knight, J.B., Morison, S.R. and Mortensen, J.K., 1999b. The relationship between placer gold particle shape, rimming, and distance of fluvial transport as exemplified by gold from the Klondike District, Yukon Territory, Canada. Economic Geology, vol. 94, p. 635-648.

LeBarge, W.P. and Morison, S.R., 1990. Yukon Placer Mining and Exploration 1985-1988. Exploration and Geological Services Division, Yukon Region, Indian and Northern Affairs Canada, 151 p.

MacDonald, N., 2001. Geology of the intrusive-hosted Longline gold prospect, Moosehorn Range, Yukon Territory. Mineral Deposit Research Unit Technical Notes, p. 29-38.

Morrison, G.W., Rose, W.J. and Jaireth, S., 1991. Geological and geochemical controls on the silver content (fineness) of gold in gold-silver deposits. Ore Geology Reviews, vol. 6, no. 4, p. 333-364.

Mortensen, J.K., Hart, C.J.R., Murphy, D.C. and Heffernan S., 2000. Temporal evolution of Early and mid-Cretaceous magmatism in the Tintina gold belt. *In:* The Tintina Gold Belt: Concepts, Exploration, and Discoveries, British Columbia and Yukon Chamber of Mines Cordilleran Roundup, January, 2000, T.L. Tucker and M.T. Smith (session chairs), Special Volume 2, p. 49-57.

Palacios, C., Herail, G., Rivas, P., Sepulveda, F., Townley, B., Maksaev, V., Lahsen, A. and Parada, M., 1999a. Geochemistry of gold grains in the Cerro Casale porphyry gold deposit, Maricunga Belt, Northern Chile. Comunicaciones, no. 50, p. 43-47.

Palacios, C., Herail, G., Ulloa, C., Maksaev, V., Townley, B., Parseval, P., Orellana, R., Lahsen, A. and Parada, M., 1999b. Geochemistry of gold crystals in epithermal, gold porphyry, and gold-rich copper porphyry deposits: A discrimination model. Comunicaciones, no. 50, p. 65-69.

Palacios, C., Sepulveda, F., Parseval, P., Herail, G., Maksaev, V., Townley, B., Lahsen, A. and Parada, M., 1999c. Vertical zonation of copper and silver in gold crystals at the Cerro Casale gold porphyry deposit, Maricunga Belt, Northern Chile. Comunicaciones, no. 50, p. 77-79.

Palacios, C., Ulloa, C., Sepulveda, F., Maksaev, V., Herail, G., Townley, B., Lahsen, A. and Parada, M., 1999d. Morphologic and chemical characteristics of gold grains: Methodologic improvements for gold-bearing deposit exploration. *In:* Active Continental Margins. Comunicaciones, no. 50, p. 97-100.

Rushton, R.W., Nesbitt, B.E., Muelenbachs, K. and Mortensen, J.K., 1998. Au-quartz veins in the Klondike District, Yukon Territory, Canada: A section through a mesothermal vein system. Economic Geology, vol. 88, p. 647-678.

## APPENDIX 1. ELECTRON MICROPROBE ANALYSES OF GOLD FROM THE STEWART RIVER MAP AREA.

| Location | Sample | Label | wt%(Cu) | wt%(Ag) | wt%(Au) | wt%(Hg) | Total wt% | Fineness | Comments |
|---|---|---|---|---|---|---|---|---|---|
| Black Hills Creek | B61-1 | 121 | 0.0051 | 33.0565 | 65.8841 | 0.2821 | 99.2278 | 666 | |
| Black Hills Creek | B61-2 | 122 | 0.0108 | 30.327 | 68.0415 | 0.6301 | 99.0094 | 692 | |
| Black Hills Creek | B63-1 | 119 | 0.0086 | 25.574 | 72.6265 | 0.0065 | 98.2156 | 740 | |
| Black Hills Creek | B63-2 | 120 | 0.0001 | 25.7951 | 74.9958 | 0.0002 | 100.7912 | 744 | |
| Black Hills Creek | B64-1 | 117 | 0.0001 | 24.0108 | 70.2388 | 0.3235 | 94.5732 | 745 | |
| Black Hills Creek | B64-2 | 118 | 0.0001 | 23.7912 | 72.5753 | 0.2867 | 96.6533 | 753 | |
| Black Hills Creek | B65-1 | 115 | 0.0067 | 17.8754 | 75.7641 | 0.7002 | 94.3464 | 809 | |
| Black Hills Creek | B65-2 | 116 | 0.0047 | 24.7398 | 72.5193 | 0.8943 | 98.1581 | 746 | |
| Blueberry Creek | BL412-1 | 161 | 0.0154 | 11.5705 | 73.1558 | 0.1148 | 84.8565 | 863 | |
| Blueberry Creek | BL412-2 | 162 | 0.0118 | 8.8298 | 89.4832 | 0.0395 | 98.3643 | 910 | |
| Blueberry Creek | BL412-3 | 163 | 0.0062 | 12.1037 | 75.743 | 0.1491 | 88.002 | 862 | |
| Blueberry Creek | BL44-1 | 158 | 0.0452 | 16.9353 | 81.962 | 0.4406 | 99.3831 | 829 | |
| Blueberry Creek | BL44-2 | 159 | 0.0173 | 13.9772 | 72.2925 | 0.4595 | 86.7465 | 838 | |
| Blueberry Creek | BL44-3 | 160 | 0.1583 | 16.2542 | 73.5348 | 0.948 | 90.8953 | 819 | |
| Blueberry Creek | BL46-1 | 155 | 0.0011 | 25.4025 | 72.2542 | 0.1263 | 97.7841 | 740 | |
| Blueberry Creek | BL46-2 | 156 | 0.0001 | 25.9478 | 73.716 | 0.189 | 99.8529 | 740 | |
| Blueberry Creek | BL46-3 | 157 | 0.0056 | 25.9285 | 72.2916 | 0.1643 | 98.39 | 736 | |
| Blueberry Creek | BL47-1 | 152 | 0.0312 | 9.5868 | 87.1051 | 0.0002 | 96.7233 | 901 | |
| Blueberry Creek | BL47-2 | 153 | 0.0478 | 9.6251 | 90.3232 | 0.0002 | 99.9963 | 904 | |
| Blueberry Creek | BL47-3 | 154 | 0.0406 | 9.5614 | 90.5075 | 0.0002 | 100.1097 | 905 | |
| Eureka A | EA41-1 | 138 | 0.0037 | 27.7033 | 71.5273 | 0.4427 | 99.677 | 721 | |
| Eureka A | EA41-2 | 139 | 0.0194 | 27.2009 | 72.5891 | 0.6185 | 100.4279 | 727 | |
| Eureka A | EA42-1 | 135 | 0.0011 | 10.5026 | 88.5586 | 0.7633 | 99.8256 | 894 | |
| Eureka A | EA42-2 | 136 | 0.0054 | 40.5154 | 55.6893 | 4.9956 | 101.2057 | 579 | |
| Eureka A | EA42-3 | 137 | 0.0023 | 44.0119 | 49.6139 | 5.6998 | 99.3279 | 530 | |
| Eureka A | EA43-1 | 132 | 0.0001 | 33.1876 | 58.9802 | 6.5669 | 98.7348 | 640 | |
| Eureka A | EA43-2 | 133 | 0.0153 | 33.0263 | 65.1166 | 1.6726 | 99.8308 | 664 | |
| Eureka A | EA43-3 | 134 | 0.0026 | 32.5716 | 65.3651 | 0.3612 | 98.3005 | 667 | |
| Eureka A | EA45-1 | 124 | 0.0156 | 22.0504 | 72.5024 | 0.3 | 94.8684 | 767 | |
| Eureka A | EA45-2 | 125 | 0.0097 | 24.415 | 74.559 | 0.1643 | 99.148 | 753 | |
| Eureka A | EA45-3 | 126 | 0.0001 | 20.1857 | 67.9107 | 0.1915 | 88.288 | 771 | |
| Eureka A | EA46-1 | 127 | 0.0001 | 38.3207 | 58.7876 | 1.3319 | 98.4403 | 605 | |
| Eureka A | EA46-2 | 128 | 0.0029 | 34.4636 | 63.3305 | 0.3787 | 98.1757 | 648 | |
| Eureka A | EA46-3 | 129 | 0.0001 | 4.6393 | 94.2369 | 0.2287 | 99.105 | 953 | |
| Eureka A | EA47-1 | 130 | 0.0057 | 33.5499 | 64.7491 | 0.4779 | 98.7826 | 659 | |
| Eureka A | EA47-2 | 131 | 0.0111 | 33.363 | 65.0891 | 0.4625 | 98.9257 | 661 | |
| Eureka A | EA51-1 | 177 | 0.0001 | 39.4004 | 58.6173 | 0.4306 | 98.4484 | 598 | |
| Eureka A | EA51-2 | 178 | 0.0001 | 39.2774 | 58.5177 | 0.4658 | 98.261 | 598 | |
| Eureka A | EA51-3 | 179 | 0.0095 | 39.3824 | 59.0048 | 0.5258 | 98.9225 | 600 | |
| Eureka A | EA52-1 | 174 | 0.0175 | 22.711 | 76.2937 | 0.2795 | 99.3017 | 771 | |
| Eureka A | EA52-2 | 175 | 0.0042 | 22.2436 | 73.8917 | 1.722 | 97.8615 | 769 | |
| Eureka A | EA52-3 | 176 | 0.0073 | 22.8723 | 75.4993 | 0.7552 | 99.1341 | 768 | |
| Eureka A | EA53-1 | 170 | 0.0044 | 23.998 | 74.5884 | 0.2594 | 98.8502 | 757 | |
| Eureka A | EA53-2 | 171 | 0.0197 | 24.0547 | 74.0605 | 0.2565 | 98.3914 | 755 | |
| Eureka A | EA53-3 | 172 | 0.0147 | 24.7135 | 74.7927 | 0.2924 | 99.8133 | 752 | |
| Eureka A | EA53-4 | 173 | 0.0266 | 24.2574 | 74.3936 | 0.2543 | 98.9319 | 754 | |
| Eureka A | EA54-1 | 168 | 0.0065 | 49.9837 | 47.9719 | 0.1065 | 98.0686 | 490 | |
| Eureka A | EA54-2 | 169 | 0.0008 | 49.9375 | 47.6639 | 0.0912 | 97.6934 | 488 | |
| Eureka A | EA55-1 | 166 | 0.013 | 21.4004 | 77.9871 | 0.0358 | 99.4363 | 785 | |
| Eureka A | EA55-2 | 167 | 0.0037 | 22.4378 | 77.3999 | 0.0251 | 99.8665 | 775 | |
| Eureka A | EA56-1 | 164 | 0.0089 | 24.5026 | 74.1425 | 0.0066 | 98.6606 | 752 | |
| Eureka A | EA56-2 | 165 | 0.0222 | 24.6193 | 74.4335 | 0.0945 | 99.1695 | 752 | |
| Eureka B | EB210-1 | 92 | 0.0056 | 10.1897 | 83.301 | 0.0117 | 93.508 | 891 | apparent high fineness zone |
| Eureka B | EB210-2 | 93 | 0.003 | 30.5071 | 68.1082 | 0.3183 | 98.9366 | 691 | |
| Eureka B | EB210-3 | 94 | 0.0107 | 33.1343 | 65.7022 | 0.4088 | 99.256 | 665 | |
| Eureka B | EB21-1 | 81 | 0.0035 | 25.7178 | 73.1064 | 1.4029 | 100.2306 | 740 | |

| Location | Sample | Label | wt%(Cu) | wt%(Ag) | wt%(Au) | wt%(Hg) | Total wt% | Fineness | Comments |
|---|---|---|---|---|---|---|---|---|---|
| Eureka B | EB21-2 | 82 | 0.0071 | 26.0642 | 71.0795 | 1.8322 | 98.983 | 732 | |
| Eureka B | EB21-3 | 83 | 0.0106 | 0.2085 | 101.7449 | 0.0002 | 101.9642 | 998 | |
| Eureka B | EB23-1 | 84 | 0.0001 | 33.9145 | 64.5252 | 0.6456 | 99.0854 | 656 | non porous rim |
| Eureka B | EB23-2 | 85 | 0.0001 | 34.0763 | 64.3886 | 0.3317 | 98.7967 | 654 | non porous rim |
| Eureka B | EB23-3 | 86 | 0.0001 | 33.6481 | 65.7676 | 0.3503 | 99.7661 | 662 | |
| Eureka B | EB25-1 | 87 | 0.0109 | 27.0076 | 71.5542 | 0.1399 | 98.7126 | 726 | non porous rim |
| Eureka B | EB25-2 | 88 | 0.0044 | 14.6799 | 53.5989 | 0.1352 | 68.4184 | 785 | |
| Eureka B | EB27-1 | 89 | 0.0019 | 39.2067 | 57.3121 | 0.6327 | 97.1534 | 594 | |
| Eureka B | EB27-2 | 90 | 0.0001 | 41.4151 | 53.5232 | 0.6409 | 95.5793 | 564 | |
| Eureka B | EB27-3 | 91 | 0.0044 | 45.3771 | 52.1863 | 1.5979 | 99.1657 | 535 | |
| Eureka B | EB32-1 | 15 | 0.0018 | 27.999 | 70.6941 | 0.2721 | 98.967 | 716 | |
| Eureka B | EB32-2 | 16 | 0.0001 | 28.1248 | 70.8061 | 0.3863 | 99.3173 | 716 | |
| Eureka B | EB32-3 | 17 | 0.0051 | 27.9543 | 71.1281 | 0.6154 | 99.7029 | 718 | |
| Eureka B | EB33-1 | 20 | 0.0012 | 30.5388 | 68.6153 | 0.1234 | 99.2787 | 692 | |
| Eureka B | EB33-2 | 21 | 0.0039 | 33.9782 | 65.3188 | 0.2427 | 99.5436 | 658 | |
| Eureka B | EB33-3 | 22 | 0.0034 | 35.092 | 63.641 | 0.349 | 99.0854 | 645 | |
| Eureka B | EB36-1 | 13 | 0.0001 | 27.036 | 68.5753 | 4.6321 | 100.2435 | 717 | |
| Eureka B | EB36-2 | 14 | 0.0052 | 29.3352 | 67.3682 | 3.3143 | 100.0229 | 697 | |
| Eureka B | EB38-1 | 18 | 0.0033 | 30.2587 | 69.2431 | 0.5813 | 100.0864 | 696 | |
| Eureka B | EB38-2 | 19 | 0.0034 | 29.4626 | 68.3247 | 0.6069 | 98.3976 | 699 | |
| Eureka C | EC110-1 | 203 | 0.0001 | 47.916 | 50.4128 | 0.1627 | 98.4916 | 513 | |
| Eureka C | EC110-2 | 204 | 0.0001 | 54.6545 | 44.5311 | 0.2824 | 99.4681 | 449 | |
| Eureka C | EC110-3 | 205 | 1.1994 | 70.7129 | 1.0019 | 0.0001 | 72.9143 | 14 | |
| Eureka C | EC110-4 | 206 | 0.0001 | 55.7306 | 42.7809 | 0.3232 | 98.8348 | 434 | apparent low fineness zone |
| Eureka C | EC110-5 | 207 | 0.0001 | 56.7407 | 41.3486 | 0.5252 | 98.6146 | 422 | apparent low fineness zone |
| Eureka C | EC110-6 | 208 | 0.0054 | 57.1608 | 41.398 | 0.4611 | 99.0253 | 420 | apparent low fineness zone |
| Eureka C | EC110-7 | 209 | 0.0089 | 37.7129 | 61.5227 | 0.0661 | 99.3106 | 620 | |
| Eureka C | EC11-1 | 219 | 0.0101 | 23.3535 | 75.233 | 0.0777 | 98.6743 | 763 | |
| Eureka C | EC11-2 | 220 | 0.0001 | 44.1172 | 54.754 | 0.1403 | 99.0116 | 554 | apparent low fineness zone |
| Eureka C | EC11-3 | 221 | 0.0061 | 22.7457 | 69.0457 | 0.0522 | 91.8497 | 752 | apparent low fineness zone |
| Eureka C | EC11-4 | 222 | 0.0001 | 24.0322 | 75.2617 | 0.0602 | 99.3542 | 758 | |
| Eureka C | EC11-5 | 223 | 0.0001 | 40.6123 | 49.9337 | 0.176 | 90.7221 | 552 | apparent low fineness zone |
| Eureka C | EC11-6 | 224 | 0.0001 | 30.6173 | 66.869 | 0.0718 | 97.5582 | 686 | |
| Eureka C | EC14-1 | 210 | 0.0007 | 53.6973 | 43.7068 | 0.3871 | 97.7919 | 449 | |
| Eureka C | EC14-2 | 211 | 0.0001 | 55.3421 | 43.3427 | 0.3791 | 99.064 | 439 | |
| Eureka C | EC14-3 | 212 | 0.0028 | 53.0426 | 45.1445 | 0.3844 | 98.5743 | 460 | apparent high fineness zone |
| Eureka C | EC14-4 | 213 | 0.0033 | 63.8096 | 34.6371 | 0.2787 | 98.7287 | 352 | apparent low fineness zone |
| Eureka C | EC14-5 | 214 | 0.0001 | 45.0384 | 53.4669 | 0.2935 | 98.7989 | 543 | apparent high fineness zone |
| Eureka C | EC14-6 | 215 | 0.0001 | 58.4793 | 41.0188 | 0.3561 | 99.8543 | 412 | |
| Eureka C | EC14-7 | 216 | 0.0028 | 63.3957 | 35.5142 | 0.3534 | 99.2661 | 359 | apparent low fineness zone |
| Eureka C | EC14-8 | 217 | 0.0003 | 58.0284 | 41.1341 | 0.3735 | 99.5363 | 415 | apparent high fineness zone |
| Eureka C | EC14-9 | 218 | 0.0001 | 56.226 | 42.1127 | 0.4023 | 98.7411 | 428 | |
| Eureka C | EC16-10 | 188 | 0.0001 | 5.1358 | 82.2321 | 0.0002 | 87.3682 | 941 | apparent high fineness zone |
| Eureka C | EC16-11 | 189 | 0.001 | 6.5999 | 83.6255 | 0.0113 | 90.2377 | 927 | apparent high fineness zone |
| Eureka C | EC16-12 | 190 | 0.0009 | 62.5167 | 36.2876 | 0.3583 | 99.1635 | 367 | apparent low fineness zone |
| Eureka C | EC16-13 | 191 | 0.0001 | 56.4232 | 41.9928 | 0.454 | 98.8701 | 427 | |
| Eureka C | EC16-14 | 192 | 0.0001 | 53.7948 | 45.1017 | 0.3195 | 99.2161 | 456 | |
| Eureka C | EC16-2 | 180 | 0.0001 | 56.3395 | 42.5876 | 0.421 | 99.3482 | 431 | |
| Eureka C | EC16-3 | 181 | 0.0001 | 54.4016 | 44.2276 | 0.3911 | 99.0204 | 448 | |
| Eureka C | EC16-4 | 182 | 0.0001 | 56.9745 | 40.906 | 0.4176 | 98.2982 | 418 | |
| Eureka C | EC16-5 | 183 | 7.1248 | 60.6203 | 0.0356 | 0.0001 | 67.7808 | 1 | dark inclusion |
| Eureka C | EC16-6 | 184 | 0.9954 | 80.5636 | 0.0416 | 0.0001 | 81.6007 | 1 | dark inclusion |
| Eureka C | EC16-7 | 185 | 0.0001 | 64.5939 | 33.6624 | 0.6958 | 98.9522 | 343 | apparent low fineness zone |
| Eureka C | EC16-8 | 186 | 0.0001 | 62.4505 | 34.6841 | 0.6678 | 97.8025 | 357 | apparent low fineness zone |
| Eureka C | EC16-9 | 187 | 0.0037 | 55.5269 | 43.9045 | 0.3673 | 99.8024 | 442 | |
| Eureka C | EC18-1 | 193 | 0.0021 | 51.1991 | 44.9088 | 1.7376 | 97.8476 | 467 | |
| Eureka C | EC18-10 | 202 | 0.0069 | 55.6354 | 40.9148 | 2.4729 | 99.03 | 424 | |
| Eureka C | EC18-2 | 194 | 0.0042 | 56.6073 | 40.2823 | 2.607 | 99.5008 | 416 | |

| Location | Sample | Label | wt%(Cu) | wt%(Ag) | wt%(Au) | wt%(Hg) | Total wt% | Fineness | Comments |
|---|---|---|---|---|---|---|---|---|---|
| Eureka C | EC18-3 | 195 | 0.0001 | 37.0573 | 61.2832 | 0.4386 | 98.7792 | 623 | |
| Eureka C | EC18-4 | 196 | 0.0001 | 59.7751 | 37.2897 | 0.5984 | 97.6633 | 384 | apparent low fineness zone |
| Eureka C | EC18-5 | 197 | 0.0009 | 61.2038 | 36.9557 | 0.7346 | 98.895 | 377 | apparent low fineness zone |
| Eureka C | EC18-6 | 198 | 0.0001 | 52.8345 | 44.7961 | 1.7678 | 99.3985 | 459 | apparent low fineness zone |
| Eureka C | EC18-7 | 199 | 0.0063 | 52.2884 | 44.3163 | 1.8576 | 98.4686 | 459 | apparent low fineness zone |
| Eureka C | EC18-8 | 200 | 0.0001 | 60.9166 | 35.6184 | 1.3257 | 97.8608 | 369 | apparent low fineness rim |
| Eureka C | EC18-9 | 201 | 0.0068 | 57.6464 | 38.9087 | 0.911 | 97.4729 | 403 | apparent low fineness zone |
| Eureka C | EC21-1 | 51 | 0.0082 | 42.8388 | 54.0743 | 0.4012 | 97.3225 | 558 | |
| Eureka C | EC21-2 | 52 | 0.0089 | 42.7896 | 55.9925 | 0.4203 | 99.2113 | 567 | |
| Eureka C | EC23-1 | 48 | 0.0001 | 27.1708 | 70.0304 | 1.8644 | 99.0657 | 721 | |
| Eureka C | EC23-2 | 49 | 0.0024 | 27.0635 | 70.5767 | 1.6746 | 99.3172 | 723 | |
| Eureka C | EC23-3 | 50 | 0.0001 | 28.141 | 69.6634 | 1.5488 | 99.3533 | 712 | |
| Eureka C | EC24-1 | 53 | 0.0001 | 25.2172 | 72.842 | 0.1158 | 98.1751 | 743 | |
| Eureka C | EC24-2 | 54 | 0.0001 | 25.0333 | 73.7363 | 0.1276 | 98.8973 | 747 | |
| Eureka C | EC24-3 | 55 | 0.0001 | 25.3562 | 74.9986 | 0.0946 | 100.4495 | 747 | |
| Eureka C | EC24-4 | 56 | 0.0016 | 25.1687 | 74.0406 | 0.0707 | 99.2816 | 746 | discoloured area |
| Eureka C | EC25-1 | 62 | 0.0028 | 47.1933 | 50.2076 | 0.6698 | 98.0735 | 516 | |
| Eureka C | EC25-2 | 63 | 0.0001 | 46.9067 | 51.1791 | 0.636 | 98.7219 | 522 | |
| Eureka C | EC26-1 | 60 | 0.0001 | 59.7083 | 36.7888 | 1.4865 | 97.9837 | 381 | |
| Eureka C | EC26-2 | 61 | 0.0082 | 60.7464 | 37.0495 | 1.5323 | 99.3364 | 379 | |
| Eureka C | EC27-1 | 57 | 0.0063 | 27.8172 | 71.1757 | 0.2934 | 99.2926 | 719 | |
| Eureka C | EC27-2 | 58 | 0.0065 | 27.0256 | 71.3076 | 0.2732 | 98.6129 | 725 | discoloured area |
| Eureka C | EC27-3 | 59 | 0.0073 | 27.7891 | 71.4157 | 0.2741 | 99.4862 | 720 | |
| Eureka E | ECR21-1 | 64 | 0.0057 | 43.6994 | 55.3569 | 0.3779 | 99.4399 | 559 | |
| Eureka E | ECR21-2 | 65 | 0.0001 | 43.2948 | 55.6023 | 0.2937 | 99.1909 | 562 | |
| Eureka E | ECR22-1 | 66 | 0.0001 | 19.8473 | 70.4067 | 0.7136 | 90.9677 | 780 | |
| Eureka E | ECR22-2 | 67 | 0.0067 | 19.9955 | 79.988 | 0.7927 | 100.7829 | 800 | |
| Eureka E | ECR23-1 | 70 | 0.0066 | 29.7232 | 69.5414 | 0.0716 | 99.3428 | 701 | |
| Eureka E | ECR23-2 | 71 | 0.0044 | 1.04 | 106.7786 | 0.0002 | 107.8232 | 990 | |
| Eureka E | ECR24-1 | 72 | 0.0001 | 34.3376 | 59.188 | 0.6568 | 94.1825 | 633 | |
| Eureka E | ECR24-2 | 73 | 0.0006 | 37.2338 | 61.9338 | 0.6473 | 99.8155 | 625 | non porous rim |
| Eureka E | ECR24-3 | 74 | 0.0001 | 35.5365 | 61.4073 | 0.6091 | 97.553 | 633 | non porous rim |
| Eureka E | ECR24-4 | 75 | 0.0001 | 35.6024 | 63.0836 | 0.6277 | 99.3138 | 639 | |
| Eureka E | ECR26-1 | 68 | 0.0043 | 23.163 | 65.4338 | 0.1004 | 88.7015 | 739 | |
| Eureka E | ECR26-2 | 69 | 0.0038 | 26.7552 | 71.7163 | 0.1092 | 98.5845 | 728 | |
| Eureka E | ECR27-1 | 76 | 0.0001 | 0.1981 | 101.2947 | 0.0002 | 101.4931 | 998 | leached rim |
| Eureka E | ECR27-2 | 77 | 0.0001 | 34.5927 | 63.9519 | 0.4721 | 99.0168 | 649 | non porous rim |
| Eureka E | ECR27-3 | 78 | 0.0001 | 20.9961 | 52.2343 | 0.187 | 73.4175 | 713 | leached rim |
| Eureka E | ECR27-4 | 79 | 0.0001 | 34.1077 | 64.0432 | 0.4331 | 98.5841 | 653 | non porous rim |
| Eureka E | ECR27-5 | 80 | 0.0101 | 0.1267 | 56.871 | 0.0002 | 57.008 | 998 | porous core |
| Eureka Pit | EPA1-1 | 108 | 0.0072 | 33.7783 | 62.3452 | 0.1679 | 96.2986 | 649 | |
| Eureka Pit | EPA2-1 | 106 | 0.0001 | 21.3845 | 76.1589 | 0.1057 | 97.6492 | 781 | |
| Eureka Pit | EPA2-2 | 107 | 0.0001 | 20.7408 | 77.502 | 0.1567 | 98.3996 | 789 | |
| Eureka Pit | EPB-1 | 109 | 62.6228 | 0.0135 | 0.0002 | 0.0002 | 62.6367 | 15 | |
| Eureka Pit | EPB-2 | 110 | 62.7491 | 0.0143 | 0.0002 | 0.0002 | 62.7638 | 14 | |
| Eureka Pit | EPB-3 | 111 | 59.5423 | 0.0226 | 0.0706 | 0.0002 | 59.6357 | 758 | |
| Eureka Pit | EPC-1 | 112 | 0.0001 | 36.347 | 63.7347 | 0.7583 | 100.8401 | 637 | |
| Eureka Pit | EPC-2 | 113 | 0.0001 | 35.0884 | 62.2482 | 0.7778 | 98.1145 | 640 | |
| Eureka Pit | EPD-1 | 114 | 0.0008 | 34.2047 | 65.6553 | 0.198 | 100.0588 | 658 | |
| Kirkman Creek | K35-1 | 10 | 0.0011 | 0.975 | 98.6065 | 0.0002 | 99.5828 | 990 | |
| Kirkman Creek | K35-2 | 11 | 0.017 | 14.0759 | 84.8735 | 0.3042 | 99.2706 | 858 | |
| Kirkman Creek | K35-3 | 12 | 0.032 | 13.4753 | 86.1109 | 0.2875 | 99.9057 | 865 | |
| Kirkman Creek | K36-1 | 2 | 0.0079 | 26.6696 | 72.1117 | 0.5784 | 99.3676 | 730 | |
| Kirkman Creek | K36-2 | 3 | 0.0001 | 26.5498 | 73.3883 | 0.5877 | 100.5259 | 734 | |
| Kirkman Creek | K36-3 | 4 | 0.0001 | 1.1267 | 100.4156 | 0.0002 | 101.5426 | 989 | |
| Kirkman Creek | K37-1 | 5 | 0.0258 | 10.4684 | 89.7602 | 0.2542 | 100.5086 | 896 | |
| Kirkman Creek | K37-2 | 6 | 0.0252 | 10.4276 | 89.0346 | 0.2881 | 99.7755 | 895 | |
| Kirkman Creek | K38-1 | 7 | 0.0135 | 15.2787 | 84.1345 | 0.0723 | 99.499 | 846 | |

| Location | Sample | Label | wt%(Cu) | wt%(Ag) | wt%(Au) | wt%(Hg) | Total wt% | Fineness | Comments |
|---|---|---|---|---|---|---|---|---|---|
| Kirkman Creek | K38-2 | 8 | 0.0121 | 15.2831 | 84.9732 | 0.1017 | 100.3701 | 848 | |
| Kirkman Creek | K38-3 | 9 | 0.0195 | 15.2989 | 84.6022 | 0.1025 | 100.0231 | 847 | |
| Mine Creek | M1_-1 | 228 | 0.0001 | 19.6056 | 79.5554 | 0.2174 | 99.3785 | 802 | |
| Mine Creek | M1_-2 | 229 | 0.0099 | 19.7723 | 79.5969 | 0.2418 | 99.6209 | 801 | |
| Mine Creek | M1_-3 | 230 | 0.0073 | 19.8971 | 77.805 | 0.2508 | 97.9602 | 796 | |
| Mine Creek | M24-1 | 33 | 0.0316 | 11.0932 | 89.0289 | 0.0002 | 100.1539 | 889 | non porous rim |
| Mine Creek | M24-2 | 34 | 0.0198 | 11.521 | 88.0436 | 0.0759 | 99.6603 | 884 | |
| Mine Creek | M25-1 | 31 | 0.0282 | 12.6252 | 83.354 | 0.0002 | 96.0076 | 869 | |
| Mine Creek | M25-2 | 32 | 0.0301 | 12.5095 | 87.1935 | 0.0522 | 99.7853 | 875 | |
| Mine Creek | M26-1 | 37 | 0.0018 | 21.6471 | 78.5043 | 0.0081 | 100.1613 | 784 | non porous rim |
| Mine Creek | M26-2 | 38 | 0.0162 | 22.0024 | 77.301 | 0.0002 | 99.3198 | 778 | |
| Mine Creek | M27-1 | 35 | 0.0393 | 11.0079 | 87.1669 | 0.0532 | 98.2673 | 888 | |
| Mine Creek | M27-2 | 36 | 0.0308 | 10.6252 | 90.5433 | 0.0241 | 101.2234 | 895 | |
| Roo Pup | R11-2 | 225 | 0.0083 | 20.2528 | 79.0478 | 0.1103 | 99.4192 | 796 | |
| Roo Pup | R11-4 | 226 | 0.0157 | 20.7475 | 78.2012 | 0.1037 | 99.0681 | 790 | |
| Roo Pup | R11-5 | 227 | 0.0072 | 20.5459 | 77.1724 | 0.0867 | 97.8122 | 790 | |
| Roo Pup | R22-1 | 46 | 0.0001 | 11.3257 | 56.6972 | 0.0002 | 68.0232 | 834 | |
| Roo Pup | R22-2 | 47 | 0.0077 | 10.5621 | 76.624 | 0.0049 | 87.1987 | 879 | |
| Roo Pup | R23-1 | 44 | 0.0001 | 20.1886 | 77.3295 | 1.4992 | 99.0174 | 793 | |
| Roo Pup | R23-2 | 45 | 0.0033 | 19.5444 | 76.465 | 1.4712 | 97.4839 | 796 | |
| Roo Pup | R25-1 | 42 | 0.0268 | 10.1824 | 86.5844 | 0.0994 | 96.893 | 895 | |
| Roo Pup | R25-2 | 43 | 0.0252 | 11.2316 | 88.555 | 0.0946 | 99.9064 | 887 | |
| Roo Pup | R27-1 | 39 | 0.0001 | 9.5213 | 41.3648 | 0.0002 | 50.8864 | 813 | non porous rim |
| Roo Pup | R27-2 | 40 | 0.0085 | 17.9392 | 81.1917 | 0.0002 | 99.1396 | 819 | non porous rim |
| Roo Pup | R27-3 | 41 | 0.0134 | 8.6459 | 54.6138 | 0.0002 | 63.2733 | 863 | |
| Swamp Creek | S210-1 | 97 | 0.01 | 25.8041 | 73.0054 | 0.0371 | 98.8566 | 739 | |
| Swamp Creek | S210-2 | 98 | 0.0116 | 30.8435 | 67.5814 | 0.0977 | 98.5342 | 687 | |
| Swamp Creek | S211-1 | 103 | 0.0001 | 0.98 | 87.2088 | 0.0002 | 88.1891 | 989 | apparent high fineness zone |
| Swamp Creek | S211-2 | 104 | 0.0114 | 13.8506 | 86.2736 | 0.0893 | 100.2249 | 862 | |
| Swamp Creek | S211-3 | 105 | 0.0131 | 13.3214 | 86.0048 | 0.0775 | 99.4168 | 866 | |
| Swamp Creek | S22-1 | 101 | 0.0103 | 17.3756 | 82.0233 | 0.0516 | 99.4608 | 825 | |
| Swamp Creek | S22-2 | 102 | 0.0129 | 17.0807 | 82.2481 | 0.0362 | 99.3779 | 828 | |
| Swamp Creek | S23-1 | 99 | 0.0035 | 16.4334 | 82.8393 | 0.0029 | 99.2791 | 835 | |
| Swamp Creek | S23-2 | 100 | 0.0113 | 16.689 | 83.3921 | 0.0077 | 100.1001 | 833 | |
| Swamp Creek | S29-1 | 95 | 0.0053 | 17.3445 | 81.9638 | 0.0002 | 99.3138 | 825 | |
| Swamp Creek | S29-2 | 96 | 0.0073 | 17.8731 | 79.7841 | 0.0002 | 97.6647 | 817 | |
| Swamp Creek | S34-1 | 23 | 0.0139 | 18.4154 | 80.6337 | 0.3807 | 99.4437 | 814 | |
| Swamp Creek | S34-2 | 24 | 0.0189 | 10.4241 | 89.8392 | 0.0002 | 100.2824 | 896 | |
| Swamp Creek | S34-3 | 25 | 0.0261 | 10.0604 | 89.9649 | 0.0002 | 100.0516 | 899 | |
| Swamp Creek | S35-1 | 26 | 0.0004 | 15.4613 | 84.8864 | 0.0002 | 100.3483 | 846 | |
| Swamp Creek | S35-2 | 27 | 0.0012 | 15.8516 | 84.3385 | 0.0002 | 100.1915 | 842 | |
| Swamp Creek | S37-1 | 28 | 0.0001 | 18.9519 | 80.0133 | 0.0002 | 98.9655 | 809 | |
| Swamp Creek | S37-2 | 29 | 0.0001 | 19.5936 | 80.4232 | 0.0002 | 100.0171 | 804 | |
| Swamp Creek | S37-3 | 30 | 0.0047 | 18.7612 | 79.9007 | 0.4004 | 99.067 | 810 | |
| Thistle Creek | T410-1 | 146 | 0.0122 | 16.4388 | 82.5962 | 0.3879 | 99.4351 | 834 | |
| Thistle Creek | T410-2 | 147 | 0.0103 | 17.0131 | 81.5868 | 0.4197 | 99.0299 | 828 | |
| Thistle Creek | T410-3 | 148 | 0.0197 | 15.4376 | 83.8467 | 0.4291 | 99.7331 | 845 | |
| Thistle Creek | T412-1 | 140 | 0.0088 | 10.312 | 69.5651 | 0.1099 | 79.9958 | 871 | |
| Thistle Creek | T412-2 | 141 | 0.0252 | 14.902 | 82.9216 | 0.3819 | 98.2307 | 848 | |
| Thistle Creek | T412-3 | 142 | 0.0215 | 14.9953 | 83.1564 | 0.341 | 98.5142 | 847 | |
| Thistle Creek | T45-1 | 149 | 0.0257 | 10.3849 | 88.299 | 0.619 | 99.3286 | 895 | |
| Thistle Creek | T45-2 | 150 | 0.0287 | 11.3179 | 85.4118 | 0.6047 | 97.3631 | 883 | non porous rim |
| Thistle Creek | T45-3 | 151 | 0.0157 | 10.3516 | 87.6619 | 0.6224 | 98.6516 | 894 | |
| Thistle Creek | T49-1 | 143 | 0.026 | 7.6273 | 89.6418 | 0.0002 | 97.2953 | 922 | |
| Thistle Creek | T49-2 | 144 | 0.0283 | 7.7078 | 91.9233 | 0.0002 | 99.6596 | 923 | |
| Thistle Creek | T49-3 | 145 | 0.0006 | 1.3794 | 90.7548 | 0.0002 | 92.135 | 985 | |
| Standard | S254 | 1 | 0.0001 | 20.1445 | 79.2806 | 0.0002 | 99.4254 | 797 | standard |
| Standard | S254A | 123 | 0.0001 | 20.1159 | 78.8039 | 0.0002 | 98.9201 | 797 | standard |
| Standard | S254B | 231 | 0.0001 | 20.0959 | 79.3642 | 0.0002 | 99.4604 | 798 | standard |

# Geology at the contact between Yukon-Tanana and Cassiar terranes, southeast of Little Salmon Lake (105L/1), south-central Yukon

***Kaesy Gladwin***[1]
*University of Victoria*[2]

***Maurice Colpron***
*Yukon Geology Program*

***Stephen T. Johnston***[3] ***and Robin Black***[4]
*University of Victoria*

Gladwin, K., Colpron, M., Johnston, S.T. and Black, R., 2002. Geology at the contact between Yukon-Tanana and Cassiar terranes, southeast of Little Salmon Lake (105 L/1), south central Yukon. *In:* Yukon Exploration and Geology 2001, D.S. Emond, L.H. Weston and L.L. Lewis (eds.), Exploration and Geological Services Division, Yukon Region, Indian and Northern Affairs Canada, p. 103-109.

## ABSTRACT

Paleozoic platformal and basinal strata of Cassiar Terrane are separated from rocks of Yukon-Tanana Terrane to the west by an unexposed fault in southeast Glenlyon map area.

Quartzite, marble, phyllite, and amphibolite are grouped in Cassiar Terrane, and no rocks of Slide Mountain Terrane are recognized. The mid-Cretaceous Glenlyon batholith contains pendants of Cassiar Terrane and is intruded by at least five andesite dykes. West of the fault, the Yukon-Tanana Terrane includes: (1) mafic volcaniclastic rocks with preserved primary textures; (2) coarse-grained quartz-feldspar grit; and (3) metasiltstone and semi-pelitic schist. The grit is intruded by foliated hornblende granodiorite, likely of early Mississippian age. Small outcrops of tectonized serpentinite were tectonically emplaced into Yukon-Tanana Terrane, and a positive magnetic anomaly parallel to the fault suggests an unexposed extension to the southwest.

Two mylonite localities and evidence of brittle cataclasis up to 1 km on either side of the presumed buried fault suggest a complex structural history along this terrane boundary.

## RÉSUMÉ

Les roches de marge continentale d'âge Paléozoïque du terrane de Cassiar sont séparées des roches du terrane de Yukon-Tanana (à l'ouest) par une faille dissimulée dans le secteur sud-est de la carte de Glenlyon.

Le terrane de Cassiar consiste de quartzite, de marbre, de phyllade, et d'amphibolite; aucune de ces roche est apparentée au terrane de Slide Mountain (tel que suggéré au préalable). Le batholite de Glenlyon, datant du Crétacé moyen, contient des enclaves du terrane de Cassiar et est recoupé par au moins cinq dykes d'andésite. À l'ouest de la faille, le terrane de Yukon-Tanana comprend : (1) des roches volcaniclastiques mafiques dont les textures primaires sont intactes; (2) un grès grossier à quartz et feldspath; et (3) du méta-siltstone et du schiste argilleux. Le grès est recoupé par un granodiorite à hornblende folié, dont l'âge est vraisemblablement du Mississippien précoce. De petits affleurements de serpentinite tectonisée sont présents au sein du terrane de Yukon-Tanana; une anomalie magnétique positive qui parallèle la faille suggère que la serpentinite se continue vers le sud-ouest.

Deux affleurements de mylonite et des indications de structures cataclastiques cassantes sur près d'un kilomètre de distance de l'emplacement présumé de la faille suggère une évolution structurale complexe le long de ce contact entre les deux terranes.

---

[1] kaesy@uvic.ca

[2] *School of Earth and Ocean Sciences, University of Victoria, Box 3055, STN CSC, Victoria, British Columbia, Canada V8W 3P6*

[3] stj@uvic.ca

[4] billyroc@uvic.ca

# INTRODUCTION

A northwest-trending fault system regionally separates Paleozoic platformal and basinal strata of Cassiar Terrane to the east from crystalline rocks of Yukon-Tanana Terrane to the west (Fig. 1). In eastern Laberge map area (NTS 105E), the southern part of this fault system corresponds to the d'Abbadie Fault (Tempelman-Kluit, 1979). It was originally interpreted by Tempelman-Kluit (1979) as a thrust fault that emplaced Yukon-Tanana Terrane over Cassiar Terrane in pre-Cretaceous time. It was later interpreted by Hansen (1989) as a strike-slip fault which formed the eastern boundary of a north-trending Jurassic transpressional shear zone. Harvey et al. (1997) estimated right-lateral strike-slip displacement of 4 km along the fault and demonstrated that d'Abbadie Fault is intruded by the synkinematic Last Peak granite, dated at 98 Ma (Brown et al., 1998). More recently, d'Abbadie Fault has been interpreted as a mid-Cretaceous brittle normal fault that cuts an older thrust fault that emplaced Yukon-Tanana Terrane onto Cassiar Terrane (de Keijzer et al., 1999).

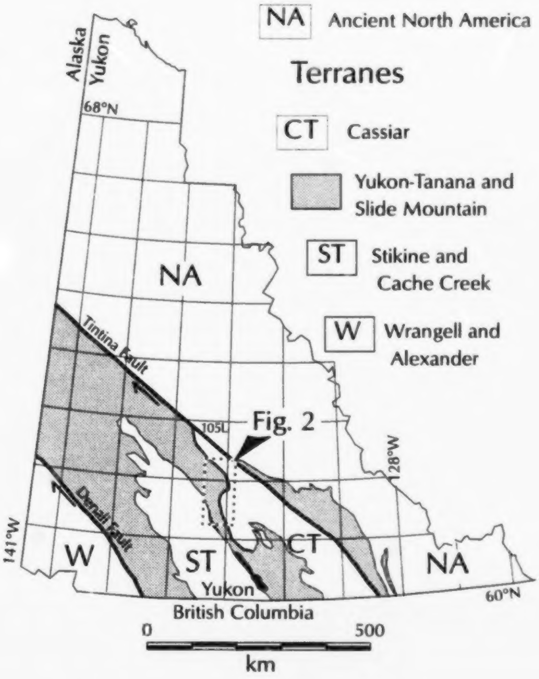

***Figure 1.*** *The study area is located in the southeast corner of Glenlyon map area (NTS 105L), along d'Abbadie Fault. Simplified tectonic boundaries are modified after Wheeler and McFeely (1991).*

When traced northward, d'Abbadie Fault takes a sharp northeast-trending bend in the northeast corner of Laberge map area (105E; Fig. 2). Its northern extent is less certain. In southeastern Glenlyon map area (105L), the contact between Yukon-Tanana and Cassiar terranes is once again defined by a steep, northwest-trending fault system (Campbell, 1967) that has been correlated with the d'Abbadie Fault (Gordey and Makepeace, 2000). It is currently unclear whether the fault system mapped in southeastern Glenlyon map area shares the same deformation history as the d'Abbadie Fault mapped in eastern Laberge map area. Furthermore, the fault system in southeastern Glenlyon map area is displayed, in part, on recent geological compilations to separate Yukon-Tanana Terrane, to the west, from Slide Mountain Terrane to the east (Gordey and Makepeace, 1999, 2000). An objective of the current study is to clarify these relations.

Recent paleomagnetic studies from Late Cretaceous volcanic rocks (Carmacks Group), which disconformably overlie the Yukon-Tanana Terrane immediately west of the d'Abbadie Fault, suggest that these rocks were 2000 km south of their present location during deposition (Johnston et al., 2001). This is consistent with the findings of earlier paleomagnetic work in central Yukon (Johnston et al., 1996; Wynne et al., 1998). However, a maximum of 450 km of Cretaceous or younger dextral strike-slip displacement can be accommodated by the strike-slip faults east of Solitary Mountain (Gabrielse, 1985; Roddick, 1967). If the paleolatitude implied by these rocks is correct, a major Late Cretaceous-Early Tertiary structure northeast of Solitary Mountain must have accommodated large-scale northward translation of Yukon-Tanana Terrane. This study aims to provide further constraints on the nature of the contact between Yukon-Tanana Terrane and Cassiar Terrane in Glenlyon map area.

The study area was previously mapped by Campbell (1967) at a scale of 1:250 000, from fieldwork carried out in the 1950s. Limited exploration work was completed in the 1980s and 1990s in connection with mineral prospects peripheral to mid-Cretaceous intrusions (Yukon MINFILE, 1997, 105L 001). More recently, Colpron (1999, 2000) has mapped Yukon-Tanana Terrane in the areas north and southwest of Little Salmon Lake at a scale of 1:50 000.

This paper presents the preliminary results of detailed 1:50 000-scale mapping of a northwest-trending, 200-km$^2$ area straddling the boundary between Yukon-Tanana, Slide Mountain and Cassiar terranes in southeast Glenlyon map area. Access to the study area was by

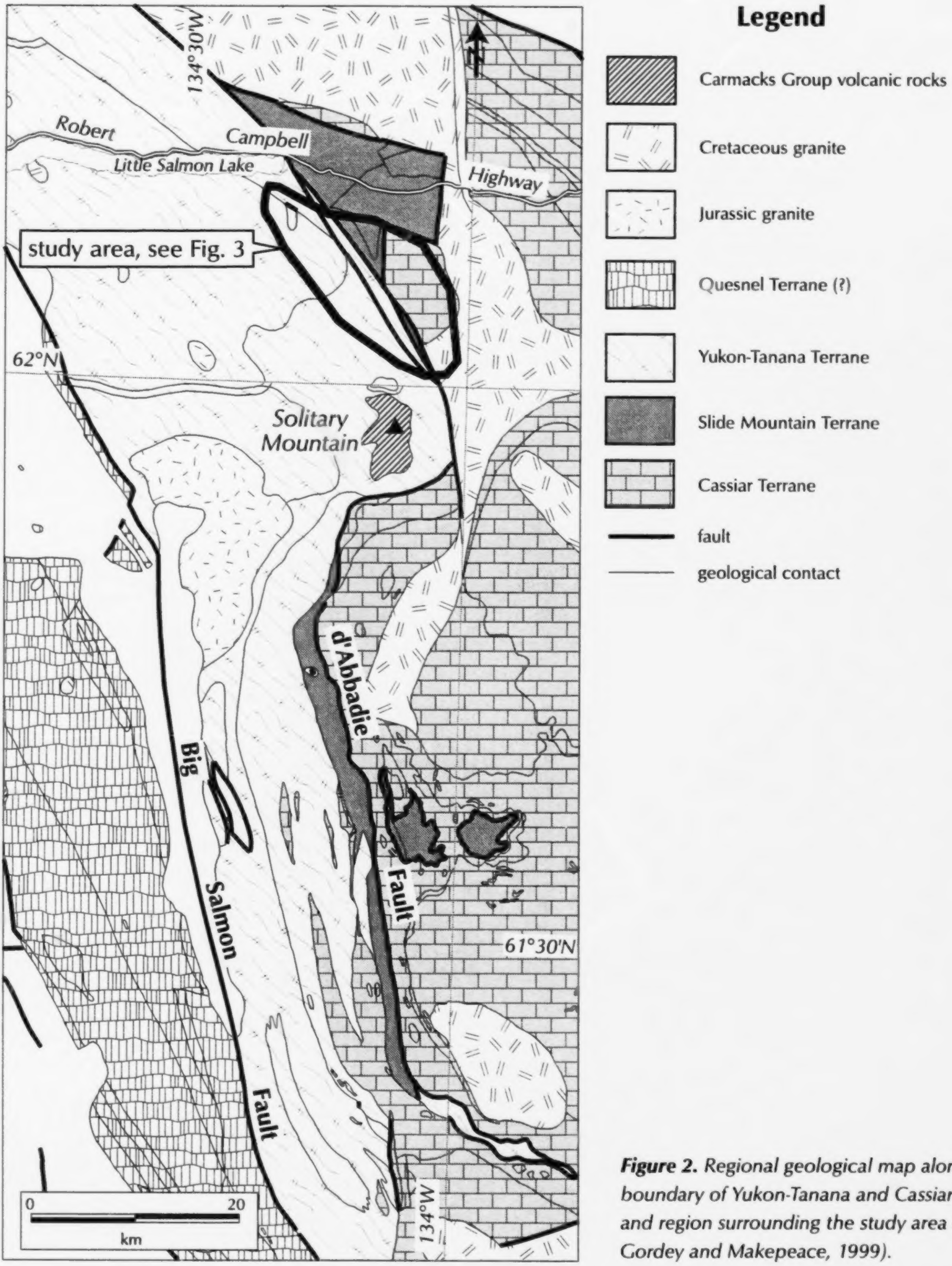
Legend
▨ Carmacks Group volcanic rocks
Cretaceous granite
Jurassic granite
Quesnel Terrane (?)
Yukon-Tanana Terrane
Slide Mountain Terrane
Cassiar Terrane
fault
geological contact
134°30'W
Robert
Campbell
Highway
Little Salmon Lake
study area, see Fig. 3
62°N
Solitary Mountain
d'Abbadie
Fault
Big
Salmon
Fault
61°30'N
134°W
0
20
km

*Figure 2. Regional geological map along the boundary of Yukon-Tanana and Cassiar terranes, and region surrounding the study area (from Gordey and Makepeace, 1999).*

helicopter. The eastern side of the d'Abbadie Fault is predominantly alpine with good outcrop exposure, in contrast to the low-lying areas to the west (Yukon-Tanana Terrane), which have poor outcrop exposure.

## GEOLOGY OF SOUTHEASTERN GLENLYON MAP AREA

A north-northwest-trending fault system bisects the study area (Fig. 3). The northeast side of the fault is underlain by a low-grade (greenschist facies) metamorphosed package of sedimentary rocks, including: (1) marble; (2) phyllite; (3) calc-silicate rocks; (4) amphibolite; and (5) pure and impure quartzite. Quartzite and marble are the most common lithologies. The quartzite commonly has a light green colour, is locally calcareous, and contains minor black, locally graphitic, phyllite. The thickness of the quartzite unit is unconstrained but is probably greater than 1 km. The quartzite unit underlies a marble unit which also includes minor amphibolite, quartzite and calc-silicate rocks. A thinly (centimetre-scale) interbedded gradational contact between the quartzite and marble was observed in several locations. Both quartzite and marble units are deformed by a steep foliation defined by mica growth that is axial planar to folds of lithological contacts. Open to closed folds on scales of tens to hundreds of metres have horizontal axes that are parallel

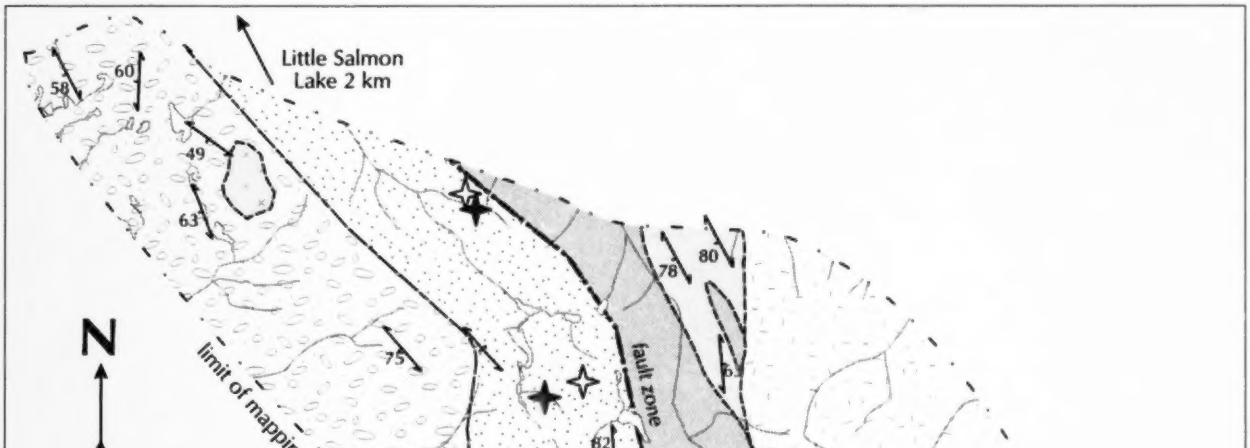
Little Salmon Lake 2 km
N
limit of mapping
fault zone
limit of mapping
58
60
49
63
75
78
80
63
82
77
65
73
43
85
76
28
80
41
69
Legend
Glenlyon Batholith: biotite granodiorite, hornblende-quartz monzodiorite, biotite-muscovite granite, pegmatite
coarse-grained foliated hornblende granodiorite
mafic volcaniclastic unit
coarse-grained arkosic grit
marble, quartzite, quartz-muscovite schist, calc-silicate, and amphibolite
quartzite, phyllite, marble, quartz-mica schist
76
foliation
serpentinite
mylonite
fault
geological contact
0
4
km

*Figure 3. Preliminary geological map of study area based on mapping completed in the 2001 field season.*

to the terrane-bounding fault. Small, centimetre- to metre-scale chevron folds were observed locally, and are thought to be contemporaneous with the larger-scale folds. These rocks were likely deposited in a continental margin setting and are probably part of Cassiar Terrane.

This metasedimentary succession is intruded by the mid-Cretaceous Glenlyon batholith (Gordey and Makepeace, 2000; Figs. 3, 4). The batholith is characterized by an early phase of hornblende-quartz monzodiorite, a voluminous phase of biotite granodiorite, and a late phase of two-mica granite and pegmatite. The two-mica granite is locally plagioclase-megacrystic. These rocks are unfoliated, but are locally cut by north-northwest-trending brittle faults. These faults are defined by chloritized fracture planes with slickenlines. Where present, release steps indicate dextral motion.

Large xenoliths of quartz + muscovite ± biotite ± garnet schist, marble, garnet + diopside calc-silicate rock, and amphibolite are common near the margin of the batholith and best exposed on hilltops. They range in size from one metre to hundreds of metres. The Glenlyon batholith imposes a contact metamorphic aureole on the metasedimentary rocks. The contact aureole extends 1-1.5 km from the southwestern margin of the batholith, with garnet-grade metamorphism at the batholith margin giving way to biotite- and chlorite-grade rocks farther to the southwest.

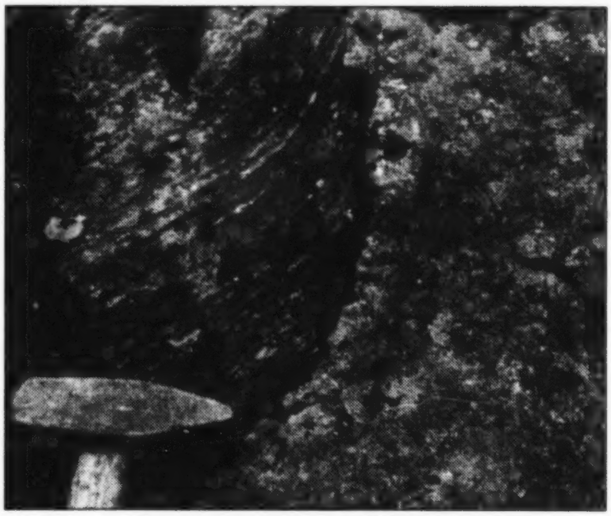

***Figure 4.*** *Coarse-grained granite of Glenlyon batholith intruding laminated marble of Cassiar Terrane. Rock hammer for scale.*

Five porphyritic andesite dykes, trending south-southeast to north-northwest, were observed in the Glenlyon batholith. The dykes are sub-vertical, 0.3 to 1.5 m wide, with chilled margins and small wall-rock xenoliths. Clinopyroxene and plagioclase phenocrysts are common. No dykes were observed in Yukon-Tanana Terrane to the west.

Southwest of the fault, the Yukon-Tanana Terrane is dominated by siliciclastic and mafic volcaniclastic rocks. Coarse-grained arkosic grit in the northwestern part of the study area (Fig. 3) is intruded by a coarse-grained, foliated hornblende granodiorite. This association of arkosic grit and foliated granodiorite is similar to that described by Colpron and Reinecke (2000) from the north shore of Little Salmon Lake. There, the arkosic grit is intruded by a hornblende granodiorite which has yielded two discordant early Mississippian preliminary U-Pb zircon dates (Oliver and Mortensen, 1998; Colpron and Reinecke, 2000). The granodiorite mapped in the study area (Fig. 3) is of similar composition and is possibly of early Mississippian age.

West of the volcaniclastic unit, and south of the grit, several outcrops of meta-siltstone and a single exposure of quartz-feldspar-sericite-chlorite schist are exposed. The schist could represent a deformed grit or an intermediate volcanic protolith. It is therefore uncertain whether these rocks are associated with the grit unit or the volcaniclastic unit.

Mafic volcaniclastic rocks occur in a 3-km-wide, northwest-trending belt that separates the grit unit from the fault system (Fig. 3). Primary porphyritic texture is commonly preserved in the basaltic lithic clasts. Epidote and chlorite development indicate greenschist facies regional metamorphism. Foliation, defined by an alignment of chlorite, dips steeply to the west. An interpreted disconformity, along which the volcaniclastic rocks overlie siliciclastic rocks to the north and west, is constrained to within 100 m at one location. Both the volcaniclastic rocks and the grit unit are interpreted to be part of the Yukon-Tanana Terrane.

Five outcrops of serpentinite, 50-200 m long, have been found within the volcaniclastic unit, 50-500 m west of the contact between Yukon-Tanana and Cassiar terranes (Fig. 3). Lineations on facoid surfaces in two of the outcrops plunge shallowly to the south. In thin section, magnetite surrounded by felty masses of chlorite, can be seen. This association probably represents pseudomorphs of spinel with plagioclase coronae, which would suggest that the rock was changed from the spinel to the plagioclase stability field as it was exhumed. This association therefore implies tectonic emplacement of the ultramafic rocks, rather than an intrusive origin (D. Canil, pers. com., 2001). A strong positive magnetic anomaly spatially associated with these outcrops suggests a larger mass may lie further southwest in an area where there is no outcrop exposure (Gordey and Makepeace, 1999).

Due to limited outcrop exposure in some areas, the exact trace of the fault cannot be precisely located, but has been constrained to an area 50 to 150 m wide. A cataclastic texture was observed in some quartzite outcrops of Cassiar Terrane. A similar texture was noted in several exposures of volcaniclastic rocks southwest of the fault. This brittle fabric was generally observed within about 1 km of the presumed fault location, although it was less apparent in the volcaniclastic unit.

Outcrops of mylonitic rocks occur at intervals along strike from the ultramafic rocks (Fig. 3). The mylonitic fabric is complexly folded at one locality, but the authors are uncertain whether this deformation of the mylonitic fabric is in response to a later event, or to progressive localized deformation. Another outcrop of mylonitic rocks occurs 50 m north of the northernmost outcrop of serpentinite (Fig. 3). At this locality, the mylonitic fabric strikes parallel to the adjacent serpentinite cliff face and dips steeply southwest beneath it. The spatial association and similar orientation suggests that the fabric may have formed during ductile deformation associated with tectonic emplacement of the serpentinite.

## DISCUSSION AND NEW INTERPRETATIONS

Platformal metasedimentary rocks and granitic intrusive rocks of Cassiar Terrane on the east side of the study area contrast with arkosic grit, quartz-muscovite schist, foliated granodiorite and mafic volcaniclastic rocks of Yukon-Tanana Terrane to the west. The contact between the terranes has been spatially constrained to a narrow (100- to 500-m-wide), north-northwest-trending zone coincident with the presumed location of the d'Abbadie Fault. Occurrences of serpentinite and mylonitic rocks near this contact, and the local presence of late, brittle structures, suggest that the terrane boundary has experienced a complex structural history.

The boundaries of lithological units in Cassiar Terrane, previously shown as faulted contacts (Campbell, 1967), are explained by observed folding patterns and contact metamorphism (Figs. 2, 3). Therefore, these metasedimentary rocks (northeast of the fault) are grouped as quartzite and marble units of the Cassiar Terrane. Rocks that were formerly assigned to Slide Mountain Terrane (Fig. 2) were observed by the authors to be lithologically and structurally similar to the Cassiar Terrane rocks to the south, and are therefore shown herein as Cassiar Terrane. The authors also note that the Glenlyon batholith extends 5 km farther to the northwest than previously mapped (compare Figs. 2 and 3). A large portion of the area previously mapped as Cassiar Terrane (Fig. 2; unit 2a of Campbell, 1967) corresponds to a series of large xenoliths at the western margin of the batholith (Fig. 3).

The 2002 field season will build upon the geological map produced this season, focusing on the nature of the contact between Yukon-Tanana and Cassiar terranes and its relation to the d'Abbadie Fault, as defined to the south in Laberge map area.

## ACKNOWLEDGEMENTS

Results presented in this paper are from five weeks of fieldwork completed during the summer of 2001. This study is a work in progress towards the completion of a M.Sc. project by the first author at the University of Victoria. Funding for this project was provided in part by the Yukon Geology Program, and in part by a National Science and Engineering Research Council (NSERC) grant to S.T. Johnston. Helicopter transport was provided by Trans North, Ross River. Discussions with Dante Canil, Joe English, and Greg Shellnutt benefited this paper. A review of the manuscript by Charlie Roots was much appreciated.

## REFERENCES

Brown, R.L., de Keijzer, M., Carr, S.D., Williams, P.F. and Gallagher, C.S., 1998. Structure of the Teslin zone, Yukon, Canada. *In:* Slave-Northern Cordillera Lithospheric Evolution (SNORCLE) and Cordilleran Tectonics Workshop, F. Cook and P. Erdmer, (eds.), Lithoprobe Report no. 64, p. 152-157.

Campbell, R.B., 1967. Geology of Glenlyon map area, Yukon Territory (105L). Geological Survey of Canada, Memoir 352, 92 p.

Colpron, M., 1999. Glenlyon Project: Preliminary stratigraphy and structure of Yukon-Tanana Terrane, Little Kalzas Lake area, central Yukon (105L/13). *In:* Yukon Exploration and Geology 1998, C.F. Roots and D.S. Emond (eds.), Exploration and Geological Services Division, Yukon Region, Indian and Northern Affairs Canada, p. 63-72.

Colpron, M., 2000. Geological map of Little Salmon Lake (parts of NTS 105L/1, 2 & 7), central Yukon (1:50 000 scale). Exploration and Geological Services Division, Yukon Region, Indian and Northern Affairs Canada, Open File 2000-10, 1:50 000 scale.

Colpron, M. and Reinecke, M., 2000. Glenlyon Project: Coherent stratigraphic succession from Little Salmon Range (Yukon-Tanana Terrane), and its potential for volcanic-hosted massive sulphide deposits. *In:* Yukon Exploration and Geology 1999, D.S. Emond and L.H. Weston (eds.), Exploration and Geological Services Division, Yukon Region, Indian and Northern Affairs Canada, p. 87-100.

de Keijzer, M., Williams, P.F. and Brown, R.L., 1999. Kilometre-scale folding in the Teslin zone, northern Canadian Cordillera, and its tectonic implications for the accretion of the Yukon-Tanana terrane to North America. Canadian Journal of Earth Sciences, vol. 36, p. 479-494.

Gabrielse, H., 1985. Major dextral transcurrent displacements along the Northern Rocky Mountain Trench and related lineaments in north-central British Columbia. Geological Society of America Bulletin, vol. 96, p. 1-14.

Gordey, S.P. and Makepeace, A.J. (comps.), 1999. Yukon Digital Geology. Geological Survey of Canada Open File D3826, and Exploration and Geological Services Division, Yukon Region, Indian and Northern Affairs, Canada, Open File 1999-1 (D), 2 CD-ROMs.

Gordey, S.P. and Makepeace, A.J. (comps.), 2000. Bedrock geology, Yukon Territory. Geological Survey of Canada, Open File 3754, and Exploration and Geological Services Division, Yukon Region, Indian and Northern Affairs Canada, Open File 2001-1, 1:1 000 000 scale.

Hansen, V.L., Mortensen, J.K. and Armstrong, R.L., 1989. U-Pb, Rb-Sr, and K-Ar isotopic constraints for ductile deformation and related metamorphism in the Teslin suture zone, Yukon-Tanana terrane, south-central Yukon. Canadian Journal of Earth Sciences, vol. 26, p. 2224-2235.

Harvey, J.L., Carr, S.D., Brown, R.L. and Gallagher, C., 1997. Deformation history and geochronology of plutonic rocks near the d'Abbadie Fault, Big Salmon Range, Yukon. *In:* Slave-Northern Cordillera Lithospheric Evolution (SNORCLE) and Cordilleran Tectonics Workshop, F. Cook and P. Erdmer (eds.), Lithoprobe Report no. 56, p. 103-114.

Johnston, S.T., Wynne, P.J., Francis, D., Hart, C.J.R., Enkin, R.J. and Engebretson, D.C., 1996. Yellowstone in Yukon: The Late Cretaceous Carmacks Group. Geology, vol. 24, p. 997-1000.

Johnston, S.T., Enkin, R., Baker, J., Francis, D., Colpron, M. and Larson, K., 2001. Solitary Mountain, Yukon: Preliminary paleomagnetic results strengthen the correlation with the Carmacks Formation. F. Cook and P. Erdmer (eds.), Lithoprobe SNORCLE – Cordilleran Tectonics Workshop, Victoria, BC, vol. 79, p. 85.

Oliver, D.H. and Mortensen, J.K., 1998. Stratigraphic succession and U-Pb geochronology from the Teslin suture zone, south central Yukon. *In:* Yukon Exploration and Geology 1997, Exploration and Geological Services Division, Yukon Region, Indian and Northern Affairs Canada, p. 69-75.

Roddick, J.A., 1967. Tintina Trench. Journal of Geology, vol. 75, p. 23-32.

Tempelman-Kluit, D.J., 1979. Transported cataclasite, ophiolite and granodiorite in Yukon: Evidence of arc-continent collision. Geological Survey of Canada, Paper 79-14, 27 p.

Wheeler, J.O. and McFeely, P., 1991. Tectonic assemblage map of the Canadian Cordillera and adjacent parts of the United States of America. Geological Survey of Canada, Map 1712A, 1:2 000 000 scale.

Wynne, P.J., Enkin, R.J., Baker, J., Johnston, S.T. and Hart, C.J.R., 1998. The Big Flush – Paleomagnetic signature of a 70 Ma regional hydrothermal event in displaced rocks of the northern Canadian Cordillera. Canadian Journal of Earth Sciences, vol. 35, p. 657-671.

Yukon MINFILE, 1997. Exploration and Geological Services Division, Yukon Region, Indian and Northern Affairs Canada.

# No remagnetization in plutonic rocks of the Whitehorse Trough, southern Yukon: An extensive paleomagnetic conglomerate test

***M.J. Harris[1] and D.T.A. Symons[1]***
*Earth Sciences, University of Windsor[1]*

***C.J.R. Hart[2]***
*Yukon Geology Program*

Harris, M.J., Symons, D.T.A. and Hart, C.J.R., 2002. No remagnetization in plutonic rocks of the Whitehorse Trough, southern Yukon: An extensive paleomagnetic conglomerate test. *In:* Yukon Exploration and Geology 2001, D.S. Emond, L.H. Weston and L.L. Lewis (eds.), Exploration and Geological Services Division, Yukon Region, Indian and Northern Affairs Canada, p. 111-124.

## ABSTRACT

Paleomagnetic conglomerate tests were run at three localities in the Conglomerate formation of the Jurassic Laberge Group in the southern Yukon. The localities are located within the Whitehorse Trough about 5, 20 and 40 km east of its margin with the intruded Coast Plutonic Complex. At each locality, 2.5-cm-diameter cores were drilled from 32 clasts of mainly igneous provenance and 8 more from the conglomerate matrix, totaling 120 cores, and yielding 190 specimens in all. The specimens were analysed using standard paleomagnetic demagnetization and testing techniques. The matrix, mostly greywacke in composition, yields characteristic remanent magnetization (ChRM) directions carried by pyrrhotite that give coherent steep downward directions. The clasts, at all three localities, yield paleomagnetic conglomerate tests that show statistically random ChRM directions. This leads to the conclusion that the clasts were not remagnetized by the event that remagnetized the matrix, which was likely caused by hydrothermal fluid flow during the Late Cretaceous to Eocene Laramide Orogeny. Furthermore, these conclusions support earlier studies by demonstrating that felsic plutons in the Whitehorse Trough likely carry primary ChRM directions, e.g., the 75 Ma Mount Lorne stock, the 109 Ma Mount McIntyre pluton, the 112 Ma Whitehorse batholith, and the 186 Ma Teslin Crossing stock.

## RÉSUMÉ

Des tests paléomagnétiques sur du conglomérat ont été effectués à trois endroits dans la formation de conglomérat du Groupe de Laberge du Jurassique, dans la partie sud du Yukon. Ces endroits se trouvent dans la dépression de Whitehorse, à environ 5, 20 et 40 km à l'est de sa marge intrusive avec le Complexe plutonique côtier. À tous ces endroits, on a extrait des carottes d'un diamètre de 2,5 cm de 32 clastes d'origine principalement magmatique et 8 autres carottes de la matrice du conglomérat, soit un total de 120 carottes, desquelles on a obtenu 190 échantillons. On a eu recours à des méthodes courantes de démagnétisation paléomagnétique et d'essai pour analyser les échantillons. La matrice, qui est principalement consituée de grauwacke, présente dans la pyrrhotine des directions de magnétisation rémanente caractéristique (ChRM) uniformément orientées vers le bas de façon abrupte. Les clastes ont donnés, aux trois endroits, des tests paléomagnétiques sur le conglomérat qui présentent des directions de ChRM statistiquement aléatoires. On en conclue donc que les clastes n'ont pas été remagnétisés lors de l'événement ayant remagnétisé la matrice qui a probablement été provoqué par l'écoulement d'un fluide hydrothermal pendant l'orogenèse du Laramide, du Crétacé tardif à l'Éocène. Par ailleurs, ces conclusions viennent appuyer des études précédentes en démontrant que les plutons felsiques dans la dépression de Whitehorse présentent vraisemblablement des directions de ChRM primaires, comme, p. ex., le batholite de Whitehorse datant de 112 millions d'années (m.a.), le stock de Mount Lorne datant de 75 m.a. et le stock de Teslin Crossing datant de 186 m.a.

---

[1] *Earth Sciences, University of Windsor, Windsor, Ontario, Canada, N9B 3P4, mjh@uwindsor.ca, dsymons@uwindsor.ca*

[2] *craig.hart@gov.yk.ca*

## INTRODUCTION

There have been many suggestions that pre-Tertiary rock units in the Canadian Cordillera, including large plutons, were remagnetized by regional metamorphism or by fluid flow during the Late Cretaceous – Paleocene Laramide Orogeny (Irving et al., 1985; Johnston et al., 1996b; Smuk et al., 1997; Wynne et al., 1998). The authors have used several versions of the paleomagnetic conglomerate test to examine this hypothesis. Ninety-six clasts (including their sedimentary matrix), which are found in the Conglomerate formation of the Early Jurassic Laberge Group in the southern Yukon, were tested; these clasts are predominantly igneous in origin. The conglomerate was sampled at three Localities, A, B, and C. These localities are approximately 5, 20 and 40 km to the east of the Whitehorse Trough's western contact with the Coast Plutonic Complex, respectively, and cover an area of over 1700 km$^2$ (Figs. 1, 2).

The original paleomagnetic conglomerate test of Graham (1949) is based on two points: (1) the magnetic vectors of the clasts in a conglomerate are randomly oriented; and, (2) the natural remanent magnetization (NRM), or one of its components in the clasts, has been directionally stable since deposition from its parent unit. To explain the first assumption, a clast formed by erosion will possess a characteristic remanent magnetization (ChRM) direction

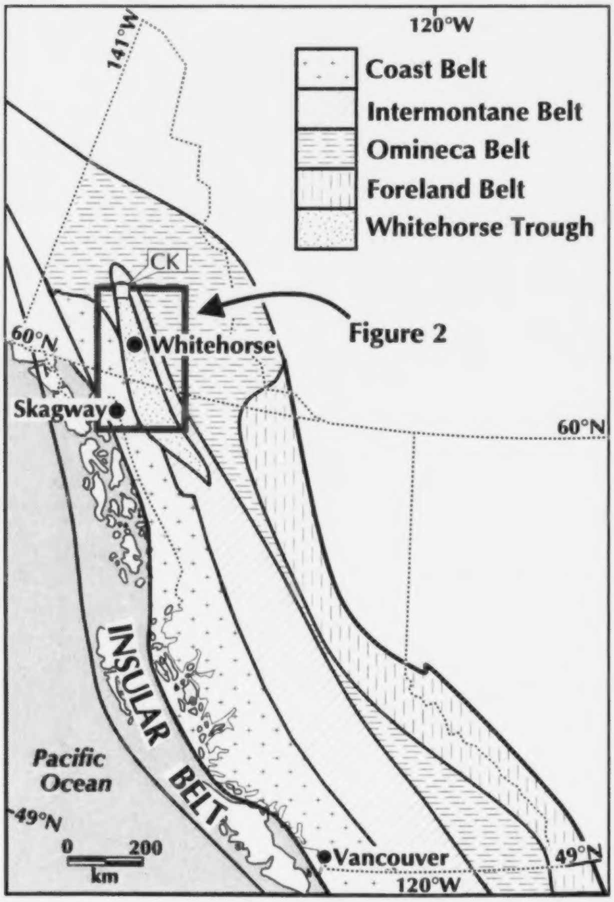
120°W
141°W
Coast Belt
Intermontane Belt
Omineca Belt
Foreland Belt
Whitehorse Trough
CK
Figure 2
60°N
Whitehorse
Skagway
60°N
INSULAR BELT
Pacific Ocean
49°N
0 200 km
Vancouver
49°N
120°W

*Figure 1. Morphogeological belts of the Canadian Cordillera (after Gabrielse et al., 1991), and location of the study area. CK = Carmacks paleomagnetic sampling area.*

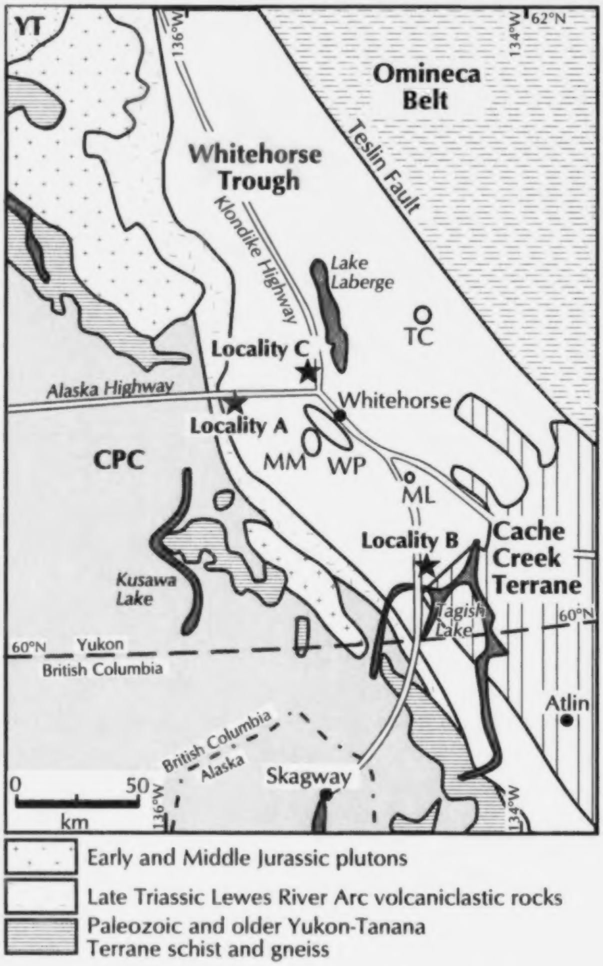
YT
136°W
134°W
62°N
Omineca Belt
Whitehorse Trough
Teslin Fault
Klondike Highway
Lake Laberge
TC
Locality C
Alaska Highway
Whitehorse
Locality A
CPC
MM
WP
ML
Locality B
Cache Creek Terrane
Kusawa Lake
Tagish Lake
60°N
60°N
Yukon
British Columbia
Atlin
British Columbia
Alaska
Skagway
0 50 km
136°W
134°W
Early and Middle Jurassic plutons
Late Triassic Lewes River Arc volcaniclastic rocks
Paleozoic and older Yukon-Tanana Terrane schist and gneiss

*Figure 2. Generalized tectonic map of the south-central Yukon and collection Localities (A, B and C) for the Conglomerate formation of the Laberge Group (YT = Yukon-Tanana Terrane; CPC = Coast Plutonic Complex; MM = Mount McIntyre pluton; WP = Whitehorse pluton; TC = Teslin Crossing stock; ML = Mount Lorne stock).*

of its parent rock unit. Upon deposition, all clasts within the conglomerate should settle with random orientations and, therefore, they should have a statistically random distribution of ChRM directions. If, later in its geological history, the conglomerate is exposed to hydrothermal fluid, metamorphic heating, or deformation events, then the clasts may be remagnetized and their ChRM directions will become realigned. The conglomerate test is considered 'positive' if the clasts have a random distribution of ChRM directions indicating that the rocks in the test area have not suffered a significant post-depositional geological event to cause remagnetization of their magnetic minerals. Alternatively, the test is 'negative' if the clasts yield a cluster of similar ChRM directions, indicating that some post-depositional event has remagnetized the rocks. The nature of the remagnetization must be understood before interpreting data from other paleomagnetic investigations in the area.

Three approaches have been employed to determine if the ChRM directions of the clasts are randomly distributed: (1) an interpretive approach, using the precision parameter, k, of Fisher (1953) as a simple estimate of randomness; (2) a statistical approach, using the Watson (1956) test for randomness that compares the length of the resultant vector, R, to calculated significance points of $R_0$ at the 95% confidence level; and, (3) a statistical approach, using the conglomerate test of Shipunov et al. (1998) that compares the directions of the clasts with a secondary component, commonly the matrix of the host rock, to determine if the host rock component is found within the clasts.

For the first approach, values of $k > 10$ are considered generally to be non-random, that is, it is not random chance that the ChRM directions of the samples came from one population (Butler, 1992). Conversely, values of $k \leq 3$ typically describe a population of random ChRM directions. This is a realistic limit because sample populations that have 5 to 15 specimens and have k values of $\leq 3$ generally have $\alpha_{95}$ values over 20° (see Table 1), and these are often rejected in paleomagnetic studies because they are statistically unacceptably large values.

The Watson (1956) test is based on the fact that $k = 0$ when the distribution of ChRM vectors is uniform or essentially random. Thus the hypothesis states that the density of vector directions is random if the resultant vector, R, is less than the significance point, $R_0$, at the 95% confidence level. If $R > R_0$, then the alternative hypothesis is accepted that there is a significant cluster of directions. Therefore, for the conglomerate test, if $R < R_0$ for the clasts, then there has been no remagnetization of the ChRM directions within the clasts. It is duly noted here that the significance points, $R_0$, were revised by Stephens (1964), however, for $N = 5$ to 20 at the 95% confidence level there are no differences in the values at two decimal places.

The conglomerate test of Shipunov et al. (1998) adds a third point that the direction of possible remagnetization is known. This direction may be measured in specimens from the matrix of the conglomerate or even from an overlying layer of remagnetized rocks. The test uses the equation $\rho = 1/n\Sigma \cos \varphi_i$, where $n$ is the number of specimens, $i = 1$ to $n$, and $\varphi$ is the angle between the $i^{th}$ unit vector and the given or known direction. The hypothesis is that if $\rho < \rho_o$, then the inferred direction is not present, that is, the clasts were not remagnetized by the event that magnetized or remagnetized the hosting rock.

Several studies have indicated that a regional scale hydrothermal event (Hart, 1995; Smuk et al., 1997) occurred throughout the southern Yukon, during the Late Cretaceous to Eocene, that resulted in remagnetization of permeable units in the Whitehorse Trough (Wynne et al., 1998). This event may be related to the Laramide Orogeny, the timing of which varies considerably along the length of the Cordillera. For example, along the west side of the Whitehorse Trough, the Coast Plutonic Complex contains plutons ranging from Eocene to as old as the Early Jurassic (Hart, 1995). However, there was a particularly large magmatic pulse in the Eocene at 55 ± 5 Ma that formed the bulk of the Coast Plutonic Complex at this latitude (Morrison et al., 1979; Armstrong, 1988; Hart, 1995, 1997). Furthermore, it has been suggested that wide-scale hydrothermal systems circulated through permeable formations in the Whitehorse Trough during the Late Cretaceous and Paleocene (105 – 61 Ma; Smuk et al., 1997) and were related to the extrusion of the Carmacks Group volcanic rocks (Johnston et al., 1996b; Wynne et al., 1998). Thus, if pre-Eocene plutons have been affected by any of these events, then clearly, clasts of the Conglomerate formation should have clustered magnetization remanence directions with orientations similar to those of the 70 Ma Carmacks Group volcanic rocks, or even younger Paleocene – Eocene rock bodies. This study provides evidence to the contrary.

*Table 1. Results of tests for randomness at the specimen (Spec.) and clast level.*

| Sample | N/n[a] | R | $\alpha_{95}$ (°) | k | Spec. $\rho$ | Spec. $\rho_o$ | Cong. test[b] | Clast $\rho$ | Clast $\rho_o$ | Cong. test[b] |
|---|---|---|---|---|---|---|---|---|---|---|
| **Matrix** | | | | | | | | | | |
| Locality A all | 13 | 6.91 | 41.4 | 2 | | | | | | |
| well-sorted | 7 | 5.46 | 49.6 | 3 | | | | | | |
| poorly sorted | 6 | 4.20 | 35.2 | 4 | | | | | | |
| Locality B | 16 | 15.54 | 6.6 | 38 | | | | | | |
| Locality C | 13 | 12.69 | 6.8 | 33 | | | | | | |
| **Locality A** | | | | | | | | | | |
| igneous mafic rocks | 9/6 | 6.05 | 38.9 | 3 | 0.156 | 0.319 | A | 0.225 | 0.392 | A |
| porphyritic rocks | 16/14 | 9.80 | 30.7 | 2 | 0.035 | 0.237 | A | 0.136 | 0.254 | A |
| granitoid rocks vi[c] | 26/19 | 24.29 | 7.7 | 15 | 0.118 | 0.186 | A | 0.178 | 0.218 | A |
| all specimens | 57 | 39.40 | 12.7 | 3 | 0.003 | 0.126 | A | | | |
| all clasts | 43 | 32.72 | 12.4 | 4 | | | | 0.204 | 0.143 | Rj, 83 |
| AF[d] | 14 | | | 3 | 0.197 | 0.254 | A | | | |
| pyrrhotite | 2 | | | | | | | | | |
| magnetite | 43/29 | | | 5 | 0.150 | 0.148 | Rj, 94 | 0.068 | 0.176 | A |
| **Locality B** | | | | | | | | | | |
| igneous mafic rocks | 20/16 | 13.00 | 24.8 | 3 | 0.287 | 0.212 | Rj, 85 | 0.241 | 0.237 | Rj, 94 |
| porphyritic rocks | 5/4 | 3.36 | 62.9 | 2 | 0.575 | 0.430 | Rj, 85 | 0.316 | >0.430 | A |
| metasedimentary rocks | 5/4 | 4.00 | 43.8 | 4 | 0.192 | 0.430 | A | 0.284 | >0.430 | A |
| granitoid rocks iv[c] | 7 | 4.02 | 58.7 | 2 | 0.207 | 0.362 | A | | | |
| all specimens | 37 | 21.05 | 20.9 | 2 | 0.091 | 0.156 | A | | | |
| all clasts | 31 | 18.19 | 22.2 | 2 | | | | 0.071 | 0.171 | A |
| AF[d] | 14 | | | 3 | 0.136 | 0.254 | A | | | |
| pyrrhotite | 12/11 | | | 4 | 0.042 | 0.274 | A | 0.092 | 0.286 | A |
| magnetite | 11/7 | | | 1 | 0.086 | 0.286 | A | 0.111 | 0.362 | A |
| **Locality C** | | | | | | | | | | |
| metasedimentary rocks | 5/3 | 2.28 | 70.6 | 1 | 0.145 | 0.430 | A | 0.145 | >0.430 | A |
| granitoid rocks ii[c] | 12/8 | 7.91 | 33.1 | 3 | 0.205 | 0.274 | A | 0.241 | 0.338 | A |
| granitoid rocks vi[c] | 19/14 | 13.19 | 23.1 | 3 | 0.080 | 0.218 | A | 0.117 | 0.254 | A |
| granitoid rocks vii[c] | 12/10 | 10.52 | 17.1 | 7 | 0.279 | 0.274 | Rj, 94 | 0.124 | 0.301 | A |
| all specimens | 54 | 34.99 | 14.4 | 3 | 0.054 | 0.129 | A | | | |
| all clasts | 41 | 25.30 | 17.9 | 3 | | | | 0.067 | 0.148 | A |
| AF[d] | 22/18 | | | 4 | 0.166 | 0.202 | A | 0.099 | 0.224 | A |
| pyrrhotite | 7 | | | 5 | 0.188 | 0.362 | A | | | |
| magnetite | 25/20 | | | 2 | 0.016 | 0.190 | A | 0.099 | 0.212 | A |

[a] number of specimens used to calculate all (N) and number used in reduced average (n)

[b] conglomerate test of Shipunov et al. (1998), where accepted when $\rho < \rho_o$ ; A – accept, Rj – reject at the 95% confidence level. The number after the Rj indicates the % confidence level at which the null hypothesis would be accepted.

[c] see Table 2 for granitoid rock types

[d] AF – alternating field

# GEOLOGY

The Whitehorse Trough (Figs. 1, 2) is a 500-km-long marine basin in the Stikine Terrane that contains ~6000 m of Middle Triassic to Middle Jurassic strata. These strata were derived from a tectonically active, present-day western source region (Wheeler, 1961; Hart et al., 1995). The Carnian to Norian Aksala Formation of the Lewes River Group was deposited as arc-marginal, coarse volcanogenic clastic rocks that grade upward into fine-grained clastic rocks and limestones. The overlying ~2500-m-thick Laberge Group contains two dominant formations: (1) the Richthofen formation comprising Sinemurian to Toarcian sandstones, mudstones and shales; and, of present interest, (2) the overlying Conglomerate formation comprising Sinemurian to Bajocian marine conglomerate (Dickie, 1989; Hart et al., 1995).

The Conglomerate formation is dominated by a polymictic, clast- and matrix-supported cobble- and boulder-rich conglomerate with well-rounded clasts that range up to 2 m in size (Fig. 3). They were deposited as debris flows, sheet floods and bar deposits of fan deltas. Plutonic clasts dominate with smaller percentages of volcanic, sedimentary and metamorphic clasts, respectively (Table 2; Hart et al., 1995). The plutonic clasts are lithologically diverse, and many authors have noted petrographic similarities of the clasts with plutons to the west of the Whitehorse Trough. However, most of these potential source plutons have returned reliable U-Pb zircon dates that are younger than ~190 Ma, indicating that these plutons are too young to provide clasts to Pliensbachian and older strata (Hart, 1995; Hart et al., 1995; Johnston et al., 1996a). Some of the volcanic clasts have been lithologically correlated to the Late Triassic volcanic Povoas Formation of the Lewes River Group, however, sparse rhyolitic and dacitic clasts cannot be correlated to a source.

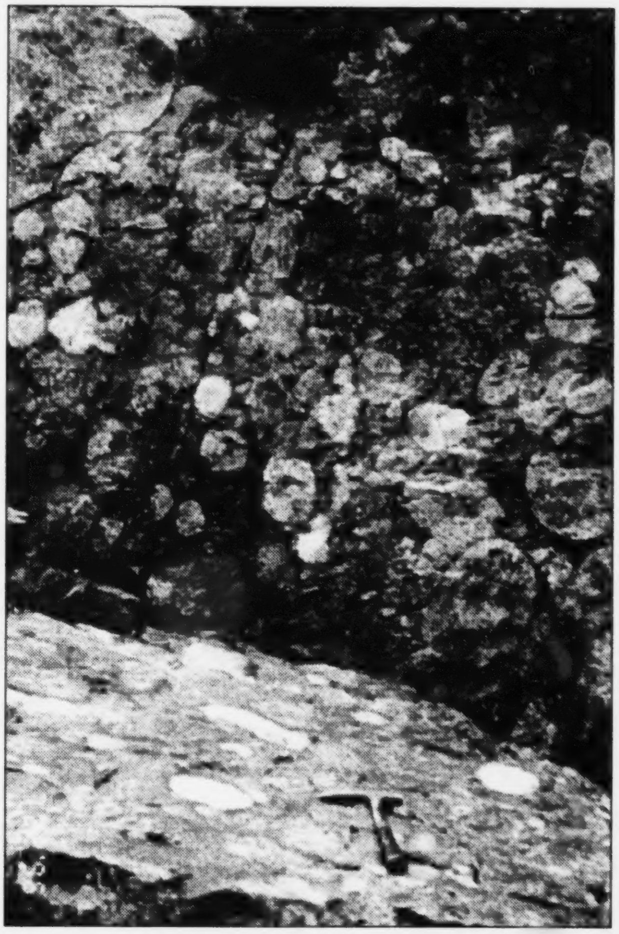

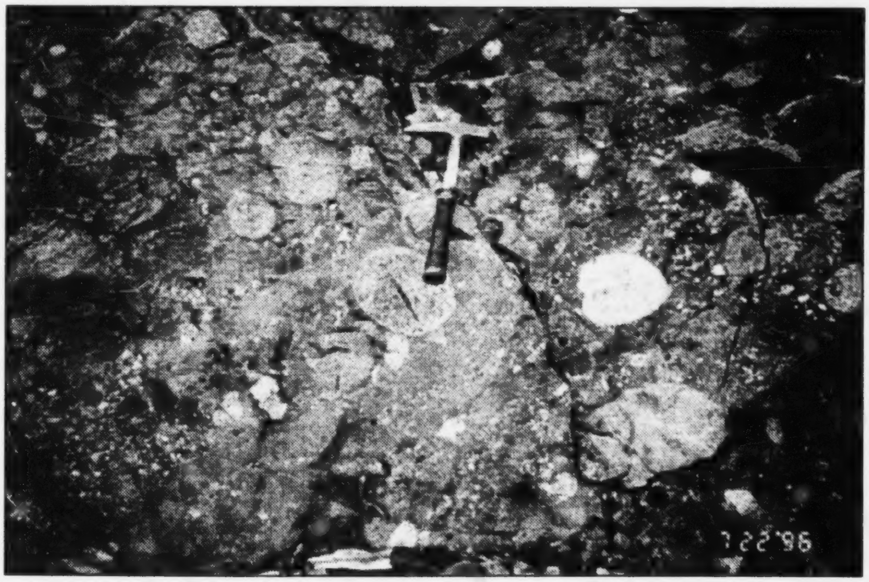

***Figure 3.*** *Field photos of the Conglomerate formation. Hammer is about 30 cm long.*

*Table 2.* The petrographic distribution of clast specimens per locality.

| | **Locality A**<br>**60°51' N**<br>**135°26' W** | **Locality B**<br>**60°16' N**<br>**134°46' W** | **Locality C**<br>**60°58' N**<br>**135°11' W** |
|---|---|---|---|
| igneous mafic rocks (undifferentiated) | 9 | 21 | 2 |
| porphyritic rocks (undifferentiated) | 16 | 5 | 1 |
| metasedimentary rocks (undifferentiated) | 0 | 5 | 5 |
| granitoids | | | |
| i) fgr, pink | 2 | 0 | 0 |
| ii) melanocratic, recrystallized | 2 | 0 | 12 |
| iii) mgr, altered | 2 | 0 | 0 |
| iv) fgr to mgr, leucocratic, recrystallized | 0 | 6 | 0 |
| v) melanocratic, fgr to mgr | 0 | 0 | 3 |
| vi) mgr, leucocratic diorite | 26 | 0 | 19 |
| vii) mgr to cgr, leucocratic diorite with amphibole/pyroxene megacrysts | 0 | 0 | 1 |
| | 57 | 37 | 54 |

Notes: fgr, mgr, cgr – fine-, medium-, and coarse-grained, respectively

The sedimentary clasts of sandstone, shale and limestone are intrabasinal, originating from the underlying Lewes River Group. Finally, sparse metamorphic clasts have only been observed in strata on the western side of the Trough, and are similar to rocks of the Yukon-Tanana Terrane (Jackson et al., 1991; Hart et al., 1995).

Four granitic clasts have been dated by U-Pb zircon techniques from two different localities and at different stratigraphic levels (Hart et al., 1995). Two clasts from Locality A (Fig. 2) yielded an interpreted age of 208 +10/-3 Ma and a discordant upper-intercept age of 215 ± 4 Ma. Two granitic clasts from Locality C (Fig. 2) yielded an interpreted age of 210 +6/-3 Ma and a weighted mean $^{207}$Pb/$^{206}$Pb age for three fractions of 210 ± 8 Ma. These data indicate that Late Triassic plutons (ca. 215 - 208 Ma) were present in the source region during the deposition of the conglomerate.

## EXPERIMENTAL METHODS

At each of the three localities (Fig. 2), 40 drill core samples of standard 2.5-cm-diameter were taken, with 32 core samples of varying clasts and 8 core samples of the matrix. At Locality A, 2 variations of matrix grain size were encountered, as a result 4 core samples were taken from each size. Overall, from the 3 localities, 54% of the 96 clasts comprise felsic plutonic rocks, 21% comprise mafic igneous rocks, and the remaining 25% comprise a variety of metasedimentary and undifferentiated porphyritic rocks (Table 2).

The paleomagnetic measurements were carried out in the Paleomagnetic Laboratory at the University of Windsor using an automated Canadian Thin Films DRM-420 cryogenic magnetometer, a Sapphire Instruments SI-4 alternating field (AF) demagnetizer, a Sapphire Instruments SI-5 spinner magnetometer, a Sapphire Instruments SI-6 pulse magnetizer, and a Magnetic Measurements MMTD-1 thermal demagnetizer. All the instruments are in a magnetically shielded room which has an ambient field of ~0.2% of the Earth's magnetic field intensity.

The natural remanent magnetization (NRM), that is, the magnetic intensity and direction before any treatment, was measured for each of the 190 specimens. The 42 matrix specimens had NRM intensities ranging from $1.3 \times 10^{-3}$ to $2.1 \times 10^{-1}$ amperes/metre (A/m) with a median intensity of $1.1 \times 10^{-2}$ A/m (lower quartile, $Q_1 = 2.4 \times 10^{-3}$ A/m; upper quartile, $Q_3 = 2.4 \times 10^{-2}$ A/m). The 148 specimens from the clasts had NRM intensities ranging from $1.0 \times 10^{-3}$ to $2.7 \times 10^{0}$ A/m with a median intensity of $1.5 \times 10^{-1}$ ($Q_1 = 1.9 \times 10^{-2}$ A/m; $Q_3 = 4.5 \times 10^{-1}$ A/m).

For the matrix specimens at Localities B and C, three pilot specimens were selected that had average intensities and directions. Two of the pilot specimens underwent detailed thermal demagnetization of 11 steps from 200°C to 580°C, while the third pilot specimen underwent detailed alternating field (AF) demagnetization of 10 steps from 5 milli tesla (mT) to 130 mT. The remaining specimens for each location were evenly divided in numbers and demagnetized either by AF demagnetization in at least five steps or thermally in at least eight steps. Locality A contained two types of matrix, and thus three pilot specimens were selected from each type. They were demagnetized in a similar manner to those pilot specimens from the other two localities. The remaining specimens for Locality A were also divided evenly for either AF or thermal demagnetization in at least five or eight steps, respectively.

Each petrographic group of clasts per locality (Table 2) had individual schedules of demagnetization. In general, two thermal pilot specimens and one AF pilot specimen underwent detailed schedules as described above for the matrix pilot specimens. In most cases, the remaining specimens per group were split evenly for either AF or thermal demagnetization. The granitoids at Locality A are the only exception, having all remaining specimens undergo a minimum of eight steps of thermal demagnetization because the AF pilot specimen showed that this method did not significantly demagnetize the specimens.

Saturation isothermal remanent magnetization (SIRM) testing was performed on 23 representative specimens to further define the mineralogy and domain size of the magnetic carriers. Each specimen was magnetized in 13 steps in a direct field from 10 mT to 900 mT, followed by 10 steps of AF demagnetization from 10 mT to 140 mT, with the specimen being measured after each step.

Specimen ChRM directions were calculated using the end-point method of Kirschvink (1980) and were accepted for statistical analysis if the best-fit stable direction had a maximum angular deviation of <15° over at least three consecutive steps. Averages for the various groups were calculated using the statistical method of Fisher (1953).

## PALEOMAGNETIC RESULTS

### LOCALITY A

Locality A, ~5 km east of the western margin of the Whitehorse Trough (Fig. 2), had two types of matrix: a fine-grained, well-sorted, homogeneous greywacke, and a fine-grained, poorly sorted, greywacke, with pebbles that are up to ~1 cm in diameter. The well-sorted matrix specimens that were thermally demagnetized have a large viscous component, gradually losing more than 75% of their NRM intensity by 290°C (Fig. 4a). Orthogonal decay plots (Zijderveld 1967) show that these specimens have a single vector component (e.g., Figs. 5a, b). SIRM testing suggests that the magnetic carriers are pseudosingle to multidomain pyrrhotite (Fig. 6a). The majority of these specimens have steep downward ChRM directions (Fig. 7a). The pebbly matrix specimens show unblocking temperature spectra of magnetite, generally having a large percentage of their intensity decreasing in the magnetite

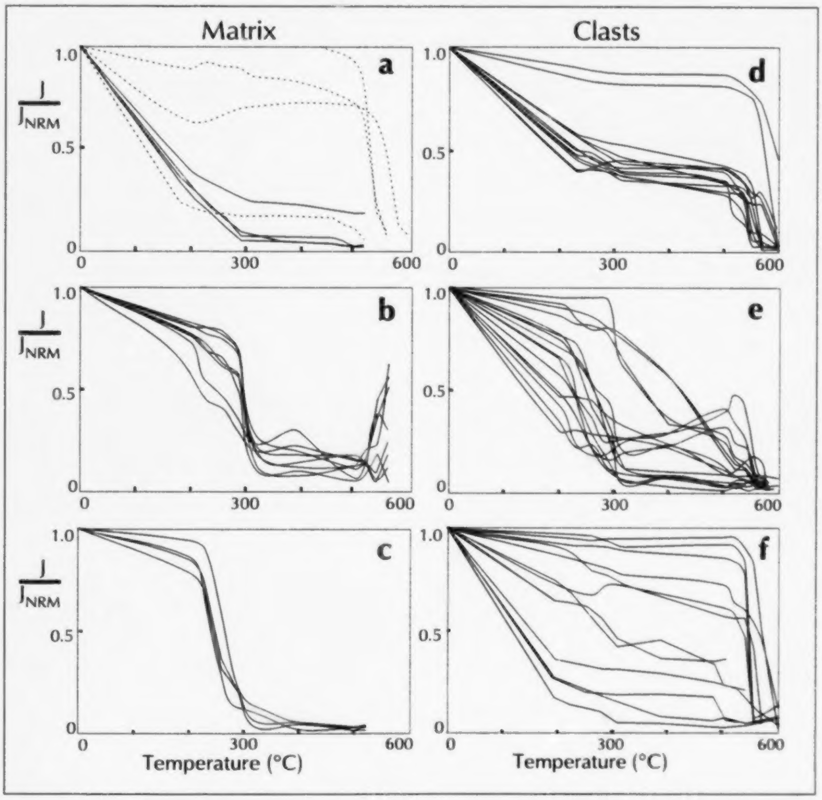

*Figure 4. Thermal decay curves for matrix (a-c) and clast (d-f) specimens. $J/J_{NRM}$ is the specimen's magnetic intensity after treatment divided by its NRM intensity; (a, d) Locality A, (b, e) Locality B, (c, f) Locality C. In (a) the solid lines represent the well-sorted matrix and the dashed lines are the pebbly matrix.*

range of 550°C to 570°C (Fig. 4a). Orthogonal decay plots generally show two components, a low temperature component that is inclined steeply downward, and a ChRM that is inclined moderately upward (Fig. 5c). SIRM testing suggests that the ChRM is carried in multidomain magnetite (Fig. 6b). Although the ChRM directions show a bimodal distribution (Fig. 7a), it is noted that the three specimens that plot to the west are from one core sample, whereas the southwest cluster is composed of specimens from three core samples.

The clasts at Locality A (Table 2) show thermal demagnetization spectra typical of magnetite (Fig. 4d), although some specimens have a greater viscous component than others, that is, more gradual decay. Specific orthogonal decay plots for Locality A include a mafic intrusive specimen (Fig. 5f) and two porphyritic specimens (Figs. 8a, b). Eight specimens were selected for SIRM testing and all plot within the pseudosingle to multidomain magnetite range (Fig. 6b). In situ geographic ChRM directions for the 57 specimens are plotted in Fig. 8d.

## LOCALITY B

Locality B is situated ~20 km east of the western margin of the Whitehorse Trough (Fig. 2). The matrix consists of fine-grained, well-sorted greywacke. All specimens that were thermally demagnetized show pyrrhotite-unblocking temperatures (Fig. 4b). Orthogonal decay curves are

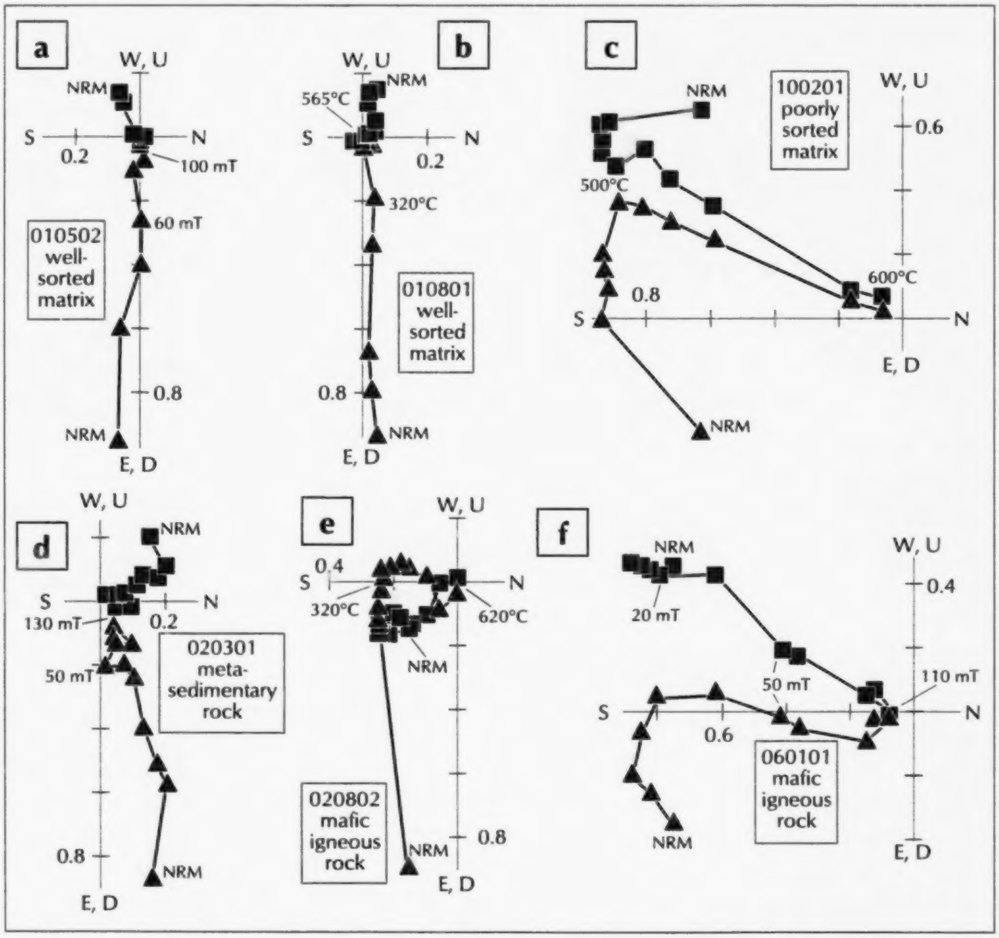

*Figure 5. Orthogonal demagnetization plots (Zijderveld, 1967). Triangles are in the vertical plane, up-north-down-south (U-N-D-S) and the squares are in the horizontal plane, west-north-east-south (W-N-E-S).*

similar to those seen in Figures 5a and b, having steep downward inclinations. SIRM testing shows the magnetic carriers to be pseudosingle to multidomain pyrrhotite (Fig. 6a). Most of the specimens have ChRM directions inclined steeply downward to the east (Fig. 7b).

Thermal decay curves for the clasts at Locality B show several patterns. About one-third of the clasts have large intensity decreases in the 270°C to 320°C range, characteristic of pyrrhotite (Fig. 4e). Several other specimens show a gradual decay with only ~50% of their NRM intensities at ~400°C and <10% of their intensities by 570°C, suggesting that either coarse-grained magnetite or titanomagnetite is present. Several other specimens show intensity decreases to ~30% by ~290°C before increasing up to ~550°C, where they decay rapidly in the magnetite temperature range. This decrease-increase-decrease pattern evidently records their polarity reversal from normal to reverse (see Figure 5e). One specific example of how the granitoids change in direction and intensity is shown in Figure 8f. Five specimens were selected for SIRM testing and yielded curves that plot within the pseudosingle to multidomain magnetite range (Fig. 6b). All four groups of clasts exhibited both downward and upward inclinations (Fig. 7e).

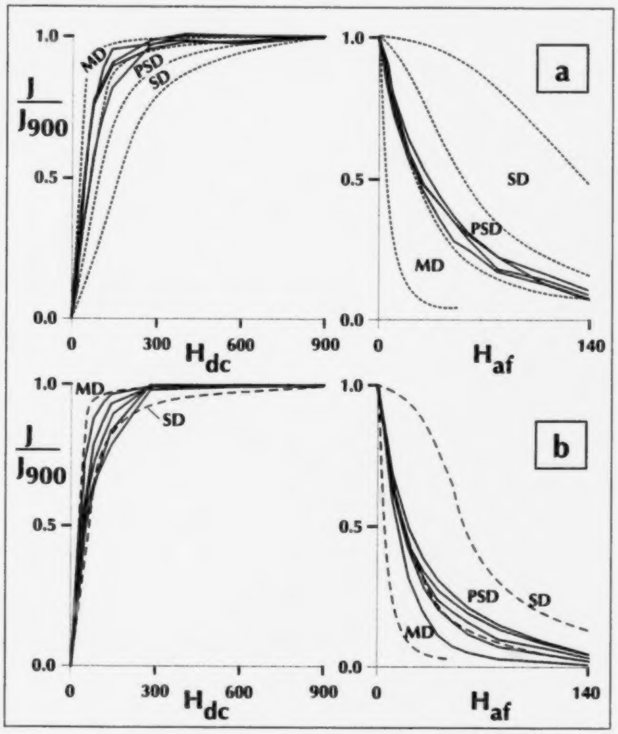

*Figure 6. Representative SIRM acquisition and decay curves for (a) the matrix specimens and (b) the clast specimens. The horizontal axes represent the magnetization acquired ($H_{dc}$) and decayed ($H_{af}$), measured in mT, and the y-axis is the measured intensity as a ratio of the saturation intensity (at 900 mT). The reference curves in (a and b) are for multidomain (MD), pseudosingle domain (PSD), and single domain (SD) pyrrhotite and magnetite, respectively.*

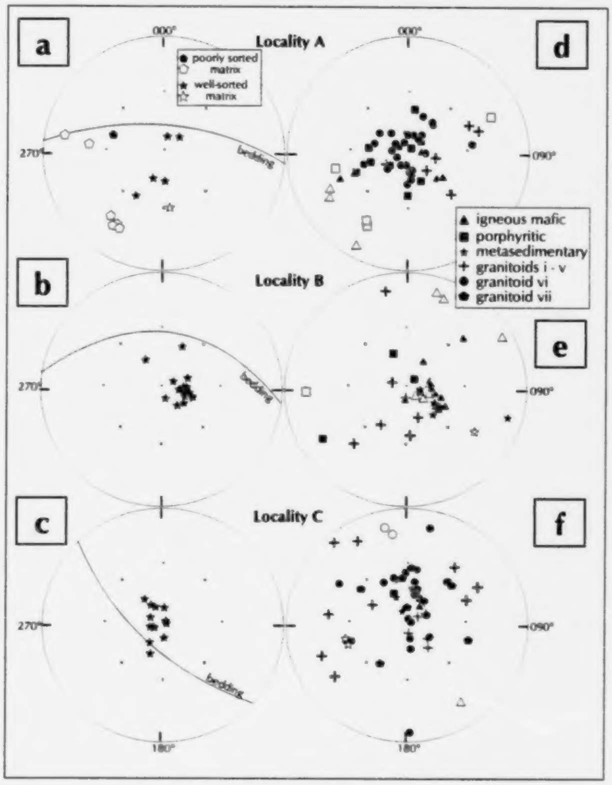

***Figure 7.*** *Equal-area stereonets showing the geographic in situ ChRM directions for the matrix (a-c) and clast (d-f) specimens. Closed symbols represent directions in the lower hemisphere of the net and represent normal polarity directions, while open symbols represent directions in the upper hemisphere and reverse polarity directions. The orientation of the bedding planes are shown on the matrix stereonets.*

## LOCALITY C

The matrix at Locality C, which lies ~40 km east of the Coast Plutonic Complex boundary and near the present centre of the Whitehorse Trough (Fig. 2), consists of a fine-grained, well-sorted greywacke. The matrix specimens that were thermally demagnetized show pyrrhotite-unblocking temperatures (Fig. 4c) and have only single vector components with steep downward inclinations (Figs. 5a, b). SIRM testing suggests that the magnetic carriers are pseudosingle to multidomain pyrrhotite (Fig. 6a). ChRM directions for all the specimens are well clustered and are inclined steeply downward towards the west (Fig. 7c).

All clast specimens showed magnetite or titanomagnetite unblocking temperature spectra, although several specimens had a large viscous component and lost ~75% of their NRM intensity by 200°C (Fig. 4f). Specific orthogonal demagnetization plots for Locality C includes a metasedimentary specimen (Fig. 5d), a mafic dyke specimen (Fig. 5e), and several granitoids (Fig. 8c,d,e). SIRM testing on seven specimens suggests that the magnetic carriers are pseudosingle to multidomain magnetite (Fig. 6b). Most of the groups of clasts show both upward and downward inclinations, except for the granitoid vii group (Table 2) that shows only downward inclinations (Fig. 7f).

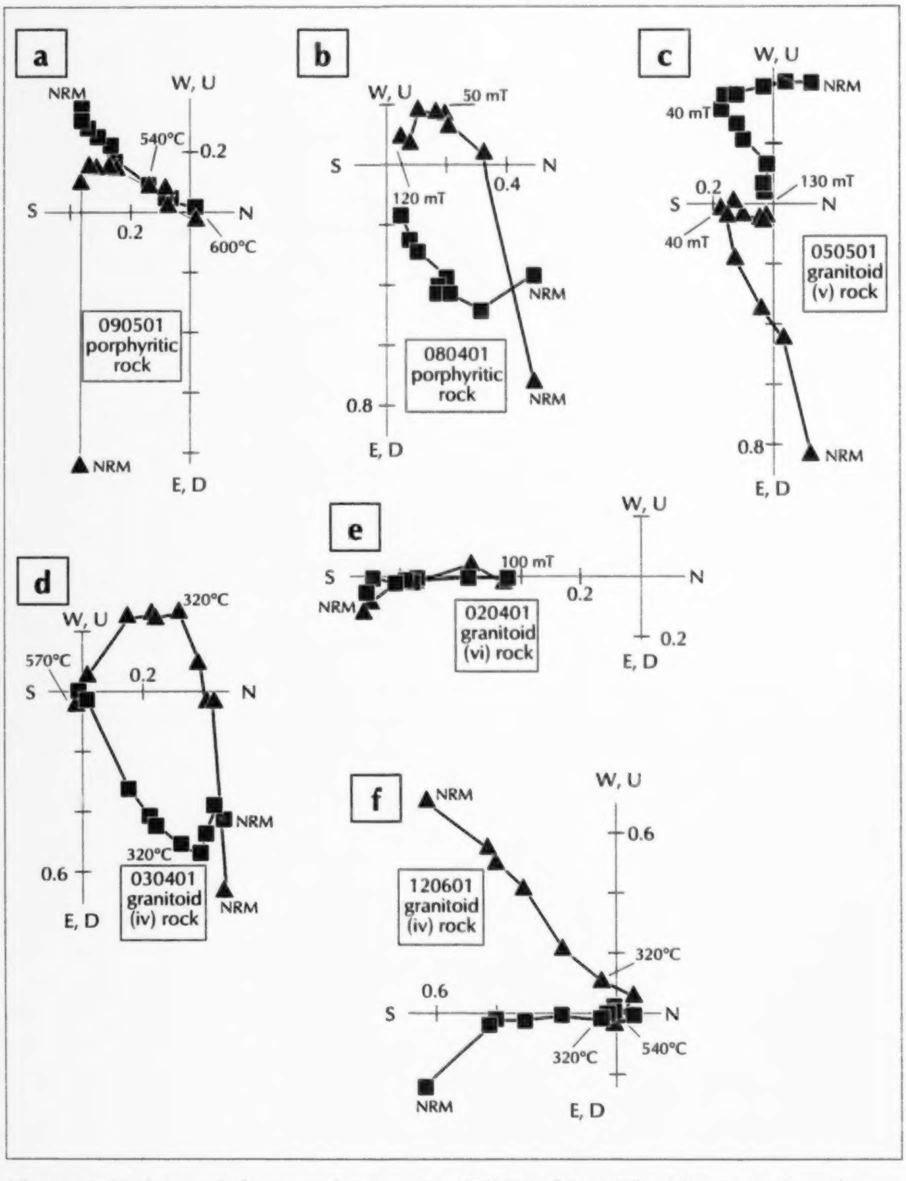

*__Figure 8.__ Orthogonal demagnetization plots (Zijderveld, 1967) with conventions the same as in Figure 5.*

## CONGLOMERATE TESTS

The Watson (1956) test was run and the majority of the tests failed, suggesting significant remagnetization of both the matrix and clasts. However, the Watson (1956) test is deemed inappropriate for this study because it does not factor in the potential effects of dual polarities. This potential needs to be considered for Jurassic-aged rocks that could have been remagnetized, if at all, over a period of several million years between the Jurassic and the present, during which time the Earth's magnetic field underwent numerous polarity reversals (Cande and Kent, 1995; Opdyke and Channell, 1996).

The other two conglomerate tests were performed for each locality using groups based on clast and matrix petrology (Table 1). Only those groups with five or more specimens are listed because the critical values of Shipunov et al. (1998) commence at $N = 5$. Two averages were calculated for the clasts per locality: one average used directions from all the specimens and the second average used a 'reduced' data set. The latter data set used the averages for cores from clasts that yielded two or more specimens, in addition to the clasts that yielded only one specimen. The precision parameter, k, was evaluated as a guideline, given that many groups are represented by only a few specimens.

### MATRIX

The ChRM directions for the matrix specimens at Localities B and C both give well-defined clusters of steep downward, single-component vectors, with low radii of 95% cones of confidence ($\alpha_{95}$) and high k values (Table 1; Figs. 7b,c). As previously noted, two types of matrix were collected at Locality A. Neither carried a well-clustered magnetization direction (Fig. 7a), presumably because of the pea-sized pebbles in the poorly sorted matrix, and because of the relatively coarse grain size of the 'well-sorted' matrix. Nevertheless, the latter population gives a ChRM direction that is similar to that of Localities B and C if the results from one core sample are excluded (Fig. 7a), and this direction is used for the Locality A mean matrix population. Thus the mean matrix directions used to compare with the clast directions in the Shipunov et al. (1998) conglomerate test for Localities A, B and C are declination ($D_A$) = 193°, inclination ($I_A$) = 77°, $\alpha_{95A}$ = 24°, $D_B$ = 095°, $I_B$ = 76°, $\alpha_{95B}$ = 6.5°, and $D_C$ = 083°, $I_C$ = 85°, $\alpha_{95C}$ = 6.8°, respectively.

### CLASTS

The results of the conglomerate tests are given in Table 1. Based on the k values, most petrologic groups of clasts are randomly oriented except for the granitoid vi rocks at Locality A, and possibly the granitoid vii rocks at Locality C.

Applying the Shipunov et al. (1998) test at Locality A, and using all the acceptable specimens for all petrologic groups and all specimens in total, the ChRM directions indicate that the null hypothesis should be accepted, that is, that the clast specimens do not carry the ChRM direction found in the matrix. Acceptance of the null hypothesis is also found for the averaged clast ChRM directions for all petrologic groups. However, when all clast directions at only Locality A are grouped, the test rejects the null hypothesis at the 95% confidence level. Nevertheless, the null hypothesis is accepted at a high 83% confidence level. This result suggests that there may be a minor remagnetization contribution, possibly from the failure of AF step demagnetization to entirely remove the steep downward components of all specimens at Locality A.

At Locality B, two petrologic groups pass and two fail the Shipunov et al. (1998) test at the 95% confidence level when specimen ChRM directions are used. However, the two groups that fail, do reach acceptance at a relatively high 85% confidence level. All specimens combined together pass the test. When the clast ChRM directions are considered, two petrologic groups accept the null hypothesis at 95% and a third at 94% confidence, and all clasts together provide acceptance.

For Locality C, all groupings indicate acceptance of the null hypothesis at the 95% confidence level that the matrix magnetization direction is not present in the clasts except for the granitoid vii rocks at the specimen level, which do accept the hypothesis at the 94% confidence level.

Overall, it is evident that the Shipunov et al. (1998) conglomerate test provides a high degree of assurance that the clasts within the conglomerate have not suffered statistically significant remagnetization since deposition. By simple random chance at the 95% confidence level, a 5% rejection rate would be expected, that is, about two of the 27 groupings should fail. Out of the five that did fail, the two populations indicating acceptance at 94% confidence, but not 95% confidence, are not worthy of concern, thus leaving a statistically insignificant three groups. However, the three groups at ~84% confidence merits some attention. There are two possible explanations. One is that AF step demagnetization is not entirely successful in removing all viscous remanent magnetization that the specimens might retain from the present Earth's magnetic field prior to isolation of the ChRM. Alternatively, either AF and/or thermal step demagnetization may not have entirely removed the effects of the event that magnetized the matrix. To evaluate these options, the tests were rerun for each locality and for the entire collection, grouping the specimens by demagnetization method (Table 1).

The specimens that were AF demagnetized at all three locations accepted the null hypothesis (Table 1), confirming that this method was successful in removing the magnetization direction found in the matrix. The three tests involving specimens from clasts with their ChRM directions in the pyrrhotite range also accepted the null hypothesis. Finally, five of the six tests involving specimens and clasts that have their ChRM directions in magnetite, also pass the conglomerate test at the 95% confidence level, with the sixth test passing at the 94% confidence level. Therefore, the few petrologic groups that failed the Shipunov et al. (1998) test appear to be due to statistical methods and not geological concerns.

## DISCUSSION

Using the procedure of Shipunov et al. (1998), the clasts at all three localities pass the conglomerate test. A few of the lithologic groups fail the conglomerate test by rejecting the null hypothesis, but as noted above, with 27 groups being tested, it is expected that a few tests should fail at the 95% confidence level. Therefore, it is suggested that the preferred magnetization found in the matrix at each locality is not present within the clasts. Thus the clasts contain ChRM directions that are older than the matrix directions because most tests accept the null hypothesis regardless of clast composition or demagnetization method, thereby providing a regional paleomagnetic conglomerate test.

There is an apparent visual cluster of downward directions in the clast specimen ChRMs (Fig. 7). There are two possible explanations for this. Firstly, there may be some minor remagnetization. Secondly, the specimens may not be sufficiently demagnetized. It should be noted, however, that the majority of the specimens showing reverse polarity were thermally demagnetized and have their ChRM vectors in the magnetite unblocking range. Conversely, those specimens that were AF demagnetized, or had their ChRM found in pyrrhotite (about one-third to one-half of the specimens per locality), may not be completely demagnetized. Thus they may be showing either minor residual remagnetization vectors or residual viscous magnetization, not their true ChRM directions. This hypothesis is supported by the results from several clasts that yielded more than one specimen. They show a steep downward normal polarity direction for the AF demagnetized specimen, and a reverse-polarity direction for the specimen that was thermally demagnetized.

The result presented here, that the Conglomerate formation of the Laberge Group passes the paleomagnetic conglomerate test, conflicts with the result presented by Wynne et al. (1998) who sampled one site near Locality A (Fig. 2). They took two core samples, each from three different boulders in a single bed, and suggested that the conglomerate test fails ($N = 3$, $R = 2.93 > R_{crit} = 2.71$) by extrapolating the critical values from Stephens (1964). Firstly, as noted earlier, the Watson test (1956) and thus Stephens' (1964) variant were deemed inappropriate because they do not factor in the possibility of dual polarity directions. Secondly, Wynne et al. (1998) used a statistically very small sample size. Thirdly, no critical values were given by Stephens (1964) for $N = 3$, however, it does appear that the conglomerate test performed by Wynne et al. (1998) would pass at the 90% confidence level. Thus the test result of Wynne et al. (1998) is considered controversial.

The age of the conglomerate matrix remagnetization is a dilemma. It appears to be post regional folding because the mean ChRM directions for the three localities diverge from each other as the sites are unfolded (e.g., the paleomagnetic fold test; see Figures 7a,c,e). However, if the three mean directions are averaged, the overall mean is found at $D = 161.2°$, $I = 84.8°$, $\alpha_{95} = 19.4°$. The resulting paleopole is located at 50.8°N, 130.0°W and it provides no reasonable geological interpretation. This result is likely caused by the very small sample size of the matrix, that is, only three poorly clustered sites. Note also that unfolding of the clast directions does not decrease the random nature of their directions because many more directions flip from normal to reverse directions rather than vice versa.

Two lines of evidence may provide an approximate age of magnetization for the matrix. The permeable rock units in the southern Yukon are thought by some to be remagnetized from hydrothermal alteration related to the extrusion of the Carmacks Group volcanic rocks at around 70 Ma (e.g., Smuk et al., 1997; Wynne et al., 1998). Another indicator comes from a region to the north of the study area, where volcanic rocks of the 105 Ma Mt. Nansen suite yield a range of partially reset ages between 94 and 61 Ma (Hart, 1995; Smuk et al., 1997). These indicators suggest that the porous matrix of the conglomerate likely acquired its present magnetization during the latest Cretaceous to Paleocene. The fact that the clasts do not carry the matrix magnetization direction, but rather are statistically random, suggests that they have not been significantly remagnetized since deposition.

Results from this study show that clasts of variable composition that range in size from ~10 cm to ~200 cm in diameter, have not been significantly remagnetized. Although other studies suggest that permeable units may be remagnetized, the majority of the clasts in this study were derived from generally impermeable felsic intrusive rock units. Given that small clasts are not remagnetized, it is most unlikely that stocks and batholiths in the Whitehorse Trough have been remagnetized unless evidently fractured and altered. Therefore, the results of this study advocate that intrusive bodies in strata of the Whitehorse Trough will carry magnetic remanences that predate any potential Late Cretaceous or Tertiary hydrothermal events and hence are likely to be primary remanences. This conclusion supports earlier published studies that report primary remanences in large plutons in the Whitehorse Trough including the Late Cretaceous Mount Lorne stock (Harris et al., 1999b), the mid-Cretaceous Mount McIntyre pluton (Harris et al., 1996), the mid-Cretaceous Whitehorse batholith (Harris et al., 1997), and the Middle Jurassic Teslin Crossing stock (Harris et al., 1999a; Fig. 2). It is noted that these plutons are not significantly fractured nor altered, and that the ChRM is carried by magnetite in all four studies and therefore further supports the conclusions of the tectonic movements of these units.

## CONCLUSIONS

Clasts at three widely separated sites in the Jurassic Conglomerate formation of the Laberge Group of the Whitehorse Trough statistically pass the paleomagnetic conglomerate test. The 96 clasts of variable compositions carry a random population of ChRM directions, showing that they have not been significantly remagnetized since deposition. The matrix carries a ChRM direction that was likely acquired during the Late Cretaceous to Eocene, probably through hydrothermal alteration during the Laramide Orogeny. The conclusion of this regional conglomerate test indicates, in all probability, that most intrusive rock bodies within strata of the Whitehorse Trough will carry a primary remanence, as has been shown in four previously published studies on large felsic plutons.

## ACKNOWLEDGEMENTS

The authors wish to thank the Natural Sciences and Engineering Research Council (NSERC) for funding through LITHOPROBE grants. This is LITHOPROBE publication number 1262.

## REFERENCES

Armstrong, R.L., 1988. Mesozoic and Early Cenozoic magmatic evolution of the Canadian Cordillera. *In:* Processes in Continental Lithospheric Deformation, S.P. Clark, B.C. Burchfiel and J. Suppe (eds.), Geological Society of America, Special Paper 218, p. 55-91.

Butler, R.F., 1992. Paleomagnetism: Magnetic Domains to Geologic Terranes. Blackwell Scientific Publications, Oxford, 319 p.

Cande, S.C. and Kent, D.V., 1995. Revised calibration of the geomagnetic polarity time scale for the Late Cretaceous and Cenozoic. Journal of Geophysical Research, vol. 100, p. 6093-6095.

Dickie, J.R., 1989. Sedimentary response to arc-continent transpressive tectonics, Laberge Conglomerates (Jurassic), Whitehorse Trough, Yukon Territory. Unpublished M.Sc. thesis, Dalhousie University, Halifax, Nova Scotia, Canada, 361 p.

Fisher, R.A., 1953. Dispersion on a sphere. Proceedings of the Royal Society of London, vol. A217, p. 295-305.

Gabrielse, H., Monger, J.W.H., Wheeler, J.O. and Yorath, C.J., 1991. Tectonic framework, Chapter 2. *In:* Geology of the Cordilleran Orogen in Canada, H. Gabrielse and C.J. Yorath (eds.), Geological Survey of Canada, Geology of Canada, no. 4, p. 15-28.

Graham, J.W., 1949. The stability and significance of magnetism in sedimentary rocks. Journal of Geophysical Research, vol. 54, p. 131-167.

Harris, M.J., Symons, D.T.A., Blackburn, W.H. and Hart, C.J.R., 1996. Paleomagnetic study of the mid-Cretaceous Mount McIntyre pluton, Whitehorse map area (105D), southern Yukon Territory. Yukon Exploration and Geology 1996, Exploration and Geological Services Division, Yukon Region, Indian and Northern Affairs Canada, p. 124-132.

Harris, M.J., Symons, D.T.A., Blackburn, W.H. and Hart, C.J.R., 1997. Paleomagnetic and geobarometric study of the mid Cretaceous Whitehorse pluton, Yukon Territory. Canadian Journal of Earth Sciences, vol. 34, p. 1379-1391.

Harris, M.J., Symons, D.T.A., Hart, C.J.R. and Blackburn, W.H., 1999a. Jurassic plate motions of the Yukon: A paleomagnetic study of the Teslin Crossing stock (NTS 105E/7). Yukon Exploration and Geology 1998, C.F. Roots and D.S. Emond (eds.), Exploration and Geological Services Division, Yukon Region, Indian and Northern Affairs Canada, p. 155-166.

Harris, M.J., Symons, D.T.A., Blackburn, W.H. and Hart, C.J.R., 1999b. Paleomagnetic and geobarometric study of the Late Cretaceous Mount Lorne stock, southern Yukon Territory. Canadian Journal of Earth Sciences, vol. 34, p. 905-915.

Hart, C.J.R., 1995. Magmatic and tectonic evolution of the Intermontane Superterrane and Coast Plutonic Complex in southern Yukon Territory. Unpublished M.Sc. thesis, University of British Columbia, Vancouver, British Columbia, Canada, 196 p.

Hart, C.J.R., 1997. A transect across northern Stikinia: Geology of the northern Whitehorse map area, southern Yukon Territory (105D/13-16). Exploration and Geological Services Division, Yukon Region, Indian and Northern Affairs Canada, Bulletin 8, 112 p.

Hart, C.J.R., Dickie, J.R., Ghosh, D.K. and Armstrong, R.L., 1995. Provenance constraints for Whitehorse Trough conglomerate: U-Pb zircon dates and initial Sr ratios of granitic clasts in Jurassic Laberge Group, Yukon Territory. *In:* Jurassic Magmatism and Tectonics of the North American Cordillera, D.M. Miller and C. Busby (eds.), Geological Society of America Special Paper 299, p. 47-63.

Irving, E., Woodsworth, G.J., Wynne, P.J. and Morrison, A., 1985. Paleomagnetic evidence for displacement from the south of the Coast Plutonic Complex, British Columbia. Canadian Journal of Earth Sciences, vol. 22, p. 584-598.

Jackson, J.L., Gehrels, G.E., Patchett, P.J. and Mihalynuk, M.G., 1991. Stratigraphic and isotopic link between the northern Stikinia and an ancient continental margin assemblage, Canadian Cordillera. Geology, vol. 19, p. 1177-1180.

Johnston, S.T., Mortensen, J.K. and Erdmer, P., 1996a. Igneous and metaigneous age constraints for the Aishihik metamorphic suite, southwest Yukon. Canadian Journal of Earth Sciences, vol. 33, p. 1543-1555.

Johnston, S.T., Wynne, P.J., Francis, D., Hart, C.J.R., Enkin, R.J. and Engebretson, D.C., 1996b. Yellowstone in Yukon: The Late Cretaceous Carmacks Group. Geology, vol. 24, p. 997-1000.

Kirschvink, J.L., 1980. The least squares line and plane and the analysis of paleomagnetic data. Geophysical Journal of the Royal Astronomical Society, vol. 62, p. 699-718.

Morrison, G.W., Godwin, C.I. and Armstrong, R.L., 1979. Interpretation of isotopic ages and $^{87}Sr/^{86}Sr$ initial ratios for plutonic rocks in the Whitehorse map area, Yukon. Canadian Journal of Earth Sciences, vol. 16, p. 1988-1997.

Opdyke, N.D. and Channell, J.E.T., 1996. Magnetic Stratigraphy. Academic Press Inc., San Diego, USA.

Shipunov, S.V., Muraviev, A.A. and Bazhenov, M.L., 1998. A new conglomerate test in palaeomagnetism. Geophysical Journal International, vol. 133, p. 721-725.

Smuk, K.A., Williams-Jones, A.E. and Francis, D., 1997. The Carmacks hydrothermal event: An alteration study in the southern Dawson range, Yukon. Yukon Exploration and Geology 1996, Exploration and Geological Services Division, Yukon Region, Indian and Northern Affairs Canada, p. 92-106.

Stephens, M.A., 1964. The testing of unit vectors for randomness. Journal of the American Statistical Association, vol. 59, p. 160-167.

Watson, G.S., 1956. A test for randomness of directions. Monthly Notice of the Royal Astronomical Society Geophysics Supplement, vol. 7, p. 160-161.

Wheeler, J.O., 1961. Whitehorse map-area, Yukon Territory. Geological Survey of Canada, Memoir 312, 156 p.

Wynne, P.J., Enkin, R.J. Baker, J., Johnston, S.T. and Hart, C.J.R., 1998. The big flush: Paleomagnetic signature of a 70 Ma regional hydrothermal event in displaced rocks of the northern Canadian Cordillera. Canadian Journal of Earth Sciences, vol. 35, p. 657-671.

Zijderveld, J.D.A., 1967. A.C. demagnetization of rocks: analysis of results. *In:* Methods in Paleomagnetism, D.E.W. Collison, K.K. Crier and S.K. Runcorn (eds.), Elsevir, Amsterdam, The Netherlands, p. 254-286.

# New mapping around the Slab iron oxide-copper-gold occurrence, Wernecke Mountains (parts of NTS 106C/13, 106D/16, 106E/1 and 106F/4), Yukon

***Julie A. Hunt***[1]
*Yukon Geology Program*[2]

***John R. Laughton, Marc-Andre Brideau and Derek J. Thorkelson***
*Simon Fraser University*[3]

***Melanie L. Brookes and Tim Baker***
*James Cook University*[4]

Hunt, J.A., Laughton, J.R., Brideau, M-A., Thorkelson, D.J., Brookes, M.L. and Baker, T., 2002. New mapping around the Slab iron oxide-copper-gold occurrence, Wernecke Mountains (parts of NTS 106C/13, 106D/16, 106E/1 and 106F/4), Yukon. *In:* Yukon Exploration and Geology 2001, D.S. Emond, L.H. Weston and L.L. Lewis (eds.), Exploration and Geological Services Division, Yukon Region, Indian and Northern Affairs Canada, p. 125-138.

## ABSTRACT

Bedrock underlying the Slab iron oxide-copper-gold occurrence consists of fine-grained sedimentary rocks and schist of the Fairchild Lake Group (oldest unit of the Early Proterozoic Wernecke Supergroup), intermediate to mafic Slab volcanics, dioritic Bonnet Plume River Intrusions, and Early Proterozoic Wernecke Breccia that crosscuts all other units. The Wernecke Breccia was divided into two units: Type 1 and Type 2. Type 1 is limited in extent and consists of sedimentary and locally abundant massive magnetite clasts in a carbonate-magnetite matrix. Type 2 cuts Type 1 and comprises sedimentary clasts in a micro-breccia matrix. Iron oxide-copper-gold mineralization is associated with Wernecke Breccia. It occurs disseminated in quartz-carbonate veins cutting metasomatized sedimentary rocks, as sulphide veins that cut Type 1 breccia, as sulphide clasts in Type 2 breccia, as well as disseminated in the matrix of Type 2 breccia, and finally as sulphide veinlets crosscutting Type 2 breccia.

## RÉSUMÉ

Le substratum de l'occurrence Slab d'oxyde de fer-cuivre-or est constitué des roches sédimentaires et du schiste à grain fin du Groupe de Fairchild Lake, la plus ancienne unité du Supergroupe de Wernecke du Protérozoïque précoce, des roches volcaniques intermédiaires à mafiques de Slab, des roches intrusives dioritiques de Bonnet Plume River ainsi que de brèche de Wernecke datant du Protérozoïque précoce, qui recoupe toutes les autres unités. La brèche de Wernecke a été subdivisée en deux unités : le type 1 et le type 2. Le type 1 occupe une étendue limitée et consiste en clastes sédimentaires de magnétite massive abondants par endroits dans une matrice de carbonate-magnétite. Le type 2 recoupe le type 1 et est constitué de clastes sédimentaires dans une matrice de microbrèche. La minéralisation en oxyde de fer-cuivre-or est associée à la brèche de Wernecke. Elle est disséminée dans des veines de quartz-carbonate recoupant des roches sédimentaires métasomatisées. Elle recoupe sous forme de veines de sulfures la brèche de type 1, se présente sous forme de clastes de sulfures dans la brèche de type 2, est disséminée dans la matrice de la brèche de type 2 et recoupe sous forme de veinules de sulfures la brèche de type 2.

---

[1] *Current address: Economic Geology Research Unit, James Cook University, Townsville, 4811, Queensland, Australia, julie.hunt@jcu.edu.au*

[2] *Yukon Geology Program, 345-300 Main Street, Whitehorse, Yukon, Canada Y1A 2B5*

[3] *Earth Sciences, Simon Fraser University, Burnaby, British Columbia, Canada V5A 1S6*

[4] *Economic Geology Research Unit, James Cook University, Townsville, 4811, Queensland, Australia*

## INTRODUCTION

This paper briefly describes the results of new geological mapping carried out in the 'Slab Mountain'[5] area (Fig. 1) and is a companion to Open File map 2002-6 (Fig. 2; Hunt et al., in press). The mapping was carried out mainly at 1:5000 scale, with more detailed mapping in part of 'Slab Creek' (Brookes et al., this volume), on the eastern part of Slab Mountain and the western part of 'Slab Ridge' (Laughton et al., this volume; Brideau et al., this volume). Parts of Slab Ridge and Slab Mountain are cliff forming and inaccessible, and were mapped in less detail. This work builds on local mapping by/for Newmont Mines Limited (Vance et al., 1995; Owerko, 1995) and on regional mapping by Thorkelson (2000). This study is part of a research program on Proterozoic mineral occurrences and geology in the Yukon which is being undertaken by the Yukon Geology Program, Simon Fraser University (British Columbia) and James Cook University (Queensland, Australia).

## LOCATION, PHYSIOGRAPHY AND ACCESS

The map area is located in northeastern Yukon Territory about 150 km northeast of the town of Mayo (Fig. 1). It covers an area of approximately 10 $km^2$ around Slab Mountain on the northeast side of the Bonnet Plume River, and includes parts of NTS map sheets 106C/13, 106D/16, 106E/1 and 106F/4. The northern boundary of the study area is the informally named Slab Creek, which drains into the Bonnet Plume River (Fig. 2). The Slab Mountain area is remote and mountainous with elevations from 560 to 1500 m.

Access to the map area is by fixed-wing aircraft to the 'Copper Point' airstrip immediately west of Slab Mountain, or the Bonnet Plume River, or by helicopter. In winter, access is also possible along the Wind River Trail, a rough winter road that begins near Keno (Fig. 1).

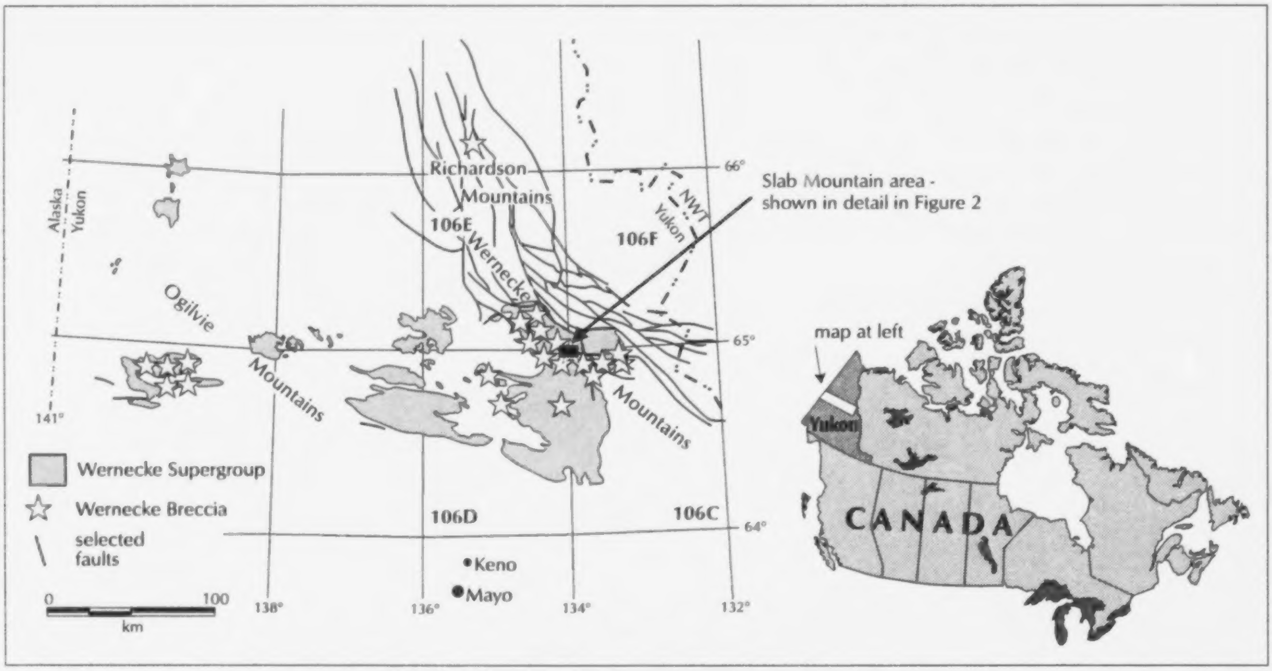
Alaska
Yukon
141°
Ogilvie
Mountains
Richardson
Mountains
106E
Wernecke
Mountains
106F
NWT
Yukon
66°
65°
64°
Slab Mountain area - shown in detail in Figure 2
map at left
Yukon
CANADA
106D
106C
Keno
Mayo
138°
136°
134°
132°
Wernecke Supergroup
Wernecke Breccia
selected faults
0
100
km

***Figure 1.*** *Location of the Slab Mountain map area and distribution of Wernecke Breccia occurrences and Wernecke Supergroup rocks in the Yukon. Modified from Thorkelson (2000).*

---

[5] *Many of the names used in this report are informal and are initially shown in quotation marks.*

# GEOLOGY OF THE MAP AREA

## INTRODUCTION

The map area is underlain by four main geological units (Fig. 2): 1) Early Proterozoic Fairchild Lake Group sedimentary rocks that are part of the Wernecke Supergroup (*cf.* Delaney, 1981; Thorkelson, 2000); 2) crosscutting Early Proterozoic Bonnet Plume River intrusions (ca. 1.71 Ga; Thorkelson et al., 2001a); 3) undated, but possibly correlative, Slab volcanics (Thorkelson, 2000); and 4) Middle Proterozoic Wernecke Breccia that crosscuts the three older units and is, at least in part, ca. 1.6 Ga (*cf.* Thorkelson et al., 2001b). These geological units, and the contacts between them, are well exposed and provide a firm basis for clarifying aspects of the Early to Middle Proterozoic evolution of the Yukon.

The geological units are described below and their distribution is shown in Figure 2 (for more detail see Open File map 2002-6 by Hunt et al., in press).

## FAIRCHILD LAKE GROUP (WERNECKE SUPERGROUP)

A large part of the Slab Mountain area is underlain by the Fairchild Lake Group (Fig. 2), the lowest of the three groups that make up the Wernecke Supergroup (Fig. 3). The base of the Fairchild Lake Group is not exposed, but is assumed to lie on ≥1.85 Ga basement (Thorkelson, 2000). The Fairchild Lake Group is conformably overlain by the Quartet Group. Delaney (1981) subdivided the Fairchild Lake Group into five formations, F1 to F5. Thorkelson (2000) was unable to consistently recognize all of these formations during regional mapping, and instead divided the Fairchild Lake Group into two units: the dominantly clastic lower Fairchild Lake Group, corresponding to formations F1 to F4, and the carbonate-dominant upper Fairchild Lake Group, equivalent to F5.

According to Delaney (1981), the Slab Mountain area is underlain by formation F4 which consists of "... at least 500 m of grey- to greenish-grey-weathering siltstone, fine sandstone and mudstone." Thorkelson (2000) included these rocks in the lower Fairchild Lake Group. Mapping in the Slab Mountain area during this study identified two general lithologies within the Fairchild Lake Group: 1) fine-grained sedimentary rock and minor carbonate that occurs as discrete outcrops and as clasts (up to 250 m across) within Wernecke Breccia; and 2) fine-grained schist and phyllite that largely form a distinct belt approximately 550 m wide within the sedimentary rocks. Following are descriptions of these two lithologies.

### *Fine-grained sedimentary rocks and minor carbonate*

Fine-grained sedimentary rocks underlying the Slab Mountain area generally weather dark brown to grey but are locally grey to rusty brown. Fresh surfaces are pale grey. The rocks are well layered and locally banded with alternating dark and light layers (Fig. 4a). Original sedimentary textures are visible in several locations and include crossbedding, scours, laminations and grading. In some exposures, banding is defined by 'spherulitic texture' with spheres up to 0.5 cm in diameter. This texture was described by Delaney (1981) as characteristic of mudstone within formation F4. He determined that the spheres are composed of silica, or in some instances, chlorite. Locally, the fine-grained sedimentary rocks are pyritic and weather rusty. The most prominent pyritic sedimentary rocks form a rusty-weathering band about 80 m wide that trends northwest across Slab Mountain (Figs. 2, 4b).

Minor carbonate occurs locally as interbeds 0.05 to 2 m thick within the fine-grained sedimentary rocks. The carbonate generally weathers pale to medium grey with a hackly surface. Fresh surfaces are white to pale grey. In some locations, the carbonate is coarsely crystalline or contains white mica flakes up to 1 cm across.

At the west end of Slab Mountain, the sedimentary rocks have undergone pervasive biotite alteration. Locally, chlorite alteration overprints the biotite; elsewhere, chlorite alteration occurs as alternating dark and light green layers in the sedimentary rocks. Quartz-chlorite-biotite alteration also occurs in the matrix of brecciated and folded sedimentary rocks. Other alteration in Fairchild Lake Group rocks includes white spots (carbonate and/or scapolite?) and the development of a pervasive purple colouration, likely due to the presence of finely disseminated hematite. Where the sedimentary rocks are proximal to Wernecke Breccia bodies, they are commonly crackle brecciated and highly fractured. At breccia contacts, the sedimentary rocks are commonly bleached (albite?) and silicified. In the 'Canyon zone' in Slab Creek, the sedimentary rocks are locally intensely carbonate-magnetite altered.

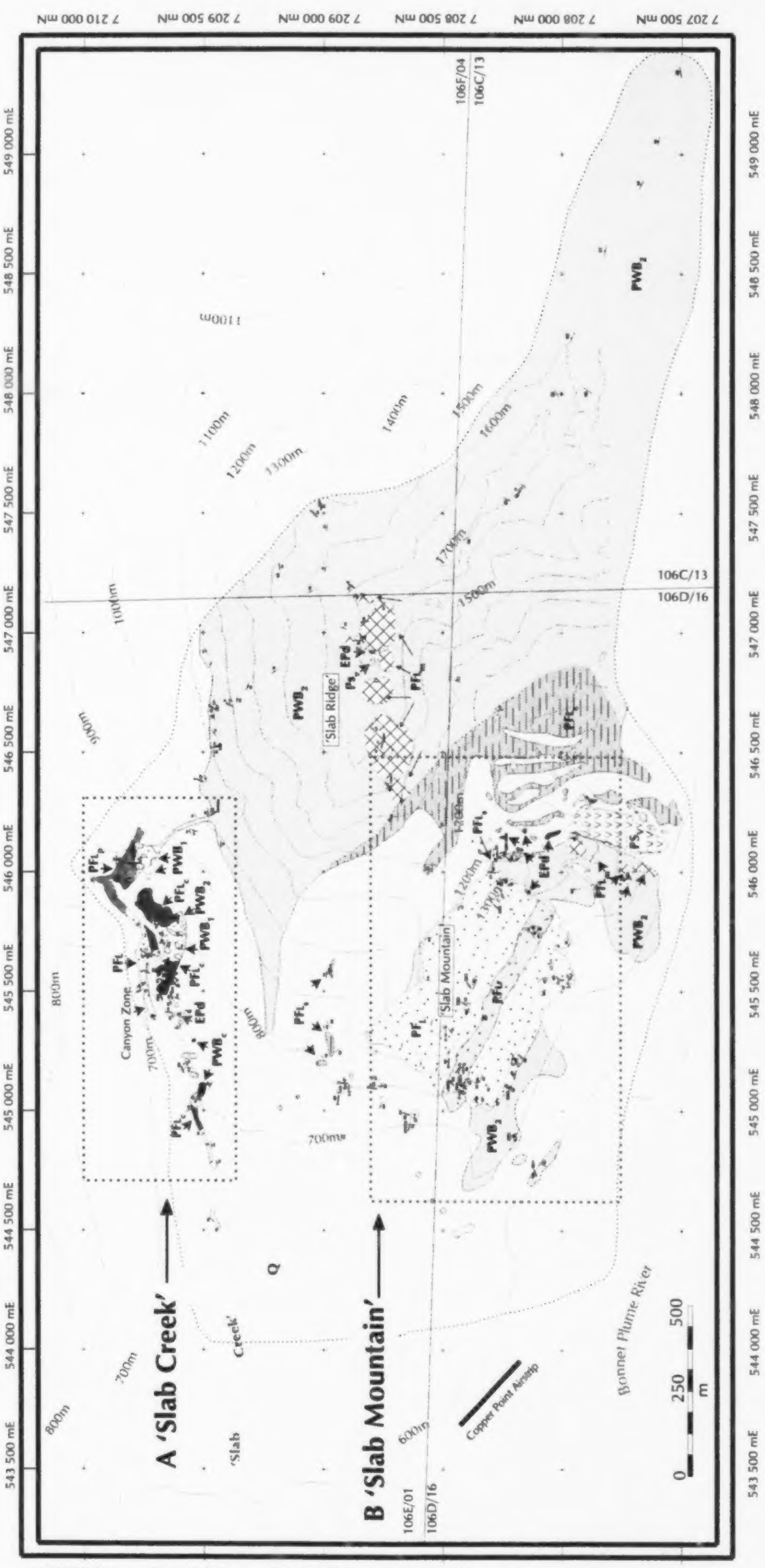
A 'Slab Creek'
B 'Slab Mountain'
Canyon Zone
'Slab Ridge'
'Slab Mountain'
'Slab Creek'
Q
Copper Point Airstrip
Bonnet Plume River
106E/01
106D/16
106C/13
106F/04
0
250
500
m
543 500 mE
544 000 mE
544 500 mE
545 000 mE
545 500 mE
546 000 mE
546 500 mE
547 000 mE
547 500 mE
548 000 mE
548 500 mE
549 000 mE
7 210 000 mN
7 209 500 mN
7 209 000 mN
7 208 500 mN
7 208 000 mN
7 207 500 mN
600m
700m
800m
900m
1000m
1100m
1200m
1300m
1400m
1500m
1600m
1700m
PWB$_2$
PWB$_c$
PFL$_c$
EPd

**QUATERNARY**

Q unconsolidated deposits

**INTRUSIVE ROCKS**

**PROTEROZOIC**

EPd dykes and megaclasts of diorite

**VOLCANIC ROCKS**

**LOWER PROTEROZOIC**

Slab volcanics

PSv mafic to intermediate lava flows; minor interbeds of conglomerate, sandstone and volcanic breccia; the volcanic rocks are present as clasts and megaclasts within zones of Wernecke Breccia

**LAYERED ROCKS**

**LOWER PROTEROZOIC**

WERNECKE SUPERGROUP

Fairchild Lake Group

PFL undivided fine-grained sedimentary rocks

PFL phyllitic fine-grained sedimentary rocks; weakly foliated, crenulated and kinked; locally contain magnetite porphyroblasts

PFL$_s$ chloritoid-muscovite-quartz-chlorite schist and phyllite containing magnetite and chloritoid porphyroblasts

PFL$_r$ rusty-weathering fine-grained sedimentary rocks

PFL$_c$ carbonate-magnetite altered fine-grained sedimentary rocks

**BRECCIATED ROCKS**

Wernecke Breccia

PWB$_c$ crackle-brecciated fine-grained sedimentary rocks

PWB$_1$ **Breccia Type 1** - dark purple-brown to brown-grey weathering breccia with dominantly grey clasts, brown to grey carbonate and magnetite matrix; locally contains numerous angular to sub-angular clasts of massive magnetite

PWB$_2$ **Breccia Type 2** - tan to grey-weathering breccia with dominantly grey clasts and fewer pale pink, white and purple clasts, fragmental matrix; locally contains clasts of Breccia Type1, Fairchild Lake Group schist and phyllite, carbonate-magnetite altered sedimentary rocks, and rare rounded sulphide clasts

PFL$_m$ examples of megaclasts of Fairchild Lake Group (fine-grained sedimentary rock) in Breccia Type 2

***Figure 2.** Bedrock geology map of the Slab Mountain area. Modified from Open File Map 2002-6 (Hunt et al., 2002).*

**A 'Slab Creek'**

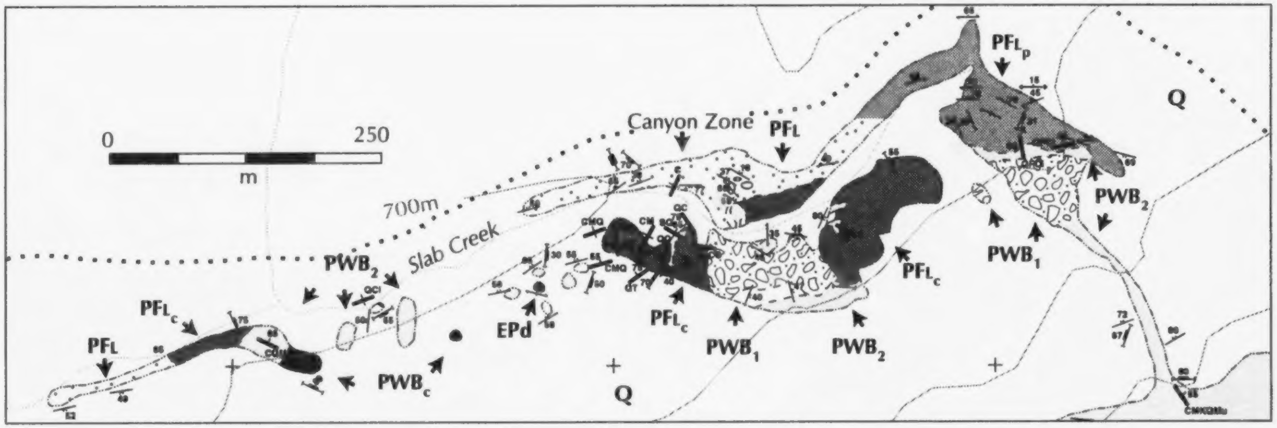
0
250
m
Canyon Zone
700m
Slab Creek
PFL
PFLp
PFLc
PWB1
PWB2
PWBc
EPd
Q

**B 'Slab Mountain'**

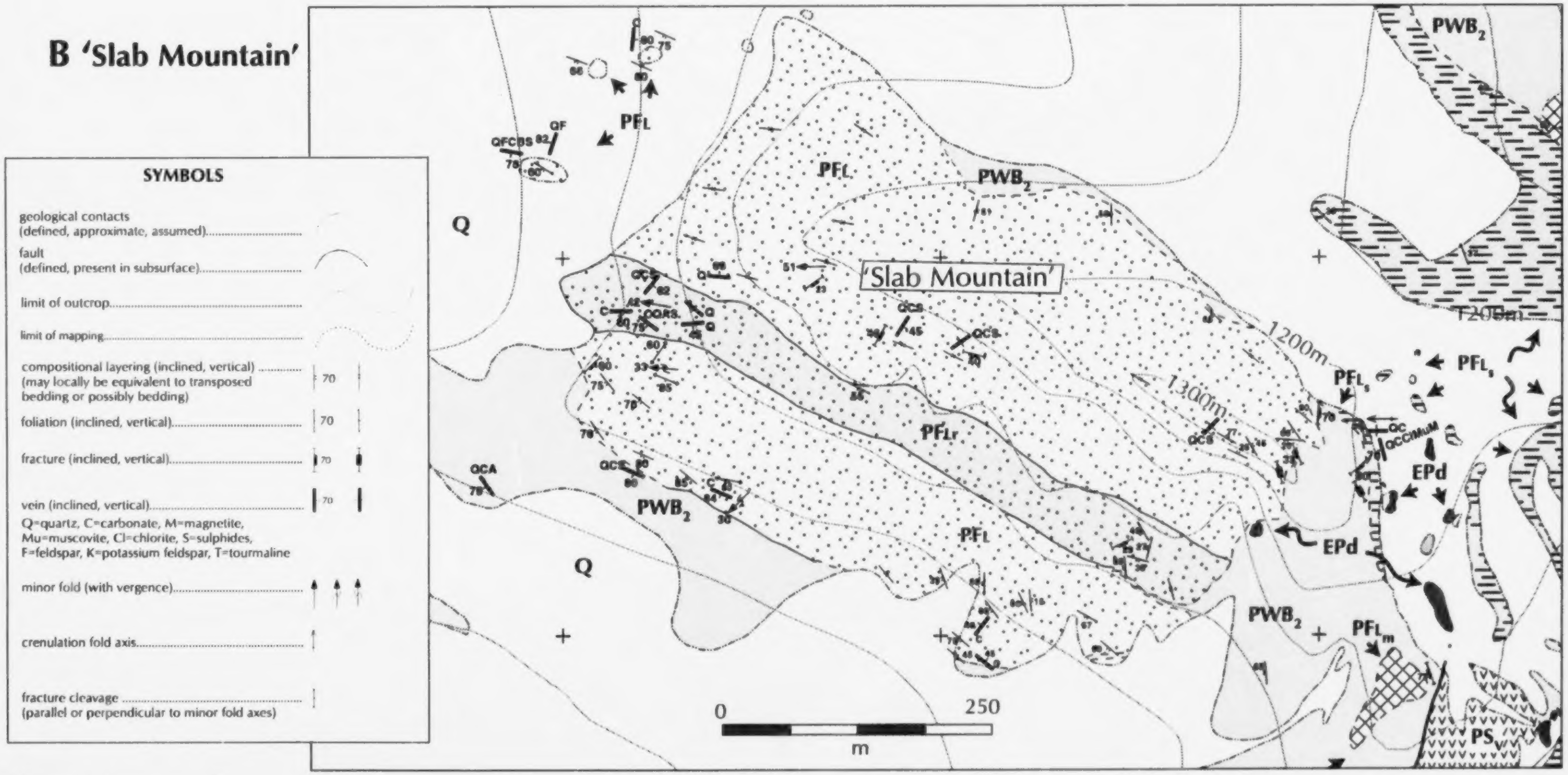
'Slab Mountain'
1200m
1300m
PFL
PFLr
PFLs
PFLm
PWB2
PSv
EPd
Q
0
250
m
SYMBOLS
geological contacts (defined, approximate, assumed)
fault (defined, present in subsurface)
limit of outcrop
limit of mapping
compositional layering (inclined, vertical) (may locally be equivalent to transposed bedding or possibly bedding)
foliation (inclined, vertical)
fracture (inclined, vertical)
vein (inclined, vertical)
Q=quartz, C=carbonate, M=magnetite, Mu=muscovite, Cl=chlorite, S=sulphides, F=feldspar, K=potassium feldspar, T=tourmaline
minor fold (with vergence)
crenulation fold axis
fracture cleavage (parallel or perpendicular to minor fold axes)
70

***Figure 2.*** *(continued)*

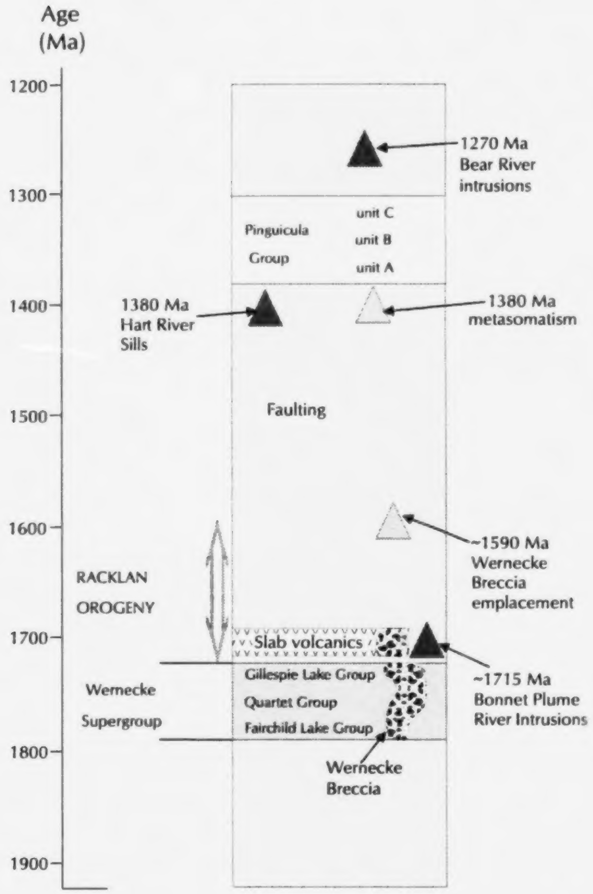
Age
(Ma)
1200
1300
1400
1500
1600
1700
1800
1900
1270 Ma
Bear River
intrusions
Pinguicula
Group
unit C
unit B
unit A
1380 Ma
Hart River
Sills
1380 Ma
metasomatism
Faulting
~1590 Ma
Wernecke
Breccia
emplacement
RACKLAN
OROGENY
Slab volcanics
Gillespie Lake Group
Quartet Group
Fairchild Lake Group
~1715 Ma
Bonnet Plume
River Intrusions
Wernecke
Supergroup
Wernecke
Breccia

***Figure 3.*** *Generalized partial area stratigraphic column for the Wernecke Mountains. Modified from Thorkelson (2000).*

### *Schist and phyllite*

Chloritoid-muscovite-quartz-chlorite schist and phyllite with magnetite and chloritoid porphyroblasts occur mainly in a recessive-weathering, northwest-trending belt between Slab Mountain and Slab Ridge (Figs. 2, 4c). The rocks weather blue-grey to green-grey with green to grey-blue fresh surfaces. They are commonly compositionally banded, crenulated and kinked, and host rare veins of quartz and orange feldspar. More detail on this area is given in Brideau et al. (this volume). Schistose, kinked, fine-grained sedimentary rocks also occur at the east end of the Canyon zone in Slab Creek (see Brookes et al., this volume).

The schist and phyllite are interpreted to be the deformed and metamorphosed equivalent of flanking fine-grained clastic rocks of the Fairchild Lake Group that formed in a high strain zone and were subsequently crenulated and kinked by two separate deformational events (Brideau et al., this volume).

## SLAB VOLCANICS

The informally named Slab volcanics were first recognized in 1992 and are regarded as relics of a stratigraphic succession, younger than the Wernecke Supergroup and older than the Pinguicula Group (Fig. 3; Thorkelson, 2000). Within the map area, the volcanic rocks are exposed on Slab Mountain and Slab Ridge (Fig. 2) where they appear to be fragments of a larger volcanic succession engulfed by Wernecke Breccia (see Laughton et al., this volume for a detailed description). The main locality, on the east side of Slab Mountain, is a block ($0.6 \times 0.25$ km$^2$) comprising about 40 steeply dipping lava flows and minor, intercalated volcaniclastic and epiclastic units (Fig. 5). The volcanic rocks are resistant and weather dark green-brown; fresh surfaces are green-grey. Individual flows are commonly about 4 m thick, but range from 0.8 m to 14 m thick. The lavas are aphyric to rarely plagioclase-phyric, with mafic to intermediate compositions. They are variably vesicular, and host amygdules of quartz, white and pink calcite, tremolite, biotite, chlorite and apatite. The groundmass of the lavas typically consists of interlocking laths of plagioclase and anhedral grains of biotite and magnetite. Locally, the rock has a spotty appearance caused by the replacement of plagioclase and other minerals by scapolite.

## BONNET PLUME RIVER INTRUSIONS

In the Wernecke Mountains, numerous small ca. 1710 Ma igneous bodies known as the Bonnet Plume River Intrusions, crosscut the Wernecke Supergroup and occur as clasts in zones of Wernecke Breccia (Thorkelson, 2000).

In the Slab Mountain, area the intrusions are fine grained, dioritic and weather green-grey; fresh surfaces are grey. Dykes range from 0.2 to 15 m across and outcrop mainly in the recessive-weathering area between Slab Mountain and Slab Ridge (Fig. 2). Intrusive clasts within Wernecke Breccia are locally abundant. For example, several large sub-rounded to sub-angular clasts of diorite occur in Wernecke Breccia (Type 2) at the eastern end of Slab Mountain, just west of the Slab volcanics (Fig. 6).

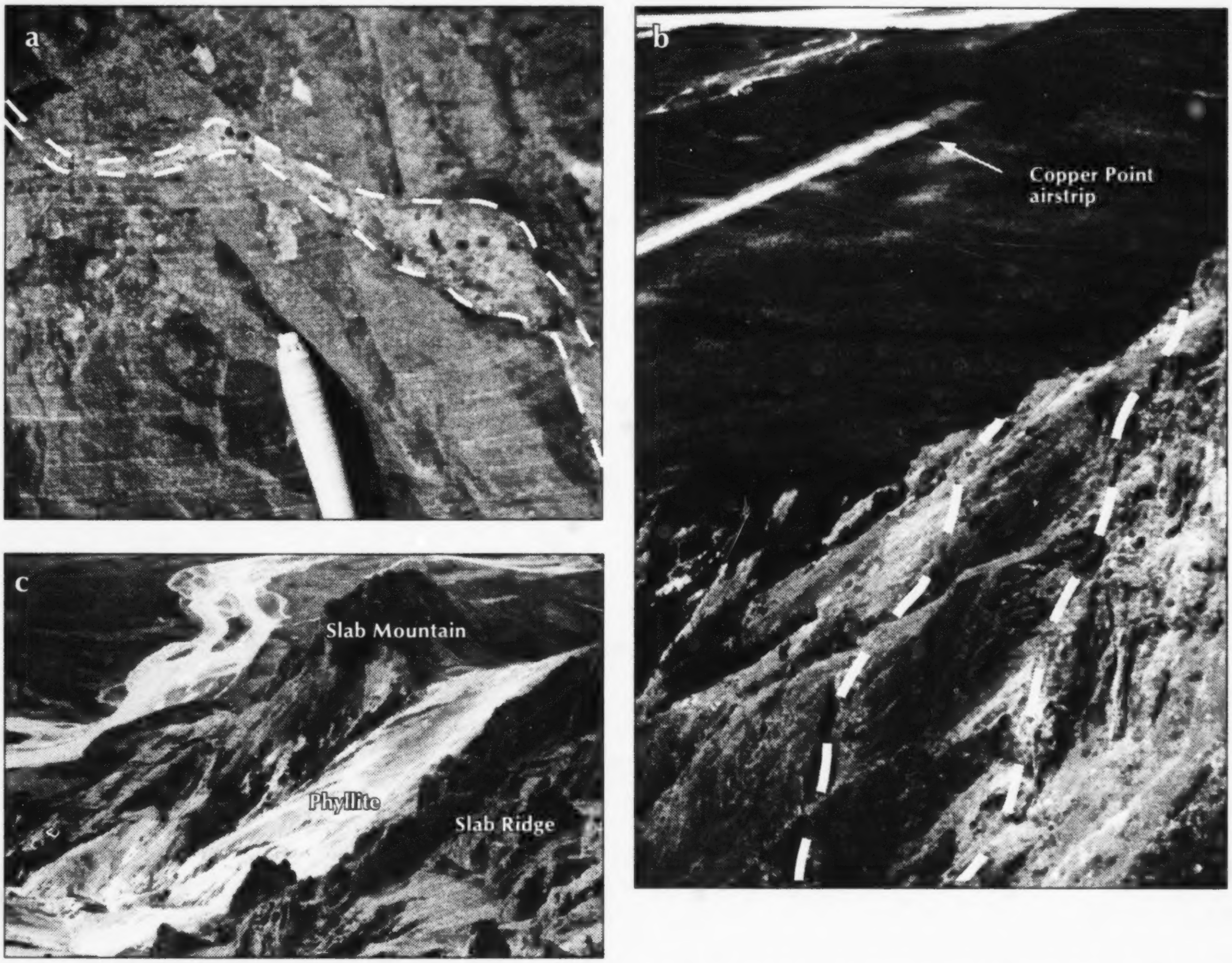
a
b
Copper Point airstrip
c
Slab Mountain
Phyllite
Slab Ridge

***Figure 4.*** *(a) Fine-grained sedimentary rocks of the Fairchild Lake Group cut by Type 2 Wernecke Breccia (within dashed lines); (b) band of pyritic siltstone on the southwest side of Slab Mountain; and (c) band of recessive-weathering phyllite (about 500 m across) exposed between Slab Mountain and Slab Ridge.*

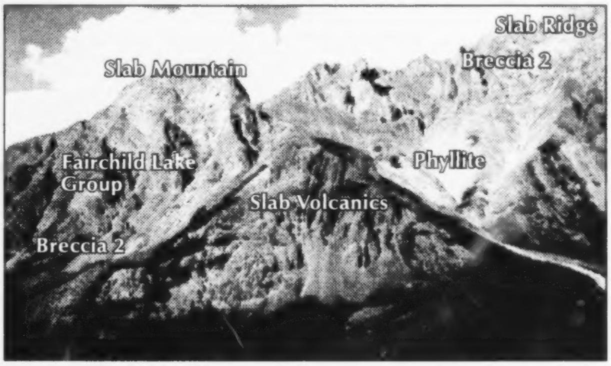
Slab Ridge
Breccia 2
Slab Mountain
Fairchild Lake Group
Phyllite
Slab Volcanics
Breccia 2

***Figure 5.*** *Slab volcanics exposed at the east end of Slab Mountain (photo by Grant Abbott).*

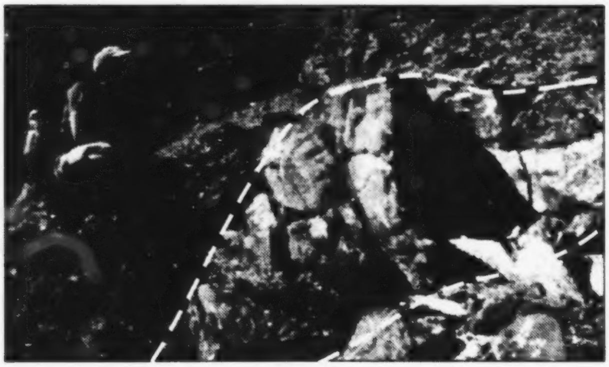

***Figure 6.*** *Large clast of Bonnet Plume River diorite in Type 2 Wernecke Breccia.*

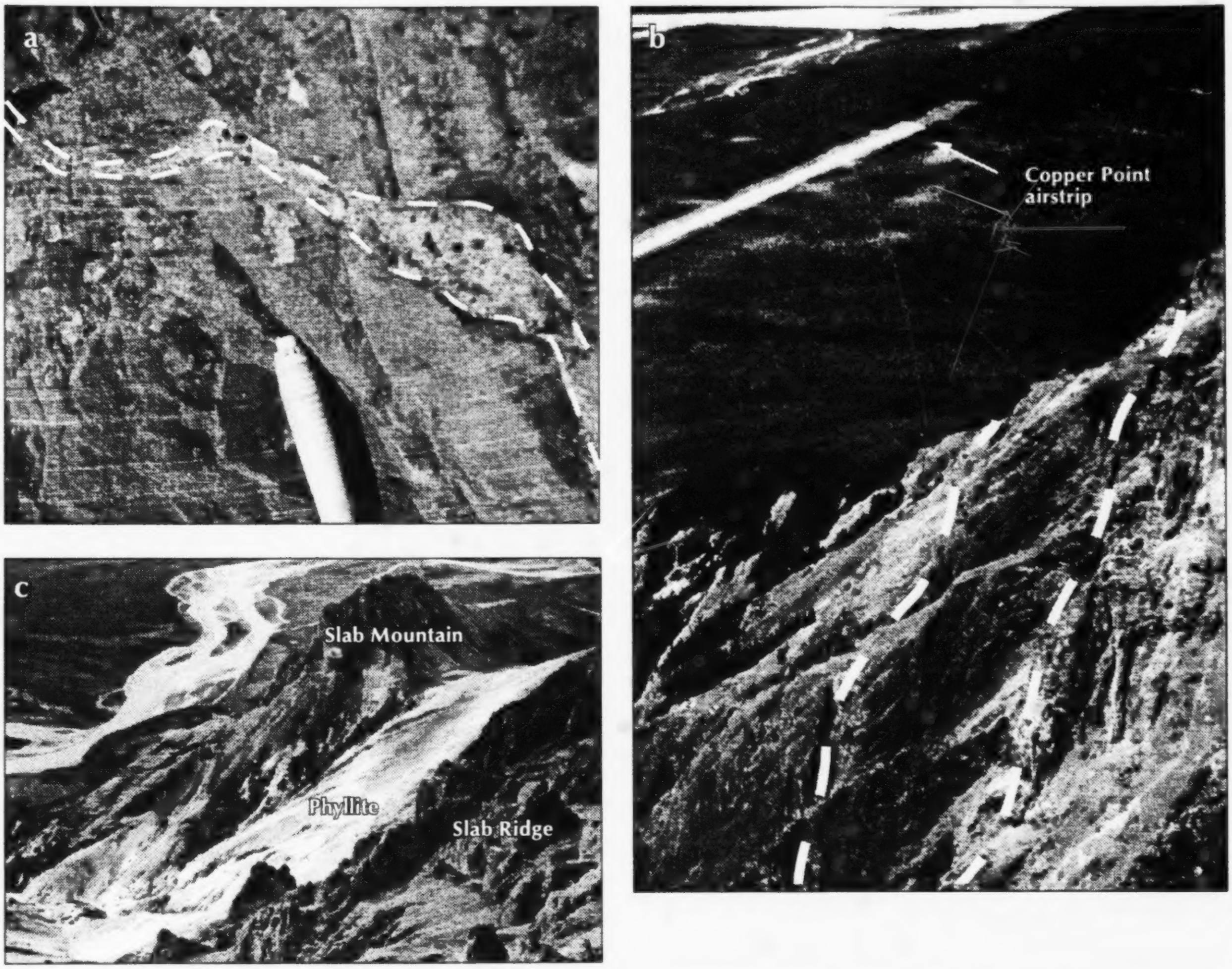
a
b
Copper Point airstrip
c
Slab Mountain
Phyllite
Slab Ridge

***Figure 4.*** *(a) Fine-grained sedimentary rocks of the Fairchild Lake Group cut by Type 2 Wernecke Breccia (within dashed lines); (b) band of pyritic siltstone on the southwest side of Slab Mountain; and (c) band of recessive-weathering phyllite (about 500 m across) exposed between Slab Mountain and Slab Ridge.*

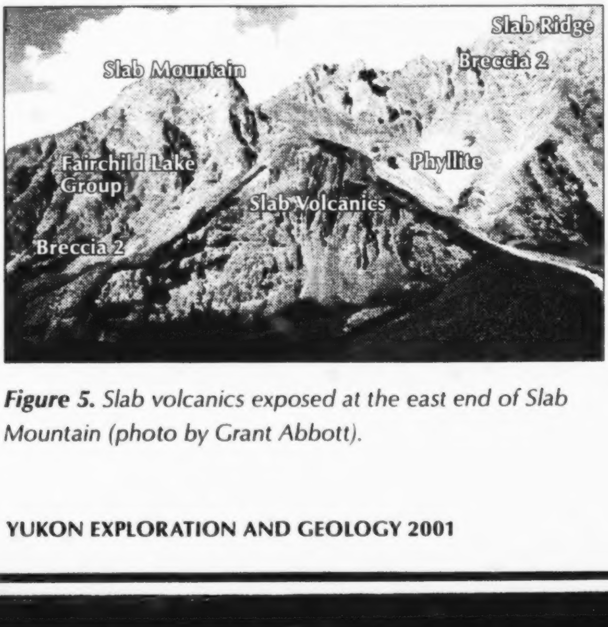
Slab Ridge
Breccia 2
Slab Mountain
Fairchild Lake Group
Phyllite
Slab Volcanics
Breccia 2

***Figure 5.*** *Slab volcanics exposed at the east end of Slab Mountain (photo by Grant Abbott).*

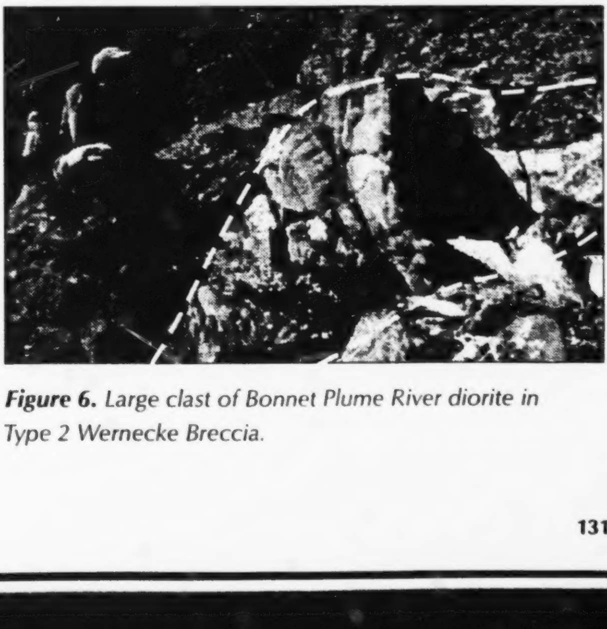

***Figure 6.*** *Large clast of Bonnet Plume River diorite in Type 2 Wernecke Breccia.*

## WERNECKE BRECCIA

Wernecke Breccia is a collective term for numerous breccia zones in the Wernecke Mountains (Fig. 1). The breccia zones range from 0.1-10 $km^2$ and occur in curvilinear arrays over about 3500 $km^2$ (Archer and Schmidt, 1978; Bell, 1986a,b; Wheeler and McFeeley, 1991; Thorkelson, 2000). Breccia emplacement took place after the deposition of the Wernecke Supergroup and Slab volcanics, but before deposition of the ca. 1.38 Ga Pinguicula Group (Fig. 3; Thorkelson, 2000).

At least two types of Wernecke Breccia occur in the Slab Mountain area based on crosscutting relationships; they are referred to informally as Type 1 and Type 2. Type 1 Wernecke Breccia is limited in extent and was observed only in the Slab Creek area where it is cut by Type 2 breccia (Fig. 2). Type 2 Wernecke Breccia is the most extensive unit in the map area and underlies large parts of Slab Ridge, Slab Mountain and Slab Creek (Fig. 2). The two breccia types are described below.

### *Type 1 Wernecke Breccia*

Type 1 Wernecke Breccia generally weathers dark purple-brown to brown-grey with dominantly grey clasts and varies from clast- to matrix-supported (Fig. 7a). The breccia matrix is typically brown to grey and made up of carbonate and magnetite; locally, the matrix contains sulphide crystals (dominantly pyrite, lesser chalcopyrite). Clasts make up 40-70% of the breccia and are primarily fine-grained, dark to medium grey to maroon sedimentary rock. The clasts vary from angular to sub-rounded, but are mainly sub-angular. They range in size from 1-12 cm, but are generally <5 cm across. Some Type 1 breccia exposures contain numerous angular to sub-angular clasts of fine-grained, massive black magnetite up to 5 cm across. Rarely, the breccia contains angular, glassy quartz clasts from 2-5 cm across.

Type 1 Wernecke Breccia is in gradational contact with carbonate-magnetite altered sedimentary rocks (Fig. 2). In one location, Type 1 breccia is in sharp contact with fine-grained sedimentary rock (non-carbonate magnetite altered), however, this is close to a contact with Type 2 breccia, and the sedimentary rock may be a clast in this breccia. Type 1 breccia was not observed cutting any of the other units.

### *Type 2 Wernecke Breccia*

Type 2 Wernecke Breccia generally weathers tan to grey with dominantly grey clasts and fewer pale pink, white and purple clasts. The breccia varies from clast- to matrix-supported. The matrix itself is fragmental (herein referred to as micro-breccia). It is typically green to pale grey and made up of carbonate and grey fine-grained sedimentary rock clasts from < 1 cm to 3 cm across, and lesser pink, purple and white clasts (Fig. 7b). Commonly, the matrix contains magnetite crystals up to 5 mm across, flakes of white mica up to 1 cm across, and biotite crystals up to 0.5 cm across. Locally, the matrix is composed of feldspar.

Clasts make up 40-75% of Type 2 breccia and are dominantly composed of fine-grained, grey sedimentary rock. The clasts are generally sub-angular to sub-rounded and range from 5 cm to several hundred metres across. Less abundant clasts include rounded to sub-angular clasts of diorite up to 3 m x 2 m; sub-angular to sub-rounded clasts of Slab volcanics up to 250 m x 600 m (see Laughton et al., this volume); sub-rounded clasts of cream-coloured carbonate up to 0.5 m x 3 m; sub-angular clasts of dark brown-weathering carbonate-magnetite up to 3 m x 7 m; sub-rounded clasts of fine-grained sedimentary rock, with white alteration spots, cut by quartz-sulphide veinlets; sub-rounded clasts of fine-grained sedimentary rock with dark alteration spots (biotite or chlorite or chloritoid); sub-rounded clasts of limey, fine-grained sedimentary rock up to 15 m x 15 m; rare sub-rounded, glassy quartz vein clasts <5 cm across; rare, rounded sulphide clasts up to 20 cm x 8 cm across; rare fine-grained sedimentary clasts containing disseminated malachite; and rare micro-breccia clasts <5 cm across.

At the western end of Slab Mountain, Type 2 breccia is locally dominated by two types of clasts: 1) 1-25 cm, angular to sub-rounded clasts of pink to grey, fine-grained sedimentary rock, with biotite porphyroblasts, in a non-calcareous matrix; and 2) sub-angular to sub-rounded, laminated, grey to pink silty dolomite clasts >2 m across, locally containing up to 1-cm-thick bands of actinolite crystals. On Slab Ridge, Type 2 breccia is dominated by very large clasts (several hundred metres across) of sedimentary rock with fingers (<1 m to 80 m across) of matrix between them. These large clasts are dominantly composed of fine-grained, grey sedimentary rock; less common are clasts of brecciated, deformed limey siltstone in a white carbonate matrix (Fig. 7c).

Contacts between Type 2 Wernecke Breccia and sedimentary rocks of the Fairchild Lake Group are sharp to gradational. Where gradational, the fine-grained sedimentary rocks are crackle brecciated. The extent of crackle brecciation ranges from a few centimetres to several tens of metres. At the eastern end of Slab Mountain and at the eastern end of the Canyon zone in Slab Creek, Type 2 breccia cuts schist and phyllite. At the breccia-schist/phyllite contacts, the breccia contains angular clasts of schist/phyllite up to 0.5 m x 1 m. Away from the breccia-schist/phyllite contacts, the breccia contains fine-grained sedimentary rock clasts up to 0.3 m x 1 m and no schist/phyllite clasts. Contacts between Type 2 breccia and large clasts of Slab volcanics or Bonnet Plume River diorite are sharp to crackle brecciated for a few centimetres. Type 2 breccia is in sharp contact with Type 1 breccia and, close to contacts, locally contains clasts of Type 1 breccia.

## STRUCTURE

The Slab Mountain area has been affected by contractional deformation associated with the Racklan Orogeny, a period of mountain building that occurred after deposition of the Wernecke Supergroup and before emplacement of Wernecke Breccia (Thorkelson, 2000). This deformation produced northeast- to east-trending folds, schistosity, crenulations and kink bands (Thorkelson, 2000; Brideau et al., this volume). A large south-verging

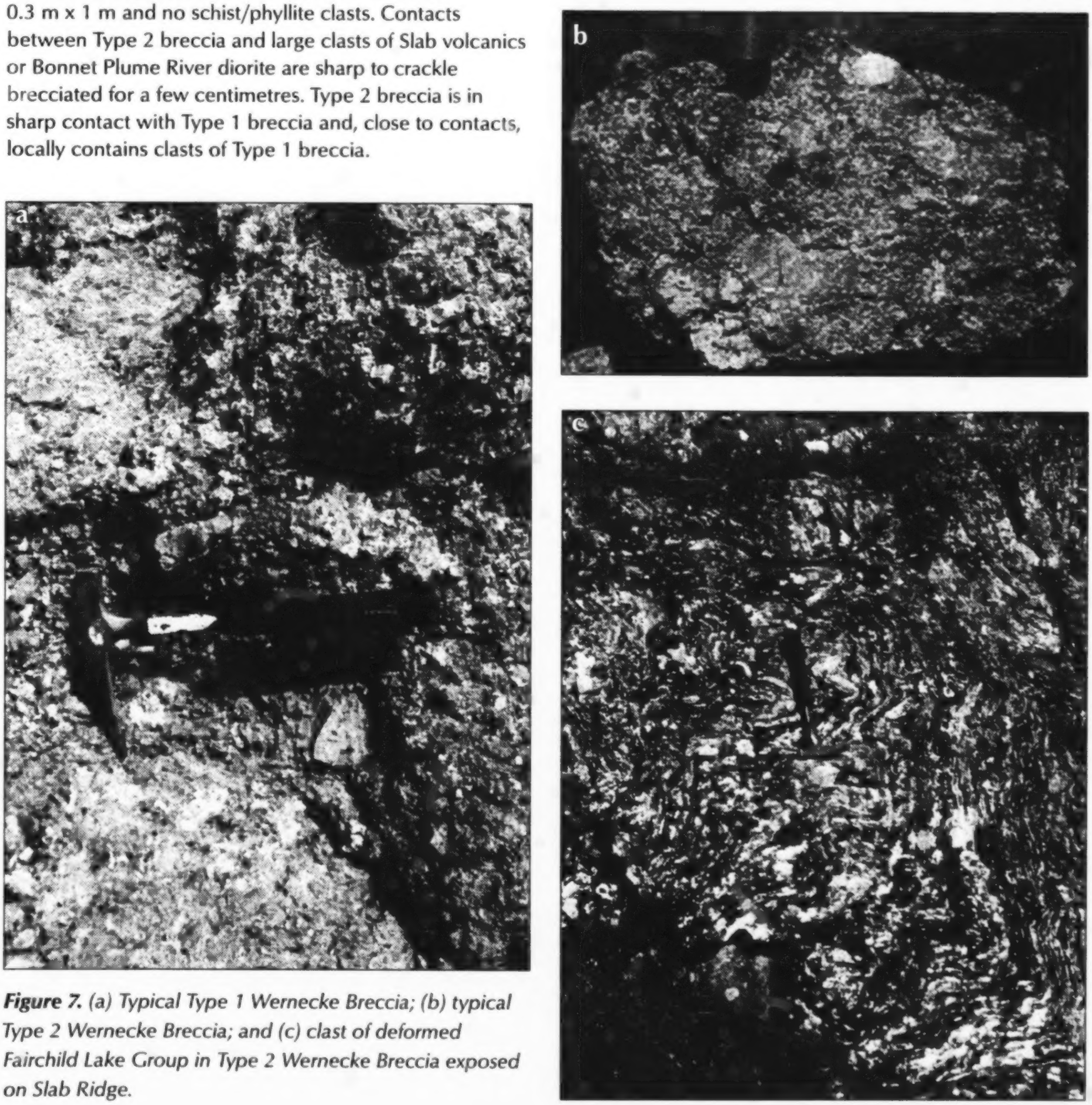

***Figure 7.*** *(a) Typical Type 1 Wernecke Breccia; (b) typical Type 2 Wernecke Breccia; and (c) clast of deformed Fairchild Lake Group in Type 2 Wernecke Breccia exposed on Slab Ridge.*

anticline related to this period of deformation was identified by Delaney (1981), Bell (1986a) and Thorkelson (2000) about 1.5 km south of the Slab Mountain area in the Bonnet Plume River valley. In this area, the anticline generally trends west, but bends to the northwest near Slab Mountain. Schistose rocks form a northwest-trending belt between Slab Mountain and Slab Ridge (Fig. 2), roughly parallel to the trend of the anticline. Brideau et al. (this volume) suggest that the schist belt represents a region of high strain, possibly developed in a region of tight parasitic folding. Schistose to phyllitic rocks also occur at the eastern end of the Canyon zone in Slab Creek (Fig. 2). Here, foliation trends roughly west and dips shallowly to moderately to the north.

Fairchild Lake Group strata on Slab Mountain have been deformed into a moderate to steep southwest-dipping monocline (Fig. 8). Minor folds within this sequence generally trend west and plunge gently to the west (Fig. 2). Fairchild Lake Group rocks in Slab Creek, where undisturbed by breccia emplacement, generally trend northeast. On the north side of the creek, compositional layering commonly dips to the north, and on the south side of the creek, to the south (Fig. 2), suggesting a northeast-southwest trending fold axis may lie in Slab Creek; rare minor folds with this orientation occur on Slab Mountain.

## VEINING AND MINERALIZATION

Iron oxide-copper-gold mineralization, dominantly hematite-magnetite-chalcopyrite, is associated with Wernecke Breccia and occurs within breccia zones and in adjacent metasomatized country rock throughout the Wernecke Mountains (*cf.* Hitzman et al., 1992; Thorkelson, 2000; Yukon MINFILE, 2001).

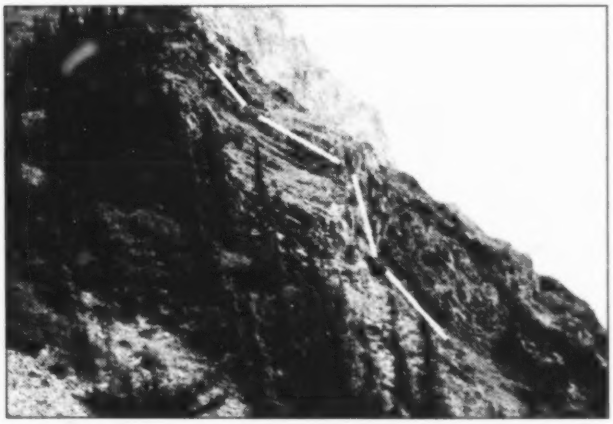

***Figure 8.*** *Fairchild Lake Group strata folded into a southwest-dipping monocline on Slab Mountain.*

The map area is host to the Slab mineral occurrence (Yukon MINFILE 106D 070), which has been explored sporadically since 1910, the most recent exploration taking place between 1992 and 1997 by the Newmont-Westmin-Equity-Pamicon joint venture. Highly visible mineralization occurs in this area as large patches of malachite staining on the peak of Slab Mountain (Fig. 9a). Here chalcopyrite is disseminated in <1-cm- to 10-cm-thick quartz-carbonate veins that trend from north-northeast to east, to east-southeast, parallel to prominent fractures. Mineralization also occurs in the band of pyritic sedimentary rocks that trends northwest across Slab Mountain, roughly parallel to a monoclinal fold hinge. Here, chalcopyrite is disseminated in quartz-carbonate veins that trend approximately east-northeast to east-southeast, roughly parallel to minor fold axial planes.

Elsewhere in the map area, mineralization includes up to 10-cm-thick, northwest-trending, steeply dipping, pyrite-chalcopyrite veins with quartz-white mica selvages. These veins cut carbonate-magnetite altered sedimentary rocks (Fig. 9b), rare clasts of massive pyrite-chalcopyrite up to 20 cm across in Type 2 Wernecke Breccia (Fig. 9c), local occurrences of disseminated chalcopyrite in the breccia matrix of Type 2 breccia, and rare chalcopyrite veinlets that cut Type 2 breccia.

In the Slab Mountain area, veins and alteration are abundant, and crosscutting relationships suggest the following **preliminary** paragenesis:

1. Quartz-feldspar-white mica ± carbonate ± chlorite veins. These veins are rare and were observed only in phyllitic siltstone at the eastern end of the Canyon zone in Slab Creek. They are, however, significant because they are deformed by kink-bands and hence formed prior to the Racklan Orogeny.
2. Quartz-magnetite veins cut deformed Fairchild Lake Group rocks prior to carbonate-magnetite alteration.
3. a) Carbonate-magnetite alteration of Fairchild Lake Group sedimentary rocks occurs locally and varies from partial to complete replacement.

   b) Emplacement of Type 1 Wernecke Breccia. Type 1 breccia contains clasts of carbonate-magnetite altered rock, but occurs only in areas with carbonate-magnetite altered rocks, and is therefore likely a continuation of the same event.

4. Dark brown carbonate-magnetite ± quartz veins crosscut kink-banded phyllite and Type 1 breccia in Slab Creek. These occur mainly in the Canyon zone where they are up to 0.5 m thick (Fig. 9b). Rare carbonate-magnetite veins cut Fairchild Lake Group rocks on Slab Mountain.
5. Hematite deposition on fractures and in veinlets that crosscut earlier veins and breccia. Locally, hematite replaces magnetite.
6. Light brown carbonate ± quartz ± hematite ± pyrite-chalcopyrite ± chlorite veins. These veins crosscut the dark brown carbonate-magnetite veins, and hematite veinlets and fractures. They are very coarse grained with carbonate and quartz crystals up to 3 cm across.

Pink carbonate ± quartz ± hematite veins also occur prior to the emplacement of Type 2 breccia, but their relation to other veins is not clear. Pyrite-chalcopyrite-quartz-white mica veins cut carbonate-magnetite altered rock, but their timing is not clear, as crosscutting relationships with other veins or breccia were not seen. However, the veins are likely pre-Type 2 breccia as the breccia contains clasts of massive pyrite-chalcopyrite (Fig. 9c) and clasts of mineralized siltstone (Fig. 9d).

7. Emplacement of Type 2 Wernecke Breccia. This breccia is extensive and contains clasts of Fairchild Lake Group, kink-banded phyllite, Bonnet Plume River diorite, Slab volcanics, Type 1 breccia and massive sulphide. It also contains rare clasts of the micro-breccia that forms the Type 2 breccia matrix, suggesting that more than one phase of Type 2 brecciation occurred.

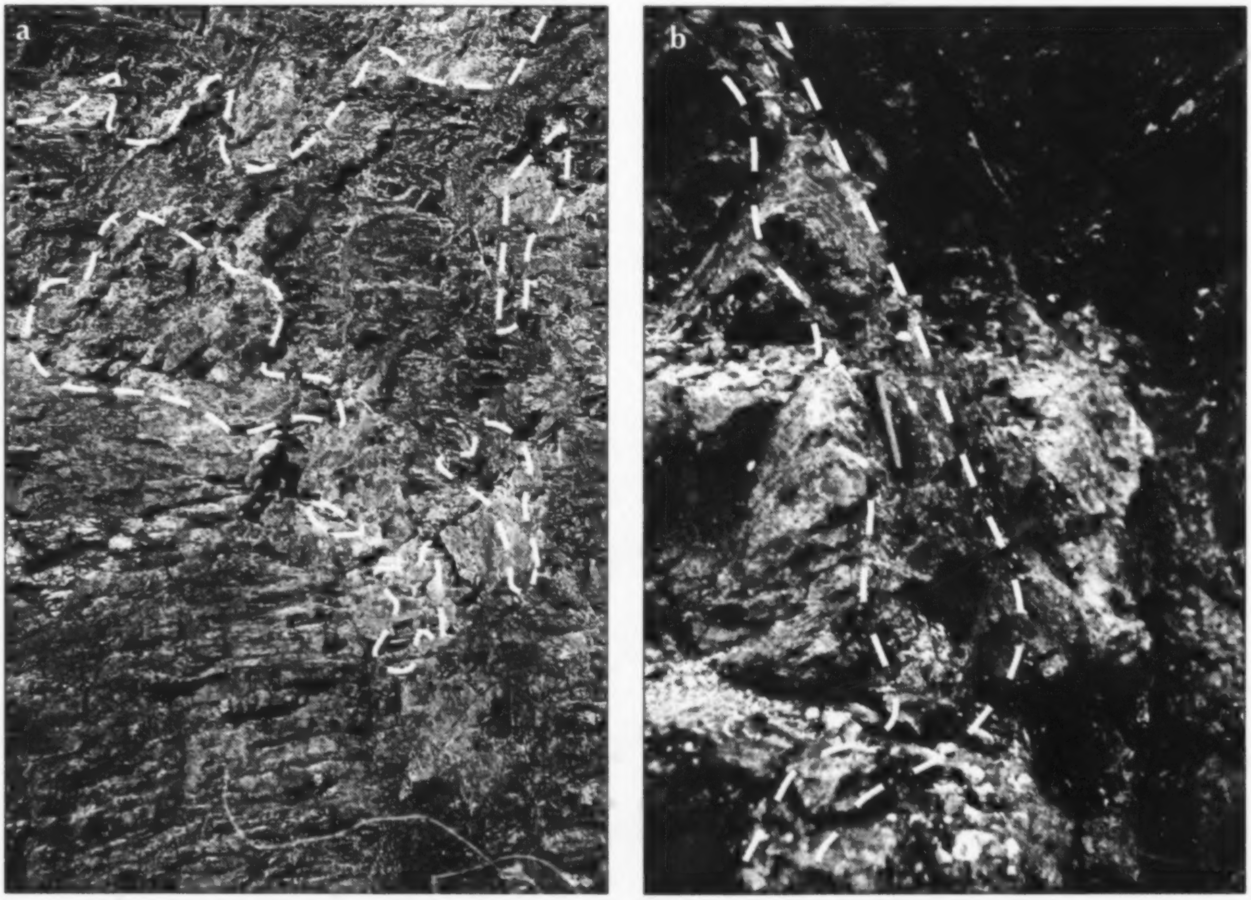

***Figure 9.*** *(a) Malachite-stained (area inside dashed lines) Fairchild Lake Group sedimentary rocks form the peak of Slab Mountain (person for scale). (b) A 10-cm-thick pyrite-chalcopyrite-quartz-white mica vein (inside dashed lines) cutting carbonate-magnetite altered rock in the Canyon zone.*

8. Veins that crosscut Type 2 Wernecke Breccia, but have unclear timing relationships to one another, including:
    - Quartz ± carbonate ± fluorite ± white mica ± chlorite ± biotite ± feldspar ± hematite ± actinolite ± pyrite ± chalcopyrite veins. These veins are locally coarsely crystalline with large (up to 2 cm) quartz, carbonate, fluorite and white mica crystals.
    - Carbonate ± quartz ± hematite ± magnetite ± pyrite veins. A prominent vein of this type occurs on the southwest side of Slab Mountain at the contact between Fairchild Lake Group sedimentary rocks and Type 2 Wernecke Breccia (Fig. 9e). This vein is 0.2-1 m thick and dominantly composed of 5 mm pink to white carbonate crystals that are loosely held together, giving the vein a sandy/crumbly texture. The vein contains sparse euhedral, grey to white quartz crystals from 0.2 cm to 1 cm long, euhedral magnetite crystals up to 3 mm across and rare disseminated 2-3 mm pyritahedrons.
    - Quartz-tourmaline veins
    - Pale pink feldspar-white mica veins that crosscut the quartz-tourmaline veins

## SUMMARY

New mapping in the Slab Mountain area indicates that it is underlain by Fairchild Lake Group fine-grained sedimentary rocks and their schistose equivalents, intermediate to mafic Slab volcanics, dioritic Bonnet Plume River dykes, and Wernecke Breccia; all are cut by numerous veins. Wernecke Breccia is herein divided into two units known informally as Type 1 and Type 2, based

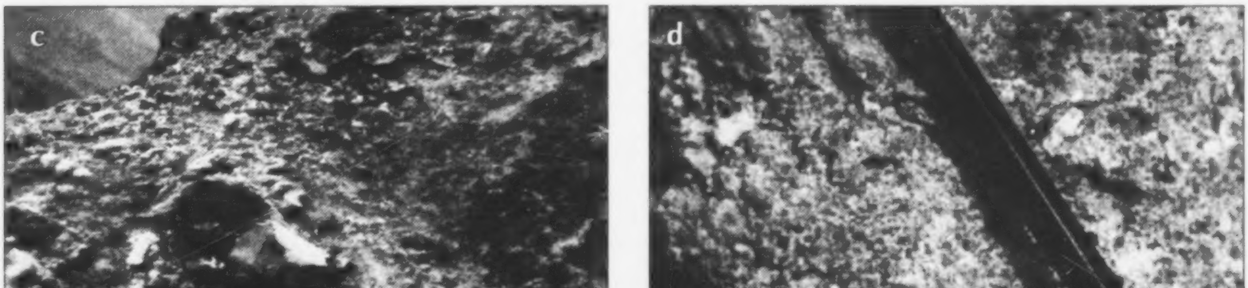

*__Figure 9.__ (c) Massive sulphide clast in Type 2 Wernecke Breccia at Slab Creek; (d) chalcopyrite bleb (dashed line) in a siltstone clast (dotted line) in Type 2 Wernecke Breccia on Slab Mountain.*

on crosscutting relationships. Type 1 breccia typically weathers dark purple to brown and consists of grey sedimentary rock clasts in a matrix of carbonate mineral(s) and magnetite. Type 2 breccia cuts Type 1 and is typically tan to grey. Clasts are generally grey with fewer pink and purple clasts. The matrix is generally green to grey and is itself fragmental. Magnetite-hematite-chalcopyrite mineralization in this area is associated with Wernecke Breccia. Crosscutting relationships suggest that this mineralization likely occurred after the emplacement of Type 1 breccia and continued until after the emplacement of Type 2 breccia. Evidence for this sequence includes pyrite-chalcopyrite-quartz-white mica veins that cut carbonate-magnetite altered rock, massive pyrite-chalcopyrite clasts up to 20 cm across in Type 2 breccia, clasts of Fairchild Lake Group with sulphide veinlets in Type 2 breccia, disseminated sulphides in the matrix of Type 2 breccia, and rare sulphide veinlets that crosscut Type 2 breccia.

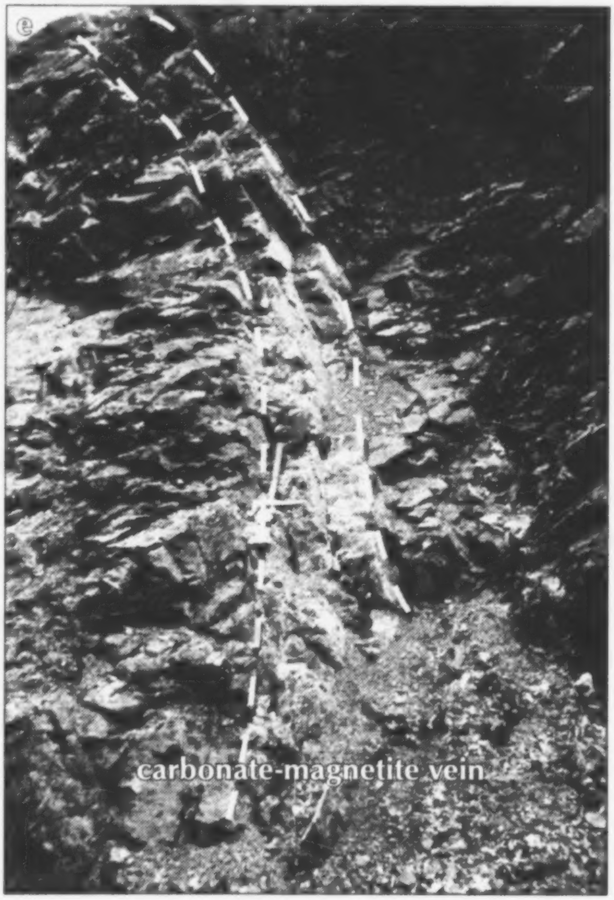

***Figure 9.*** *(e) Carbonate-magnetite vein (inside dashed lines) cutting carbonate-magnetite altered rock in the Canyon zone, Slab Creek.*

## ACKNOWLEDGEMENTS

This project was funded by the Yukon Geology Program, a Society of Economic Geologists Student Grant to Julie Hunt, a Lithoprobe grant to Derek Thorkelson, a Northern Studies Training Program grant to John Laughton, and an NSERC undergraduate scholarship to Marc-Andre Brideau.

The authors thank Richard Gorton of Newmont Mines Limited for access to confidential information, properties and drill core in the Wernecke Mountains; Mike Stammers, Dave Caulfield and Mark Baknes for sharing geological ideas and information; Trevor Ellis, Chad Santo, Monique Raichey and Rod Hill for logistical support; Grant Redfern for logistical support and assistance; and Trans North Helicopters, especially pilot Curtis Humphrey, for providing competent and reliable helicopter service.

## REFERENCES

Archer, A.R. and Schmidt, U., 1978. Mineralised breccias of Early Proterozoic age, Bonnet Plume River District, Yukon Territory. CIM Bulletin, vol. 71, p. 53-58.

Bell, R.T., 1986a. Geological map of north-eastern Wernecke Mountains, Yukon Territory. Geological Survey of Canada, Open File 1027.

Bell, R.T., 1986b. Megabreccias in north-eastern Wernecke Mountains, Yukon Territory. *In:* Current Research, Part A, Geological Survey of Canada, Paper 86-1A, p. 375-384.

Brideau, M-A., Thorkelson, D.J., Godin, L. and Laughton, J.R., 2002 (this volume). Paleoproterozoic deformation of the Racklan Orogeny, Slats Creek (106D/16) and Fairchild Lake (106C/13) map areas, Wernecke Mountains, Yukon. *In:* Yukon Exploration and Geology 2001, D.S. Emond, L.H. Weston and L.L. Lewis (eds.), Exploration and Geological Services Division, Yukon Region, Indian and Northern Affairs Canada, p. 65-72.

Brookes, M.L., Baker T. and Hunt, J.A., 2002 (this volume). Alteration zonation, veining and mineralization associated with Wernecke Breccias in 'Slab Creek' (NTS 106E/1), Wernecke Mountains, Yukon, Canada. *In:* Yukon Exploration and Geology 2001, D.S. Emond, L.H. Weston and L.L. Lewis (eds.), Exploration and Geological Services Division, Yukon Region, Indian and Northern Affairs Canada, p. 249-258.

Delaney, G.D., 1981. The mid-Proterozoic Wernecke Supergroup, Wernecke Mountains, Yukon Territory. *In:* Proterozoic Basins of Canada, F.H.A. Campbell (ed.), Geological Survey of Canada, Paper 81-10, p. 1-23.

Hitzman, M.W., Oreskes, N. and Einaudi, M.T., 1992. Geological characteristics and tectonic setting of Proterozoic iron oxide (Cu-U-Au-REE) deposits. *In:* Precambrian Metallogeny Related to Plate Tectonics, G. Gall and K. Schulz (eds.), Precambrian Research, vol. 58, p. 241-287.

Hunt, J.A., Laughton, J.R., Brideau, M-A, Thorkelson, D.J., Brookes, M. and Baker, T., (in press). Bedrock geology of the 'Slab Mountain' area, Wernecke Mountains (parts of 106C/13, 106D/16, 106E/1, 106F/4), Yukon Territory. Exploration and Geological Services Division, Yukon Region, Indian and Northern Affairs Canada, Open File 2002-6, 1:5000 scale map.

Laughton, J.R., Thorkelson, D.J., Brideau, M-A. and Hunt, J.A., 2002 (this volume). Paleoproterozoic volcanism and plutonism in the Wernecke Mountains, Yukon. *In:* Yukon Exploration and Geology 2001, D.S. Emond, L.H. Weston and L.L. Lewis (eds.), Exploration and Geological Services Division, Yukon Region, Indian and Northern Affairs Canada, p. 139-145.

Owerko, K.A., 1995. 1995 Summary Report on the Slab 1-222 claims. Private report prepared for Newmont Exploration Limited. (Part of this information is available in Assessment Report 093363, Mineral Resources Directorate, Yukon Region, Indian and Northern Affairs Canada).

Thorkelson, D.J., 2000. Geology and mineral occurrences of the Slats Creek, Fairchild Lake and "Dolores Creek" areas, Wernecke Mountains (106D/16, 106C/13, 106C/14), Yukon Territory. Exploration and Geological Services Division, Yukon Region, Indian and Northern Affairs Canada, Bulletin 10, 73 p.

Thorkelson, D.J., Mortensen, J.K., Creaser, R.A., Davidson, G.J. and Abbott, J.G., 2001a. Early Proterozoic magmatism in Yukon, Canada: Constraints on the evolution of northwestern Laurentia. Canadian Journal of Earth Science, vol. 38, p. 1479-1494.

Thorkelson, D.J., Mortensen, J.K., Davidson, G.J., Creaser, R.A., Perez, W.A. and Abbott, J.G., 2001b. Early Mesoproterozoic intrusive breccias in Yukon, Canada: The role of hydrothermal systems in reconstructions of North America and Australia. Precambrian Research, vol. III, p. 31-55.

Vance, R.B., Stammers, M.A. and Owerko, K.A., 1995. 1994 Summary Report on the Slab 1-222 claims. Private report prepared for Newmont Exploration Limited. (Part of this information is available in Assessment Report 093224, Mineral Resources Directorate, Yukon Region, Indian and Northern Affairs Canada).

Wheeler, J.O. and McFeeley, P., 1991. Tectonic assemblage map of the Canadian Cordillera and adjacent parts of the United States of America. Geological Survey of Canada, Map 1712A, 1:2 000 000 scale.

Yukon MINFILE, 2001. Exploration and Geological Services Division, Yukon Region, Indian and Northern Affairs Canada.

# Paleoproterozoic volcanism and plutonism in the Wernecke Mountains, Yukon

**John R. Laughton, Derek J. Thorkelson[1], Marc-André Brideau**
Simon Fraser University[2]

**Julie A. Hunt**
James Cook University[3]

Laughton, J.R., Thorkelson, D.J., Brideau, M-A. and Hunt, J.A., 2002. Paleoproterozoic volcanism and plutonism in the Wernecke Mountains, Yukon. *In:* Yukon Exploration and Geology 2001, D.S. Emond, L.H. Weston and L.L. Lewis (eds.), Exploration and Geological Services Division, Yukon Region, Indian and Northern Affairs Canada, p. 139-145.

## ABSTRACT

The Paleoproterozoic Slab volcanics occur in three localities in the Wernecke Mountains. The largest exposure is at Slab Mountain and consists of a 0.6 x 0.25 km block of thin, steeply dipping mafic to intermediate lava flows. A zone of Wernecke Breccia (1.60 Ga), which crops out along the exposed margin of this volcanic block suggests that the megaclast foundered into the breccia zone from a higher crustal level. The volcanic rocks are typically aphyric. The groundmass consists mainly of laths of plagioclase (commonly altered to scapolite), anhedral biotite and magnetite. The scapolite, and possibly the biotite and magnetite, likely grew during hydrothermal alteration associated with Wernecke Breccia emplacement. Primary igneous mineralogy is uncertain. The Slab volcanics appear geochemically similar and are probably comagmatic with some of the 1.71 Ga Bonnet Plume River Intrusions. No correlative volcanic strata have been found in the Wernecke Mountains or in the neighbouring Ogilvie Mountains.

## RÉSUMÉ

On retrouve les roches volcaniques de Slab, d'âge Paléoprotérozoïque, à trois endroits dans les monts Wernecke. Le plus grand affleurement se situe sur le mont Slab et consiste d'un bloc qui mesure 0,6 sur 0,25 km contenant de minces coulées de lave mafique à intermédiaire abruptement inclinées. Une zone de brèche de Wernecke (1,60 milliard d'années) affleure le long de la marge exposée de ce bloc volcanique; ce dernier serait un mégaclaste qui se serait effondré dans la zone de brèche depuis un niveau supérieur de la croûte. Les roches volcaniques sont typiquement aphyriques. La pâte est principalement constituée de biotite anédrique, de magnétite et de cristaux prismatiques de plagioclase (généralement altérés en scapolite). La scapolite, et peut-être la biotite ainsi que la magnétite, s'est probablement formée pendant l'altération hydrothermale associée à la mise en place de la brèche de Wernecke. La minéralogie des roches ignées primaires est incertaine. Les roches volcaniques de Slab semblent être d'une composition géochimique similaire aux intrusions de la rivière Bonnet Plume, datant de 1,71 milliard d'années; elles sont probablement comagmatiques. Aucune strate volcanique corrélative n'a été trouvée dans les monts Wernecke ni dans les monts Ogilvie avoisinants.

---

*[1] dthorkel@sfu.ca*

*[2] Department of Earth Sciences, Simon Fraser University, Burnaby, British Columbia, Canada V5A 1S6*

*[3] School of Earth Sciences, James Cook University, Townsville, Queensland 4811, Australia*

## INTRODUCTION

Geological mapping and research was carried out in the summer of 2001 in the northeastern corner of Slats Creek (106D/16) and southeastern corner of Quartet Lakes (106E/1) map areas in a remote part of the Wernecke Mountains approximately 180 km north-northeast of Mayo (Fig. 1). The study area includes 'Slab Mountain' and 'Slab Ridge', informally named features north of the Bonnet Plume River near Latitude 65°N and Longitude 134°W. The terrain is rugged and exposure is excellent. The study area has been of interest to exploration companies since the 1970s and is the site of the Slab mineral occurrence (Yukon MINFILE, 2001, 106O 070). The current investigation is part of a larger program involving personnel from Simon Fraser University (British Columbia), James Cook University (Australia), and the Yukon Geology Program.

In 1992, geologists of the Pamicon-Equity-Westmin mineral exploration venture first recognized the presence of volcanic rocks on Slab Mountain and Slab Ridge. These rocks were subsequently described, and named the Slab volcanics, by Thorkelson and Wallace (1993) as part of a regional 1:50 000-scale mapping project for the Canada/Yukon Geoscience Office. The Slab volcanics do not appear to correlate with other strata in the Yukon or elsewhere and therefore represent a unique and essentially unstudied geological formation (Thorkelson, 2000). Research in 2001 consisted of detailed mapping, examination, and geochemical sampling of the Slab volcanics. Emphasis was placed on the main exposure of the volcanic rocks, a succession of mainly lava flows on the eastern side of Slab Mountain (Thorkelson, 1993; Fig. 2). Two smaller localities originally noted by members of the Pamicon-Equity-Westmin-Newmont joint venture were also examined (Fig. 1, Localities 2 and 3). This report provides new field observations and petrographic descriptions of all three localities and a brief description of volcanic rock intersected in drill core on the Arch claims, south of the Bonnet Plume River (Fig. 1, Locality 1).

## GEOLOGICAL FRAMEWORK

Four main geological units occur in the study area (Fig. 3). The oldest is the ~4-km-thick Fairchild Lake Group of the Wernecke Supergroup, which consists mainly of siltstone and carbonate (Delaney, 1981; Thorkelson, 2000). In the study area, much of the Fairchild Lake Group has been metamorphosed to fine-grained, low-grade schist

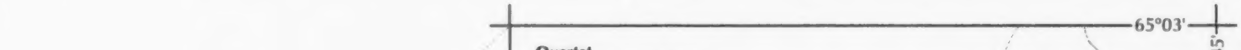

***Figure 1.*** *Region of interest in the Wernecke Mountains. Boxed area indicates location of study area. Locations marked with crosses indicate: 1. Arch claims, 2. unnamed locality of Slab volcanic rocks, 3. Fairchild MINFILE occurrence (Yukon MINFILE, 2001, 106C 007).*

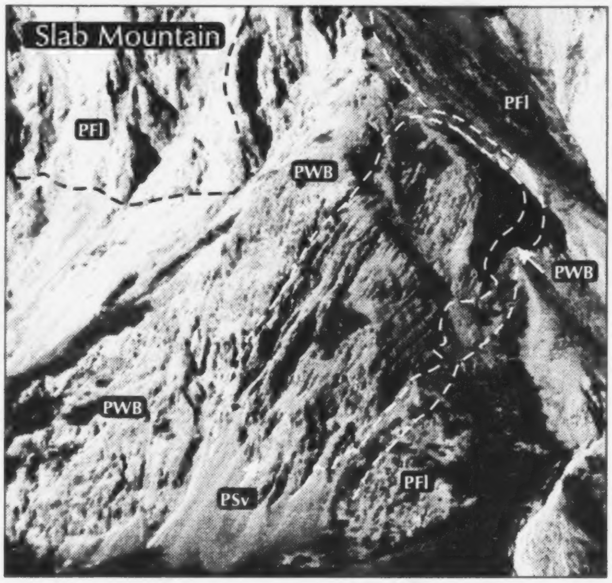
Slab Mountain
PFl
PFl
PWB
PWB
PWB
PSv
PFl

***Figure 2.*** *Eastern side of Slab Mountain, view is approximately north. Wernecke Breccia (PWb) occurs between Fairchild Lake Group (PFl) and Slab volcanics (PSv). Width of frame is approximately 600 m.*

(Brideau et al., this volume). The Bonnet Plume River Intrusions, of mainly dioritic composition, crosscut the Fairchild Lake Group, and have been dated by U-Pb zircon to be ca. 1.71 Ga (Thorkelson et al., 2001a). These relations constrain the age of the Wernecke Supergroup to >1.71 Ga. The Slab volcanics were considered by Thorkelson (2000) to be younger than the Wernecke Supergroup, and possibly comagmatic with the Bonnet Plume River Intrusions. The youngest units in the study area are zones of hydrothermal breccia and megabreccia, collectively called Wernecke Breccia, which crosscut the entire Wernecke Supergroup and Bonnet Plume River Intrusions (Bell and Delaney, 1977; Thorkelson et al., 2001b) and nonconformably underlie the Pinguicula Group (Thorkelson 2000, 2001b; Fig. 3). The zone of Wernecke Breccia at the eastern end of Slab Mountain (Fig. 2) was dated by U-Pb titanite to be ca. 1.60 Ga (Thorkelson et al., 2001b). The main succession of Slab volcanics at Slab Mountain was regarded by Thorkelson et al. (2001b) as a megaclast within this breccia zone (Fig. 4). New field observations presented in this report support the megaclast model for the Slab volcanics and

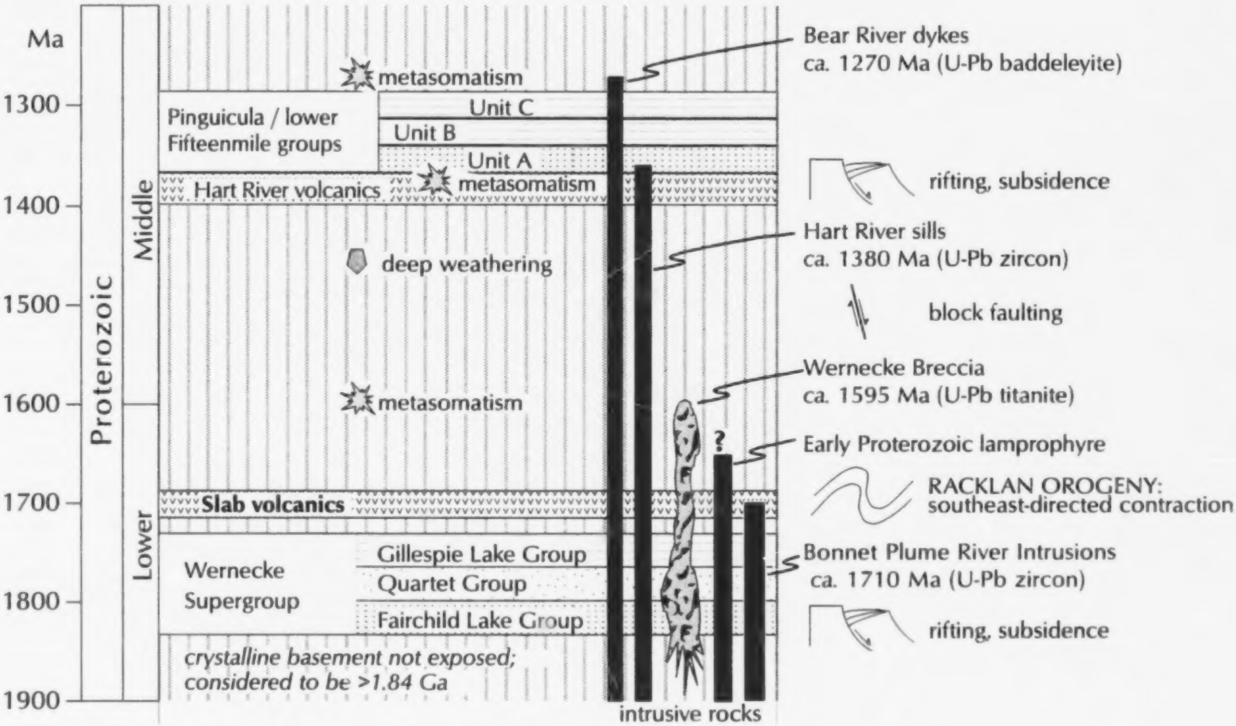
Ma
1300
1400
1500
1600
1700
1800
1900
Proterozoic
Middle
Lower
metasomatism
Pinguicula / lower Fifteenmile groups
Unit C
Unit B
Unit A
Hart River volcanics
metasomatism
deep weathering
metasomatism
Slab volcanics
Wernecke Supergroup
Gillespie Lake Group
Quartet Group
Fairchild Lake Group
crystalline basement not exposed; considered to be >1.84 Ga
intrusive rocks
?
Bear River dykes
ca. 1270 Ma (U-Pb baddeleyite)
rifting, subsidence
Hart River sills
ca. 1380 Ma (U-Pb zircon)
block faulting
Wernecke Breccia
ca. 1595 Ma (U-Pb titanite)
Early Proterozoic lamprophyre
RACKLAN OROGENY:
southeast-directed contraction
Bonnet Plume River Intrusions
ca. 1710 Ma (U-Pb zircon)
rifting, subsidence

***Figure 3.*** *Representative time stratigraphic column demonstrating the relations between sedimentary deposition, volcanism, plutonism, deformation, brecciation and metasomatism in the Wernecke Mountains. Modified after Thorkelson (2000).*

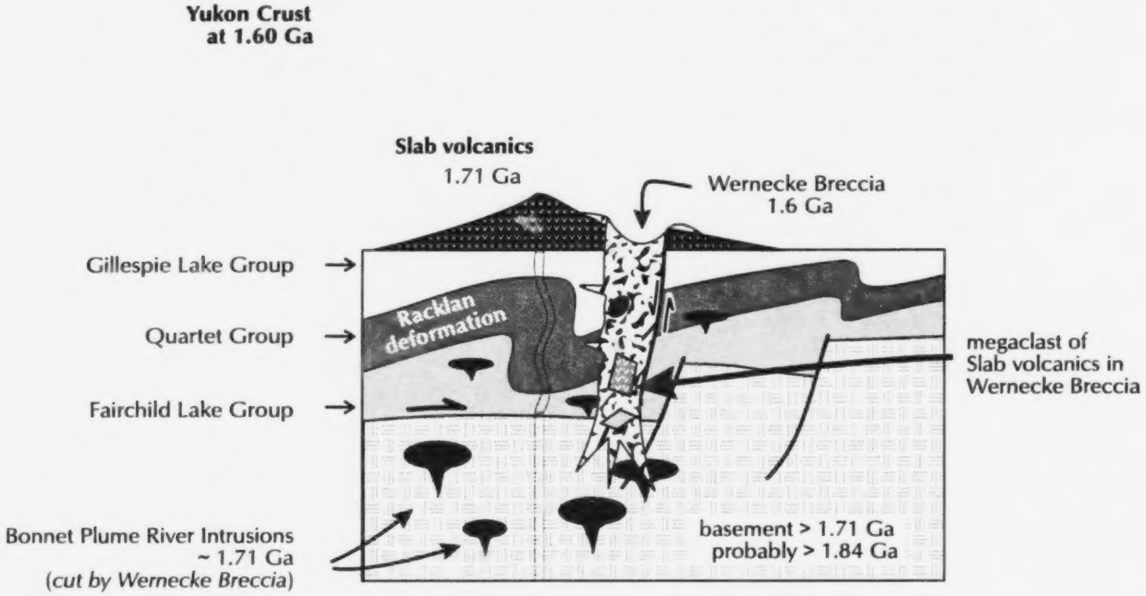
Yukon Crust
at 1.60 Ga
Slab volcanics
1.71 Ga
Wernecke Breccia
1.6 Ga
Gillespie Lake Group
Quartet Group
Racklan deformation
Fairchild Lake Group
megaclast of
Slab volcanics in
Wernecke Breccia
Bonnet Plume River Intrusions
~ 1.71 Ga
(cut by Wernecke Breccia)
basement > 1.71 Ga
probably > 1.84 Ga

***Figure 4.*** *Cartoon illustrating a hypothetical crustal cross-section, showing relations between Wernecke Supergroup, Slab volcanics, Bonnet Plume River Intrusions and Wernecke Breccia (modified after Thorkelson et al., 2001a).*

suggest that the volcanic rocks are coeval with, or older than, the Bonnet Plume River Intrusions.

## SLAB VOLCANICS

The Slab volcanics crop out at one main and two minor localities. At each locality, the volcanic rocks appear to be fragments of a larger succession engulfed by zones of Wernecke Breccia. Physical connections between the volcanic rocks and intact stratigraphic units are absent. Original volcanic textures are commonly visible, whereas deformational features, such as schistosity, crenulations and kink bands, which are locally prominent in nearby exposures of the Fairchild Lake Group, are not evident. Metamorphic grade, although not rigorously determined, appears to be no higher than lower greenschist grade.

### MAIN LOCALITY

The largest exposure of the Slab volcanics lies on the eastern end of Slab Mountain (Fig. 2). The volcanic block is roughly rectangular in outcrop, measuring about 250 m in the east-west direction and about 600 m north-south. The volcanic block consists mainly of steeply dipping lava flows with tops to the west. On the west side, a narrow (< 2-m-wide) fault zone, characterized by abundant slickensides, separates the uppermost lava flow from a broad zone (> 300 m wide) of Wernecke Breccia to the west. Along the north and east sides, a thin zone of breccia (0.1 m to 50 m) separates the volcanic rocks from schist of the Fairchild Lake Group and diorite of the Bonnet Plume River Intrusions. At one location, the eastern margin of the volcanic succession is separated from breccia by a 10-m-wide block of diorite. The diorite is chilled against the lowest unit of the volcanic succession and progressively coarsens toward the interior of the intrusion. At approximately 1 m from the chilled margin, the intrusion is a fine-grained diorite composed mainly of interlocking feldspar and pyroxene grains, typical of the intrusions in this area. The southern end of the volcanic succession is overlain by talus.

The volcanic rocks on eastern Slab Mountain consist of 35 mafic-intermediate lava flows that dip roughly 70° to the northwest. Flow thickness averages 4 m, but ranges from 0.8 m to 14 m. Lava flows throughout the succession commonly display prominent, amygdaloidal and locally auto-brecciated bottoms, typically 1.5 m to 2 m thick, which grade into massive, recessive lava, ~1 m thick, which grades upward into a prominent 2-m-thick scoriaceous flow top. The flows are variably amygdaloidal, with vesicles commonly filled with quartz, white and pink calcite, tremolite, biotite, chlorite and apatite. The distribution of pipe vesicles and scoria in the lava flows confirms the tops-to-the-northwest facing direction of the succession.

The basal volcanic unit is a 14-m-thick volcanic breccia. A 6-m-thick, blocky weathering, moderately vesiculated lava flow lies between the basal breccia and a 10-m-thick, prominent, volcanic tuff breccia. A succession of conformable vesiculated, aphyric lava flows of variable thickness overlies this volcaniclastic unit. A thin (1.4 m) sandstone interbed is located approximately one-third of the way up the succession. Load structures in the sandstone indicate stratigraphic tops to the northwest. Clastic units are absent above the sandstone interbed. Pipe vesicles up to 1.5 cm in diameter and 12 cm in length occur in the basal part of the lava flow that directly overlies the sandstone. Hydrothermal veins composed of powdery, white, fine-grained minerals cut many of the flows. Where the veins are thick (> 2 cm) and abundant, the lavas are deformed into local zones of crackle breccia.

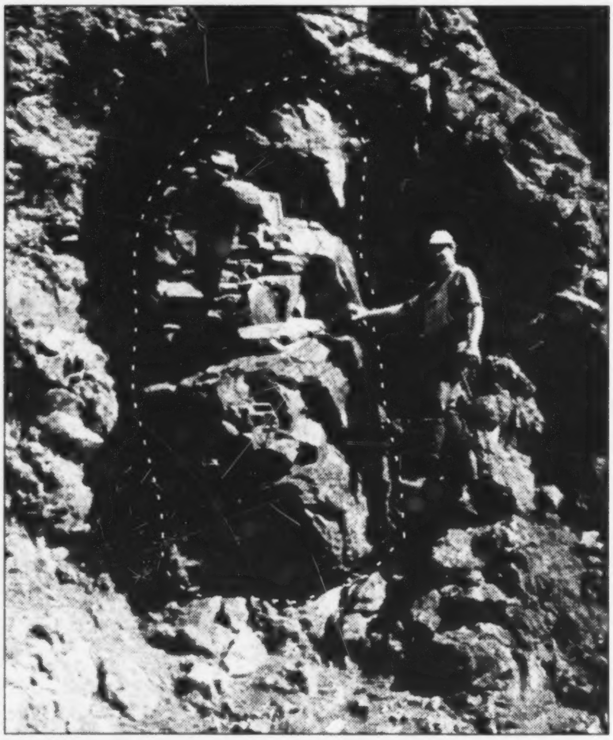

*Figure 5. Megaclast of Bonnet Plume River Intrusion in Wernecke Breccia on Slab Mountain.*

The thinness and scoriaceous character of the lava flows suggests that they were deposited as pahoehoe lavas in a subaerial environment. No indicators of subaqueous deposition, such as pillows, pillow breccias, or intercalations of hyaloclastite, have been recorded. The abundance of these thin lava flows, and a paucity of clastic rock at all localities indicate that the volcanic succession was dominated by mafic flows and is likely to have formed part of a shield volcano.

The Slab volcanics are mainly aphyric and composed of plagioclase, biotite and magnetite. Rare thick flows (> 8 m) show no noticeable differences in grain size throughout. Towards the bottom of the succession, a 6-m-thick flow contains conspicuous, large (up to 2 cm) trachytically aligned laths of euhedral plagioclase which are concentrated in the lower 30 cm. The groundmass of ~0.4-mm-long interlocking laths of plagioclase feldspar is commonly weakly flow aligned. Replacement and recrystallization of plagioclase by scapolite is seen in many of the flows examined. Expected mafic minerals such as hornblende and augite are conspicuously absent. Subhedral groundmass magnetite is ubiquitous. The biotite exists as 0.1 mm grains that occur both individually and in clusters. Whether this assemblage is primary (of igneous origin) or secondary (caused by alteration) is under investigation.

Two small, nearby occurrences of the Slab volcanics are included in this locality. Both occur as clasts within Wernecke Breccia. On Slab Mountain and Slab Ridge, Wernecke Breccia mainly consist of angular to well rounded clasts of siltstone and schist derived from the surrounding Fairchild Lake Group, and subordinate clasts of diorite derived from the Bonnet Plume River Intrusions. Clasts range from pebble-size fragments, to 60-m blocks located on the south side of Slab Mountain (Fig. 5). One clast of the Slab volcanics is boulder-sized (1.5 m in diameter) and crops out in a thick zone of Wernecke Breccia, approximately 5 m west of the top lava flow. It is petrographically similar to the lava flows of the main succession. The other clast is a 2 m by 3 m, fine-grained, amygdaloidal and locally auto-brecciated fragment of lava within Wernecke Breccia on the crest of Slab Ridge.

## OTHER LOCALITIES

Volcanic rocks have been found at two other localities in the region. One locality is situated about 10 km east-southeast of Slab Mountain, north of the Bonnet Plume River (Fig. 1, Locality 2). The outcrop is a 150-m-high cliff face that is continuous for 500 m. Exposure is excellent and field relations are discernable. Three separate 50-m-wide blocks of dark grey volcanic rocks outcrop along the face. Each block is surrounded on all exposed sides by large (> 70 m) bodies of Wernecke Breccia. A 2-m-diameter rounded boulder of Slab volcanics was found and sampled in the breccia at the west end of the outcrop and appears to be a milled fragment derived from the larger succession. The groundmass consists of interlocking laths of plagioclase and anhedral grains of biotite and magnetite, and is indistinguishable from typical groundmass in the flows at the main succession on Slab Mountain.

The other locality is approximately 1 km south of Fairchild Lake, 14 km east-southeast of Slab Mountain (Fig. 1, Locality 3), at the Fairchild mineral occurrence (Yukon MINFILE, 2001, 106C 007). The outcrop is on a low, 200-m-wide rocky knob situated in the valley bottom east of the Bonnet Plume River. The exposure is continuous and consists of dark grey, fine-grained aphyric lava. Two exposures of Wernecke Breccia, each about 20 m across, appear to crosscut the volcanic rocks. The rock has a conspicuous spotty hornfels appearance caused by replacement of plagioclase and other minerals by scapolite. Anhedral biotite and subhedral magnetite occur throughout. The rocks are petrographically similar to flows of the main volcanic succession at Slab Mountain and are tentatively correlated with them.

Rock that appears to be correlative with the Slab volcanics was intersected in core at the Arch claims south of the Bonnet Plume River (Fig. 1, Locality 1). The suspected volcanic rocks occur in a 70-cm interval of core and are bounded by Wernecke Breccia. Mineralogically and texturally, they are similar to the volcanic rocks at the locality south of Fairchild Lake, including conspicuous light-coloured, spherical patches (2 mm) of scapolite.

## INTERPRETATION OF FIELD RELATIONS

The chilling of a dioritic Bonnet Plume River Intrusion against a lava flow of the Slab volcanics on Slab Mountain indicates that Bonnet Plume River Intrusion magmatism post-dates, or is coeval with, the Slab volcanics. The Slab volcanics are therefore constrained in age to > 1.71 Ga. The two igneous units may be comagmatic, and part of the same volcano-plutonic complex.

We interpret all blocks of volcanic rocks discussed as megaclasts derived from a volcanic succession that became incorporated into zones of Wernecke Breccia through explosive brecciation and foundering (Fig. 4; Thorkelson et al., 2001b). The smaller exposures, such as those on Slab Ridge and northwest of the main succession on Slab Mountain, are clearly visible as clasts in the breccia. The main block of volcanic rocks on Slab Mountain is also surrounded by breccia, except where the volcanic rocks are intruded by a Bonnet Plume River Intrusion. At that location, the breccia engulfs both the volcanic rocks and the intrusion. Slickensides between breccia and the northwest side of the main block indicate that subsequent faulting occurred; however, we contend that the displacements are minor and that the fundamental process linking the breccia to the volcanic rocks is hydrothermal brecciation. Engulfment of the volcanic rocks by breccia is also evident at the locality 10 km southeast of Slab Mountain.

If the Slab volcanics are relics of a larger volcanic succession, at what stratigraphic position did this succession lie? No proximal volcanic rocks are known from the Wernecke Supergroup, in the immediate vicinity or elsewhere, despite excellent exposure (Thorkelson, 2000). Moreover, the volcanic rocks were deposited subaerially, in contrast to the marine environment of the Wernecke Supergroup (Delaney, 1981), making the Wernecke Supergroup an unsuitable stratigraphic unit to host the volcanism. If the Slab volcanics were deposited prior to the Wernecke Supergroup, then their current position within breccia flanked by the Fairchild Lake Group would require upward motion from depth. This option seems unlikely because of the enormous size of some of the blocks, especially the main succession on Slab Mountain. In addition, the metamorphic grade of the volcanic rocks appears to be no higher than the Wernecke Supergroup, inferring that they did not originally underlie the Wernecke succession. Consequently, the most suitable stratigraphic position for the volcanic succession is above the Wernecke Supergroup.

In this scenario, the volcanic succession, probably a shield volcano, would have been fragmented, along with the underlying zones of Wernecke Supergroup and the Bonnet Plume River Intrusions, by explosive hydrothermal activity during formation and emplacement of two zones of Wernecke Breccia (Thorkelson et al., 2001b). Large blocks of the volcanic succession would have fallen into dilatant zones near the tops of the breccia zones and become surrounded by hydrothermal fluids and clasts derived predominantly from the Wernecke Supergroup. Local scapolite alteration of the Slab volcanics supports the foregoing model of hydrothermal brecciation and foundering. Scapolite-after-plagioclase is present in clasts of the Bonnet Plume River Intrusions (Thorkelson et al., 2001a, b) and appears to be an alteration signature of igneous rock incorporated into the breccias.

## CONCLUSIONS

The Slab volcanics occur at three main localities in the Wernecke Mountains. They are characterized by their dark grey, vesicular, aphyric appearance. Petrographically, they consist of a groundmass of interlocking laths of plagioclase, anhedral biotite and magnetite. Scapolite occurs locally as light grey patches and spherical porphyroblasts, commonly replacing plagioclase. The mineral assemblage, including scapolite, may be a product of metasomatism related to brecciation. In all localities, the volcanic rocks are in contact with zones of Wernecke Breccia and are interpreted to be megaclasts within the breccia. At one locality, the volcanic rocks are intruded by an Early Proterozoic Bonnet Plume River Intrusion, constraining the age of the volcanic rocks to > 1.71 Ga. The megaclasts of the Slab volcanics are relics of a larger but entirely eroded volcanic succession, probably a shield volcano that overlay the Wernecke Supergroup.

## ACKNOWLEDGEMENTS

Access to the study area and samples of drill core were provided by Richard Gorton of Newmont Mines Limited. Funding was provided by a LITHOPROBE grant to D.J. Thorkelson, a Northern Studies Training Program grant to J.R. Laughton, an NSERC undergraduate scholarship to M-A. Brideau, and the Yukon Geology Program.

## REFERENCES

Bell, R.T. and Delaney, G.D., 1977. Geology of some uranium occurrences in Yukon Territory. Current Research, Part A, Geological Survey of Canada, Paper 77-1A, p. 33-37.

Brideau, M-A., Thorkelson, D.J., Godin, L. and Laughton, J.R., 2002 (this volume). Paleoproterozoic deformation of the Racklan Orogeny, Slats Creek (106D/16) and Fairchild Lake (106C/13) map areas, Wernecke Mountains, Yukon. *In:* Yukon Exploration and Geology 2001, D.S. Emond, L.H. Weston and L.L. Lewis (eds.), Exploration and Geological Services Division, Yukon Region, Indian and Northern Affairs Canada, p. 65-72.

Delaney, G.D., 1981. The mid-Proterozoic Wernecke Supergroup, Wernecke Mountains, Yukon Territory. *In:* Proterozoic Basins of Canada, F.H.A. Campbell (ed.), Geological Survey of Canada, Paper 81-10, 23 p.

Thorkelson, D.J., 2000. Geology and mineral occurrences of the Slats Creek, Fairchild Lake and "Dolores Creek" areas, Wernecke Mountains, Yukon Territory (106D/16, 106C/13, 106C/14). Exploration and Geological Services Division, Yukon Region, Indian and Northern Affairs Canada, Bulletin 10, 73 p.

Thorkelson, D.J. and Wallace, C.A., 1993. Development of Wernecke Breccias in Slats Creek (106D/16) map area, Wernecke Mountains, Yukon. *In:* Yukon Exploration and Geology 1992, Exploration and Geological Services Division, Yukon Region, Indian and Northern Affairs Canada, p. 19-30.

Thorkelson, D.J., Mortensen, J.K., Creaser, R.A., Davidson, G.J. and Abbott, J.G., 2001a. Early Proterozoic magmatism in Yukon, Canada: Constraints on the evolution of northwestern Laurentia. Canadian Journal of Earth Sciences, vol. 38, p. 1479-1494.

Thorkelson, D.J., Mortensen, J.K., Davidson, G.J., Creaser, R.A., Perez, W.A. and Abbott, J.G., 2001b. Early Mesoproterozoic intrusive breccias in Yukon, Canada: The role of hydrothermal systems in reconstructions of North America and Australia. Precambrian Research, vol. 111, p. 31-55.

Yukon MINFILE, 2001. Fairchild Lake and Nash Creek areas, 106C and 106D. Exploration and Geological Services Division, Yukon Region, Indian and Northern Affairs Canada.

# White Channel Gravel alteration revisited

***Grant W. Lowey***[1]
*Yukon Geology Program*

Lowey, G.W., 2002. White Channel Gravel alteration revisited. *In:* Yukon Exploration and Geology 2001, D.S. Emond, L.H. Weston and L.L. Lewis (eds.), Exploration and Geological Services Division, Yukon Region, Indian and Northern Affairs Canada, p. 147-162.

## ABSTRACT

The White Channel Gravel (Pliocene) is the most important gold-bearing unit in the world famous Klondike goldfields of west-central Yukon. It is up to 46 m thick and consists of framework-supported, poorly bedded, slightly muddy sandy gravel that was deposited by braided rivers. Historically, this unit is subdivided into a lower 'white gravel' and an upper 'yellow gravel'. The colour of the white gravel is due to an abundance of quartz clasts and an alteration of the sand-mud matrix that has been referred to as 'leaching' or 'bleaching'. Previous researchers concluded that the alteration is hydrothermal in origin, but a review of this research shows that there is no unequivocal evidence supporting hydrothermal alteration. Petrographic examination of in situ samples from both the white and yellow gravel reveals a depositional fabric and an alteration fabric, although the alteration is better developed in the white gravel. The alteration is reinterpreted as the result of weathering, and particularly diagenesis due to groundwater flow.

## RÉSUMÉ

Les graviers de White Channel (Pliocène) constituent l'unité aurifère la plus importante des champs aurifères de la région ouest-centre du Yukon, de renommée mondiale. D'une épaisseur pouvant atteindre 46 mètres, ces graviers sableux légèrement boueux et mal lités furent déposés par des cours d'eau anastomosés. Historiquement, cette unité comprend des « graviers blancs » inférieurs et des « graviers jaunes » supérieurs. La couleur des graviers blancs s'explique par une abondance de clastes quartzeux et par une altération, qualifiée de « lessivage » ou de « blanchiment », de la matrice sable-boue. Des chercheurs avaient conclu précédemment que l'altération était d'origine hydrothermale, mais un examen des résultats de cette recherche révèle qu'aucune donnée non équivoque ne milite en faveur de cette explication. Un examen pétrographique d'échantillons in situ prélevés sur des graviers blancs et des graviers jaunes a révélé une fabrique de dépôt et une fabrique d'altération, l'altération étant plus accentuée dans les graviers blancs. Selon la réinterprétation, l'altération des graviers serait le résultat de la météorisation et plus particulièrement de la diagénèse provoquée par l'écoulement des eaux souterraines.

---

[1] grant.lowey@geology.gov.yk.ca

# INTRODUCTION

The White Channel Gravel is the most important placer gold-bearing unit in the world famous Klondike goldfields. The Klondike goldfields are located in the unglaciated part of west-central Yukon (Fig. 1), and extend from the Klondike River, south to the Indian River (Fig. 2), and from the Yukon River, east to Flat Creek, covering an area of approximately 2000 km$^2$. Since their discovery over 100 years ago, they have produced an estimated 311 million tonnes of gold, primarily from bench and creek placers that are fluvial in origin and range from Pliocene to Holocene in age (Lowey, 1998, 2001a; McConnell, 1905, 1907). The dominant forcing mechanisms controlling the formation of the placer deposits were isostatically compensated exhumation and climatic change related to the repeated glaciation of the Yukon (Lowey, 2001b,c). Historically, the Klondike goldfields are classified into three levels of gravel with four main units (McConnell, 1905, 1907). The 'high-level' gravel includes the Pliocene age White Channel Gravel, which McConnell (1905, 1907) subdivided into a lower 'white gravel' and an upper 'yellow gravel' (Figs. 3, 4). McConnell (1905, 1907) described the white gravel as being dominated by rounded pebbles and boulders of vein quartz, with minor amounts of schist and gneiss pebbles, all in a compact matrix of 'sericite plates' and angular quartz grains; whereas the yellow gravel consists mostly of flat schist pebbles in a significantly less compact, coarse sandy matrix. Overall, the White Channel Gravel is up to 46 m thick and consists of framework-supported, poorly bedded, slightly muddy, sandy pebble to cobble gravel (Fig. 5). It was deposited by braided rivers such as the paleo-Bonanza and paleo-Hunker creeks (Lowey, 1998).

According to McConnell (1905), the White Channel Gravel was named for its dominant white or light grey colour, which he attributed to the abundance of quartz clasts and an alteration of the sand-mud matrix that he thought was due to the 'leaching of iron'. McConnell (1905, 1907) also recognized that some igneous clasts in the gravel decomposed and crumbled easily when thawed. Tempelman-Kluit (1982) referred to the alteration as 'bleaching' and suggested that it was caused by groundwater. He further suggested that the gold in the gravel had precipitated from the mixing of deep, warm, ascending groundwater with shallow, cool, descending groundwater, and proposed that the gold was 'growing' in the gravel. This prompted a detailed study of the origin of gold in the White Channel Gravel by Dufresne (1987). Dufresne (1987) concluded that the alteration and gold were due to low temperature (i.e., 120-130°C), low

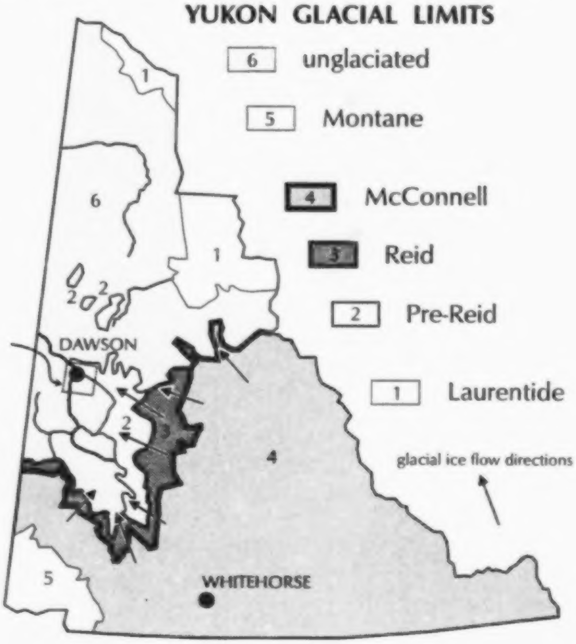

*Figure 1. Location map of the Klondike goldfields (box) and Yukon glacial limits (modified from Bostock, 1966; Hughes, 1968).*

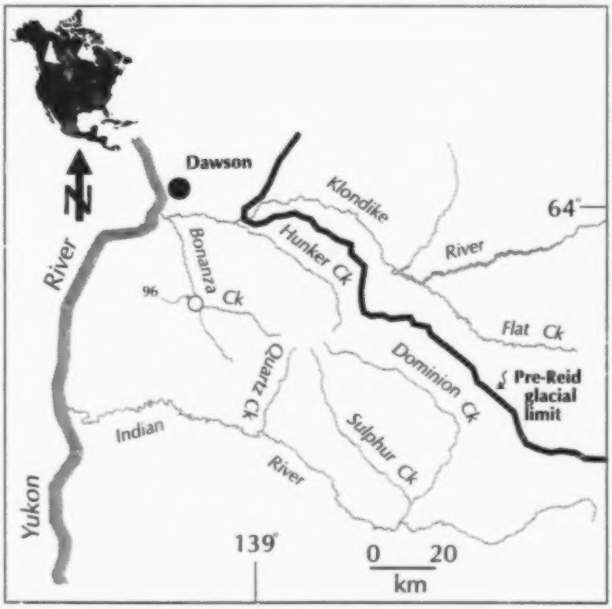

*Figure 2. Klondike goldfields, west-central Yukon, and major drainages (96 = 1896, the year and location of gold discovery).*

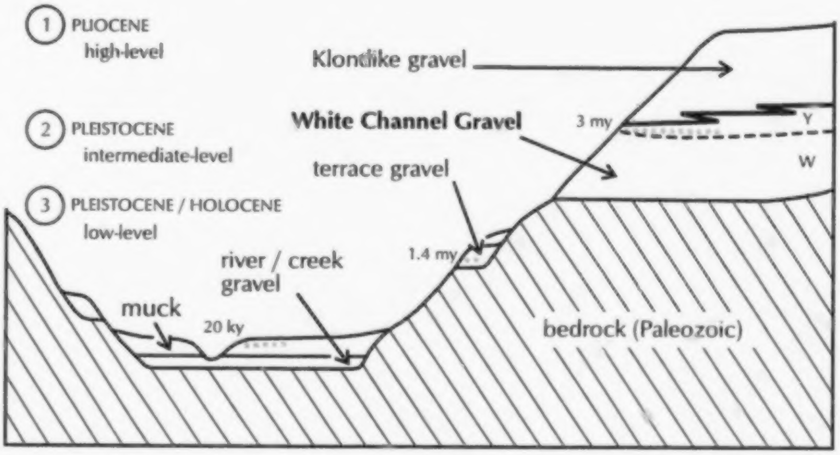
1 PLIOCENE high-level
2 PLEISTOCENE intermediate-level
3 PLEISTOCENE / HOLOCENE low-level
Klondike gravel
White Channel Gravel
3 my
Y
W
terrace gravel
1.4 my
river / creek gravel
muck
20 ky
bedrock (Paleozoic)

**Figure 3.** *Schematic cross-section of Bonanza Creek, showing the stratigraphy of the Klondike goldfields; W = white gravel; Y = yellow gravel; 3 my and 1.4 my = age of tephra in million years; 20 ky = age of tephra in thousand years (modified from McConnell, 1905, 1907; Westgate et al., 2000).*

salinity (i.e., 1-2 wt.% NaCl) hydrothermal fluids characteristic of epithermal mineralization. The hypogene alteration proposed by Dufresne (1987) resembles argillic-type wall-rock alteration (Peters, 1987). Dufresne (1987, p. 150) further proposed that "Current gravitational techniques employed in the evaluation and mining of clay-altered White Channel gravel and footwall rocks are vastly inadequate to recover the large amount of fine-grained hydrothermal gold suspected to be present in these units." However, Knight et al. (1994, 1999), using major and minor trace element compositions of gold particles from placer and lode deposits in the Klondike goldfields, determined that "most if not all" of the gold was derived from the lodes, similar to what McConnell (1905, 1907) had reported nearly one hundred years ago.

Perplexingly, Knight et al. (1999) did not discount a hydrothermal origin for the alteration. Instead, they stated (Knight et al., 1999, p. 652) that Dufresne (1987) "demonstrated clearly that the White Channel alteration is the result of ... hydrothermal activity." The statement by Knight et al. (1999) is confusing because the alteration is still considered hydrothermal in origin even though the gold is not. The author has worked on the White Channel Gravel for the last four years, and has observed and described only sedimentary processes (i.e., Lowey, 1998, 1999a,b, 2001a,b,c,d). The purpose of this paper is to review the evidence for and against hyrothermal alteration, present new evidence regarding the alteration from transmitted light petrography, and reinterpret the origin of the alteration in terms of sedimentary processes.

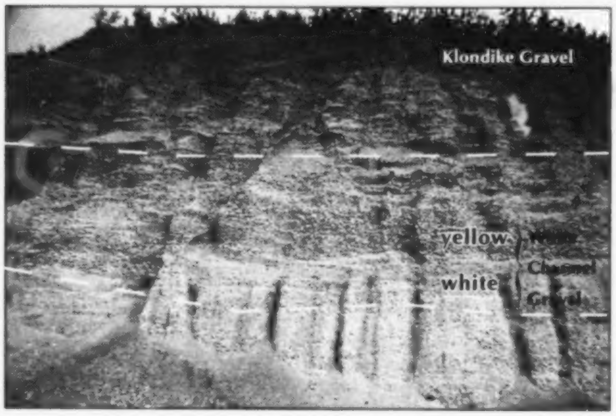
Klondike Gravel
yellow
white
White Channel Gravel

**Figure 4.** *White Channel Gravel, showing the white gravel and yellow gravel sub-units and the overlying Klondike Gravel, Australia Hill.*

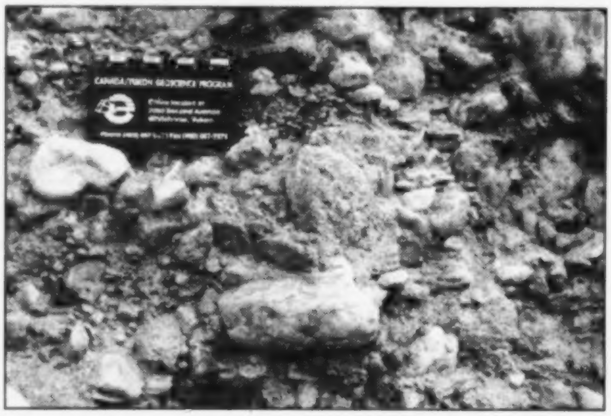

**Figure 5.** *White gravel, showing the preserved texture, Jackson Hill.*

## EVIDENCE FOR AND AGAINST HYDROTHERMAL ALTERATION

Dufresne (1987) presented seven major lines of evidence for hydrothermal alteration of the White Channel Gravel: 1) distribution of the alteration; 2) grain-size analysis; 3) mineralogy; 4) crystallinity of clay minerals; 5) geochemistry; 6) discovery of new veins; and 7) distribution of gold.

### DISTRIBUTION OF ALTERATION

Dufresne (1987) classified the degree of alteration as ranging from unaltered (1) to altered (6), and mapped its lateral distribution in the White Channel Gravel and in the bedrock (Fig. 6). He also recognized three alteration zones (i.e., the footwall zone in bedrock, the iron zone in gravel adjacent to bedrock, and the bleached zone in gravel above bedrock) based on their physical characteristics (Fig. 7). Note that both the iron and bleached zones correspond to McConnell's (1905, 1907) white gravel sub-unit, whereas the unaltered gravel corresponds to McConnell's (1905, 1907) yellow gravel sub-unit. Dufresne (1987) suggested that the distribution of the alteration, particularly the three alteration zones, was evidence that it was hydrothermal in origin.

The White Channel Gravel is not restricted to Bonanza and Hunker creeks. It also occurs along Dominion Creek, Quartz Creek and the Indian River (Lowey, 1998, 1999a,b; McConnell, 1905, 1907). Hence, the distribution of the gravel is widespread, indicating that the alteration is regional in extent. In addition, the degree of alteration in the White Channel Gravel along Bonanza and Hunker

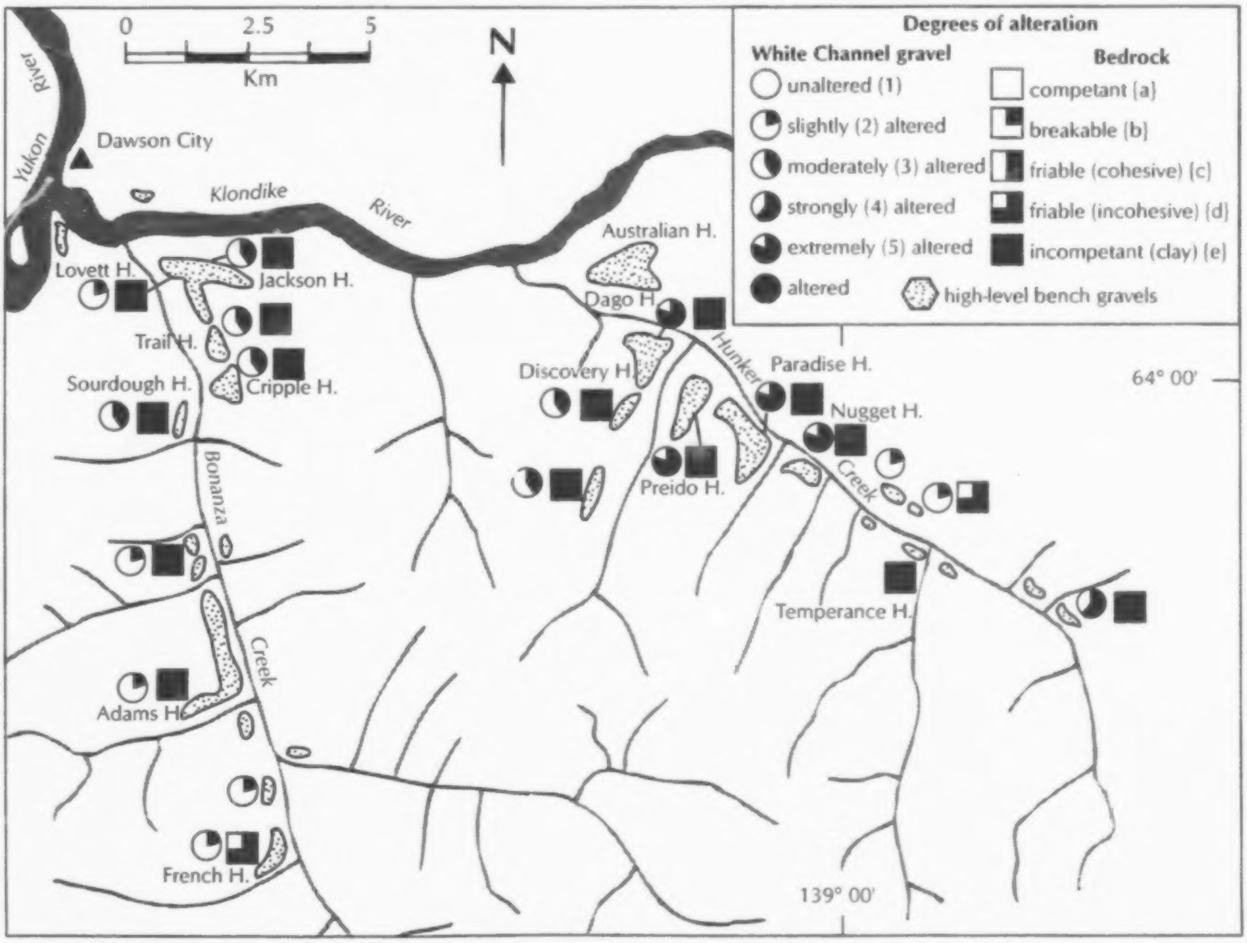
0
2.5
5
Km
N
Yukon River
Dawson City
Klondike River
Lovett H.
Jackson H.
Trail H.
Cripple H.
Sourdough H.
Bonanza Creek
Adams H.
French H.
Australian H.
Dago H.
Hunker Creek
Discovery H.
Paradise H.
Nugget H.
Preido H.
Temperance H.
64° 00'
139° 00'
Degrees of alteration
White Channel gravel
unaltered (1)
slightly (2) altered
moderately (3) altered
strongly (4) altered
extremely (5) altered
altered
Bedrock
competant (a)
breakable (b)
friable (cohesive) (c)
friable (incohesive) (d)
incompetant (clay) (e)
high-level bench gravels

*__Figure 6.__ Map showing the degree and distribution of alteration in the White Channel Gravel and bedrock (modified from Dufresne, 1987, Figure 2.5). H = Hill.*

creeks tends to increase downstream, indicating that groundwater flow may be an important process in the formation of the alteration. With regards to the three alteration zones, note that Figure 7 is an idealized, schematic section (modified from Dufresne, 1987), and the author could not find the three zones vertically juxtaposed in the field during placer deposit mapping.

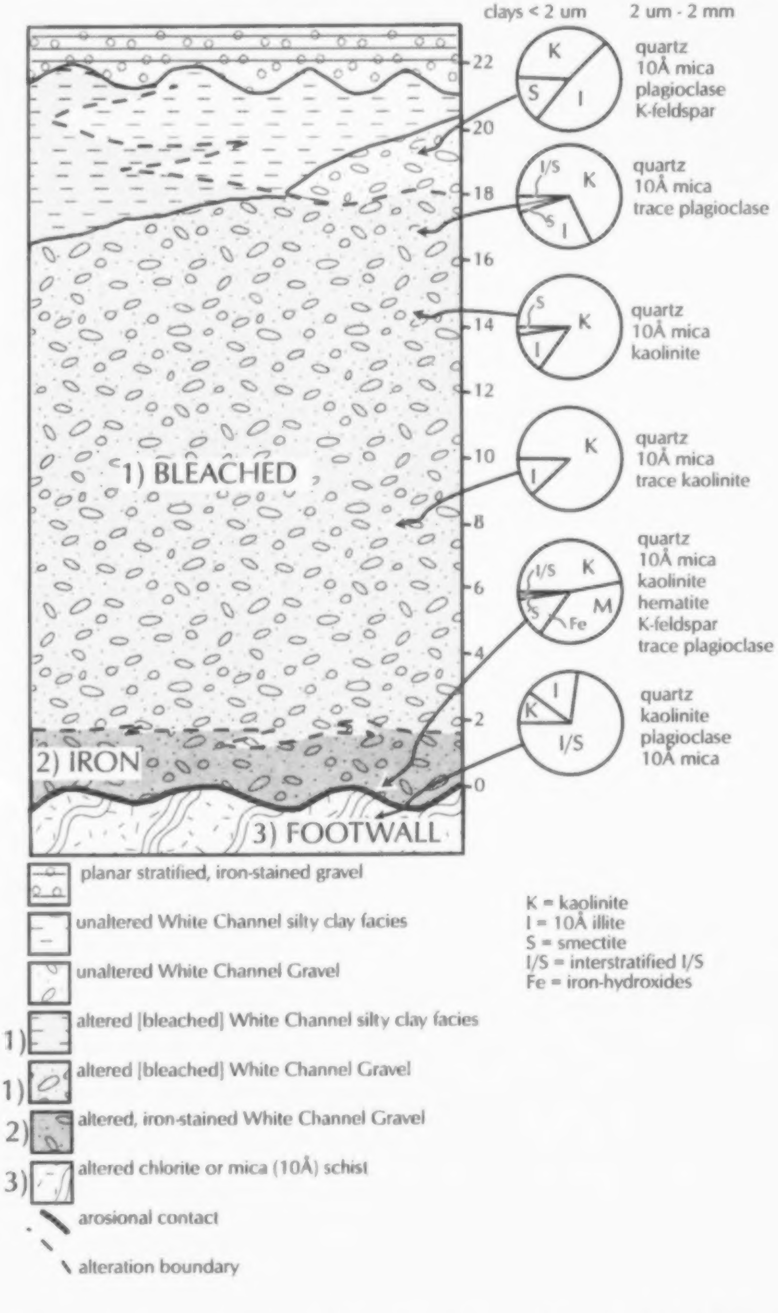
clays < 2 um
2 um - 2 mm
22
20
18
16
14
12
10
8
6
4
2
0
K
S
I
quartz
10Å mica
plagioclase
K-feldspar
I/S
K
S
I
quartz
10Å mica
trace plagioclase
S
K
I
quartz
10Å mica
kaolinite
K
I
quartz
10Å mica
trace kaolinite
I/S
K
S
M
Fe
quartz
10Å mica
kaolinite
hematite
K-feldspar
trace plagioclase
I
K
I/S
quartz
kaolinite
plagioclase
10Å mica
1) BLEACHED
2) IRON
3) FOOTWALL
planar stratified, iron-stained gravel
unaltered White Channel silty clay facies
unaltered White Channel Gravel
1) altered [bleached] White Channel silty clay facies
1) altered [bleached] White Channel Gravel
2) altered, iron-stained White Channel Gravel
3) altered chlorite or mica (10Å) schist
arosional contact
alteration boundary
K = kaolinite
I = 10Å illite
S = smectite
I/S = interstratified I/S
Fe = iron-hydroxides

*Figure 7. Schematic diagram of the White Channel Gravel, displaying the three alteration zones and clay mineralogy (modified from Dufresne, 1987; Figure 2.8).*

## GRAIN-SIZE ANALYSIS

The grain-size distribution of gravel samples was determined using standard hydrometer analyses (Dufresne, 1987). Based on this technique, Dufresne (1987, Table 2.1) demonstrated that there was more clay in the iron and bleached zones (i.e., 6-14 wt.% and 5-14 wt.%, respectively) than in the unaltered gravel (i.e., 2 wt.%), and concluded that this was evidence that the clay was due to post-depositional alteration.

The abundance of clay (the grain size) does not imply a secondary origin – the clay could be detrital in origin and related to deposition: Dufresne (1987) reported one sample from 'overbank sediments' of the unaltered gravel that contained 31 wt.% clay. Note that Dufresne (1987) confuses the grain-size definition of clay with the mineral definition of clay. In addition, only the sand-mud matrix was sampled and all grains larger than 2 mm were screened off (Dufresne, 1987). Sampling only the matrix of the gravel (and ignoring the framework or gravel-sized fraction) results in a 'relative abundance', which changes if the framework component of the gravel is included. For example, assume that one sample of gravel contains 70% gravel (framework), 24% sand, 2% silt and 4% clay, and that another sample contains 91% gravel, 6% sand, 1% silt and 2% clay. Obviously, the first sample contains more clay. However, by recalculating the weight percentages using only the sand, silt and clay fraction (i.e., ignoring the framework or gravel-sized fraction), the first sample appears to have less clay (i.e., 13%) compared to the second sample (i.e., 22%). Dufresne's (1987) sampling method is thus biased: the results show only variability within a sample and not between samples. Unfortunately, this sampling bias affects most of the other lines of evidence Dufresne (1987) puts forward for hydrothermal alteration.

Table 1 summarizes the results of three particle-size analyses of the White Channel Gravel. The gravel samples were collected using proper sampling methods and were analysed using standard sieve and hydrometer techniques. Note that the absolute or actual amount of clay in the various gravel sub-units is ≤1%, much less than the maximum 14% in the gravel sub-unit that Dufresne (1987) reported.

## MINERALOGY

The mineralogy of the gravel samples was determined using standard X-ray diffraction analyses (Dufresne, 1987). Based on this technique, Dufresne (1987, Table 2.2, 2.3, 2.4) demonstrated that, in the <2 µm fraction, there was more kaolinite in the iron and bleached zones (i.e., ~65% and ~70%, respectively) than in the unaltered gravel (i.e., 41%), but that there was less illite in the iron and bleached zones (i.e., ~30% and ~27%, respectively) than in the unaltered gravel (i.e., ~41%). He also calculated the abundance of several other minerals in the <2 µm fraction (e.g., smectite and mixed illite/smectite) and in the <2 mm fraction (e.g., muscovite, feldspar, chlorite, kaolinite, hematite and goethite). Dufresne (1987) concluded that the iron and bleached zones were characterized by extensive secondary clay mineral development, which he attributed to hydrothermal alteration.

The mineralogy results are based on the relative abundance of clay-sized grains in the matrix, and as it was pointed out previously, Dufresne's (1987) sampling method is biased. In addition, the abundance of the various minerals was calculated from X-ray diffractograms, and the resulting percentages are only semi-quantitative (Hardy and Tucker, 1988). Dufresne (1987) also assumes that all of the <2-µm-sized clay minerals are secondary in origin (hence, the 10 Å phyllosilicate minerals in the <2-µm fraction are referred to as illite rather than muscovite). Note that similar clay mineral assemblages have been found in the pre-Reid, Wounded Moose paleosol (Foscolos et al., 1977) and in the 'clay cliffs' of Whitehorse, Yukon (Mougeot, 1994).

## CRYSTALLINITY OF CLAY MINERALS

The crystallinity of minerals was based primarily on the 'Hinckley crystallinity index' of kaolinite (Dufresne, 1987), which is derived from the $1\dot{1}0$ and $11\dot{1}$ peaks on diffractograms (Hinckley, 1963). Based on this technique, Dufresne (1987, Table 2.2, 2.4) obtained kaolinite crystallinities of 1.03 for the footwall zone, 1.3 and 1.59 for the iron zone, 0.53, 0.59 and 0.61 for the bleached zone, and <0.3 for unaltered gravel. He concluded that the high crystallinity of kaolinite in the iron zone indicates that it is hydrothermal in origin.

The Hinckley crystallinity index provides a value indicating only a 'relative degree of crystal perfection' and not what caused it (Hinckley, 1963). Hinckley (1963) reported crystallinity index values ranging from 0.25-1.5 for very pure, detrital kaolinite. In addition, the Hinckley crystallinity index is not widely used because it is influenced by the presence of quartz, feldspar, iron oxides and other clay minerals (Aparico et al., 1997), all of which are present in the White Channel Gravel, especially Dufresne's (1987) iron zone.

## GEOCHEMISTRY

The geochemistry of the gravel samples was based on whole rock analyses of major and minor trace elements (Dufresne, 1987). These analyses revealed an apparent depletion in certain oxides (i.e., $Fe_20_3$, Mg0, $Na_20$ and $K_20$) in the bleached zone, which Dufresne (1987, Table 2.1) concluded was due to hydrothermal alteration.

Again, the geochemistry results are based on only the relative abundance of the matrix, which limits their

***Table 1.*** *Particle-size analysis of the White Channel Gravel, Australia Hill, Klondike goldfields, Yukon.*

| SUB-UNIT | SAMPLE NUMBER | % GRAVEL >2 mm | % SAND <2 mm >0.0625 mm | % SILT <0.0625 mm >0.0039 mm | % CLAY <0.0039 mm |
|---|---|---|---|---|---|
| yellow | GL98-08B | 80.5 | 17.3 | 2.0 | 0.2 |
| white | GL98-08A | 73.9 | 20.8 | 4.6 | 0.7 |
| iron-stained | GL98-09A | 70.1 | 24.3 | 4.6 | 1.0 |

applicability. In addition, the depletion of the oxides could be due to other processes, such as weathering. Also, if it is assumed that the geochemical results are applicable, then they can be statistically tested to determine if they are significant. When using geochemical results expressed as major oxides for sediments, it is often convenient to calculate a 'chemical index of alteration', or CIA: high CIAs indicate greater chemical weathering [CIA= $(100\ Al_2O_3)/(Al_2O_3+CaO+Na_2O+K_2O)$, Fairchild, et al., 1988]. Using Dufresne's (1987, Table 2.5) data, the unaltered gravel (three samples) has a mean CIA of 71.5, with a standard deviation of 4.8; whereas the bleached zone gravel (eleven samples) has a mean CIA of 79.0, with a standard deviation of 6.0. Testing the difference between these means with a t-test (based on independent samples, Bluman, 1992) reveals a calculated t-statistic of -2.27. This value lies outside the critical region of ±4.303 (based on two degrees of freedom and a 95% confidence interval), indicating that there is not enough evidence to support the claim that the CIA of the unaltered gravel differs from the CIA of the bleached or altered gravel.

## DISCOVERY OF NEW VEINS

Dufresne (1987) reported that the footwall zone contained three types of previously unrecognized veins: 1) Type 1 - quartz; 2) Type 2 - carbonate and quartz; and 3) Type 3 - clay iron oxide and amorphous silica. Fluid inclusion data from Type 1 and 2 veins revealed homogenization temperatures ranging from ~90-300°C, and 0-4.6 wt.% NaCl (Dufresne, 1987). Using these results, Dufresne (1987) concluded that the veins were emplaced during the alteration by ascending hydrothermal fluids, which resulted in epithermal gold mineralization in the bedrock and altered gravel.

The age of the veins is unknown and they only 'appear' to be related to the alteration (Dufresne, 1987). In addition, Dufresne (1987, p. 82) stated that the veins have been observed at most hills in the Klondike goldfields, but that the "vein occurrences are usually rare, with erratic distribution and extent." One would expect that the veins should be more common and predictable in distribution and extent if they caused the regional alteration observed in the White Channel Gravel. Also, Knight et al. (1999) demonstrated that the gold in the gravel was mainly derived from mesothermal quartz veins: that is, the gold in the gravel is detrital or placer gold and did not originate through precipitation of hydrothermal fluids.

## DISTRIBUTION OF GOLD

McConnell (1907, p. 220) observed that the "greater part of the gold in the hill and creek gravels occurs on or near bedrock, either in the lower four to six feet (1.2-1.8 m) of gravel or sunk for some distance in the bedrock itself." He (McConnell, 1907, p. 221) noted also several exceptions to this general rule, such as at Dago Hill where a "considerable enrichment takes place at a point sixty feet (18 m) above bedrock," and at Paradise Hill where the "main gold zone here is in many places not found on bedrock, but at elevations of from three to twelve feet (0.9-3.7 m) or more above it." McConnell (1905, p. 105) concluded that there is "little doubt that the Klondike gold, or the greater part of it, at least, is detrital in origin, and has been largely derived from the auriferous quartz veins cutting the older schists." However, he (McConnell, p. 106) suggested that a "small percentage may have been precipitated from water carrying gold in solution," citing as evidence a boulder from the Sixtymile River placer area, the upper surface of which was partially covered with dendritic gold.

McConnell's comments were interpreted by Dufresne (1987) as evidence for a hydrothermal origin of the gold, and because Dufresne (1987) thought that the alteration was related to the gold mineralization, he concluded that the alteration was also hydrothermal in origin. In addition, Dufresne (1987) based his interpretation on personal communications with two placer miners (i.e., Mike Stutter and Benny Warmsby) and on a student completing a Master thesis on the White Channel Gravel (i.e., Steve Morison). According to the two placer miners (who provided calculations of gold grade), the bleached zone gravel contains higher concentrations of gold than the unaltered gravel (Dufresne, 1987, p. 67). Unfortunately, there is no information on how the calculations were done or what the calculations are based on. Also, Morison (Dufresne, 1987, p. 67) suggested that the distribution of gold in the altered gravel is atypical and "contrasts distinctly with the normal distribution of placer gold in unaltered gravel," but Morison does not explain its variation from 'normal'.

The distribution of gold in the Klondike goldfields was discussed by McConnell (1907). He reported that the distribution partly depended on the underlying bedrock: bedrock underlying the White Channel Gravel is more decomposed (i.e., clay-rich) than that under gravel along Bonanza and Hunker creeks. Excessive clay in the bedrock prevents gold from descending further (i.e., into fractures), thereby allowing its concentration at the gravel-bedrock contact (McConnell, 1907). The slight enrichment of gold above bedrock in the White Channel Gravel at Dago Hill was attributed by McConnell (1907) to the development of a 'clayey stratum' or false-bedrock, which prevented the gold from settling further through the gravel. Similarly, the enrichment of gold above bedrock in the yellow gravel of the White Channel Gravel at Paradise Hill was due to the more 'compact nature' of the white gravel, which resulted in gold being concentrated at the white gravel/yellow gravel contact (McConnell, 1907). Also, as it was pointed out previously (i.e., in the Introduction and in the section Discovery of New Veins), gold in the White Channel Gravel is detrital in origin and so Dufresne's (1987) reasoning that 'if the gold is hydrothermal in origin, then the alteration is too,' is no longer valid.

## NEW EVIDENCE FROM TRANSMITTED LIGHT PETROGRAPHY

There appears to be no compelling evidence for hydrothermal alteration, but perhaps by looking at the texture of the White Channel Gravel, it may be possible to recognize an alteration fabric and distinguish this from a depositional fabric. Carrigy and Mellon (1964), Dickinson (1970), Moraes and De Ros (1990), Pettijohn et al. (1987), Thomas (1983), and Wilson and Pitman (1977) present criteria for distinguishing between depositional and alteration textures based on observations of thin sections. A total of 32 undisturbed gravel samples were collected from the White Channel Gravel (including both the white and yellow gravel sub-units and the iron-stained gravel) by carefully excavating 'cylindrical' mounds of gravel and saturating these with epoxy resin. After the epoxy hardened, the samples were removed and sent to Vancouver Petrographics Ltd., where they were made into oversized thin sections and off-cuts (which were stained for potassium feldspar). The thin sections were subsequently examined with a petrographic microscope.

### DESCRIPTION OF FABRIC

Representative photomicrographs displaying the observed fabric are presented in Figures 8 and 9. Figure 8a is a view in plane light of the white gravel, showing the wide range in grain size from pebbles to sand, silt and clay. Note that the silt-clay groundmass has a turbid or cloudy colour. Figure 8b is the same view in crossed polars, showing a vein-quartz pebble and angular quartz grains 'floating' in a groundmass of degraded muscovite and possibly illite. In a study of the heavy minerals in the Klondike area, Gleeson (1970) reported that 'muscovite' was present in all gravel samples from the goldfields. The muscovite was thought to be a mixture of 'hydromica' (i.e., illite), sericite and muscovite, and ranged from < 1 to 81% in the fine sand fraction (Gleeson, 1970). Figure 8c is a view in plane light of the white gravel, showing the angular quartz grains surrounded by the cloudy groundmass. Figure 8d is the same view in crossed polars, showing degraded muscovite between the angular quartz grains. Note that the sample displays very little porosity. Also observed in the white gravel were slightly bent muscovite grains, very mildly squished labile grains, local microcline grains, well developed 'books' of kaolinite, and undifferentiated illite/smectite.

Figure 9a is a view in plane light of the yellow gravel, showing the wide range in grain size from pebbles to sand, silt and clay. Note the erratic distribution of limonite and that the silt-clay groundmass has a less turbid or cloudy colour than in the white gravel. Figure 9b is the same view in crossed polars, showing a vein-quartz pebble, angular quartz grains and muscovite grains that are not as degraded as those in the white gravel. Also observed in the yellow gravel were slightly bent muscovite grains, very mildly squished labile grains, many microcline grains, local plagioclase grains, and undifferentiated kaolinite/illite/smectite. Figure 9c is a view in plane light (approximately 5 mm wide) of iron-stained gravel, showing the wide range in grain size from pebbles to sand, all surrounded by hematite and probably goethite. Figure 9d is the same view in crossed polars, showing a vein-quartz pebble, angular quartz grains and muscovite surrounded by hematite and probable goethite.

### INTERPRETATION OF FABRIC

Transmitted-light microscopy reveals a depositional fabric characterized by quartz grains 'floating' in a matrix of allogenic muscovite (degraded) and possibly illite. In addition, an alteration fabric is evident, characterized by mild compaction and the formation of a 'pseudomatrix' due to the precipitation of authigenic kaolinite, limonite and hematite, and possibly illite, smectite, and goethite, and probably the recrystallization of detrital clay minerals. Precipitation and recrystallization has also resulted in a reduction in the porosity of the White Channel Gravel. Hence, the fabric is due to deposition and alteration, although the degree of alteration is greater in the white

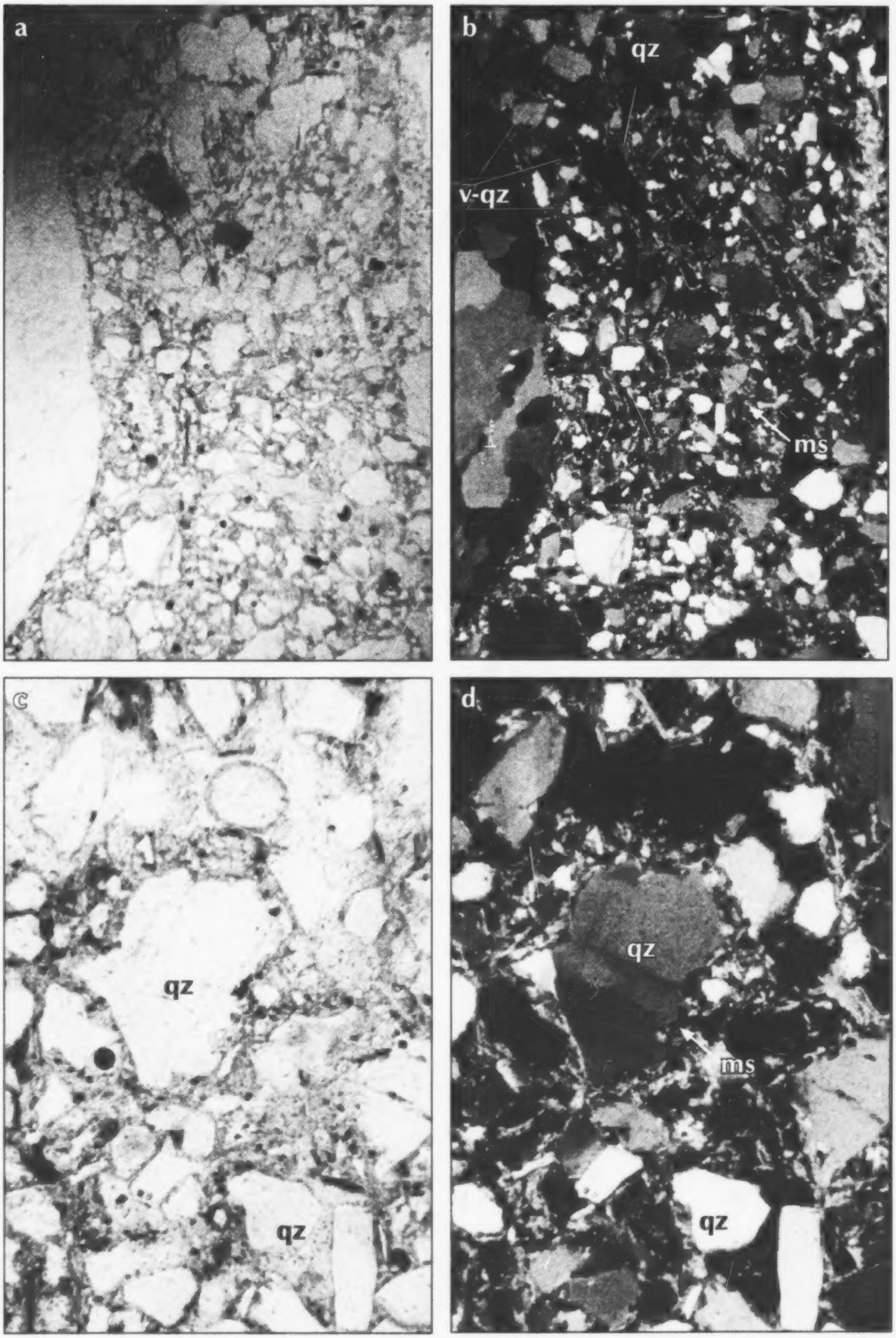

***Figure 8.*** *Thin-section photomicrographs of the white gravel. (a) wide range in grain size from pebbles to sand, silt and clay with the silt-clay groundmass displaying a turbid or cloudy colour (view approximately 5 mm wide, plane light); (b) vein-quartz pebble (v-qz) and angular quartz (qz) grains 'floating' in a groundmass of degraded muscovite (ms) and possibly illite (view approximately 5 mm wide, crossed polars); (c) angular quartz grains surrounded by the cloudy groundmass (view approximately 1.4 mm wide, plane light); (d) degraded muscovite between the angular quartz grains (view approximately 1.4 mm wide, crossed polars).*

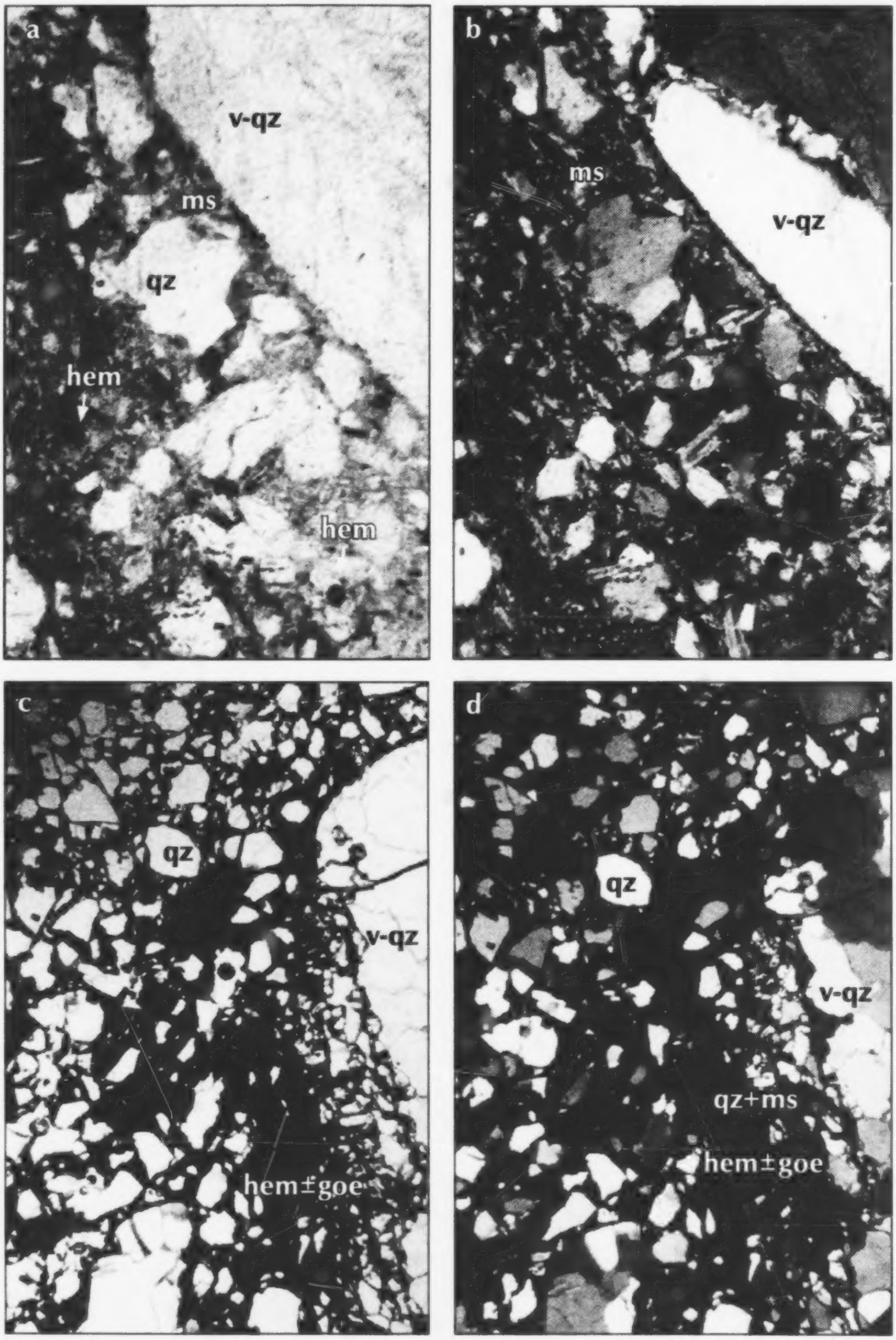

***Figure 9.*** *Thin-section photomicrographs of the yellow gravel: (a) wide range in grain size from pebbles to sand, silt and clay, with an erratic distribution of hematite (hem) and a silt-clay groundmass that has a less turbid or cloudy colour than in the white gravel (view approximately 5 mm wide, plane light); (b) vein-quartz pebble (v-qz), angular quartz grains (qz) and muscovite grains (ms) that are not as degraded as those in the white gravel (view approximately 5 mm wide, crossed polars). Thin-section photomicrographs of the iron-stained gravel: (c) wide range in grain size from pebbles to sand, all surrounded by hematite (hem) and probably goethite (goe) (view approximately 5 mm wide, plane light); (d) vein-quartz pebble, angular quartz grains and muscovite surrounded by hematite and probable goethite (view approximately 5 mm wide, crossed polars).*

gravel than in the yellow gravel. The alteration can be explained as a combination of weathering and diagenetic processes. Diagenesis refers to "all chemical, physical, and biologic changes undergone by a sediment after its initial deposition, and during and after its lithification, exclusive of surficial alteration (weathering) and metamorphism," (Bates and Jackson, 1987); it includes "compaction, cementation, authigenesis, recrystallization, inversion, replacement, dissolution and bioturbation" (Boggs, 1987). According to Morrow and McIlreath (1990), it is not possible to assign unique ranges of temperature and pressure conditions to diagenesis, although it is generally accepted that diagenesis is characterized by temperatures of 0-300°C and pressures of 0.1-10 MPa. Surprisingly, diagenesis has not been mentioned in any previous research on the geology of placer deposits in the Klondike goldfields, particularly those studies examining the alteration or sedimentology of the White Channel Gravel (i.e., Dufresne, 1987; Dufresne and Morison, 1985; Dufresne et al., 1986; Froese, 1997; Milner, 1976; Morison, 1985; Morison et al., 1998; Tempelman-Kluit, 1982). The degree of alteration observed in the White Channel Gravel is classified as early diagenesis (i.e., characterized by changes occurring during burial to a few metres and temperatures not 'appreciably' exceeding 25°C; Berner, 1980), rather than the more advanced late diagenesis (i.e., characterized by deeper burial and higher temperatures; Thomas, 1983; Tucker, 1981).

## REINTERPRETATION OF ALTERATION

Figure 10 presents a schematic diagram of paleo-Bonanza Creek, showing how weathering and diagenesis produced the alteration observed in the White Channel Gravel. Clay minerals can originate in at least the following five ways:

1) The Klondike goldfields (and most of west-central Yukon) are mainly underlain by Paleozoic metasedimentary (i.e., Klondike Assemblage and Nasina Assemblage) and meta-igneous rocks belonging to the Yukon-Tanana Terrane, and minor amounts of altered ultramafic rocks that are assigned to the Slide Mountain Terrane (Mortensen, 1990, 1996). This area is thought to have been a mature, subdued landscape by Miocene time, which underwent a period of uplift and erosion in the Pliocene (Tempelman-Kluit, 1980). Common bedrock lithologies throughout the goldfields include schist, gneiss and quartzite, which contain abundant muscovite, biotite, chlorite and feldspar (Mortensen, 1996). These minerals alter during weathering to clay minerals such as illite, smectite, vermiculite and kaolinite (Blatt, 1992; Bloom, 1969; Grim, 1968; Velde, 1985), all of which were probably produced during the long period of weathering

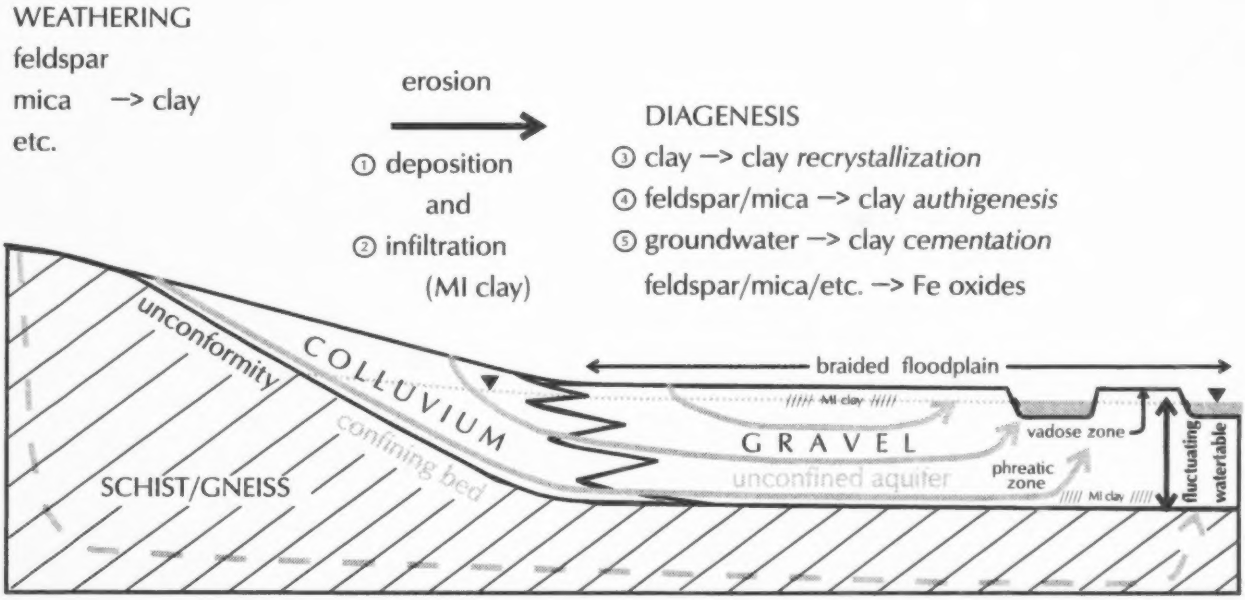
WEATHERING
feldspar
mica —> clay
etc.
erosion
① deposition
and
② infiltration
(MI clay)
DIAGENESIS
③ clay —> clay *recrystallization*
④ feldspar/mica —> clay *authigenesis*
⑤ groundwater —> clay *cementation*
feldspar/mica/etc. —> Fe oxides
unconformity
COLLUVIUM
confining bed
SCHIST/GNEISS
braided floodplain
MI clay
GRAVEL
unconfined aquifer
vadose zone
phreatic zone
MI clay
fluctuating
watertable

***Figure 10.*** *Schematic diagram summarizing the origin of alteration in the White Channel Gravel, Klondike goldfields, Yukon; MI = mechanically infiltrated; = water table.*

required to develop the subdued Miocene landscape. During subsequent uplift and erosion in the Pliocene, the clays may have been transported and deposited as allogenic clay minerals with other sediments to form the White Channel Gravel. This long period of weathering followed by uplift and erosion may also explain the formation and distribution of tors throughout the goldfields (Easterbrook, 1993). In addition, Johnson and Meade (1990), and Morton and Hallsworth (1999) have shown that further weathering of sediment occurs during periods of alluvial storage on floodplains, which may have resulted in additional clay minerals being produced.

2) The seepage of muddy water through gravel alluvium may result in the deposition of mechanically infiltrated clays (Moraes and De Ros, 1990). Mechanically infiltrated clays tend to be concentrated within the vadose zone (due to the evaporation of infiltrated water), within the water table (due to a decrease in the velocity of percolating water in the phreatic zone) and above impermeable barriers, such as bedrock-gravel contacts (due to the filtering of clay particles above barriers in the phreatic zone, Moraes and De Ros, 1990). During floods, the White Channel Gravel floodplain would have been repeatedly inundated with muddy water that enhanced the formation of mechanically infiltrated clays. In addition, the White Channel Gravel represents a water table aquifer, or unconfined aquifer, that is confined to the relatively impermeable bedrock walls of the valley. Hence, the floodplain water table, which is closely associated with the river stage, changes as groundwater flow through the aquifer varies (Fetter, 1988). According to Moraes and De Ros (1990), fluctuations in the water table can result in the formation of subhorizontal clay-rich zones that may or may not cut across sedimentary structures. These zones, which correspond to former positions of the water table, can be relatively narrow (i.e., centimetres) or thick (i.e., up to tens of metres), depending on the length of time the water table was maintained at a particular level (Moraes and De Ros, 1990). Dufresne (1987) described similar clay-rich zones that occur above the gravel-bedrock contact and which transect primary sedimentary structures, but he interpreted these zones as evidence of ascending hydrothermal fluids.

3) Once deposited, allogenic and mechanically infiltrated clay minerals may recrystallize. This diagenetic process mainly involves a change in size (usually an increase) or shape of mineral crystals, without significant changes in composition (Boggs, 1987).

4) Other allogenic minerals (such as feldspar, mica and chlorite) deposited with the White Channel Gravel may undergo diagenetic alteration to authigenic clay minerals (i.e., kaolinite, illite and smectite), similar to the weathering process described previously. Depending on their abundance, these new minerals may or may not act as a cement in the White Channel Gravel (Boggs, 1987).

5) New clay minerals (particularly kaolinite) may have precipitated from interstitial pore water and circulating groundwater as diagenetic pore filling cement (Boggs, 1987). Groundwater flow would have been enhanced by the large differences in hydraulic conductivities (i.e., the capacity of sediment to transmit water) between the White Channel Gravel and the underlying bedrock. This may have resulted in a concentration of groundwater flow near the gravel-bedrock contact, which could account also for the formation of the iron oxide cement at this contact, (i.e., Dufresne's [1987] 'iron zone'). The iron for the cement was most likely supplied by intrastratal solution of detrital silicate minerals such as hornblende, chlorite, and biotite, as well as detrital magnetite and pyrite (Tucker, 1981). In addition, iron oxide can be seen precipitating at the bedrock-gravel contact at almost every exposure of the White Channel Gravel and other gravel units throughout the Klondike Goldfields.

There is no evidence that groundwater flowing within the White Channel Gravel aquifer was hot or even warm, and most shallow groundwater has temperatures of <30°C (Berner, 1971; Fetter, 1988; Heath, 1983), implying that the various diagenetic processes responsible for the alteration in the White Channel Gravel would have taken considerable time to occur. Although the age of the white gravel is only loosely constrained to a post-Miocene and pre-Late Pliocene age (~5-3.3 Ma, based on paleomagnetism and paleobotany), the yellow gravel is Late Pliocene in age (~3.3-2.6 Ma, based on glass fission track argon ages of two tephras, Westgate at al., 2000). Hence, the higher degree of alteration observed in the white gravel (i.e., greater degradation of muscovite and a greater amount of authigenic kaolinite), as compared to the yellow gravel, may be due to the older age of this sub-unit. Smith et al. (1986) found a direct relationship between age and clay content of paleosols, with the older paleosol (i.e., Wounded Moose) containing a greater amount of kaolinite than the younger paleosol (i.e., Diversion Creek). In addition, climate is considered the most significant long-term control of weathering, and therefore the type of clay minerals produced during weathering is thought to reflect the climate at the time they formed (Easterbrook, 1993; Grim, 1968). Generally, kaolinite is characteristic of more temperate and humid climates, whereas smectite is characteristic of warm to subhumid climates (Berner, 1971; Foscolos et al., 1977; Smith et al., 1986). Hence, the abundance of kaolinite in the white gravel may also be due to a more temperate and humid climate at the time of its formation. Due to the greater amount of clay in the white gravel, the mining of this sub-unit may result in a slightly greater impact on water quality and effluent discharge than mining other, younger gravel units.

Although a sedimentary origin for the alteration observed in the White Channel Gravel cannot be proven, May (1994) suggested that the presence of certain iron minerals provides a method of distinguishing hydrothermal alteration from weathering: siderite and iron-rich dolomite apparently indicate low temperature hydrothermal alteration, whereas hematite and goethite are supposedly more characteristic of weathering. The White Channel Gravel contains no authigenic siderite or iron-rich dolomite, but it does contain abundant hematite and goethite in Dufresne's (1987) iron zone, which indicates that the alteration is not hydrothermal in origin. In addition, Longstaffe (1984) used oxygen-isotopic compositions of clay minerals to distinguish authigenic from allogenic clays (i.e., authigenic clays, which were mostly kaolinite, have $\delta^{18}O<+16$ SMOW, whereas allogenic clays, which were mostly illite, have $\delta^{18}O>+16$ SMOW). However, Hutcheon (1983, 1990) cautioned that for most sediment, it is practically impossible to physically separate the authigenic from the allogenic clays.

## CONCLUSIONS

Dufresne (1987) has not demonstrated clearly that the alteration observed in the White Channel Gravel is hydrothermal in origin: there is no unequivocal evidence supporting hydrothermal alteration. The alteration is reinterpreted as a result of weathering and particularly diagenesis due to groundwater flow. In addition, there is no 'hidden' epithermal gold deposit in the gravel or in the bedrock. The reinterpretation of the alteration as the product of sedimentary processes has the following implications and applications: 1) for the past ~20 years, the alteration had been incorrectly referred to as hydrothermal alteration without any compelling evidence; 2) it appears that the older the gravel, the greater the degree of alteration (i.e., it takes time for weathering and diagenetic processes to operate); 3) the alteration provides information on paleoweathering and paleoclimate; and 4) mining-altered (i.e., older) gravel has a slightly greater impact on water quality and effluent discharge (i.e., authigenic clay is more abundant in the white gravel than in the yellow gravel).

## ACKNOWLEDGEMENTS

The author is grateful to the placer miners that permitted access to their properties, and thanks Barrett Mataseje for his assistance during the 2001 summer field season and Mark Nowosad for performing the hydrometer analyses. Jim Vinnell of Vancouver Petrographics Ltd. oversaw the making of the gravel thin sections, and Lee Pigage provided many useful comments on an earlier draft of the manuscript.

## REFERENCES

Aparico, P., Galan, E. and Gonzalez, I., 1997. Selection of the most suitable XRD kaolinite crystallinity index for routine studies of kaolin according to sample composition. *In:* 11th International Clay Conference, Program with Abstracts, Clay Mineral Society, Ottawa, June 15-21, 1997.

Bates, C.C. and Jackson, J.A., 1987. Glossary of Geology, Third Edition. American Geological Institute, 784 p.

Berner, R.A., 1971. Principles of Chemical Sedimentology. McGraw-Hill Book Company, New York, 240 p.

Berner, R.A., 1980. Early Diagenesis, A Theoretical Approach. Princeton University Press, Princeton, New Jersey, 241 p.

Blatt, H., 1992. Sedimentary Petrology, Second Edition. W.H. Freeman and Company, San Francisco, 514 p.

Bloom, A.L., 1969. The surface of the Earth. Foundations in Earth Science Series, Prentice-Hall Inc., New Jersey, 152 p.

Bluman, A.G., 1992. Elementary Statistics, Second Edition. Wm. C. Brown Publishers, Dubuque, Iowa, 684 p.

Boggs, S., Jr., 1987. Principles of Sedimentology and Stratigraphy. Merril Publishing Company, Columbus, Ohio, 784 p.

Bostock, H.S., 1966. Notes on glaciation in central Yukon Territory. Geological Survey of Canada, Paper 65-56, 18 p.

Carrigy, M.A. and Mellon, G.B., 1964. Authigenic clay mineral cements in Cretaceous and Tertiary sandstones of Alberta, Journal of Sedimentary Petrology, vol. 34, p. 461-472.

Dickinson, W.R., 1970. Interpreting detrital modes of graywacke and arkose. Journal of Sedimentary Petrology, vol. 40, p. 695-707.

Dufresne, M.B., 1987. Origin of gold in the White Channel sediments of the Klondike region, Yukon Territory. Unpublished M.Sc. thesis, The University of Alberta, Edmonton, Alberta, 181 p.

Dufresne, M.B. and Morison, S.R., 1985. Stratigraphy and alteration of the White Channel Gravel at Dago Hill, a progress report, Klondike area, Yukon. *In:* Yukon Exploration and Geology 1983, Exploration and Geological Services Division, Yukon Region, Indian and Northern Affairs Canada, p. 55-59.

Dufresne, M.B., Morison, S.R. and Nesbitt, B.E., 1986. Evidence of hydrothermal alteration in the White Channel sediments and bedrock of the Klondike area, west-central Yukon. *In:* Yukon Geology Volume 1. Exploration and Geological Services Division, Yukon Region, Indian and Northern Affairs Canada, p. 44-49.

Easterbrook, D.J., 1993. Surface processes and landforms. MacMillan Publishing Company, New York, 520 p.

Fairchild, I., Hendry, G., Quest, M. and Tucker, M., 1988. Chemical analysis of sedimentary rocks. *In:* Techniques in Sedimentology, M. Tucker (ed.), Blackwell Scientific Publications Inc., California, p. 274-354.

Fetter, C.W., 1988. Applied Hydrogeology, Second Edition. Macmillan Publishing Company, New York, 592 p.

Foscolos, A.E., Rutter, N.W. and Hughes, O.L., 1977. The use of pedological studies in interpreting the Quaternary history of central Yukon. Geological Survey of Canada, Bulletin 271, 48 p.

Froese, D.G., 1997. Sedimentology and paleomagnetism of Plio-Pleistocene lower Klondike valley terraces, Yukon Territory. Unpublished M.Sc. thesis, University of Calgary, Calgary, Alberta, 152 p.

Gleeson, C.F., 1970. Heavy mineral studies in the Klondike area, Yukon Territory. Geological Survey of Canada, Bulletin 173, 63 p.

Grim, R.E., 1968. Clay Mineralogy, Second Edition. McGraw-Hill Book Co., New York, 596 p.

Hardy, R. and Tucker, M., 1988. X-ray powder diffraction of sediments. *In:* Techniques in Sedimentology, M. Tucker (ed.), Blackwell Scientific Publications Inc., California, p. 191-228.

Heath, R.C., 1983. Basic ground-water hydrology. United States Geological Survey, Water-Supply Paper 2200, 84 p.

Hinckley, D.N., 1963. Variability in "crystallinity" values among the Kaolin deposits of the Coastal Plain of Georgia and South Carolina. International Series of Monographs on Earth Sciences, vol. 13, p. 229-235.

Hughes, O.L., 1968. Glacial map of Yukon Territory (1:1 000 000 scale). Geological Survey of Canada Map 6-1968, Paper 1968-34.

Hutcheon, I., 1983. Structures and identification of clay minerals and other techniques in diagenetic studies. *In:* Clastic Diagenesis, A. Oldershaw (ed.), Canadian Society of Petroleum Geologists and The Department of Geology and Geophysics, University of Calgary, Course Notes, May 5th and 6th, 1983, University of Calgary, Calgary, Alberta, p. 2-1 - 2-36.

Hutcheon, I., 1990. Aspects of the diagenesis of coarse-grained siliclastic rocks. *In:* Diagenesis, I.A. McIlreath and D.W. Morrow (eds.), Geoscience Canada, Reprint Series 4, p. 165-176.

Johnson, M.J. and Meade, R.H., 1990. Chemical weathering of fluvial sediments during alluvial storage: The Macuai'anim Islan point bar, Solimões River, Brazil. Journal of Sedimentary Petrology, vol. 60, p. 827-842.

Knight, J.B., Mortensen, J.K. and Morison, S.R., 1994. Shape and composition of lode and placer gold from the Klondike district, Yukon, Canada. Exploration and Geological Services Division, Yukon Region, Indian and Northern Affairs Canada, Bulletin 3, 142 p.

Knight, J.B., Mortensen, J.K. and Morison, S.R., 1999. Lode and placer gold composition in the Klondike District, Yukon, Canada: Implications for the nature and genesis of Klondike placer and lode gold deposits. Economic Geology, vol. 94, p. 649-664

Longstaffe, F.J., 1984. The role of meteoric water in diagenesis of shallow sandstones: Stable isotope studies of the Milk River aquifer and gas pool, southeastern Alberta. *In:* Clastic Diagenesis, D.A. McDonald and R.C. Surdam (eds.), The American Association of Petroleum Geologists, Memoir 37, p. 81-98.

Lowey, G.W., 1998. White Channel Gravel. Exploration and Geological Services Division, Yukon Region, Indian and Northern Affairs Canada, Open File 1998-2 (1:100 000 scale map and marginal notes).

Lowey, G.W., 1999a. The fluvial geology of placer gold deposits in the Indian River area, west-central Yukon (abstract). *In:* CANQUA - CGRC 1999, Canadian Quaternary Association - Canadian Geomorphology Research Group, Program and Abstracts, August 23-27, 1999, University of Calgary, Calgary, Canada, p. 43-44.

Lowey, G.W., 1999b. The geology of placer gold deposits in the Indian River area, west-central Yukon. *In:* Yukon Exploration and Geology 1998, C.F. Roots and D.S. Emond (eds.), Exploration and Geologic Services Division, Yukon Region, Indian and Northern Affairs Canada, p. 117-124.

Lowey, G.W., 2001a. The Stewart River placer project, west-central Yukon. *In:* Yukon Exploration and Geology 2000, D.S. Emond and L.H. Weston (eds.), Exploration and Geological Services Division, Yukon Region, Indian and Northern Affairs Canada, p. 199-206.

Lowey, G.W., 2001b. The role of forcing mechanisms, base level change and accommodation space in the formation of the Klondike goldfields, Yukon, Canada (abstract). *In:* Fluvial Sedimentology 2001, 7th International Conference on Fluvial Sedimentology, Program and Abstracts, University of Nebraska- Lincoln, Lincoln, Nebraska (USA), August 6-10, 2001, p. 178.

Lowey, G.W., 2001c. The role of forcing mechanisms, base level change and accommodation space in the formation of the Klondike goldfields, Yukon, Canada (abstract). *In:* Canadian Quaternary Association Meetings, 2001, Whitehorse, Yukon, August 20-24, Program and Abstracts. Heritage Branch, Government of the Yukon, Occasional Papers in Earth Sciences no. 1, p. 50-51.

Lowey, G.W., 2001d. White Channel Alteration: Paradise Hill. *In:* Field Guide to Quaternary Research in Central and Western Yukon Territory, D.G. Froese, A. Duk-Rodkin and J.D. Bond (eds.), Heritage Branch, Government of the Yukon, Occasional Papers in Earth Sciences no. 2, p. 63-64.

May, F., 1994. Weathering or hydrothermal alteration, examples from the Rhenish Massif, Germany. Electronically published manuscript: www.geo.uni-bonn.de/publications/journals/may/may94_jou.html

McConnell, R.G., 1905. Report on the Klondike gold fields. Geological Survey of Canada, Annual Report, part B, vol. 14, p. 1-71.

McConnell, R.G., 1907. Report on gold values in the Klondike high level gravels. Geological Survey of Canada, Report no. 979, 34 p.

Milner, 1976. Geomorphology of the Klondike placer goldfields, Yukon Territory. Final Report, Contract OSV 5-0047, Supply and Services, Canada, 157 p.

Moraes, M.A. and De Ros, L.F., 1990. Infiltrated clays in fluvial Jurassic sandstones of Recôncavo Basin, northeastern Brazil. Journal of Sedimentary Petrology, vol. 60, p. 809-819.

Morison, S.R., 1985. Sedimentology of White Channel Gravels, Klondike area, west-central Yukon. Unpublished M.Sc. thesis, The University of Alberta, Edmonton, Alberta, 149 p.

Morison, S.R., Mougeot, C. and Walton, L., 1998. Surficial geology and sedimentology of Garner Creek, Ogilvie and Matson Creek map areas, western Yukon Territory (115O/13, 115O/12, 115N/9- east half). Exploration and Geological Services Division, Yukon Region, Indian and Northern Affairs Canada, Open File 1998-1, 87 p.

Morrow, D.W. and McIlreath, I.A., 1990. Diagenesis, general introduction. *In:* Diagenesis, I.A. McIlreath and D.W. Morrow (eds.), Geoscience Canada, Reprint Series 4, p. 165-176.

Mortensen, J.K., 1990. Geology and U-Pb chronology of the Klondike District, west-central Yukon Territory. Canadian Journal of Earth Sciences, vol. 27, p. 903-914.

Mortensen, J.K., 1996. Geological compilation maps of the northern Stewart River map area, Klondike and Sixtymile Districts (115N/15, 16; 115O/13, 14; and parts of 115O/15, 16). Exploration and Geological Services Division, Yukon Region, Indian and Northern Affairs Canada, Open File 1996-1 (G), 43 p.

Morton, A.C. and Hallsworth, C.R., 1999. Processes controlling the composition of heavy mineral assemblages in sandstones. Sedimentary Geology, vol. 124, p. 3-29.

Mougeot, C., 1994. Preliminary assessment of clay deposits in selected areas of the Whitehorse map sheet area (105 D) for the manufacture of clay based products (unpublished report). Yukon-Canada Co-operation Agreement for Small Business Development, 23 p.

Peters, W.C., 1987. Exploration and Mining Geology, Second Edition. John Wiley and Sons, New York, 685 p.

Pettijohn, F.J., Potter, P.E. and Siever, R., 1987. Sand and sandstone. Springer-Verlag, New York, 610 p.

Smith, C.A.S., Tornacai, C. and Hughes, O.L., 1986. Pedological investigations of Pleistocene glacial drift surfaces in central Yukon. Geographie physique et Quaternaire, vol. XL, p. 29-37.

Tempelman-Kluit, D.J., 1980. Evolution of physiography and drainage in southern Yukon. Canadian Journal of Earth Sciences, vol. 17, p. 1189-1203.

Tempelman-Kluit, D.J., 1982. White Channel Gravel of the Klondike. *In:* Yukon Exploration and Geology 1981, Exploration and Geologic Services Division, Yukon Region, Indian and Northern Affairs Canada, p. 74-79.

Thomas, R., 1983. A brief introduction to clastic diagenesis and relevant aspects of detrital texture and mineralogy. *In:* Clastic diagenesis, A. Oldershaw (ed.), Canadian Society of Petroleum Geologists and the Department of Geology and Geophysics, University of Calgary, Course Notes, May 5th and 6th, 1983, the University of Calgary, Calgary, Alberta, p. 1-1 - 1-51.

Tucker, M.E., 1981. Sedimentary Petrology, An Introduction. A Halsted Press Book, John Wiley & Sons, New York, 252 p.

Velde, B., 1985. Clay minerals, a physico-chemical explanation of their occurrence. Developments in Sedimentology, vol. 40, Elsevier, New York, 562 p.

Westgate, J.A., Sandhu, A.S. and Froese, D.G., 2000. Age of the gold-bearing White Channel Gravel, Klondike district, Yukon Territory. Canadian Journal of Earth Sciences, vol. 9, p. 19-29.

Waterhouse, H.K. 1999. Orbital forcing of palynofacies in the Jurassic of France and the United Kingdom. Geology, vol. 27, p. 511-514.

Wilson, M.D. and Pittman, E., 1977. Authigenic clays in sandstones: Recognition and influence on reservoir properties and paleoenvironmental analysis. Journal of Sedimentary Petrology. vol. 47, p. 3-31.

# Paleomagnetism and geobarometry of the Granite Mountain batholith, Yukon: Minimal geotectonic motion of the Yukon-Tanana Terrane relative to North America

*P.J.A. McCausland*[1]
*Earth Sciences, University of Western Ontario*[1]

*D.T.A. Symons*[2]
*Earth Sciences, University of Windsor*[2]

*C.J.R. Hart*[3]
*Yukon Geology Program*

*W.H. Blackburn*[2]
*Earth Sciences, University of Windsor*[2]

McCausland, P.J.A., Symons, D.T.A., Hart, C.J.R. and Blackburn, W.H., 2002. Paleomagnetism and geobarometry of the Granite Mountain batholith, Yukon: Minimal geotectonic motion of the Yukon-Tanana Terrane relative to North America. *In:* Yukon Exploration and Geology 2001, D.S. Emond, L.H. Weston and L.L. Lewis (eds.), Exploration and Geological Services Division, Yukon, Indian and Northern Affairs Canada, p. 163-177.

## ABSTRACT

Paleomagnetic and geobarometric results are reported here for the Early Jurassic Granite Mountain batholith, an ~600 km$^2$ granodiorite intrusion in the Yukon-Tanana Terrane. Paleomagnetic analyses of 331 specimens from 24 sites yield magnetite-borne characteristic remanent magnetization (ChRM) directions. Eight northerly and westerly sites display a mean direction **A** (D=337, I=69°; $\alpha_{95}$=7.6°, k=54). Another 11 sites appear to be lightning-struck, or exhibit unstable remanence, and 3 sites in a fault-bounded block to the southeast carry an anomalous northeast upwards ChRM direction **B**. Two sites in a Cretaceous andesite porphyry dyke and its contact zone give a westerly, steep-down ChRM direction, **C**. Aluminum-in-hornblende geobarometry at 10 sites defines emplacement depths of ~16 km in the north and west, and ~19 km in the southeast. The batholith has probably not been significantly tilted since its emplacement, but it may be subdivided into two separate intrusive phases or structural blocks that have experienced differential uplift. Ambient temperatures at 16-19 km were too high for magnetite to record an enduring remanence, so the observed ChRMs likely record uplift of the batholith through ~15 km depth, at 180-170 Ma. Both **A** and **C** ChRM directions are similar to those expected for Early Jurassic and Late Cretaceous reference poles, respectively, suggesting that the Yukon-Tanana Terrane is not far-traveled with respect to cratonic North America since Early Jurassic time.

## RÉSUMÉ

Les auteurs rapportent des résultats paléomagnétiques et géobarométriques relatifs au batholite de Granite Mountain, datant du Jurassique précoce, qui est une intrusion de granodiorite d'environ 600 km$^2$ dans le terrane de Yukon-Tanana. Les analyses paléomagnétiques effectuées sur 331 échantillons provenant de 24 sites fournissent des directions de magnétisation rémanente caractéristique (ChRM) dans la magnétite. Huit sites au nord et à l'ouest présentent une direction moyenne **A** (D=337, I=69°; $\alpha_{95}$=7,6°, k=54). Onze autres sites semblent avoir été frappés par la foudre ou présenter une rémanence instable, et trois sites dans un bloc limité par des failles au sud-est présentent une direction de ChRM **B** anormale ascendante nord-est. Deux sites, situés dans un dyke de porphyre d'andésite datant du Crétacé ainsi que dans la zone de contact du dyke, présentent une direction de ChRM **C** plongeant abruptement vers l'ouest. Dans dix sites, la géobarométrie de l'aluminium dans la hornblende indique que la profondeur de mise en place est d'environ 16 km, au nord et à l'ouest, et d'environ 19 km, au sud-est. Le batholite ne s'est probablement pas incliné de façon significative depuis sa mise en place, mais il peut être subdivisé en deux phases intrusives ou blocs structuraux distincts, qui ont subi un soulèvement différentiel. Entre 16 et 19 km, les températures ambiantes étaient trop élevées pour que la magnétite présente une rémanence durable; par conséquent, les directions de ChRM observées remontent probablement à l'époque du soulèvement du batholite à environ 15 km de profondeur, il y a entre 180 et 170 millions d'années. Les directions de ChRM **A** et **B** sont toutes deux similaires à celles prévues respectivement pour les pôles de références au Jurassique précoce et au Crétacé tardif, ce qui suggère que le terrane de Yukon-Tanana ne s'est pas déplacé sur une grande distance par rapport à l'Amérique du Nord cratonique depuis le Jurassique précoce.

---

[1] *Earth Sciences, University of Western Ontario, London, Ontario, Canada N6A 5B7, pjam@julian.uwo.ca*

[2] *Earth Sciences, University of Windsor, Windsor, Ontario N9B 3P4, dsymons@uwindsor.ca, blackbu@uwindsor.ca*

[3] *craig.hart@gov.yk.ca*

## INTRODUCTION

Paleomagnetic research conducted in the Northern Cordillera with the LITHOPROBE-SNORCLE transect provides regional-scale constraints upon possible past terrane motions. Paleomagnetic results from the Stikine and Cache Creek terranes have refined estimates of the timing and magnitude of their net poleward motion and clockwise rotation with respect to North America (Harris et al., 1999; Symons et al., 2000a).

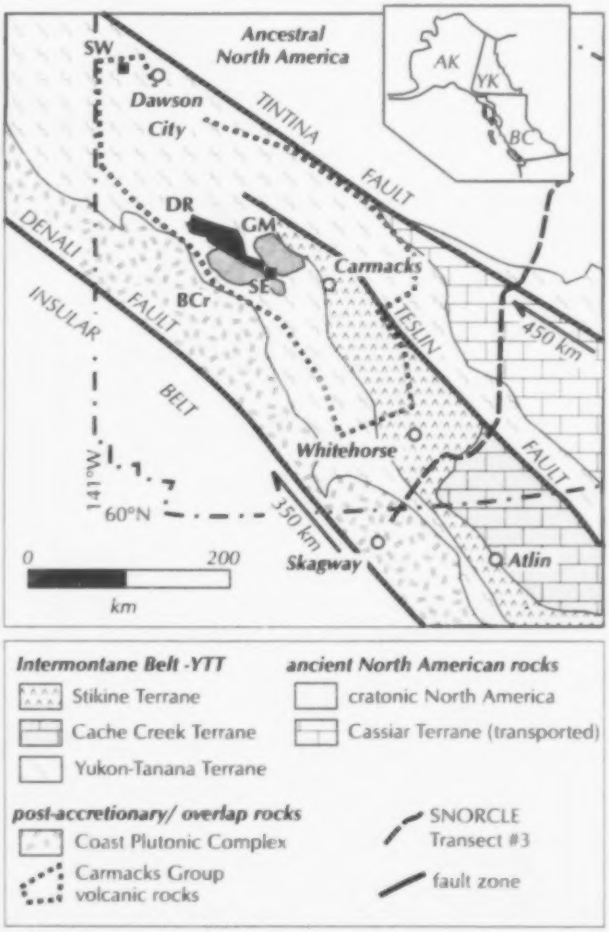
Ancestral North America
SW
Dawson City
TINTINA FAULT
DR
GM
SE
Carmacks
BCr
DENALI FAULT
INSULAR BELT
TESLIN FAULT
450 km
Whitehorse
141°W
60°N
350 km
Skagway
Atlin
0
200
km
AK
YK
BC
Intermontane Belt -YTT
Stikine Terrane
Cache Creek Terrane
Yukon-Tanana Terrane
ancient North American rocks
cratonic North America
Cassiar Terrane (transported)
post-accretionary/ overlap rocks
Coast Plutonic Complex
Carmacks Group volcanic rocks
SNORCLE Transect #3
fault zone

**Figure 1.** *Tectonic elements of the Northern Canadian Cordillera. Inset abbreviations are AK - Alaska; BC - British Columbia; and YK - Yukon. YTT units from which paleomagnetic studies are reported: BCr - 190 Ma Big Creek batholith; DR - 105 Ma Dawson Range batholith; GM - 190 Ma Granite Mountain batholith; SE - 69 Ma Seymour Creek stock; SW - 70 Ma Swede Dome stock. The extent of the 70 Ma Carmacks Group volcanic rocks is given by the dashed line.*

A complementary program of study is underway for the 'pericratonic' Yukon-Tanana Terrane (YTT) to discern its geotectonic motion history and to test its coherency since Early Jurassic time. The YTT is a poorly exposed assemblage of Paleozoic continental rocks with apparent North American affinity that underlies much of central Yukon and eastern Alaska. Its size, cratonic provenance and central position make the YTT a key tectonic element in the assembly of the Northern Cordillera (Fig. 1), but its past relations to other far-traveled terranes and to North America itself are poorly understood (Mortensen, 1992; Lowe et al., 1994). The YTT may have acted as a 'bumper' to halt the motions of other terranes in the Late Triassic (McClelland et al., 1992; Mihalynuk et al., 1994) or Eocene (Symons et al., 2000a), or it may have participated, at least in part, with other accreted terrane motions relative to North America (Irving et al., 1996; Johnston et al., 1996a).

Paleomagnetic results from the ~190 Ma Big Creek batholith of west-central Yukon indicate that the YTT has experienced minimal net latitudinal transport and counter-clockwise rotation with respect to North America since the Early Jurassic, a history that is markedly different from the significant poleward transport and clockwise rotations exhibited by Early Jurassic and younger units of the Stikine Terrane (Symons et al., 2000b). Paleomagnetic and geobarometric results from the nearby and similar-aged Granite Mountain batholith are presented here as a further exploration of YTT history since the Early Jurassic.

## GEOLOGICAL SETTING

The Early Jurassic Granite Mountain batholith is a buff-weathering, melanocratic, biotite-hornblende granodiorite intrusion of ~600 km$^2$ extent, emplaced in schists and gneisses of the YTT (Fig. 2). Along with the nearby Big Creek and Minto batholiths, the Granite Mountain batholith is part of a regional ~800-km-long belt of Late Triassic to Early Jurassic calc-alkaline intrusions extending from west of Whitehorse to east-central Alaska, consistent with a continental arc setting within the YTT (Johnston et al., 1996b; Mortensen et al., 2000).

The Granite Mountain batholith is situated within a fault-bounded block of the YTT, adjacent to rocks of the Stikine Terrane in the northeast. The dip-slip Big Creek Fault forms the southwest limit of the Granite Mountain batholith and its YTT host rocks, separating them from the ~190 Ma Big Creek batholith and the mid-Cretaceous Dawson Range batholith. Across the southern boundary of the Granite Mountain batholith, Late Cretaceous Carmacks Group volcanic rocks of Millers Ridge lie on the downthrown side of the Miller fault, with a vertical displacement of at least 800 m. To the northeast, along the Yukon River valley, Triassic volcanic breccia and tuff of the Lewes River Group (Stikine Terrane) is in contact with the batholith along the dextral Hoochekoo fault. The Granite Mountain batholith is intruded by dacite dykes related to the ~105 Ma Mt. Nansen Group volcanic rocks and by feeder dykes for the overlying basal andesite flows of the ~70 Ma Carmacks Group (Tempelman-Kluit, 1984).

Southeast and northwest of the map area depicted in Figure 2, the Big Creek and Hoochekoo fault traces appear to merge, although definitive relationships are obscured by overlying Carmacks Group volcanic flows (Tempelman-Kluit, 1984). Post-Carmacks Group motion history recorded by these northwest-trending faults is minimal, but mid- to Late-Cretaceous dextral displacement on the Big Creek fault was at least 20 km (Johnston, 1999). Johnston (1999) also documents kinematic evidence for a prior ductile history of the Big Creek fault as a shear zone that accommodated the mid-Cretaceous intrusion of the northwest-trending Dawson Range batholith, with a net dextral motion of ~65 km. These motions are not geotectonically significant, but may bear upon the Early Jurassic relationship between the coeval Granite Mountain and Big Creek batholiths, now adjacent across the Big Creek fault (Fig. 2).

Coarse (>5 mm) pink K-feldspar phenocrysts are a distinguishing feature of the batholith, in places defining a weak magmatic fabric. In the west and northwest of the study area, equally large hornblende phenocrysts impart a swarthy melanocratic appearance to the granodiorite, defining a northwest-trending magmatic fabric. In thin section, the mineral phases are fresh, including subhedral hornblende, K-feldspar and brown biotite. Fresh to mildly altered plagioclase is abundant. Quartz is ubiquitous and interstitial to the above phases. Accessory minerals are titanite, apatite, zircon and magnetite.

In the south part of the study area, sites 7 and 6 (Fig. 2) samples were from a Cretaceous andesite porphyry dyke and nearby host batholith, respectively, exposed in a roadside quarry. The dyke carries ~5 mm plagioclase phenocrysts set in a fine groundmass of microcline,

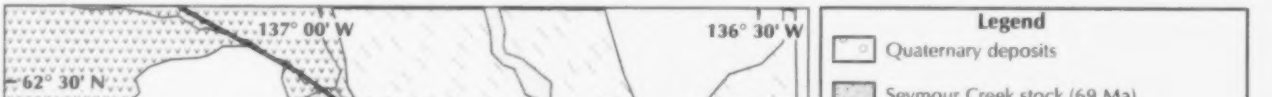
137° 00' W
136° 30' W
62° 30' N
62° 30' N
N
Yukon River
HOOCHEKOO FAULT
19
20
hb 142±10 Ma
21
22
23
24
Big Creek
BIG CREEK FAULT
Granite Mountain
Mt. Freegold
13
14
Williams Creek Cu-Au deposit
12
15
16
11
10
7
6
18 17 9 8
4 5 1-3
62° 15' N
62° 15' N
MILLER FAULT
0
10
km
137° 00' W
136° 30' W
Legend
Quaternary deposits
Seymour Creek stock (69 Ma)
Carmacks Group volcanic rocks (70 Ma)
Mount Nansen Group volcanic rocks (100 Ma)
Dawson Range batholith (105 Ma)
Big Creek batholith (190 Ma)
Granite Mountain batholith (190 Ma)
Triassic volcanic breccia + tuff (Stikine)
Devono-Mississippian quartzite
Devono-Mississippian schist + gneiss (YTT)
18 ○ paleomagnetic sampling site
✕ K-Ar date of hornblende
mining road
fault (inferred; normal)
contact (unspecified)

*Figure 2. Geology of the Granite Mountain batholith (after Tempelman-Kluit, 1984) including sampling sites.*

strongly altered plagioclase, interstitial chlorite, quartz, and well-distributed subangular iron-oxides. The dyke lacks the phenocrystic quartz that is typical of the mid-Cretaceous Mt. Nansen feeder dykes; it is most likely related to the Late Cretaceous Carmacks Group basal andesites (Smuk et al., 1997). Site 6 was sampled from a brittle, yellowed granodiorite that has undergone extensive alteration of hornblende and plagioclase, apparently in association with the dyke.

Hornblende from the northwest part of the batholith has given a K-Ar age of 142 ± 10 Ma (Stevens et al., 1982) that has likely undergone resetting. A U-Pb titanite age of ~190 Ma has been reported for the batholith, along with U-Pb zircon crystallization ages of ~194 Ma and ~193 Ma for associated gneisses hosting the deformed Minto and Williams Creek copper-gold porphyry deposits, respectively (Mortensen et al., 2000; Yukon MINFILE, 2001). The gneisses are enclosed within the batholith, possibly as roof pendants (Gordey and Makepeace, 2001). These age and geological relations imply that the Granite Mountain batholith was emplaced into the freshly deformed gneiss as the youngest magmatic product in an active shear zone. Magmatic fabric along the west margin of the batholith may indicate the nearby presence of the shear zone's northwesterly trending wall within the Early Jurassic continental magmatic arc.

## PALEOMAGNETISM

A total of 331 specimens from 24 sites were collected along mining roads in the southern and eastern parts of the batholith, as well as by helicopter along Big Creek in the northwest (Fig. 2). Each site is represented by at least six 2.54-cm diameter cores, oriented in situ by solar and/or magnetic compass. Standard specimens of 2.20 cm length were sliced from each core. The specimens underwent thermal and alternating field (AF) stepwise demagnetization at the University of Windsor Paleomagnetics Laboratory using a Sapphire Instruments SI-4 AF demagnetizer, a Magnetic Measurements MMTD-80 thermal demagnetizer, and an automated Canadian Thin Films (CTF) DRM-420 cryogenic magnetometer. All measuring instruments are set inside a magnetically shielded room, which permits entry of only 0.2% of the Earth's ambient magnetic field intensity.

Measurement of the specimens' natural remanent magnetizations (NRM) showed a median intensity of 7.7 x $10^{-2}$ A/m (1st quartile, 5.0 x $10^{-2}$ A/m; 3rd quartile, 19.0 x $10^{-2}$ A/m). Specimen volume magnetic susceptibilities, measured with a Sapphire Instruments SI-2B magnetic susceptibility meter, had a median value of 10.0 x $10^{-3}$ SI (1st quartile, 6.6 x $10^{-3}$ SI; 3rd quartile, 18.0 x $10^{-3}$ SI). Both the NRM intensities and the bulk susceptibility values found here are normal for granodioritic rocks (e.g., Lowe et al., 1994).

After NRM measurement, two pilot specimens per site were thermally demagnetized in 13-16 steps up to at least 580°C, and two other pilot specimens were AF-demagnetized in 12 steps up to 130 mT. Thermal demagnetization of 48 pilot specimens revealed distributed unblocking, punctuated in some cases by an intensity drop in the 530°C-580°C range (Fig. 3), implying that magnetite carries the characteristic remanent magnetization (ChRM). Most specimens lost ~90% of their NRM intensity by 450°C, suggesting that multidomain magnetite is likely a significant remanence carrier. At several sites, specimens broke up in the oven at temperatures >470°C. AF step demagnetization removed a 'soft' viscous remanent magnetization (VRM) by ~15 mT, whereas thermal methods required ~260°C. VRM observed in both thermal and AF demagnetizations accounted for 50%-80% of the NRM intensity, and typically was directed steeply downwards to the north-northeast, consistent with its originating from the present Earth's magnetic field in Yukon. AF demagnetization beyond 30 mT commonly led to unstable remanence behaviour, implying the presence of multidomain magnetite.

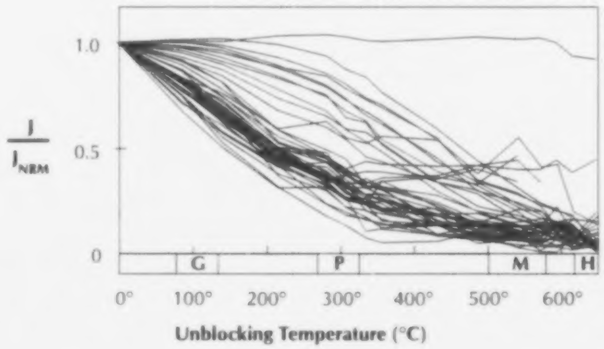

***Figure 3.*** *Thermal demagnetization intensity decay curves for 48 pilot specimens from the Granite Mountain batholith. G, P, M, and H denote the characteristic unblocking temperature ranges of goethite, pyrrhotite, magnetite and hematite, respectively.* $J/J_{NRM}$ *is the ratio of measured remanence intensity to the initial, NRM intensity.*

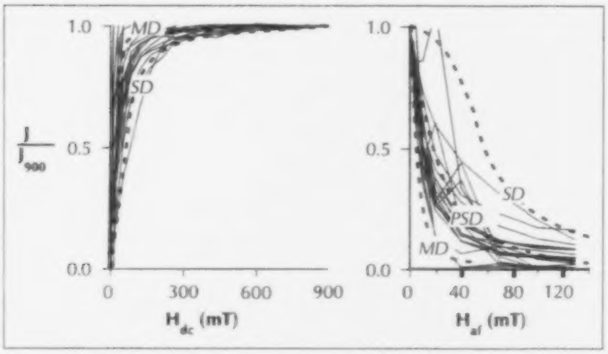

***Figure 4.*** *Saturation isothermal remanent magnetization (SIRM) acquisition and decay curves for 19 specimens from the Granite Mountain batholith. Saturation remanence acquisition is plotted as intensity normalized to saturation intensity ($J/J_{900}$) versus direct field ($H_{dc}$) steps up to 900 mT, and remanence decay is plotted versus alternating-field ($H_{af}$) steps to 130 mT. Dashed curves are given for multidomain (MD), pseudo-single domain (PSD), and single-domain (SD) magnetite.*

Saturation isothermal remanent magnetization (SIRM) acquisition and decay curves were obtained for specimens from 19 sites using a Sapphire Instruments SI-6 pulse magnetizer by magnetizing them in 14 direct-field steps up to 900 mT, and then demagnetizing them in 7 AF steps up to 130 mT. The presence of pseudosingle to multidomain magnetite remanence carriers is confirmed by the generally rapid saturation and decay SIRM behaviour of the Granite Mountain specimens (Fig. 4).

The presence of multidomain magnetite is of concern since it can acquire a remanence at relatively low temperatures (~200°C), but may require laboratory unblocking temperatures of up to 450°C to remove significantly overlapping remanence information carried by pseudosingle and single domain magnetite (Dunlop and Argyle, 1991). Also, the significant presence of multidomain magnetite tends to contribute 'noise' to higher field steps during AF demagnetization (Dunlop and Ozdemir, 1997). To address this problem, 130 specimens were subjected to low-temperature demagnetization (LTD) in field-free space prior to stepwise thermal demagnetization, to remove the multidomain magnetite contribution to remanence (Dunlop and Argyle, 1991; Warnock et al., 2000). The remaining specimens in the collection were thermally demagnetized in steps starting from 450°C. Specimens selected for LTD typically lost between 55% and 85% of their NRM intensities upon cycling through liquid Nitrogen temperature (95 K), thus matching in direction and intensity the remanence that is removed by 15 mT or 450°C. Accordingly, characteristic remanent magnetization (ChRM) directions are determined using specimens which were subjected to post-LTD thermal demagnetization, along with other specimens that exhibited stable remanence at unblocking temperatures of >450°C and coercivities of >15 mT. ChRM directions were identified using the least-squares line-fitting method over four or more consecutive AF or thermal steps (Kirschvink, 1980), with a maximum uncertainty of <15° for the fitted vector.

The paleomagnetic behaviour of specimens from the Granite Mountain batholith is complex (Fig. 5). North and west of the batholith, a ChRM **A** component with mean direction D=337, inclination I=69° (8 sites; $\alpha_{95}$=7.6°; k=54.5) is present (Fig. 5a-c). Some **A** specimens (Fig. 5a) exhibit poor northwest and down ChRM directions, requiring the anchoring of the fitted vector to the zero remanence origin. A north-and-up ChRM **B** component with mean direction (D=024, I=-54°; $\alpha_{95}$=14.0°, k=78.3) exists in three southeastern sites (Fig. 5d). The Cretaceous andesite porphyry dyke and its contact zone give a steep down remanence direction, **C** (Fig. 5e). ChRM components **A, B** and **C** are mutually exclusive. Specimens from 11 other sites either did not carry a stable remanence, or had inconsistent directions from sample to sample, possibly due to lightning strikes. Site mean paleomagnetic results are set out in Table 1 and depicted in Figure 6.

## PALEODEPTH ESTIMATES

To be meaningful, paleomagnetic directions must be referenced to the paleohorizontal at the time of remanence acquisition. Estimates of paleohorizontal are usually obtained from bedded depositional strata, but this is not possible for massive crystalline intrusions. Instead, we employ the aluminum-in-hornblende geobarometer (Anderson and Smith, 1995) to estimate crystallization pressures and therefore emplacement depths at various locations in the batholith, thus providing a batholith-scale estimate of paleohorizontal at the time of emplacement.

Following petrographic inspection of a polished thin section from each site, 10 sites were chosen to represent the Granite Mountain batholith. Each chosen site contained the requisite mineral assemblage of amphibole,

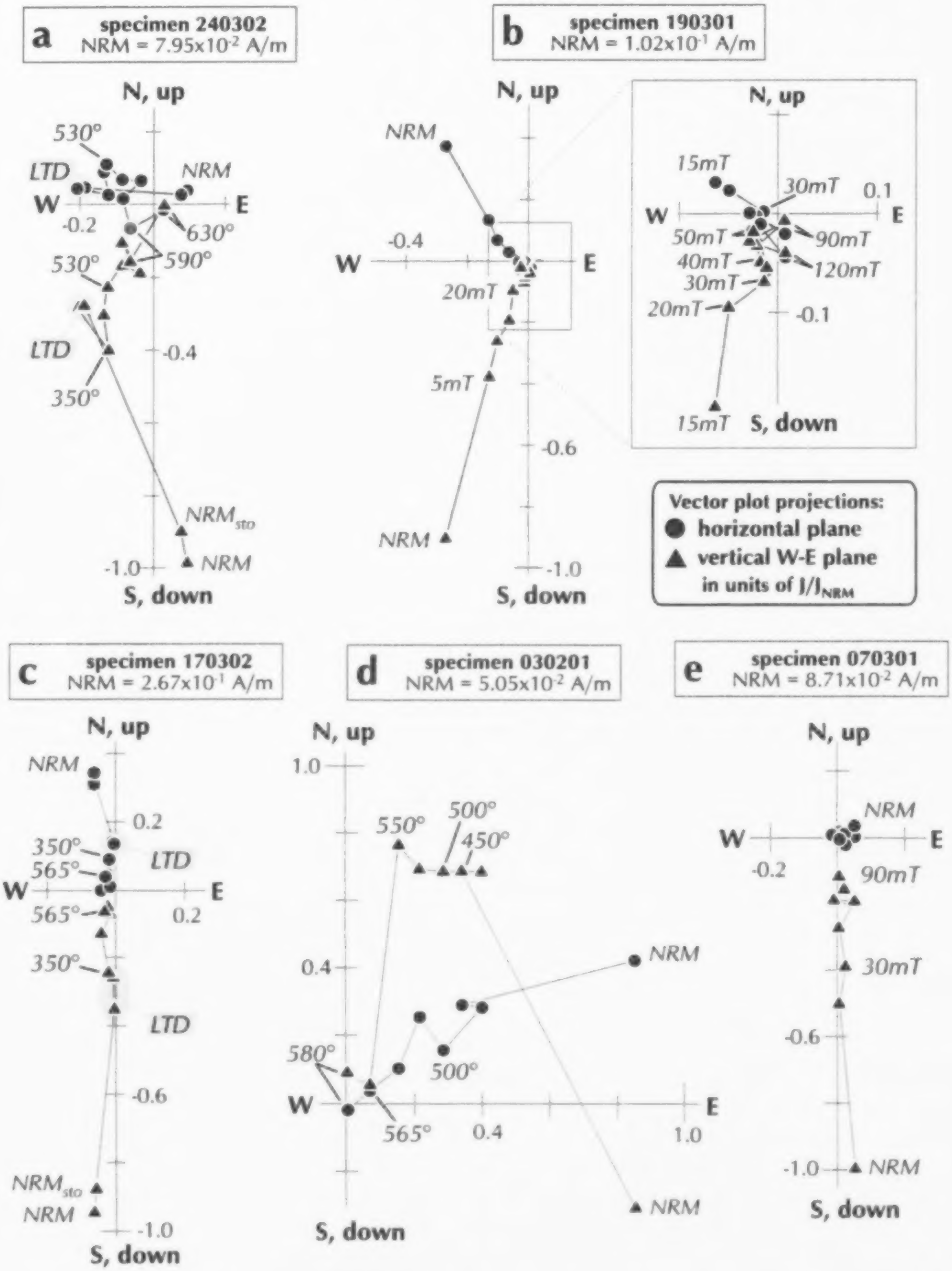

***Figure 5.*** *NRM intensity-normalized orthogonal step demagnetization plots (Zijderveld, 1967) for representative specimens carrying the **A** remanence (a-c), the **B** remanence (d), and the **C** remanence (e). See text for discussion. NRM$_{sto}$ is the natural remanent magnetization remaining in the specimen after decay during one year of storage in field-free space, prior to the stepwise demagnetization. LTD marks the low-temperature demagnetization steps discussed in the text. Circles mark the remaining remanence direction and intensity at each demagnetization step projected into the map-like horizontal north-south, east-west plane, whereas triangles mark the same stepwise demagnetization vectors projected into the vertical, east-west plane.*

plagioclase, K-feldspar, quartz, biotite, titanite, apatite, and magnetite or ilmenite, with minimal or no alteration of the primary igneous phases. It has been shown empirically (Hammarstrom and Zen, 1986) and experimentally (Schmidt, 1992) that the aluminum content in Ca-amphiboles increases linearly with greater pressure of crystallization under equilibrium $H_2O$-saturated conditions. Pressure estimates may be corrected for effect of temperature through the plagioclase-hornblende geothermometer (Blundy and Holland, 1990).

Electron microprobe elemental abundance analyses of two hornblende and plagioclase pairs in each site were performed using a JEOL JXA-8600 Superprobe at the University of Western Ontario, using standards as reported in Symons et al. (2000b). Analytical data were reduced for elemental abundances using structural formulae with 32 oxygens for plagioclase (Blundy and Holland, 1990), and by the ferric-iron maximizing method of Schumacher (1997) for amphibole. Plagioclase and amphibole were each analysed three to five times near their common boundaries for averaging and to test reproducibility. Within-crystal variation between analyses was typically less than 1% of the measured elemental abundances. Additionally, both the calcium (Ca) content in plagioclase and the aluminum (Al) content in hornblende are consistent between crystal pairs within each site (Table 2; Fig. 7). Plagioclase analyses range from $An_{19}$ to $An_{33}$, within the calibrated limits of the geothermometer, and amphiboles are tschermakites to ferrotschermakites in the classification of Leake et al. (1997), with $Al^{TOT}$ ranging from 1.8 to 2.1 atomic formula units (Table 2).

Initial pressure estimates (method of Schmidt, 1992), crystallization temperatures, and temperature-corrected pressure estimates for the 10 sites are given in Table 3. Emplacement depths, calculated assuming a baric gradient of 0.036 km/MPa (density 2.8 g/cm$^3$), and corrected for relative topographic differences between

***Table 1.*** *Site mean remanence data for the Granite Mountain batholith, Yukon.*

| **Site**[a] | **n/N** | **ChRM Direction** | | | |
|---|---|---|---|---|---|
| | | **Dec (°)** | **Inc (°)** | **$\alpha_{95}$ (°)** | **k** |
| 02[b] | 6/15 | 024.2 | -52.7 | 7.2 | 87.1 |
| 03[b] | 11/13 | 021.8 | -63.6 | 6.2 | 55.3 |
| 05[b] | 5/12 | 025.3 | -45.5 | 13.1 | 35.2 |
| 06[c] | 11/15 | 258.1 | 81.6 | 7.6 | 36.9 |
| 07[c] | 13/13 | 344.7 | 85.4 | 5.8 | 52.8 |
| 08 | 7/13 | 328.1 | 76.5 | 10.9 | 31.9 |
| 09 | 7/15 | 002.7 | 64.3 | 11.8 | 27.1 |
| 17 | 8/15 | 350.6 | 75.3 | 6.9 | 65.7 |
| 18 | 7/15 | 353.0 | 61.1 | 10.0 | 37.7 |
| 19 | 8/14 | 308.1 | 70.5 | 7.5 | 55.0 |
| 20 | 7/11 | 310.1 | 61.3 | 9.6 | 40.4 |
| 23 | 6/12 | 002.8 | 64.4 | 10.2 | 44.1 |
| 24 | 7/11 | 310.5 | 68.5 | 9.5 | 41.3 |
| **B** = 3 sites | | 024.0 | -53.9 | 14.0 | 78.3 |
| **A** = 8 sites | | 336.8 | 69.4 | 7.6 | 54.5 |

[a] Sites 1, 4, 10-13, 15, 21 and 22 carry unstable remanence; sites 14, 16 carry stable remanence with inconsistent between-sample directions, probably due to lightning strike.

[b] Sites exhibiting **B** ChRM directions.

[c] Sites from a Cretaceous dyke and its contact zone, exhibiting **C** ChRM directions.

n/N: Number of specimens useable for site mean ChRM calculation/total number of specimens in site. Site mean ChRM directions are given by: Dec - declination; Inc - inclination; $\alpha_{95}$ - radius of 95% cone of confidence, and k - precision parameter.

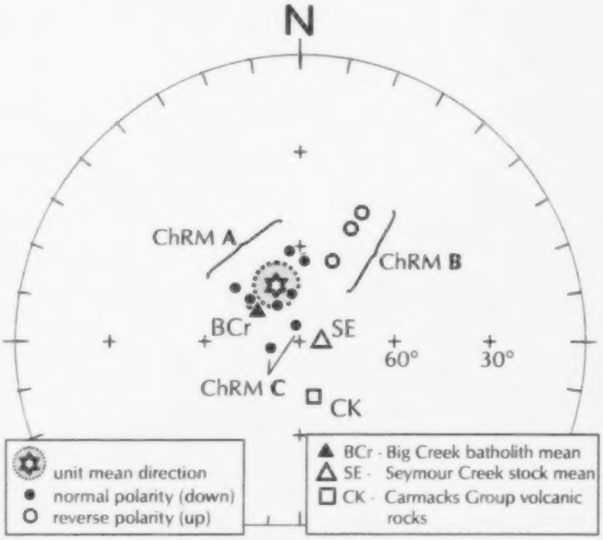

***Figure 6.*** *Equal-area stereonet projection showing all site means from the Granite Mountain batholith (Table 1), along with reported mean direction for the Big Creek batholith (Symons et al., 2000b), the Seymour Creek stock (McCausland et al., 2001) and the Carmacks Group volcanic rocks (Wynne et al., 1998). Closed and open symbols represent down and up directions, respectively.*

***Table 2.** Averaged amphibole analyses from the Granite Mountain batholith, using the structural formula calculation procedure of Schumacher (1997).*

| | 04-A | 04-B | 11-A | 11-B | 12-A | 12-B | 14-A | 14-B | 15-A | 15-B |
|---|---|---|---|---|---|---|---|---|---|---|
| $SiO_2$ (wt.%) | 40.46 | 40.67 | 41.07 | 40.94 | 41.81 | 41.52 | 41.13 | 40.94 | 40.73 | 41.23 |
| $TiO_2$ | 0.91 | 0.91 | 0.96 | 1.05 | 0.94 | 0.78 | 0.61 | 0.73 | 0.91 | 0.9 |
| $Al_2O_3$ | 11.48 | 11.23 | 11.21 | 11.34 | 10.51 | 10.8 | 11.09 | 11.11 | 11.56 | 11.58 |
| $Fe_2O_3$* | 4.75 | 4.29 | 4.73 | 4.94 | 4.25 | 4.32 | 4.66 | 4.5 | 4.89 | 4.09 |
| $Cr_2O_3$ | 0.04 | 0.04 | 0.02 | 0.00 | 0.05 | 0.05 | 0.05 | 0.01 | 0.00 | 0.01 |
| FeO | 15.72 | 15.78 | 16.32 | 16.23 | 15.79 | 16.03 | 15.23 | 15.8 | 16 | 16.77 |
| MnO | 0.51 | 0.59 | 0.47 | 0.45 | 0.61 | 0.62 | 0.58 | 0.59 | 0.56 | 0.49 |
| MgO | 8.33 | 8.32 | 8.14 | 8.15 | 8.99 | 8.66 | 8.76 | 8.5 | 8.21 | 8.05 |
| CaO | 11.68 | 11.74 | 11.76 | 11.72 | 11.48 | 11.49 | 11.5 | 11.69 | 11.63 | 11.7 |
| $Na_2O$ | 1.4 | 1.3 | 1.32 | 1.33 | 1.56 | 1.54 | 1.47 | 1.49 | 1.37 | 1.37 |
| $K_2O$ | 1.41 | 1.37 | 1.24 | 1.26 | 1.29 | 1.33 | 1.31 | 1.33 | 1.45 | 1.38 |
| $H_2O$* | 1.88 | 1.88 | 1.91 | 1.9 | 1.91 | 1.91 | 1.9 | 1.89 | 1.9 | 1.92 |
| F | 0.05 | 0.04 | 0.02 | 0.04 | 0.03 | 0.00 | 0.02 | 0.04 | 0.03 | 0.01 |
| Cl | 0.07 | 0.05 | 0.06 | 0.04 | 0.07 | 0.07 | 0.05 | 0.03 | 0.05 | 0.04 |
| Total | 98.67 | 98.23 | 99.22 | 99.4 | 99.29 | 99.12 | 98.36 | 98.64 | 99.29 | 99.56 |
| Si(cations) | 6.256 | 6.308 | 6.314 | 6.284 | 6.401 | 6.379 | 6.351 | 6.323 | 6.263 | 6.317 |
| $^{[4]}$Al | 1.744 | 1.692 | 1.686 | 1.716 | 1.599 | 1.621 | 1.649 | 1.677 | 1.737 | 1.683 |
| $^{[6]}$Al | 0.347 | 0.362 | 0.345 | 0.335 | 0.297 | 0.333 | 0.369 | 0.347 | 0.357 | 0.408 |
| Ti | 0.106 | 0.107 | 0.111 | 0.122 | 0.108 | 0.09 | 0.07 | 0.084 | 0.105 | 0.104 |
| Cr | 0.005 | 0.004 | 0.002 | 0.001 | 0.006 | 0.006 | 0.006 | 0.002 | 0.00 | 0.002 |
| $Fe^{3+}$ | 0.553 | 0.501 | 0.547 | 0.57 | 0.49 | 0.499 | 0.541 | 0.523 | 0.565 | 0.472 |
| $^{[C]}Fe^{2+}$ | 2.032 | 2.047 | 2.098 | 2.083 | 2.022 | 2.059 | 1.967 | 2.04 | 2.057 | 2.149 |
| $^{[C]}$Mn | 0.037 | 0.055 | 0.033 | 0.025 | 0.025 | 0.03 | 0.03 | 0.047 | 0.034 | 0.026 |
| Mg | 1.92 | 1.924 | 1.865 | 1.864 | 2.052 | 1.983 | 2.017 | 1.957 | 1.881 | 1.839 |
| $^{[B]}$Mn | 0.031 | 0.023 | 0.029 | 0.034 | 0.054 | 0.051 | 0.046 | 0.031 | 0.039 | 0.037 |
| $^{[B]}Fe^{2+}$ | 0.00 | 0.00 | 0.00 | 0.00 | 0.00 | 0.00 | 0.00 | 0.00 | 0.00 | 0.00 |
| Ca | 1.934 | 1.951 | 1.937 | 1.928 | 1.884 | 1.891 | 1.902 | 1.934 | 1.916 | 1.921 |
| $^{[B]}$Na | 0.035 | 0.026 | 0.034 | 0.038 | 0.062 | 0.058 | 0.052 | 0.035 | 0.045 | 0.042 |
| $^{[A]}$Na | 0.384 | 0.366 | 0.361 | 0.358 | 0.399 | 0.401 | 0.386 | 0.41 | 0.365 | 0.364 |
| K | 0.279 | 0.271 | 0.243 | 0.248 | 0.252 | 0.261 | 0.259 | 0.262 | 0.284 | 0.27 |
| OH* | 1.958 | 1.967 | 1.978 | 1.969 | 1.967 | 1.981 | 1.977 | 1.972 | 1.973 | 1.984 |
| F | 0.025 | 0.02 | 0.008 | 0.021 | 0.014 | 0.00 | 0.01 | 0.019 | 0.013 | 0.005 |
| Cl | 0.017 | 0.013 | 0.015 | 0.01 | 0.018 | 0.019 | 0.013 | 0.009 | 0.014 | 0.011 |
| $Al_{[TOT]}$ | 2.091 | 2.054 | 2.031 | 2.052 | 1.896 | 1.955 | 2.018 | 2.023 | 2.094 | 2.092 |
| $Fe^{3+}$# | 0.214 | 0.197 | 0.207 | 0.215 | 0.195 | 0.195 | 0.216 | 0.204 | 0.216 | 0.18 |
| Fe# | 0.574 | 0.57 | 0.586 | 0.587 | 0.55 | 0.563 | 0.554 | 0.567 | 0.582 | 0.588 |

*$Fe_2O_3$ and $H_2O$ are back-calculated from the structural formula. $Fe^{3+}$# = $Fe^{3+}/(Fe^{3+} + Fe^{2+})$; Fe# = $(Fe^{3+} + Fe^{2+})/(Fe^{3+} + Fe^{2+} + Mg)$.

*(continued)* ***Table 2.***

| | 09-A | 09-B | 18-A | 18-B | 20-A | 20-B | 21-A | 21-B | 23-A | 23-B |
|---|---|---|---|---|---|---|---|---|---|---|
| $SiO_2$ (wt.%) | 42.63 | 42.51 | 42.87 | 42.49 | 42.09 | 42.44 | 42.5 | 42.44 | 41.88 | 42.25 |
| $TiO_2$ | 0.99 | 0.87 | 0.74 | 0.76 | 0.83 | 0.85 | 0.95 | 0.92 | 0.8 | 0.72 |
| $Al_2O_3$ | 9.91 | 10.12 | 10.24 | 10.7 | 10.55 | 10.36 | 9.76 | 10.24 | 10.78 | 10.62 |
| $Fe_2O_3^*$ | 3.06 | 4.35 | 4.46 | 5.05 | 4.45 | 3.9 | 4.01 | 3.03 | 4.65 | 4.02 |
| $Cr_2O_3$ | 0.07 | 0.07 | 0.04 | 0.01 | 0.01 | 0.01 | 0.02 | 0.03 | 0.01 | 0.02 |
| FeO | 14.54 | 14.1 | 12.93 | 12.73 | 13.64 | 14.09 | 14.68 | 15.22 | 13.13 | 13.51 |
| MnO | 0.52 | 0.52 | 0.64 | 0.63 | 0.47 | 0.51 | 0.49 | 0.47 | 0.59 | 0.45 |
| MgO | 10.06 | 10.02 | 10.48 | 10.41 | 10.04 | 10.03 | 9.84 | 9.68 | 10.17 | 10.26 |
| CaO | 11.82 | 11.79 | 11.89 | 11.95 | 11.68 | 11.77 | 11.67 | 11.77 | 11.87 | 11.87 |
| $Na_2O$ | 1.31 | 1.31 | 1.18 | 1.21 | 1.32 | 1.34 | 1.33 | 1.42 | 1.29 | 1.31 |
| $K_2O$ | 1.18 | 1.15 | 1.02 | 1.09 | 1.13 | 1.14 | 1.16 | 1.19 | 1.21 | 1.18 |
| $H_2O^*$ | 1.92 | 1.93 | 1.94 | 1.93 | 1.93 | 1.93 | 1.91 | 1.92 | 1.92 | 1.93 |
| F | 0.02 | 0.01 | 0.00 | 0.05 | 0.00 | 0.00 | 0.03 | 0.02 | 0.03 | 0 |
| Cl | 0.06 | 0.06 | 0.05 | 0.04 | 0.03 | 0.05 | 0.05 | 0.04 | 0.04 | 0.04 |
| Total | 98.11 | 98.81 | 98.48 | 99.05 | 98.19 | 98.42 | 98.4 | 98.4 | 98.35 | 98.2 |
| Si (cations) | 6.532 | 6.475 | 6.506 | 6.424 | 6.436 | 6.478 | 6.512 | 6.502 | 6.394 | 6.45 |
| $^{[4]}Al$ | 1.468 | 1.525 | 1.494 | 1.576 | 1.564 | 1.522 | 1.488 | 1.498 | 1.606 | 1.55 |
| $^{[6]}Al$ | 0.322 | 0.291 | 0.337 | 0.331 | 0.338 | 0.342 | 0.274 | 0.351 | 0.334 | 0.362 |
| Ti | 0.114 | 0.1 | 0.085 | 0.086 | 0.096 | 0.097 | 0.11 | 0.106 | 0.091 | 0.083 |
| Cr | 0.009 | 0.008 | 0.005 | 0.001 | 0.002 | 0.001 | 0.003 | 0.003 | 0.001 | 0.003 |
| $Fe^{3+}$ | 0.353 | 0.499 | 0.509 | 0.575 | 0.512 | 0.448 | 0.462 | 0.35 | 0.534 | 0.462 |
| $^{[C]}Fe^{2+}$ | 1.863 | 1.796 | 1.641 | 1.609 | 1.744 | 1.798 | 1.881 | 1.95 | 1.676 | 1.725 |
| $^{[C]}Mn$ | 0.04 | 0.032 | 0.052 | 0.051 | 0.02 | 0.031 | 0.024 | 0.03 | 0.05 | 0.031 |
| Mg | 2.299 | 2.275 | 2.371 | 2.347 | 2.288 | 2.283 | 2.247 | 2.211 | 2.315 | 2.334 |
| $^{[B]}Mn$ | 0.028 | 0.036 | 0.031 | 0.03 | 0.04 | 0.035 | 0.04 | 0.031 | 0.027 | 0.027 |
| $^{[B]}Fe^{2+}$ | 0.00 | 0.00 | 0.00 | 0.00 | 0.00 | 0.00 | 0.00 | 0.00 | 0.00 | 0 |
| Ca | 1.941 | 1.923 | 1.934 | 1.936 | 1.914 | 1.925 | 1.915 | 1.933 | 1.942 | 1.942 |
| $^{[B]}Na$ | 0.032 | 0.041 | 0.035 | 0.034 | 0.046 | 0.04 | 0.045 | 0.036 | 0.031 | 0.031 |
| $^{[A]}Na$ | 0.358 | 0.346 | 0.312 | 0.32 | 0.346 | 0.355 | 0.349 | 0.386 | 0.351 | 0.358 |
| K | 0.231 | 0.224 | 0.197 | 0.211 | 0.22 | 0.222 | 0.227 | 0.233 | 0.235 | 0.231 |
| $OH^*$ | 1.976 | 1.978 | 1.987 | 1.968 | 1.992 | 1.986 | 1.971 | 1.98 | 1.974 | 1.987 |
| F | 0.008 | 0.005 | 0.00 | 0.023 | 0.00 | 0.00 | 0.015 | 0.009 | 0.015 | 0.001 |
| Cl | 0.016 | 0.016 | 0.013 | 0.009 | 0.008 | 0.014 | 0.014 | 0.011 | 0.01 | 0.011 |
| $Al_{[TOT]}$ | 1.79 | 1.816 | 1.831 | 1.907 | 1.902 | 1.864 | 1.763 | 1.849 | 1.94 | 1.911 |
| $Fe^{3+}$# | 0.159 | 0.217 | 0.237 | 0.263 | 0.227 | 0.199 | 0.197 | 0.152 | 0.242 | 0.211 |
| Fe# | 0.491 | 0.502 | 0.476 | 0.482 | 0.497 | 0.496 | 0.51 | 0.51 | 0.488 | 0.484 |

sites, define two domains in the batholith (Table 3; Fig. 8): 16.1 ± 0.5 km in the north and west (five sites), and 18.8 ± 0.6 km to the southeast (five sites). Topographic correction is minor, as all sites occur within a 0.5-km-range of elevation. The paleodepth estimates imply either a west ~6° tilt of a coherent intrusive body, or more likely, a subdivision of the batholith into at least two blocks, which experienced differential uplift.

***Table 3.*** *Site-averaged compositions of co-existing amphibole and plagioclase crystal pairs and consequent thermobarometric data for the Granite Mountain batholith.*

| Site pair | Plag An# | Amph Al[TOT] | P-Sch (MPa) | Temp (°C) | P-A&S (MPa) | Depth (km) | Corr. Depth (km) |
|---|---|---|---|---|---|---|---|
| 04-A | 24.9 | 2.09 | 703 | 769 | 523 | 18.6 | 18.6 |
| 04-B | 25.4 | 2.05 | 685 | 762 | 526 | 18.7 | 18.7 |
| **11-A** | **26.2** | **2.03** | **674** | **764** | **509** | **18.1** | **18.3** |
| **11-B** | **27.0** | **2.05** | **684** | **771** | **502** | **17.8** | **18.0** |
| 12-A | 19.5 | 1.90 | 609 | 739 | 507 | 18.0 | 18.2 |
| 12-B | 19.7 | 1.96 | 638 | 739 | 532 | 18.9 | 19.1 |
| **14-A** | **22.2** | **2.02** | **668** | **746** | **545** | **19.4** | **19.5** |
| **14-B** | **22.8** | **2.02** | **671** | **754** | **531** | **18.9** | **19.0** |
| 15-A | 26.5 | 2.09 | 705 | 769 | 524 | 18.6 | 18.8 |
| 15-B | 25.5 | 2.09 | 704 | 756 | 555 | 19.7 | 19.9 |
| **09-A** | **29.6** | **1.79** | **558** | **746** | **446** | **15.9** | **16.2** |
| **09-B** | **30.1** | **1.82** | **571** | **758** | **433** | **15.4** | **15.7** |
| 18-A | 32.7 | 1.83 | 578 | 757 | 442 | 15.7 | 16.1 |
| 18-B | 32.6 | 1.91 | 615 | 769 | 446 | 15.9 | 16.2 |
| **20-A** | **31.1** | **1.90** | **612** | **762** | **461** | **16.4** | **16.3** |
| **20-B** | **32.0** | **1.86** | **594** | **758** | **452** | **16.1** | **15.9** |
| 21-A | 28.9 | 1.76 | 545 | 750 | 426 | 15.1 | 15.1 |
| 21-B | 28.6 | 1.85 | 587 | 745 | 473 | 16.8 | 16.8 |
| **23-A** | **31.5** | **1.94** | **630** | **769** | **459** | **16.3** | **16.3** |
| **23-B** | **31.3** | **1.91** | **617** | **758** | **473** | **16.8** | **16.8** |
| East | 24.0 | 2.03 | 670 | 757 | 525 | 18.7 | 18.8 |
| s.d. | ±2.6 | ±0.06 | ±29 | ±12 | ±16 | ±0.6 | ±0.6 |
| West | 30.8 | 1.86 | 591 | 757 | 451 | 16.0 | 16.1 |
| s.d. | ±1.4 | ±0.06 | ±27 | ±8 | ±15 | ±0.5 | ±0.5 |

Notes: Plagioclase An# - the atomic ratio [Ca/(Na+Ca+K)]; Amphibole Al[TOT] - the average total number of Al cations calculated in the structural formula (Table 2); P-Sch - pressure calculated using Schmidt (1992); Temp - temperature calculated using the plagioclase-amphibole geothermometer of Blundy and Holland (1992); P-A&S - the final temperature-corrected pressure estimate, calculated using Anderson and Smith (1995); Corr. Depth - paleodepth estimates that have been corrected for minor variation in present-day topography, with the correction made arbitrarily to the elevation at site 4.

Within each domain, the paleodepth estimates are consistent with present horizontal, given the relative uncertainty of the method (±0.5 km, Anderson and Smith, 1995). The depth difference between western and eastern domains therefore suggests the presence of a roughly north-northwest-trending normal fault separating the domains, with ~2.5 km east-side-up displacement. The eastern portion of the batholith may be a 'pop up' sliver, involving a west-side-up displacement on the Hoochekoo Fault. Alternatively, the ~2.5 km depth difference between domains may mark an original difference in intrusive depth between two phases of the batholith, emplaced at slightly different times.

Crystal-pair plagioclase Ca content and amphibole Al content differs markedly between western and eastern sites of the batholith (Fig. 7). Such a bimodal distribution suggests that geobarometric comparisons between the batholith domains should be made with caution; it is as if they were separate intrusions. Paleodepth estimates from the two domains almost agree within the geobarometric method's ±2 km absolute uncertainty (Anderson and Smith, 1995), which is partly based on the compositional variation amongst the intrusions used to calibrate the geobarometer (Hammarstrom and Zen, 1986). Nevertheless, the sense of depth difference between western and eastern batholith domains is probably correct.

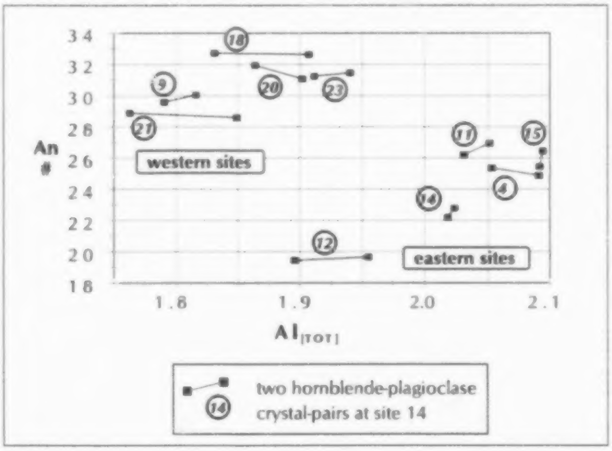

***Figure 7.*** *Plagioclase and hornblende crystal-pairs for each site plotted as calcium content in plagioclase (Anorthite # - An #) versus total number of aluminum cations ($Al_{[TOT]}$) in hornblende. Within-site consistency is indicated by the similarity of pairs from each site.*

## DISCUSSION

Given the estimated emplacement depths of 16-19 km, the ambient post-emplacement temperatures would have been >480°C (assuming ~30°/km geothermal gradient), too high for an enduring remanence to be acquired by magnetite (Pullaiah et al., 1975). Any ChRM present was likely recorded during uplift through ~15 km depth. Simple time-linear uplift of the batholith from 16-19 km at 190 Ma to surfacing, and deposition of the Carmacks Group flows at 70 Ma, indicates that the **A** and **B** ChRMs would have been acquired at 180-170 Ma. Rapid early uplift is also suggested by cooling curves obtained from the coeval Aishihik batholith to the south (Johnston et al., 1996b).

Remanence **C** is younger, related to the emplacement of the Cretaceous andesite dyke. The westerly, steep-down ChRM compares well with the ChRM recovered from 14 reversed- and 2 normal-polarity sites of the nearby 69 Ma Seymour Creek stock (McCausland et al., 2001). Alternatively, the ChRM **C** is similar to the nearly vertical-down ChRM directions found in a preliminary analysis of the 105 Ma Dawson Range batholith (McCausland et al., 2000a), although the dyke appears to be younger, and is likely a feeder for the overlying 70 Ma Carmacks andesite flows.

Remanence **B** has no clear tectonic meaning, with its direction plotting well away from the antipode to **A**, or any possible North American reference pole. It is resolved in only three sites, all sampled by road from the southeasternmost part of the Granite Mountain batholith, where the Miller and Hoochekoo faults meet (Fig. 8). The **B** ChRM direction may be resident in a local, tumbled block of km size, marking the fault-bounded corner of the exposed batholith.

Unlike ChRM **B**, the **A** ChRM is observed in eight sites distributed across the western and northern portions of the batholith. Its wide geographic distribution is coincident with the sites that show geobarometric depth estimates of ~16 km, strongly indicating that no tilt correction of the **A** ChRM direction is required. Remanence **A** gives a paleopole position of 74.7°N, 106.9°E (dp=11°, dm=13°), which has negligible rotation and is 690 km ± 1090 km near-sided compared with the 180 Ma North American reference pole of Besse and

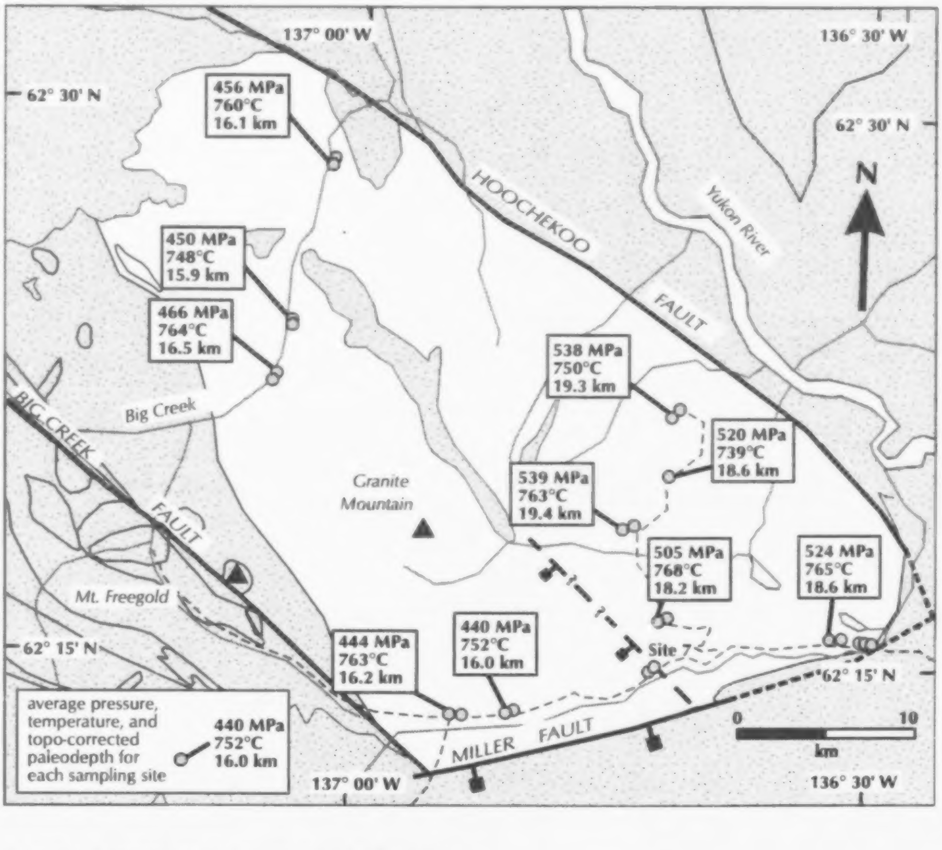
137° 00' W
136° 30' W
62° 30' N
62° 30' N
N
HOOCHEKOO
FAULT
Yukon River
456 MPa
760°C
16.1 km
450 MPa
748°C
15.9 km
466 MPa
764°C
16.5 km
538 MPa
750°C
19.3 km
520 MPa
739°C
18.6 km
539 MPa
763°C
19.4 km
505 MPa
768°C
18.2 km
524 MPa
765°C
18.6 km
440 MPa
752°C
16.0 km
444 MPa
763°C
16.2 km
Big Creek
BIG CREEK
FAULT
Granite Mountain
Mt. Freegold
62° 15' N
62° 15' N
Site 7
MILLER FAULT
0
10
km
137° 00' W
136° 30' W
average pressure, temperature, and topo-corrected paleodepth for each sampling site
440 MPa
752°C
16.0 km

*Figure 8.* Pressure, temperature and intrusion depth estimates for the Granite Mountain batholith. A possible normal fault between eastern and western portions of the batholith is marked by a dashed line. Note that such a fault might have provided a conduit for the 70 Ma Carmacks Group magmatism preserved along the centre of the batholith and as a dyke at Site 7.

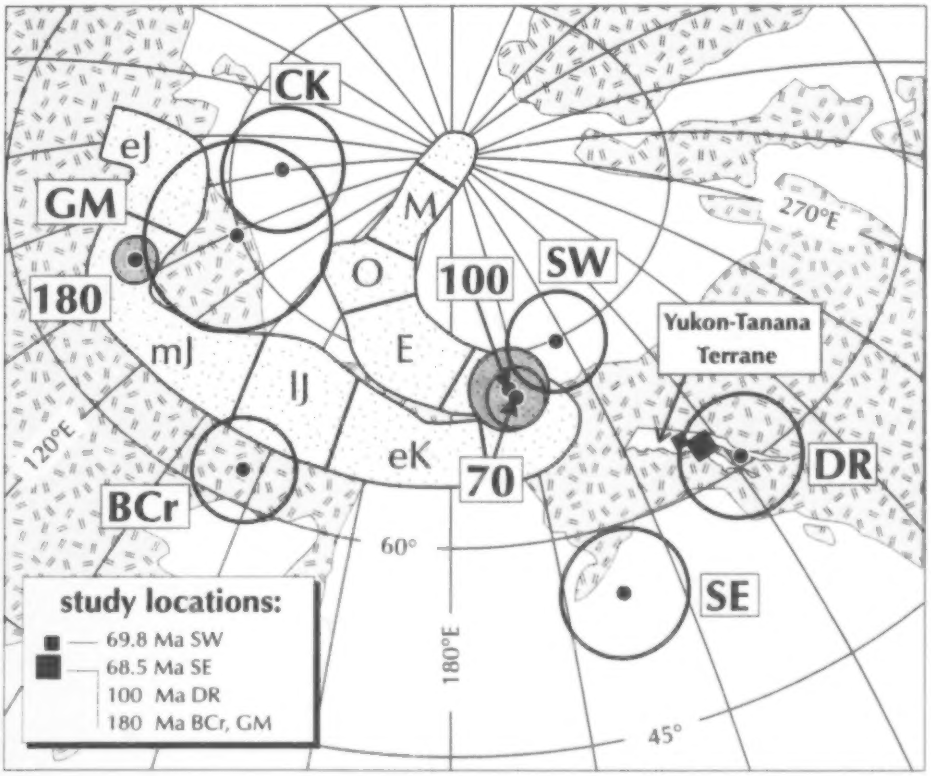

***Figure 9.*** *YTT paleopoles and their 1-sigma confidence ellipses plotted on the present-day globe with reference to the North American apparent polar wander path (stippled pattern) of Besse and Courtillot (1991), from Early Jurassic (eJ) time to the present day, with its 1-sigma bounds. CK - 70 Ma Carmacks Group volcanic rocks; mJ - Middle Jurassic; lJ - Late Jurassic; eK - Early Cretaceous; E - Eocene; O - Oligocene; M - Miocene; all other abbreviations are defined in Figure 1. See text for discussion.*

Courtillot (1991). Both **A** and **C** remanence directions are similar to those expected for Early Jurassic and Late Cretaceous North American reference poles, respectively, and are most simply interpreted as representing minimal motion of the Granite Mountain batholith relative to North America since Early Jurassic time.

All paleomagnetic results reported to date for the YTT (Table 4) are plotted in Figure 9 as paleopoles with reference to a path of past positions of the North American pole (Besse and Courtillot, 1991). Results reported here for the Granite Mountain batholith are similar to those obtained from the Early Jurassic Big Creek batholith which carries a dual-polarity uplift remanence direction in 18 sites (Symons et al., 2000b). The much larger 1σ formal error ellipse of the Granite Mountain paleopole position mainly reflects its derivation from only eight sites.

Unlike the counter-clockwise-rotated Big Creek batholith, the Granite Mountain batholith result implies no significant net rotation with respect to North America since 180 Ma. Following this observation, it would appear that the Big Creek batholith has undergone 31° ± 19° of counter-clockwise rotation with respect to the Granite Mountain batholith at some time during their history, perhaps during motion along the Big Creek fault/shear zone that brought them into their current adjacency. Note

***Table 4.*** *Net tectonic motion estimates from units of the YTT*[a]*.*

| Unit[b] | Age (Ma) | Paleopole Lat.(°N) | Paleopole Long.(°E) | $A_{95}$ | Net Transport, Poleward[c]; | Rotation Clockwise |
|---|---|---|---|---|---|---|
| GM | 180 | 74.7° | 106.9° | 12.0° | -6.2°±9.8°; | 4°±17° |
| BCr | 180 | 62.9° | 146.6° | 6.5° | -10.1°±5.6°; | -27°±10° |
| DR[d] | 105 | 61.1° | 226.3° | 8.1° | -12.3°±7.8°; | N/A |
| CK | 70 | 78.4° | 088.6° | 7.8° | 21.0°±7.0°; | 22°±16° |
| SW[e] | 70 | 77.3° | 224.7° | 6.0° | 0.5°±5.8°; | 44°±27° |
| SE | 69 | 55.2° | 202.5° | 8.4° | -2.4°±7.5°; | -79°±36° |

[a] Calculated with respect to North America paleopoles from Besse and Courtillot (1991): 180 Ma, 68.1°N, 101.2°E; $A_{95}$=2.7°; 100 Ma, 72.9°N, 191.4°E; $A_{95}$=5.4°; 70 Ma, 72.3°N, 192.7°E; $A_{95}$=4.1°.

[b] Unit abbreviations are defined in Figure 1.

[c] One degree of transport is equal to approximately 111 km.

[d] Dawson Range batholith (McCausland et al., 2000a).

[e] Swede Dome stock (McCausland et al., 2000b).

that the paleopoles also nonsignificantly imply that at 180 Ma, the Big Creek batholith was located in present-day coordinates, some 430 km ± 1200 km 'northwestwards' of the Granite Mountain batholith, requiring a net 'sinistral' motion to bring them to their present day positions. This apparent sinistral motion history is poorly resolved, but, if true, would have occurred prior to the mid-Cretaceous emplacement of the Dawson Range batholith, after which only minimal fault motions are known for the area (Johnston, 1999).

The Granite Mountain batholith paleopole overlaps that of the Late Cretaceous Carmacks Group volcanic rocks of Wynne et al. (1998), and the **A** ChRM may instead have been acquired during a thermal or hydrothermal event related to the overlying Carmacks volcanism at 70 Ma (Fig. 2). Evidence is lacking, however, for thermal paleomagnetic overprinting or hydrothermally driven creation of new magnetic material in sites carrying the **A** ChRM. The **A** remanence defined in this study unblocks at temperatures >450°C with no trace of another, higher temperature ancient component. In thin section, plagioclase shows only patchy alteration, with little or no alteration of hornblende. A pervasive hydrothermal event (Wynne et al., 1998) might be expected to produce extensive alteration along grain boundaries, a feature not observed for most sites of the Granite Mountain batholith.

Paleomagnetic results from the Granite Mountain batholith are most consistent with, but not rigorously supportive of, theories which postulate minimal tectonic motion for the YTT relative to North America since the Early Jurassic. Remanence **A** is not as well constrained as the dual-polarity results from the Big Creek batholith (Symons et al., 2000b). Additionally, the dyke- and contact-borne remanence **C** is not likely to have averaged out paleosecular variation of the Earth's magnetic field.

A major issue for future discussion is the poor agreement between the Carmacks Group paleomagnetism, which implies ~2000 km of polewards transport for the YTT and Stikine terranes since 70 Ma (Johnston et al., 1996a; Wynne et al., 1998), and paleomagnetic results from YTT intrusions, especially of 70 Ma age, which all imply minimal transport of the YTT from Early Jurassic to Eocene time (Symons et al., 2000a,b; McCausland et al., 2000a,b; 2001). Forthcoming results from other Jurassic, Cretaceous and Eocene units, along with a regional geological synthesis should further illuminate the YTT's motion history.

## ACKNOWLEDGEMENTS

The authors express their gratitude to the Yukon Geology Program for essential assistance in this study. Harmen Keiser of Trans North Air provided safe and efficient helicopter support. Rachel Comber did measurements of magnetic susceptibility. Steve Johnston, Carmel Lowe, Currie Palmer and Maurice Colpron offered helpful discussions, and Yves Thibault provided guidance with the electron microprobe. The authors acknowledge financial support from LITHOPROBE-SNorCLE to DTAS and the Ontario Government Scholarship for Science and Technology to P. McCausland. This is also known as LITHOPROBE contribution #1265.

## REFERENCES

Anderson, J.L. and Smith, D.R., 1995. The effects of temperature and $f_{O_2}$ on the Al-in-hornblende barometer. American Mineralogist, vol. 80, p. 549-559.

Besse, J. and Courtillot, V., 1991. Revised and synthetic apparent polar wander paths of the African, Eurasian, North American and Indian Plates, and true polar wander since 200 Ma. Journal of Geophysical Research, vol. 96, p. 4029-4050.

Blundy, J.D. and Holland, T.J.B., 1990. Calcic amphibole equilibria and a new amphibole-plagioclase geothermometer. Contributions to Mineralogy and Petrology, vol. 104, p. 208-224.

Dunlop, D.J. and Argyle, K.S., 1991. Separating multidomain and single-domain-like remanences in pseudo-single-domain magnetites (215-540 nm) by low-temperature demagnetization. Journal of Geophysical Research, vol. 96, p. 2007-2017.

Dunlop, D.J. and Ozdemir, O., 1997. Rock Magnetism: Fundamentals and Frontiers. Cambridge Studies in Magnetism, Cambridge University Press, 573 p.

Gordey, S.P. and Makepeace, A.J. (comps.), 2001. Bedrock Geology, Yukon Territory. Geological Survey of Canada, Open File 3754 and Exploration and Geological Services Division, Yukon Region, Indian and Northern Affairs Canada, Open File 2001-1, 1:1 000 000 scale map.

Hammarstrom, J.M. and Zen, E., 1986. Aluminum in hornblende: an empirical igneous geobarometer. American Mineralogist, vol. 71, p. 1297-1313.

Harris, M.J., Symons, D.T.A., Blackburn, W.H. and Hart, C.J.R., 1999. Paleomagnetic and geobarometric study of the Late Cretaceous Mount Lorne stock, southern Yukon Territory. Canadian Journal of Earth Sciences, vol. 36, p. 905-915.

Irving, E., Wynne, P.J., Thorkelson, D.J. and Schiarizza, P., 1996. Large (1000 to 4000 km) northward movements of tectonic domains in the northern Cordillera, 83 to 45 Ma. Journal of Geophysical Research, vol. 101, p. 17901-17916.

Johnston, S.T., 1999. Large-scale coast-parallel displacements in the Cordillera: a granitic solution to a paleomagnetic dilemma. Journal of Structural Geology, vol. 21, p. 1103-1108.

Johnston, S.T., Wynne, P.J., Francis, D., Hart, C.J.R., Enkin, R.J. and Engebretson, D.C., 1996a. Yellowstone in Yukon: the Late Cretaceous Carmacks Group. Geology, vol. 24, p. 997-1000.

Johnston, S.T., Mortensen, J.K. and Erdmer, P., 1996b. Igneous and metaigneous age constraints for the Aishihik metamorphic suite, southwest Yukon. Canadian Journal of Earth Sciences, vol. 33, p. 1534-1555.

Kirschvink, J.L., 1980. The least squares line and plane and the analysis of paleomagnetic data. Geophysical Journal of the Royal Astronomical Society, vol. 62, p. 699-718.

Leake, B.E. (chairperson) et al., 1997. Nomenclature of amphiboles: report of the Subcommittee on Amphiboles of the International Mineralogical Association, Commission on New Minerals and Mineral Names. Canadian Mineralogist, vol. 35, p. 219-246.

Lowe, C., Horner, R.B., Mortensen, J.K., Johnston, S.T. and Roots, C.F., 1994. New geophysical data from the northern Cordillera: preliminary interpretations and implications for the tectonics and deep geology. Canadian Journal of Earth Sciences, vol. 31, p. 891-904.

McCausland, P.J.A., Symons, D.T.A., Hart, C.J.R. and Blackburn, W.H., 2000a. Minimal geotectonic motion of the Yukon-Tanana Terrane relative to North America: Preliminary paleomagnetic results from the Dawson Range batholith. LITHOPROBE, Slave-Northern Cordillera Lithospheric Evolution (SNorCLE) and Cordilleran Tectonics Workshop, Report of the Combined Meeting, Calgary, Alberta, LITHOPROBE Report 72, p. 146-154.

McCausland, P.J.A., Symons, D.T.A., Hart, C.J.R. and Blackburn, W.H., 2000b. Minimal geotectonic motion of the Yukon-Tanana Terrane relative to North America: Preliminary paleomagnetic results from two Late Cretaceous intrusions. GeoCanada 2000, Calgary, Alberta.

McCausland, P.J.A., Symons, D.T.A., Hart, C.J.R. and Blackburn, W.H., 2001. Paleomagnetic study of the Late Cretaceous Seymour Creek stock, Yukon: Minimal geotectonic motion of the Yukon-Tanana Terrane. *In:* Yukon Exploration and Geology 2000, D.S. Emond and L.H. Weston (eds.), Exploration and Geological Services Division, Yukon Region, Indian and Northern Affairs Canada, p. 207-216.

McClelland, W.C., Gehrels, G.E. and Saleeby, J.B., 1992. Upper Jurassic-Lower Cretaceous basinal strata along the Cordilleran Margin: Implications for the accretionary history of the Alexander-Wrangellia-Peninsular Terrane. Tectonics, vol. 11, no. 4, p. 823-835.

Mihalynuk, M.G., Nelson, J. and Diakow, L.J., 1994. Cache Creek terrane entrapment: oroclinal paradox within the Canadian Cordillera. Tectonics, vol. 13, no. 2, p. 575-595.

Mortensen, J.K., 1992. Pre-Mid-Mesozoic tectonic evolution of the Yukon-Tanana Terrane, Yukon and Alaska. Tectonics, vol. 11, no. 4, p. 836-853.

Mortensen, J.K., Emon, K., Johnston, S.T. and Hart, C.J.R., 2000. Age, geochemistry, paleotectonic setting and metallogeny of Late Triassic-Early Jurassic intrusions in the Yukon and eastern Alaska: A preliminary report. *In:* Yukon Exploration and Geology 2000, D.S. Emond and L.H. Weston (eds.), Exploration and Geological Services Division, Yukon Region, Indian and Northern Affairs Canada, p. 139-144.

Pullaiah, G.E., Irving, E., Buchan, K.L. and Dunlop, D.J., 1975. Magnetization changes caused by burial and uplift. Earth and Planetary Science Letters, vol. 28, p. 133-143.

Schmidt, M.W., 1992. Amphibole composition in tonalite as a function of pressure and experimental calibration of the Al-in-hornblende barometer. Contributions to Mineralogy and Petrology, vol. 110, p. 304-310.

Schumacher, J.C., 1997. The estimation of the proportion of ferric iron in the electron-microprobe analysis of amphiboles. Canadian Mineralogist, vol. 35, p. 238-246 (Appendix 2).

Smuk, K.A., Williams-Jones, A.E. and Francis, D., 1997. The Carmacks hydrothermal event: an alteration study in the southern Dawson Range, Yukon. *In:* Yukon Exploration and Geology 1996, Exploration and Geological Services Division, Yukon Region, Indian and Northern Affairs Canada, p. 92-106.

Stevens, R.D., DeLabio, R.N. and LaChance, G.R., 1982. Age determinations and geological studies, K-Ar isotopic ages. Geological Survery of Canada, Report 15, p 74.

Symons, D.T.A., Harris, M.J., Gabites, J.E. and Hart, C.J.R., 2000a. Eocene (51 Ma) end to northward translation of the Coast Plutonic Complex: paleomagnetism and K-Ar dating of the White Pass Dikes. Tectonophysics, vol. 326, p. 93-109.

Symons, D.T.A., Williams, P.R., McCausland, P.J.A., Harris, M.J., Hart, C.J.R. and Blackburn, W.H., 2000b. Paleomagnetism and geobarometry of the Big Creek Batholith suggests that Yukon-Tanana Terrane has been a parautochthon since Early Jurassic. Tectonophysics, vol. 326, p. 57-72.

Tempelman-Kluit, D.J., 1984. Geology of Laberge (105E) and Carmacks (115I) map areas, Yukon. Geological Survey of Canada, Open File 1101.

Warnock, A.C., Kodama, K.P. and Zeitler, P.K., 2000. Using thermochronology and low-temperature demagnetization to accurately date Precambrian paleomagnetic poles. Journal of Geophysical Research, vol. 105, no. B8, p. 19435-19453.

Wynne, P.J., Enkin, R.J., Baker, J., Jojnston, S.T. and Hart, C.J.R., 1998. The big flush: paleomagnetic signature of a 70 Ma regional hydrothermal event in displaced rocks of the northern Canadian Cordillera. Canadian Journal of Earth Sciences, vol. 35, p. 657-671.

Zijderveld, J.D.A., 1967. A.C. demagnetization of rocks: analysis of results. *In:* Methods in Paleomagnetism, D.E.W. Collinson, K.K. Crier and S.K. Runcorn (eds.), Elsevier, Amsterdam, The Netherlands, p. 254-286.

# Lead isotopic constraints on the metallogeny of southern Wolf Lake, southeastern Teslin and northern Jennings River map areas, Yukon and British Columbia: Preliminary results

*James K. Mortensen*[1] *and Janet E. Gabites*[2]
*University of British Columbia*[3]

Mortensen, J.K. and Gabites, J.E., 2002. Lead isotopic constraints on the metallogeny of southern Wolf Lake, southeastern Teslin and northern Jennings River map areas, Yukon and British Columbia: Preliminary results. *In:* Yukon Exploration and Geology 2001, D.S. Emond, L.H. Weston and L.L. Lewis (eds.), Exploration and Geological Services Division, Yukon Region, Indian and Northern Affairs Canada, p. 179-188.

## ABSTRACT

Southern Wolf Lake (105B), southeastern Teslin (105C) and northern Jennings River (104O) map areas contain a wide variety of styles of mineralization, including carbonate replacement deposits, skarns, greisens and veins, as well as several apparently stratiform occurrences that have been interpreted to be syngenetic in origin. Lead isotopic compositions of galena and other sulphide minerals from many of these occurrences help to constrain the nature and approximate age of individual occurrences. Preliminary results of this study indicate that most mineralization in the area, including that at Dan, Logan, Logtung, Arsenault, Fiddler and Hart occurrences, is epigenetic and of Mesozoic to Early Tertiary age. Galena analyses from the Cabin Lake and Mor occurrences in southwestern Wolf Lake and southeastern Teslin map areas, respectively, yield relatively non-radiogenic compositions that are consistent with a syngenetic (VMS) origin and broadly Devono-Mississippian age.

## RÉSUMÉ

Les régions représentées par la partie sud du feuillet de Wolf Lake (105B), par la partie sud-est du feuillet de Teslin (105C) et par la partie nord du feuillet de Jennings River (104O) renferment une grande variété de types de minéralisation, y compris des gisements de remplacement des carbonates, des skarns, des greisens et des veines, ainsi que plusieurs occurrences apparemment stratiformes, que l'on estime être d'origine syngénétique. Les teneurs en isotopes du plomb dans la galène et des autres minéraux sulfurés d'un grand nombre de ces occurrences aident à en déterminer la nature et l'âge approximatif. Les résultats préliminaires de cette étude indiquent que la plupart des minéralisations dans la région, y compris celles des gisements de Dan, Logan, Logtung, Arsenault, Fiddler et Hart, sont épigéniques et datent du Mésozoïque au Tertiaire précoce. Des analyses de la galène provenant des occurrences de Mor et de Cabin Lake, situées respectivement dans la région sud-ouest de la carte de Wolf Lake et dans la région sud-est de la carte de Teslin, indiquent que ces occurrences sont relativement peu radiogéniques et de compositions compatibles avec une origine syngénétique (SMV) et un âge approximatif du Dévono-Mississippien.

---

[1] *jmortens@eos.ubc.ca*

[2] *jgabites@eos.ubc.ca*

[3] *Department of Earth & Ocean Sciences, University of British Columbia, 6339 Stores Road, Vancouver, British Columbia, Canada V6T 1Z4*

## INTRODUCTION

A wide variety of styles of mineralization are present in southern Wolf Lake (105B), southeastern Teslin (105C) and northern Jennings River (104O) map areas (Fig. 1). Carbonate replacement deposits, skarns, porphyries, greisens, veins and stratabound deposits are all represented. Recent mapping has greatly improved our understanding of the geology of this area, and in particular, the geological setting of the various mineral occurrences. The area is extensively intruded by plutons of several different ages, and some occurrences are clearly intrusion-related (e.g., skarns and porphyries). However, the exact relationship between mineralization and magmatism is not well constrained. In addition, the question of whether some of the stratabound occurrences (e.g., Dan, Yukon MINFILE, 2001, 105B 027; Cabin Lake) are intrusion-related or syngenetic in origin is in dispute. In this study, we use Pb isotopic compositions of sulphide minerals to constrain the possible age and origin of many occurrences in the study area. The authors' isotopic database includes previously published analyses

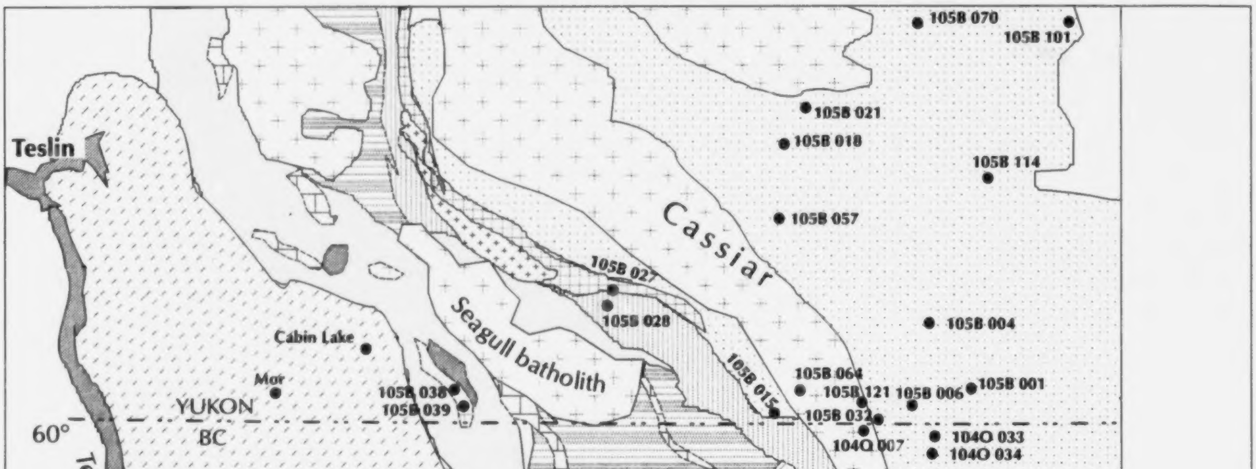
105B 070
105B 101
105B 021
105B 018
105B 114
Teslin
Cassiar
105B 057
105B 027
105B 028
Seagull batholith
105B 004
Cabin Lake
Mor
105B 038
105B 039
YUKON
BC
60°
105B 015
105B 064
105B 121
105B 006
105B 001
105B 032
104O 007
104O 033
104O 034
104O 004
104O 003, 038, 039, 048
Teslin Lake
104O 011
batholith
0
50
Km
132°
130°
Cretaceous plutons
Jurassic plutons
Permian Ram stock
Triassic Teh Formation
Klinkit Succession
Screw Creek Limestone
Swift River Succession
Big Salmon Complex
Dorsey Assemblage
Ram Creek Assemblage
Cassiar Platform

*Figure 1. Simplified geological map of the study area, showing the main supracrustal assemblages and plutonic suites present, and the locations of the main mineral occurrences discussed in the paper. Occurrences are labeled with their Yukon MINFILE (2001) occurrence numbers. Base geological map compiled by C. Roots, 2001*

as well as a number of new analyses. This contribution reports initial results of an on-going study, which in the future will be expanded to include Pb isotopic analyses of whole rocks and igneous feldspars, to better constrain possible source reservoirs for metals in the various mineral occurrences.

## GEOLOGICAL SETTING

The main supracrustal assemblages in the study area include the Big Salmon Complex and the Ram Creek, Dorsey, Swift River and Klinkit assemblages, all considered to be part of either the Yukon-Tanana Terrane, or adjacent miogeoclinal rocks of the Cassiar Terrane. The supracrustal rocks are intruded by at least three distinct suites of intrusions (Fig. 1). Brief lithological descriptions of each of the main supracrustal assemblages given below are summarized from Harms and Stevens (1996), Mihalynuk et al. (1998), Nelson (2000), Roots et al. (2000), Mihalynuk and Devine (2001), and Nelson et al. (2001).

The *Big Salmon Complex* comprises Late Devonian to late Mississippian mafic and minor felsic metavolcanic rocks, quartz-rich metaclastic rocks, and minor carbonate and metamorphosed chert-exhalite ('crinkled chert'). Broadly coeval, mafic to felsic intrusive rocks are also locally abundant. The *Ram Creek assemblage* is a package of mafic to felsic metavolcanic rocks of mainly Mississippian age that are locally interlayered with minor metasedimentary rocks including marble, meta-argillite and meta-chert. The *Dorsey assemblage* comprises highly deformed, quartz-rich metaclastic rocks, marble, mafic and felsic metavolcanic rocks (mainly of Mississippian age), and intermediate to felsic intrusions. Most metaplutonic rocks in the Dorsey assemblage yield Mississippian U-Pb ages; however, a large unfoliated body named the Ram stock gives a Late Permian U-Pb age (Mortensen, unpublished data). The *Swift River succession* is a pre-late Mississippian package of metachert, metatuff, coarse metaclastic rocks and marble. The *Screw Creek limestone* is a thick, laterally continuous band of late Mississippian to early Pennsylvanian limestone that stratigraphically overlies the Swift River succession. The Klinkit assemblage comprises mafic to intermediate volcanic and epiclastic rocks that interfinger with and overlie the Screw Creek limestone. Late Triassic, thin-bedded clastic rocks with minor chert and limestone unconformably overlie the Klinkit rocks.

Late Proterozoic through Late Triassic carbonate and siliciclastic strata of the Cassiar Platform dominate the eastern part of the study area. The Cassiar Terrane is a portion of the Cordilleran miogeoclinal margin that has been displaced approximately 425 km northwestward along the Tintina fault zone.

Post-tectonic intrusions of Early to mid-Cretaceous age (e.g., Cassiar batholith, Seagull batholith, Marker Lake batholith) occur throughout the study area (Fig. 1). Several mafic to intermediate plutons of Early Jurassic age are also present, as well as a single large, mainly unfoliated, felsic intrusion of Late Permian age (the Ram stock).

## ANALYTICAL METHODS

Small clean cubes of galena collected from various mineral occurrences were hand-picked, washed and dissolved in dilute hydrochloric acid, and approximately 10-25 nanograms of the lead in chloride form was loaded directly onto a rhenium filament. Trace sulphide samples were hand-picked and then leached in dilute hydrochloric acid to remove surface contamination before dissolution in nitric acid. The samples were passed through ion exchange columns in hydrobromic acid, and the Pb was stripped using hydrochloric acid. Isotopic compositions were measured using a Faraday collector on a modified VG54R thermal ionization mass spectrometer. The measured ratios were corrected for instrumental mass fractionation of 0.12% per mass unit based on repeated measurements of the N.B.S. SRM 981 Standard Isotopic Reference Material (composition from Thirlwall, 2000). Errors reported in Table 1 were obtained by propagating all mass fractionation and analytical uncertainties through the calculation. The average total procedural blank for the trace Pb chemistry was 300 ± 5 picograms.

## INITIAL RESULTS OF THE STUDY

Samples from which lead isotopic compositions were determined in this study and previous work (Godwin et al., 1988) represent most styles of mineralization in the study area. A total of 77 analyses are available from 26 individual deposits and occurrences. Table 1 provides information for each occurrence for which Pb isotopic data are available, including the MINFILE number, location, style of mineralization, host assemblage and the age and composition of the immediate host rocks (all information taken from Yukon MINFILE, 2001, and British

Columbia MINFILE, 2001). Appendix 1 lists new Pb isotopic analyses generated during this study; other data discussed here are from Godwin et al. (1988). The complete Pb isotopic data set is plotted on $^{208}$Pb/$^{204}$Pb *vs.* $^{206}$Pb/$^{204}$Pb, $^{207}$Pb/$^{204}$Pb *vs.* $^{206}$Pb/$^{204}$Pb and $^{208}$Pb/$^{206}$Pb *vs.* $^{207}$Pb/$^{206}$Pb diagrams in Figure 2. The latter plot is used in order to eliminate uncertainties associated with measurement of the relatively small $^{204}$Pb peak. This source of error can be significant in some of the early analyses reported in Godwin et al. (1988), and employing the $^{208}$Pb/$^{206}$Pb *vs.* $^{207}$Pb/$^{206}$Pb plot commonly results in a tighter clustering of closely related analyses and a clearer discrimination between unrelated analyses. The data on all the plots is shown relative to the 'shale curve', which is a model average Pb isotopic growth curve derived for miogeoclinal strata of Ancestral North America (Godwin and Sinclair, 1982). Lead isotopic analyses of sulphides from syngenetic base metal deposits within the Yukon-Tanana Terrane in Yukon and Alaska define an average growth curve for this terrane that is very similar to the 'shale curve' (Mortensen, unpublished data).

***Table 1.*** *Locations and brief descriptions of mineral occurrences from which lead isotopic analyses are available (summarized from current Yukon MINFILE, 2001 and BC MINFILE, 2001 descriptions).*

| Deposit name | Map sheet/ MINFILE no. | Lat. | Long. | Host lithology | Host age | Deposit type | Tectonic element |
|---|---|---|---|---|---|---|---|
| Arsenault | 104O 011 | 59.81 | 131.71 | 'crinkled chert' | Early Carboniferous | epigenetic | Big Salmon Complex |
| Midway (Silvertip) | 104O 003 | 59.92 | 130.35 | McDame Group limestone | Late Devonian | replacement | Cassiar Platform |
| Amy (Marbaco) | 104O 004 | 59.93 | 130.50 | marble, schist, Kechika Group | Cambrian-Ordovician | vein | Cassiar Platform |
| Luck Allochthon | 104O 033 | 59.98 | 130.45 | quartz diorite | Cretaceous | vein | Sylvester |
| Rancheria | 104O 034 | 59.92 | 130.48 | skarn in limestone, near Cassiar batholith | Ordovician - Devonian | skarn | Cassiar Platform |
| Midway (Discovery) | 104O 038 | 59.93 | 130.33 | McDame Gp limestone | Late Devonian | replacement | Cassiar Platform |
| Tootsee Star | 104O 039 | 59.90 | 130.30 | chert, limestone, argillite | Mississippian to Permian | vein | Cassiar Platform |
| Silverknife | 104O 048 | 59.93 | 130.36 | Rosella Fm. marble and Kechika Gp. hornfels | Lower Cambrian - Ordovician | replacement | Cassiar Platform |
| Star (YP) | 105B 001 | 60.06 | 130.37 | dolomite, near Cassiar batholith | Lower Cambrian | vein/ stratabound | Cassiar Platform |
| A and B | 105B 003 | 60.12 | 130.45 | limestone, near Cassiar batholith | Cambrian | vein | Cassiar Platform |
| Fiddler | 105B 004 | 60.13 | 130.43 | phyllite and limestone, near Cassiar batholith | Cambrian | vein | Cassiar Platform |
| Lola | 105B 007 | 60.01 | 130.48 | quartz diorite, Cassiar batholith | Cretaceous | vein | Cassiar batholith |
| Dale Mountain | 105B 007 | 60.01 | 130.48 | fault zone in Cassiar batholith | Cretaceous | vein | Cassiar batholith |
| Blackrock | 105B 015 | 60.01 | 130.78 | greenstone/Cassiar batholith | Devono-Mississipian | vein | Cassiar Platform |
| Hart | 105B 021 | 60.33 | 130.74 | Atan Gp.? Bi-qtz and calcareous schist near Cassiar batholith | Cambrian | skarn/vein | Cassiar Platform |
| Dan (Bar) | 105B 027 | 60.17 | 131.13 | garnet-diopside skarn along shear contact meta-tuff and marble | Permo-Carboniferous | skarn | Ram Creek assemblage |
| Bom | 105B 028 | 60.15 | 131.21 | hornfelsed clastic and carbonates | Carboniferous: Cretaceous related | skarn | Swift River assemblage |
| Logjam | 105B 038 | 60.02 | 131.60 | quartz diorite | Cretaceous | vein | Klinkit succession |
| Logtung | 105B 039 | 60.01 | 131.60 | banded argillite and quartzite, cut by quartz monzonite | Pennsylvanian | vein/ porphyry | Klinkit succession |
| CMC | 105B 057 | 60.29 | 130.73 | granodiorite | Cretaceous | vein | Cassiar batholith |
| MC Ridge | 105B 088 | 60.20 | 131.74 | hornfelsed clastic and carbonate near Seagull batholith | Carboniferous: Cretaceous related | skarn | Klinkit succession |
| Logan | 105B 070 | 60.50 | 130.47 | biotite schist cut by granodiorite | Cretaceous-related | vein | Marker Lake batholith |
| Wolf (Cordilleran) | 105B 101 | 60.55 | 130.05 | quartz biotite schist, calcareous phyllite | Lower Cambrian | replacement | Cassiar Platform |
| Meister | 105B 114 | 60.30 | 130.33 | phyllite, marble | Lower Cambrian | replacement | Cassiar Platform |
| Cabin Lake | 105B/4 | 60.10 | 131.78 | felsic schist (metavolcanic rock?) | Paleozoic? | stratiform | Big Salmon Complex |
| Mor | 105C/1 | 60.08 | 132.08 | felsic schist (metavolcanic rock?) | Paleozoic? | stratiform | Big Salmon Complex |

## *Carbonate replacement, skarn and vein mineralization*

Epigenetic mineral occurrences within the study area have been described by numerous authors, including Abbott (1983), Bremner and Liverton (1990), Germann et al. (1992) and D'el-Rey Silva et al. (2001). The Midway deposit (BC MINFILE, 2001, 104O 003, 038) and other epigenetic base metal occurrences in the immediate area of the deposit (Silverknife - 104O 048 and Amy - 104O 004, BC MINFILE, 2001) are massive sulphide replacements and veins in Lower Paleozoic carbonate rocks. Lead isotopic analyses from Midway, and most analyses from Amy, cluster near the shale curve and correspond to model ages of ~100 Ma (Fig. 2). One possible interpretation of these data is that metals in Midway and Amy are magmatic in origin and were derived from Early to mid-Cretaceous intrusions in the area. The tight clustering of the data from Midway and Amy indicates that lead in these deposits was either derived from a single homogeneous source (such as a body of magma), or derived from multiple sources and completely homogenized by a very large and vigorous hydrothermal circulation system. Analyses from the Silverknife occurrence are slightly more radiogenic (relatively high measured $^{206}Pb/^{204}Pb$ ratios), and plot on the shale curve in Figure 2. This suggests that Silverknife mineralization is slightly younger than that at Midway and Amy, and/or that metals in the deposits were derived from different sources.

Most other epigenetic occurrences in the study area (including skarns and porphyry occurrences that are clearly intrusion-related) also yield model ages that are younger than their immediate host rocks. There is considerable scatter in the data, however, which suggests that Pb was derived from several isotopically

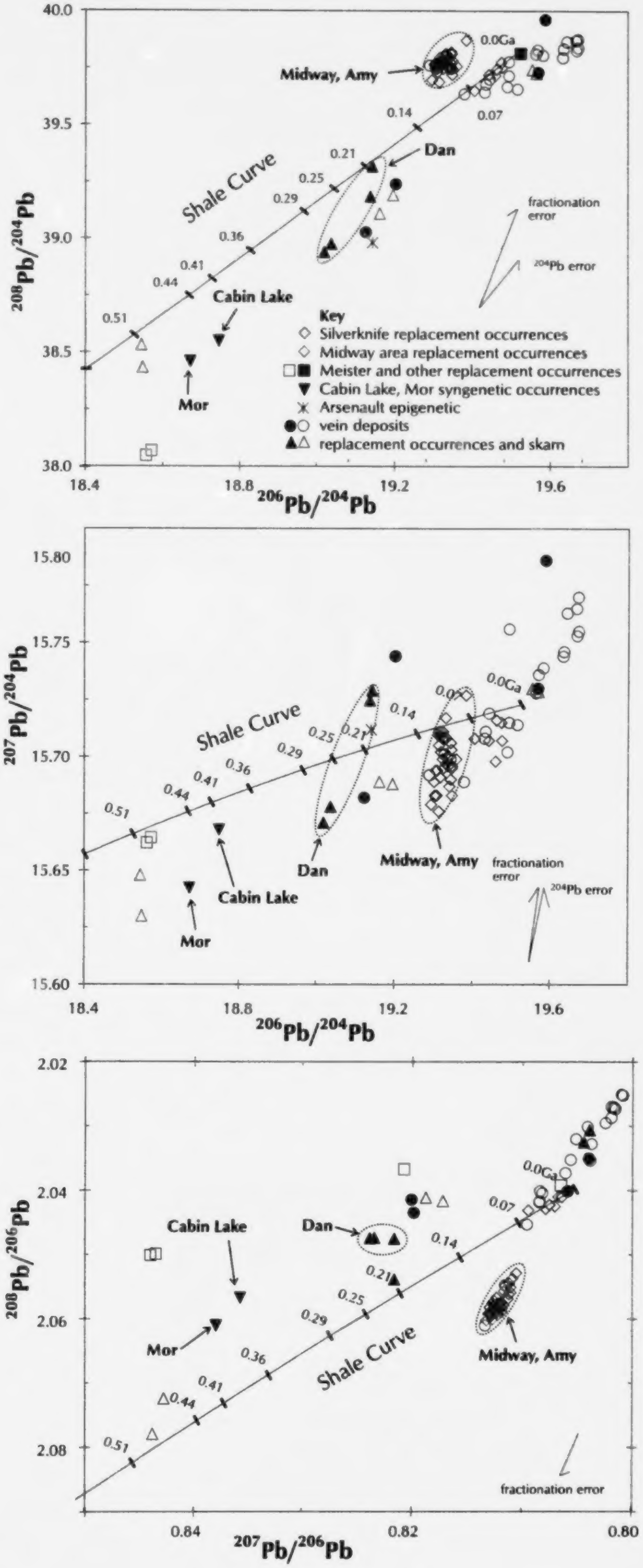

***Figure 2.*** *Plot of $^{208}Pb/^{204}Pb$ vs. $^{206}Pb/^{204}Pb$, $^{207}Pb/^{204}Pb$ vs. $^{206}Pb/^{204}Pb$, and $^{208}Pb/^{206}Pb$ vs. $^{207}Pb/^{206}Pb$ for sulphide minerals from the study area. Included are previously published data from Godwin et al. (1988) and data from this study. Analyses from occurrences within the Cassiar Platform are shown in open symbols and those from the Yukon-Tanana Terrane are shown as closed symbols.*

distinct sources (possibly magmatic Pb plus Pb leached from sedimentary and/or volcanic wall rocks of various ages and compositions). Alternatively, intrusion-related mineralization may be associated with more than one magmatic suite. Many of the vein and skarn occurrences are spatially associated with the Early and mid-Cretaceous intrusions in the area; however, Early Jurassic intrusions and at least one large Late Permian intrusion are also present in the area and may have provided a source of metals.

The MC Ridge and Meister occurrences (Yukon MINFILE, 2001, 105B 088 and 105B 114, respectively) comprise skarn and carbonate replacement style mineralization, respectively, within Lower Paleozoic phyllite and carbonate of the Cassiar Platform (Table 1). Duplicate analyses of a single sample from each occurrence yield surprisingly non-radiogenic compositions (Appendix 1; Fig. 2). Two other analyses from the MC Ridge occurrence give compositions more similar to other epigenetic occurrences in the area. The implications of the non-radiogenic analyses from these two occurrences are uncertain. Distal, intrusion-related carbonate replacement deposits with low base metal contents, such as the Ketza River deposit, have been shown to have relatively scattered Pb isotopic compositions that approach those of the host rocks that have been replaced (Fonseca, 1998). On the other hand, veins rich in base metals, such as those at the Iona Silver mine, thought to be genetically closely associated with the replacement style mineralization at Ketza River, yield tightly clustered analyses that are interpreted as more representative of Pb of magmatic derivation (Fonseca, 1998). The non-radiogenic compositions of the Meister sulphides and some from the MC Ridge occurrence may therefore indicate that metals in these occurrences were derived largely from the host rocks. Further work is required to test this model.

### *Stratabound and stratiform mineralization*

Several occurrences within the study area are broadly conformable with enclosing strata and have been postulated as syngenetic in origin. Included in this group are the Arsenault occurrence (BC MINFILE, 2001, 104O 111) which is hosted in the 'crinkled chert' (metamorphosed chert exhalite) unit of the Big Salmon complex, the Cabin Lake and Mor occurrences (no MINFILE numbers assigned) hosted by felsic metavolcanic rocks of the Big Salmon Complex, and the Dan (Bar) occurrence (Yukon MINFILE, 2001, 105B 027), which is hosted by marble, calc-silicate, metapelite and metatuffaceous rocks of the Ram Creek assemblage. Analyses of galena from the Cabin Lake and Mor occurrences (Appendix 1) fall somewhat below the shale curve and yield broadly Devono-Mississippian model ages. This is consistent with the inferred age of the host strata and thus provides strong support for a syngenetic origin for this mineralization, as has been proposed by E. Balon and W. Jakubowski (pers. comm., 2001). An analysis of sulphides from the Arsenault occurrence, however, yields a much more radiogenic Pb composition (Appendix 1; Fig. 2), suggesting that this occurrence is more likely to be epigenetic in nature.

The Dan occurrence comprises three roughly conformable bands of massive sphalerite, pyrrhotite and magnetite with minor galena that occur along the contact between underlying massive marble and calc-silicate rock, and overlying metatuffaceous rocks (Table 1; Bremner and Liverton, 1990; D'el Rey Silva et al., 2001). Previous workers have suggested a syngenetic origin for the mineralization, based, in part, on the presence of metatuffaceous rocks in the immediate hanging wall. Bremner and Liverton (1990), however, presented textural and structural evidence, observable in the field, that argues for an epigenetic, possibly intrusion-related origin. Four Pb isotopic analyses of galena and pyrrhotite from the Dan deposit have been carried out (Appendix 1), and clearly do not support the syngenetic model (Fig. 2). The Dan analyses, together with the single analysis of sulphide minerals from the Arsenault and two other analyses from veins and skarns, form a loose cluster that is less radiogenic than Pb isotopic compositions of most other epigenetic occurrences in the study area (Fig. 2). This cluster of analyses corresponds to broadly mid-Triassic to mid-Jurassic model ages. Both the Dan and Arsenault occurrences are located near Early Jurassic intrusions, and it is possible that these occurrences are temporally and genetically associated with the Early Jurassic magmatism.

## DISCUSSION

The extensive Pb isotopic database now available for sulphide occurrences from throughout the study area provides a powerful tool for understanding the metallogeny of this complex region. In particular, it makes it possible to discriminate with some confidence between a syngenetic and epigenetic origin for specific occurrences (providing the geology of the area is reasonably well understood). In some instances, the data also gives a rough indication of the age of individual occurrences. In order to gain a more complete understanding of the nature and origin of mineralization in this area, however, the Pb isotopic composition of potential source reservoirs for the metals (e.g., intrusive rocks of different ages, or sedimentary or volcanic host rocks, particularly for replacement-style mineralization) must be determined. A Pb isotopic study of igneous feldpars in intrusive rocks of various ages in the study area is now underway to constrain the possible composition(s) of magmatic Pb that may be present in mineral occurrences.

## ACKNOWLEDGMENTS

We thank Ed Balon of Fairfield Minerals for contributing samples from the Cabin Lake and Mor occurrences and for information on the Dan occurrence. The paper benefited from a review by Dick Tosdal.

## REFERENCES

Abbott, J.G., 1983. Silver-bearing veins and replacement deposits of the Rancheria District. *In:* Yukon Exploration and Geology 1983, Exploration and Geological Services Division, Yukon Region, Indian and Northern Affairs Canada, p. 34-44.

BC MINFILE, 2001. B.C. Ministry of Energy and Mines, Open File 2001-1b, CD-ROM.

Bremner, T.J. and Liverton, T., 1990. Crescent, Dan (property descriptions). *In:* Yukon Exploration and Geology 1990, Exploration and Geological Services Division, Yukon Region, Indian and Northern Affairs Canada, p. 25-30.

D'el-Rey Silva, L.J.H., Liverton, T., Paradis, S. and Roots, C., 2001. A structural analysis of the upper Swift River area (105B/3), Yukon, Part 1: Dan Zn occurrence and implications for sulphide mineralization. *In:* Yukon Exploration and Geology 1999, D.S. Emond and L.H. Weston (eds.), Exploration and Geological Services Division, Yukon Region, Indian and Northern Affairs Canada, p. 289-300.

Fonseca, A.L., 1998. Origin of carbonate hosted gold rich replacement deposits and related mineralization styles in the Ketza River deposit, Yukon Territory. Unpublished M.Sc. thesis, University of British Columbia, 136 p.

Germann, A., Friedrich, G. and Schattner, R., 1992. Ore mineralogy and formation conditions of vein and replacement-type Pb-Zn-Ag occurrences, Logan and YP properties, Rancheria District, Yukon. *In:* Yukon Geology Volume 3, Exploration and Geological Services Division, Yukon Region, Indian and Northern Affairs Canada, p. 37-44.

Godwin, C.I. and Sinclair, A.J., 1982. Average lead isotope growth curves for shale-hosted zinc-lead deposits, Canadian Cordillera. Economic Geology, vol. 77, p. 675-690.

Godwin, C.I., Gabites, J.E. and Andrew, A., 1988. Leadtable: A galena lead isotope database for the Canadian Cordillera, with a guide to its use by explorationists. B.C. Ministry of Energy, Mines and Petroleum Resources, Paper 1988-4, 188 p.

Harms, T.A. and Stevens, R.A., 1996. Assemblage analysis of the Dorsey Terrane. Slave-Northern Cordillera Lithospheric Evolution (SNORCLE) and Cordilleran Tectonics Workshop, Report of the 1996 Combined Meeting, p. 199-201.

Mihalynuk, M., Nelson, J.L. and Friedman, R.M., 1998. Regional geology and mineralization of the Big Salmon Complex (104N NE and 104O NW). *In:* Geological Fieldwork 1997, B.C. Ministry of Employment and Investment, Geological Survey Branch, Paper 1998-1, p. C-1–C-20.

Mihalynuk, M. and Devine, F., 2001. Big Salmon Complex between Teslin and Swan lakes. Unpublished 2001 NATMAP Field Trip Guidebook, p. 16-24.

Nelson, J.L., 2000. Ancient Pacific Margins Part VI: Still heading south: Potential hosts in the eastern Dorsey Terrane, Jennings River (104O/1, 7, 8, 9, 10). *In:* Geological Fieldwork 1999, B.C. Ministry of Employment and Investment, Geological Survey Branch, Paper 2000-1, p. 107-126.

Nelson, J.L., Roots, C. and Mihalynuk, M., 2001. Allochthonous units in the B.C.-Yukon border area east of Teslin Fault and west of the Cassiar Batholith. *In:* Unpublished 2001 NATMAP Field Trip Guidebook, 74 p.

Roots, C.F., de Keijzer, M. and Nelson, J.L., 2000. Wolf Lake project: Revision mapping of Dorsey Terrane assemblages in the upper Swift River area. *In:* Yukon Exploration and Geology 1999, D.S. Emond and L.H. Weston (eds.), Exploration and Geological Services Division, Yukon Region, Indian and Northern Affairs Canada, p. 115-125.

Thirlwall, M.F., 2000. Interlaboratory and other errors in Pb isotope analyses investigated using a $^{207}$Pb - $^{204}$Pb double spike. Chemical Geology, vol. 163, p. 299-322.

Yukon MINFILE, 2001. Exploration and Geological Services Division, Yukon Region, Indian and Northern Affairs Canada.

## APPENDIX 1. Pb ISOTOPE ANALYTICAL DATA

| Deposit name | Mineral | $^{206}$Pb/ $^{204}$Pb | Pb64 % err | $^{207}$Pb/ $^{204}$Pb | Pb74 % err | $^{208}$Pb/ $^{204}$Pb | Pb84 % err | $^{207}$Pb/ $^{206}$Pb | Pb76 % err | $^{208}$Pb/ $^{206}$Pb | Pb86 % err | Analyst |
|---|---|---|---|---|---|---|---|---|---|---|---|---|
| Arsenault | CP | 19.142 | 0.25 | 15.712 | 0.25 | 38.986 | 0.25 | 0.821 | 0.02 | 2.037 | 0.03 | GA |
| Midway (Silvertip)-012a | GL | 19.345 | 0.02 | 15.706 | 0.01 | 39.818 | 0.03 | 0.8119 | 0.00 | 2.058 | 0.00 | GA |
| Midway (Silvertip)-012b | GL | 19.325 | 0.04 | 15.699 | 0.03 | 39.747 | 0.05 | 0.8124 | 0.00 | 2.057 | 0.00 | GA |
| Midway (Silvertip)-013 | GL | 19.321 | 0.00 | 15.702 | 0.01 | 39.771 | 0.00 | 0.8127 | 0.00 | 2.059 | 0.00 | GA |
| Midway (Silvertip)-501 | GL | 19.303 | 0.00 | 15.689 | 0.16 | 39.765 | 0.22 | 0.8128 | 0.00 | 2.060 | 0.00 | GSC |
| Midway (Silvertip)-001a | GL | 19.315 | 0.01 | 15.676 | 0.02 | 39.688 | 0.02 | 0.8116 | 0.00 | 2.055 | 0.00 | AN |
| Midway (Silvertip)-001b | GL | 19.347 | 0.02 | 15.695 | 0.01 | 39.747 | 0.02 | 0.8112 | 0.00 | 2.054 | 0.00 | GA |
| Midway (Silvertip)-507 | GL | 19.340 | 0.11 | 15.700 | 0.16 | 39.795 | 0.22 | 0.8118 | 0.00 | 2.058 | 0.00 | UA |
| Midway (Silvertip)-508 | GL | 19.334 | 0.11 | 15.697 | 0.16 | 39.806 | 0.22 | 0.8119 | 0.00 | 2.059 | 0.00 | UA |
| Amy (Marbaco)-001 | GL | 19.406 | 0.02 | 15.708 | 0.01 | 39.649 | 0.05 | 0.8095 | 0.00 | 2.043 | 0.00 | GA |
| Amy (Marbaco)-002 | GL | 19.315 | 0.00 | 15.705 | 0.00 | 39.773 | 0.00 | 0.8131 | 0.00 | 2.059 | 0.00 | GA |
| Amy (Marbaco)-003 | GL | 19.324 | 0.00 | 15.711 | 0.01 | 39.773 | 0.00 | 0.8130 | 0.00 | 2.058 | 0.00 | GA |
| Amy (Marbaco)-004 | GL | 19.321 | 0.00 | 15.709 | 0.03 | 39.762 | 0.00 | 0.8130 | 0.00 | 2.058 | 0.00 | GA |
| Luck-001 | GL | 19.563 | 0.00 | 15.728 | 0.01 | 39.810 | 0.00 | 0.8040 | 0.00 | 2.035 | 0.00 | GA |
| Luck-501 | GL | 19.588 | 0.00 | 15.786 | 0.00 | 39.962 | 0.00 | 0.8059 | 0.00 | 2.040 | 0.00 | GSC |
| Rancheria | GL | 19.331 | 0.00 | 15.708 | 0.00 | 39.780 | 0.00 | 0.8126 | 0.00 | 2.058 | 0.00 | UA |
| Midway (Discovery)-002 | GL | 19.296 | 0.04 | 15.679 | 0.04 | 39.696 | 0.04 | 0.8126 | 0.00 | 2.057 | 0.00 | GA |
| Midway (Discovery)-003 | GL | 19.310 | 0.01 | 15.694 | 0.01 | 39.731 | 0.01 | 0.8128 | 0.00 | 2.058 | 0.00 | GA |
| Midway (Discovery)-005 | GL | 19.346 | 0.02 | 15.703 | 0.01 | 39.811 | 0.03 | 0.8117 | 0.00 | 2.058 | 0.00 | GA |
| Midway (Discovery)-006 | GL | 19.326 | 0.03 | 15.695 | 0.03 | 39.766 | 0.04 | 0.8121 | 0.00 | 2.058 | 0.00 | GA |
| Midway (Discovery)-007 | PY | 19.324 | 0.00 | 15.708 | 0.01 | 39.783 | 0.02 | 0.8129 | 0.00 | 2.059 | 0.00 | GA |
| Midway (Discovery)-008 | GL | 19.331 | 0.03 | 15.708 | 0.03 | 39.803 | 0.04 | 0.8126 | 0.00 | 2.059 | 0.00 | GA |
| Midway (Discovery)-009 | GL | 19.317 | 0.06 | 15.711 | 0.06 | 39.795 | 0.07 | 0.8133 | 0.00 | 2.060 | 0.00 | GA |
| Midway (Discovery)-010 | GL | 19.359 | 0.01 | 15.699 | 0.01 | 39.757 | 0.02 | 0.8110 | 0.00 | 2.054 | 0.00 | GA |
| Midway (Discovery)-011 | GL | 19.338 | 0.01 | 15.696 | 0.01 | 39.753 | 0.02 | 0.8117 | 0.00 | 2.056 | 0.00 | GA |
| Midway (Discovery)-502 | GL | 19.348 | 0.11 | 15.696 | 0.16 | 39.782 | 0.22 | 0.8112 | 0.00 | 2.056 | 0.00 | UA |
| Midway (Discovery)-503 | GL | 19.341 | 0.11 | 15.687 | 0.16 | 39.747 | 0.22 | 0.8111 | 0.00 | 2.055 | 0.00 | UA |
| Midway (Discovery)-504 | GL | 19.348 | 0.11 | 15.683 | 0.16 | 39.719 | 0.22 | 0.8106 | 0.00 | 2.053 | 0.00 | UA |
| Midway (Discovery)-505 | GL | 19.309 | 0.11 | 15.683 | 0.16 | 39.746 | 0.22 | 0.8122 | 0.00 | 2.058 | 0.00 | UA |
| Midway (Discovery)-506 | GL | 19.384 | 0.11 | 15.727 | 0.16 | 39.871 | 0.22 | 0.8113 | 0.00 | 2.057 | 0.00 | UA |
| Midway (Discovery)-509 | GL | 19.305 | 0.11 | 15.683 | 0.16 | 39.749 | 0.22 | 0.8124 | 0.00 | 2.059 | 0.00 | UA |
| Midway (Discovery)-510 | GL | 19.318 | 0.11 | 15.691 | 0.16 | 39.782 | 0.22 | 0.8122 | 0.00 | 2.059 | 0.00 | UA |
| Midway (Discovery)-511 | GL | 19.345 | 0.00 | 15.690 | 0.16 | 39.771 | 0.22 | 0.8111 | 0.00 | 2.056 | 0.00 | UA |
| Tootsee Star | GL | 19.291 | 0.00 | 15.692 | 0.00 | 39.760 | 0.00 | 0.8134 | 0.01 | 2.061 | 0.01 | GA |
| Silverknife-001 | GL | 19.462 | 0.01 | 15.716 | 0.02 | 39.744 | 0.02 | 0.8076 | 0.00 | 2.042 | 0.01 | GA |
| Silverknife-002 | GL | 19.459 | 0.00 | 15.698 | 0.00 | 39.717 | 0.00 | 0.8067 | 0.01 | 2.041 | 0.01 | GA |
| Silverknife-003 | GL | 19.442 | 0.00 | 15.707 | 0.00 | 39.719 | 0.00 | 0.8079 | 0.01 | 2.043 | 0.00 | GA |
| Silverknife-004 | GL | 19.476 | 0.00 | 15.707 | 0.00 | 39.751 | 0.00 | 0.8065 | 0.01 | 2.041 | 0.00 | GA |
| Silverknife-005 | GL | 19.474 | 0.00 | 15.715 | 0.00 | 39.774 | 0.00 | 0.8071 | 0.00 | 2.043 | 0.00 | GA |
| Silverknife-006 | GL | 19.462 | 0.01 | 15.716 | 0.01 | 39.744 | 0.01 | 0.8076 | 0.00 | 2.042 | 0.00 | GA |
| Star (YP)-501 | GL | 19.671 | 0.00 | 15.770 | 0.00 | 39.874 | 0.00 | 0.8017 | 0.00 | 2.027 | 0.00 | AN |
| Star (YP)-502 | GL | 19.633 | 0.00 | 15.744 | 0.00 | 39.795 | 0.00 | 0.8019 | 0.00 | 2.027 | 0.00 | AN |
| Star (YP)-503 | GL | 19.568 | 0.00 | 15.730 | 0.00 | 39.827 | 0.00 | 0.8039 | 0.00 | 2.035 | 0.00 | AN |
| Star (YP)-504 | GL | 19.635 | 0.00 | 15.746 | 0.00 | 39.833 | 0.00 | 0.8019 | 0.00 | 2.029 | 0.00 | AN |
| Star (YP)-505 | GL | 19.643 | 0.00 | 15.763 | 0.00 | 39.865 | 0.00 | 0.8025 | 0.00 | 2.029 | 0.00 | AN |
| Star (YP)-506 | GL | 19.667 | 0.00 | 15.765 | 0.00 | 39.871 | 0.00 | 0.8016 | 0.00 | 2.027 | 0.00 | AN |
| A & B | GL | 19.516 | 0.08 | 15.714 | 0.15 | 39.657 | 0.19 | 0.8052 | 0.00 | 2.032 | 0.00 | RY |
| Fiddler-101 | GL | 19.672 | 0.01 | 15.755 | 0.00 | 39.837 | 0.01 | 0.8009 | 0.00 | 2.025 | 0.00 | GA |
| Fiddler-102 | GL | 19.668 | 0.01 | 15.753 | 0.01 | 39.826 | 0.01 | 0.8010 | 0.00 | 2.025 | 0.00 | GA |
| Lola-001a | GL | 19.344 | 0.03 | 15.699 | 0.01 | 39.747 | 0.04 | 0.8116 | 0.00 | 2.055 | 0.00 | GA |

| Deposit name | Mineral | $^{206}Pb/^{204}Pb$ | Pb64 % err | $^{207}Pb/^{204}Pb$ | Pb74 % err | $^{208}Pb/^{204}Pb$ | Pb84 % err | $^{207}Pb/^{206}Pb$ | Pb76 % err | $^{208}Pb/^{206}Pb$ | Pb86 % err | Analyst |
|---|---|---|---|---|---|---|---|---|---|---|---|---|
| Lola-001b | GL | 19.431 | 0.02 | 15.708 | 0.01 | 39.642 | 0.02 | 0.8084 | 0.00 | 2.040 | 0.00 | GA |
| Lola-002 | GL | 19.330 | 0.05 | 15.701 | 0.02 | 39.776 | 0.07 | 0.8123 | 0.00 | 2.058 | 0.00 | GA |
| Lola-003 | GL | 19.434 | 0.04 | 15.711 | 0.02 | 39.678 | 0.05 | 0.8084 | 0.00 | 2.042 | 0.00 | GA |
| Lola-501 | GL | 19.443 | 0.00 | 15.719 | 0.00 | 39.699 | 0.00 | 0.8085 | 0.00 | 2.042 | 0.00 | AN |
| Dale Mountain | GL | 19.379 | 0.00 | 15.689 | 0.00 | 39.636 | 0.00 | 0.8096 | 0.00 | 2.045 | 0.00 | GSC |
| Blackrock-001a | GL | 19.490 | 0.02 | 15.702 | 0.02 | 39.667 | 0.02 | 0.8056 | 0.00 | 2.035 | 0.00 | GA |
| Blackrock-001b | GL | 19.494 | 0.03 | 15.715 | 0.01 | 39.715 | 0.03 | 0.8061 | 0.00 | 2.037 | 0.00 | GA |
| Hart-001 | GL | 19.554 | 0.02 | 15.730 | 0.02 | 39.742 | 0.02 | 0.8044 | 0.01 | 2.033 | 0.01 | GA |
| Hart (Meteorite)-101 | GL | 19.494 | 0.02 | 15.756 | 0.02 | 39.777 | 0.02 | 0.8082 | 0.01 | 2.040 | 0.01 | GA |
| Hart (Breccia)-102 | GL | 19.565 | 0.01 | 15.729 | 0.02 | 39.727 | 0.02 | 0.8039 | 0.00 | 2.031 | 0.01 | GA |
| Dan (Bar)-001 | GL | 19.038 | 0.01 | 15.678 | 0.01 | 38.976 | 0.02 | 0.8235 | 0.00 | 2.047 | 0.01 | PI |
| Dan (Bar)-002 | GL | 19.020 | 0.02 | 15.671 | 0.02 | 38.940 | 0.02 | 0.8239 | 0.01 | 2.047 | 0.01 | PI |
| Dan (Bar)-005 | SL | 19.137 | 0.04 | 15.725 | 0.05 | 39.184 | 0.07 | 0.8217 | 0.02 | 2.048 | 0.03 | GA |
| Bom | GL | 19.143 | 0.00 | 15.729 | 0.00 | 39.316 | 0.00 | 0.8217 | 0.00 | 2.054 | 0.00 | GSC |
| Logjam | GL | 19.203 | 0.00 | 15.744 | 0.00 | 39.240 | 0.00 | 0.8199 | 0.00 | 2.043 | 0.00 | GSC |
| Logtung | GL | 19.123 | 0.03 | 15.682 | 0.03 | 39.035 | 0.03 | 0.8201 | 0.00 | 2.041 | 0.00 | GA |
| CMC | GL | 19.582 | 0.00 | 15.739 | 0.00 | 39.805 | 0.00 | 0.8037 | 0.00 | 2.033 | 0.00 | AN |
| MC Ridge (K3)-001a | GL | 18.544 | 0.06 | 15.648 | 0.14 | 38.532 | 0.13 | 0.8438 | 0.00 | 2.078 | 0.00 | RY |
| MC Ridge (K3)-001b | GL | 18.547 | 0.02 | 15.630 | 0.02 | 38.433 | 0.02 | 0.8428 | 0.00 | 2.072 | 0.00 | GA |
| MC Ridge (K1)-002a | GL | 19.196 | 0.06 | 15.688 | 0.12 | 39.191 | 0.13 | 0.8173 | 0.00 | 2.042 | 0.00 | RY |
| MC Ridge (K1)-002b | GL | 19.162 | 0.02 | 15.689 | 0.02 | 39.109 | 0.02 | 0.8188 | 0.00 | 2.041 | 0.00 | GA |
| Logan | GL | 19.570 | 0.02 | 15.736 | 0.02 | 39.729 | 0.02 | 0.8041 | 0.01 | 2.030 | 0.01 | PI |
| Wolf (Cordilleran) | GL | 19.524 | 0.02 | 15.747 | 0.03 | 39.813 | 0.03 | 0.80655 | 0.01 | 2.039 | 0.02 | GA |
| Meister-002 | GL | 18.571 | 0.03 | 15.665 | 0.02 | 38.068 | 0.03 | 0.8435 | 0.00 | 2.050 | 0.00 | GA |
| Meister-002 | GL | 18.557 | 0.03 | 15.662 | 0.02 | 38.044 | 0.03 | 0.8440 | 0.00 | 2.050 | 0.00 | GA |
| Cabin Lake | PY | 18.747 | 0.14 | 15.668 | 0.21 | 38.552 | 0.28 | 0.8358 | 0.07 | 2.057 | 0.14 | GA |
| Mor | PY | 18.670 | 0.03 | 15.644 | 0.05 | 38.470 | 0.06 | 0.8379 | 0.02 | 2.061 | 0.03 | GA |

## *Notes*

Analyses by Janet E. Gabites (GA), Anne Andrew (AN), Anne Pickering (PI) and Barry Ryan (RY), Geochronology Laboratory, Department of Earth, Ocean and Atmospheric Sciences, University of British Columbia, Vancouver, B.C., and analysts at the Geological Survey of Canada (GSC) and University of Alberta, Edmonton, Alberta (UA).

Deposit names have been suffixed with sample numbers from LEADTABLE, where multiple samples were analysed.

Multiple analyses are listed as a, b. Minerals are GL = galena, CP = chalcopyrite, PY = pyrite.

Analytical errors are quoted at the 2σ level.

# Finlayson Lake Targeted Geoscience Initiative (southeastern Yukon), Part 1: Bedrock geology

*Donald C. Murphy*[1] *and Maurice Colpron*[2]
*Yukon Geology Program*

**Charlie F. Roots**[3]
*Geological Survey of Canada*
*and Yukon Geology Program*

*S.P. Gordey*[4]
*Geological Survey of Canada*[4]

*J. Grant Abbott*[5]
*Yukon Geology Program*

Murphy, D.C., Colpron, M., Roots, C.F., Gordey, S.P. and Abbott, J.G., 2002. Finlayson Lake Targeted Geoscience Initiative (southeastern Yukon), Part 1: Bedrock geology. *In:* Yukon Exploration and Geology 2001, D.S. Emond, L.H. Weston and L.L. Lewis (eds.), Exploration and Geological Services Division, Yukon Region, Indian and Northern Affairs Canada, p. 189-207.

## ABSTRACT

The Finlayson Lake Targeted Geoscience Initiative, conducted jointly by the Geological Survey of Canada and Yukon Geology Program, comprised new geological mapping and till geochemistry in the northern two-thirds of Finlayson Lake map area, in and around the Finlayson Lake massive sulphide district. The goals of the initiative were to document the nature of Yukon-Tanana Terrane in this area, and, as bedrock exposures are sparse, to use till geochemistry to remotely sense new exploration targets.

The new mapping illustrates that much of the area south of the Robert Campbell Highway is underlain by the rock units that host the Fyre Lake, Kudz Ze Kayah and GP4F deposits. These rocks are thrust northwardly over a succession of carbonaceous clastic rocks, chert and felsic meta-volcanic rocks, with potential for syngenetic deposits. The Permian Campbell Range basalt, host of the Ice deposit, unconformably overlies both sequences, and all of these rocks are thrust onto rocks of the North American miogeocline.

### RÉSUMÉ

Dans le cadre de l'Initiative géoscientifique ciblée du lac Finlayson, la Commission géologique du Canada, en collaboration avec le programme de géologie du Yukon, a dressé une nouvelle carte géologique et effectué une nouvelle analyse géochimique du till des deux tiers de la partie nord de la carte représentant la région du lac Finlayson, dans le district de sulfures massifs du lac Finlayson et aux alentours. L'Initiative avait comme objectifs de documenter la nature du terrane de Yukon-Tanana dans cette région, et d'utiliser des analyses géochimiques du till, étant donné que le substratum n'affleure que par endroits, pour « télédétecter » de nouvelles cibles d'exploration. La nouvelle carte indique que le substratum d'une grande partie de la région au sud de la route Robert Campbell est constitué d'unités rocheuses renfermant les gisements Fyre Lake, Kudz Ze Kayah et GP4F. Ces roches chevauchent vers le nord une succession de roches clastiques carbonées, de chert et de roches métavolcaniques felsiques pouvant renfermer des gisements syngénétiques. Le basalte permien de la chaîne Campbell, qui renferme le gisement Ice, repose en discordance sur les deux séquences; toutes ces roches chevauchent des roches du miogéoclinal nord-américain.

---

[1] *don.murphy@gov.yk.ca*

[2] *maurice.colpron@gov.yk.ca*

[3] *charlie.roots@gov.yk.ca*

[4] *Geological Survey of Canada, 101-605 Robson Street, Vancouver, British Columbia, Canada V6B 5J3, sgordey@gsc.nrcan.gc.ca*

[5] *abbottg@inac.gc.ca*

## INTRODUCTION

In 2001, Yukon Geology Program joined with the Geological Survey of Canada to fund and implement the Finlayson Lake Targeted Geoscience Initiative (TGI), a program of bedrock geological mapping and till geochemistry in and around the Finlayson Lake massive sulphide district (Fig. 1). The intent of the TGI was to produce new geoscience data that would enhance understanding of the district's host rocks and facilitate mineral exploration in the poorly exposed areas. Under the auspices of the TGI, personnel from both organizations worked for five weeks with a contract helicopter out of a base camp at the Finlayson airstrip. A new bedrock geological map of the northern two-thirds of Finlayson Lake area (Murphy et al., 2001; Fig. 2) and the results of the till geochemical survey are now available (Bond and Plouffe, this volume). In this report, the authors present an overview of the bedrock geology of the northern part of the Finlayson Lake map area (105G) and discuss the implications for mineral exploration.

## PREVIOUS WORK

Dawson traversed the area in 1887 (Dawson, 1888), followed by Keele's reconnaissance in 1907-08 (Keele, 1910). Wheeler, Green and Roddick (1960) outlined the distribution of many of the major rock types in the area without subdividing the metamorphic rock units. Tempelman-Kluit (1977) further refined the earlier maps and subsequently interpreted the metamorphic rocks as a subduction complex formed between an offshore arc and the North American continent (Tempelman-Kluit, 1979). Mortensen (1983), Mortensen and Jilson (1985), and Mortensen (1992a), showed that the area was underlain by a coherent regional stratigraphic sequence. The aforementioned authors used U-Pb geochronology to constrain the ages of the meta-igneous rocks, and concluded that Yukon-Tanana Terrane in the Finlayson Lake area represented a mid- and Late Paleozoic continental magmatic arc. Plint (1995), and Plint and Gordon (1995; 1996a,b; 1997) mapped part of northern Finlayson Lake map area in their study of the rocks of the Campbell Range belt, its relationship to Yukon-Tanana Terrane, and the implications of this relationship for the evolution of the Finlayson Lake fault zone.

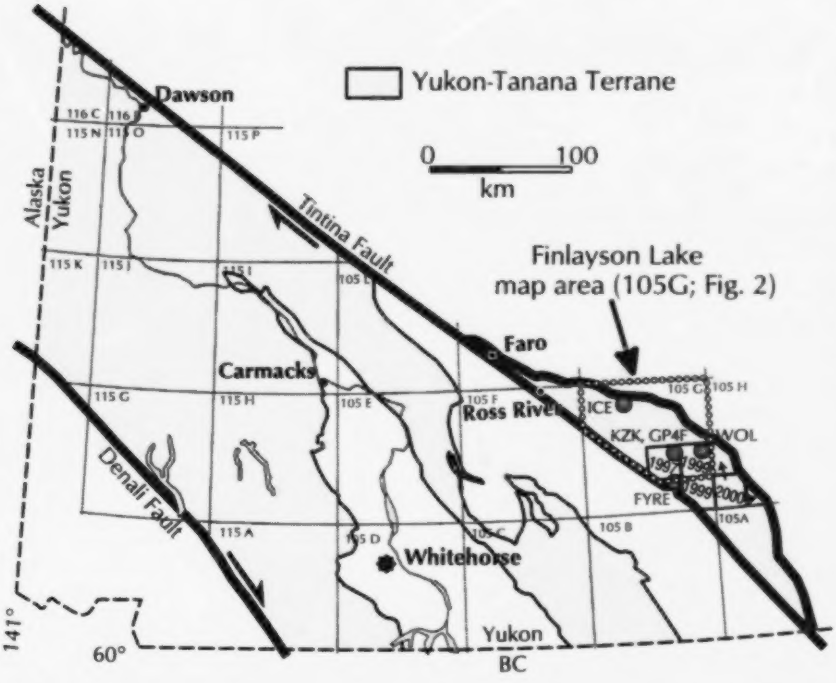

*Figure 1. Map of southern Yukon displaying location of Figure 2 with respect to the distribution of Yukon-Tanana Terrane, the main deposits of the Finlayson Lake massive sulphide district and areas that were mapped in previous years.*

Systematic geological mapping of parts of Finlayson Lake and Frances Lake areas by Murphy and others at 1:50 000 scale has been ongoing since 1996 (Murphy, 1997; Murphy and Piercey, 1999a; Murphy, 2000a,b,c, along with related reports: Murphy and Timmerman, 1997; Murphy, 1998; Hunt and Murphy, 1998; Murphy and Piercey, 1999b, 2000; Piercey and Murphy, 2000; Piercey et al., 1999, 2000, 2001a,b,c; Sebert and Hunt, 1999). Murphy and Piercey (1999c) published a 1:100 000-scale compilation that included the southeastern part of the area and neighbouring parts of 105H (105G/7 and 8; and parts of 105G/1, 2, and 9, as well as 105H/5 and 12).

## EXPOSURE AND ACCESS

With local exception, bedrock in northern Finlayson Lake area is sparsely exposed due to relatively low-relief topography and an extensive blanket of surficial sediment. Foot traversing was done where outcrops were relatively continuous, however, much of the area was covered by spot landings on isolated outcrops. Over the entire northern half of the Finlayson Lake map area, very few, if any, helicopter-accessible outcrops were not visited during the Targeted Geoscience Initiative and previous programs.

## GEOLOGY OF NORTHERN FINLAYSON LAKE AREA

Northern Finlayson Lake map area is underlain primarily by rocks belonging to Yukon-Tanana Terrane and the North American miogeocline (Fig. 2). Most of the southern part of the area consists of polydeformed and thrust-imbricated meta-igneous and meta-sedimentary rocks of Yukon-Tanana Terrane. The northernmost part of the area is underlain by weakly deformed and slightly metamorphosed Silurian to Triassic sedimentary rock units of the North American miogeocline. The boundary between the two geological assemblages is the newly defined 'Inconnu thrust'. Minor Permian and locally voluminous Jurassic granitic rocks intrude Yukon-Tanana Terrane, while variably foliated Cretaceous granite, possibly of different ages, intrude both Yukon-Tanana Terrane and North American rocks. Undeformed Eocene basalt, rhyolite and gabbro also occur throughout the area.

## YUKON-TANANA TERRANE

Yukon-Tanana Terrane north of the Tintina Fault comprises several fault- and unconformity-bound meta-sedimentary and meta-volcanic successions and affiliated meta-plutonic suites (Figs. 2 and 3; Murphy, 2001). The structurally deepest rocks are those in the footwall of the Money Creek thrust. These include the Grass Lakes succession, mid-Paleozoic granitic meta-plutonic rocks, and the unconformably overlying Wolverine succession. The hanging wall of the thrust comprises the herein defined 'Tuchitua succession', which is composed of Carboniferous limestone and quartzite, as well as meta-volcanic rocks coeval to those in both the Grass Lakes and Wolverine successions, but primarily of an intermediate composition. The footwall and hanging wall of the Money Creek thrust are both overlain by dark clastic rocks and chert of probable Late Pennsylvanian age. All of these rocks are emplaced along the Jules Creek thrust over dark clastic rocks, chert, limestone and meta-volcanic rocks of the herein defined Finlayson succession. Permian basalt and chert of the Campbell Range succession overlie all the thrust sheets. Mafic and ultramafic meta-plutonic rocks, thought to be the sub-volcanic feeders to the Campbell Range basalt, occur within most older rock units. Permian granitic dykes occur locally. Relatively weakly deformed mid-Permian to possibly Triassic conglomerate overlies all rocks of Yukon-Tanana Terrane. Three bodies of Jurassic granitic rocks intrude rocks of Yukon-Tanana Terrane in the west-central part of the map area.

### FOOTWALL OF THE MONEY CREEK THRUST

*Grass Lakes succession*

Murphy (1997), and Murphy and Piercey (1999b), described the rocks of the Grass Lakes succession in detail, therefore only a short summary is provided here. The lowest exposed unit of the Grass Lakes succession (Fig. 3), is composed of grit, psammite, meta-pelite, locally important muscovite-quartz phyllite, as well as augen phyllite of probable felsic meta-volcanic protolith, minor chloritic phyllite of mafic meta-igneous protolith, and marble and calcareous schist. It is overlain by the Fire Lake unit (Fig. 3), a mafic meta-volcanic unit composed mainly of chloritic phyllite, but also including carbonaceous phyllite and rare muscovite-quartz phyllite of probable felsic meta-volcanic protolith. The Fyre Lake massive sulphide deposit (Yukon MINFILE, 2001, 105G 034) is hosted in chloritic phyllite of the Fire Lake unit. Mafic and ultramafic meta-plutonic rocks are spatially associated with the Fire Lake unit and are inferred to be comagmatic sills and dykes (Murphy and Piercey, 2000). The Fire Lake unit is overlain by carbonaceous phyllite, lesser quartz-feldspar grit and pebble meta-conglomerate, and feldspar-muscovite-quartz phyllite and augen phyllite (felsic meta-volcanic rocks) of the Kudz Ze Kayah unit. These latter rocks host the Kudz Ze Kayah and GP4F massive sulphide deposits (Yukon MINFILE, 2001, 105G 117 and 143). The upper unit of the Grass Lakes succession is composed of carbonaceous phyllite, chloritic phyllite (mafic meta-volcanic rocks and dykes), quartzite and quartzo-feldspathic meta-conglomerate. The latter conglomerate unit was deposited on all underlying units of the Grass Lakes succession, implying an angular unconformity following a phase of deformation.

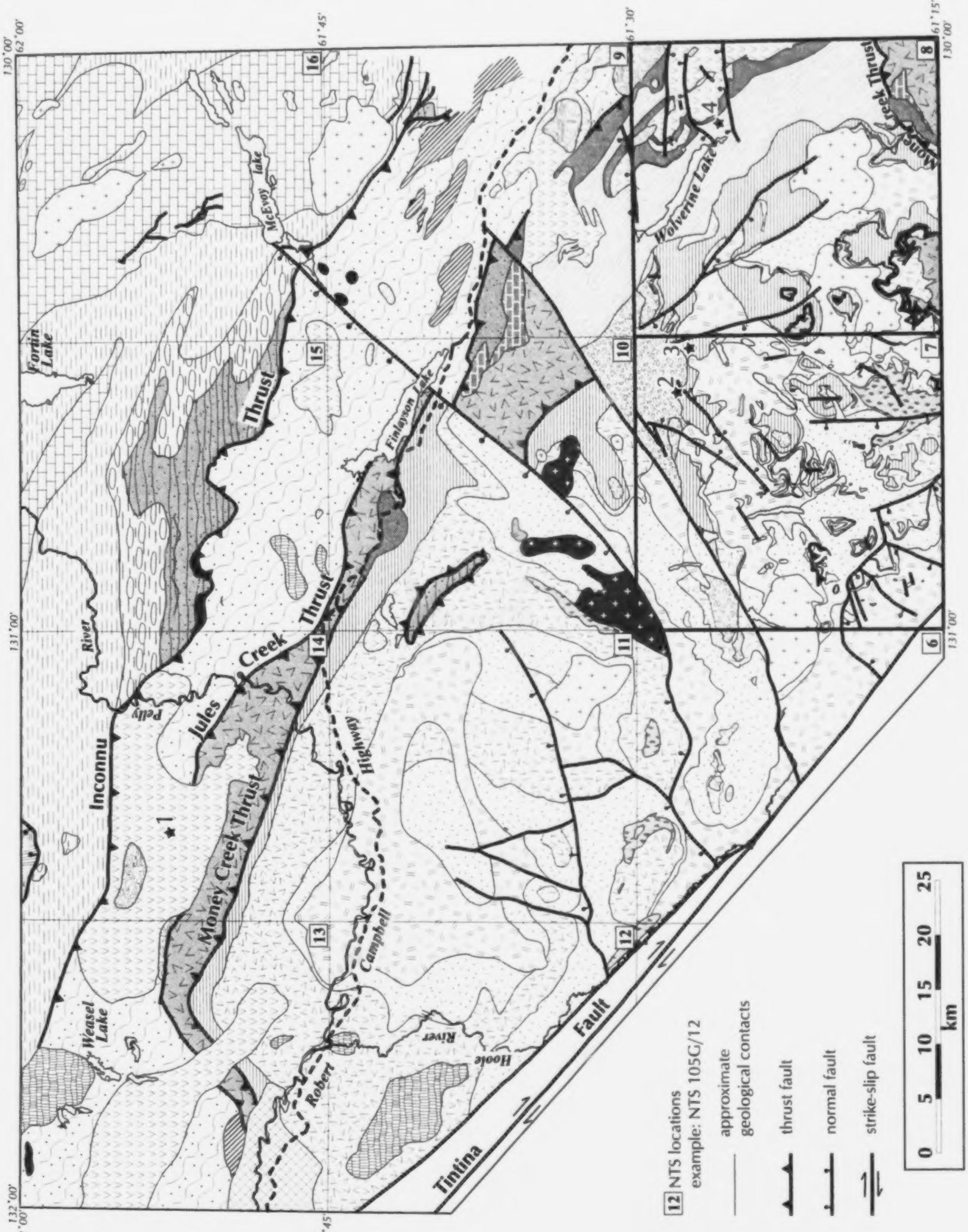
130°00'
62°00'
132°00'
62°00'
61°45'
61°45'
61°30'
61°15'
130°00'
131°00'
131°00'
Inconnu
Thrust
Jules
Creek
Thrust
Money Creek Thrust
Tintina
Fault
Weasel Lake
Fortin Lake
McEvoy lake
Finlayson Lake
Wolverine Lake
Pelly
River
Campbell
Highway
Robert
Hoole
River
Money Creek Thrust
16
15
14
13
12
11
10
9
8
7
6
1
2
3
4
12 NTS locations
example: NTS 105G/12
approximate geological contacts
thrust fault
normal fault
strike-slip fault
0
5
10
15
20
25
km

**Figure 2.** *Simplified bedrock geological map of the northern part of Finlayson Lake area. Map areas highlighted in southeastern corner (105G/7 and 8) are available at 1:50 000 scale (Murphy, 1997; Murphy and Piercey, 1999a).*

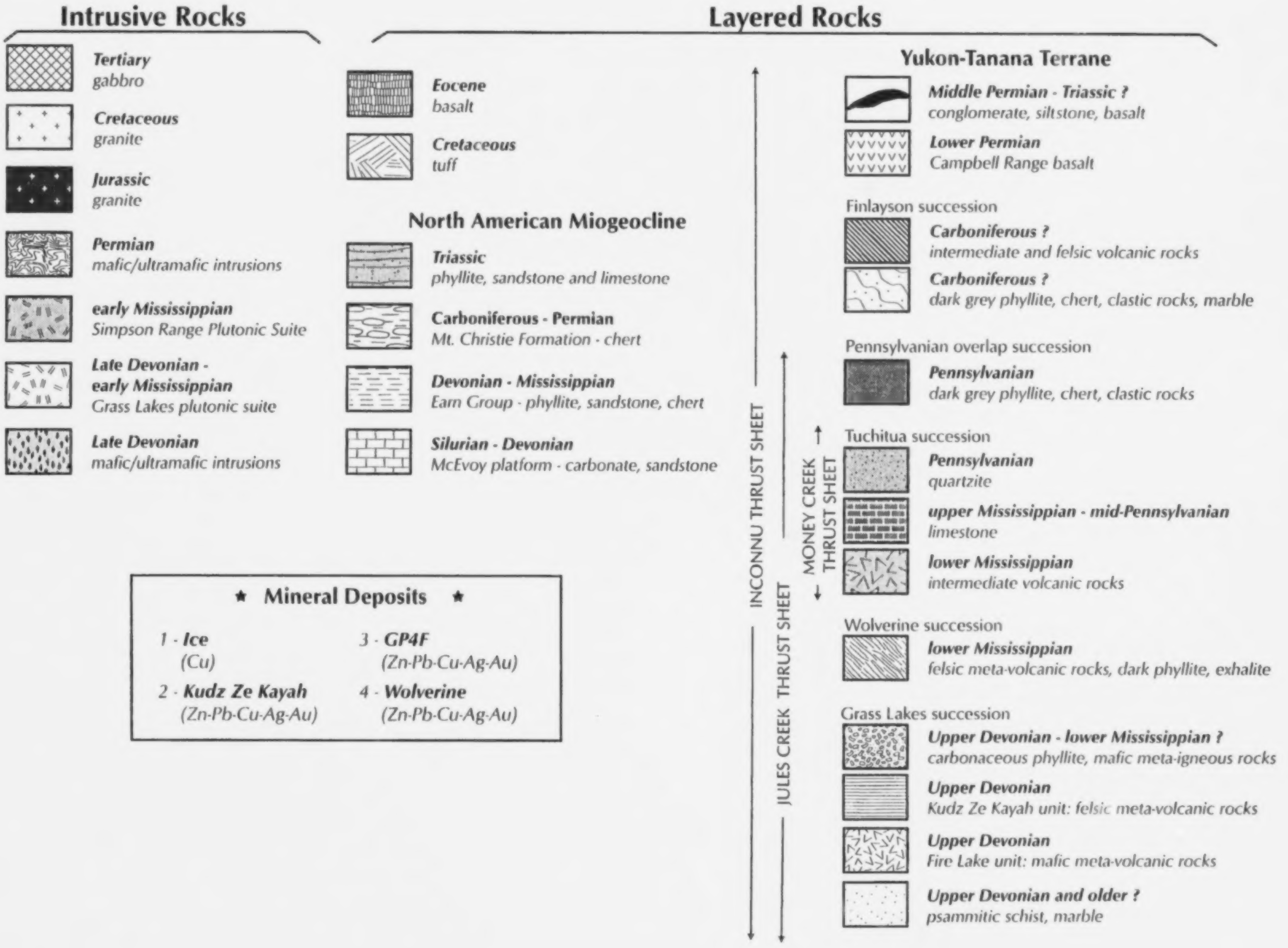
Intrusive Rocks
Tertiary
gabbro
Cretaceous
granite
Jurassic
granite
Permian
mafic/ultramafic intrusions
early Mississippian
Simpson Range Plutonic Suite
Late Devonian - early Mississippian
Grass Lakes plutonic suite
Late Devonian
mafic/ultramafic intrusions
Layered Rocks
Eocene
basalt
Cretaceous
tuff
North American Miogeocline
Triassic
phyllite, sandstone and limestone
Carboniferous - Permian
Mt. Christie Formation - chert
Devonian - Mississippian
Earn Group - phyllite, sandstone, chert
Silurian - Devonian
McEvoy platform - carbonate, sandstone
★ Mineral Deposits ★
1 - Ice
(Cu)
2 - Kudz Ze Kayah
(Zn-Pb-Cu-Ag-Au)
3 - GP4F
(Zn-Pb-Cu-Ag-Au)
4 - Wolverine
(Zn-Pb-Cu-Ag-Au)
INCONNU THRUST SHEET
JULES CREEK THRUST SHEET
MONEY CREEK THRUST SHEET
Yukon-Tanana Terrane
Middle Permian - Triassic ?
conglomerate, siltstone, basalt
Lower Permian
Campbell Range basalt
Finlayson succession
Carboniferous ?
intermediate and felsic volcanic rocks
Carboniferous ?
dark grey phyllite, chert, clastic rocks, marble
Pennsylvanian overlap succession
Pennsylvanian
dark grey phyllite, chert, clastic rocks
Tuchitua succession
Pennsylvanian
quartzite
upper Mississippian - mid-Pennsylvanian
limestone
lower Mississippian
intermediate volcanic rocks
Wolverine succession
lower Mississippian
felsic meta-volcanic rocks, dark phyllite, exhalite
Grass Lakes succession
Upper Devonian - lower Mississippian ?
carbonaceous phyllite, mafic meta-igneous rocks
Upper Devonian
Kudz Ze Kayah unit: felsic meta-volcanic rocks
Upper Devonian
Fire Lake unit: mafic meta-volcanic rocks
Upper Devonian and older ?
psammitic schist, marble

***Figure 2.*** *(continued) Legend.*

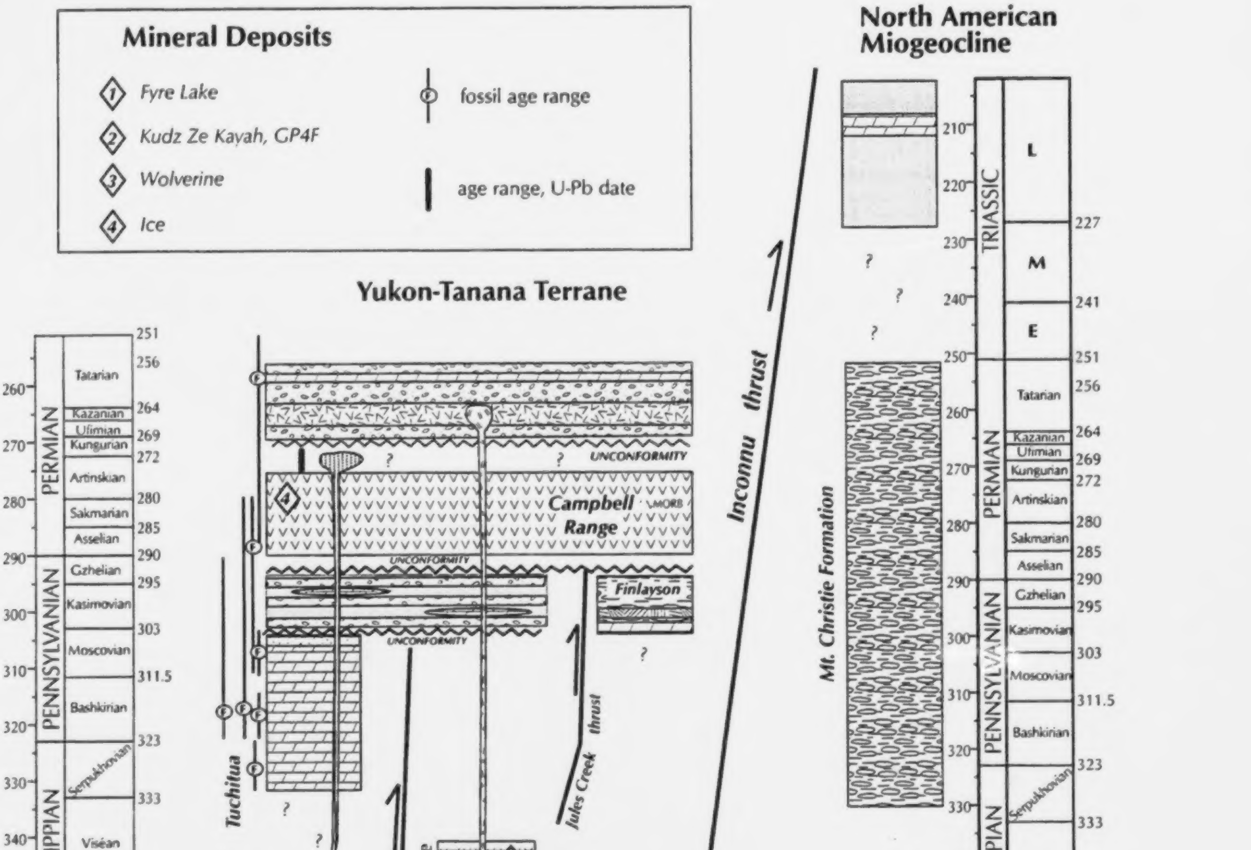
Mineral Deposits
1 Fyre Lake
2 Kudz Ze Kayah, GP4F
3 Wolverine
4 Ice
fossil age range
age range, U-Pb date
Yukon-Tanana Terrane
North American Miogeocline
Inconnu thrust
Campbell Range
MORB
UNCONFORMITY
Finlayson
Tuchitua
Jules Creek thrust
Money Creek thrust
Wolverine
Grass Lakes
BAB
Arc
BON
deformation
Mt. Christie Formation
Earn Group
McEvoy Platform
PERMIAN
PENNSYLVANIAN
MISSISSIPPIAN
DEVONIAN
TRIASSIC
SILURIAN
UNDIVIDED
L
M
E
Tatarian
Kazanian
Ufimian
Kungurian
Artinskian
Sakmarian
Asselian
Gzhelian
Kasimovian
Moscovian
Bashkirian
Serpukhovian
Viséan
Tournaisian
Famennian
Frasnian
Givetian
Eifelian
Dalejan
Emsian
Pragian
Lochkovian
Rock Types
carbonaceous phyllite/shale
chert and argillite
coarse clastic rocks
quartzite
carbonate
quartz-rich metaclastic rocks
iron formation
felsic meta-volcanic and meta-plutonic rocks
intermediate meta-plutonic rocks
intermediate meta-volcanic rocks
mafic and ultramafic meta-plutonic rocks
mafic meta-volcanic rocks

***Figure 3.*** *Summary of stratigraphy and stratigraphic relationships in northern Finlayson Lake area. MORB = mid ocean ridge basalt; BAB = back-arc basin; BON = boninite.*

The Grass Lakes succession is intruded by voluminous granitic meta-plutonic rocks of the 'Grass Lakes suite'. In the Grass Lakes area, in the heart of the Finlayson Lake massive sulphide district, the Grass Lakes suite comprises variably foliated, medium- to coarse-grained, equigranular granite to quartz monzonite. An unfoliated phase of the suite that crosscuts structures attests to a phase of deformation during intrusion of the suite, possibly the phase of deformation indicated by the unconformity beneath the upper conglomerate unit of the Grass Lakes succession. To the west and northwest, in the Mink Creek and Hoole River watersheds, the suite comprises foliated potassium feldspar megacrystic granite. Coarse-grained igneous muscovite and biotite occur in both phases indicating a peraluminous composition.

The Grass Lakes succession is constrained to the pre-Late Devonian to Earliest Mississippian. The North Lakes meta-diorite, inferred to be comagmatic with the Fire Lake unit, is 365 Ma (U-Pb, zircon, Mortensen, 1992a; Mortensen and Murphy, unpublished data, 1997). The lowest unit of the Grass Lakes succession is therefore pre-365 Ma. A number of imprecise Late Devonian to Early Mississippian U-Pb ages have been obtained from felsic meta-volcanic rocks of the Kudz Ze Kayah unit (Mortensen, 1992a; Mortensen, Murphy and Piercey, unpublished data, 1997-2001). Late Devonian to Early Mississippian U-Pb ages have been obtained from the Grass Lakes suite, one of which intrudes the youngest unit (op. cit.). The Grass Lakes succession is therefore Devonian to earliest Mississippian in age.

### *Wolverine succession*

The Wolverine succession, occurring mainly in the Wolverine Lake map area (105G/8; Fig. 2), consists of several northwesterly striking map units that cut across the mainly easterly stratigraphic trend of the underlying Grass Lakes succession (Murphy and Piercey, 1999a,b,c; Murphy et al., 2001). The Wolverine succession is truncated to the northwest by a northeast-striking normal fault, and to the southwest by the Money Creek thrust. The oldest unit in the Wolverine succession is composed of a basal, quartz-feldspar-pebble meta-conglomerate and overlying carbonaceous phyllite. This unit passes transitionally upward into carbonaceous phyllite with laterally discontinuous amounts of muscovite-quartz phyllite and quartz-feldspar meta-porphyry of volcanic, volcaniclastic and sub-volcanic protolith (Murphy and Piercey, 1999b; Piercey, 2001; Piercey et al., 2001c; Bradshaw et al., 2001). The Wolverine massive sulphide deposit (Yukon MINFILE, 2001, 105G 072; Bradshaw et al., 2001) occurs at the top of this unit. Medium- to thick-bedded siliceous phyllite (aphyric meta-rhyolite), with barite-magnetite-silica iron formation and carbonate-pyrite exhalite, overlie the deposit stratigraphy. The top of the Wolverine succession comprises chloritic phyllite of mafic meta-volcanic protolith.

## HANGING WALL OF THE MONEY CREEK THRUST

### *Tuchitua succession*

Rocks of the hanging wall of the Money Creek thrust occur in a narrow discontinuous belt that trends northwestly across the map area (Fig. 2). The thrust sheet in this area is composed mainly of Mississippian meta-volcanic rocks (primarily intermediate), and Pennsylvanian carbonate and quartzite of the Tuchitua succession. Tuchitua succession is named after the area where it is extensively and well exposed in southwestern Frances Lake map area (Murphy, 2000a,b,c; 2001). Older and structurally deeper parts of the thrust sheet also occur in the southeastern part of the Finlayson Lake map area, where the thrust sheet was originally recognized (Murphy and Piercey, 1999a,c, 2000; Tempelman-Kluit, 1977, 1979; Mortensen and Jilson, 1985). These rocks were thrust northeastwardly over the Grass Lakes and Wolverine successions in the Late Pennsylvanian (Murphy, 2001). In the northern part of the map area, the thrust sheet is discontinuously present beneath unconformably overlying Late Pennsylvanian clastic rocks and Permian Campbell Range basalt. With discontinuous preservation and the general poor exposure in the map area, it was necessary to define an undifferentiated unit to represent the Money Creek thrust sheet where individual units could not be traced.

In the northern part of the Finlayson map area, the Tuchitua succession is best exposed south of the southeast end of Finlayson Lake. In this location, massive bioclastic limestone occurs on hilltops south of the Robert Campbell Highway, underlain by mainly chlorite-muscovite-quartz phyllite of intermediate volcanic and possibly volcaniclastic protolith. Mafic rocks occur locally, consisting of calcareous chloritic phyllite with millimetre-scale calcite pods (amygdules?). Pyritic and altered felsic rocks occur 8 km south of the Robert Campbell Highway at the southeastern end of Finlayson Lake. The bioclastic limestone is inferred to be overlain by massive orthoquartzite. This unit underlies the hills south of the Robert Campbell Highway and the Finlayson River. All units are truncated to the southeast by a northeast-striking normal fault.

With the exception of orthoquartzite, a similar sequence occurs elsewhere in the northern part of the map area. Massive limestone and felsic meta-volcanic rocks, intercalated with thin limestone and dark phyllite, occurring north of the Robert Campbell Highway, west of Finlayson Lake, are also included in the Money Creek thrust sheet. Limestone and intermediate to felsic meta-volcanic rocks included in the Money Creek thrust sheet are also exposed west of the north-trending stretch of the Pelly River, southeast of the Ice deposit. In this locality, the meta-volcanic rocks include quartz- and feldspar-phyric meta-porphyritic varieties.

The Money Creek thrust sheet in the southern part of map area 105G/8 includes older and structurally deeper parts of the sheet than in the north, likely reflecting the presence of a hanging wall ramp. The older rocks include klippe of ultramafic rocks ('North Klippe' of Tempelman-Kluit, 1979) and variably deformed mafic and felsic meta-volcanic rocks, as well as overlying crinoidal limestone in the area of the original 'Money Klippe' of Tempelman-Kluit (1979). These latter rocks have been correlated with the Fire Lake unit of the Grass Lakes succession in the footwall of the thrust. The meta-volcanic rocks in the thrust sheet in the southeastern corner of the map area are intruded by variably foliated metaluminous meta-plutonic rocks of the Simpson Range suite (Hunt and Murphy, 1998; Murphy and Piercey, 2000; Piercey and Murphy, 2000).

The rocks in the Money Creek thrust sheet have been dated in various places in Finlayson Lake and Frances Lake map areas. Limestone along the Robert Campbell Highway, 7 km west of Finlayson Lake, contains Late Mississippian (Serpukhovian) conodonts (J. Hunt and M. Orchard, pers. comm., 1998). Pennsylvanian conodonts were obtained from limestone 8 km south-southeast of Finlayson Lake (Tempelman-Kluit, 1977, 1979). Correlative limestone in the headwaters of the Tuchitua River in Frances Lake map area has conodonts as young as Moscovian, as well as Serpukhovian (M. Orchard and D. Murphy, unpublished data, 2000). Felsic meta-volcanic rocks underlying the Carboniferous limestone have not been dated in Finlayson Lake map area, however, in Frances Lake map area, correlative units have Early Mississippian U-Pb zircon ages (Mortensen, 1983, 1992a; J. Mortensen and D. Murphy, unpublished data). The quartzite unit above the Carboniferous limestone has not been directly dated, but is likely to be Late Pennsylvanian. The basal contact of the limestone is likely a disconformity because all of the U-Pb dates for meta-volcanic rocks beneath the Carboniferous limestone are substantially older than Serpukhovian, the oldest age of the limestone. Quartz-porphyritic granite, inferred to be comagmatic with rhyolite in the older part of the thrust sheet, is ca. 361 Ma (Mortensen, 1992b), and intrusions of the Simpson Range Suite in the Money Creek thrust sheet range from ca. 346 Ma to 358 Ma (Mortensen, 1992a; Grant, 1997).

## UPPER PENNSYLVANIAN OVERLAP SUCCESSION

A succession of carbonaceous phyllite, grey chert, diamictite and quartzofeldspathic sandstone, grit, and local conglomerate, overlies rocks in the footwall of the Money Creek thrust, as well as those in the Money Creek thrust sheet. Bedded chert, inferred to overlie the Kudz Ze Kayah unit of the Grass Lakes succession along Campbell Creek, and carbonaceous phyllite, diamictite, grit and chert overlying the Wolverine succession north of Wolverine Lake, belong to this unit.

The relationship of this sequence to both the hanging wall and footwall of the Money Creek thrust implies that this succession overlaps the thrust itself and its age would therefore place a younger limit on the age of the thrust. There are no direct age constraints in Finlayson Lake area, but the sequence overlies limestone of Moscovian age in Frances Lake area (M. Orchard and D. Murphy, unpublished data, 2000) and is overlain by Campbell Range basalt of probable Early Permian age (Plint and Gordon, 1997; Murphy, 2000a,b,c, 2001). A Late Pennsylvanian age is thus indicated for both the clastic overlap succession and the displacement on the Money Creek thrust.

## THE JULES CREEK THRUST AND ITS FOOTWALL

Recent mapping in Frances Lake map area has shown that rocks in the footwall of the Money Creek thrust, the Money Creek thrust sheet, and the Pennsylvanian overlap succession were thrust to the northeast along the Jules Creek thrust (Murphy, 2000a,b,c, 2001). In the Frances Lake area, rocks in the footwall of the Jules Creek thrust comprise mainly carbonaceous phyllite, chert and chert-pebble conglomerate, which have been correlated with the Earn Group of the North American miogeocline (Plint and Gordon, 1997). This fault and its footwall succession, herein termed the Finlayson succession, have been traced into the Finlayson Lake area where they include rock types unlike those in the Earn Group and where a pre-mid-Permian geological history, unlike that of the Earn Group, can be demonstrated.

### *Finlayson succession*

The Finlayson succession, named for the relatively good exposures on the hills north of Finlayson Lake and Finlayson River in the eastern part of the map area (Figs. 2 and 3), is composed mainly of dark grey siliceous carbonaceous phyllite; grey, white, pink and green chert; mottled grey-white chert-pebble conglomerate; and shale chip-bearing, quartzofeldspathic grit and conglomerate. Also included in the succession are significant accumulations of felsic meta-volcanic rocks that occur east of Finlayson Lake and also north of the Pelly River, in the western part of 105G/13. Intermediate meta-volcanic rocks have been found in 105G/16, about 14 km north-northwest of where the Robert Campbell Highway exits Finlayson Lake map area. Mafic meta-volcanic rocks occur locally in 105G/14, southwest of Fortin Lake. Massive limestone occurs north of the Robert Campbell Highway, in the eastern part of 105G/16.

In 105G/15, southwest of Fortin Lake, rocks of the Finlayson succession exhibit a pronounced strain gradient. At the southern end of the north-trending ridges in this area, chert and carbonaceous phyllite are foliated and folded, but bedding is distinct. Northwards along the ridges, foliation is more intense and bedding less distinct. Where observed, bedding is thicker and isoclinally folded at the outcrop scale, suggesting transposition. Although highly strained rocks extend northwards to the post-Late Triassic Inconnu thrust, the presence of clasts of highly strained rocks of the Finlayson succession within mid-Permian (to Triassic?) conglomerate (see next section) demonstrates that the deformation was not related to the Inconnu thrust, but reflects a Paleozoic deformation event.

The age of the Finlayson succession has not been directly determined. The unit is overlain by Campbell Range basalts of late Pennsylvanian to Early Permian age. Similar rocks near Faro have Mississippian conodont ages (L. Pigage, pers. comm., 2000).

## UPPER PENNSYLVANIAN TO PERMIAN OVERLAP ASSEMBLAGES

Recent mapping in Frances Lake map area showed that the trace of the Jules Creek thrust is locally overlapped by outliers of basalt of the late Pennsylvanian to Early Permian Campbell Range succession (Murphy, 2000a,b,c, 2001). This relation has also been documented in northern Finlayson Lake area, where the Campbell Range succession lies on all older thrust sheets. In addition, mafic and ultramafic meta-plutonic rocks, inferred to be the sub-volcanic roots to the Campbell Range basalt, occur in rocks belonging to all the thrust sheets. Finally, highly strained rocks of the Finlayson succession and basalt of the Campbell Range succession are overlain by a polymictic conglomerate, sandstone, siltstone and basalt unit thought to correlate with similar rocks of mid-Permian age in Frances Lake and Watson Lake map areas (Murphy, 2000a,b,c, 2001; Mortensen et al., 1997, 1999).

### *Campbell Range succession*

Weakly deformed basalt and chert, occurring intermittently across the map area, have been included in the Campbell Range succession. The succession includes basalt and chert in the Campbell Range where the succession was originally documented (Murphy and Piercey, 1999a,b), as well as occurrences underlying the massifs in the northwestern part of the area, and smaller outliers between the two areas. The current definition, however, excludes carbonaceous meta-clastic rocks and chert of the Upper Pennsylvanian overlap succession, which were included in the original definition of the succession (Murphy and Piercey, 1999a,b). These rocks were placed into a separate unconformity-bound succession when the profound nature of the unconformity at the base of the Campbell Range basalt/chert sequence was recognized in Frances Lake area (Murphy, 2001).

Basalt is the predominant rock type of the Campbell Range succession. It is generally massive, green to brown on weathered surfaces, and dark green to black on fresh surfaces. Pillowed and fragmental varieties are locally important, especially around the Ice massive sulphide deposit in the northern part of the map area (Yukon MINFILE, 2001, 105G 118; Fig. 2). Epidote alteration is a common feature, as is pink to tan jasperoidal silica.

Chert, argillite and rarely limestone are intercalated with basalt. Maroon, pink and green chert, and siliceous argillite are locally important enough to define separate map units. Chert is ribbon-bedded (10- to 30-cm-thick beds with lesser centimetre- to decimetre-scale beds of argillite). Chert/argillite sequences are foliated and internally folded, contrasting with the relatively pristine nature of the intercalated basalt. A metre-scale bed of algal-laminated limestone was observed in one locality.

The age of the Campbell Range succession is constrained to be latest Pennsylvanian to Early Permian. It overlies the post-Moscovian clastic sequence, which overlaps the Money Creek thrust and is intruded by ca. 274 Ma leucogabbro (Mortensen, 1992b; J. Mortensen and D. Murphy, unpublished data, 2000). Plint and Gordon (1997) report Atokan to Wolfcampian (early Pennsylvanian to Early Permian) radiolaria from chert near the base of the succession. Furthermore, the Campbell Range succession is identical to, and likely correlates with, the Anvil Range Group at Rose Mountain near Faro from which Early Permian radiolaria have been obtained (L. Pigage, pers. comm., 2000).

The base of the Campbell Range succession is inferred to be a profound regional unconformity, developed after movement on the Jules Creek thrust. The succession overlies both the Finlayson succession in the footwall of the Jules Creek thrust and rocks in the hanging wall. The succession must therefore overlap the Jules Creek thrust, and thrusting must therefore be late Pennyslvanian in age.

### *Mafic and ultramafic meta-plutonic rocks*

Several aeromagnetically prominent bodies of mafic and ultramafic meta-plutonic rocks occur across the area. These range in area from hundreds of square metres to over 2 km$^2$. Leucogabbro, meta-pyroxenite and meta-peridotite occur most commonly in this area, the latter being ubiquitously serpentinized with only ghosts of the primary mineralogy preserved. The outcrop distribution of these rocks is coincident with that of the Campbell Range basalt, implying a genetic association. Where contact relations are exposed, the basalt is intruded by the meta-plutonic rocks. Two different bodies of leucogabbro have yielded Early Permian U-Pb ages (ca. 274 Ma, Mortensen, 1992b; J. Mortensen and D. Murphy, unpublished data, 2000).

### *Mid-Permian (to Triassic?) clastic rocks*

Isolated outcrops of weakly deformed polymictic conglomerate, sandstone and siltstone, and rare mafic meta-volcanic rocks, occur sporadically across the central part of the map area, mainly near the northern edge of Yukon-Tanana Terrane. The conglomerate is light green- to tan-weathering and poorly bedded. Sandstone and siltstone are tan, and locally grade to argillite. Clasts in the conglomerate are locally derived, being mainly foliated chert and phyllite where the conglomerate overlies the Finlayson succession, and basalt where the conglomerate overlies the Campbell Range basalt. Other clasts include serpentinized ultramafic rocks, limestone, and quartz- and feldspar-phyric meta-volcanic rock. Randomly oriented foliated clasts, inferred to be derived from the Finlayson succession, imply that the conglomerate post-dates the intense deformation of the succession.

The age of the conglomerate in Finlayson Lake area is poorly constrained, however, lithologic similarity to better dated conglomerate units along strike to the west and southeast imply either a mid-Permian or Triassic age. In one locality in the northern part of the map area, conglomerate clasts are mostly Campbell Range basalt, hence it must be younger than latest Pennsylvanian to Early Permian. If the clasts of serpentinized ultramafic rock were derived from the ultramafic meta-plutonic rocks that intrude the Campbell Range basalt, then the conglomerate is younger than ca. 274 Ma. Southeast of the Finlayson Lake area, throughout Frances Lake map area, and as far south as Watson Lake, lithologically similar polymictic conglomerate occurs at a similar structural position near the leading edge of Yukon-Tanana Terrane. Near Simpson Lake, conglomerate is interbedded with limestone containing Permian conodonts (J. Mortensen, pers. comm., 1999; identification by M.J. Orchard) and with felsic volcanic rocks that have mid-Permian U-Pb dates (J. Mortensen, pers. comm., 2000). Clasts within the conglomerate have mid-Permian to Triassic cooling ages (Mortensen et al., 1999). A mid-Permian age is therefore indicated for the conglomerate unit in Watson Lake area. However, west of the Finlayson Lake area near Faro, lithologically similar polymictic conglomerate is interbedded with limy shales that contain Late Triassic conodonts (Tempelman-Kluit, 1979; Mortensen and Jilson, 1985; Mortensen, et al., 1997, 1999). The Faro conglomerate differs from the Finlayson Lake-Frances Lake-Watson Lake conglomerates in that it does not lie along the leading edge of Yukon-Tanana Terrane. The Faro conglomerate occurs southwest of the belt of basalt of the Anvil Range Group that extends almost to Finlayson Lake map area, and which likely correlates with basalt of the Campbell Range succession. Owing to the overall similarity with the Watson Lake conglomerate, a mid-Permian age for the Finlayson Lake conglomerate succession is preferred.

## POST-THRUSTING INTRUSIVE ROCKS OF YUKON-TANANA TERRANE

In addition to the mid-Paleozoic meta-plutonic rocks of the various thrust sheets, rocks of Yukon-Tanana Terrane are intruded by two suites of plutonic rocks that are absent in the North American miogeocline. These include rare, narrow, variably foliated dykes of granite and hornblende granodiorite of probable mid-Permian age

(J. Mortensen and D. Murphy, unpublished data), as well as stocks of weakly foliated Jurassic hornblende granodiorite (Mortensen, 1992a).

## NORTH AMERICAN MIOGEOCLINE

Rocks of the North American miogeocline include four units: Silurian to Devonian rocks of McEvoy Platform (S. Gordey, pers. comm., 2001); unconformably overlying dark clastic rocks and chert of the Devonian-Mississippian Earn Group; chert of the Carboniferous to Permian Mt. Christie Formation; and Triassic clastic rocks and limestone. Miogeoclinal rocks are folded and locally weakly foliated, but show no evidence of multiple regional deformations, as do rocks of Yukon-Tanana Terrane.

### McEVOY PLATFORM

S. Gordey (pers. comm., 2001) defines McEvoy Platform as the belt of dominantly shallow water siltstone, carbonate and quartzite of Siluro-Devonian age that extends northwestward from Watson Lake map area to southern Sheldon Lake map area, crossing the northeastern corner of Finlayson Lake map area. The platformal rocks in Finlayson Lake area have been subdivided into four map units, which are intermittently exposed beneath the unconformity at the base of the overlying Earn Group. The oldest unit is composed of tan to orange-brown platy siltstone of Silurian age (unit Ss of Tempelman-Kluit, 1977; Poulton et al., 1999). This unit passes upward into a unit of cream-weathering, sandy dolostone and grey quartzite (unit Sdq of Tempelman-Kluit, 1977), which grades upwardly into massive grey orthoquartzite (unit Sq of Tempelman-Kluit, 1977). The top of the McEvoy Platform succession is a unit of dark grey limestone containing two-hole crinoids suggesting a middle Devonian age (unit Sd of Tempelman-Kluit, 1977).

### EARN GROUP

Dark clastic rocks of the Earn Group underlie an extensive, east-striking belt across the northern part of the map area. The Earn Group is primarily dark grey, pin-striped slate, but also includes dark chert, chert-pebble conglomerate, bedded barite, and, rarely, sandstone and grit/pebble conglomerate with quartz and feldspar. The basal rocks of the Earn Group overlie different units of McEvoy Platform in the northeastern corner of the map area, suggesting that the regional unconformity that has been documented elsewhere in the Selwyn Basin region (Gordey et al., 1982, 1987) also occurs in Finlayson Lake map area.

The age span of the Earn Group in Finlayson Lake area is not known as no fossils have been reported. Regionally, the Earn Group ranges in age from Middle Devonian to earliest Mississippian (Gordey et al., 1982; Gordey and Anderson, 1993).

### MT. CHRISTIE FORMATION

Chert and shale overlying the dark clastic rocks of the Earn Group have been assigned to the Mt. Christie Formation. The unit occurs in an east-striking belt from the Pelly River to McEvoy Creek, south of, and parallel to, the belt of underlying Earn Group. Mt. Christie chert is massive to thick-bedded, pale green to black, and alternates with thinner interbeds of similarly coloured dark shale. Differential erosion of alternating chert and shale lends a corrugated appearance to the terrain underlain by the Mt. Christie Formation.

The age of the Mt. Christie Formation in Finlayson Lake area is not known. Elsewhere, fossils ranging in age from Late Mississippian to Late Permian have been reported (S. Gordey, pers. comm., 2001).

### UNNAMED TRIASSIC FORMATION

The Mt. Christie Formation is overlain to the south by a sequence of dark clastic rocks and limestone of Late Triassic age. The sequence consists mostly of tan-brown-weathering, weakly calcareous, grey-green, finely laminated, platy siltstone and fine sandstone. Ripple cross-lamination occurs locally and detrital mica is visible on most parting surfaces. One member of light grey, sandy, bioclastic limestone occurs in the middle of the sequence. This unit has been traced for about 14 km within the Triassic outcrop belt midway between Finlayson and Fortin lakes. Conodonts obtained from this unit are consistently Early Norian in age (Poulton et al., 1999).

An 11-km-long outlier of Triassic rocks occurs 9 km southwest of the western end of Finlayson Lake. At this locality, folded dark silty shale; fine-grained, laminated and ripple cross-laminated, tan-brown weathering, detrital mica-bearing sandstone; and fetid, dark grey limestone of Late Carnian age (Poulton, et al., 1999) alternate with fragmental basalt and greenstone, and serpentinized ultramafic rock. Although poorly exposed, the repetitions are inferred to be thrust imbricates of an original unconformable depositional contact between the Triassic rocks and the fragmental basalt, greenstone and ultramafic rock. Poly-deformed, pre-Upper Devonian meta-sedimentary and meta-volcanic rocks of the Grass Lakes succession surround the imbricated rocks at higher elevations, as well as structurally overlying them to the south and north (Murphy et al., 2001). This relation suggests that the imbricated rocks are exposed in a structural window through Yukon-Tanana Terrane.

## THE INCONNU THRUST

Rocks of Yukon-Tanana Terrane are in contact with rocks of the North American miogeocline along the Inconnu thrust. Although unexposed, the thrust was initially recognized in the 105G/15 mapsheet, southwest of Fortin Lake (Fig. 2). At this locality, polymictic, mid-Permian (to Triassic?) conglomerate and unconformably underlying intensely foliated siliceous phyllite and chert of the Finlayson succession are juxtaposed against dark, south-dipping shale, siltstone and bioclastic limestone of Late Triassic age (see below). Between the Pelly River and the western edge of the map area, progressively older strata are present in the footwall. Similarly, south and southeast of Fortin Lake (Fig. 2), Triassic rocks occur intermittently in the immediate footwall, but locally, the Finlayson succession is juxtaposed against Early Paleozoic quartzite and dolomite of McEvoy Platform.

The structural window through Yukon-Tanana Terrane into Upper Triassic rocks southwest of Finlayson Lake is inferred to be a window through the Inconnu thrust sheet. The Inconnu thrust is the only thrust in the area with Upper Triassic rocks in its footwall; all other faults are Paleozoic in age. Therefore, a geometrically plausible interpretation is that the Upper Triassic rocks under the leading edge of the thrust in 105G/15 are continuous in the subsurface with the Upper Triassic rocks in the window. If so, then the Inconnu thrust must be a gently folded, low angle, large displacement thrust fault.

## MESOZOIC AND CENOZOIC IGNEOUS ROCKS

Cretaceous and Tertiary igneous rocks underlie about 5% of northern Finlayson Lake area. The Cretaceous and Eocene episodes are represented by both volcanic and plutonic rocks, suggesting that the present erosion level in some parts of the map area approximates the Cretaceous and Eocene erosion level.

### CRETACEOUS IGNEOUS ROCKS

The Cretaceous episode is mainly represented by weakly foliated to unfoliated peraluminous granitic plutons. Weakly foliated intrusions occur mainly in the southeastern part of the area, where the country rock is at a higher metamorphic grade. Crosscutting relationships in this area suggest that the weakly foliated suite is late kinematic with respect to deformation in the host rock (Murphy, 1997; Murphy and Timmerman, 1997; Murphy and Piercey, 1999b). Unfoliated granitic stocks intrude poly-deformed rocks of Yukon-Tanana Terrane in the southern and south-central parts of the map area (Murphy et al., 2001). Two unfoliated granitic stocks with aeromagnetically prominent hornfels zones occur in the northeastern corner of the map area where they intrude rocks of the North American miogeocline.

A small outlier of Cretaceous South Fork volcanics extends into the northern part of the Finlayson Lake map area from Sheldon Lake map area (S. Gordey, pers. comm., 2001; Gordey and Makepeace, 1999). The South Fork volcanics consist of massive, poorly stratified, dacitic crystal-lithic tuff. Lithic clasts can be several cubic metres in size and include blocks of Silurian dolostone suggesting that the volcanic rocks erupted through rocks of McEvoy Platform.

U-Pb crystallization ages suggest that there is more than one episode of Cretaceous magmatism in the area (J.K. Mortensen, 2001). Zircon and monazite ages on weakly foliated to unfoliated intrusions in the southern part of the area are mainly 110 Ma to 112 Ma. No U-Pb dates have been obtained from the intrusions into the miogeocline in the northeastern corner of the map area. The South Fork volcanics, however, have been dated as 97 ± 1 Ma (Mortensen, 1999).

### EOCENE IGNEOUS ROCKS

Eocene magmatism was compositionally diverse (Jackson et al., 1986). Basalt is the most extensive product, occurring in a variety of settings ranging from thick pillowed flows and tuff breccia in a massif west of Starr Creek ('Pillow Mountain' locality of Jackson et al., 1986), to a columnar-jointed volcanic neck and flow complex near Weasel Lake. Massive flows occur along Starr Creek near the Robert Campbell Highway and along the Hoole River. Aeromagnetically prominent gabbro and pyroxenite in the Pelly River valley in the western part of the map area are inferred to be the sub-volcanic equivalents of the basalt. Quartz-feldspar porphyritic volcanic rocks occur in

Starr Creek in a fault block within the Tintina fault zone, west of the limit of mapping (Jackson et al., 1986). These may be continuous with the Grew Creek volcanic rocks located in the Tintina Trench northwest of the map area (Jackson et al., 1986). Isolated bodies of quartz-feldspar porphyritic intrusions occur north of Finlayson Lake.

K-Ar ages on both basalt and felsic volcanic rocks range from ca. 46 Ma to ca. 58 Ma confirming the Eocene age of these rocks, and attesting to the bimodal nature of Eocene magmatism (Jackson et al., 1986; Mortensen, 1999).

## MINERAL OCCURRENCES AND POTENTIAL

The Finlayson Lake map area contains 143 known mineral occurrences (Yukon MINFILE, 2001), and therefore has a correspondingly high potential for new discoveries. The 1994 discovery of the Kudz Ze Kayah volcanic-hosted massive sulphide deposit (op. cit., 105G 117; Schultze, 1996) led to Yukon's largest staking rush. This staking rush lead to the discovery of new volcanic-hosted deposits such as GP4F near Kudz Ze Kayah (Yukon MINFILE, 2001, 105G 143) and Ice (op. cit., 105G 118) in Permian basalt of the Campbell Range succession, as well as the delineation of reserves on previously known occurrences such as Wolverine (Yukon MINFILE, 2001, 105G 072; Tucker et al., 1997) and Fyre Lake (Yukon MINFILE, 2001, 105G 032; Foreman, 1998). In the northern part of Finlayson Lake map area, dark shale of the Earn Group and carbonaceous phyllite in Yukon-Tanana Terrane contain Zn-Pb-Ag-Ba sedimentary-exhalative (SEDEX) deposits (e.g., Dwonk; Yukon MINFILE, 2001, 105G 094) and have seen sporadic interest, especially following discoveries in the Anvil district near Faro. Exploration around mid-Cretaceous granitic intrusions in the area has uncovered skarn, vein and other types of intrusion-related occurrences. Eocene igneous rocks near the Tintina Fault have been the focus of some exploration for epithermal gold deposits similar to the Grew Creek deposit in the Tintina Trench, located about 50 km northwest of the western edge of the map area (Duke and Godwin, 1986; Christie et al., 1992). The area's potential for this type of deposit was recently affirmed by a coincident Hg-As-Sb-Tl-Au-Ag till geochemical anomaly defined in northwestern Weasel Lake map area (105G/13; Bond, 2001; Bond and Plouffe, this volume). A recent addition to this impressive mineral inventory are emeralds, discovered in 1998 in the southern part of the map area. They occur in pockets along quartz-tourmaline-beryl veins in mafic meta-volcanic rocks near where a mid-Cretaceous pluton intrudes ultramafic and mafic meta-plutonic rocks (Crown showing on Goal Net property, Yukon MINFILE, 2001, 105G 123; L.A. Groat, pers. comm., 2001).

The new map of the northern part of Finlayson Lake map area (Murphy et al., 2001) extends to the northwest, to areas known to be underlain by the prospective meta-volcanic rock units that host the syngenetic deposits in the core of the Finlayson Lake district. Most of the area west and southwest of Finlayson Lake, between the Robert Campbell Highway and the Tintina Fault, is underlain by the Grass Lakes succession and Mississippian augen orthogneiss. The lowest unit of the Grass Lakes succession contains a greater abundance of felsic meta-volcanic rocks in this area than in the better exposed eastern part of the area (105G/7 and 8) and is locally mineralized (e.g. Yukon MINFILE, 2001, 105G 016). Several occurrences have been found in the area underlain by the Fire Lake unit (Yukon MINFILE, 2001). Higher in the Grass Lakes succession, chloritic phyllite (mafic meta-volcanic rock) of the Fire Lake unit occurs extensively, commonly associated with large and extensive masses of mafic and ultramafic meta-plutonic rocks, an association found near the Fyre Lake deposit. Part of the area shown on previous maps as being underlain by augen orthogneiss (Tempelman-Kluit, 1977; Mortensen and Jilson, 1985) is now known to be underlain by a large roof pendant in the meta-plutonic body consisting of rocks of the Fire Lake unit and the underlying quartz-rich meta-clastic unit (Fig. 2). A new

***Table 1.*** *New mineral showings in northern Finlayson Lake area.*

| **Name** | **Type** | **Easting (83)** | **Northing (83)** |
|---|---|---|---|
| CAM | volcanogenic massive sulphide | 408105 | 6836588 |
| STEVE | volcanogenic massive sulphide | 384404 | 6838698 |
| PAT | volcanogenic massive sulphide | 401302 | 6844329 |
| BEAR | sedimentary exhalative | 439637 | 6837687 |

showing was discovered in rocks of the Fire Lake unit within the pendant (Steve showing, Table 1; Murphy et al., 2001). The Kudz Ze Kayah unit, host of the deposit of the same name, is less extensive in the western part of the Finlayson Lake area than in the heart of the massive sulphide district, and for the most part, is represented by carbonaceous phyllite. Felsic meta-volcanic rocks of this unit occur in a northeast-trending belt east of the headwaters of Big Campbell Creek, where they host the League occurrence (Yukon MINFILE, 2001, 105G 130), and in the area south of the northwest end of Finlayson Lake, between Campbell Creek and the Robert Campbell Highway. A new showing and kill zone were discovered in rocks of the Kudz Ze Kayah unit along Campbell Creek (Cam showing, Table 1; Murphy et al., 2001).

Intermediate to felsic meta-volcanic rocks of the Money Creek thrust sheet are locally porphyritic, pyritic or altered, suggesting that they may have potential to host massive sulphide deposits. Yukon MINFILE (2001) occurrence 105G 108 is located near outcrops of sericite-altered, pyritic, felsic meta-volcanic rocks, south of the southeastern end of Finlayson Lake. A new showing of pyritic and silicified felsic meta-volcanic rocks was found north of the Robert Campbell Highway, east of the bridge over Campbell Creek (Pat showing, Table 1; Murphy et al., 2001). Pale greenish-white feldspar-quartz meta-porphyry that occurs about 8 km north-northwest of the confluence of Big Campbell Creek and the Pelly River, may be a sub-volcanic intrusion and may possibly indicate a volcanic centre for the meta-volcanic rocks of the thrust sheet.

The Finlayson succession has potential for both volcanic-hosted and sedimentary exhalative massive sulphide deposits. Significant thicknesses of felsic meta-volcanic rocks occur in the succession north of the Finlayson River in the eastern part of the map area, and north of the Pelly River, in the western part of the map area. Porphyritic varieties occur in both localities. A barite occurrence (also noted by Cominco Ltd., B. Mauer, pers. comm., 2001), is hosted by carbonaceous phyllite north of the Finlayson River in the eastern part of the map area (Bear showing, Table 1).

## DISCUSSION

The 1996-2001 mapping of Yukon-Tanana Terrane in Finlayson Lake and Frances Lake map areas (Fig. 1) and associated petrochemical (Piercey et al., 1999, 2000, 2001a,b; Piercey, 2001), geochronological and biochronological studies have led to a new understanding of the geological evolution of this complex terrane. The picture that emerges from this work is one of a continental or transitional crustal fragment evolving through rapidly changing convergent margin geodynamic settings during the mid- and Late Paleozoic, and ultimately amalgamating with the North American miogeocline in Jura-Cretaceous time. During Late Devonian and early Mississippian time, a southwest-facing (current geographic coordinates) continental arc and back-arc magmatic system was established on this crustal block. Following the early Mississippian cessation of arc-back-arc magmatism in this area, a mid-Mississippian hiatus and a late Mississippian to mid-Pennsylvanian period of carbonate deposition, the arc rocks and overlying carbonates were thrust to the northeast over the back-arc rocks along the Money Creek thrust. In the late Pennsylvanian, this thrust-shortened terrane became the locus of uplift, erosion, and sedimentation of basinal coarse-grained clastic rocks derived from the hinterland of the thrust belt. The shortened arc-back-arc complex, and the overlapping clastic rocks were subsequently thrust to the northeast over basinal rocks of the Finlayson succession in the latest Pennsylvanian, before the Early Permian deposition of the Campbell Range succession. Originally considered to be part of Slide Mountain Terrane (e.g., Plint and Gordon, 1997 and references therein), the Campbell Range succession is now inferred to be a manifestation of rifting of the thrust-imbricated Yukon-Tanana Terrane, possibly in the back-arc region of an Early Permian arc, which was recently recognized in Wolf Lake map area (Roots et al., in press). Mid-Permian time is represented by a polymictic conglomerate made up of clasts of Yukon-Tanana Terrane lithologies that was likely deposited in a fore-arc setting along the eastern (present geographic coordinates) margin of Yukon-Tanana Terrane (Mortensen et al., 1997, 1999). The switch to subduction along the northern/eastern side of the terrane led to the consumption of the Slide Mountain Terrane ocean rocks that commonly occur between Yukon-Tanana Terrane and North America (Nelson, 1993; Ferri, 1997 and references therein). This subduction is believed to have initiated the process of convergence between Yukon-Tanana Terrane and North America that culminated with the post-Late Triassic thrusting of the terrane onto the North American miogeocline along the Inconnu thrust.

The recognition of the several different and sequentially developed paleogeographic settings within Yukon-Tanana Terrane has implications for the exploration for new mineral deposits. With the exception of the Fyre Lake deposit, all of the known volcanic-hosted massive sulphide deposits occur within rocks inferred to have been deposited in back-arc settings (Piercey and Murphy, 2000; Piercey, 2001b). The Kudz Ze Kayah and GP4F deposits formed in the Late Devonian back-arc region, while Wolverine Lake formed in the early Mississippian back-arc region, all of these in the footwall of the Money Creek thrust. The Ice deposit formed during rifting behind a coeval Early Permian arc recently recognized in southern Yukon (Roots et al., in press). As was noted by Piercey et al. (2000, 2001b), back-arc settings have the structural and thermal characteristics necessary for the generation and maintenance of large-scale hydrothermal circulatory systems that lead to the development of sea floor massive sulphide deposits.

The back-arc regions are clearly prospective for mineral deposits, however, the arc region also holds promise for new discoveries. This region contains one deposit and several occurrences. The Fyre Lake deposit occurs in boninitic rocks that Piercey et al. (2001a) concluded formed in an intra-arc rift. Piercey et al. (2001a) noted that the structural and thermal characteristics of arc-rift settings are similar to those in a back-arc region (high heat-flow and extensional syn-volcanic faults). Numerous gossanous areas occur in felsic intervals within the dominantly intermediate Mississippian meta-volcanic rocks in the hanging wall of the Money Creek thrust of southwestern Frances Lake map area (Murphy, 2001). The new showing in felsic rocks in the hanging wall of the Money Creek thrust, north of the Robert Campbell Highway, was documented in this study (Pat showing, Table 1).

Further insight into the mineral potential of specific areas within northern Finlayson Lake map area can be gained by considering the new bedrock map in conjunction with the results of the concurrently conducted till geochemistry program (Bond and Plouffe, this volume). Several coincident base metal geochemical anomalies occur in the map area, which can be correlated with meta-volcanic units that lie in the 'up-ice' direction. Altogether, this bedrock, and surficial mapping and till geochemistry initiative, provide comprehensive coverage and a firm foundation for systematic regional mineral exploration.

## ACKNOWLEDGEMENTS

This project was jointly funded by Yukon Geology Program and the Geological Survey of Canada under the auspices of the Targeted Geoscience Initiative. The authors would especially like to thank the following: Lee Manderson (pilot) and Gord and Amos Marsden (engineers) of West Coast Helicopters for safe and reliable flying services; Louise Levesque and Karen van der Laars for great camp cooking; Joe Haggett for making, maintaining and taking down a warm and comfortable camp; Monique Raitchey of the Yukon Geology Program for patient expediting and administration; and Dorothy Dick and Gary McLaughlin for being great neighbours. Camp security and comic relief for the project generously provided by Canine Companions, Inc. This paper benefitted greatly from a critical review by Robert Stroshein of Yukon Geology Program.

## REFERENCES

Bond, J.D., 2001. Surficial geology and till geochemistry of Weasel Lake map area (105G/13), east-central Yukon. *In:* Yukon Exploration and Geology 2000, D.S. Emond and L.H. Weston (eds.), Exploration and Geological Services Division, Yukon Region, Indian and Northern Affairs Canada, p. 73-96.

Bond, J.D. and Plouffe, A., 2002 (this volume). Finlayson Lake Targeted Geoscience Initiative (southeastern Yukon), Part 2: Quaternary geology and till geochemistry. *In:* Yukon Exploration and Geology 2001, D.S. Emond, L.H. Weston and L.L. Lewis (eds.), Exploration and Geological Services Division, Yukon Region, Indian and Northern Affairs Canada, p. 209-228 plus 10 fold-out maps.

Bradshaw, G.D., Tucker, T.L., Peter, J.M., Paradis, S. and Rowins, S.M., 2001. Geology of the Wolverine polymetallic volcanic-hosted massive sulphide deposit, Finlayson Lake district, Yukon Territory, Canada. *In:* Yukon Exploration and Geology 2000, D.S. Emond and L.H. Weston (eds.), Exploration and Geological Services Division, Yukon Region, Indian and Northern Affairs Canada, p. 269-287.

Christie, A.B., Duke, J.L. and Rushton, R., 1992. Grew Creek epithermal gold-silver deposit, Tintina Trench, Yukon (105K/2). *In:* Yukon Geology, Volume 3, T.J. Bremner (ed.), Exploration and Geological Services Division, Yukon Region, Indian and Northern Affairs Canada, p. 223-259.

Dawson, G.M., 1888. The Yukon district and British Columbia, Annual Report of the Geological and Natural History Survey of Canada, Volume III, Part I. B, 277 p.

Duke, J.L. and Godwin, C.I., 1986. Geology and alteration of the Grew Creek epithermal gold-silver prospect, south-central Yukon. *In:* Yukon Geology, Volume 1, Exploration and Geological Services Division, Yukon Region, Indian and Northern Affairs Canada, p. 72-82.

Ferri, F., 1997. Nina Creek Group and Lay Range Assemblage, north-central British Columbia: Remnants of late Paleozoic oceanic and arc terranes. Canadian Journal of Earth Sciences, vol. 34, p. 854-874.

Foreman, I., 1998. The Fyre Lake project 1997: Geology and mineralization of the Kona massive sulphide deposit. *In:* Yukon Exploration and Geology 1997, Exploration and Geological Services Division, Yukon Region, Indian and Northern Affairs Canada, p. 105-113.

Gordey, S.P. and Anderson, RG., 1993. Evolution of the northern Cordilleran miogeocline, Nahanni map area (105I), Yukon and Northwest Territories. Geological Survey of Canada Memoir 428, 214 p.

Gordey, S.P. and Makepeace, A.J., 1999. Yukon Digital Geology. S.P. Gordey and A.J. Makepeace (comps.), Geological Survey of Canada, Open File D3826, and Exploration and Geological Services Division, Yukon Region, Indian and Northern Affairs Canada, Open File 1999-1(D), 2 CD-ROMs.

Gordey, S.P., Abbott, J.G. and Orchard, M.J., 1982. Devono-Mississippian Earn Group and younger strata in east-central Yukon. *In:* Current Research, Part B, Geological Survey of Canada, Paper 82-1B, p. 93-100.

Gordey, S.P., Abbott, J.G., Tempelman-Kluit, D.J. and Gabrielse, H., 1987. "Antler" clastics in the Canadian Cordillera. Geology, vol. 15, p. 103-107.

Grant, S.L., 1997. Geochemical, radiogenic tracer isotopic, and U-Pb geochronological studies of Yukon-Tanana Terrane rocks from the Money Klippe, southeastern Yukon, Canada. Unpublished MSc. Thesis, University of Alberta, 177 p.

Hunt, J.A. and Murphy, D.C., 1998. A note on preliminary bedrock mapping in the Fire Lake area. *In:* Yukon Exploration and Geology 1997. Exploration and Geological Services Division, Yukon Region, Indian and Northern Affairs Canada, p. 59-68.

Jackson, L.E., Gordey, S.P., Armstrong, R.L. and Harakal, J.E., 1986. Bimodal Paleogene volcanics near Tintina Fault, east-central Yukon, and their possible relationship to placer gold. *In:* Yukon Geology, Volume 1, J.A. Morin and D.S. Emond (eds.), Exploration and Geological Services Division, Yukon Region, Indian and Northern Affairs Canada, p. 139-147.

Keele, J., 1910. A Reconnaissance Across the Mackenzie Mountains on the Pelly, Ross and Gravel Rivers, Yukon and Northwest Territories. Geological Survey Branch, Canada Department of Mines, Publication No. 1097, 54 p.

Mortensen, J.K., 1983. Age and evolution of the Yukon-Tanana terrane, southeastern Yukon Territory. Unpublished Ph.D thesis, University of California, Santa Barbara, 155 p.

Mortensen, J.K., 1992a. Pre-mid-Mesozoic tectonic evolution of the Yukon-Tanana Terrane, Yukon and Alaska. Tectonics, vol. 11, p. 836-853.

Mortensen, J.K., 1992b. New U-Pb zircon ages for the Slide Mountain Terrane in southeastern Yukon Territory. *In:* Radiogenic Age and Isotopic Studies: Report 5, Geological Survey of Canada, Paper 91-2, p. 167-173.

Mortensen, J.K. (comp.), 1999. YUKONAGE, An isotopic age database for the Yukon Territory. *In:* Yukon Digital Geology, S.P. Gordey and A.J. Makepeace (comps.), Geological Survey of Canada, Open File D3826, and Exploration and Geological Services Division, Yukon Region, Indian and Northern Affairs Canada, Open File 1999-1(D), 2 CD-ROMs.

Mortensen, J.K. and Jilson, G.A., 1985. Evolution of the Yukon-Tanana terrane: evidence from southeastern Yukon Territory. Geology, vol. 13, p. 806-810.

Mortensen, J.K., Erdmer, P. and Ghent, E.D., 1997. Westerly-derived Upper Triassic clastic sedimentary rocks in southeastern Yukon: Evidence for Early Mesozoic terrane interaction with the western margin of ancestral North America. *In:* Slave – Northern Cordillera Lithospheric Evolution (SNORCLE) Transect and Cordilleran Tectonics Workshop Meeting, Abstracts, F. Cook and P. Erdmer (comp.), Lithoprobe Report No. 56, p. 76.

Mortensen, J.K., Erdmer, P., Piercey, S.J. and Ghent, E.D., 1999. Evidence for Late Triassic terrane accretion in the northern Canadian Cordillera in southeastern Yukon. Geological Survey of Canada/Geological Association of Canada, Terrane Paths 99, Circum-Pacific Terrane Conference, Abstracts and Program, p. 55.

Murphy, D.C., 1997. Preliminary geological map of Grass Lakes area, Pelly Mountains, southeastern Yukon (105G/7). Exploration and Geological Services Division, Yukon Region, Indian and Northern Affairs Canada, Open File 1997-3, 1:50 000 scale.

Murphy, D.C., 1998. Stratigraphic framework for syngenetic mineral occurrences, Yukon-Tanana Terrane south of Finlayson Lake: A progress report. *In:* Yukon Exploration and Geology 1997, Exploration and Geological Services Division, Yukon Region, Indian and Northern Affairs Canada, p. 51-58.

Murphy, D.C., 2000a. Preliminary geological map of part of the Klatsa River area (105H/3), southeastern Yukon, 1:50 000 scale. Exploration and Geological Services Division, Yukon Region, Indian and Northern Affairs Canada, Open File 2000-15.

Murphy, D.C., 2000b. Preliminary geological map of part of the 'Tuchitua River-north' (105H/4), southeastern Yukon (1:50 000 scale). Exploration and Geological Services Division, Yukon Region, Indian and Northern Affairs Canada, Open File 2000-15.

Murphy, D.C., 2000c. Preliminary geological map of part of the Money Creek area (105H/5), southeastern Yukon (1:50 000 scale). Exploration and Geological Services Division, Yukon Region, Indian and Northern Affairs Canada, Open File 2000-15.

Murphy, D.C., 2001. Yukon-Tanana Terrane in southwestern Frances Lake area (105H/3, 4, and 5), southeastern Yukon. *In:* Yukon Exploration and Geology 2000, D.S. Emond and L.H. Weston (eds.), Exploration and Geological Services Division, Yukon Region, Indian and Northern Affairs Canada, p. 217-233.

Murphy, D.C. and Piercey, S.J., 1999a. Geological map of Wolverine Lake area, Pelly Mountains (NTS 105G/8), southeastern Yukon. Exploration and Geological Services Division, Yukon Region, Indian and Northern Affairs Canada, Open-File 1999-3, 1:50 000 scale.

Murphy, D.C. and Piercey, S.J., 1999b. Finlayson Project: Geological evolution of Yukon-Tanana Terrane and its relationship to the Campbell Range belt, northern Wolverine Lake map area, southeastern Yukon. *In:* Yukon Exploration and Geology 1998, D.S. Emond and C.F. Roots (eds.), Exploration and Geological Services Division, Yukon Region, Indian and Northern Affairs Canada, p. 47-62.

Murphy, D.C. and Piercey, S.J., 1999c. Geological map of parts of Finlayson Lake (105G/7, 8 and parts of 1, 2, and 9) and Frances Lake (parts of 105H/5 and 12) areas, southeastern Yukon. Exploration and Geological Services Division, Yukon Region, Indian and Northern Affairs Canada, Open-File 1999-4, 1:100 000 scale.

Murphy, D.C. and Piercey, S.J., 2000. Syn-mineralization faults and their re-activation, Finlayson Lake massive sulphide district, Yukon-Tanana Terrane, southeastern Yukon. *In:* Yukon Exploration and Geology 1999, D.S. Emond and L.H. Weston (eds.), Exploration and Geological Services Division, Yukon Region, Indian and Northern Affairs Canada, p. 55-66.

Murphy, D.C. and Timmerman, J.R.M., 1997. Preliminary geology of the northeast third of Grass Lakes map area (105G/7), Pelly Mountains, southeastern Yukon. *In:* Yukon Exploration and Geology 1996, Exploration and Geological Services Division, Yukon Region, Indian and Northern Affairs Canada, p. 62-73.

Murphy, D.C., Colpron, M., Gordey, S.P., Roots, C., Abbott, J.G. and Lipovsky, P.S., 2001. Preliminary bedrock geological map of northern Finlayson Lake area (NTS 105G), Yukon Territory. Exploration and Geological Services Division, Yukon Region, Indian and Northern Affairs Canada, Open File 2001-33, 1:100 000 scale.

Nelson, J.L., 1993. The Sylvester Allochthon: Upper Paleozoic marginal-basin and island-arc terranes in northern British Columbia. Canadian Journal of Earth Sciences, vol. 30, p. 631-643.

Piercey, S.J., 2001. Petrology and tectonic setting of felsic and mafic volcanic and intrusive rocks in the Finlayson Lake volcanic-hosted massive sulphide (VHMS) district, Yukon, Canada: A record of mid-Paleozoic arc and back-arc magmatism and metallogeny. Unpublished PhD thesis, University of British Columbia, 304 p.

Piercey, S.J. and Murphy, D.C., 2000. Stratigraphy and regional implications of unstrained Devono-Mississippian volcanic rocks in the Money Creek Thrust Sheet, Yukon-Tanana Terrane, southeastern Yukon. *In:* Yukon Exploration and Geology 1999, D.S. Emond and L.H. Weston (eds.), Exploration and Geological Services Division, Yukon Region, Indian and Northern Affairs Canada, p. 67-78.

Piercey, S.J., Hunt, J.A. and Murphy, D.C., 1999. Lithogeochemistry of meta-volcanic rocks from Yukon-Tanana Terrane, Finlayson Lake region, Yukon: Preliminary results. *In:* Yukon Exploration and Geology 1998, D.S. Emond and C.F. Roots (eds.), Exploration and Geological Services Division, Yukon Region, Indian and Northern Affairs Canada, p. 125-138.

Piercey, S.J., Murphy, D.C., Mortensen, J.K. and Paradis, S., 2000. Arc-rifting and ensialic back-arc basin magmatism in the northern Canadian Cordillera: Evidence from the Yukon-Tanana Terrane, Finlayson Lake region, Yukon. *In:* Slave-Northern Cordilleran Lithospheric Experiment (SNORCLE)-Lithoprobe Report 72, Vancouver, British Columbia, Lithoprobe Secretariat, p. 129-138.

Piercey, S.J., Murphy, D.C., Mortensen, J.K. and Paradis, S., 2001a. Boninitic magmatism in a continental margin setting, Yukon-Tanana Terrane, southeastern Yukon, Canada. Geology, vol. 29, p. 731-734.

Piercey, S.J., Paradis, S., Murphy, D.C. and Mortensen, J.K., 2001b (in press). Petrological constraints on the tectonic setting of felsic volcanic-hosted volcanogenic massive sulfide (VMS) mineralization in the Finlayson Lake district, Yukon, Canada. Economic Geology.

Piercey, S.J., Peter, J.M., Bradshaw, G.D., Tucker, T. and Paradis, S., 2001c. Geological characeristics of high-level subvolcanic porphyritic intrusions associated with the Wolverine Zn-Pb-Cu volcanic-hosted massive sulphide deposit, Finlayson Lake District, Yukon, Canada. *In:* Yukon Exploration and Geology 2000, D.S. Emond and L.H. Weston (eds.), Exploration and Geological Services Division, Yukon Region, Indian and Northern Affairs Canada, p. 335-346.

Plint, H.E., 1995. Geological mapping in the Campbell Range, southeastern Yukon (parts of 105G/8/9 and 105H/12). *In:* Yukon Exploration and Geology 1994, Exploration and Geological Services Division, Yukon Region, Indian and Northern Affairs Canada, p. 47-57.

Plint, H.E. and Gordon, T.M., 1995. The Slide Mountain terrane and Finlayson Lake fault zone: Marginal basin rocks in a transpressive setting? Evidence from the Campbell Range, southeastern Yukon. *In:* F. Cook and P. Erdmer (eds.), Lithoprobe Slave – Northern Cordillera Lithospheric Evolution Report No. 44, p. 33-50.

Plint, H.E. and Gordon, T.M., 1996a. Structural evolution and rock types of the Slide Mountain and Yukon-Tanana terranes in the Campbell Range, southeastern Yukon Territory. *In:* Current Research, Part A, Geological Survey of Canada, Paper 96-1A, p. 19-28.

Plint, H.E. and Gordon, T.M., 1996b. Geology of Campbell Range near Wolverine Lake, southeastern Yukon (parts of 105H/5, 9, 12 and 105G/8, 9). Geological Survey of Canada, Open File 3303, 1:50 000 scale.

Plint, H.E. and Gordon, T.M., 1997. The Slide Mountain Terrane and the structural evolution of the Finlayson Lake Fault Zone, southeastern Yukon. Canadian Journal of Earth Sciences, vol. 34, p. 105-126.

Poulton, T., Orchard, M.J., Gordey, S.P. and Davenport, P., 1999. Selected Yukon fossil determinations. *In:* Yukon Digital Geology, S.P. Gordey and A.J. Makepeace (comps.), Geological Survey of Canada, Open File D3826, and Exploration and Geological Services Division, Yukon Region, Indian and Northern Affairs Canada, Open File 1999-1(D).

Roots, C.F., Harms, T.A., Simard, R.L., Orchard, M.J. and Heaman, L., 2002 (in press). Constraints on the age of the Klinkit assemblage east of Teslin Lake, northern British Columbia, Geological Survey of Canada, Current Research 2002-A7.

Schultze, H.C., 1996. Summary of the Kudz Ze Kayah Project, volcanic-hosted massive sulphide deposit, Yukon Territory. *In:* Yukon Exploration and Geology 1995, Exploration and Geological Services Division, Yukon Region, Indian and Northern Affairs Canada, p. 29-32.

Sebert, C. and Hunt, J.A., 1999. A note on preliminary lithogeochemistry of the Fire Lake area. *In:* Yukon Exploration and Geology 1998, C.F. Roots and D.S. Emond (eds.), Exploration and Geological Services Division, Yukon Region, Indian and Northern Affairs Canada, p. 139-142.

Tempelman-Kluit, D.J., 1977. Quiet Lake (105F) and Finlayson Lake (105G) map areas, Yukon Territory. Geological Survey of Canada, Open File 486, 1:250 000 scale.

Tempelman-Kluit, D.J., 1979. Transported cataclasite, ophiolite and granodiorite in Yukon Territory: Evidence of arc-continent collision. Geological Survey of Canada, Paper 79-14, 27 p.

Tucker, T.L., Turner, A.J., Terry, D.A. and Bradshaw, G.D., 1997. Wolverine massive sulphide project. *In:* Yukon Exploration and Geology 1996, Exploration and Geological Services Division, Yukon Region, Indian and Northern Affairs Canada, p. 53-55.

Wheeler, J.O., Green, L.H. and Roddick, J.A., 1960. Geology, Finlayson Lake, Yukon Territory. Geological Survey of Canada Map 7-1960, 1:250 000 scale.

Yukon MINFILE, 2001. Finlayson Lake area – 105G. Exploration and Geological Services Division, Yukon Region, Indian and Northern Affairs Canada.

# Finlayson Lake Targeted Geoscience Initiative (southeastern Yukon), Part 2: Quaternary geology and till geochemistry

***Jeffrey D. Bond***[1]
*Yukon Geology Program*

***Alain Plouffe***
*Geological Survey of Canada*[2]

Bond, J.D. and Plouffe, A., 2002. Finlayson Lake Targeted Geoscience Initiative (southeastern Yukon), Part 2: Quaternary geology and till geochemistry. *In:* Yukon Exploration and Geology 2001, D.S. Emond, L.H. Weston and L.L. Lewis (eds.), Exploration and Geological Services Division, Yukon Region, Indian and Northern Affairs Canada, p. 209-228 plus 10 fold-out maps.

## ABSTRACT

A regional till geochemistry survey and Quaternary geology investivations were carried out across poorly exposed terrain of the Finlayson Lake map area. Two sampling teams collected 331 till samples, including regional and deposit orientation samples from Wolverine, Kudz Ze Kayah and the Argus properties. In total, 489 till samples were analysed by ICP-MS, including 158 samples collected in 2000. Quaternary exposures were logged and interpreted in order to reconstruct the Late Wisconsinan glacial history of the area (McConnell Glaciation). Ice-flow patterns during glacial maximum generally trended towards the west-northwest. Basal till is widespread across plateau surfaces and glaciofluvial sand and gravel dominate in low-lying terrain. Multi-element anomalies are present near known mineralized zones. High lead and zinc concentrations are measured in till down-ice from the massive sulphide bedrock mineralization at Kudz Ze Kayah. In addition, multi-element anomalies particularly enriched in base metals are found northwest of Wolverine Lake and southwest of Finlayson Lake, where no mineral occurrences are known. Results of the 2000 survey indicated the presence of a multi-element anomaly suggestive of epithermal mineralization in the northwest corner of the study area. Staking has ensued in the area. Follow-up sampling on the anomaly confirmed the 2000 results and has yielded highly anomalous gold levels. Another sample collected south (up-ice) from the Kudz Ze Kayah deposit returned an unexpected high gold concentration. Samples with high copper/nickel/chromium concentrations are located in the northwest part of the study area and southwest of Finlayson Lake.

## RÉSUMÉ

Un programme d'échantillonage régional du till et une étude de la géologie du Quaternaire ont été entrepris dans une région située à l'intérieur des limites du feuillet topographique de Finlayson Lake où il y a peu d'affleurements rocheux. Deux équipes ont recueilli 331 échantillons de till afin d'en analyser la composition géochimique incluant des échantillons régionaux et des échantillons obtenus près de gisements connus tels Wolverine, Kudz Ze Kayah et Argus. Des données géochimiques sont maintenant disponible pour un total de 489 échantillons de till incluant 158 échantillons receuillis en 2000. Des coupes stratigraphiques de sédiments quaternaires ont été mesurées et interprétées dans le but de reconstituer l'histoire de la Glaciation de McConnell dans la région, au Wisconsinien tardif. En général, la glace s 'est écoulée vers l'ouest-nord-ouest pendant le maximum glaciaire. Le till de fond est largement répandu sur les plateaux alors que du sable et gravier fluvioglaciaires dominent dans les régions plus basses. Plusieurs éléments sont présents en concentrations anomales dans le till près des zones minéralisées connues. De hautes teneurs en plomb et zinc sont mesurées dans le till en aval glaciaire de la minéralisation de sulfure massif de Kudz Ze Kayah. D'autres éléments, plus particulièrement des métaux de base, sont présents en fortes teneurs au nord-ouest du lac Wolverine et au sud-ouest du lac Finlayson où il n'y a pas de minéralisation connue. Suite au programme d'échantillonnage effectué en 2000, de fortes concentrations de plusieurs éléments ont été détectées dans la partie nord-ouest de la région d'étude suggérant la présence d'une zone de minéralisation épithermale. Par la suite, la région a été jalonnée. Un échantillonnage subséquent de l'anomalie a confirmé les résultats obtenus en 2000 et permis de trouver des concentrations hautement anomales en or. On a également découvert des valeurs d 'or anomalement élevées au sud du gisement Kudz Ze Kayah. De fortes valeurs en cuivre, nickel et chrome ont été observées dans la partie nord-ouest de la région d'étude et au sud-ouest du lac Finlayson.

---

[1] *jdbond@gov.yk.ca*

[2] *Geological Survey of Canada, 601 Booth Street, Ottawa, Ontario, Canada K1A 0E8, APlouffe@NRCan.gc.ca; GSC Contribution No. 2001159*

## INTRODUCTION

As part of the Targeted Geoscience Initiative (TGI), the Geological Survey of Canada and the Yukon Geology Program carried out a joint bedrock geology mapping (see TGI , Part 1, Murphy et al., this volume) and a regional till geochemistry survey in the northern sector of the Finlayson Lake map area (NTS 105G; Fig. 1, this report). The goal of this part of the TGI project is to enhance the regional geochemical database with the intention of finding new exploration targets in this poorly exposed area. The objective of this paper is to present the results of the till geochemistry, along with new data on the Quaternary stratigraphy.

The abundance of mineral occurrences and deposits in the Finlayson Lake region (e.g., Kudz Ze Kayah, Wolverine, Fyre Lake, Ice, Yukon MINFILE, 2001; Fig. 1) clearly reflect the high mineral potential of the area. Combined probable reserves from the Kudz Ze Kayah and Wolverine deposits are estimated at 14.57 million tonnes grading 7.23% Zn, 1.53% Pb, 0.97% Cu, 184.5 g/t Ag and 1.39 g/t Au (Burke, 2001). Poor bedrock exposure has hindered mineral exploration in the northern half of the Finlayson Lake map area. Previous regional geochemical surveys in the area made use of stream sediments. This was successful in areas of high relief where drainage density is high. In low-relief terrain, where drainage density is low, stream sediment geochemistry provided limited regional coverage. Till was favoured as a sampling medium in this regional geochemical drift prospecting survey for the following reasons: 1) it occurs abundantly on plateaus and hills in areas of poor bedrock exposure; 2) it is considered as the first derivative of bedrock (Shilts, 1976, 1993), which implies that mineralized debris found in till generally has a simple transport history; and 3) one dominant ice-flow direction persisted during most of the last glaciation, which also suggests a simple transport history and facilitates tracing to the potential bedrock source of anomalies in till.

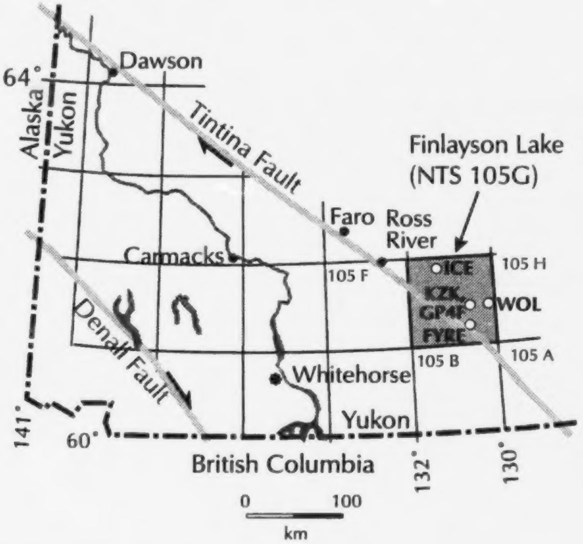

*Figure 1. Location of Finlayson Lake map area (NTS 105G). Major mineral deposits are shown: KZK = Kudz Ze Kayah, Wol = Wolverine and Fyre = Fyre Lake.*

## PREVIOUS STUDIES

Surficial geological mapping and Quaternary stratigraphic investigations were carried out by Jackson (1994) for the Pelly River region, including the Finlayson Lake map area. The surficial geology of the Frances Lake map area (105H) was mapped by Dyke (1990), the Wolf Lake map area (105B) by Klassen (1983), and the Watson Lake map area (105A) by Klassen and Morison (1982) (see Fig. 1). Building on the stratigraphic framework developed by Jackson (1989) and Plouffe (1989), Plouffe and Jackson (1992) presented a detailed study of the Quaternary succession and the regional till geochemistry of a region extending from Wolverine Lake to Faro. More recently, two studies on surficial geology and till geochemistry were completed in the Anvil district (105K) and the Weasel Lake map area (105G/13) with the objective of promoting exploration and developing the application of drift prospecting in Yukon (Bond, 2001a,b).

## PHYSIOGRAPHY AND GEOLOGY

The northern sector of the Finlayson Lake map area is part of the Yukon Plateau, which consists of a low-lying region with isolated plateaus reaching 1219 m in elevation and intermittent summits reaching 1828 m in elevation. Inter-plateau regions are generally poorly drained (Figs. 2,3). The Yukon Plateau is flanked by the Pelly and Logan mountains to the south and east, respectively. Till sampling was only conducted over the Yukon Plateau.

The drainage west and north of Finlayson Lake is part of the Pelly River watershed. The main tributaries include Hoole River and Big Campbell, Campbell, Mink and Fortin creeks. The region east of Finlayson Lake drains easterly via the Finlayson River. The continental drainage divide between the Liard River (Beaufort Sea) and Pelly River (Bering Sea) is part of the study area.

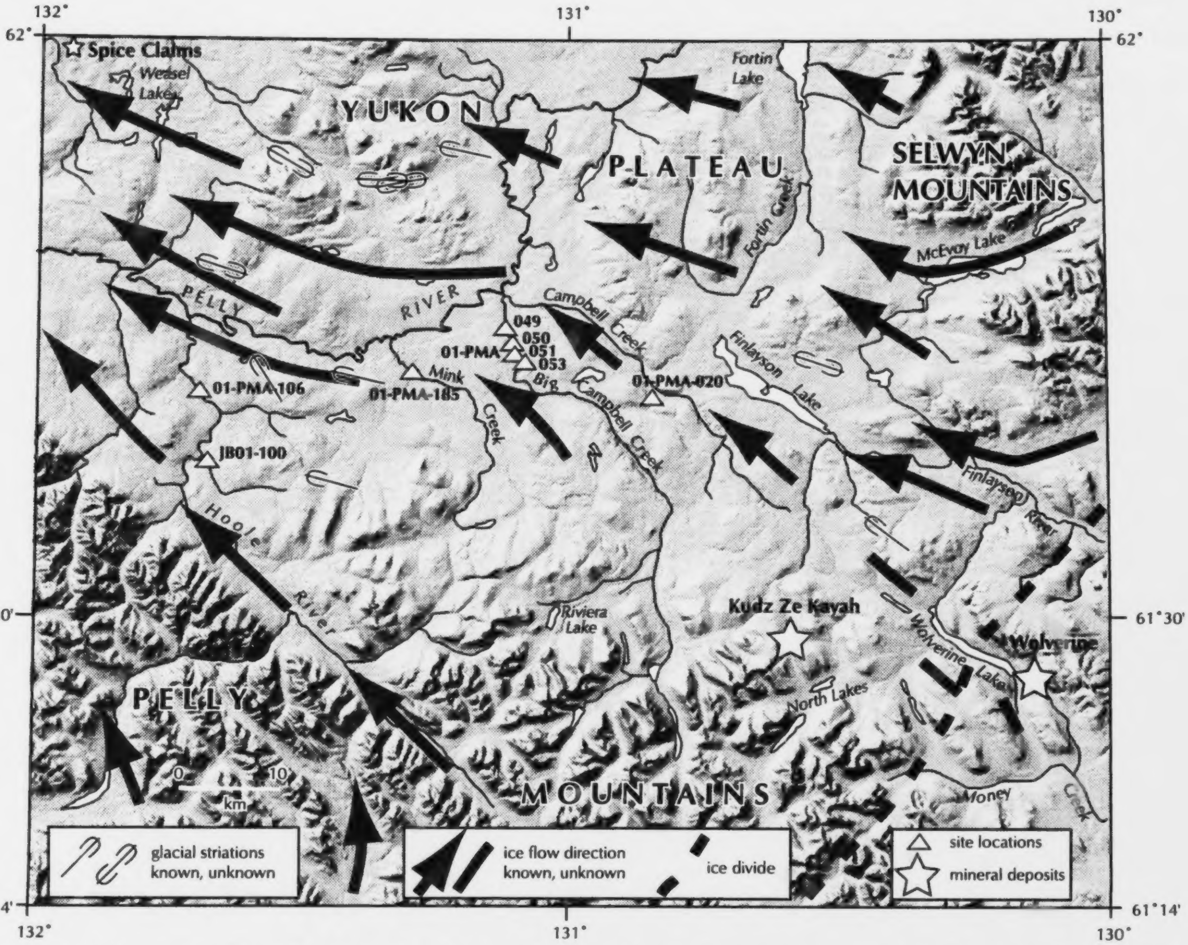
132°
131°
130°
62°
62°
Spice Claims
Weasel Lake
YUKON
PLATEAU
Fortin Lake
SELWYN MOUNTAINS
McEvoy Lake
Fortin Creek
PELLY RIVER
Campbell Creek
049
050
051
053
01-PMA
Mink
01-PMA-185
01-PMA-106
Big Campbell Creek
01-PMA-020
Finlayson Lake
JB01-100
Creek
Finlayson River
Hoole River
Riviera Lake
Kudz Ze Kayah
Wolverine Lake
Wolverine
North Lakes
61°30'
61°30'
PELLY
MOUNTAINS
0
10
km
Money Creek
glacial striations known, unknown
ice flow direction known, unknown
ice divide
site locations
mineral deposits
61°14'
61°14'
132°
131°
130°

*Figure 2. Location map with 2001 section locations, and regional ice-flow patterns simplified from Jackson (1993a,b,c,d). Glacial striations measured during the 2001 field season are also shown.*

The study area lies at the boundary between the Yukon-Tanana Terrane (YTT) and ancient North America. The YTT consists of a large crustal fragment of mafic and felsic meta-volcanic rocks, carbonaceous meta-clastic rocks, marble and granitic orthogneiss that was accreted to North America in Mesozoic time. The YTT is host of the most significant mineral deposits of the area: e.g., Fyre Lake, Kudz Ze Kayah and GP4F. See Murphy et al. (2001, 2002, this volume) for details on the bedrock geology.

## METHODOLOGY

Existing surficial geology, bedrock geology and geophysical maps, along with Yukon MINFILE (2001) occurrences, were compiled and evaluated prior to the

*Figure 3. Low rolling topography with isolated uplands in northern Finlayson Lake map area (105G).*

field season. Existing surficial geology maps by Jackson (1994) were used as the primary guide to the distribution of surficial deposits. Air photo interpretation was also completed prior to sample collection to confirm the surficial geology.

Fieldwork was completed from a base camp located at the Finlayson air strip (105G/10). Bedrock geologists, surficial geologists, a Geographic Information System (GIS) technician, and the helicopter pilot and mechanic shared the base camp. A Bell 206 helicopter provided access to the survey areas. Road traverses were also completed along the Robert Campbell Highway and the Kutz Ze Kayah exploration road. All samples, apart from those taken on the road traverses, were collected during daily foot traverses. Till samples were collected along traverse lines oriented perpendicular to sub-perpendicular to the former ice-flow direction. Such orientation of the traverse lines provides the maximum coverage of the underlying geology. Sample spacing was approximately 1 km and an average of 6-8 samples were collected on a daily traverse.

At each sample station, a 2-kg and a 1-kg bulk sediment sample were collected for geochemical analysis of the silt plus clay-size fraction (-230 mesh or <0.063 mm) and the clay-size fraction (<0.002 mm), respectively. In addition to the geochemical samples, approximately 50 pebbles were collected for a lithologic record. Emphasis was placed on sampling basal till, although colluviated basal till and meltout till were also collected. Samples were collected from the C-horizon (the unweathered parent material) at an average depth of 55 cm, in hand-dug pits (Fig. 4). Natural exposures from stream cuts were sampled along the Hoole River, Pelly River, Big Campbell Creek, Mink Creek and some unnamed streams. Where thick till is exposed, samples were collected at different depths to assess the vertical variability of the till geochemistry.

*Figure 4. Digging for a till sample, northwest of Wolverine Lake.*

Site and sample information were recorded onto data sheets, or digitized in the field using a hand-held device (Compaq iPAQ). Both techniques were used in order to test the efficiency of the latter method. The information was downloaded at base camp into an Access database. The database, which includes site and sample descriptions and results of geochemical analyses, will be released in digital form (CD-ROM) in 2002. Additional information that was recorded in the field included the location of outcrops (where samples were taken), general bedrock descriptions, and presence and orientation of glacial ice-flow features.

Unreported exposures of Quaternary sediments present along stream banks were logged during the 2001 field season in order to reconstruct the glacial history of the study area. Each stratigraphic unit was characterized with respect to its texture, sedimentary structures, colour, clast composition, contact relationships, and lateral continuity. A proper understanding of the glacial and ice-flow histories of a region is crucial for the interpretation of the till geochemistry. Tracing the source of a geochemical anomaly in till depends directly on the understanding of local and regional ice-flow patterns.

## SAMPLE PREPARATION AND ANALYSIS

Preparation of the silt and clay-size fractions for asssay was conducted by Acme Analytical Laboratories in Vancouver, British Columbia. Samples were oven dried at 60°C and dry-sieved to separate the silt and clay-size fractions (<0.062 mm or -230 mesh). Samples of 15 g of combined silt and clay were analysed for 39 elements by inductively coupled plasma mass spectrometry (ICP-MS) after an aqua regia digestion. The aqua regia attack dissolves most sulphide minerals and therefore can be considered as a total digestion for base and precious metals held in sulphide minerals. On the other hand, aqua regia is a partial leach for silicate minerals and does not dissolve barite. Therefore, certain elemental concentrations (e.g., Cr, Ti, Fe, Mg, Ba) should be considered as partial concentrations. Detection limits for ICP-MS analyses are shown in Table 1. Separations of the clay-size fraction were conducted in the Sedimentology Laboratory of the Geological Survey of Canada. Results of the geochemical analyses of the clay-size fractions were not available at the time this paper was prepared, but will be released in a later publication.

***Table 1.*** *Detection limits for elements analysed in the 2000/2001 study.*

| Element | Detection limit | Element | Detection limit |
|---|---|---|---|
| **Au** | 0.2 ppb | **Na** | 0.001 % |
| **Ag** | 2 ppb | **Ni** | 0.1 ppm |
| **Al** | 0.01 % | **P** | 0.001 % |
| **As** | 0.1 ppm | **Pb** | 0.01 ppm |
| **B** | 1 ppm | **Pd** | 10 ppb |
| **Ba** | 0.5 ppm | **Pt** | 2 ppb |
| **Bi** | 0.02 ppm | **S** | 0.02 % |
| **Ca** | 0.01 % | **Sb** | 0.02 ppm |
| **Cd** | 0.01 ppm | **Sc** | 0.1 ppm |
| **Co** | 0.1 ppm | **Se** | 0.1 ppm |
| **Cr** | 0.5 ppm | **Sr** | 0.5 ppm |
| **Cu** | 0.01 ppm | **Te** | 0.02 ppm |
| **Fe** | 0.01 % | **Th** | 0.1 ppm |
| **Hg** | 5 ppb | **Ti** | 0.001 % |
| **Ga** | 0.02 ppm | **Tl** | 0.02 ppm |
| **K** | 0.01 % | **U** | 0.1 ppm |
| **La** | 0.5 ppm | **V** | 2 ppm |
| **Mg** | 0.01 % | **W** | 0.2 ppm |
| **Mn** | 1 ppm | **Zn** | 0.1 ppm |
| **Mo** | 0.01 ppm | | |

## QUALITY CONTROL

Quality control measures were carried out during the till sampling program to ensure data reliability. In every block of 20 samples, 2 field duplicates and 1 control standard were inserted. In total, 33 field duplicates and 16 control standards were included with the 331 samples collected during the 2001 field survey. The control standards were obtained from the Canada Centre for Mineral and Energy Technology (CANMET). The field duplicates consist of an additional sample collected at random from one in every ten till sampling stations. These duplicates are used to test the geochemical variation within the till, whereas the control standards test the accuracy of the analytical laboratory. Analytical duplicates (sieved splits) were inserted by the analytical laboratory during sample preparation to evaluate analytical precision. Similarly, 16 pairs of field duplicates and 9 control standards were inserted in the 156 samples from the 2000 field season (Bond, 2001a).

Analytical precision is judged as satisfactory based on the good correlation between the field and laboratory duplicate pairs (Fig. 5). The analytical accuracy is also judged as satisfactory for all of the elements herein

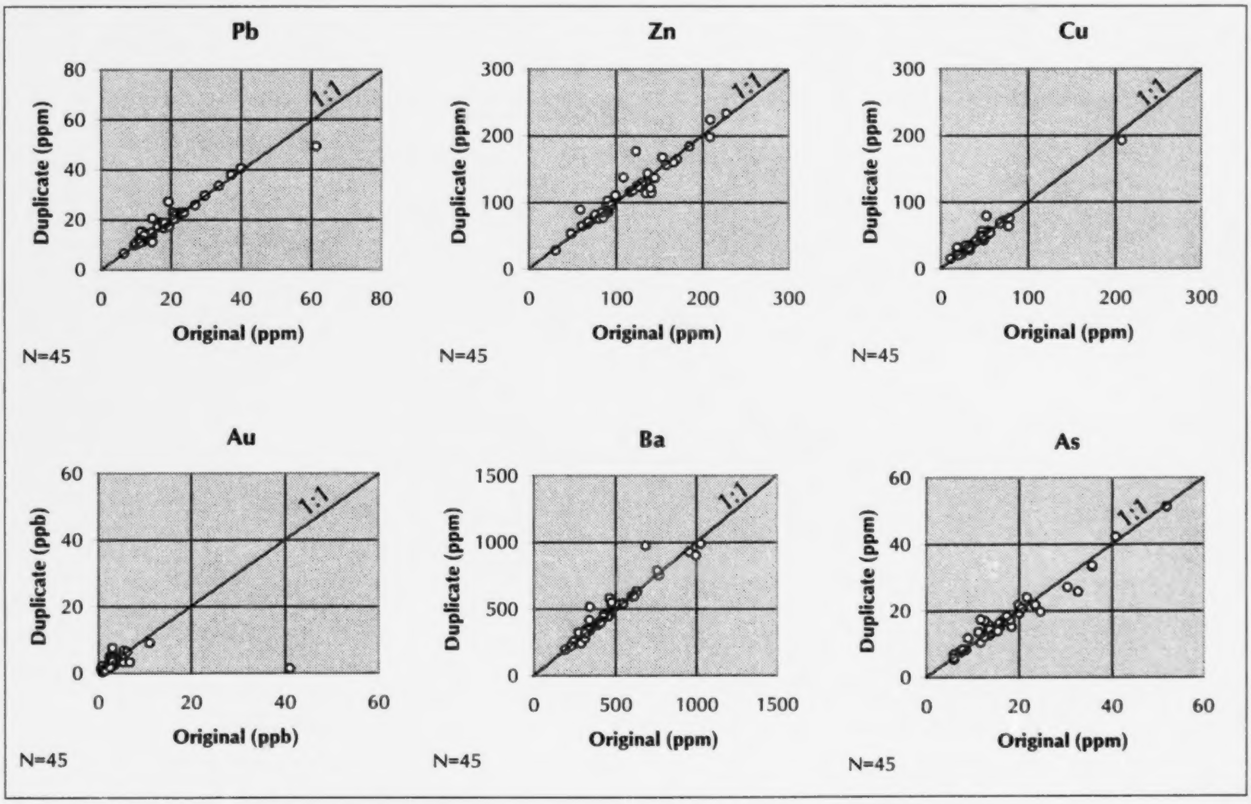

***Figure 5.*** *Correlation plots of field and laboratory duplicate samples. N = the number of samples.*

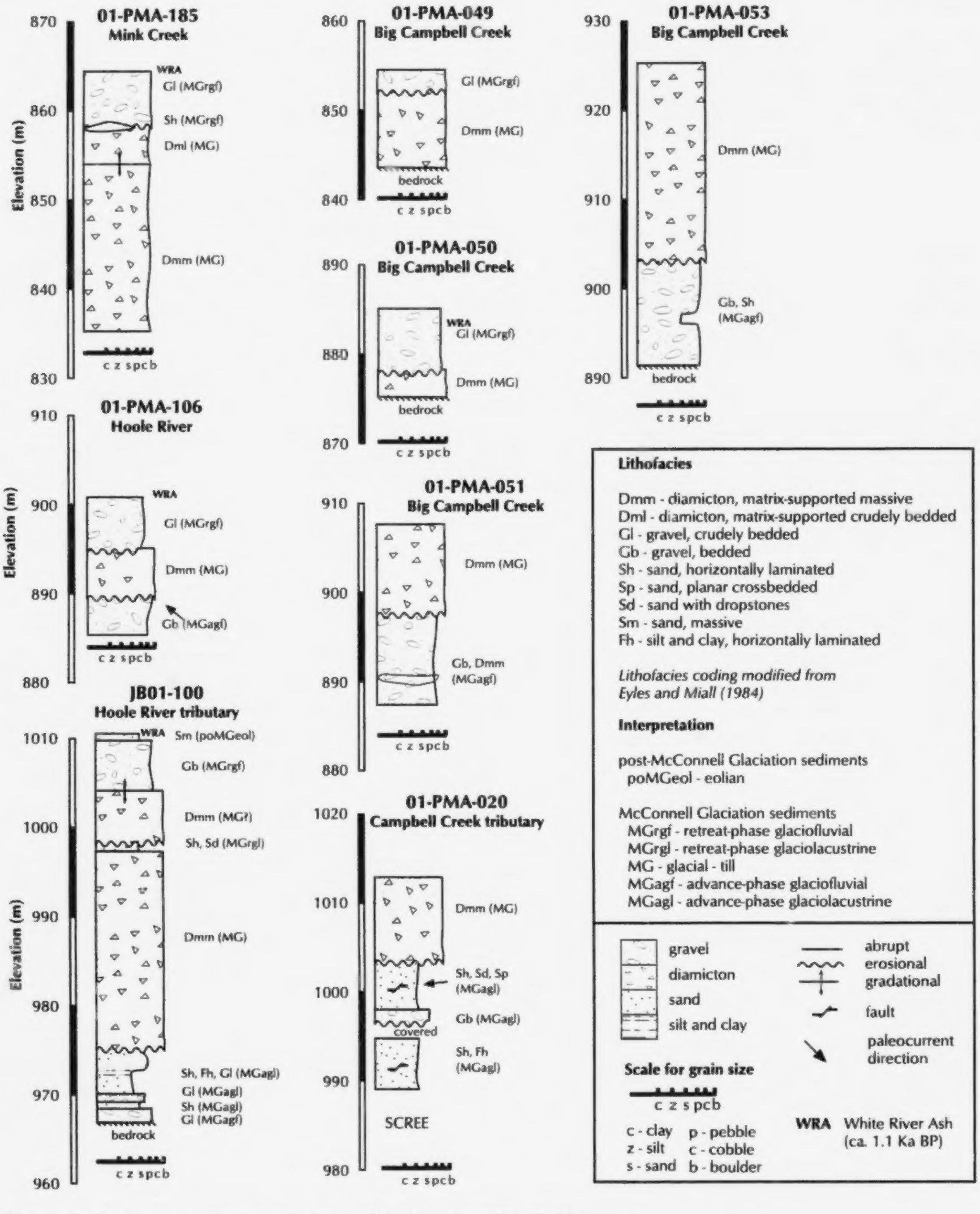
01-PMA-185
Mink Creek
01-PMA-106
Hoole River
JB01-100
Hoole River tributary
01-PMA-049
Big Campbell Creek
01-PMA-050
Big Campbell Creek
01-PMA-051
Big Campbell Creek
01-PMA-020
Campbell Creek tributary
01-PMA-053
Big Campbell Creek
Elevation (m)
WRA
Gl (MGrgf)
Sh (MGrgf)
Dml (MG)
Dmm (MG)
Gb (MGagf)
Sm (poMGeol)
Gb (MGrgf)
Dmm (MG?)
Sh, Sd (MGrgl)
Sh, Fh, Gl (MGagl)
Gl (MGagl)
Sh (MGagl)
Gl (MGagf)
Gb, Dmm (MGagf)
Sh, Sd, Sp (MGagl)
Gb (MGagl)
Sh, Fh (MGagl)
Gb, Sh (MGagf)
covered
SCREE
bedrock
c z s p c b
Lithofacies
Dmm - diamicton, matrix-supported massive
Dml - diamicton, matrix-supported crudely bedded
Gl - gravel, crudely bedded
Gb - gravel, bedded
Sh - sand, horizontally laminated
Sp - sand, planar crossbedded
Sd - sand with dropstones
Sm - sand, massive
Fh - silt and clay, horizontally laminated
Lithofacies coding modified from Eyles and Miall (1984)
Interpretation
post-McConnell Glaciation sediments
poMGeol - eolian
McConnell Glaciation sediments
MGrgf - retreat-phase glaciofluvial
MGrgl - retreat-phase glaciolacustrine
MG - glacial - till
MGagf - advance-phase glaciofluvial
MGagl - advance-phase glaciolacustrine
gravel
diamicton
sand
silt and clay
abrupt
erosional
gradational
fault
paleocurrent direction
Scale for grain size
c - clay
z - silt
s - sand
p - pebble
c - cobble
b - boulder
WRA White River Ash (ca. 1.1 Ka BP)

***Figure 6.*** *Quaternary stratigraphy logged during the 2001 field season.*

***Table 2.*** *Elemental concentrations of standard Till-2 obtained in this study compared to reported values.*

| **Elements** | **Pb ppm** | **Zn ppm** | **Cu ppm** | **Ba ppm** | **Ni ppm** | **Cr ppm** | **Co ppm** | **Au ppb** | **Ag ppb** | **As ppm** | **Hg ppb** |
|---|---|---|---|---|---|---|---|---|---|---|---|
| Till-2; average value, this study | 25.48 | 108.21 | 142.45 | 105.47 | 31.95 | 38.75 | 13.86 | 1.7 | 218.62 | 22.2 | 65.75 |
| Elemental values (Till-2; Lynch, 1996) | 21 | 116 | 149 | 95 | 31 | 40 | 13 | n/a | 200 | 22 | 74 |

reported, based on comparison between the nine analyses of the standard conducted during this study and values obtained from previous reports (Till 2 - Lynch, 1996; Table 2).

## QUATERNARY STRATIGRAPHY

Most of the sediments observed in sections are deposits of the Late Wisconsinan McConnell Glaciation, that is the last glacial event that affected the region (Fig 6; Bostock, 1966; Jackson, 1994). The oldest sediments were deposited during the advance phase of the McConnell Glaciation. These sediments are overlain by the McConnell till and retreat-phase deposits.

### ADVANCE-PHASE SEDIMENTS

Sediments directly under the McConnell till that show a degree of weathering similar to the overlying till, and that contain, in places, clasts of distal lithologies, are interpreted to have been deposited during the advance-phase of the last glaciation. However, in the absence of absolute dating, the greater antiquity of these sediments can not be ruled out.

Advance-phase sediments were observed in the Campbell Creek, Big Campbell Creek, Hoole River, and Pelly River valleys. Advance-phase sediments were deposited into two broad depositional environments: glaciolacustrine and glaciofluvial. Glaciolacustrine sediments are typically well-sorted fine sand and silt, horizontally laminated and bedded, and contain sporadic dropstones (Fig. 7). Sporadic sand and gravel beds and lenses observed within the units of glaciolacustrine sediments were likely deposited near the mouth of meltwater streams. Advance-phase glaciolacustrine sediments indicate that the drainage was blocked by glaciers during glacial advance.

Units of clast-supported sand and gravel, which are generally poorly sorted and crudely to well bedded, are thought to reflect glaciofluvial sedimentation (Fig. 8). Diamicton lenses were observed within the advance-phase glaciofluvial sediments, and they are interpreted as sediment gravity flow or flow till. Advance-phase glaciofluvial sediments indicate free drainage conditions during glacial advance.

Advance-phase glaciofluvial and glaciolacustrine sediments are well compacted. Some faults observed in the advance-phase sediments are likely the product of glacio-tectonic deformations as suggested by their consistent orientation transverse to the known ice-flow

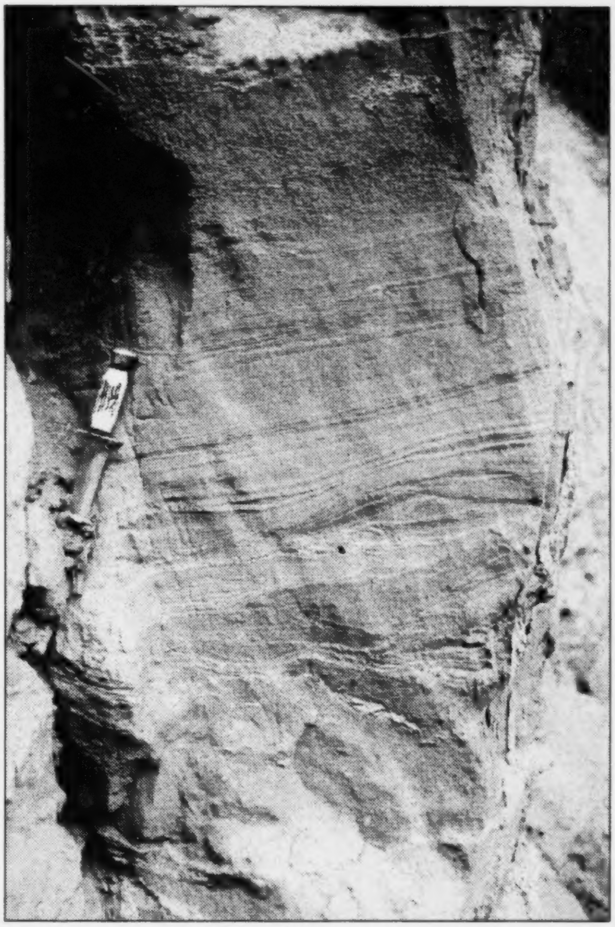

***Figure 7.*** *Advance-phase glaciolacustrine sediments exposed at section 01-PMA-020 in a tributary valley of Campbell Creek. Knife measures 20 cm.*

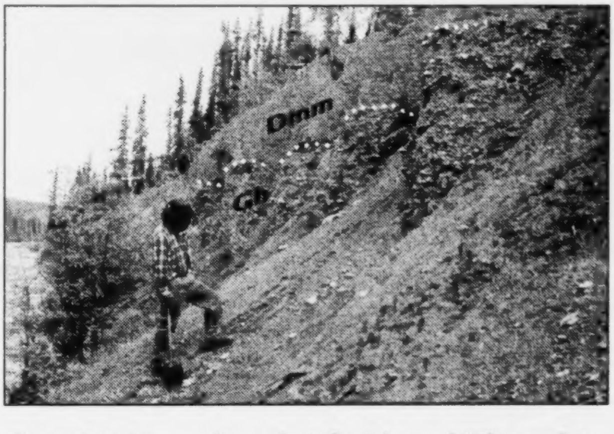

***Figure 8.*** *Advance-phase glaciofluvial gravel (Gb) overlain by till (Dmm) at section 01-PMA-106 in the Hoole River valley.*

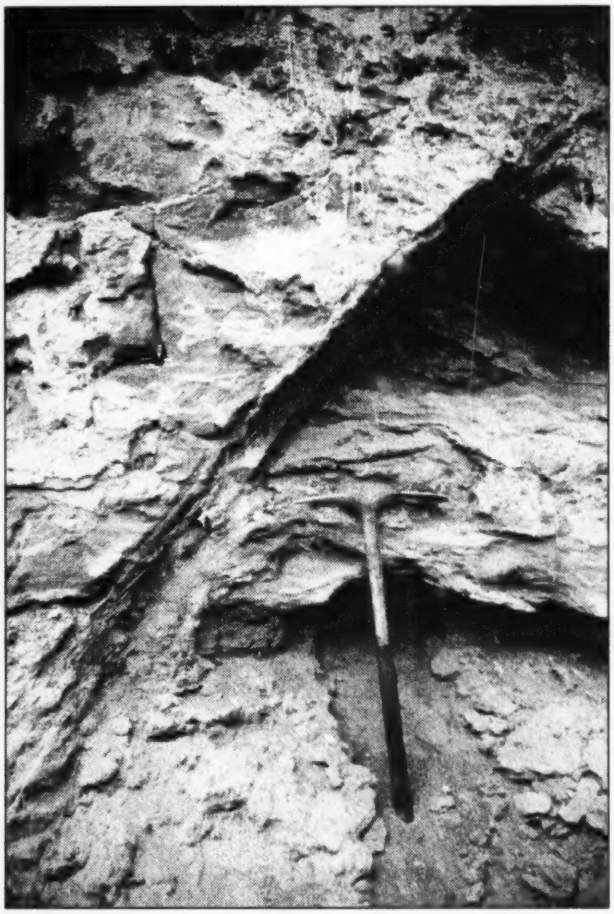

*Figure 9. Fault in advance-phase glacial lake sediments of section 01-PMA-020. Pick measures approximately 65 cm.*

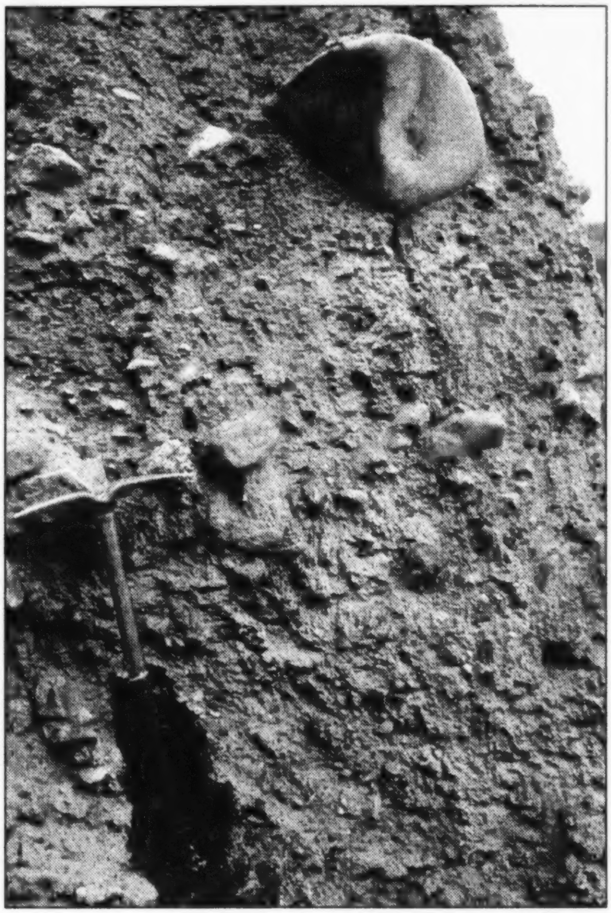

*Figure 10. McConnell Till exposed at section JB01-100 in a tributary valley of the Hoole River. Pick measures approximately 65 cm.*

movement and dip in the up-ice direction (up-paleo-ice flow; Fig. 9).

## McCONNELL TILL

Till is a sediment that is directly deposited by glacier ice. Only one lithostratigraphic unit of till found within the study area represents the till deposited during the McConnell Glaciation. McConnell Till consists of a poorly sorted diamicton with clasts of pebble to boulder size in a sandy to clayey matrix (Fig. 10). Abundant faceted and striated clasts are found in the till reflecting the glacial origin of the sediment. McConnell Till is on average 1-3 m thick on plateaus and hills but can reach a thickness of up to 20 m in some valleys (e.g., Big Campbell Creek, Hoole River; Fig. 6). On plateau summits where the till is thin, it contains abundant angular to subangular clasts of local lithologies. However, in the valleys, till contains a mixture of subangular to rounded clasts with lithologies from distal and local sources. Therefore, the provenance region of the till in a valley could be distal or proximal.

McConnell Till was likely deposited by a combination of meltout and lodgement processes. Plouffe (1989), and Plouffe and Jackson (1992) have reported strong till fabrics parallel to ice flow in McConnell Till suggesting lodgement sedimentation. However, sand and gravel lenses and crude layering were generally observed in the upper portion of McConnell Till (see section 01-PMA-185, Fig. 6) suggesting sedimentation by meltout.

### RETREAT-PHASE SEDIMENTS

As for the advance-phase, the retreat-phase of the last glaciation was also marked by glaciofluvial and glaciolacustrine sedimentation. Jackson (1993c) reported several metres of well-sorted fine sand, silt and clay underlain by McConnell Till in the Pelly River valley, which he interpreted to be glaciolacustrine sediments. Elsewhere in the study area, clast-supported, pebbly to cobbly, and crudely to well-bedded gravel overlying McConnell Till was interpreted as retreat-phase glaciofluvial sediments deposited by meltwater streams. Therefore, the stratigraphic evidence found by Jackson (1993c) indicates that a glacial lake developed in the Pelly River valley during the retreat-phase of the glaciation (Jackson, 1994). Elsewhere, the drainage was free during ice retreat, except where local glacial lakes formed in tributary valleys by drainage impoundment.

### NONGLACIAL SEDIMENTS

A thin veneer, generally less than 1 m, of eolian sediments caps several sections in the study area. Only in the Hoole River valley, at section JB01-100, is this unit thick enough to be represented on the stratigraphic log. The White River Ash, dated at 1147 calendric years BP (Clague et al., 1995), is often present near the top of the eolian sediments indicating that these deposits are Holocene in age. The Stewart neosol (modern brunisolic soil) is visible in the eolian cap.

## GLACIAL LANDFORMS

During the field investigation, particular attention was paid to micro- and macro-landforms indicative of ice-flow patterns: streamlined landforms (drumlins, flutes and crag-and-tails), glacial striations, and roche moutonnée. Streamlined landforms predominantly occur in the less rugged portion of the northern sector of the Finlayson Lake map sheet. They reveal a general westward to northwestward ice-flow direction with minor deflections near topographic highs (Jackson, 1993a,b,c,d).

Glacial striations measured on bedrock surfaces generally represent important ice-flow indicators, but very few striated sites were observed in the study area (Fig. 2). Only two roches moutonnées were recorded during fieldwork. Roches moutonnées and striations were found to be parallel to sub-parallel to streamlined landforms.

Ice marginal features such as frontal and lateral moraines, and lateral meltwater channels are used to reconstruct ice configuration during ice retreat (e.g., Dyke, 1990). Potential late glacial ice-flow patterns can be suggested knowing the ice configuration during deglaciation. Few moraines are present in the Finlayson Lake map area (see Jackson, 1994), but two provide clues on the pattern of deglaciation. North and east of Riviera Lake, and at about 8 km west of Wolverine Lake, Jackson (1993b,d) mapped morainic complexes that suggested high ground was deglaciated before the valleys. In other words, an ice mass was probably still present in the Wolverine Lake valley and in the vicinity of Finlayson Lake while most of the Pelly Mountains were deglaciated. The lack of lateral continuity in these morainic complexes suggests that the still stand of the ice front might have only been local. The amount of glacial transport that occurred during this late glacial episode is yet to be evaluated.

## GLACIAL HISTORY

What is known to date of the ice-flow patterns at the onset of the McConnell Glaciation comes from the detailed stratigraphic investigation of the Lapie River region presented by Plouffe (1989). Plouffe suggested, based on the interpretation of till fabrics and lithologies, that ice first formed in the Pelly Mountains. Valley glaciers advancing from the Pelly Mountains later coalesced in the Tintina Trench to form an ice tongue advancing to the northwest, parallel to the Tintina Trench. Valley glaciers likely formed also in the portion of the Selwyn Mountains north and south of McEvoy Lake. During the ice advance, trunk valleys and low areas were invaded first, and glacial lakes developed in tributary valleys as their drainages were blocked by ice in the main valleys. For example, such glacial lakes developed in tributaries of the Hoole River (JB01-100, Fig. 6) and Campbell Creek (01-PMA-020, Fig. 6).

At glacial maximum, ice was generally flowing to the northwest within the Finlayson Lake map area and was thick enough to cover the highest mountains (Jackson, 1994). However, ice-flow patterns were influenced by topography, such as east of Weasel Lake where striations and streamlined landforms indicate a deflection around a topographic high (Fig. 2). In the rugged portion of the Pelly Mountains, ice flow was more complex than on the Yukon Plateau, and was highly controlled by topography (Jackson, 1994). On the Glacial Map of Canada (Prest et al., 1967), orientation of streamlined landforms suggests the presence of an ice divide centred on the Selwyn Mountains, northwest of Frances Lake. The position of the ice divide was refined following mapping by Jackson (1994) and Dyke (1990) and is thought to have been located in the Wolverine Lake region. Consequently, east and southeast of Wolverine Lake, ice flow was generally to the southeast for a good part of the McConnell Glaciation. This is corroborated by the presence of abundant boulders of Cretaceous granite (see Murphy and Piercey, 1999) transported to the south of their bedrock source. The presence of an ice divide in the Wolverine Lake region indicates that an ice dome was continuous between the Pelly and Selwyn mountains. As a result, the greatest ice thicknesses in the study area were likely located over lowlands immediately north of the Pelly and west of the Selwyn mountains.

Jackson (1994) envisaged a rapid down-wasting of the Selwyn Lobe of the Cordilleran Ice Sheet at the close of the McConnell Glaciation. This was initiated by a rapid rise in the firn line (equilibrium line). The alpine regions, where ice was thinnest, were the first to be deglaciated. However, it is possible that local valley glaciers remained active for some time during deglaciation. Deglaciation was marked by local glacial readvance(s) originating from glaciers in the lowlands (Plouffe, 1989; Jackson, 1994; Bond, 2001a). For instance, during an ice readvance, clasts of South Fork volcanics, originating north of the Tintina Trench, were transported at least 9 km into the Lapie River valley (Plouffe, 1989). Bond (2001a) documented two tills in the Anvil district, the upper one being associated to a late glacial readvance originating from the Tintina Trench. Morainic complexes that surround the Anvil Range also supported this glacial readvance. However, no evidence of a late glacial readvance was identified in the Finlayson Lake map area during the 2001 field season. If a readvance occurred in the study area, it was likely related to the ice mass that occupied the Finlayson Lake and Wolverine Lake region at the end of the glaciation. Jackson (1994) suggested that the retreat-phase glacial lake that developed in the Pelly River valley was at least partly ponded by isostatic rebound.

In summary, in tracing the source of geochemical anomalies in till, the best estimate of the main vector of glacial transport corresponds to the regional ice-flow pattern at glacial maximum, which is generally to the northwest for most of the northern sector of the Finlayson Lake map area. Only in the Pelly Mountains region was ice flow dominantly controlled by topography.

# TILL GEOCHEMISTRY: RESULTS

## ORIENTATION SURVEY – KUDZ ZE KAYAH

More detailed sampling was completed near the Kudz Ze Kayah (KZK) massive sulphide mineralization to define the level of metal enrichment in till in areas of known mineralization. This data was used to aid regional data interpretation elsewhere in the study area. At Kudz Ze Kayah, the ice-flow direction was to the north and topographically confined by the valley.

In total, 14 till samples were collected in a north transect that passes directly over the deposit (Appendix 1). All samples were derived from hand-dug pits, stream-cuts or road cuts. The sampling and analytical methods are the same as those used during the regional survey.

### *Lead*

Lead concentrations in till are only enriched immediately down-ice of the massive sulphide deposit (maximum of 559 ppm; Appendix 1). Such enrichment is directly related to northward glacial transport. A value of 441 ppm was derived from glaciofluvial gravel in a kame terrace, also down-ice flow of the KZK deposit. A stratigraphic sample from a stream cut on Fault Creek returned a value of 250 ppm. A source area for this anomaly could lie immediately south of Fault Creek.

### *Zinc*

Zinc values north of the KZK deposit range from 1068 to 1711 ppm. Similar to lead, the zinc levels in till clearly reflect the presence of the massive sulphide deposit in the valley bottom. The three low zinc values to the northeast may be derived from the east, rather than from the south. Samples derived from the Fault Creek exposure also contain high zinc levels, ranging from 534 to 861 ppm. Sample 01-PMA-047-01 is high in zinc (637 ppm) and may indicate a down-slope dispersion of zinc from a similar source area as the Fault Creek samples. Site notes from 01-PMA-047 indicate the sample was derived from a colluviated till.

### *Silver*

The distribution pattern of silver concentrations in till in the KZK valley is similar to the ones of lead and zinc. Silver enrichment in till is only found north of the mineralization. Immediately down-ice of the deposit, a maximum value of 5387 ppb was measured in till.

### *Gold*

Gold enrichment in till is more subtle compared to the previous elements. The transport of gold from the massive sulphide is clearly reflected in sample JB01-067 (73 ppb). Sample 01-PMA-045-01, located nearly 3 km south of the known mineralization at KZK, yielded an unexpected gold concentration of 153 ppb. A source area for this sample is likely proximal (to the south) and somewhat up-slope from the station. Mississippian granite underlies this region (Murphy et al., 2000) and could be the host of intrusion-related mineralization.

## REGIONAL TILL GEOCHEMISTRY

The till geochemistry presented here combines data from the 2000 and 2001 field seasons (number of samples, N=489). The element maps present the data in percentiles and concentration range. The elements discussed here are considered to be significant for mineral exploration in the northern half of the Finlayson Lake map area. See Appendix 2 for the sample location map and the related element concentration maps. All references to bedrock geology are derived from Murphy et al. (2001).

### *Lead*

The lead values range from 2 ppm to 559 ppm with a mean concentration of 15 ppm and a median value of 15 ppm. The four highest lead values, corresponding to values above the 97th percentile, are discussed below.

The highest lead values were obtained from the orientation surveys conducted at the Kudz Ze Kayah (559 ppm) and Wolverine (275 ppm) deposits. The highest lead value from the regional data set was 234 ppm collected from JB01-001-08 in the northwest part of 105G. The sample was derived from a follow-up survey conducted near a multi-element mercury/gold anomaly identified during the 2000-sampling program (JB00-155; Bond, 2001). As part of the follow-up survey, nine samples were collected on a sample spacing of 200 m. The purpose was to test the reproducibility of the 2000 anomaly that is now staked as the Spice claims on NTS 105G/13 (Fig. 11). The sample line spans the width of a Permian conglomerate, which is expected to host mineralization; the mineralization might extend into the adjacent Carboniferous dark grey phyllite. Sample JB01-001-08 was collected over the Carboniferous dark grey phyllite. In addition to a high lead level, sample JB01-001-08 contains high copper (161 ppm), zinc (362 ppm), manganese (1165 ppm), arsenic (157 ppm), mercury (5892 ppb) and gold (29 ppb) concentrations. This sample contains numerous angular clasts suggesting a potential proximal volcanogenic massive sulphide (VMS) or sedimentary exhalative (SEDEX) deposit source. The multi-element anomaly could also be related to mineralization at the nearby Spice target. The elemental signature at Spice, which is discussed further under 'Gold' (later in this section), is suggestive of an epithermal source focused in the conglomerate. Epithermal fluids may have interacted with the nearby phyllites and re-deposited base metals within the conglomerate unit.

The second highest concentration of lead, 67 ppm, was collected from station 01-PMA-169-01, approximately 14 km south of Wolverine Lake. The sample also contains moderately elevated levels of zinc (147 ppm), antimony (12 ppm) and gold (6 ppb) and is located within muscovite-quartz phyllite of the Wolverine succession. This sample site is not located on the regional maps. Its UTM location is 439001E, 6797333N.

The third highest lead value, 67 ppm, was collected from station 01-PMA-027-01. The sample is located southwest of Finlayson Lake within Devonian schist. The location of the sample is immediately down-ice from a large area of Fire Lake metavolcanic rocks, which are considered a favourable target for mineralization. This sample also yielded high zinc (182 ppm) and arsenic (32 ppm) values.

The fourth highest concentration of lead, 61 ppm, is from sample 01-PMA-176-01. This sample is located immediately down-ice from the northwestern extent of the Wolverine succession. Samples in this area generally contain high zinc (95th percentile), silver (99th percentile), molybdenum, gold, selenium and mercury concentrations.

### *Zinc*

Zinc concentrations range from 20 ppm to 4900 ppm, with mean and median values of 137 ppm and 104 ppm, respectively. The six highest values (>96.5th percentile) are discussed below.

The highest zinc concentrations are derived from the orientation surveys at Wolverine (4900 ppm), Kudz Ze Kayah (1711 ppm) and Argus (457 ppm). Sample JB01-114, located along the Pelly River in the northern sector of the study area, yielded the highest zinc value of the regional samples (387 ppm). Numerous high zinc values are present in till in this area and are attributed to the high background level of zinc in the underlying Earn

Group shale. A potential bedrock source area for the high zinc value in JB01-114 could lie within 2 km to the east.

The second highest concentration of zinc, 361 ppm, was recorded from a colluviated basal till veneer overlying Carboniferous dark grey phyllite on the Spice claims. See the reference to this sample (JB01-001-08) under 'Lead'.

The third and fourth highest zinc values, 348 ppm and 337 ppm, overlie Carboniferous dark grey phyllite at stations JB00-047 and JB00-006. Based on metal association, VMS or SEDEX-style mineralization could be present in the phyllite.

The fifth highest zinc anomaly, 299 ppm, is from sample JB01-133, southwest of Fortin Lake above dark grey phyllite of the North American miogeocline. SEDEX-style mineralization may be the source of this high value.

The sixth highest concentration of zinc, 295 ppm, is derived from the Mink Creek drainage. The sample overlies black carbonaceous phyllite of the Fire Lake metavolcanic unit. These rocks may have a high background level in zinc, which could explain the high zinc level in till.

### *Copper*

Copper concentrations range from 6 to 480 ppm with mean and median values of 48 ppm and 43 ppm, respectively. The four highest regional copper values, corresponding to values above the 98th percentile, are discussed below.

Orientation samples taken at Kudz Ze Kayah (KZK; 315-480 ppm) and Wolverine (247 ppm) contain the highest copper concentrations. A sample collected along the KZK road, approximately 10 km north of the deposit, yielded the highest copper value of the regional data (218 ppm). A bedrock source for this anomaly could lie to the east-southeast, probably within 2 km of the sampling site. The sample was collected from a relatively thin till unit and the local bedrock consists of lower Mississippian chlorite-muscovite phyllite. Rocks of the Wolverine succession lie approximately 3 km to the east.

The second highest regional copper value, 208 ppm, is from a sample collected in upper Big Campbell Creek, northeast of Riviera Lake. Sample JB01-040 was collected from a thin till deposit overlying Jurassic granite.

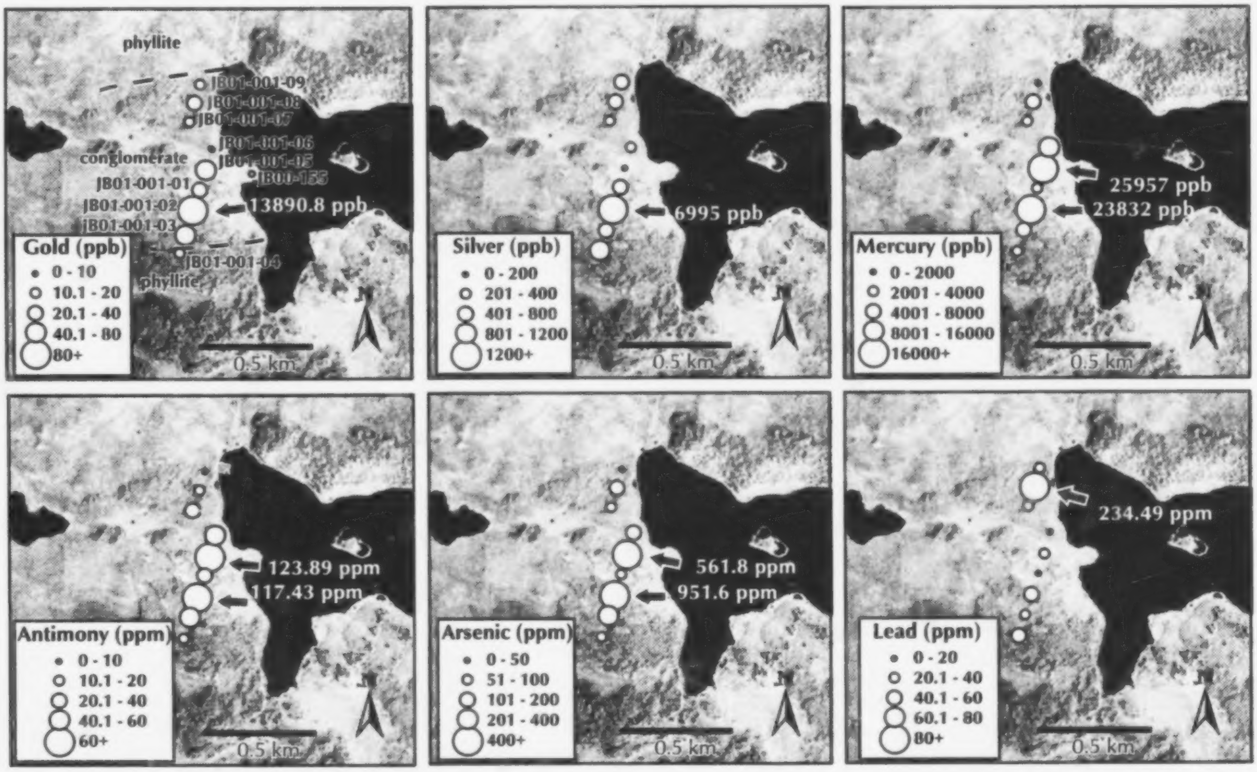
phyllite
JB01-001-09
JB01-001-08
JB01-001-07
JB01-001-06
JB01-001-05
JB00-155
conglomerate
JB01-001-01
JB01-001-02
JB01-001-03
13890.8 ppb
JB01-001-04
phyllite
Gold (ppb)
0 - 10
10.1 - 20
20.1 - 40
40.1 - 80
80+
0.5 km
6995 ppb
Silver (ppb)
0 - 200
201 - 400
401 - 800
801 - 1200
1200+
0.5 km
25957 ppb
23832 ppb
Mercury (ppb)
0 - 2000
2001 - 4000
4001 - 8000
8001 - 16000
16000+
0.5 km
123.89 ppm
117.43 ppm
Antimony (ppm)
0 - 10
10.1 - 20
20.1 - 40
40.1 - 60
60+
0.5 km
561.8 ppm
951.6 ppm
Arsenic (ppm)
0 - 50
51 - 100
101 - 200
201 - 400
400+
0.5 km
234.49 ppm
Lead (ppm)
0 - 20
20.1 - 40
40.1 - 60
60.1 - 80
80+
0.5 km

***Figure 11.*** *Spice claims exploration till geochemical survey, overlaid on aerial photograph (northwest corner of 105G/13, see Figure 2).*

Ultramafic rocks in the area could be the source of copper in till.

The third highest regional copper value, 189 ppm, was obtained near Late Devonian ultramafic bedrock, within the Fire Lake metavolcanic unit. The sample JB01-028 also contains high cobalt and chromium values. Approximately 94% of the pebbles collected from the sample site are angular to subangular chloritic phyllite, suggesting a source within the metavolcanic unit.

Sample 01-PMA-178-01 yielded the fourth highest regional copper value of 145 ppm. The sample is derived from a basal till veneer located between two outcrops. A source for the anomaly could be proximal (within 2 km) to the east-southeast. The sample is located immediately down-ice of prospective Wolverine stratigraphy and also contains elevated cobalt (41 ppm), iron (8.75%), vanadium (255 ppm) and barium (1974 ppm) concentrations. This element suite may correspond to the baritic iron formation of the Wolverine succession.

### *Barium*

Barium concentrations range from 76 to 2906 ppm with a mean value of 521 ppm and a median value of 476 ppm. The four highest values (>99th percentile) are discussed below.

The highest barium concentration, 2906 ppm, was collected from station JB00-064, in the northwest part of the study area. The sample was collected from a till blanket which contains some oxidized clasts and overlies Carboniferous phyllite, chert, sandstone and conglomerate. This sample also contains high copper (96 ppm), gold (12 ppb) and mercury (1062 ppb) levels. Platinum and palladium concentrations are 2 ppb and 5 ppb, respectively.

The second highest barium concentration, 2780 ppm, was collected southwest of Fortin Lake at station 01-PMA-139-01. The sample was collected from a till veneer that overlies chert of the Permian Mount Christie Formation. No other elements are anomalous in this sample.

The third highest barium concentration, 1974 ppm, was previously discussed under 'Copper' and is derived from sample 01-PMA-178-01.

The fourth highest barium concentration, 1893 ppm, is from sample JB00-147 collected in the northwest part of the study area. The area is underlain by Earn Group rocks, which could have potential for SEDEX mineralization. Station JB00-146, located 400 m to the southeast, also contains a high barium level (1562 ppm). No other elements were anomalous in these two samples.

### *Nickel/Chromium/Cobalt/Platinum/Palladium*

Given the common association of high nickel, chromium and cobalt concentrations in bedrock (e.g., ultramafic rocks), these three elements will be discussed together. Notes on platinum and palladium are included as these elements generally occur in ultramafic rocks. Nickel concentrations range from 4 to 1015 ppm, with a mean value of 65 ppm and a median value of 51 ppm. Chromium concentrations range from 9 to 1073 ppm, with mean and median values of 52 ppm and 39 ppm, respectively. Cobalt concentrations range from 1 to 63 ppm, with a mean value of 14 ppm and a median value of 12 ppm. Five of the most significant multi-element anomalies are discussed below.

The highest concentrations for each of nickel, chromium and cobalt are derived from sample JB01-026 (Ni: 1015 ppm; Cr: 1073 ppm; Co: 63 ppm). The sample is located immediately down-ice from a Late Devonian ultramafic unit, southwest of Finlayson Lake. The underlying bedrock consists of the Fire Lake metavolcanic unit. Pebbles consist of 88% ultramafic rocks. Other elements are present in high concentration in this sample including gold (15 ppb), magnesium (7.06%) and boron (22 ppm). Copper, platinum and palladium levels are not anomalous in this sample.

Sample JB00-112 yielded high nickel (897 ppm), chromium (322 ppm) and cobalt (34 ppm) concentrations. The sample was collected above Campbell Range basalts. Numerous samples collected near JB00-112 also contain high nickel, chromium and cobalt values. Platinum and palladium values were at, or near, the detection limit (2 ppb) in this area. Gold values reached 13 ppb at station JB00-110, which is 1 km south of JB00-112.

Sample JB00-046 contained high chromium (368 ppm) and cobalt (43 ppm) concentrations, but only a moderately elevated nickel (132 ppm) level. This sample is located over Campbell Range basalts and likely reflects nearby ultramafic rocks. Other elements also present in elevated concentrations in these samples are vanadium (182 ppm), scandium (21 ppm) and gallium (18 ppm).

Sample JB01-149, located in the Mink Creek drainage, contains high nickel (199 ppm), chromium (191 ppm) and cobalt (55 ppm) concentrations. This sample was collected from a till blanket that overlies highly altered, pyritic, felsic metavolcanic bedrock exposed along Mink Creek (Murphy et al., this volume). Chip samples from the outcrop assayed 835 ppm Cu, 3079 ppm As and up to 163 ppb Au. JB01-149 also contains elevated arsenic (386 ppm) and moderately elevated copper (88 ppm) values. The topography of this area is very flat and blanketed by glacial meltout deposits. This sample was collected from a stratigraphically lower level in the till unit. Samples collected stratigraphically higher in the till would most likely reflect distal sources.

Sample 01-PMA-083-01, located on the Kudz Ze Kayah road about 8 km north of the deposit, contains the following concentrations: nickel 179 ppm, chromium 341 ppm, and cobalt 43 ppm. The sample was collected from a till veneer containing angular and subangular clasts, which suggests a relatively nearby source for the anomalies. The underlying bedrock consists of phyllite and schist of the Kudz Ze Kayah felsic metavolcanic unit. Carbonaceous phyllite and quartzite of the Grass Lakes succession lie to the east (up-ice).

### Gold

As indicated in the methodology section, gold concentrations were determined by ICP-MS analyses but some re-analyses were conducted by fire assay for comparison purposes. The mean and median concentrations of gold are 5 ppb and 3 ppb, respectively. Values ranged from 0.4 to 153 ppb for the 489 samples analysed. Discussion will also include results from the exploration survey completed at the Spice claims. The four highest gold values are discussed below.

The highest concentration of gold, 153 ppb, was recorded about 2.5 km south of the Kudz Ze Kayah deposit. The sample was collected at station 01-PMA-045-01 from a colluvial apron on the valley side. The colluvium consists of both local bedrock fragments and till. Ice flow in this valley was to the north, so a source for this anomaly would lie up-slope and to the south. The bedrock in the area consists of granite of the early Mississippian Grass Lakes plutonic suite. This anomaly suggests potential for intrusive-hosted gold in the Mississippian granite of the Finlayson Lake district.

The second highest regional gold anomaly, 41 ppb, was collected at station 01-PMA-075-01, approximately 10 km southeast of the confluence of the Hoole and the Pelly rivers. The sample is derived from a till veneer collected on a small outcrop, suggesting a proximal bedrock source for the anomaly. The underlying bedrock consists of the early Mississippian granite with augen texture.

The third highest regional gold anomaly, 39 ppb, was collected at station JB01-073. This sample is located near the margin of the same granite mentioned in the previous anomaly, and is less than 1 km east of the Robert Campbell Highway. A till blanket covers the area, and meltout deposits are widespread in surrounding low areas. A duplicate sample was also collected at this station and returned a gold value of 5 ppb. Such a large difference between both analyses is related to the well-known nugget effect, that is, the heterogeneous distribution of gold in till.

The fourth highest regional gold anomaly, 28 ppb, was collected during the 2000 field season at station JB00-155. The sample was taken from a mudflow-like deposit on a small peninsula of a lake. The soil at the site was highly iron-oxidized. Numerous other elements are anomalous at this site including arsenic (485 ppm), antimony (151 ppm), mercury (21,020 ppb), thallium (1 ppm) and silver (1374 ppb). Most notable is the extremely high mercury concentration. As suggested by Bond (2001b), such elemental association could be indicative of gold epithermal mineralization. The area was staked early in 2001 as the Spice claims by Tanana Exploration. As part of a follow-up survey, nine samples were taken in 2001 along a north transect that appears to crosscut a bedrock structure (Fig. 11). The line traversed across, from south to north, Carboniferous dark grey phyllite, into Permian conglomerate, and back into dark grey phyllite. All samples have a high mercury concentration, with the highest reaching 25,957 ppb. A significant multi-element anomaly is present at JB01-001-02 (Fig. 11) including gold (13,891 ppb), silver (6995 ppb), arsenic (952 ppm), antimony (117 ppm) and mercury (23,832 ppb). Re-analysis of the remaining pulp by fire assay, as well as ICP-MS assays on the –230 mesh and -80 mesh from the sample split, confirmed the anomaly with nearly identical gold values. Angular pebbles of grey quartz with breccia fragments and hair-like black veinlets, collected from the till pit, gave a gold concentration of 1.05 g/t. Given the thin till cover and the abundance of angular bedrock fragments in till at this site, the source of the anomaly is likely proximal, possibly within 50 m of the sample site.

### *Silver*

Silver concentrations ranged from 14 to 5387 ppb with a mean concentration of 305 ppb and a median concentration of 221 ppb. The four highest regional values are discussed below.

The highest silver values were obtained from the orientation survey at Kudz Ze Kayah (5387 ppb). The highest regional values, 2980 ppb and 2582 ppb, were obtained from stations 01-PMA-177-01 and 01-PMA-176-01, down-ice of the Wolverine succession rocks, northwest of Wolverine Lake. These samples also contain high concentrations of lead, gold, antimony, mercury and selenium.

The second highest regional silver value was collected at the Spice claims (JB00-155). See discussions under the 'Gold' section for follow-up sampling completed at this location.

The third highest regional silver value, 1243 ppb, was collected southwest of Fortin Lake at station JB01-135. The underlying bedrock consists of Permian chert and upper Triassic dark grey phyllite.

The fourth highest regional silver value, 1153 ppb, was collected at station JB00-076. The sample was collected from a till blanket exposed along a creek cut. The sample site is near the contact between Carboniferous dark grey phyllite and early Permian Campbell Range basalt. Zinc (172 ppm) and mercury (988 ppb) are also elevated in this sample.

### *Arsenic*

The concentration of arsenic ranged from 2 to 485 ppm, with mean and median concentrations of 21 ppm and 15 ppm, respectively. Stations with the four highest arsenic concentrations are discussed below.

The highest arsenic concentration from the regional data, 485 ppm, was collected from the Spice claims or regional station JB00-155 (Fig. 11). The geochemistry of this station was discussed previously under the 'Gold' section.

The second highest arsenic concentration in till, 386 ppm, was found at station JB01-149. This station was also discussed earlier for its anomalous nickel, chromium and cobalt values.

The third highest regional arsenic value, 230 ppm, was collected at station 01-PMA-185-01, located along Mink Creek, immediately south of the Robert Campbell Highway. The sample was collected from a thick till unit exposed on a stream cut. The underlying bedrock consists of early Mississippian granite of the Grass Lakes plutonic suite. No other elements are anomalous at this station.

The fourth highest regional arsenic value, 96 ppm, was collected south of the Wolverine deposit at station 01-PMA-169-01. This sample was discussed earlier for its high lead concentration.

## CONCLUSIONS

The northern sector of the Finlayson Lake map area lies within the influence of the Late Wisconsinan McConnell Glaciation. At the onset of the glaciation, ice advanced from the Pelly and Selwyn mountains. Local ice-marginal ponding occurred in tributary valleys. At glacial maximum, the highest peaks were glaciated and ice flow maintained a general west-northwest trajectory, with only minor deviations across isolated highlands. Jackson (1994) indicated that deglaciation was marked by a rapid raise in the firn line. The last ice mass to disappear was located in the Finlayson and Wolverine lake areas.

Massive sulphide mineralization at KZK is well reflected in till with strong enrichment of lead, zinc, silver and gold down-ice (north) of the deposit. In addition, high base-metal concentrations in till near Fault Creek, and a high gold value almost 3 km south of the deposit might be related to concealed bedrock mineralization.

Data from the 2000 and 2001 regional till geochemistry surveys highlighted elevated concentrations of gold and base metals. High base-metal concentrations were identified northwest of Wolverine Lake, on the Spice claims, between Big Campbell Creek and Mink Creek, and west of Fortin Creek. High gold values were identified over Mississippian granite 10 km southeast of the confluence of the Hoole and the Pelly rivers, and results of the follow-up survey over the Spice claims define a multi-element gold anomaly characterized by gold concentrations reaching 13,891 ppb in till.

## ACKNOWLEDGEMENTS

This project was coordinated by the Geological Survey of Canada and the Yukon Geology Program. Funding was provided through the Targeted Geoscience Initiative of the Federal Government (Exploration and Geological Services Division of Indian and Northern Affairs Canada) and Yukon Government (Economic Development). The field assistance of Louis (Super G) Robertson and Patrick (off-road) Sack is much appreciated. Don Murphy and Steve Gordey initiated and coordinated the project planning. Their efforts were extensive. Panya Lipovsky provided excellent GIS support at the Finlayson camp and during the post-field season. Gary Stronghill constructed the element maps and his swift cooperation is much appreciated. Lee Manderson of West Coast Helicopters provided safe and accurate flying expertise. Thank you to the camp support personnel, Joe, Louise and Karen for helping us survive the bush experience. Gratitude is also owed to Terry Tucker of Expatriate Resources for spending time with us at Kudz Ze Kayah and Wolverine. Finally, thanks to Leyla and Sofia for enduring a pesty field season. The first version of the manuscript was improved following comments by R.N.W. Dilabio. This is also known as Geological Survey of Canada contribution number 2001159.

## REFERENCES

Bond, J.D., 2001a. Quaternary geology and till geochemistry of the Anvil district (parts of 105K/2, 3, 5, 6 and 7), central Yukon Territory. Exploration and Geological Services Division, Yukon Region, Indian and Northern Affairs Canada, Bulletin 11, 38 p.

Bond, J.D., 2001b. Surficial geology and till geochemistry of Weasel Lake map area (105G/13), east-central Yukon. *In:* Yukon Exploration and Geology 2000, D.S. Emond and L.H. Weston (eds.), Exploration and Geological Services Division, Yukon Region, Indian and Northern Affairs Canada, p. 73-96.

Bostock, H.S., 1966. Notes on glaciation in central Yukon Territory. Geological Survey of Canada, Paper 65-36, 18 p.

Burke, M., 2001. Yukon mining and exploration overview, 2000. *In:* Yukon Exploration and Geology 2000, D.S. Emond and L.H. Weston (eds.), Exploration and Geological Services Division, Yukon Region, Indian and Northern Affairs Canada, p. 2-27.

Clague, J.J., Evans, S.G., Rampton, V.N. and Woodsworth, G.J., 1995. Improved age estimates for the White River and Bridge River tephras, western Canada. Canadian Journal of Earth Sciences, vol. 32, p. 1172-1179.

Dyke, A.S., 1990. Quaternary geology of the Frances Lake map area, Yukon and Northwest Territories. Geological Survey of Canada, Memoir 426, 39 p.

Eyles, N. and Miall, A.D., 1984. Glacial facies. *In:* Facies Models, R.G. Walker (ed.), Geological Association of Canada, Geoscience Canada Reprint Series no. 1, p. 15-38.

Jackson, L.E. Jr., 1989. Paleoglaciology of the Selwyn Lobe of the Cordilleran Ice Sheet and Quaternary Stratigraphy of east central Yukon. *In:* Late Cenozoic History of the Interior Basins of Alaska and the Yukon, L.D. Carter, T.D. Hamilton and J.P. Galloway (eds.), United States Geological Survey, Circular 1026, p. 46-48.

Jackson, L.E. Jr., 1993a. Surficial geology, Fortin Lake, Yukon Territory. Geological Survey of Canada, Map 1795A, 1:100 000 scale.

Jackson, L.E. Jr., 1993b. Surficial geology, Rainbow Creek, Yukon Territory. Geological Survey of Canada, Map 1797A, 1:100 000 scale.

Jackson, L.E. Jr., 1993c. Surficial geology, Hoole River, Yukon Territory. Geological Survey of Canada, Map 1794A, 1:100 000 scale.

Jackson, L.E. Jr., 1993d. Surficial geology, Lonely Creek, Yukon Territory. Geological Survey of Canada, Map 1796A, 1:100 000 scale.

Jackson, L.E. Jr., 1994. Terrain inventory and Quaternary history of the Pelly River area, Yukon Territory. Geological Survey of Canada, Memoir 437, 41 p.

Klassen, R.W., 1983. Surficial geology, Wolf Lake, Yukon Territory. Geological Survey of Canada, Map 14-1982, 1:250 000 scale.

Klassen, R.W. and Morison, S.R., 1982. Surficial geology, Watson Lake, Yukon Territory. Geological Survey of Canada, Map 21-1981, 1:250 000 scale.

Lynch, J., 1996. Provisional Elemental Values for Four New Geochemical Soil and Till Reference Materials, Till-1, Till-2, Till-3 and Till-4. Geostandards Newsletter, vol. 20, No. 2, p. 277-287.

Murphy, D.C. and Piercey, S.J., 1999. Syn-mineralization faults and their re-activation Finlayson Lake massive sulphide district, Yukon-Tanana Terrane, southeastern Yukon. *In:* Yukon Exploration and Geology 1999, D.S. Emond and L.H. Weston (eds.), Exploration and Geological Services Division, Yukon Region, Indian and Northern Affairs Canada, p. 55-66.

Murphy, D.C., Colpron, M., Gordey, S.P., Roots, C.F., Abbott, G. and Lipovsky, P.S., 2001. Preliminary bedrock geological map of northern Finlayson Lake area (NTS 105G), Yukon Territory (1:100 000 scale). Exploration and Geological Services Division, Yukon Region, Indian and Northern Affairs Canada, Open File 2001-33.

Murphy, D.C., Colpron, M., Roots, C.F., Gordey, S.P. and Abbott, J.G., 2002 (this volume). Finlayson Lake Targeted Geoscience Initiative (southeastern Yukon), Part 1: Bedrock geology. *In:* Yukon Exploration and Geology 2001, D.S. Emond, L.H. Weston and L.L. Lewis (eds.), Exploration and Geological Services Division, Yukon Region, Indian and Northern Affairs Canada, p. 189-207.

Plouffe, A., 1989. Drift prospecting and till geochemistry in Tintina Trench, southeastern Yukon. M.Sc. thesis, Carleton University, Ottawa, 112 p.

Plouffe, A. and Jackson, L.E. Jr., 1992. Drift prospecting for gold in the Tintina Trench. *In:* Yukon Geology, Volume 3, T.J. Bremner (ed.), Exploration and Geological Services Division, Yukon Region, Indian and Northern Affairs Canada, p. 196-213.

Prest, V.K., Grant, D.R. and Rampton, V.N., 1967. Glacial map of Canada. Geological Survey of Canada, Map 1253A, 1:5 000 000 scale.

Shilts, W.W., 1976. Glacial till and mineral exploration. *In:* Glacial Till: An Interdisciplinary Study, R.F. Legget (ed.), Royal Society of Canada, Special Publication 12, Toronto, Ontario, p. 205-224.

Shilts, W.W., 1993. Geological Survey of Canada' s contributions to understanding the composition of glacial sediments. Canadian Journal of Earth Sciences, vol. 30, p. 333-353.

Yukon MINFILE, 2001. Exploration and Geological Services Division, Yukon Region, Indian and Northern Affairs Canada.

## APPENDIX 1. Kudz Ze Kayah orientation till geochemistry

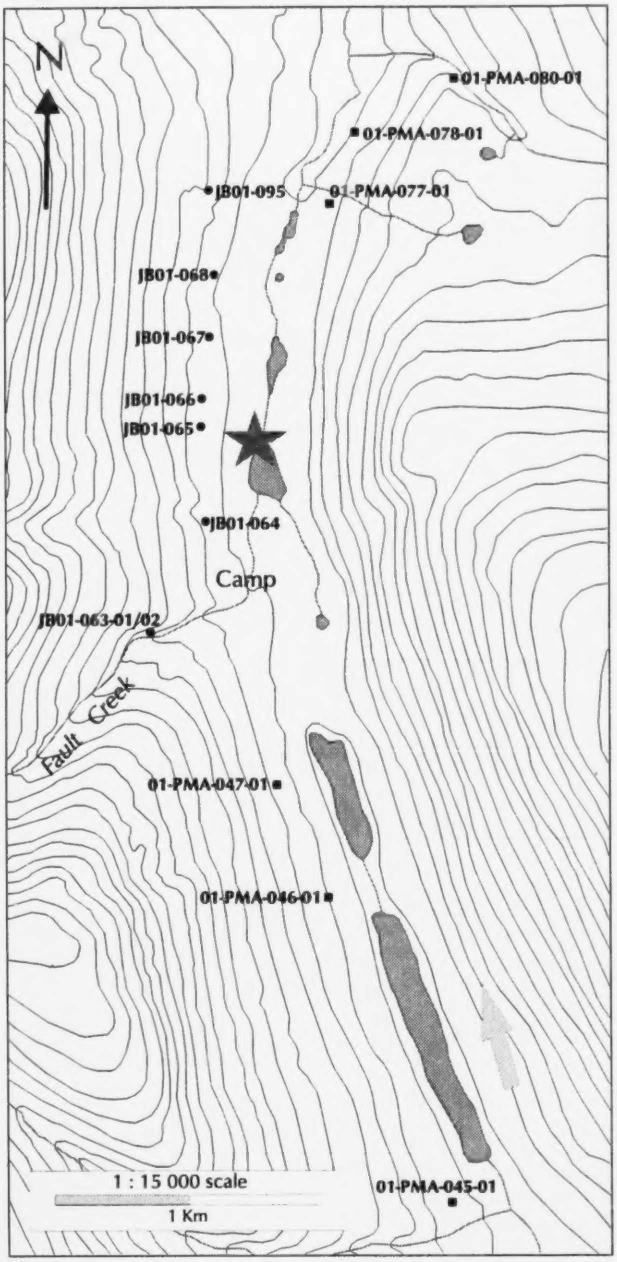
N
01-PMA-080-01
01-PMA-078-01
JB01-095
01-PMA-077-01
JB01-068
JB01-067
JB01-066
JB01-065
JB01-064
Camp
JB01-063-01/02
Fault Creek
01-PMA-047-01
01-PMA-046-01
1 : 15 000 scale
1 Km
01-PMA-045-01

Till sample locations, Kudz Ze Kayah – 2001

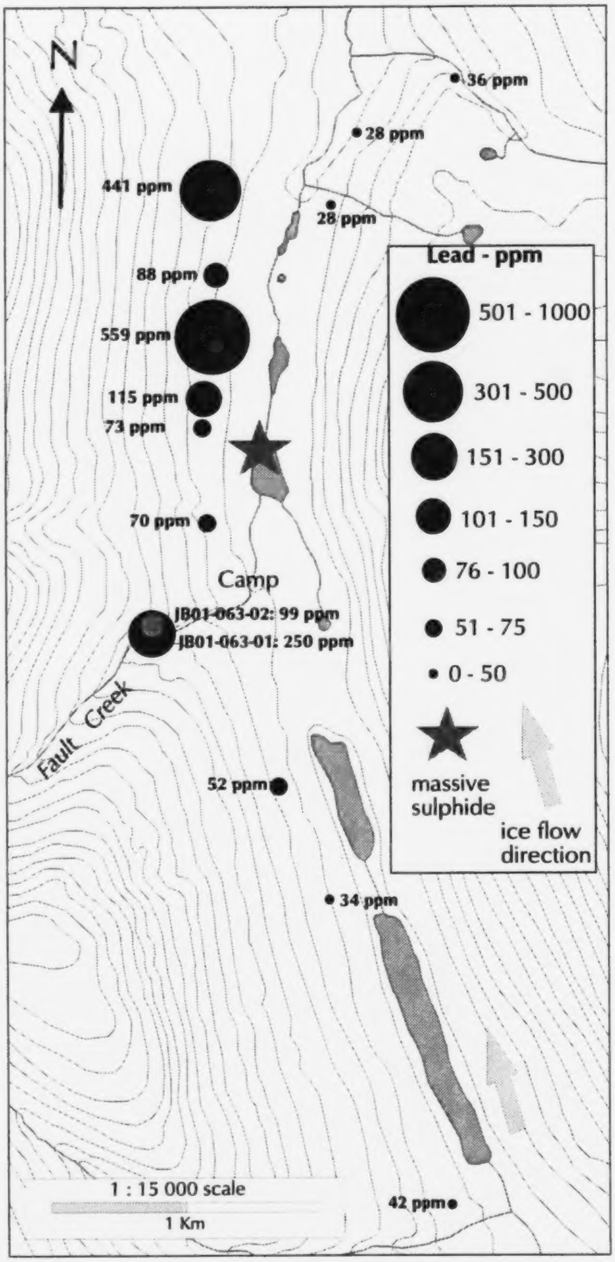
N
36 ppm
28 ppm
441 ppm
28 ppm
88 ppm
559 ppm
115 ppm
73 ppm
70 ppm
Camp
JB01-063-02: 99 ppm
JB01-063-01: 250 ppm
Fault Creek
52 ppm
34 ppm
42 ppm
1 : 15 000 scale
1 Km
Lead - ppm
501 - 1000
301 - 500
151 - 300
101 - 150
76 - 100
51 - 75
0 - 50
massive sulphide
ice flow direction

Lead

## APPENDIX 1. Kudz Ze Kayah orientation till geochemistry (continued)

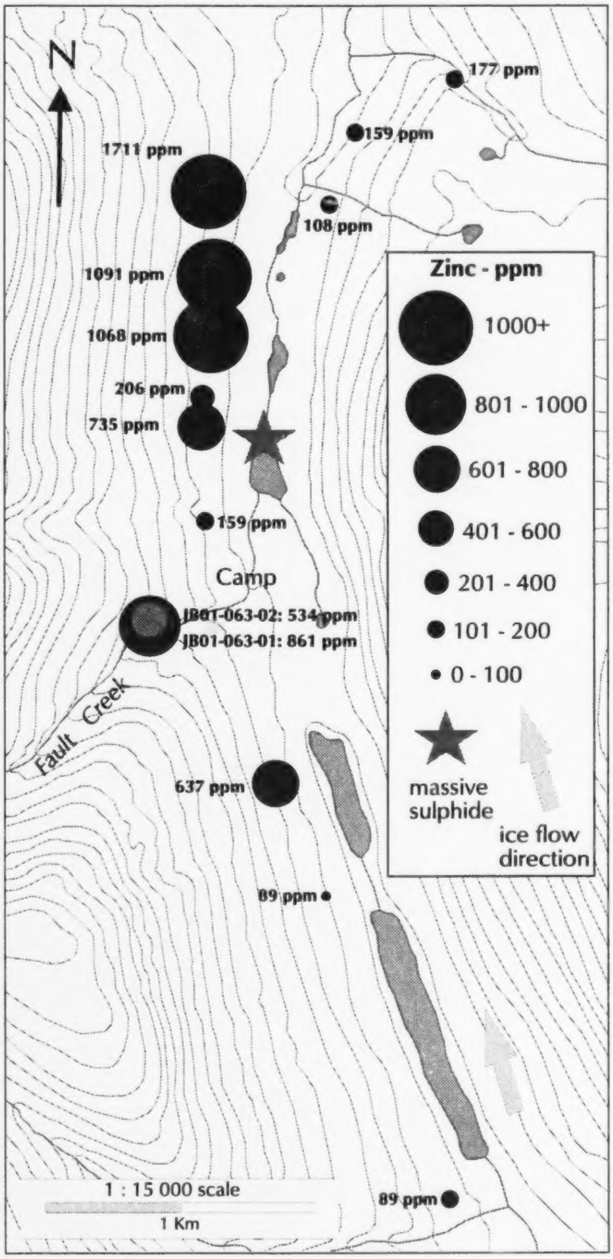
N
177 ppm
159 ppm
1711 ppm
108 ppm
1091 ppm
1068 ppm
206 ppm
735 ppm
159 ppm
Camp
JB01-063-02: 534 ppm
JB01-063-01: 861 ppm
Fault Creek
637 ppm
89 ppm
89 ppm
1 : 15 000 scale
1 Km
Zinc - ppm
1000+
801 - 1000
601 - 800
401 - 600
201 - 400
101 - 200
0 - 100
massive sulphide
ice flow direction

**Zinc**

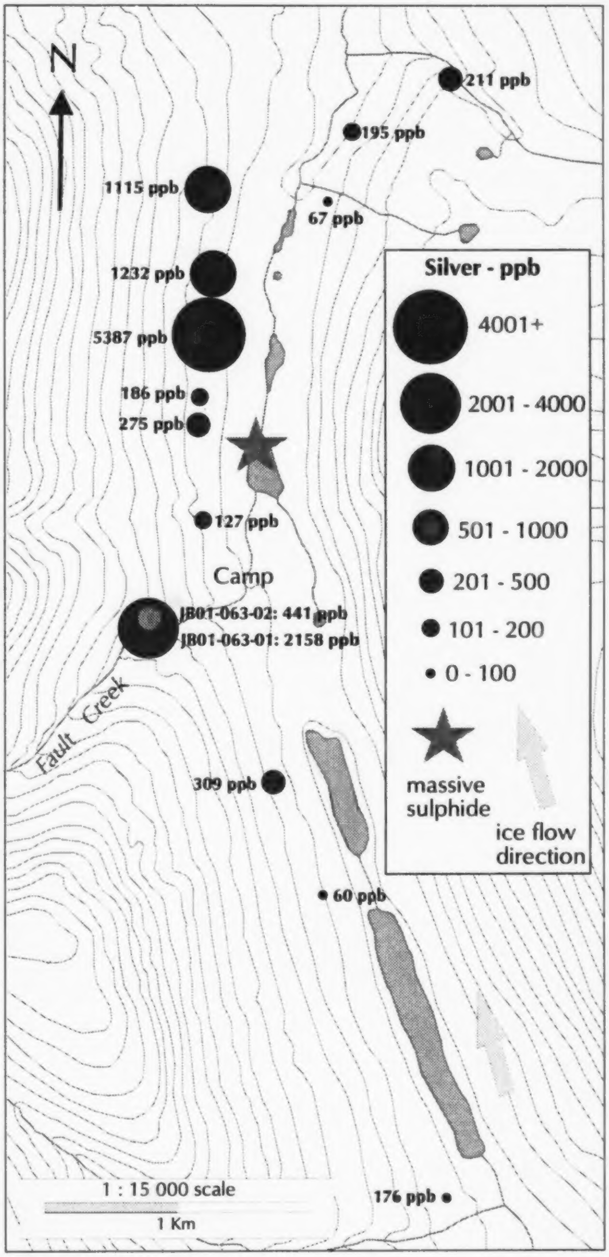
N
211 ppb
195 ppb
1115 ppb
67 ppb
1232 ppb
5387 ppb
186 ppb
275 ppb
127 ppb
Camp
JB01-063-02: 441 ppb
JB01-063-01: 2158 ppb
Fault Creek
309 ppb
60 ppb
176 ppb
1 : 15 000 scale
1 Km
Silver - ppb
4001+
2001 - 4000
1001 - 2000
501 - 1000
201 - 500
101 - 200
0 - 100
massive sulphide
ice flow direction

**Silver**

## APPENDIX 1. Kudz Ze Kayah orientation till geochemistry (continued)

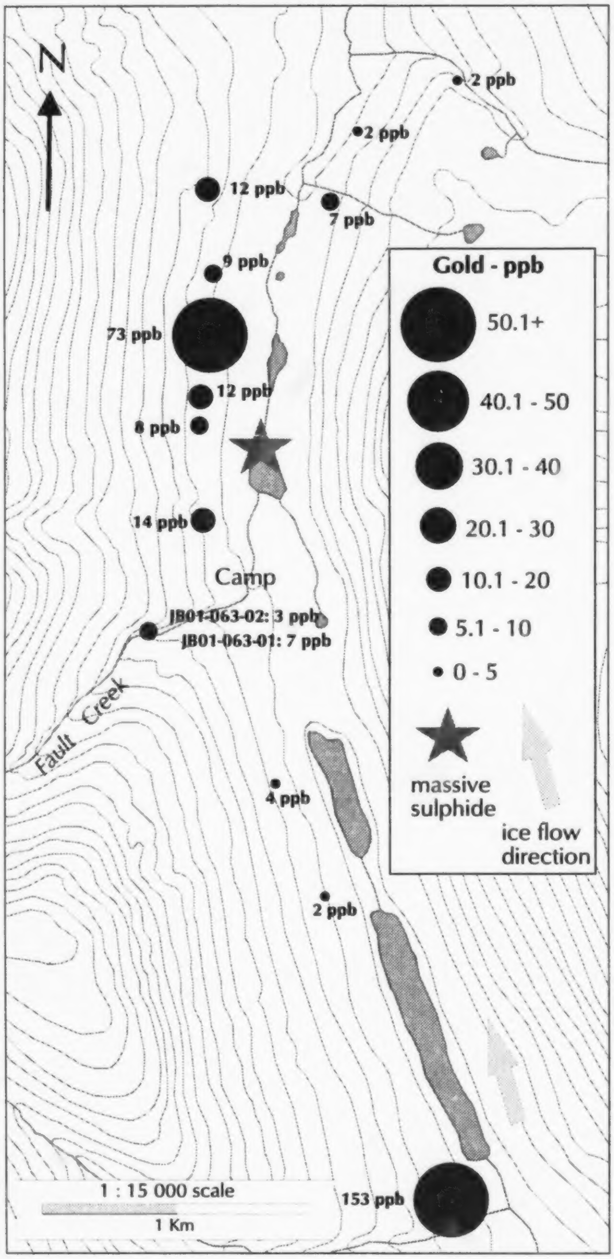
N
2 ppb
2 ppb
12 ppb
7 ppb
9 ppb
73 ppb
12 ppb
8 ppb
14 ppb
Camp
JB01-063-02: 3 ppb
JB01-063-01: 7 ppb
Fault Creek
4 ppb
2 ppb
153 ppb
1 : 15 000 scale
1 Km
Gold - ppb
50.1+
40.1 - 50
30.1 - 40
20.1 - 30
10.1 - 20
5.1 - 10
0 - 5
massive sulphide
ice flow direction

**Gold**

## Appendix 2: Regional till geochemistry maps

**Map 1 of 10, Sample locations**

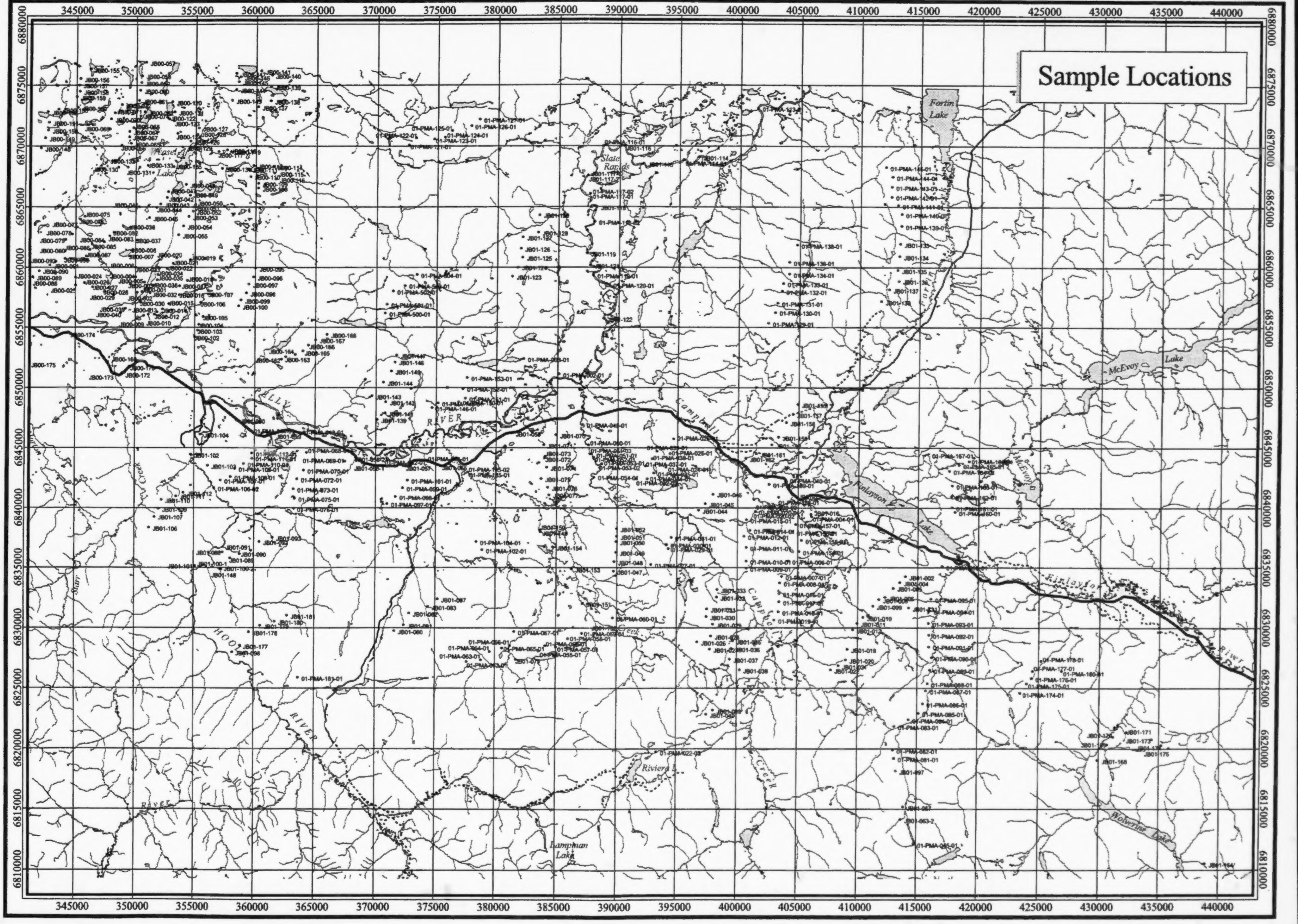
Sample Locations
345000
350000
355000
360000
365000
370000
375000
380000
385000
390000
395000
400000
405000
410000
415000
420000
425000
430000
435000
440000
6880000
6875000
6870000
6865000
6860000
6855000
6850000
6845000
6840000
6835000
6830000
6825000
6820000
6815000
6810000
Fortin Lake
Weasel Lake
Slate Rapids
McEvoy Lake
Finlayson Lake
Pelly River
Campbell
Campbell Creek
Finlayson River
Hoole River
Riviera L.
Lapman Lake
Wolverine Lake

**Appendix 2: Regional till geochemistry maps**

**Map 2 of 10, Lead**

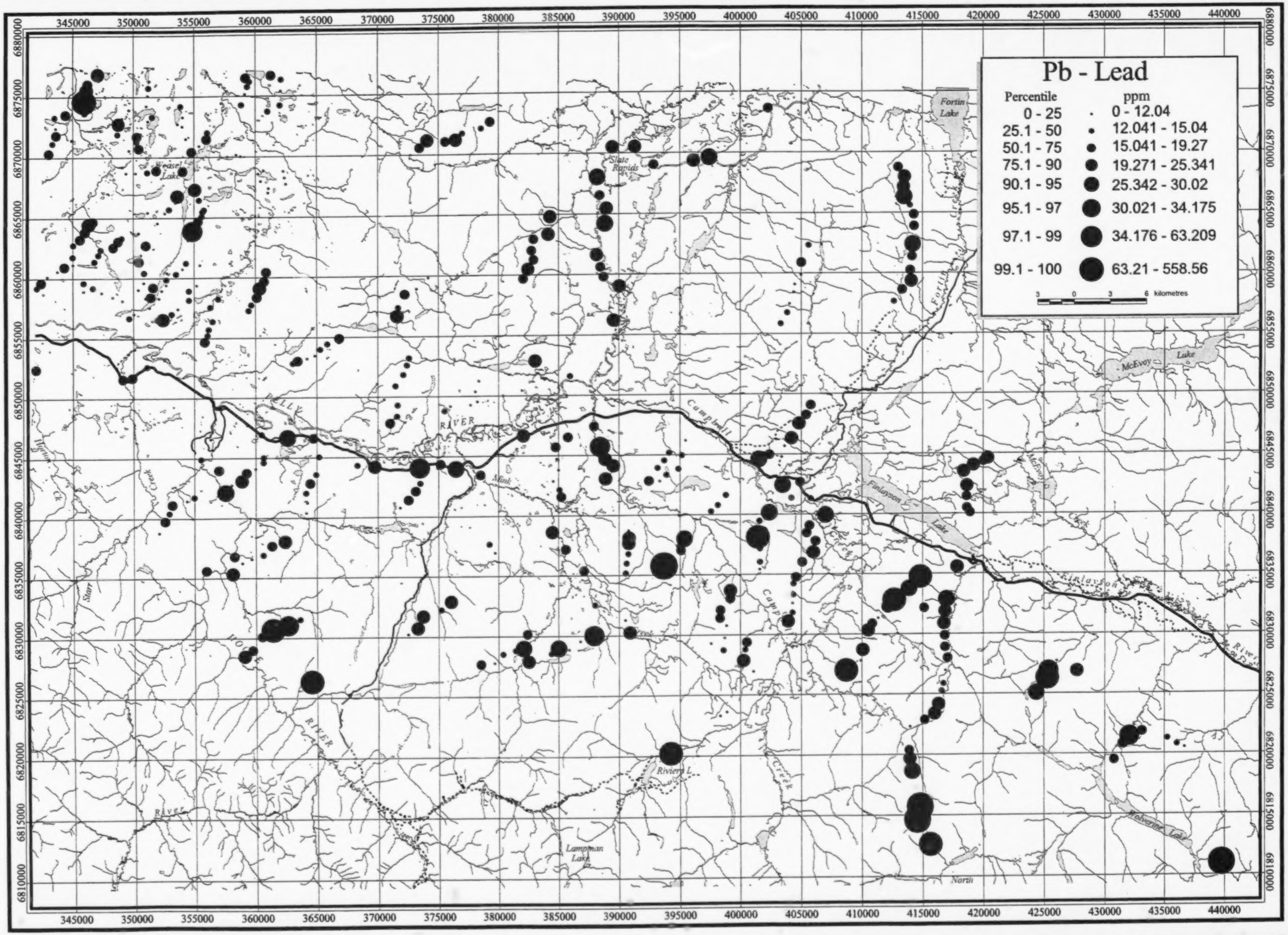
Pb - Lead
Percentile
ppm
0 - 25 · 0 - 12.04
25.1 - 50 ● 12.041 - 15.04
50.1 - 75 ● 15.041 - 19.27
75.1 - 90 ● 19.271 - 25.341
90.1 - 95 ● 25.342 - 30.02
95.1 - 97 ● 30.021 - 34.175
97.1 - 99 ● 34.176 - 63.209
99.1 - 100 ● 63.21 - 558.56
3 0 3 6 kilometres
345000
350000
355000
360000
365000
370000
375000
380000
385000
390000
395000
400000
405000
410000
415000
420000
425000
430000
435000
440000
6880000
6875000
6870000
6865000
6860000
6855000
6850000
6845000
6840000
6835000
6830000
6825000
6820000
6815000
6810000
Fortin Lake
Weasel Lake
Slate Rapids
Fortin Creek
McEvoy Lake
PELLY
RIVER
Campbell
Mink
Finlayson Lake
McEvoy Creek
Finlayson
River
Starr
Creek
Hoole
RIVER
Campbell
Creek
Riviera L.
Creek
River
Wolverine Lake
Lapman Lake
North

**Appendix 2:
Regional till geochemistry maps**

**Map 3 of 10, Zinc**

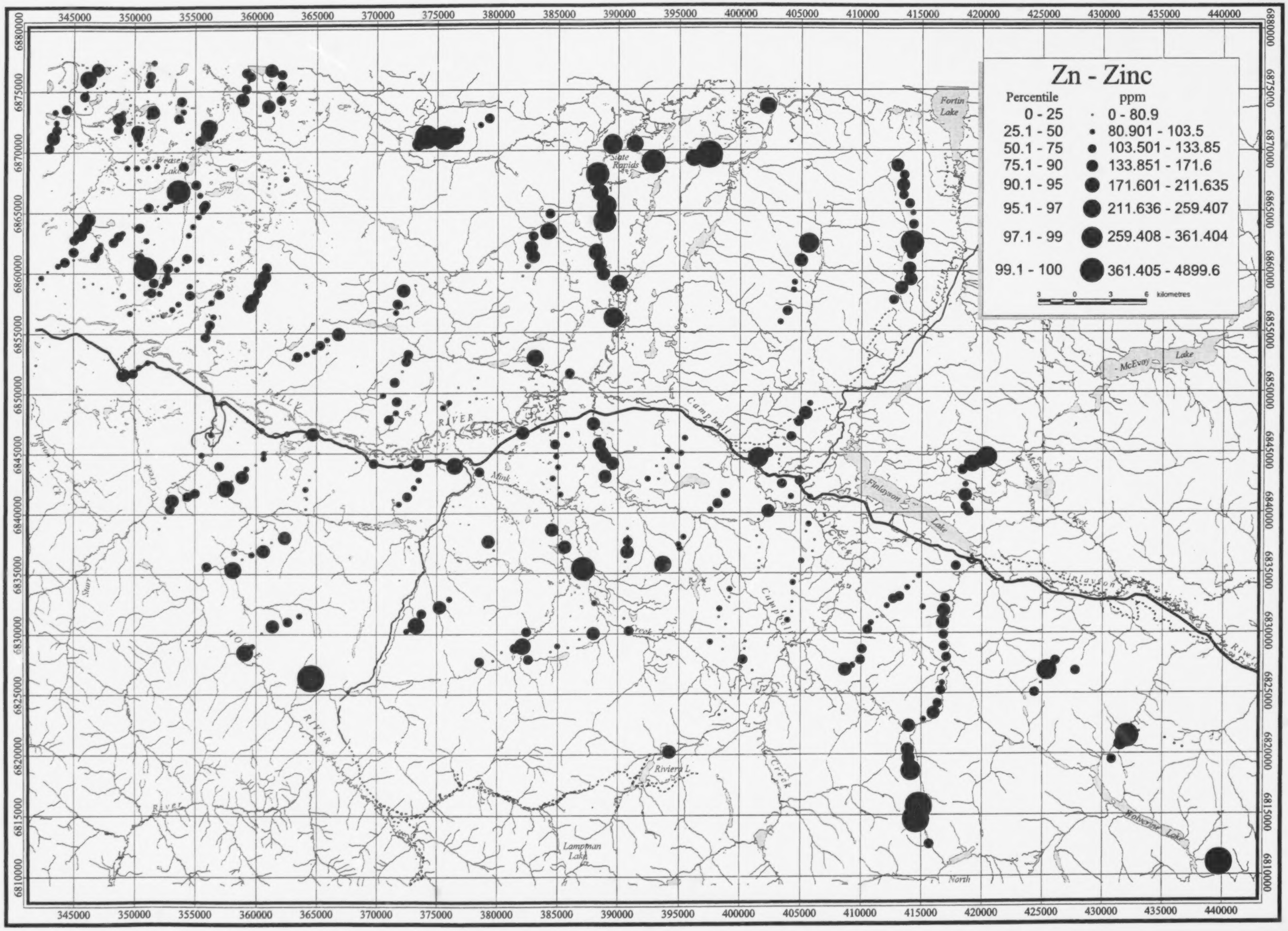
Zn - Zinc
Percentile
ppm
0 - 25 · 0 - 80.9
25.1 - 50 ● 80.901 - 103.5
50.1 - 75 ● 103.501 - 133.85
75.1 - 90 ● 133.851 - 171.6
90.1 - 95 ● 171.601 - 211.635
95.1 - 97 ● 211.636 - 259.407
97.1 - 99 ● 259.408 - 361.404
99.1 - 100 ● 361.405 - 4899.6
3 0 3 6 kilometres
345000
350000
355000
360000
365000
370000
375000
380000
385000
390000
395000
400000
405000
410000
415000
420000
425000
430000
435000
440000
6880000
6875000
6870000
6865000
6860000
6855000
6850000
6845000
6840000
6835000
6830000
6825000
6820000
6815000
6810000
Weasel Lake
State Rapids
Fortin Lake
Fortin Creek
McEvoy Lake
PELLY RIVER
Campbell
Mink
Finlayson Lake
Finlayson
McEvoy Creek
Campbell Creek
Hoole River
Riviera L.
Lampman Lake
Wolverine Lake
North
River
Starr

**Appendix 2:
Regional till
geochemistry
maps**

**Map 4 of 10,
Copper**

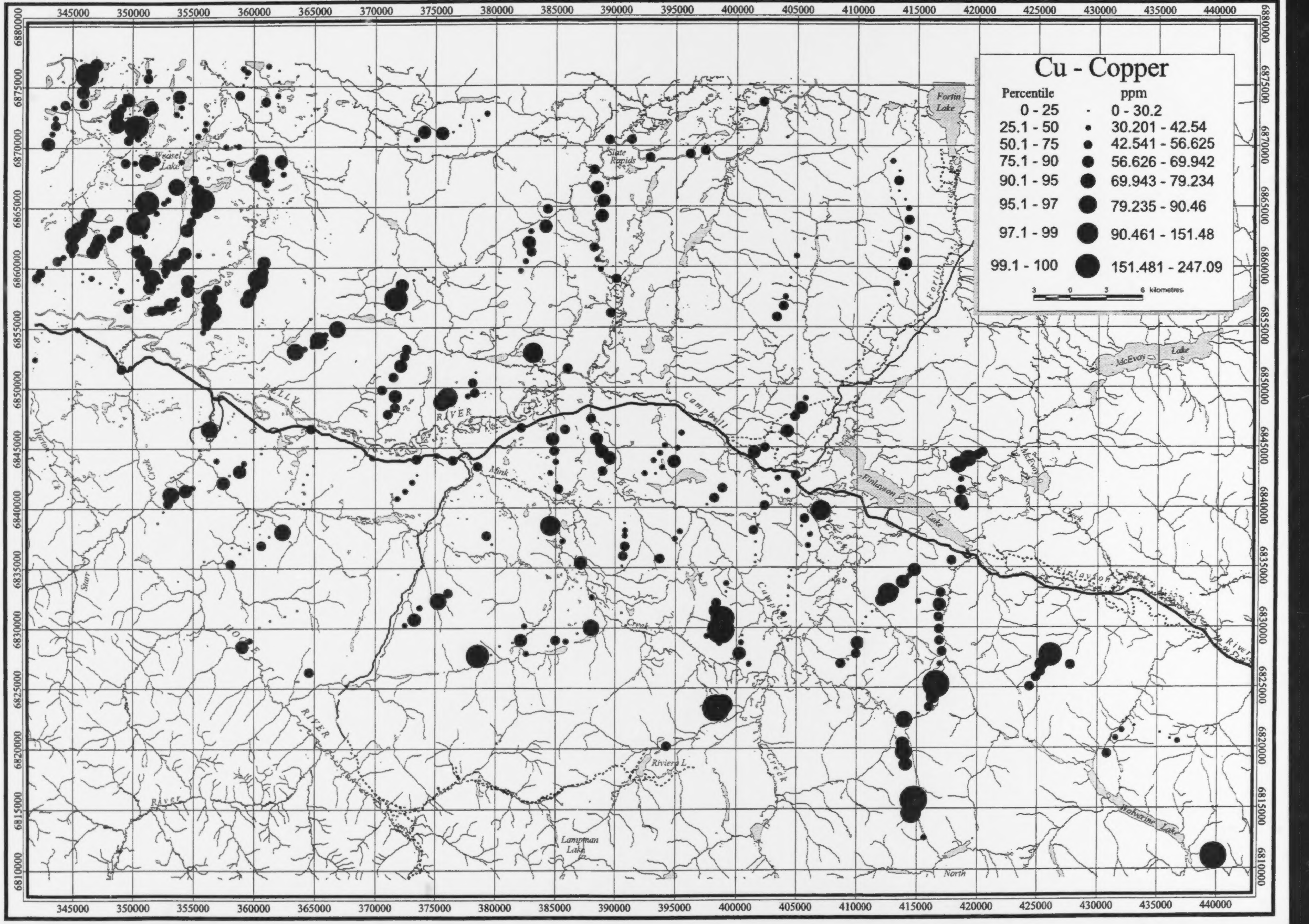
Cu - Copper
Percentile
ppm
0 - 25
0 - 30.2
25.1 - 50
30.201 - 42.54
50.1 - 75
42.541 - 56.625
75.1 - 90
56.626 - 69.942
90.1 - 95
69.943 - 79.234
95.1 - 97
79.235 - 90.46
97.1 - 99
90.461 - 151.48
99.1 - 100
151.481 - 247.09
3 0 3 6 kilometres
345000
350000
355000
360000
365000
370000
375000
380000
385000
390000
395000
400000
405000
410000
415000
420000
425000
430000
435000
440000
6880000
6875000
6870000
6865000
6860000
6855000
6850000
6845000
6840000
6835000
6830000
6825000
6820000
6815000
6810000
Fortin Lake
Weasel Lake
Slate Rapids
Fortin Creek
McEvoy Lake
PELLY RIVER
Campbell
Finlayson Lake
Finlayson River
Mink
Big Creek
McEvoy Creek
Campbell Creek
HOOLE RIVER
Starr
Horton Ck
Creek
Riviera L.
Creek
River
Lampman Lake
Wolverine Lake
North

**Appendix 2: Regional till geochemistry maps**

**Map 5 of 10, Barium**

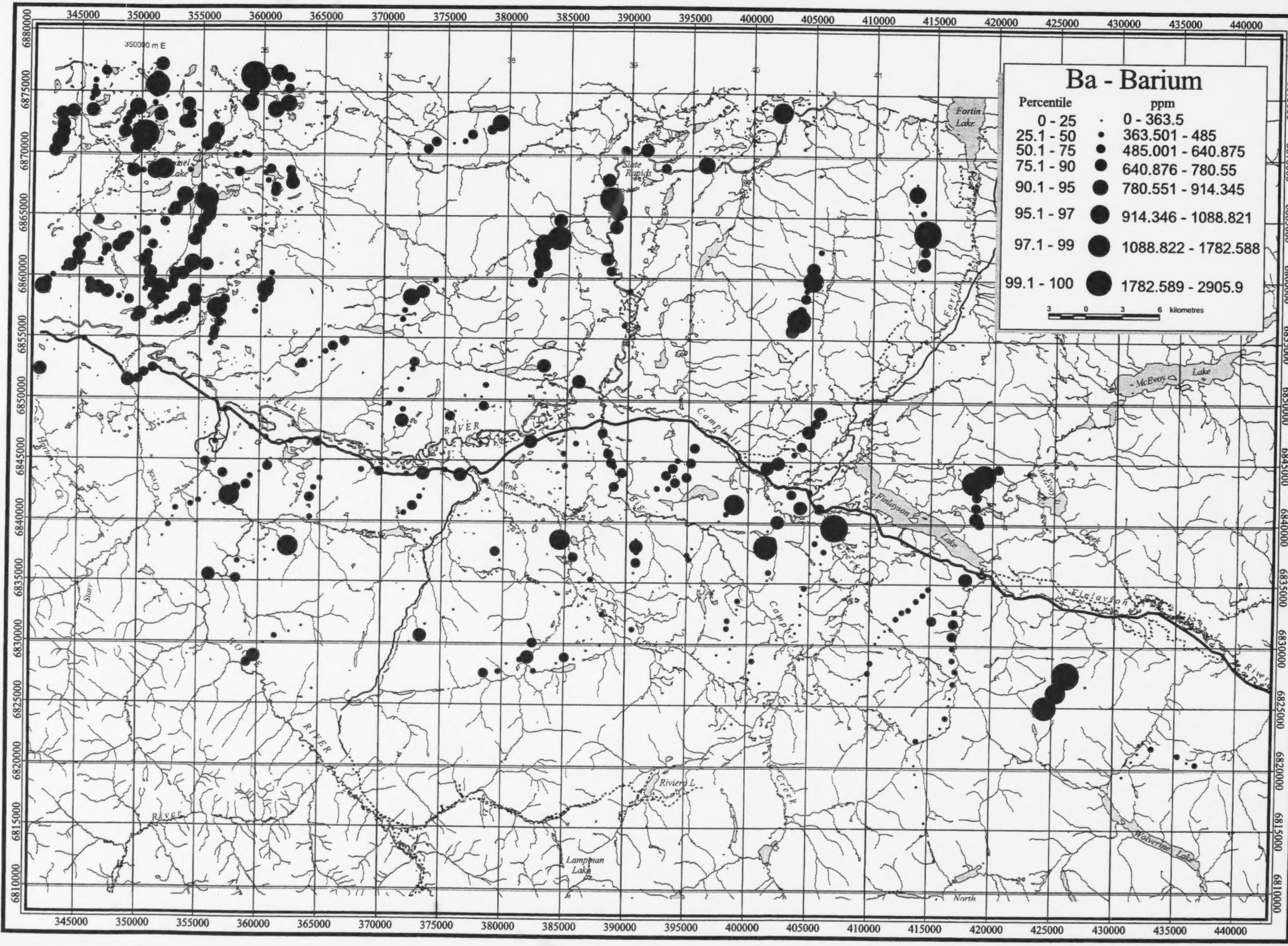
Ba - Barium
Percentile
ppm
0 - 25 · 0 - 363.5
25.1 - 50 ● 363.501 - 485
50.1 - 75 ● 485.001 - 640.875
75.1 - 90 ● 640.876 - 780.55
90.1 - 95 ● 780.551 - 914.345
95.1 - 97 ● 914.346 - 1088.821
97.1 - 99 ● 1088.822 - 1782.588
99.1 - 100 ● 1782.589 - 2905.9
3 0 3 6 kilometres
350000 m E
345000
350000
355000
360000
365000
370000
375000
380000
385000
390000
395000
400000
405000
410000
415000
420000
425000
430000
435000
440000
6880000
6875000
6870000
6865000
6860000
6855000
6850000
6845000
6840000
6835000
6830000
6825000
6820000
6815000
6810000
Fortin Lake
Slate Rapids
Fortin Creek
McEvoy Lake
PELLY RIVER
Campbell
Mink
Big
Finlayson Lake
Finlayson
River
Campbell Creek
Creek
Riviera L.
Lampman Lake
Wolverine Lake
North
RIVER
River
Creek

## Appendix 2: Regional till geochemistry maps

Map 6 of 10, Nickel

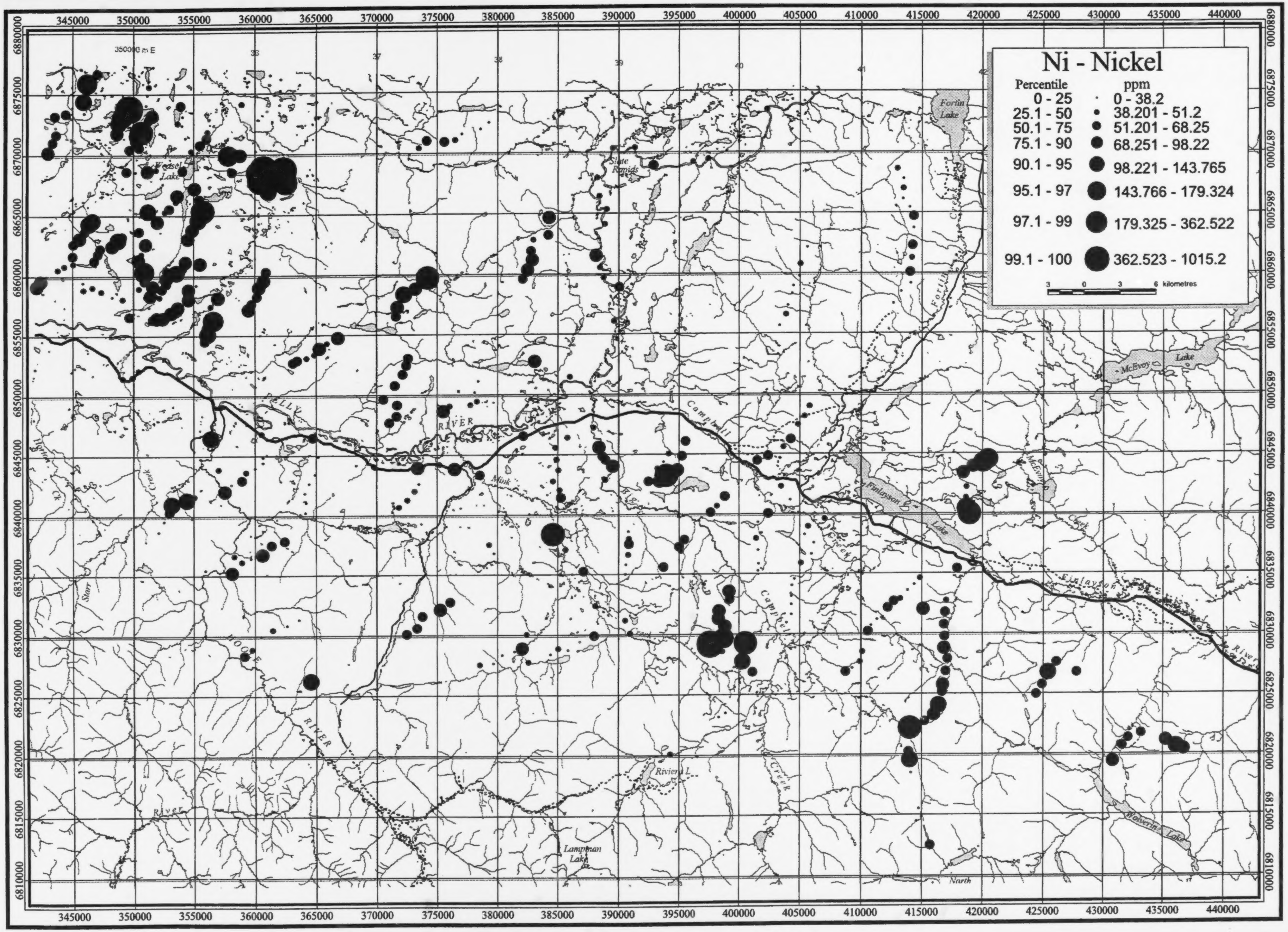
Ni - Nickel
Percentile
ppm
0 - 25
0 - 38.2
25.1 - 50
38.201 - 51.2
50.1 - 75
51.201 - 68.25
75.1 - 90
68.251 - 98.22
90.1 - 95
98.221 - 143.765
95.1 - 97
143.766 - 179.324
97.1 - 99
179.325 - 362.522
99.1 - 100
362.523 - 1015.2
3 0 3 6 kilometres
350000 m E
Weasel Lake
Slate Rapids
Fortin Lake
Fortin Creek
McEvoy Lake
PELLY RIVER
Campbell
Finlayson Lake
Finlayson River
Money Creek
Big Creek
Starr Creek
HOOLE RIVER
River
Riviera L.
Lapie Lake
Wolverine Lake
North
345000
350000
355000
360000
365000
370000
375000
380000
385000
390000
395000
400000
405000
410000
415000
420000
425000
430000
435000
440000
6880000
6875000
6870000
6865000
6860000
6855000
6850000
6845000
6840000
6835000
6830000
6825000
6820000
6815000
6810000

**Appendix 2: Regional till geochemistry maps**

**Map 7 of 10, Chromium**

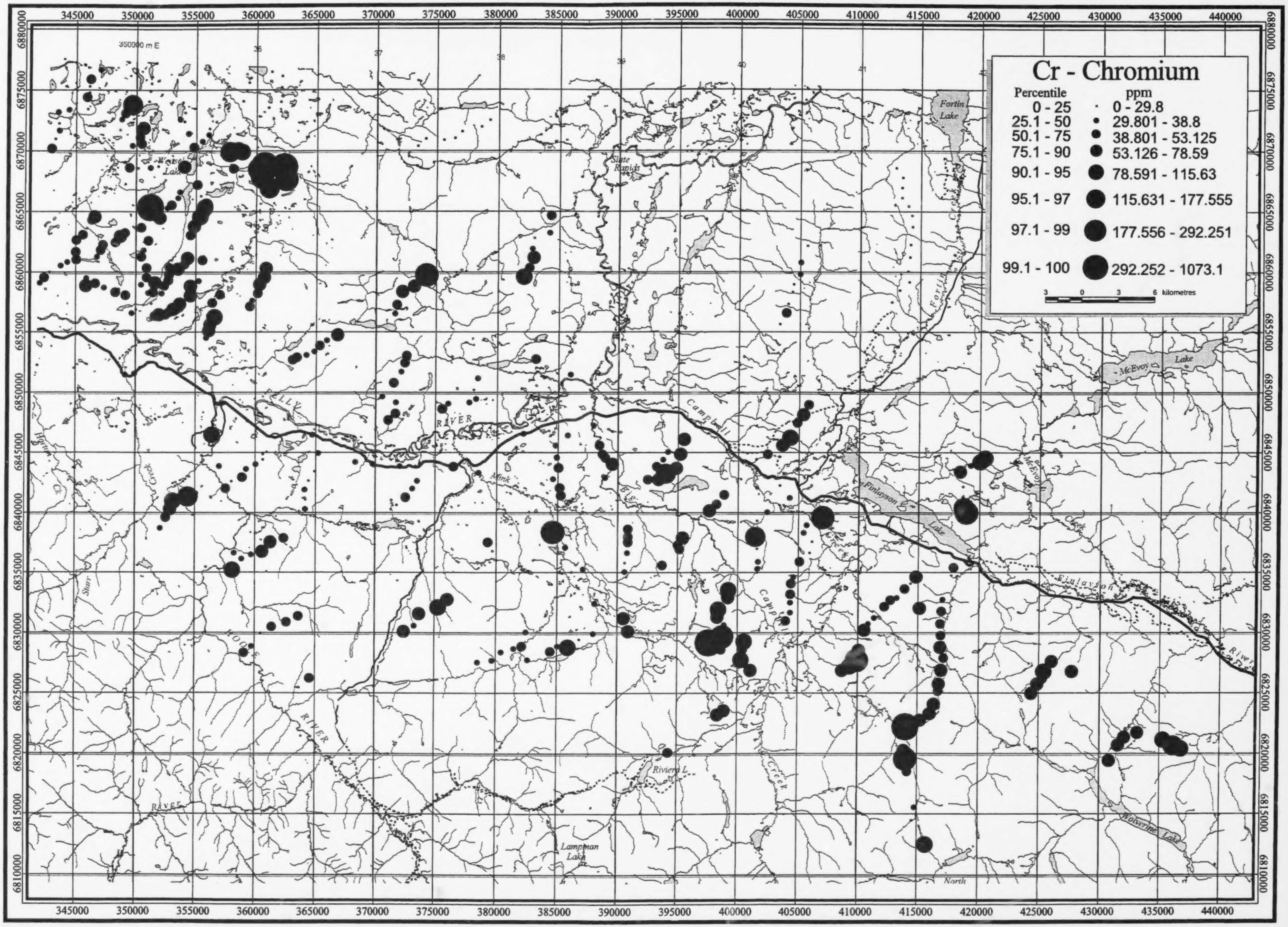
Cr - Chromium
Percentile
ppm
0 - 25
0 - 29.8
25.1 - 50
29.801 - 38.8
50.1 - 75
38.801 - 53.125
75.1 - 90
53.126 - 78.59
90.1 - 95
78.591 - 115.63
95.1 - 97
115.631 - 177.555
97.1 - 99
177.556 - 292.251
99.1 - 100
292.252 - 1073.1
3 0 3 6 kilometres
345000
350000
355000
360000
365000
370000
375000
380000
385000
390000
395000
400000
405000
410000
415000
420000
425000
430000
435000
440000
6880000
6875000
6870000
6865000
6860000
6855000
6850000
6845000
6840000
6835000
6830000
6825000
6820000
6815000
6810000
350000 m E
Wolverine Lake
Fortin Lake
Slate Rapids
PELLY RIVER
Campbell
McEvoy Lake
Finlayson Lake
Finlayson
River
Mink
Big
Campbell
Creek
Star
Hoole
RIVER
River
Riviera L.
Lapman Lake
Wolverine Lake
North

**Appendix 2: Regional till geochemistry maps**

**Map 8 of 10, Gold**

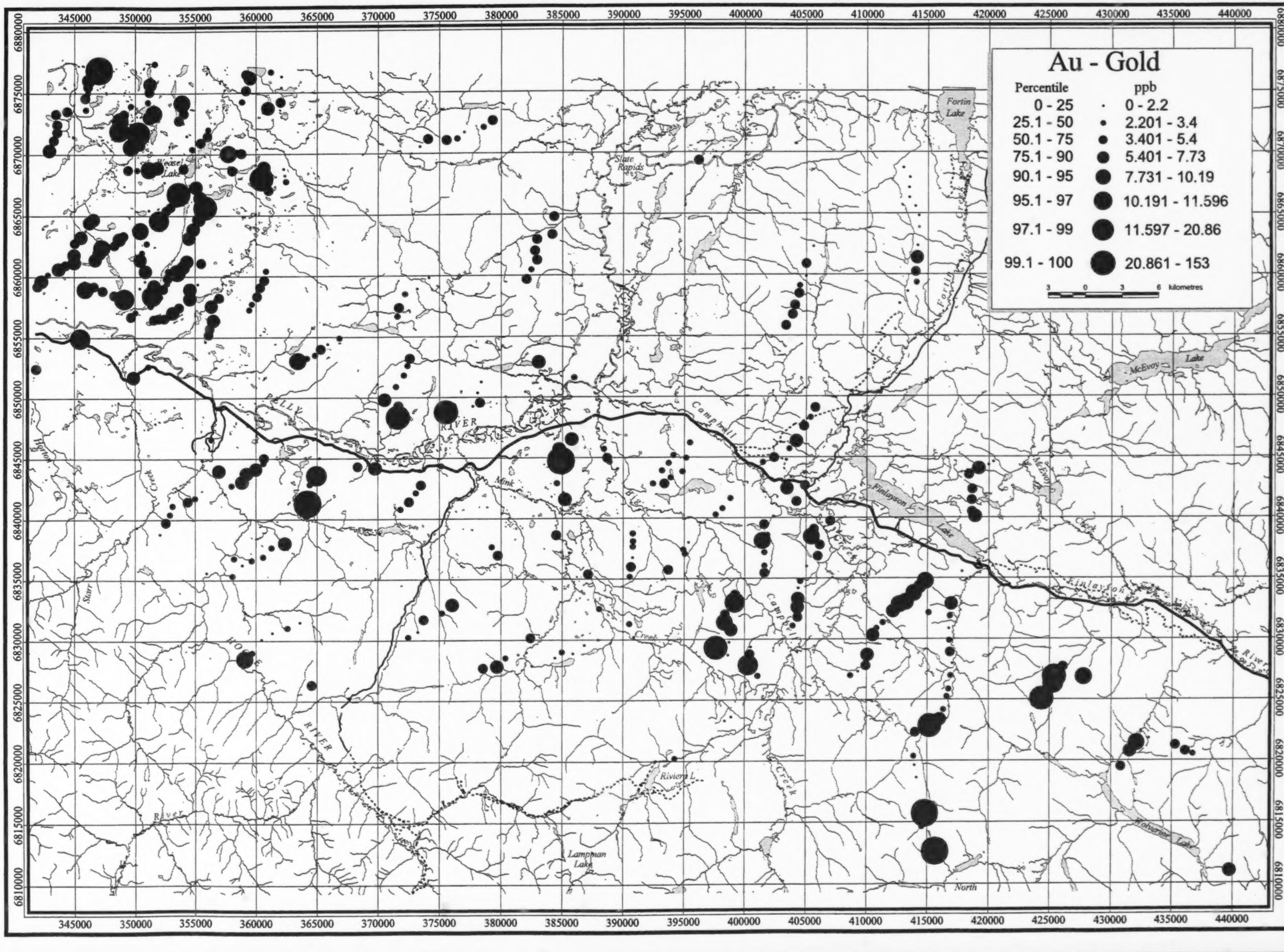
Au - Gold
Percentile
ppb
0 - 25 · 0 - 2.2
25.1 - 50 · 2.201 - 3.4
50.1 - 75 ● 3.401 - 5.4
75.1 - 90 ● 5.401 - 7.73
90.1 - 95 ● 7.731 - 10.19
95.1 - 97 ● 10.191 - 11.596
97.1 - 99 ● 11.597 - 20.86
99.1 - 100 ● 20.861 - 153
3 0 3 6 kilometres
345000
350000
355000
360000
365000
370000
375000
380000
385000
390000
395000
400000
405000
410000
415000
420000
425000
430000
435000
440000
6880000
6875000
6870000
6865000
6860000
6855000
6850000
6845000
6840000
6835000
6830000
6825000
6820000
6815000
6810000
Weasel Lake
Slate Rapids
Fortin Lake
Fortin Creek
McEvoy Lake
McEvoy Creek
Finlayson Lake
Finlayson River
Pelly River
Campbell
Campbell Creek
Big Campbell Creek
Mink
Hoole River
Starr
Horton Ck
Creek
Riviera L.
Lapman Lake
Wolverine Lake
North
River

## Appendix 2: Regional till geochemistry maps

Map 9 of 10, Silver

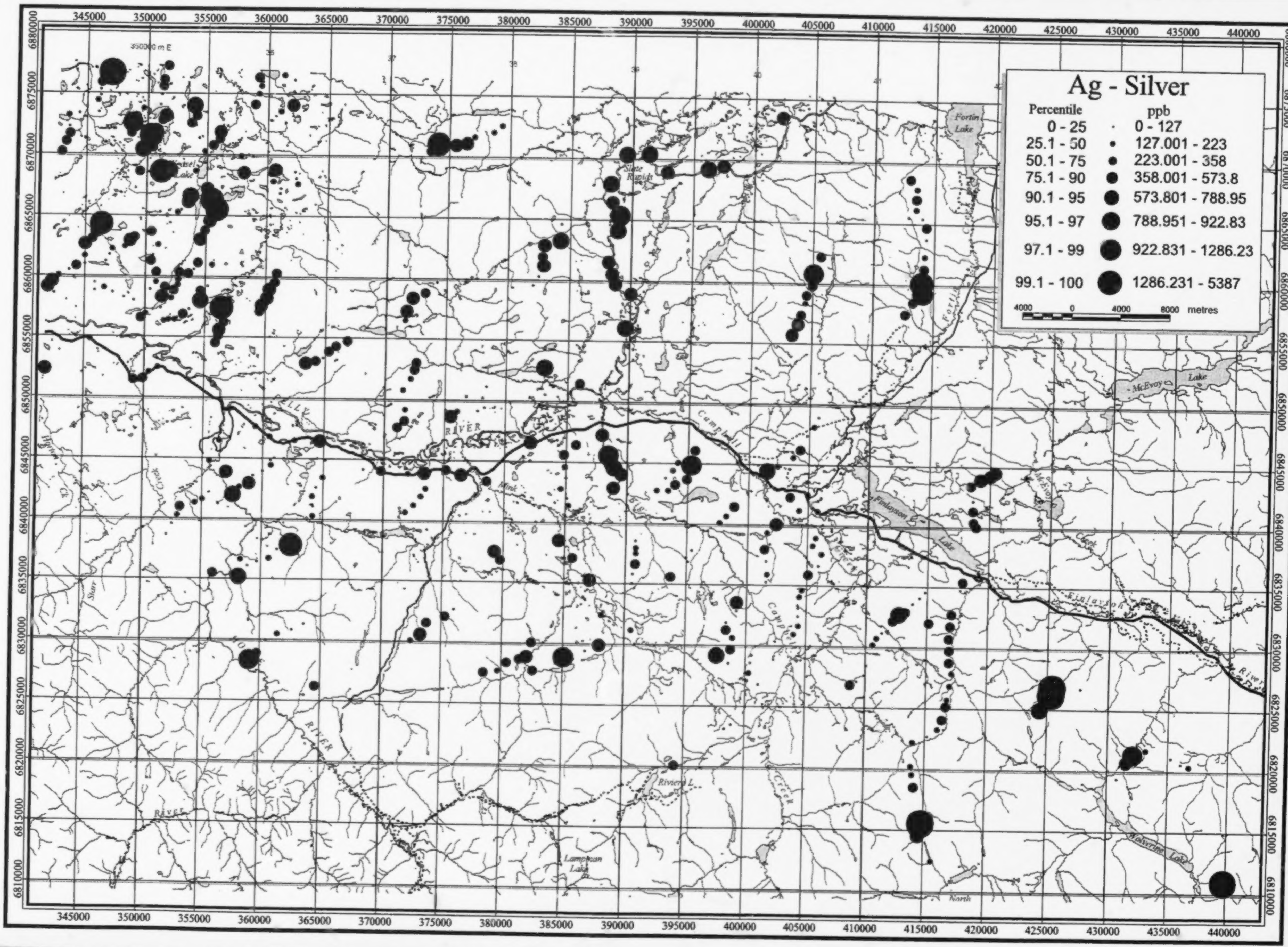
Ag - Silver
Percentile
ppb
0 - 25 · 0 - 127
25.1 - 50 ● 127.001 - 223
50.1 - 75 ● 223.001 - 358
75.1 - 90 ● 358.001 - 573.8
90.1 - 95 ● 573.801 - 788.95
95.1 - 97 ● 788.951 - 922.83
97.1 - 99 ● 922.831 - 1286.23
99.1 - 100 ● 1286.231 - 5387
4000 0 4000 8000 metres
350000 m E
Fortin Lake
McEvoy Lake
Slate Rapids
Pelly River
Campbell
Mink
Big
Finlayson Lake
Finlayson
Riviera L.
Lapman Lake
Wolverine Lake
Starr Creek
River
North

**Appendix 2: Regional till geochemistry maps**

**Map 10 of 10, Arsenic**

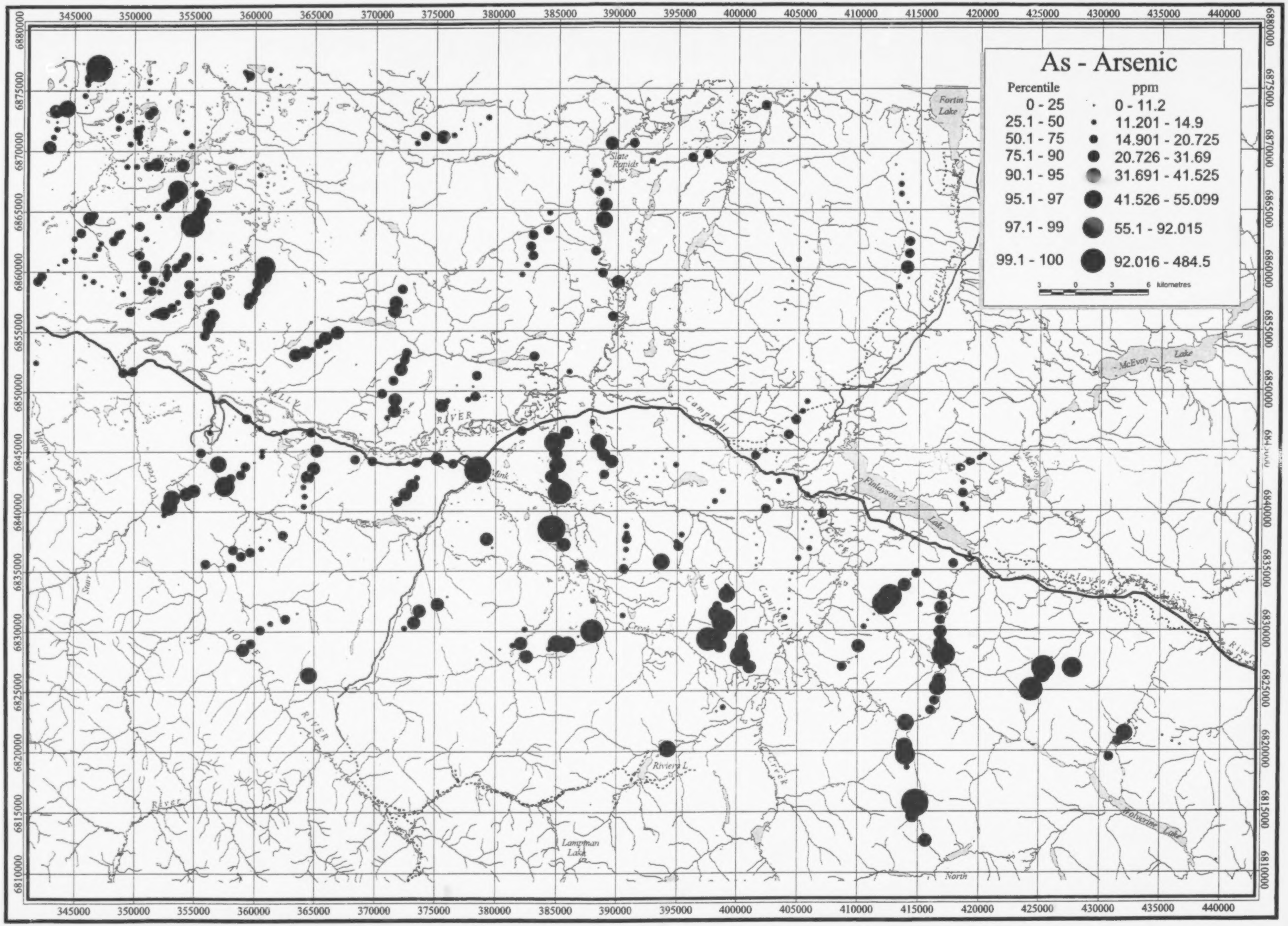
As - Arsenic
Percentile
ppm
0 - 25
0 - 11.2
25.1 - 50
11.201 - 14.9
50.1 - 75
14.901 - 20.725
75.1 - 90
20.726 - 31.69
90.1 - 95
31.691 - 41.525
95.1 - 97
41.526 - 55.099
97.1 - 99
55.1 - 92.015
99.1 - 100
92.016 - 484.5
3 0 3 6 kilometres
345000
350000
355000
360000
365000
370000
375000
380000
385000
390000
395000
400000
405000
410000
415000
420000
425000
430000
435000
440000
6880000
6875000
6870000
6865000
6860000
6855000
6850000
6845000
6840000
6835000
6830000
6825000
6820000
6815000
6810000
Fortin Lake
Slate Rapids
McEvoy Lake
Campbell
Finlayson Lake
Finlayson River
Wolverine Lake
Riviera L.
Lampman Lake
North
Mink
VALLY
RIVER
Creek
Big
Campbell
Creek
Stars
RIVER
River
Creek
Fortin
McEvoy
Creek

# Preliminary results of a petrological study of ultramafic rocks of the Northern Cordillera

*J. Gregory Shellnutt*[1]*, Dante Canil and Stephen T. Johnston*[2]
University of Victoria[3]

Shellnutt, J.G., Canil, D. and Johnston, S.T., 2002. Preliminary results of a petrological study of ultramafic rocks of the Northern Cordillera. *In:* Yukon Exploration and Geology 2001, D.S. Emond, L.H. Weston and L.L. Lewis (eds.), Exploration and Geological Services Division, Yukon Region, Indian and Northern Affairs Canada, p. 229-237.

## ABSTRACT

The Cache Creek (CCT) and Slide Mountain terranes (SMT, including the Seventymile Terrane in Alaska) of the Northern Cordillera consist of oceanic assemblages that have been tectonically emplaced. The CCT has been enclosed by a series of arc terranes, whereas the SMT has been thrust onto pericratonic North America. Detailed studies of ultramafic rocks in CCT, SMT, Livengood Terrane and the Kluane metamorphic assemblage across Yukon, Alaska and British Columbia were conducted at nine site locations. The most common type of ultramafic rock present at these localities is serpentinized harzburgite. The ultramafic rocks from the CCT and SMT have been interpreted as the lower layers from dismembered ophiolite complexes. Samples collected from the CCT are consistently harzburgite, whereas samples from the SMT are both mantle-derived harzburgite and lherzolite. The variety of ultramafic rock present in the SMT suggests they were generated within contrasting geological settings.

## RÉSUMÉ

Les terranes de Cache Creek (TCC) et de Slide Mountain (TSM, y compris le terrane de Seventymile, en Alaska) de la Cordillère septentrionale sont constitués d'assemblages océaniques mis en place par tectonisation. Le TCC est encaissé dans une série de terranes d'arc, alors que le TSM a été poussé sur l'Amérique du Nord péricratonique. On a effectué des études détaillées des roches ultramafiques provenant de neuf sites représentant les terranes de TCC, TSM, Livengood, et de l'assemblage métamorphique de Kluane, au Yukon, en Alaska et en Colombie-Britannique. La variété de péridotite préservée la plus répandue dans ces sites est l'harzburgite serpentinisée. Les roches ultramafiques du TCC et du TSM constitueraient les couches inférieures de complexes ophiolitiques démembrés. Les échantillons provenant du TCC sont uniformément du même type de roche (harzburgite), alors que ceux extraits du TSM proviennent d'un plus vaste éventail de types de roche (harzburgite et lherzolite mantelliques). Les divers types de roche ultramafique (péridotites mantelliques et intrusions ultramafiques) du TSM suggèrent que ces roches se sont formées dans différents cadres géologiques (p. ex., tectonique et magmatique).

---

[1] *jgshelln@uvic.ca*

[2] *stj@uvic.ca*

[3] *University of Victoria, School of Earth and Ocean Science, P.O. Box 3055 STN CSC, Victoria, British Columbia, Canada V8W 3P6*

## INTRODUCTION

Ultramafic rocks characterize all orogenic belts, and include structurally interleaved mantle and metasedimentary rocks (orogenic peridotite massifs), oceanic mantle and crust (ophiolites), and concentrically zoned intrusions (Alaskan-type intrusions). Numerous ultramafic occurrences are known in the Northern Cordillera, and many of these have been interpreted as ophiolite, in some cases, despite the absence of other ophiolite components (Terry, 1977; Tempelman-Kluit, 1979; Keith et al., 1981; Leaming, 1982; Patton et al., 1994; Mihalynuk et al., 1994). The purpose of this study is to assess, through mapping, petrological and geochemical studies, the tectonic affinity of ultramafic occurrences between the Tintina and Denali faults in Yukon and adjacent portions of Alaska and British Columbia. This paper is an initial summary of petrographic and field observations of ultramafic rocks from the Northern Cordillera.

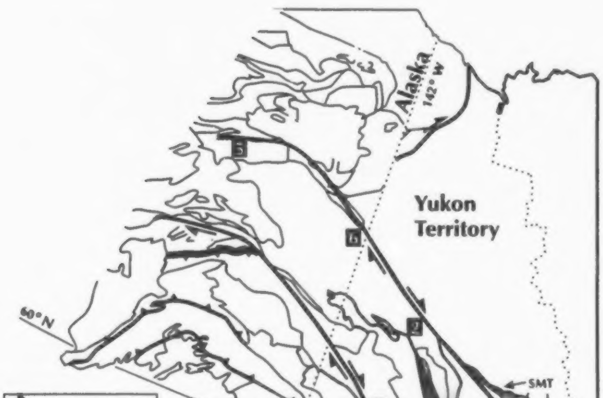

***Figure 1.*** *Regional map of the Northern Cordillera showing site locations of ultramafic rocks, and the extent of the Cache Creek and Slide Moutain terranes.*

## SITE LOCATIONS

During the summer of 2001, nine ultramafic rock occurrences were chosen for detailed geological investigation: four sites in Yukon, two in Alaska and three in British Columbia (Fig. 1). The nomenclature for peridotites of Harte (1977) is adopted for the petrographic textures. All samples are serpentinized, however the extent of serpentinization varies. Petrographic interpretation of these rocks is based on the recognition of relict minerals and their associated characteristic pseudomorph textures. Serpentine is primarily found along fractures and grain boundaries and locally as large veins (≤ 2 mm). Serpentinized olivine is recognized by crystal shape, fractures and remnant outline. Pyroxenes are identified by relict crystal shape, distinct cleavage and appearance of former exsolution lamellae. Orthopyroxene and clinopyroxene pseudomorphs can be distinguished by their extinction angle provided both crystals have preserved cleavage planes. Other common features include magnetite derived from serpentinized olivine and primary red-brown spinel.

## YUKON

### *Kluane Lake*

Mezger (2000) mapped a series of southeast-trending ultramafic lenses within the 150-km-long Kluane metamorphic assemblage, a southeast-trending belt of graphitic mica schist and gneiss located between Yukon-Tanana Terrane and Wrangellia in western Yukon. An ultramafic body along the Talbot Arm of Kluane Lake was selected for geological reconnaissance (Fig. 2). The outcrop is 500 m long, and is a continuation of a larger body that extends 5 km to the west (Fig. 2). The ultramafic body is in contact with the Ruby Range batholith to the north and muscovite-chlorite schist to the south. The contact relationships were not visible in the study area and have been inferred from aeromagnetic data (Mezger, 2000).

The ultramafic rocks weather red-brown with 1-3 mm orthopyroxene, irregular, blocky, 1-10 mm olivine and acicular, 2-4 cm long talc. The rocks consist of 40-90%, coarse (≤ 10 mm), anhedral olivine that has altered to serpentine and talc. Talc (0-35%; 0.5 to 2 mm) has a radiating fibrous texture. Orthopyroxene (~5%) grains (≤ 2 mm) have exsolution lamellae of clinopyroxene and commonly enclose talc. The remainder of the rock is made up of secondary magnetite, tremolite, and chlorite, however the textures of olivine and orthopyroxene suggest the protolith was a mantle harzburgite.

### *Flat Creek*

The ultramafic rocks of Flat Creek were collected along a northwest-trending, semi-continous ridge located less than 1 km southwest of the Klondike-Dempster highway junction (Fig. 3). Mortensen (1996) assigned the ultramafic rocks to the SMT and interpreted thrust fault contact relationships with surrounding Yukon-Tanana Terrane rocks (Nasina Assemblage). Other ultramafic rocks of the SMT in this region are found along the Klondike River (west of the Tintina Trench) and continue northwest into Alaska.

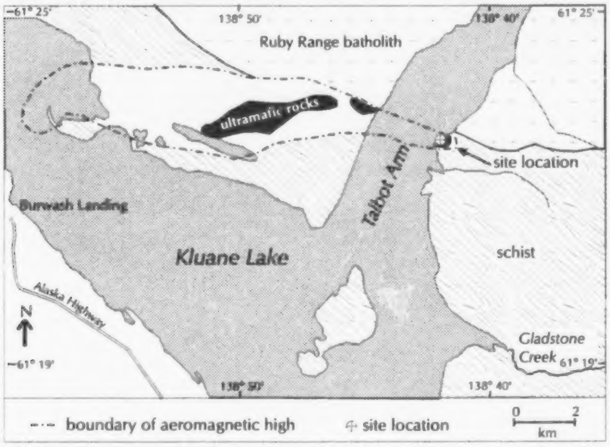
61° 25'
138° 50'
Ruby Range batholith
138° 40'
61° 25'
ultramafic rocks
site location
Talbot Arm
Burwash Landing
Kluane Lake
schist
Alaska Highway
N
61° 19'
Gladstone Creek
61° 19'
138° 50'
138° 40'
boundary of aeromagnetic high
site location
0
2
km

***Figure 2.*** *Simplified geological map of Kluane Lake area with site location (modified from Mezger, 2000).*

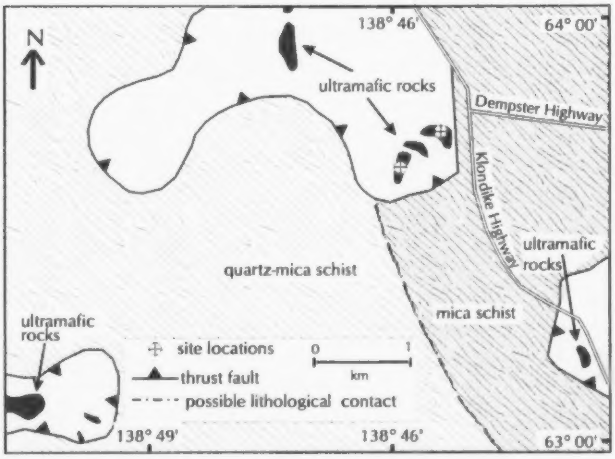
N
138° 46'
64° 00'
ultramafic rocks
Dempster Highway
Klondike Highway
ultramafic rocks
quartz-mica schist
mica schist
ultramafic rocks
site locations
thrust fault
possible lithological contact
0
1
km
138° 49'
138° 46'
63° 00'

***Figure 3.*** *Simplified geological map of Flat Creek area with site location (modified from Mortensen, 1996).*

The weathered surface of the ultramafic rock is bluish-grey with white to light beige talc and carbonate alteration. The fresh surface is greasy with black serpentine, olivine porphyroclasts, clear crystalline green lenses, and thin (≤ 1 mm) veins of secondary magnetite. The rock is generally brittle and fractured with asbestos-bearing slickensides.

Samples from Flat Creek show (~10%) relict coarse, equant olivine (≤ 0.1 mm). Carbonate is found as an aggregate alteration texture of either olivine or pyroxene within serpentine veins. Spinel is the only other primary mineral that has remained and is typically bright red, (rarely exceeds 0.5 mm) with corroded irregular grain boundaries. The protolith is not easily ascertained because the remaining primary textures cannot be differentiated between a mantle tectonite and a cumulate igneous rock.

### *Frances Lake*

Ultramafic rocks occur west of Frances Lake on the King Arctic jade mine (Yukon MINFILE, 2001, 105H 014) road (west of the Robert Campbell Highway) in eastern Yukon (Murphy, 2001, 2000; Fig. 4). The ultramafic rock at this locality is interpreted by Murphy (2001) to represent a

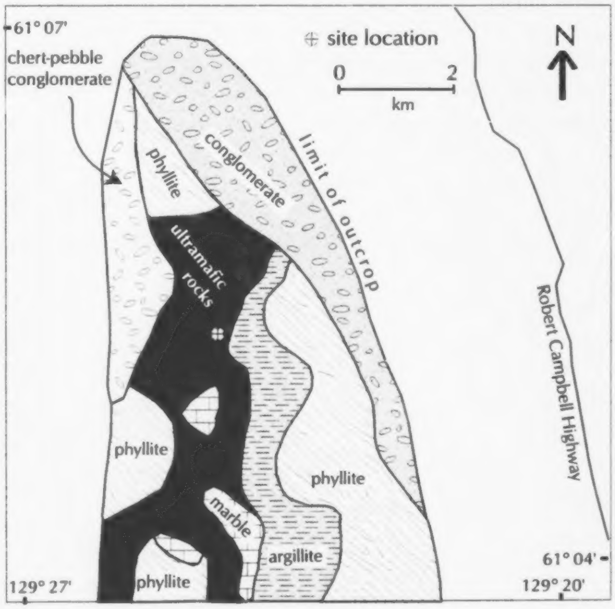
61° 07'
site location
N
chert-pebble conglomerate
0
2
km
phyllite
conglomerate
limit of outcrop
ultramafic rocks
Robert Campbell Highway
phyllite
phyllite
marble
argillite
61° 04'
129° 27'
phyllite
129° 20'

***Figure 4.*** *Simplified geological map of Frances Lake area with site location (modified from Murphy, 2001).*

Pennsylvanian-Permian intrusion into carbonate rocks of Yukon-Tanana Terrane and may be correlative with similar age Campbell Range basalts (Murphy, 2000).

Samples from Frances Lake area are composed of olivine (80-95%), orthopyroxene (10-15%), secondary magnetite (5%) and a minor amount of clinopyroxene (≤ 2%). Orthopyroxene is curviplanar, displays exsolution lamellae of clinopyroxene and is ≤ 4 mm long, subhedral and porphyroclastic. Clinopyroxene is equant, subhedral, typically ≤ 2 mm and has corroded boundaries. The clinopyroxene crystals form rims around a mineral with clay-like (dirty brown) edges and red-brown centres (remnant olivine or orthopyroxene). The textures of clinopyroxene were not observed in any other mantle harzburgite in this study and suggest these samples are lherzolite. Spinel (bright red) is a minor phase, has an irregular shape, and is less than 0.5 mm long. The corona-like rims of clinopyroxene around relict olivine/orthopyroxene (?) are not indicative of tectonized peridotites and suggest these samples did not originate from the mantle.

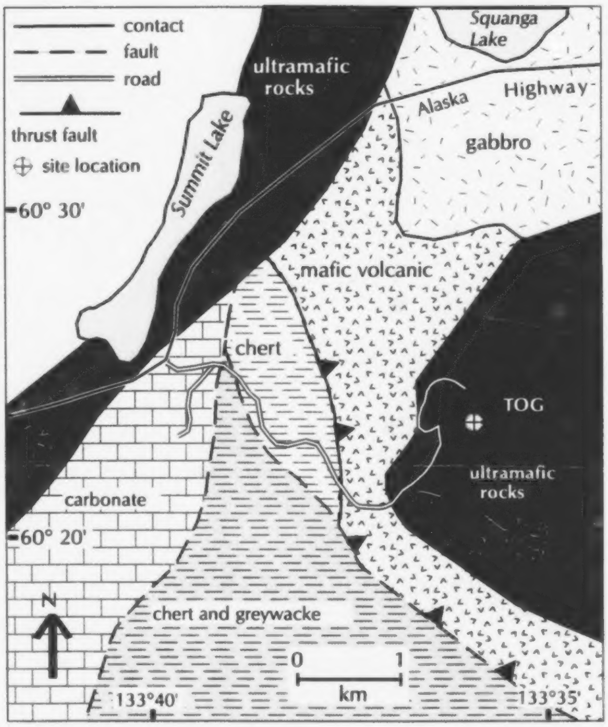
contact
fault
road
thrust fault
site location
60° 30'
60° 20'
Squanga Lake
ultramafic rocks
Summit Lake
Alaska Highway
gabbro
mafic volcanic
chert
TOG
ultramafic rocks
carbonate
chert and greywacke
N
0
1
km
133°40'
133°35'

*Figure 5. Simplified geological map of Tonnes of Gold area with site location (modified from Hart, 1996).*

### *Tonnes of Gold*

The Tonnes of Gold (TOG) site is located 20 km east of Jakes Corner and is one of many ultramafic outcrops within a 10 km radius of Squanga Lake (Gordey and Stevens, 1994; Hart, 1996; Fig. 5). The TOG ultramafic occurrence is in contact with mafic volcanic rocks to the west and gabbro to the north. The site has been the focus of gold-vein exploration and is located within the northern CCT (Hart, 1996).

The ultramafic rock collected at the TOG site consists of carbonate (30-40%) and serpentine (40-50%) with secondary magnetite (10%) and chlorite veins. The carbonate is likely an alteration of clinopyroxene, is typically ≤ 4 mm, and forms euhedral rhombs. Magnetite forms small (< 0.1 mm) euhedral cubes (locally rounded) distributed throughout the carbonate and serpentine veins, and is related to the breakdown of an unknown predecessor (olivine or orthopyroxene?). Serpentine is found between carbonate crystals, and has completely replaced any interstitial mineral that was present. The mineralogy and textures are not consistent with mantle rocks and may indicate the TOG ultramafic has an intrusive origin.

## ALASKA

### *Livengood*

The Livengood ultramafic body is located approximately 100 km north of Fairbanks along the Elliot Highway (Fig. 6) and has been assigned to the Livengood Terrane of east-central Alaska (Loney and Himmelberg, 1988;

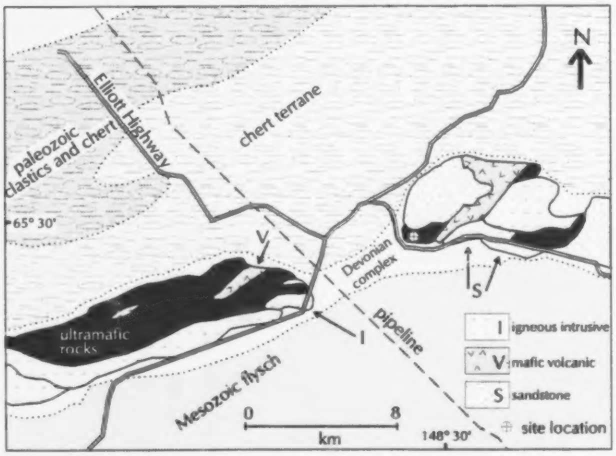
N
paleozoic clastics and chert
Elliott Highway
chert terrane
65° 30'
V
Devonian complex
S
ultramafic rocks
I
pipeline
Mesozoic flysch
0
8
km
148° 30'
I igneous intrusive
V mafic volcanic
S sandstone
site location

*Figure 6. Simplified geological map of Livengood area with site location (modified from Albanese et al., 1986).*

Patton et al., 1994). Two elongate ultramafic occurrences that strike east-northeast have been mapped as members of a Devonian ultramafic-mafic-clastic complex (Weber et al., 1992; Albanese et al., 1986; Fig. 6). The ultramafic bodies form areas of higher topography or ridges (Amy Dome and Cascaden Ridge) and are bound to the north by a thrust fault and to the south by Mesozoic flysch. The ultramafic rocks have been intruded by gabbro and diorite dykes with K-Ar hornblende dates of 633 Ma to 518 Ma (Patton et al., 1994).

Samples collected from Cascaden Ridge are brittle, fractured, greasy, black to dark green serpentinites. The rocks are nearly 100% serpentine with minor amounts of relict orthopyroxene, olivine and spinel. The rocks of the Livengood area are interpreted as serpentinized harzburgite (Loney and Himmelberg, 1988), however the amount of alteration of the samples makes classification difficult.

### *American Creek*

The American Creek peridotite is located 4 km south of Eagle along the Taylor Highway (Fig. 7). The peridotite is one member of a group of tectonically emplaced ultramafic complexes known as the Salcha-Seventymile Terrane (70MT) that extends west-southwest for 350 km from the Yukon-Alaska border to Fairbanks and is considered to be correlative to the SMT in Canada (Foster and Keith, 1994; Mortensen, 1992). The American Creek peridotite is fault bounded by quartz-mica schist and greenstone, and is mapped as an orogenic (tectonite) peridotite (harzburgite and dunite) with olivine ($Fo_{95-85}$), enstatite, minor clinopyroxene and accessory chromite (Foster, 1976).

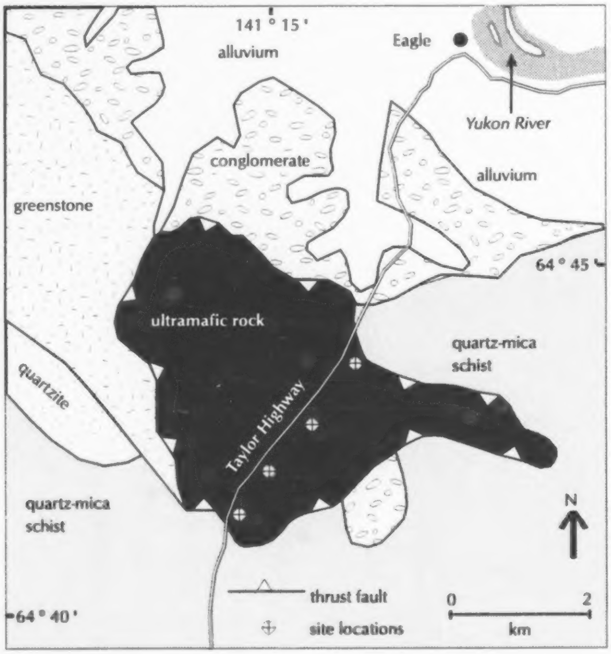

***Figure 7.*** *Simplified geological map of American Creek area with site locations (modified from Foster, 1976).*

The American Creek peridotite is bluish-grey to black with abundant beige carbonate and light green asbestos; it has a greasy feel and is fractured in outcrop. The fresh surface shows serpentinized olivine, relict grey orthopyroxene crystals and thin (1 mm) black magnetite veins. The samples collected from the centre of the peridotite body tend to be less altered (i.e., less serpentinization and carbonatization).

Olivine (50%) is coarse and less than 6 mm in diameter. Orthopyroxene (up to 15%) is typically smaller (≤ 3 mm), more altered, and contains exsolution lamellae of clinopyroxene. Some orthopyroxene grains have feathery grain boundaries that grade into amphibole. Amphibole (< 2%) forms tabular radiating laths approximately 0.5 mm long. Clinopyroxene (0-5%) is typically less altered. Spinel is intergrown with orthopyroxene to form a symplectic texture. The American Creek peridotite displays classic textures and mineralogy of a mantle tectonite (Harte, 1977; Ross, 1977; Tardy et al., 2001).

## BRITISH COLUMBIA

### *Pinchi Lake*

Harzburgite with dunite and pyroxenite veins at the Pinchi Lake locality is located in central British Columbia (Fig. 8) and forms part of the Cache Creek Terrane. These rocks are fault-bounded to the west by Upper Paleozoic to Jurassic Stikine Terrane and to the east by the Triassic Takla Group and Early Jurassic Quesnel Terrane (Tardy et al., 2001; Ross, 1977).

Samples were collected from a quarry located 8 km north of Fort St. James. A series of linear, northwest-striking outcrops, a few hundred metres apart, are exposed along a seasonal logging road. The rock is characteristic dun brown to dark bluish-grey (serpentine alteration) with (~5 mm) bronze coloured orthopyroxene porphyroclasts, thin magnetite veins and slickensides.

Petrographically, the rock consists of olivine (80%), orthopyroxene (10%) and spinel (2%). Olivine forms equant, anhedral to subhedral neoblasts and in some

Pennsylvanian-Permian intrusion into carbonate rocks of Yukon-Tanana Terrane and may be correlative with similar age Campbell Range basalts (Murphy, 2000).

Samples from Frances Lake area are composed of olivine (80-95%), orthopyroxene (10-15%), secondary magnetite (5%) and a minor amount of clinopyroxene (≤ 2%). Orthopyroxene is curviplanar, displays exsolution lamellae of clinopyroxene and is ≤ 4 mm long, subhedral and porphyroclastic. Clinopyroxene is equant, subhedral, typically ≤ 2 mm and has corroded boundaries. The clinopyroxene crystals form rims around a mineral with clay-like (dirty brown) edges and red-brown centres (remnant olivine or orthopyroxene). The textures of clinopyroxene were not observed in any other mantle harzburgite in this study and suggest these samples are lherzolite. Spinel (bright red) is a minor phase, has an irregular shape, and is less than 0.5 mm long. The corona-like rims of clinopyroxene around relict olivine/orthopyroxene (?) are not indicative of tectonized peridotites and suggest these samples did not originate from the mantle.

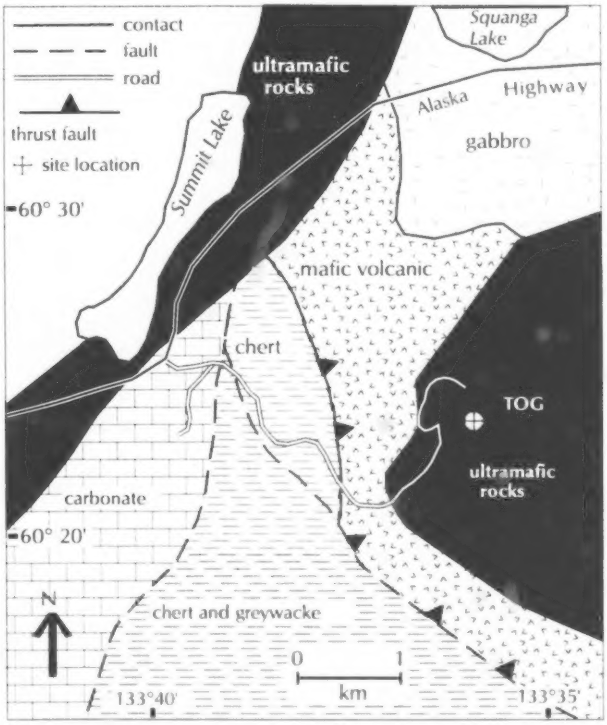
contact
fault
road
thrust fault
site location
60° 30'
60° 20'
133°40'
133°35'
Squanga Lake
ultramafic rocks
Summit Lake
Alaska Highway
gabbro
mafic volcanic
chert
TOG
ultramafic rocks
carbonate
chert and greywacke
N
0
1
km

*Figure 5. Simplified geological map of Tonnes of Gold area with site location (modified from Hart, 1996).*

## *Tonnes of Gold*

The Tonnes of Gold (TOG) site is located 20 km east of Jakes Corner and is one of many ultramafic outcrops within a 10 km radius of Squanga Lake (Gordey and Stevens, 1994; Hart, 1996; Fig. 5). The TOG ultramafic occurrence is in contact with mafic volcanic rocks to the west and gabbro to the north. The site has been the focus of gold-vein exploration and is located within the northern CCT (Hart, 1996).

The ultramafic rock collected at the TOG site consists of carbonate (30-40%) and serpentine (40-50%) with secondary magnetite (10%) and chlorite veins. The carbonate is likely an alteration of clinopyroxene, is typically ≤ 4 mm, and forms euhedral rhombs. Magnetite forms small (< 0.1 mm) euhedral cubes (locally rounded) distributed throughout the carbonate and serpentine veins, and is related to the breakdown of an unknown predecessor (olivine or orthopyroxene?). Serpentine is found between carbonate crystals, and has completely replaced any interstitial mineral that was present. The mineralogy and textures are not consistent with mantle rocks and may indicate the TOG ultramafic has an intrusive origin.

## ALASKA

## *Livengood*

The Livengood ultramafic body is located approximately 100 km north of Fairbanks along the Elliot Highway (Fig. 6) and has been assigned to the Livengood Terrane of east-central Alaska (Loney and Himmelberg, 1988;

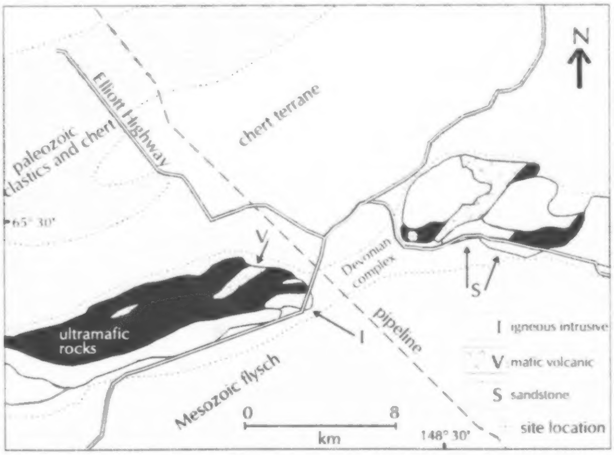
N
Elliott Highway
chert terrane
paleozoic clastics and chert
65° 30'
V
Devonian complex
S
ultramafic rocks
I
pipeline
Mesozoic flysch
I igneous intrusive
V mafic volcanic
S sandstone
site location
0
8
km
148° 30'

*Figure 6. Simplified geological map of Livengood area with site location (modified from Albanese et al., 1986).*

Patton et al., 1994). Two elongate ultramafic occurrences that strike east-northeast have been mapped as members of a Devonian ultramafic-mafic-clastic complex (Weber et al., 1992; Albanese et al., 1986; Fig. 6). The ultramafic bodies form areas of higher topography or ridges (Amy Dome and Cascaden Ridge) and are bound to the north by a thrust fault and to the south by Mesozoic flysch. The ultramafic rocks have been intruded by gabbro and diorite dykes with K-Ar hornblende dates of 633 Ma to 518 Ma (Patton et al., 1994).

Samples collected from Cascaden Ridge are brittle, fractured, greasy, black to dark green serpentinites. The rocks are nearly 100% serpentine with minor amounts of relict orthopyroxene, olivine and spinel. The rocks of the Livengood area are interpreted as serpentinized harzburgite (Loney and Himmelberg, 1988), however the amount of alteration of the samples makes classification difficult.

### American Creek

The American Creek peridotite is located 4 km south of Eagle along the Taylor Highway (Fig. 7). The peridotite is one member of a group of tectonically emplaced ultramafic complexes known as the Salcha-Seventymile Terrane (70MT) that extends west-southwest for 350 km from the Yukon-Alaska border to Fairbanks and is considered to be correlative to the SMT in Canada (Foster and Keith, 1994; Mortensen, 1992). The American Creek peridotite is fault bounded by quartz-mica schist and greenstone, and is mapped as an orogenic (tectonite) peridotite (harzburgite and dunite) with olivine ($Fo_{95-85}$), enstatite, minor clinopyroxene and accessory chromite (Foster, 1976).

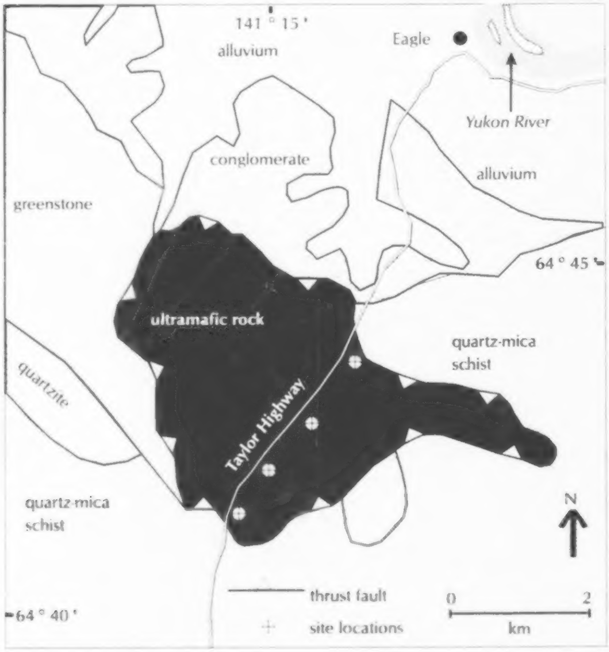

***Figure 7.*** *Simplified geological map of American Creek area with site locations (modified from Foster, 1976).*

The American Creek peridotite is bluish-grey to black with abundant beige carbonate and light green asbestos; it has a greasy feel and is fractured in outcrop. The fresh surface shows serpentinized olivine, relict grey orthopyroxene crystals and thin (1 mm) black magnetite veins. The samples collected from the centre of the peridotite body tend to be less altered (i.e., less serpentinization and carbonatization).

Olivine (50%) is coarse and less than 6 mm in diameter. Orthopyroxene (up to 15%) is typically smaller (≤ 3 mm), more altered, and contains exsolution lamellae of clinopyroxene. Some orthopyroxene grains have feathery grain boundaries that grade into amphibole. Amphibole (< 2%) forms tabular radiating laths approximately 0.5 mm long. Clinopyroxene (0-5%) is typically less altered. Spinel is intergrown with orthopyroxene to form a symplectic texture. The American Creek peridotite displays classic textures and mineralogy of a mantle tectonite (Harte, 1977; Ross, 1977; Tardy et al., 2001).

## BRITISH COLUMBIA

### Pinchi Lake

Harzburgite with dunite and pyroxenite veins at the Pinchi Lake locality is located in central British Columbia (Fig. 8) and forms part of the Cache Creek Terrane. These rocks are fault-bounded to the west by Upper Paleozoic to Jurassic Stikine Terrane and to the east by the Triassic Takla Group and Early Jurassic Quesnel Terrane (Tardy et al., 2001; Ross, 1977).

Samples were collected from a quarry located 8 km north of Fort St. James. A series of linear, northwest-striking outcrops, a few hundred metres apart, are exposed along a seasonal logging road. The rock is characteristic dun brown to dark bluish-grey (serpentine alteration) with (~5 mm) bronze coloured orthopyroxene porphyroclasts, thin magnetite veins and slickensides.

Petrographically, the rock consists of olivine (80%), orthopyroxene (10%) and spinel (2%). Olivine forms equant, anhedral to subhedral neoblasts and in some

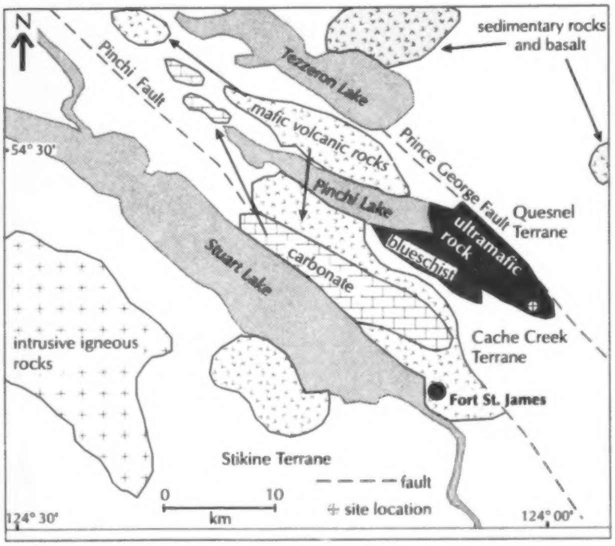
N
sedimentary rocks and basalt
Pinchi Fault
Tezzeron Lake
mafic volcanic rocks
Prince George Fault
54° 30'
Pinchi Lake
ultramafic rock
Quesnel Terrane
blueschist
Stuart Lake
carbonate
intrusive igneous rocks
Cache Creek Terrane
Fort St. James
Stikine Terrane
fault
site location
0
10
km
124° 30'
124° 00'

**Figure 8.** *Simplified geological map of Pinchi Lake area with site location (modified from Tardy et al., 2001).*

instances is fluidal. Other olivine grains are 1 cm in size. Curviplanar orthopyroxene porphyroclasts (≤ 3.5 mm) show exsolution lamellae of clinopyroxene. Spinel is a bright red colour and forms ≤ 0.5 mm euhedral cubes. The ultramafic rocks of the Pinchi Lake area are tectonized mantle harzburgite.

### *Atlin*

The ultramafic rocks near Atlin are located within the Cache Creek Terrane and have been the focus of other studies (e.g., Ash and Arksey, 1990; Ash, 1994; Mihalynuk et al., 1999; Fig. 9). Harzburgite and associated dunite and pyroxenite have been interpreted to represent the base of an ophiolite sequence that includes the Nahlin ultramafic suite (Aitken, 1959; Souther, 1971; Terry, 1977; Ash and Arksey, 1990) and may be correlative with samples collected from Pinchi Lake.

Harzburgite contains lenses of dunite (Fig. 10) and 2- to 6-cm-wide pyroxenite dykes. The weathered surface of the harzburgite is rough, red-brown, with protruding porphyroclasts of pink-red orthopyroxene (1-5 mm in diameter) and 1- to 2-mm-thick black veins of magnetite. The fresh surface is bluish-grey, showing conspicuous grey orthopyroxene porphyroclasts. Serpentinization of these rocks ranges from 50 to 60%. Dunite pods are a few centimetres to tens of metres in length and have characteristic smooth dun-brown weathered surface.

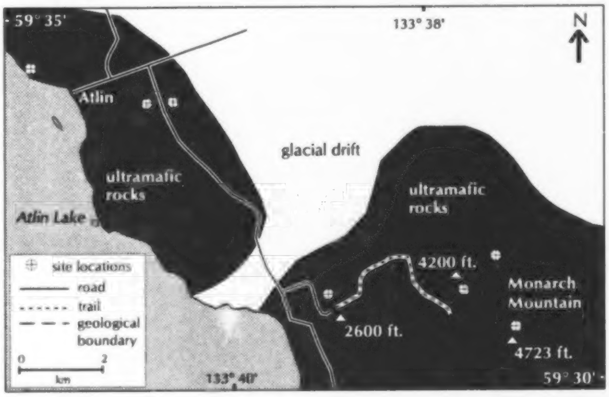
59° 35'
133° 38'
N
Atlin
glacial drift
ultramafic rocks
ultramafic rocks
Atlin Lake
site locations
road
trail
geological boundary
0
2
km
4200 ft.
Monarch Mountain
2600 ft.
4723 ft.
133° 40'
59° 30'

**Figure 9.** *Simplified geological map of Atlin area with site locations (modified from Aitken, 1959).*

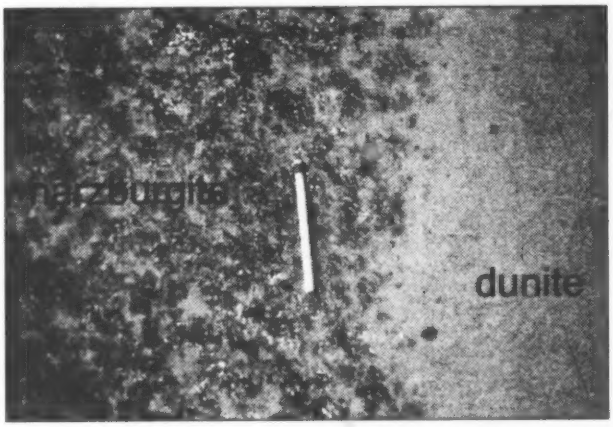
harzburgite
dunite

**Figure 10.** *Coarse harzburgite with dunite lense from Atlin. Match is six centimetres.*

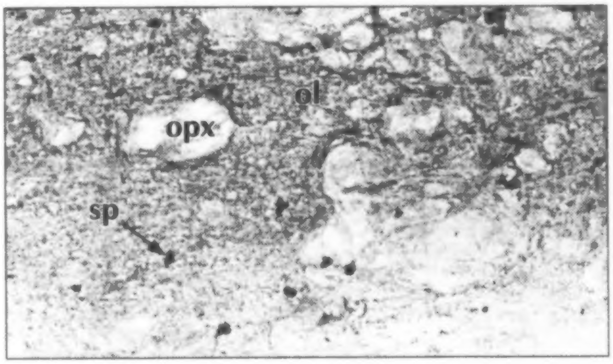

**Figure 11.** *Plane-polarized light image of coarse harzburgite with olivine (ol), orthopyroxene (opx) and spinel (sp). Thin section is about 3.6 cm long by 2.1 cm wide.*

The harzburgite contains (60-75%) coarse, equant olivine that is subhedral and less than 1 mm in diameter. Olivine is altered to both serpentine and carbonate. Orthopyroxene typically represents 20% of the bulk mineralogy and encloses small clinopyroxene crystals. Many orthopyroxene crystals are tabular to irregular shapes, are ≤ 5 mm in length, and show exsolution lamellae of clinopyroxene. Bright red spinel (≤ 2 mm) is irregular to euhedral and represents 2% of the modal mineralogy. Textures from the dunite are similar to harzburgite, except that olivine crystals are larger (≤ 5 mm; Fig. 11).

### *Nahlin*

The Nahlin ultramafic suite is located along the western boundary of the Cache Creek Terrane south of Atlin (Fig. 12). It is the largest (260 km$^2$) ultramafic body in the Northern Cordillera and is fault-bounded in the west against Triassic-Jurassic Laberge Group and in the east by Upper Paleozoic sedimentary rocks of the Cache Creek Group (Aitken, 1959; Souther, 1971; Terry, 1977).

Souther (1971) and Terry (1977) described ultramafic rocks from the Nahlin suite to be very similar to ultramafic rocks found in the town of Atlin. However, rocks collected for this study from the Nahlin ultramafic body differ from those collected in the Atlin area. They are brittle, black to dark green, greasy, almost entirely serpentinized and are not associated with dunite or pyroxenite dykes.

The rocks are 80% to 100% serpentinized. Relict olivine, when present, forms groups of small (≤ 1 mm), equant, anhedral to subhedral neoblasts, which define a mosaic porphyroclastic texture. Coarse orthopyroxene (≤ 4 mm) shows exsolution lamellae and encloses small (< 0.5 mm) grains of clinopyroxene. Spinel is bright red with irregular boundaries (< 1 mm). Since most of the samples consist of serpentinite, it is difficult to assign a rock name other than serpentinite. Based on the presence of remnant spinel and neoblastic olivine, it appears that these samples were mantle harzburgites and possibly represent tectonized equivalents found elsewhere in the Nahlin suite or in Atlin Group (Aitken, 1959; Souther, 1971; Terry, 1977).

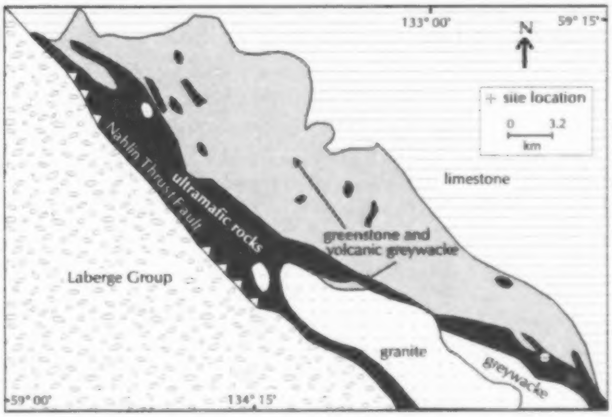

**Figure 12.** *Simplified geological map of Nahlin ultramafic suite with site location (modified from Aitken, 1959).*

## SUMMARY

Future geochemical research will provide better constraints on the origin of ultramafic rocks from the Cache Creek (CCT), Slide Mountain (SMT) and Livengood terranes and the Kluane metamorphic assemblage. The results will lead to firmer conclusions regarding the geological history of each terrane. The ultramafic rock types from the CCT are homogeneous while those from SMT are heterogeneous .

## ACKNOWLEDGEMENTS

The authors would like to thank Don Murphy of the Yukon Geology Program for his guidance at the Frances Lake site and Mitch Mihalynuk of the British Columbia Geological Survey Branch for accommodations and helicopter support while in Atlin. The first author would also like to thank Bert Goodvin of Johnson's Crossing, Yukon for his generous hospitality and assistance.

## REFERENCES

Aitken, J.D., 1959. Atlin map-area, British Columbia. Geological Survey of Canada, Memoir 307, 89 p.

Albanese, M.D., Smith, T.E., Robinson, M.S. and Bundtzen, T.K., 1986. Summary of DGGS investigations at Livengood, Alaska: Geology, mineral potential, and regional correlations with east-central Yukon. *In:* Yukon Geology Volume 1, Exploration and Geological Services Division, Yukon Region, Indian and Northern Affairs Canada, p. 171-175.

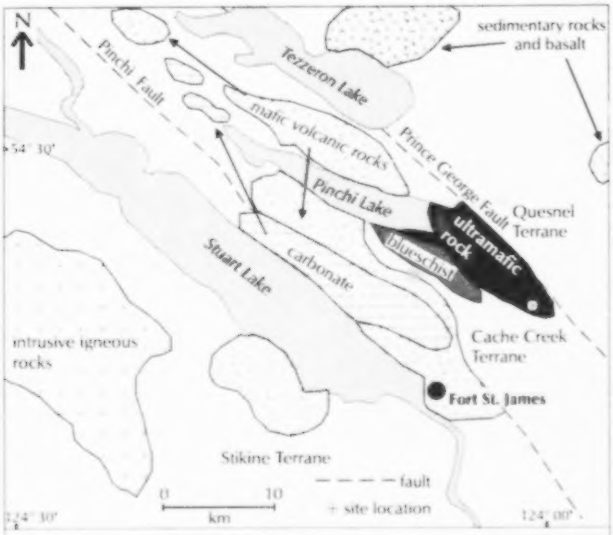
N
sedimentary rocks and basalt
Tezzeron Lake
Pinchi Fault
mafic volcanic rocks
Prince George Fault
54° 30'
Pinchi Lake
Quesnel Terrane
ultramafic rock
blueschist
Stuart Lake
carbonate
Cache Creek Terrane
intrusive igneous rocks
Fort St. James
Stikine Terrane
fault
site location
0
10
km
124° 30'
124° 00'

**Figure 8.** *Simplified geological map of Pinchi Lake area with site location (modified from Tardy et al., 2001).*

instances is fluidal. Other olivine grains are 1 cm in size. Curviplanar orthopyroxene porphyroclasts (≤ 3.5 mm) show exsolution lamellae of clinopyroxene. Spinel is a bright red colour and forms ≤ 0.5 mm euhedral cubes. The ultramafic rocks of the Pinchi Lake area are tectonized mantle harzburgite.

### *Atlin*

The ultramafic rocks near Atlin are located within the Cache Creek Terrane and have been the focus of other studies (e.g., Ash and Arksey, 1990; Ash, 1994; Mihalynuk et al., 1999; Fig. 9). Harzburgite and associated dunite and pyroxenite have been interpreted to represent the base of an ophiolite sequence that includes the Nahlin ultramafic suite (Aitken, 1959; Souther, 1971; Terry, 1977; Ash and Arksey, 1990) and may be correlative with samples collected from Pinchi Lake.

Harzburgite contains lenses of dunite (Fig. 10) and 2- to 6-cm-wide pyroxenite dykes. The weathered surface of the harzburgite is rough, red-brown, with protruding porphyroclasts of pink-red orthopyroxene (1-5 mm in diameter) and 1- to 2-mm-thick black veins of magnetite. The fresh surface is bluish-grey, showing conspicuous grey orthopyroxene porphyroclasts. Serpentinization of these rocks ranges from 50 to 60%. Dunite pods are a few centimetres to tens of metres in length and have characteristic smooth dun-brown weathered surface.

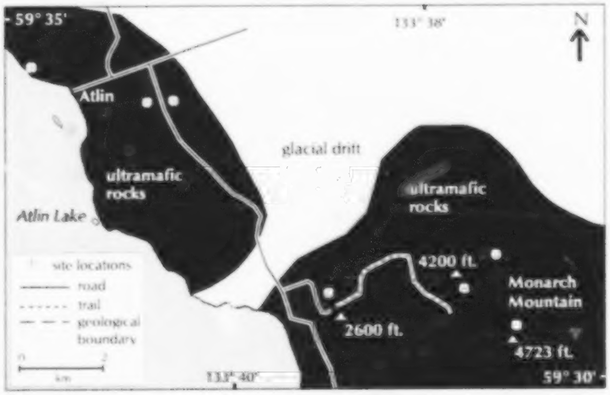
59° 35'
133° 38'
N
Atlin
glacial drift
ultramafic rocks
Atlin Lake
ultramafic rocks
site locations
road
trail
geological boundary
0
2
km
4200 ft.
Monarch Mountain
2600 ft.
4723 ft.
133° 40'
59° 30'

**Figure 9.** *Simplified geological map of Atlin area with site locations (modified from Aitken, 1959).*

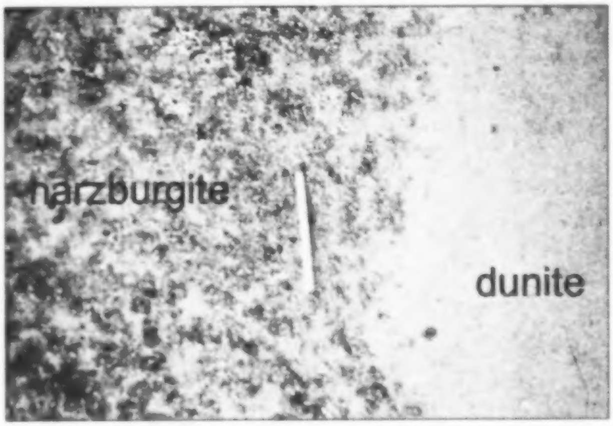
harzburgite
dunite

**Figure 10.** *Coarse harzburgite with dunite lense from Atlin. Match is six centimetres.*

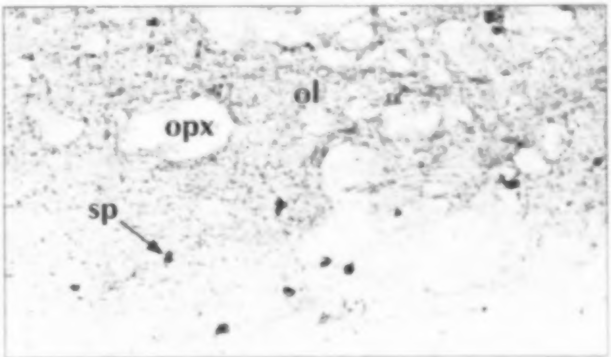

**Figure 11.** *Plane-polarized light image of coarse harzburgite with olivine (ol), orthopyroxene (opx) and spinel (sp). Thin section is about 3.6 cm long by 2.1 cm wide.*

The harzburgite contains (60-75%) coarse, equant olivine that is subhedral and less than 1 mm in diameter. Olivine is altered to both serpentine and carbonate. Orthopyroxene typically represents 20% of the bulk mineralogy and encloses small clinopyroxene crystals. Many orthopyroxene crystals are tabular to irregular shapes, are ≤ 5 mm in length, and show exsolution lamellae of clinopyroxene. Bright red spinel (≤ 2 mm) is irregular to euhedral and represents 2% of the modal mineralogy. Textures from the dunite are similar to harzburgite, except that olivine crystals are larger (≤ 5 mm; Fig. 11).

### *Nahlin*

The Nahlin ultramafic suite is located along the western boundary of the Cache Creek Terrane south of Atlin (Fig. 12). It is the largest (260 km$^2$) ultramafic body in the Northern Cordillera and is fault-bounded in the west against Triassic-Jurassic Laberge Group and in the east by Upper Paleozoic sedimentary rocks of the Cache Creek Group (Aitken, 1959; Souther, 1971; Terry, 1977).

Souther (1971) and Terry (1977) described ultramafic rocks from the Nahlin suite to be very similar to ultramafic rocks found in the town of Atlin. However, rocks collected for this study from the Nahlin ultramafic body differ from those collected in the Atlin area. They are brittle, black to dark green, greasy, almost entirely serpentinized and are not associated with dunite or pyroxenite dykes.

The rocks are 80% to 100% serpentinized. Relict olivine, when present, forms groups of small (≤ 1 mm), equant, anhedral to subhedral neoblasts, which define a mosaic porphyroclastic texture. Coarse orthopyroxene (≤ 4 mm) shows exsolution lamellae and encloses small (< 0.5 mm) grains of clinopyroxene. Spinel is bright red with irregular boundaries (< 1 mm). Since most of the samples consist of serpentine, it is difficult to assign a rock name other than serpentinite. Based on the presence of remnant spinel and neoblastic olivine, it appears that these samples were mantle harzburgites and possibly represent tectonized equivalents found elsewhere in the Nahlin suite or in Atlin Group (Aitken, 1959; Souther, 1971; Terry, 1977).

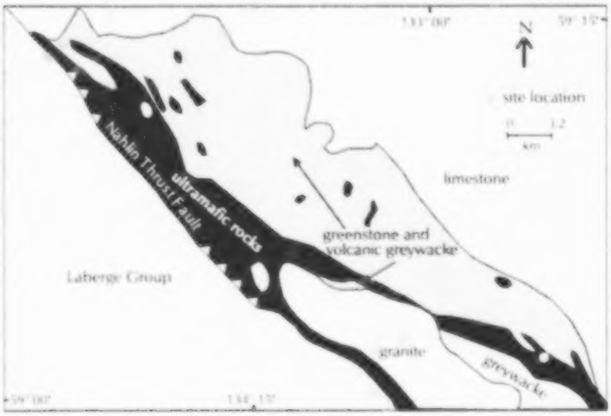

***Figure 12.*** *Simplified geological map of Nahlin ultramafic suite with site location (modified from Aitken, 1959).*

## SUMMARY

Future geochemical research will provide better constraints on the origin of ultramafic rocks from the Cache Creek (CCT), Slide Mountain (SMT) and Livengood terranes and the Kluane metamorphic assemblage. The results will lead to firmer conclusions regarding the geological history of each terrane. The ultramafic rock types from the CCT are homogeneous while those from SMT are heterogeneous .

## ACKNOWLEDGEMENTS

The authors would like to thank Don Murphy of the Yukon Geology Program for his guidance at the Frances Lake site and Mitch Mihalynuk of the British Columbia Geological Survey Branch for accommodations and helicopter support while in Atlin. The first author would also like to thank Bert Goodvin of Johnson's Crossing, Yukon for his generous hospitality and assistance.

## REFERENCES

Aitken, J.D., 1959. Atlin map-area, British Columbia. Geological Survey of Canada, Memoir 307, 89 p.

Albanese, M.D., Smith, T.E., Robinson, M.S. and Bundtzen, T.K., 1986. Summary of DGGS investigations at Livengood, Alaska: Geology, mineral potential, and regional correlations with east-central Yukon. *In:* Yukon Geology Volume 1, Exploration and Geological Services Division, Yukon Region, Indian and Northern Affairs Canada, p. 171-175.

Ash, C.H., 1994. Origin and tectonic setting of the ophiolitic ultramafic and related rocks in the Atlin area, British Columbia (NTS 104N). British Columbia Ministry of Energy, Mines and Petroleum Resources, Bulletin 94, 48 p.

Ash, C.H. and Arksey, R.L., 1990. The Atlin ultramafic allochthon: Ophiolite basement within the Cache Creek Terrane; tectonic and metallogenic significance (104N/12). *In:* British Columbia Ministry of Energy, Mines and Petroleum Resources, Geological Fieldwork 1989, Paper 1990-1, p. 365-374.

Foster, H.L., 1976. Geological map of the Eagle quadrangle, Alaska. United States Geological Survey, Miscellaneous Investigation Series Map I-922, 1:250 000 scale.

Foster, H.L. and Keith, T.E.C., 1994. Geology of the Yukon-Tanana area of east-central Alaska. *In:* The Geology of Alaska, G. Plafker and H.C. Berg (eds.), The Geology of North America Volume G-1, p. 205-240.

Gordey, S.P. and Stevens, R.A., 1994. Preliminary interpretation of bedrock geology of the Teslin area (105C), southern Yukon. Geological Survey of Canada, Open File 2886, 1:250 000 scale.

Hart, C.J.R., 1996. Geology and mineralization of the TOG listwanite-hosted gold occurrence in southern Yukon Territory. *In:* Yukon Exploration and Geology, 1995, Exploration and Geological Services Division, Yukon Region, Indian and Northern Affairs Canada, p. 49-56.

Harte, B., 1977. Rock nomenclature with particular relation to deformation and recrystallization textures in olivine-bearing xenoliths. Journal of Geology, vol. 85, p. 279-288.

Keith, T.E.C., Foster, H.L., Foster, R.L., Post, E.V. and Lehmbeck, W.L., 1981. Geology of an alpine-peridotite in the Mount Sorenson area, east-central Alaska. United States Geological Survey Professional Paper 1170-A, p. A1-A9.

Leaming, S., 1982. Ultramafic and related rocks in the Cassiar district, British Columbia. *In:* Current Research, Geological Survey of Canada, Paper 82-1A, p. 417-418.

Loney, R.A. and Himmelberg, G.R., 1988. Ultramafic rocks of the Livengood Terrane. *In:* Geologic Studies in Alaska by the U.S. Geological Survey during 1987, J.P. Galloway and T.D. Hamilton (eds.), United States Geological Survey Circular 945, p. 46-48.

Mezger, J.E., 2000. 'Alpine-type' ultramafic rocks of the Kluane metamorphic assemblage, southwest Yukon: Oceanic crust fragments of a late Mesozoic back-arc basin along the northern Coast Belt. *In:* Yukon Exploration and Geology 1999, D.S. Emond and L.H. Weston (eds.), Exploration and Geological Services Division, Yukon Region, Indian and Northern Affairs Canada, p. 127-138.

Mihalynuk, M.G., Nelson, J. and Diakow, L., 1994. Cache Creek entrapment: Oroclinal paradox within the Canadian Cordillera. Tectonics, vol. 13, p. 575-595.

Mihalynuk, M.G., Mountjoy, K.J., Smith, M.T., Currie, L.D., Gabites, J.E., Tipper, H.W., Orchard, M.J., Poulton, T.P. and Cordey, F., 1999. Geology and mineral resources of the Tagish Lake area (NTS 104M/8,9,10E,15 and 104N/12W), northwestern British Columbia. British Columbia Ministry of Energy, Mines and Petroleum Resources, Bulletin 105, 217 p.

Mortensen, J.K., 1992. Pre-Mesozoic tectonic evolution of the Yukon-Tanana Terrane, Yukon and Alaska. Tectonics, vol. 11, p. 836-853.

Mortensen, J.K., 1996. Northern Stewart River map area Klondike and Sixtymile Districts (115N/15,16; 115O/13,14 and parts of 115O/15,16). Exploration and Geological Services Division, Yukon Region, Indian and Northern Affairs Canada, Open File 1996-1(G), 1:50 000 scale.

Murphy, D.C., 2000. Preliminary geological map of part of the Klatsa River area (105H/3), southeastern Yukon (1:50 000 scale). Exploration and Geological Services Division, Yukon Region, Indian and Northern Affairs Canada, Open File 2000-15.

Murphy, D.C., 2001. Yukon-Tanana Terrane in southwestern Frances Lake area (105H/3,4 and 5), southeastern Yukon. *In:* Yukon Exploration and Geology 2000, D.S. Emond and L.H. Weston (eds.), Exploration and Geological Services Division, Yukon Region, Indian and Northern Affairs Canada, p. 217-233.

Patton Jr., W.W., Box, S.E. and Grybeck, D.J., 1994. Ophiolites and other mafic-ultramafic complexes in Alaska. *In:* The Geology of Alaska, G. Plafker and H.C. Berg (eds.), The Geology of North America, vol. G-1, p. 671-686.

Ross, J.V., 1977. The internal fabric of an alpine peridotite near Pinchi Lake, central British Columbia. Canadian Journal of Earth Science, vol. 14, p. 32-44.

Souther, J.G., 1971. Geology and mineral deposits of Tulsequah map-area, British Columbia. Geological Survey of Canada, Memoir 362, 84 p.

Tardy, M., Lapierre, H., Struik, L.C., Bosch, D. and Brunet, P., 2001. The influence of mantle plume in the genesis of the Cache Creek oceanic igneous rocks: Implications for the geodynamic evolution of the inner accreted terranes of the Canadian Cordillera. Canadian Journal of Earth Science, vol. 38, p. 515-534.

Tempelman-Kluit, D.J., 1979. Transported cataclasite, ophiolite and granodiorite in Yukon. Geological Survey of Canada, Paper 79-14, 27 p.

Terry, J., 1977. Geology of the Nahlin ultramafic body, Atlin and Tulsequah map-areas, northwestern British Columbia. *In:* Current Research, Geological Survey of Canada, Paper 77-1A, p. 263-266.

Weber, F.R., Wheeler, K.L., Rinehart, C.D., Chapman, R.M. and Blodgett, R.B., 1992. Geologic map of the Livengood quadrangle, Alaska. United States Geological Survey, Open File Report 92-562, 19 p., 1: 250 000 scale.

Yukon MINFILE, 2001. Frances Lake and western half of Flat River - 105H and 95E. Exploration and Geological Services Division, Yukon Region, Indian and Northern Affairs Canada.

# Resedimentation of the late Holocene White River tephra, Yukon Territory and Alaska

***K.D. West*[1] *and J.A. Donaldson*[2]**
*Carleton University*[3]

West, K.D. and Donaldson, J.A. 2002. Resedimentation of the late Holocene White River tephra, Yukon Territory and Alaska. *In:* Yukon Exploration and Geology 2002, D.S. Emond, L.H. Weston and L.L. Lewis (eds.), Exploration and Geological Services Division, Yukon Region, Indian and Northern Affairs Canada, p. 239-247.

## ABSTRACT

The Wrangell region of eastern Alaska represents a zone of extensive volcanism marked by intermittent pyroclastic activity during the late Holocene. The most recent and widely dispersed pyroclastic deposit in this area is the White River tephra, a distinct tephra-fall deposit covering 540 000 km$^2$ in Alaska, Yukon, and the Northwest Territories. This deposit is the product of two Plinian eruptions from Mount Churchill, preserved in two distinct lobes, created ca. 1887 years B.P. (northern lobe) and 1147 years B.P. (eastern lobe). The tephra consists of distal primary air-fall deposits and proximal, locally resedimented volcaniclastic deposits.

Distinctive layers such as the White River tephra provide important chronostratigraphic control and can be used to interpret the cultural and environmental impact of ancient large magnitude eruptions. The resedimentation of White River tephra has resulted in large-scale terraces, which flank the margins of Klutlan Glacier. Preliminary analysis of resedimented deposits demonstrates that the volcanic stratigraphy within individual terraces is complex and unique.

## RÉSUMÉ

Au cours de l'Holocène tardif, des matériaux pyroclastiques ont été projetés lors d'importantes et nombreuses éruptions volcaniques, dans la région de Wrangell de l'est de l'Alaska. Le plus récent et vaste gisement pyroclastique de cette région est le téphra de White River; c'est un gisement de téphra unique d'une superficie de 540 000 km$^2$, qui couvre une partie de l'Alaska, du Yukon et des Territoires du Nord-Ouest. Il résulte de deux éruptions du mont Churchill et est préservé dans deux lobes distincts, qui se sont formés il y a environ 1887 (lobe septentrional) et 1147 (lobe oriental) ans avant le présent. Le téphra est constitué de dépôts pyroclastiques distaux principalement projetés et de dépôts proximaux resédimentés.

Des couches distinctives de téphra, comme le téphra de White River, fournissent d'importantes données chronostratigraphiques et peuvent servir à interpréter l'impact culturel et environnemental des anciennes éruptions de grande magnitude. La resédimentation du téphra de White River a entraîné la formation de terrasses de téphra de grandes dimensions en bordure du glacier Klutlan. D'après une analyse préliminaire des dépôts resédimentés, la stratigraphie volcanique de chacune des terrasses est complexe et unique.

---

[1] *kim.west@usask.ca*

[2] *jadonald@ccs.carleton.ca*

[3] *Ottawa-Carleton Geoscience Centre, Carleton University, Ottawa, Ontario, Canada K1S 5B6*

## GEOLOGIC SETTING

The White River tephra deposit (540 000 km$^2$) is one of the most widely dispersed tephra-fall units in the Yukon-Alaska region (Fig. 1). It is comparable in size and magnitude to some of the largest tephra-fall deposits in the circum-Pacific, including Krakatoa in 1883 and Novarupta in 1912. The bilobate deposit of rhyodacitic tephra is the product of two Plinian eruptions from Mount Churchill (McGimsey et al., 1992), a stratovolcano located approximately 25 km (15 miles) west of the Yukon-Alaska border in Wrangell-St. Elias National Park (61°25'N, 141°70'W; Fig. 2). Mount Churchill belongs to the Wrangell volcanic field (WVF), a late Cenozoic continental volcanic arc system located 400 km from the more recently active Aleutian volcanic arc system in southeastern Alaska (Richter et al., 1990).

The division of the White River deposit into elongate northern and eastern lobes indicates that strong unidirectional northward and eastward blowing winds prevailed during the times of their respective deposition. Radiocarbon dating, based on numerous peat and wood samples at sites distal and proximal to the vent, indicate that the northern-lobe tephra was deposited ca. 1887 years B.P. (Lerbekmo et al., 1975). The most recent radiocarbon estimate for the eastern-lobe tephra (ca. 1147 years B.P.) is based on a sample taken from a stump killed in growth position from the latest eruption (Clague et al., 1995). This estimate is consistent with several other radiocarbon ages taken from sediments above and below the White River tephra east of Mount Churchill (Clague et al., 1995).

The White River tephra is primarily composed of glass, plagioclase, hornblende, hypersthene and magnetite (Lerbekmo and Campbell, 1969), with minor amounts of biotite. An abundance of long tube vesicles in both eastern and northern lobe tephras (Fig. 3) indicates that the eruptions responsible for both lobes were extremely violent. Although eruption cloud heights are estimated to be between 30 and 35 km for both eruptions (Downes, 1979), temperatures are estimated to be higher for the eastern lobe eruption (995-1030°C) than for the northern lobe eruption (950-990°C; Downes, 1985). This has been taken to suggest that the eastern-lobe eruption was more violent than the northern-lobe eruption (Lerbekmo et al., 1975). If so, the latest White River eruption may have been responsible for destroying a much larger massif between Mount Churchill and Mount Bona, which may be remnants of a much older, single volcano.

Primary air-fall deposits of eastern lobe tephra have been found in peatland areas up to 1300 km from the vent (Robinson, 2001), indicating that environmental disruption from the latest White River eruption was widespread over a large portion of northern Canada. In addition, several anthropologists have indicated that the cultural impact of this eruption on the region's Athapaskan peoples was substantial (Moodie et al., 1992; Workman, 1977, 1979). Although no clear evidence of this eruption has been found in Athapaskan oral traditions, it has been suggested that the migration and linguistic diversification of the ancestral Athapaskan peoples occurred as the result of the latest White River eruption.

Recent stratigraphic and sedimentological evidence bearing on the cultural impact of this event suggests that the eastern lobe tephra was deposited during the late fall

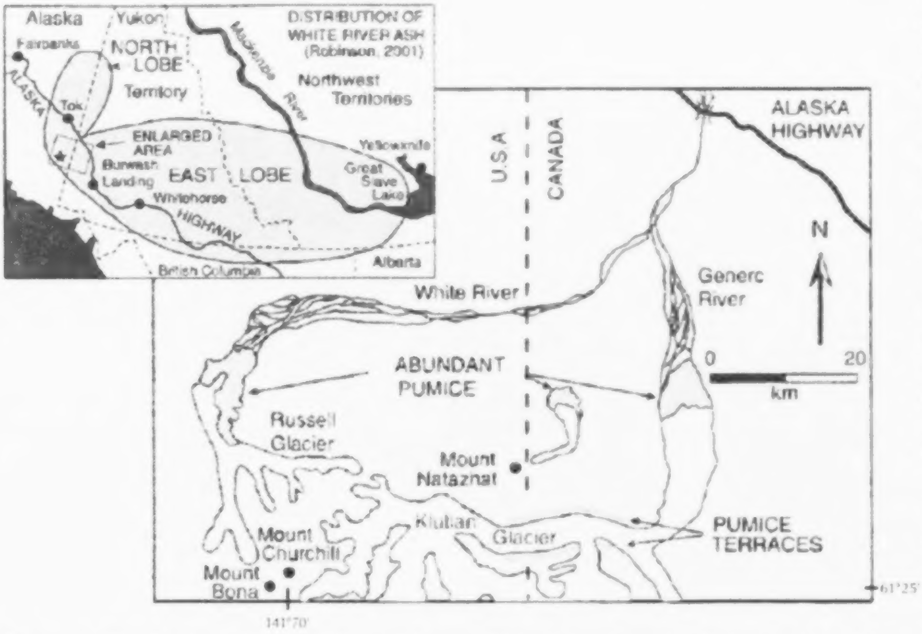
Alaska
Yukon
Fairbanks
NORTH LOBE
ALASKA
Tok
Territory
Mackenzie River
DISTRIBUTION OF WHITE RIVER ASH (Robinson, 2001)
Northwest Territories
ENLARGED AREA
Burwash Landing
EAST LOBE
Whitehorse
HIGHWAY
Yellowknife
Great Slave Lake
British Columbia
Alberta
U.S.A.
CANADA
ALASKA HIGHWAY
N
White River
Generc River
0
20
km
ABUNDANT PUMICE
Russell Glacier
Mount Natazhat
Mount Churchill
Mount Bona
Klutlan Glacier
PUMICE TERRACES
61°25'
141°70'

***Figure 1.*** *Distribution of White River tephra, and location of proximal terrace deposits.*

## GEOLOGIC SETTING

The White River tephra deposit (540 000 km$^2$) is one of the most widely dispersed tephra-fall units in the Yukon-Alaska region (Fig. 1). It is comparable in size and magnitude to some of the largest tephra-fall deposits in the circum-Pacific, including Krakatoa in 1883 and Novarupta in 1912. The bilobate deposit of rhyodacitic tephra is the product of two Plinian eruptions from Mount Churchill (McGimsey et al., 1992), a stratovolcano located approximately 25 km (15 miles) west of the Yukon-Alaska border in Wrangell-St. Elias National Park (61°25'N, 141°70'W; Fig. 2). Mount Churchill belongs to the Wrangell volcanic field (WVF), a late Cenozoic continental volcanic arc system located 400 km from the more recently active Aleutian volcanic arc system in southeastern Alaska (Richter et al., 1990).

The division of the White River deposit into elongate northern and eastern lobes indicates that strong unidirectional northward and eastward blowing winds prevailed during the times of their respective deposition. Radiocarbon dating, based on numerous peat and wood samples at sites distal and proximal to the vent, indicate that the northern-lobe tephra was deposited ca. 1887 years B.P. (Lerbekmo et al., 1975). The most recent radiocarbon estimate for the eastern-lobe tephra (ca. 1147 years B.P.) is based on a sample taken from a stump killed in growth position from the latest eruption (Clague et al., 1995). This estimate is consistent with several other radiocarbon ages taken from sediments above and below the White River tephra east of Mount Churchill (Clague et al., 1995).

The White River tephra is primarily composed of glass, plagioclase, hornblende, hypersthene and magnetite (Lerbekmo and Campbell, 1969), with minor amounts of biotite. An abundance of long tube vesicles in both eastern and northern lobe tephras (Fig. 3) indicates that the eruptions responsible for both lobes were extremely violent. Although eruption cloud heights are estimated to be between 30 and 35 km for both eruptions (Downes, 1979), temperatures are estimated to be higher for the eastern lobe eruption (995-1030°C) than for the northern lobe eruption (950-990°C; Downes, 1985). This has been taken to suggest that the eastern-lobe eruption was more violent than the northern-lobe eruption (Lerbekmo et al., 1975). If so, the latest White River eruption may have been responsible for destroying a much larger massif between Mount Churchill and Mount Bona, which may be remnants of a much older, single volcano.

Primary air-fall deposits of eastern lobe tephra have been found in peatland areas up to 1300 km from the vent (Robinson, 2001), indicating that environmental disruption from the latest White River eruption was widespread over a large portion of northern Canada. In addition, several anthropologists have indicated that the cultural impact of this eruption on the region's Athapaskan peoples was substantial (Moodie et al., 1992; Workman, 1977, 1979). Although no clear evidence of this eruption has been found in Athapaskan oral traditions, it has been suggested that the migration and linguistic diversification of the ancestral Athapaskan peoples occurred as the result of the latest White River eruption.

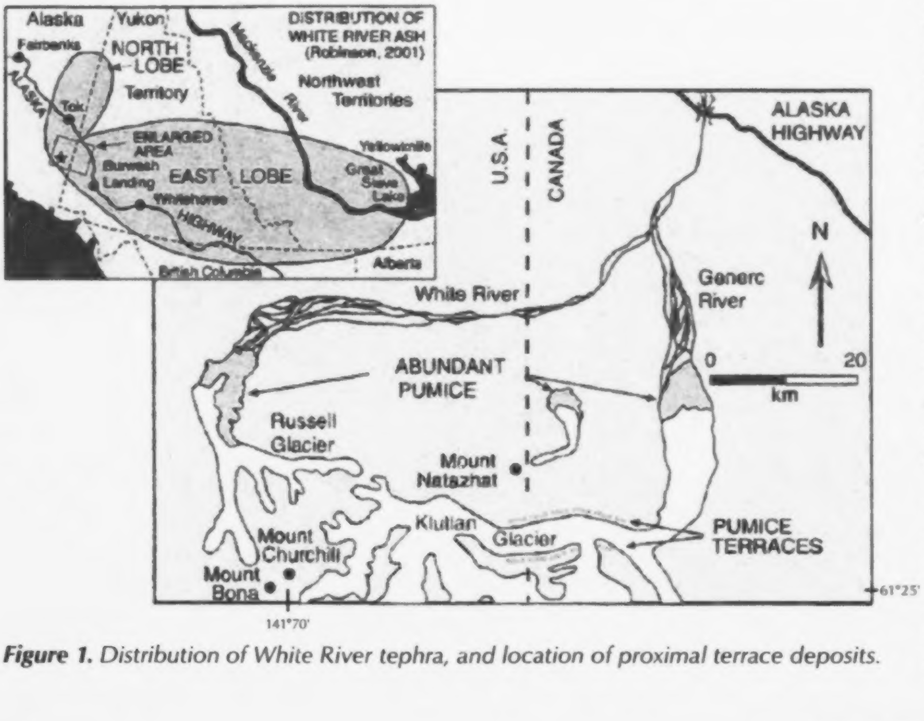
Alaska
Yukon
Fairbanks
NORTH LOBE
Territory
ALASKA
Tok
DISTRIBUTION OF WHITE RIVER ASH (Robinson, 2001)
Mackenzie
River
Northwest Territories
ENLARGED AREA
Burwash Landing
EAST LOBE
Whitehorse
HIGHWAY
Yellowknife
Great Slave Lake
British Columbia
Alberta
U.S.A.
CANADA
ALASKA HIGHWAY
White River
Generc River
N
0
20
km
ABUNDANT PUMICE
Russell Glacier
Mount Natazhat
Klutlan Glacier
PUMICE TERRACES
Mount Churchill
Mount Bona
141°70'
61°25'

***Figure 1.*** *Distribution of White River tephra, and location of proximal terrace deposits.*

Recent stratigraphic and sedimentological evidence bearing on the cultural impact of this event suggests that the eastern lobe tephra was deposited during the late fall

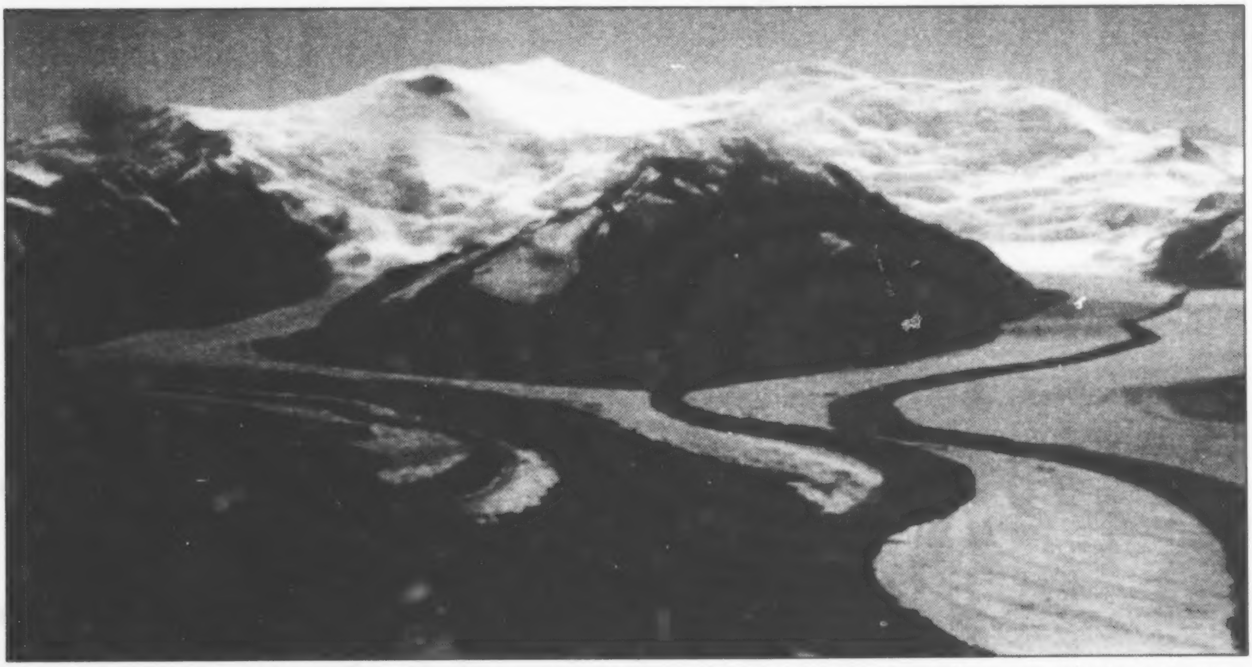

**Figure 2.** *Source of the White River tephra, the Bona-Churchill complex. This is a view from the west, with Mount Bona (5005 m, 16,421 ft.) on the right, Mount Churchill (4766 m, 15,638 ft.) on the left, and Russell Glacier in the foreground.*

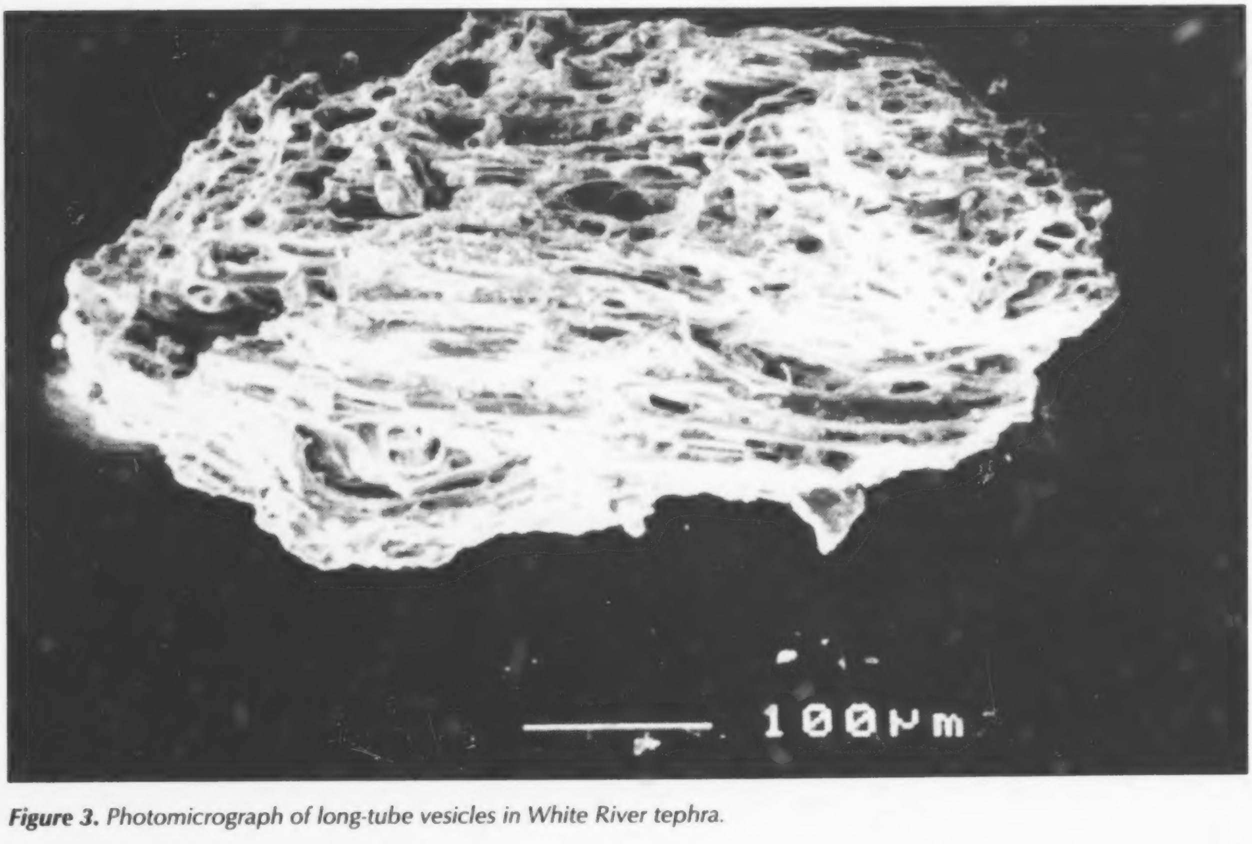

**Figure 3.** *Photomicrograph of long-tube vesicles in White River tephra.*

or early winter (West and Donaldson, 2001). Fieldwork in 2001 has provided preliminary stratigraphic data for resedimented tephra that forms terraces along the margins of Klutlan Glacier. Currently, work is being done to complete a detailed facies analysis and interpretation of these terrace deposits. Such information is essential in volcanic hazard assessment of the region, because pyroclastic activity in ice-covered regions can cause sudden melting of glaciers and snowfields, resulting in catastrophic flooding of surrounding drainage areas as demonstrated by the 1990 eruption of Mount Redoubt in Alaska (Alaska Volcano Observatory, 1990).

## DISTAL TEPHRA DEPOSITS

Distal deposits of White River tephra display characteristic features of tephra-fall deposits, which form as pyroclastic material settles from a large-scale eruption column. These features include a good to moderate sorting of angular to sub-rounded fragments in slightly graded or laminated beds. In contrast, the proximal deposits of the White River tephra are commonly reworked, displaying less angular grains and an improvement in sorting (Donaldson et al., 1996). In addition, bed thickness and particle size show a gradual decrease as distance increases from the site of eruption.

In distal regions, the deposit occurs as a pristine, compositionally homogeneous layer of unconsolidated white to beige-coloured tephra. The white colour of the tephra is due to the presence of numerous glass shards, and the slight beige tinting of the ash is attributed to organic staining from the overlying organic horizon (Crampton, 1982). Deposits occur less than 1 m below the present surface level of the soil, commonly between beds of silt or peat. The tephra is commonly redistributed onto lower slopes and is notably thicker on slopes facing west towards Mount Churchill (Crampton, 1982). Distal deposits of eastern lobe tephra are significantly more coarse grained than their northern lobe equivalents. Differences in the Fe-Ti composition of hematite-ilmenite minerals in the northern and eastern lobes of tephra allow for geochemical distinction between the lobes (Lerbekmo et al., 1975).

## PROXIMAL TEPHRA DEPOSITS

Proximal deposits of White River tephra are commonly reworked, and are primarily concentrated at the base and along the margins of Klutlan Glacier. As a result of reworking, these deposits are better-sorted and less angular in shape than their distal equivalents. At the summit region, resedimented deposits of ash, lapilli and blocks may reach thicknesses up to 50 m, and individual tephra blocks may be up to 50 cm in diameter (Richter et al., 1995). At 40 km east of Mount Churchill, thicknesses of sedimented deposits decrease to approximately 30 m. Geochemical analysis indicates that all proximal deposits from the summit of Mount Churchill represent material from the eastern lobe eruption of White River tephra (Richter et al., 1995).

## EVIDENCE FOR WINTER ERUPTION OF EASTERN-LOBE TEPHRA

Modern high-atmosphere wind patterns in the Alaska-Yukon region indicate that winds blow eastward in the winter and northward in the summer. Similar wind patterns during White River tephra deposition may indicate that the eastern lobe tephra was deposited during the winter months, and the northern lobe tephra was deposited during the summer months (Hanson, 1965; Workman, 1979). The exceptional preservation of White River tephra on steep slopes throughout the region may provide further evidence that the eastern-lobe tephra was erupted during the winter season (Hanson, 1965). The following section summarizes recent evidence from a frozen layer of airfall tephra near Destruction Bay, Yukon, and from ice-cemented tephra clasts near the Donjek River, Yukon, which both illustrate that the eruption of eastern-lobe tephra must have occurred during the late fall or early winter (West and Donaldson, 2000).

## BOCK'S BROOK

Evidence for late fall/early winter deposition of the eastern lobe tephra is based on a layer of airfall tephra preserved between beds of fluvial sand and gravel in the southern bank of Bock's Brook. This site is cut by the Alaska Highway, 4.2 km (3 miles) south of Destruction Bay and 100 km east of Mount Churchill. On the west side of the highway, the unit of tephra may be seen as a white granular layer with sharp boundaries that extends uninterrupted for more than 8 m. On the east side of the highway, the same bed may be followed discontinuously for 3-4 m. At this point, the bed disappears for another 3-4 m and is continuous thereafter, as far as can be seen downstream, along the banks of the channel.

The Bock's Brook tephra layer occurs as a distinctive, white, unconsolidated layer within an exposed succession of silt and gravel (Fig. 4). Minor amounts of sand occur within the vertical section, and discontinuous horizons of peat are abundant within the silt units (Fig. 5). The tephra layer displays normal graded bedding and faint horizontal laminations, attesting to its origin as an airfall deposit (Fig. 6). Particles within the tephra layer are granular, consisting of medium sand-sized ash, likely derived from the eastern lobe eruption. The tephra layer has a consistent thickness of 3.5 cm along its length and it

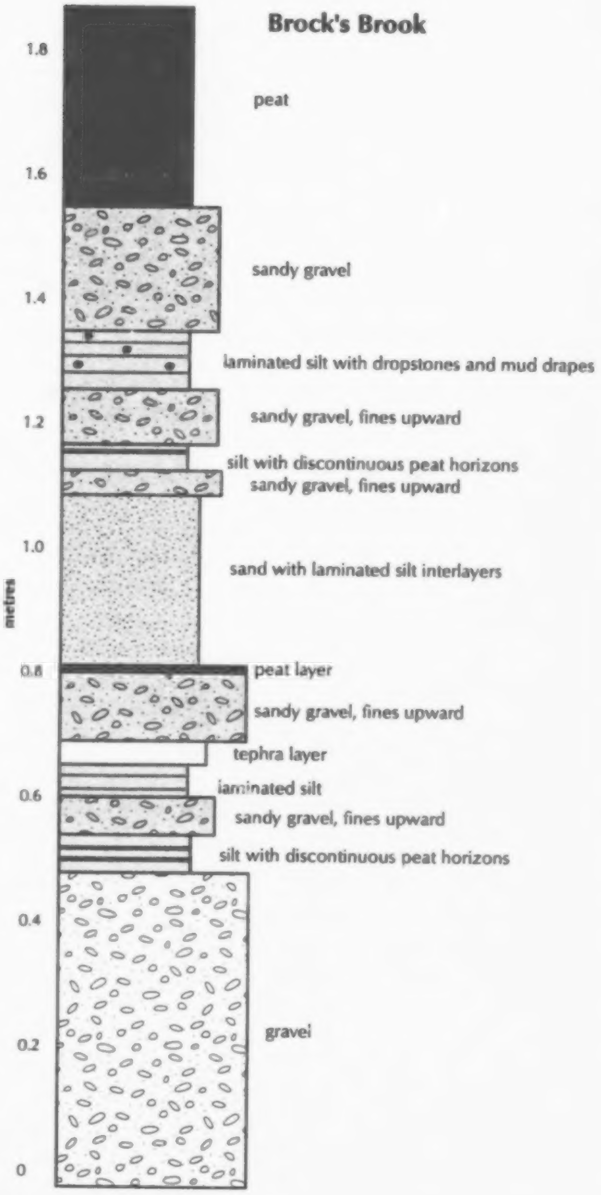
Brock's Brook
1.8
peat
1.6
sandy gravel
1.4
laminated silt with dropstones and mud drapes
sandy gravel, fines upward
1.2
silt with discontinuous peat horizons
sandy gravel, fines upward
1.0
sand with laminated silt interlayers
metres
0.8
peat layer
sandy gravel, fines upward
tephra layer
laminated silt
0.6
sandy gravel, fines upward
silt with discontinuous peat horizons
0.4
gravel
0.2
0

***Figure 5.*** *Stratigraphy of the Bock's Brook vertical section.*

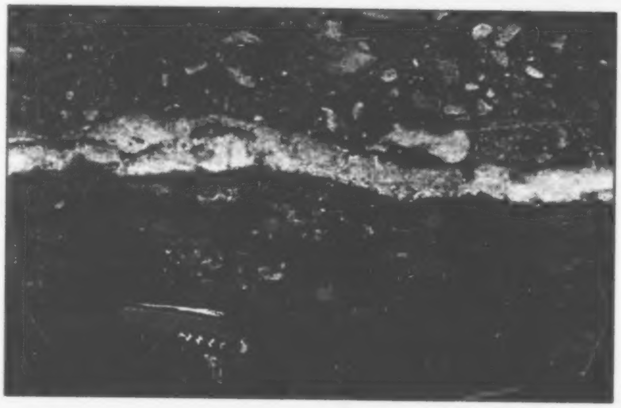

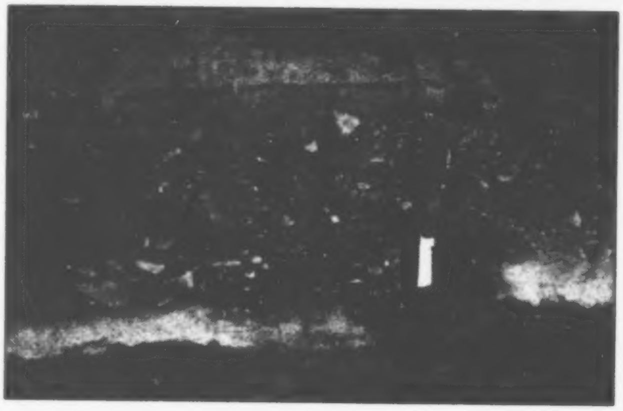

*(above)* ***Figure 4.*** *Overview of the vertical section exposed in the southern bank of Bock's Brook, 4.2 km south of Destruction Bay, Yukon. Trowel is approximately 30 cm in length. (middle)* ***Figure 6.*** *Airfall tephra embedded in a section of fluvial gravel and silt, Bock's Brook. This layer of tephra must have been frozen in order to escape reworking by fluvial currents. Penknife body is 8 cm long. (bottom)* ***Figure 7.*** *Truncation of airfall tephra layer by channel-fill deposits, Bock's Brook, Yukon. Penknife body is 8 cm long.*

occurs approximately 70 cm above the base of the vertical section. In some places, channel-fill deposits of sand and gravel abruptly truncate the tephra layer (Fig. 7).

The preservation of such a distinct layer of airfall tephra beneath deposits of fluvial sand and gravel requires that the tephra had to have been frozen in order to escape reworking. The tephra layer is inferred to have been deposited on a subaerially exposed overbank flood plain in the late fall or early winter, prior to the first major snowfall. Over the remainder of the winter season, it is inferred that the tephra layer would have become frozen and buried under a canopy of snow and ice. In the spring, the still-frozen tephra layer was subsequently buried by flood deposits of sand and gravel, sealing and protecting the layer against future erosion. Subsequent melting of ice in the pore spaces of the tephra layer produced post-depositional loading of epiclastic sediment along the boundaries of the tephra layer.

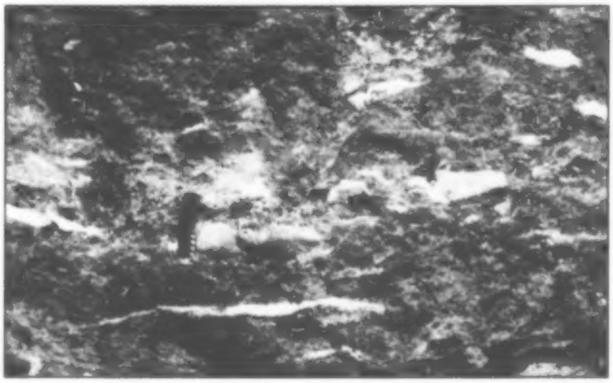

***Figure 9.*** *Unconsolidated tephra clasts in unit of fluvial silt. Angularity of the clasts and internal laminations suggest they were frozen prior to deposition. Penknife is 8 cm long.*

## DONJEK RIVER

Further evidence for a late fall/early winter timing of the eastern lobe eruption is provided by ice-cemented tephra clasts of the Donjek River section. This site is located 200 m west of the Donjek River bridge on the Alaska Highway and 130 km southeast of Mount Churchill, within the north bank of the Donjek River. The section comprises glacial till, overlain by fluvial silt and an upper unit of sandy to pebbly silt (Fig. 8). The ice-cemented tephra clasts are embedded within the upper 30 cm of the fluvial silt unit. These tephra clasts are unconsolidated, consist entirely of medium sand-sized tephra particles, and are tabular, ovoid and irregular in shape (Fig. 9). Internally, the clasts display faint horizontal lamination parallel to elongation.

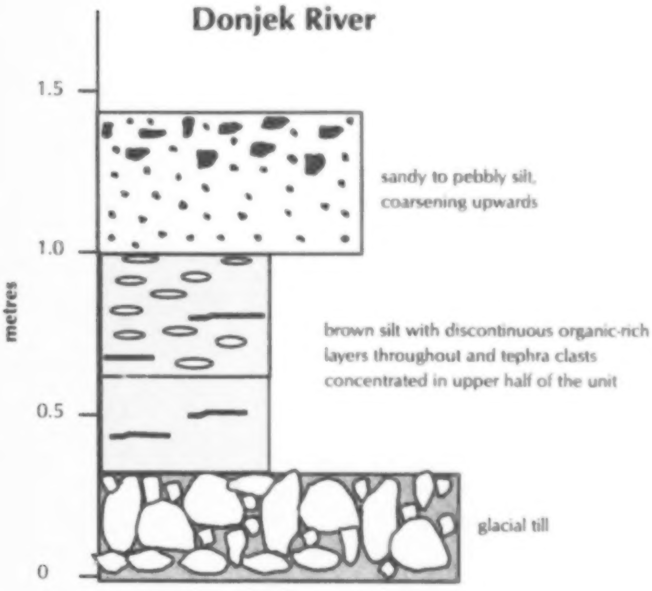
Donjek River
1.5
1.0
0.5
0
metres
sandy to pebbly silt, coarsening upwards
brown silt with discontinuous organic-rich layers throughout and tephra clasts concentrated in upper half of the unit
glacial till

***Figure 8.*** *Stratigraphy of the Donjek River vertical section.*

The compositional homogeneity and internal laminations of the Donjek River clasts indicate they were originally deposited as an airfall layer of tephra, comparable to the Bock's Brook tephra layer. This tephra layer was similarly deposited on a subaerially exposed overbank plain during the late fall or early winter, and was subsequently frozen over the remainder of the season. During spring flooding, fragmentation of the ice-cemented tephra layer yielded the clasts now embedded in fluvial silt. In order to remain morphologically intact, the tephra clasts had to have remained ice-cemented during fragmentation in order to survive minimal abrasion, transport, and their subsequent burial in fluvial silt.

Stratigraphic evidence of ice-cemented tephra from the Donjek River and Bock's Brook sections indicate that the eastern lobe eruption of tephra must have occurred during the late fall or early winter in order for the tephra in both sections to be preserved as it is today. Further preliminary evidence supporting a late fall or early winter timing for the eastern lobe tephra is provided by locally resedimented proximal terrace deposits.

## PROXIMAL TERRACE DEPOSITS

Discontinuous, locally resedimented terraces are prominent features along the lateral margins of Klutlan Glacier. These terraces extend for approximately 30 km on both sides of the Yukon-Alaska border in Kluane National Park (Yukon Territory) and Wrangell-St. Elias National Park (Alaska; Fig. 1). Individual terraces may reach more than 30 m in height and consist almost entirely of reworked pyroclastic material. The terraces stand more than 100 m above the present surface of Klutlan Glacier, indicating that significant melt-back of the glacier has occurred in the last 1200 years (Donaldson et al., 1996). The terraces are composed of white to light grey unconsolidated pyroclastics, and display steep (> 30 degree) angle of repose margins (Fig. 10). A discontinuous layer of granular airfall tephra up to 1 m thick caps individual terraces.

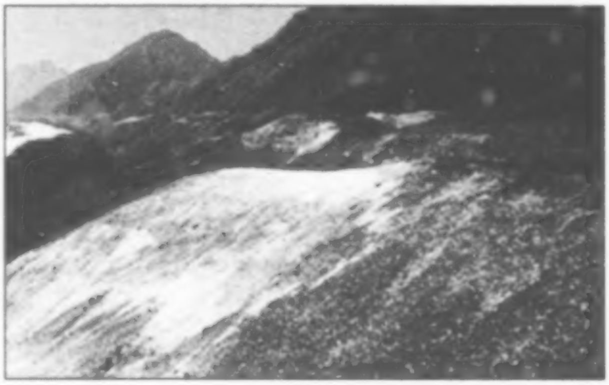

***Figure 10.*** *Proximal terrace deposit, north side of Klutlan Glacier. Terrace is approximately 30 m in height.*

Detailed facies analysis of one terrace deposit, located 4 km east of the Yukon-Alaska border on the north side of Klutlan Glacier, has already been completed (Donaldson et al., 1996). Measured sections of this terrace contain silt and lithic-rich interlayers, in addition to pyroclastic material (ash, lapilli, agglomerate). Sedimentary structures within the terrace (large-scale crossbedding, normal and inverse graded bedding, linguoid and climbing ripples, and channels) indicate water transport. These terraces were likely deposited subglacially as a hyperconcentrated flow. Consensus has not been reached on whether pyroclastic deposits from the terraces represent eastern-lobe tephra, northern lobe tephra, or a combination of both.

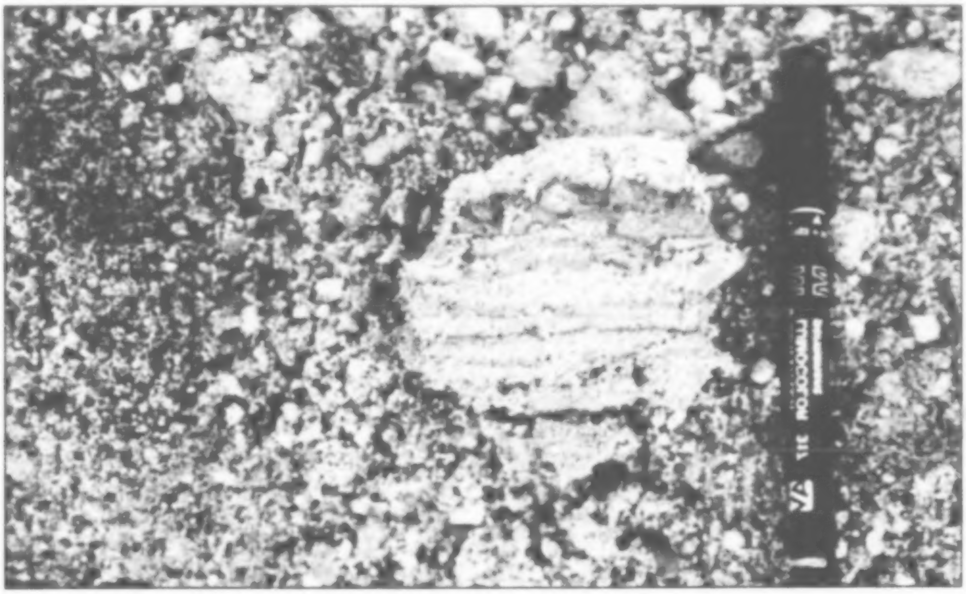

***Figure 11.*** *Internally laminated tephra clast embedded in pyroclastic sediments, proximal terrace deposit, south side of Klutlan Glacier. Black marker is 14 cm in length.*

Further study of terraces 5 km west of the Yukon-Alaska border on the south side of Klutlan Glacier, and 15.5 km east of the Yukon-Alaska border on the north side of Klutlan Glacier indicates that the stratigraphy of individual terraces is unique. These terraces contain interlayers of clay, lithic-rich layers and finer-grained pyroclastic material (ash, lapilli). Sedimentary structures include horizontal laminations, crossbedding, asymmetric ripples, normal and inverse grading, channels, clay clasts/wisps, and internally laminated clasts of pumice grains, similar to the ice-cemented clasts discovered within the Donjek River section. Such clasts are inferred to have been frozen before reworking, thus providing an excellent analogue for our inference regarding origin of the Donjek River clasts (Fig. 11). Preliminary analysis of these terrace deposits indicates accumulation may have occurred in an area ponded by ice-blocks adjacent to Klutlan Glacier.

## CONCLUSIONS

Recent stratigraphic evidence indicates that the eruption of eastern-lobe White River tephra occurred during the late fall or early winter. A precise timing of the eastern lobe eruption is essential for elucidation of the cultural and environmental effects of this volcanic event. The impact of such a large-magnitude eruption on vegetation, fauna, and the Athapaskan peoples subsisting on the land would vary during different times of the year. In addition, the effect of landslides, mudslides, and erosion in proximal and surrounding regions would also vary according to the season in which the eruption occurred. Detailed facies analysis of proximal terrace deposits, where they exist, is essential in documentation of the processes of volcanic resedimentation in glacial environments and provides essential background for comprehensive hazard assessment.

## ACKNOWLEDGEMENTS

Fieldwork for our study of terrace deposits in the summer of 2001 would not have been possible without the extensive logistical support provided by Game McGimsey and Don Richter, USGS, Anchorage, Alaska. Excellent accommodation was provided by Urban Rahoe of Ptarmigan Lake Lodge, Alaska and Bob Beatty of 1202 Lodge, Beaver Creek, Yukon. Reliable helicopter transport was provided by Tim Gaffney of Coastal Helicopters, Haines, Alaska.

## REFERENCES

Alaska Volcano Observatory, 1990. Debris flows and floods generated by eruption of Redoubt volcano, Alaska - Consequences of interaction between snow and ice and volcanic debris. Geological Society of America, Abstracts with Programs, vol. 22, no. 7, p. A55.

Clague, J.J., Evans, S.G., Rampton, V.N. and Woodsworth, G.J., 1995. Improved age estimates for the White River and Bridge River tephras, western Canada. Canadian Journal of Earth Sciences, vol. 32, p. 1172-1179.

Crampton, C.B., 1982. Volcanic ash soils in the southern Yukon of Canada. Muskox, vol. 30, p. 81-84.

Donaldson, J.A., Guerstein, P.G. and Mueller, W., 1996. Facies analysis of a pumiceous terrace beside Klutlan Glacier, Yukon Territory. Canadian Journal of Earth Sciences, vol. 12, p. 1233-1242.

Downes, H., 1979. The White River ash, Yukon Territory: A petrologic study. Unpublished M.Sc. Thesis, University of Calgary, Calgary, Alberta, 137 p.

Downes, H., 1985. Evidence of magma heterogeneity in the White River ash (Yukon Territory). Canadian Journal of Earth Sciences, vol. 22, p. 929-934.

Hanson, L.W., 1965. Size distribution of the White River ash, Yukon Territory. Unpublished M.Sc. Thesis, University of Alberta, Edmonton, Alberta, 59 p.

Lerbekmo, J.F. and Campbell, F.A., 1969. Distribution, composition, and source of the White River ash, Yukon Territory. Canadian Journal of Earth Sciences, vol. 6, p. 109-116.

Lerbekmo, J.F., Westgate, J.A., Smith, D.G.W. and Denton, G.H., 1975. New data on the character and history of the White River volcanic eruption, Alaska. *In:* Quaternary Studies, R.P. Suggate and M.M. Cresswell (eds.), Royal Society of New Zealand, Wellington, p. 203-209.

McGimsey, R.G., Richter, D.H., DuBois, G.D. and Miller, T.P., 1992. A postulated new source of the White River ash, Alaska. *In:* Geological Studies in Alaska, D.C. Bradley and A.C. Ford (eds.), United States Geological Survey, Bulletin 1999, p. 212-218.

Moodie, D.W., Catchpole, A.J.W. and Abel, K., 1992. Northern Athapaskan oral traditions and the White River volcano. Ethnohistory, vol. 39, p. 148-171.

Richter, D.H., Smith, J.G., Lanphere, M.A., Dalrymple, G.B., Reed, B.L. and Shew, N., 1990. Age and progression of volcanism, Wrangell volcanic field, Alaska. Bulletin of Volcanology, vol. 53, p. 29-44.

Richter, D.H., Preece, S.J., McGimsey, R.G. and Westgate, J.A., 1995. Mount Churchill, Alaska: Source of the late Holocene White River ash. Canadian Journal of Earth Sciences, vol. 32, p. 741-748.

Robinson, S.D., 2001. Extending the late Holocene White River ash distribution, northwestern Canada. Arctic, vol. 54, no. 2, p. 157-161.

West, K.D. and Donaldson, J.A., 2000. Evidence for winter eruption of the White River Ash (eastern lobe), Yukon Territory, Canada. Geocanada 2000 - The Millenium Geoscience Summit, Conference CD.

West, K.D. and Donaldson, J.A., 2001. Eruptive timing of White River ash deposit (Yukon, Northwest Territories, and Alaska). Canadian Quaternary Association Meetings, Programs and Abstracts, p. 67.

Workman, W.B., 1977. The prehistory of the southern Tutchone area: Problems in the prehistory of the North American subarctic. *In:* The Athapaskan Question, J.W. Helmer, S. Van Dyke and F.J. Kense (eds.), Archaeological Association of the University of Calgary, p. 46-54.

Workman, W.B., 1979. The significance of volcanism in the prehistory of subarctic northwest North America. *In:* Volcanic Activity and Human Ecology, P. Sheets and D.K. Grayson (eds.), Academic Press (New York), p. 339-371.

# PROPERTY DESCRIPTIONS

Alteration zonation, veining and mineralization associated with the Wernecke Breccias at Slab Creek, Yukon Territory, Canada
*M. Brookes, T. Baker and J. Hunt* .......... 249

Ray Gulch tungsten skarn, Dublin Gulch, central Yukon: Gold-tungsten relationships in intrusion-related ore systems and implications for gold exploration
*V.S. Brown, T. Baker and J.R. Stephens* .......... 259

Geology, mineralization and sampling results from the Kalzas tungsten property, central Yukon
*G.G. Carlson* .......... 269

# Alteration zonation, veining and mineralization associated with the Wernecke Breccias at Slab Creek, Yukon Territory, Canada

***Melanie Brookes and Tim Baker***[1]
*James Cook University*[1]

***Julie Hunt***[2]
*Yukon Geology Program*

Brookes, M.L., Baker, T. and Hunt, J., 2002. Alteration zonation, veining and mineralization associated with the Wernecke Breccias at Slab Creek, Yukon Territory, Canada. *In:* Yukon Exploration and Geology 2002, D.S Emond, L.H. Weston and L.L. Lewis (eds.), Exploration and Geological Services Division, Yukon Region, Indian and Northern Affairs Canada, p. 249-258.

## ABSTRACT

Detailed vertical-face mapping of 'Slab Creek' was carried out in the summer of 2001 to evaluate the relations of Wernecke Breccia bodies with alteration, veining and iron oxide-copper-gold mineralization. Slab Creek is situated near the 'Slab' mineral occurrence in the Bonnet Plume River district of the Wernecke Mountains. Meta-sedimentary rocks in the area consist of meta-siltstone, meta-silty dolomite and phyllite of the lower succession of the Early Proterozoic Wernecke Supergroup, known as the Fairchild Lake Group. These rocks were folded and metamorphosed to lower greenschist facies, and were subsequently intruded by the Wernecke Breccias during the Mid Proterozoic. Three alteration zones can be recognized within Slab Creek, an inner feldspar zone coinciding with the large breccia bodies, surrounded by a chlorite-quartz-carbonate zone, grading outward into a sericite-chlorite zone. Alteration, veining and mineralization is most intense within the albite alteration zone where iron oxide-copper-gold (cobalt-uranium) mineralization is disseminated and occurs as vein infill.

## RÉSUMÉ

Au cours de l'été 2001, on a dressé une carte détaillée de la paroi verticale au « ruisseau Slab » afin d'établir les relations entre les corps de brèche de Wernecke et l'altération, la disposition des filons ainsi que la minéralisation en oxyde de fer-cuivre-or. Le ruisseau Slab est situé à proximité de l'occurrence minérale « Slab », dans la région de la rivière Bonnet Plume, des monts Wernecke. Les roches métasédimentaires dans la région sont du métasiltstone, de la dolomie silteuse métamorphisée et du phyllade de la succession inférieure du Supergroupe de Wernecke (Groupe de Fairchild Lake), qui date du Protérozoïque précoce. Ces roches ont été plissées et métamorphisées au faciès des schistes verts inférieur; elles ont été ultérieurement pénétrées par les brèches de Wernecke pendant le Protérozoïque moyen. On peut reconnaître trois zones d'altération au ruisseau Slab : une zone intérieure d'albite recouvrant les gros corps de brèche, qui est entourée par une zone de chlorite-quartz-carbonates passant vers l'extérieur à une zone de séricite-chlorite. L'altération, la disposition des filons et la minéralisation sont les plus marquées dans la zone d'altération en albite, où la minéralisation en oxyde de fer-cuivre-or (cobalte-uranium) est disséminée et se présente sous forme de matériaux de remplissage de filons.

---

[1] *Economic Geology Research Unit, James Cook University, Townsville, Queensland, Australia, tim.baker@jcu.edu.au*

[2] *Yukon Geology Program, 300-345 Main Street, Whitehorse, Yukon, Canada Y1A 2B6. Current address: Economic Geology Research Unit, James Cook University, Townsville, Queensland, Australia, julie.hunt@jcu.edu.au*

## INTRODUCTION

'Slab Creek' is located on NTS map sheet 106E/1 as a tributary of the Bonnet Plume River, adjacent to an area unofficially known as 'Slab Mountain' (Fig. 1; Fig. 2 of Hunt et al., this volume). Approximately 150 km northeast of the town of Mayo, the Slab Mountain area is isolated and mountainous, with elevations of 560 to 1500 m above sea level. The geomorphology and remoteness of the area permits only access by air during the summer months, and by vehicle along the Wind River Trail during the winter (Hunt et al., this volume).

The region is host to numerous sub-economic occurrences of iron oxide, copper, gold, uranium and cobalt. Mineral exploration programs carried out in the region since the 1960s recognized a correlation between mineralization and extensive breccia bodies (Archer and Schmidt, 1978). More recent work carried out by Newmont Exploration Ltd. from 1994 to 1997 resulted in a 1:5000-scale geological and lithological interpretation of the Slab Mountain area. This map formed the basis on which detailed mapping of Slab Creek was undertaken. Vertical exposure of up to 50 m in the 'Canyon Zone' of Slab Creek allowed 1:400-scale mapping of geology, alteration, veining and mineralization along horizontal intervals totalling 630 m in length (Figs. 2a and 2b). Intervals were measured in 10-m increments along base lines from which detailed mapping of each face was made.

The purpose of this study was to determine the association between alteration, veining and mineralization with respect to that of the Slab Creek breccia bodies. The orientation of veins, crosscutting relationships, relative timing of mineralization and alteration styles, and their distribution were mapped and sampled. This paper primarily covers field observations with petrographic and geochemical data to follow in April of 2002 in the form of a fourth year Honours thesis, currently being completed at James Cook University, Australia.

## REGIONAL GEOLOGY

The Wernecke Mountains consist of meta-sedimentary rocks, meta-volcanic rocks, igneous intrusive rocks and breccias. Sedimentation took place throughout the Early Proterozoic to Palaeozoic and was punctuated by

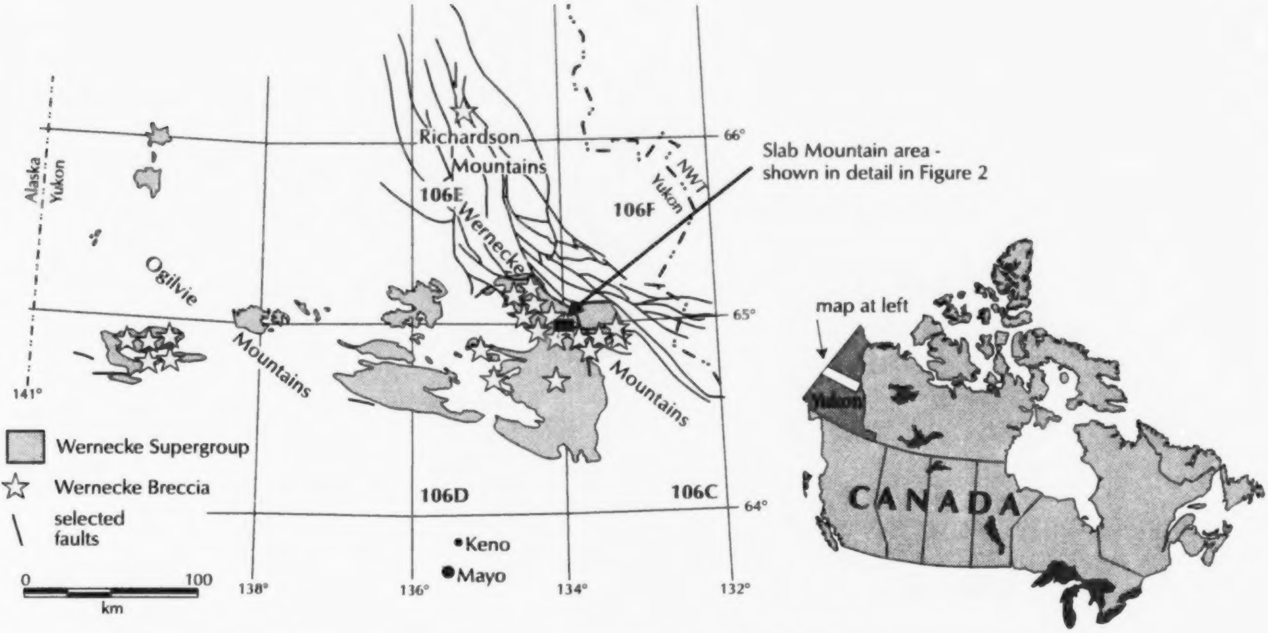
Alaska
Yukon
Ogilvie
Mountains
Richardson
Mountains
106E
Wernecke
Mountains
106F
NWT
Yukon
66°
65°
64°
Slab Mountain area - shown in detail in Figure 2
141°
Wernecke Supergroup
Wernecke Breccia
selected faults
0
100
km
138°
136°
134°
132°
106D
106C
Keno
Mayo
map at left
Yukon
CANADA

***Figure 1.*** *Location of the Slab Mountain map area and distribution of Wernecke Breccia occurrences and Wernecke Supergroup rocks in the Yukon (Hunt, this volume, modified from Thorkelson (2000)).*

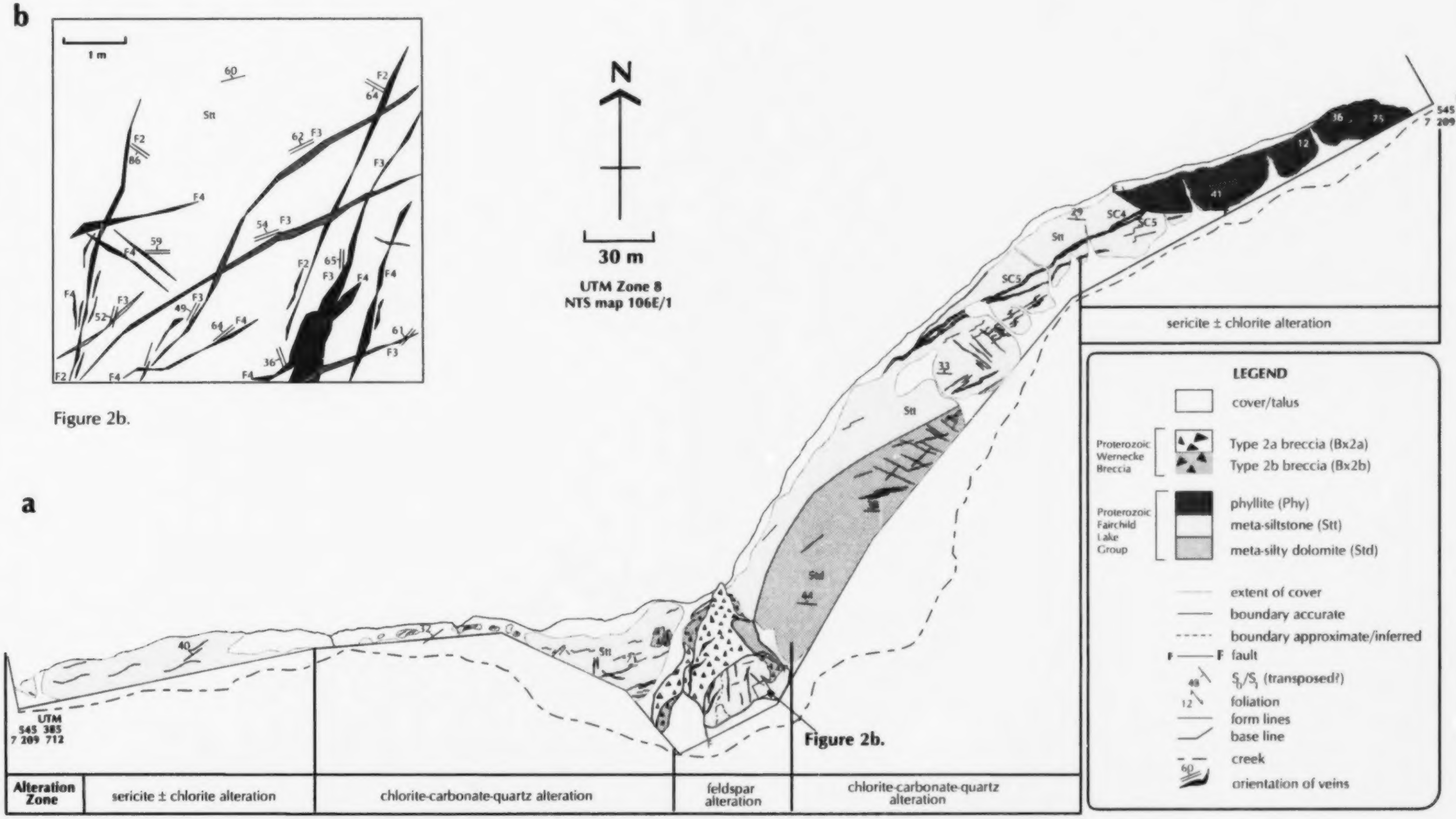
b
1 m
60
Stt
F2
86
F4
59
F4
F3
52
F3
49
F3
54
F3
62
F3
F2
64
F3
F2
65
F3
F4
F4
64
F4
36
F4
61
F3
F2
F4
Figure 2b.
N
30 m
UTM Zone 8
NTS map 106E/1
a
UTM
545 385
7 209 712
40
Stt
Std
44
Stt
33
SC5
Stt
29
SC4
SC5
41
12
36
75
UTM
545 964
7 209 885
Figure 2b.
Alteration Zone
sericite ± chlorite alteration
chlorite-carbonate-quartz alteration
feldspar alteration
chlorite-carbonate-quartz alteration
sericite ± chlorite alteration
LEGEND
cover/talus
Proterozoic Wernecke Breccia
Type 2a breccia (Bx2a)
Type 2b breccia (Bx2b)
Proterozoic Fairchild Lake Group
phyllite (Phy)
meta-siltstone (Stt)
meta-silty dolomite (Std)
extent of cover
boundary accurate
boundary approximate/inferred
F F fault
49
S0/S1 (transposed?)
12
foliation
form lines
base line
creek
60
orientation of veins

**Figure 2.** *(a) Near vertical face map of the Slab Creek showing 'Canyon zone' general geology and alteration zones (from Hunt et al., this volume). For explanation of vein stages SC4 and SC5 in the sericite-chlorite alteration zone see Figure 5. (b) Inset showing meta-siltstone of the feldspar alteration zone and crosscutting vein relationships typical of this alteration zone. Veins were mapped in the vertical plane and orientated in the horizontal plane. Feldspar alteration zone vein stages (see also Fig. 7): F2=feldspar ± quartz, F3=carbonate ± quartz, F4=chalcopyrite-magnetite-carbonate-quartz ± feldspar and F5=chlorite-carbonate-quartz.*

numerous phases of deformation, igneous activity, metasomatism and mineralization (see Fig. 3 of Hunt et al., this volume; Thorkelson et al., 2000).

The oldest rocks in the region are that of the Wernecke Supergroup. These rocks were deposited during the Early Proterozoic and are interpreted to unconformably overlie a crystalline basement of Archean or Early Proterozoic age (Thorkelson et al., 2000). The Wernecke Supergroup comprises the lowermost Fairchild Lake Group, middle Quartet Group and upper Gillespie Lake Group. The Wernecke Supergroup is ~14 km thick and as a whole, represents two carbonate-dominated cycles, of which the deposition of siltstone, shale, sandstone and dolostone represent initial basin development followed by subsidence and marine transgression (Delaney, 1981).

Intrusion of dioritic to syenitic dykes and stocks (the Bonnet Plume River Intrusions ~1.72 Ga), and undated biotite lamprophyre, possibly took place prior to the onset of a southeast-directed compression in the Racklan Orogeny (Thorkelson et al., 2001; Gabrielse, 1967). The 'Slab volcanics' (possibly a comagmatic extrusive component of the Bonnet Plume River Intrusions) is preserved as a single down-dropped block at the Slab Mountain mineral occurrence (Yukon MINFILE, 2001, 106D 070). The undated Slab volcanics exist as a megaclast (0.25 x 0.6 km) within an extensive brecciated zone of Slab Mountain. It is assumed that uplift and erosion associated with orogenesis left no in-situ remnants of the Slab volcanics (Thorkelson, 2000).

Individual breccia zones collectively form an extensive breccia system covering 3500 km$^2$ (Archer and Schmidt, 1978). Previous terminology of the breccias has included 'pre-breccia', 'slurry', 'homolithic', 'typical', 'Wernecke', 'colourful' and 'heterolithic' breccia (Archer and Schmidt, 1978; Laznicka and Edwards, 1979; Laznicka and Gaboury, 1988). Mapping carried out this summer by Hunt et al. (this volume) defined two breccia types, herein termed Type 1 and Type 2 breccias. In the Canyon zone of Slab Creek, Type 2 breccia was recognized and further divided into Type 2a and 2b breccias on the basis of crosscutting relationships (see Fig. 2). The breccias have been dated at ~1.6 Ga using U-Pb dating on titanite (Thorkelson et al., 2000). Clasts of folded, metamorphosed sedimentary rocks, dykes and sills, and the Slab volcanics further constrain the relative timing of brecciation.

The Pinguicula Group unconformably overlies the brecciated, sheared and faulted Wernecke Supergroup. Sedimentation within a basinal to platformal environment during the Middle Proterozoic resulted in the deposition of carbonate and siliciclastic rocks that were intruded by the Hart River sills at ~1.38 Ga and later by the Bear River dykes at ~1.27 Ga (Thorkelson et al., 2001). Unconformably overlying the Pinguicula Group is the Hematite Creek Group. The uncomformity represents a hiatus in which sedimentation ceased for some 300 million years, recommencing around 1033 Ma (Thorkelson, 2000). The Hematite Creek Group consists of shallow-water carbonates and clastics derived largely from rocks affected by the Grenvillian Orogeny (~1250-1000 Ma; Hoffman, 1989). The Hematite Creek Group, older Pinguicula Group and localized portions of the Wernecke Supergroup were later folded and thrust faulted during the Corn Orogeny, possibly a late phase of Grenvillian orogenesis (Thorkelson, 2000).

The Late Proterozoic (~755 Ma) saw the deposition of the Windemere Supergroup as two distinct sedimentary packages, the Lower and Upper Rapitan groups, both of which are divided into several formations. The Lower Rapitan Group consists of tillites, whilst the Upper Rapitan Group consists of three clastic carbonate cycles. The Windemere Supergroup is overlain by dolostone, arenite, conglomerate and siltstone of Upper Proterozoic to Lower Paleozoic age. In the western portion of the Wernecke Mountains, mostly shelf environment carbonates and clastics of Cambro-Devonian age overlie the Werenecke Supergroup. The Laramide Orogeny of the Mesozoic to Early Tertiary produced large-scale folding that affected all geological units, with more localized thrust faulting.

## LOCAL GEOLOGY

The meta-sedimentary rocks of Slab Creek are part of the lowermost sedimentary succession of the Early Proterozoic Wernecke Supergroup, the Fairchild Lake Group (see Fig. 2 of Hunt et al., this volume). Outcrop in the study area extends over approximately 650 m and runs parallel to the canyon forming Slab Creek, in which the rocks are exposed to a height of up to 50 m (Fig. 3a). A thin cover, commonly less than 5 m, marks the boundary between strata of the Fairchild Lake Group and that of overlying, unconsolidated Quarternary glacial sediments.

### STRUCTURE

Deformation, associated with Racklan orogenesis, accompanied lower greenschist facies metamorphism and

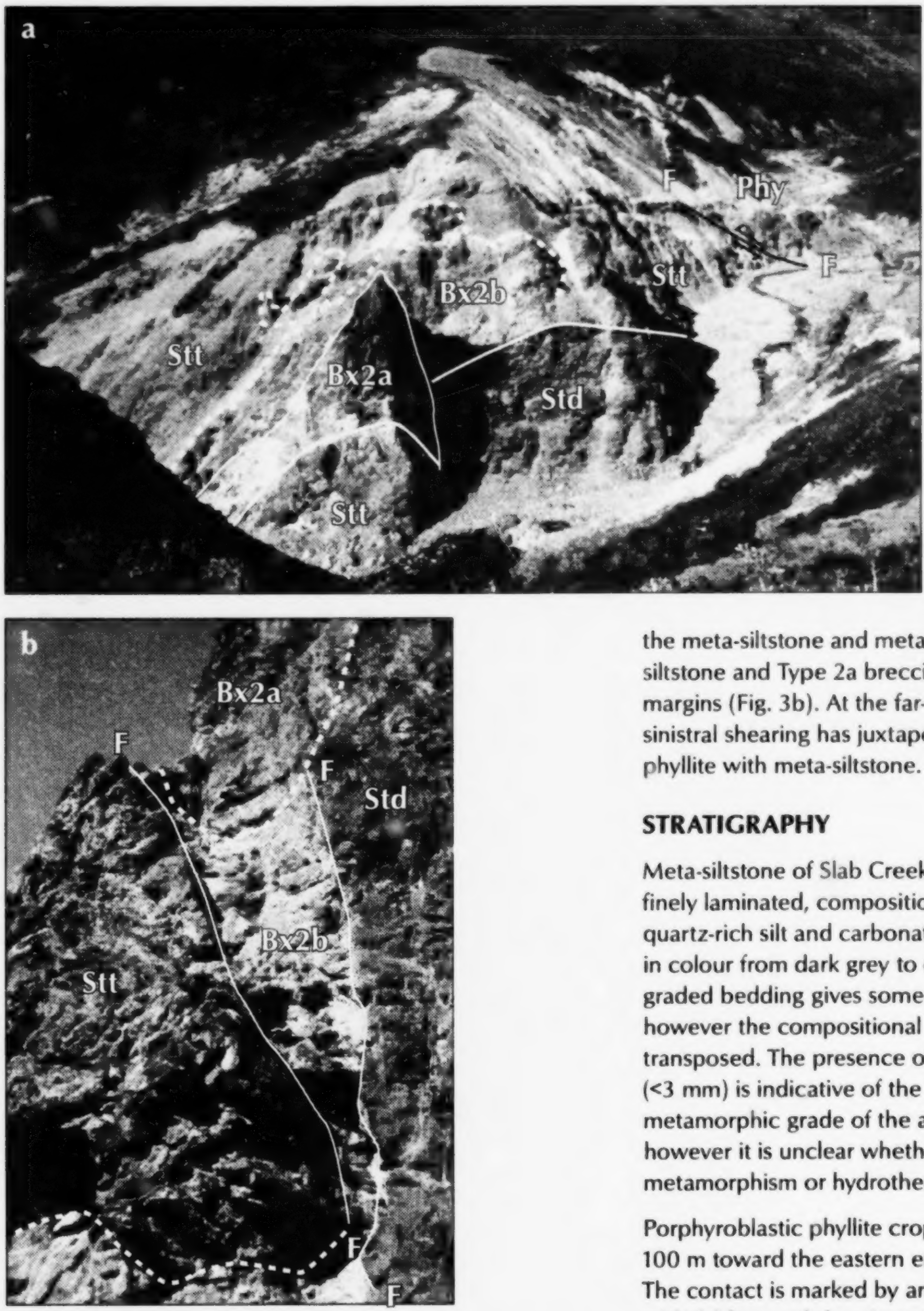

***Figure 3.*** *(a) 'Canyon Zone' of Slab Creek, looking north. Scale east to west is approximately 600 m. Phy = phyllite; other abbreviations, see below. (b) Lithological contacts between Type 2a breccia (Bx2a), feldspathically altered meta-siltstone (Stt) and meta-silty dolomite (Std; dashed lines). Their faulted margins (F-F) are intruded by Type 2b breccia (Bx2b; full lines). Outcrop is approximately 7 m in height.*

resulted in schistosity, crenulations and kink banding of the more micaceous meta-sedimentary rocks of Slab Creek (Brideau et al., this volume). Compositional layering of the meta-sedimentary rocks has a northerly trend, dipping shallowly at the distal margins of the outcrop and gradually steepening toward the central brecciated zone (Fig. 2a). Both brittle faulting and ductile shearing postdate the layering. East-trending faults are evident as sharp contacts and fault gouge between the meta-siltstone and meta-silty dolomite, and meta-siltstone and Type 2a breccia sits within these faulted margins (Fig. 3b). At the far-eastern end of the outcrop, sinistral shearing has juxtaposed the fine, micaceous phyllite with meta-siltstone.

## STRATIGRAPHY

Meta-siltstone of Slab Creek consists of finely to very finely laminated, compositional layering of micaceous quartz-rich silt and carbonate-quartz-rich layers that vary in colour from dark grey to off white, respectively. Relict graded bedding gives some direction of younging, however the compositional layering may have been transposed. The presence of chloritoid porphyroblasts (<3 mm) is indicative of the lower greenschist facies metamorphic grade of the area. Chlorite is also common, however it is unclear whether this relates to regional metamorphism or hydrothermal activity.

Porphyroblastic phyllite crops out for approximately 100 m toward the eastern end of the section (Fig. 2a). The contact is marked by an area of high strain associated with folding and shearing where the phyllite has been juxtaposed against the meta-siltstone. The light-green coloured phyllite consists of fine- to medium-grained micas and quartz, mineralogically differentiated to form intercalated chlorite-muscovite and muscovite-rich bands averaging 3 to 10 mm in width.

A sharp contact defines the boundary between the meta-siltstone and that of a lower dolomitic unit

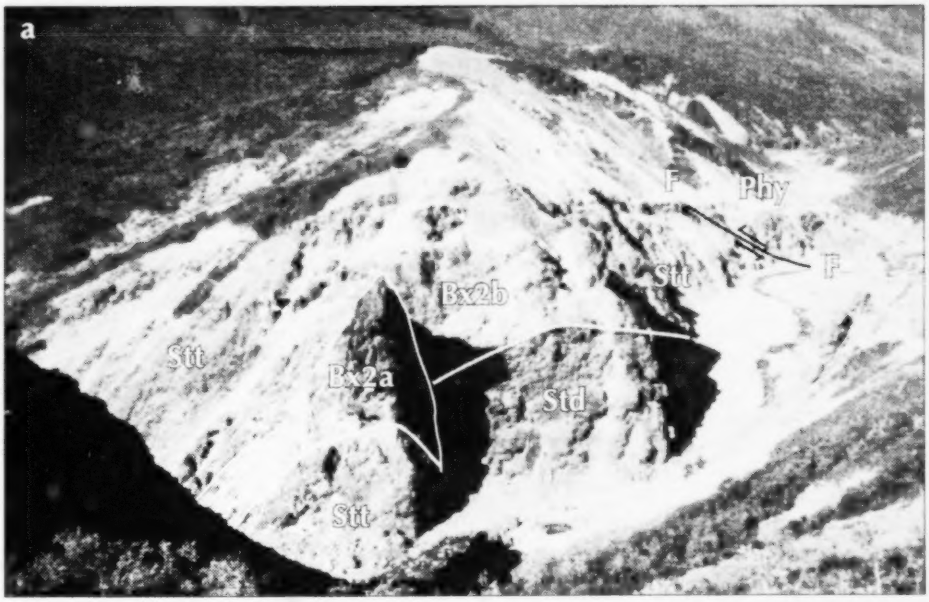

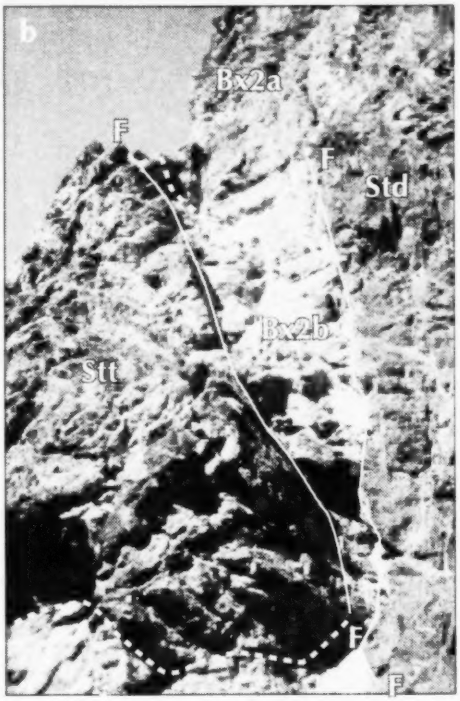

***Figure 3.*** *(a) 'Canyon Zone' of Slab Creek, looking north. Scale east to west is approximately 600 m. Phy = phyllite; other abbreviations, see below. (b) Lithological contacts between Type 2a breccia (Bx2a), feldspathically altered meta-siltstone (Stt) and meta-silty dolomite (Std; dashed lines). Their faulted margins (F-F) are intruded by Type 2b breccia (Bx2b; full lines). Outcrop is approximately 7 m in height.*

resulted in schistosity, crenulations and kink banding of the more micaceous meta-sedimentary rocks of Slab Creek (Brideau et al., this volume). Compositional layering of the meta-sedimentary rocks has a northerly trend, dipping shallowly at the distal margins of the outcrop and gradually steepening toward the central brecciated zone (Fig. 2a). Both brittle faulting and ductile shearing postdate the layering. East-trending faults are evident as sharp contacts and fault gouge between the meta-siltstone and meta-silty dolomite, and meta-siltstone and Type 2a breccia sits within these faulted margins (Fig. 3b). At the far-eastern end of the outcrop, sinistral shearing has juxtaposed the fine, micaceous phyllite with meta-siltstone.

## STRATIGRAPHY

Meta-siltstone of Slab Creek consists of finely to very finely laminated, compositional layering of micaceous quartz-rich silt and carbonate-quartz-rich layers that vary in colour from dark grey to off white, respectively. Relict graded bedding gives some direction of younging, however the compositional layering may have been transposed. The presence of chloritoid porphyroblasts (<3 mm) is indicative of the lower greenschist facies metamorphic grade of the area. Chlorite is also common, however it is unclear whether this relates to regional metamorphism or hydrothermal activity.

Porphyroblastic phyllite crops out for approximately 100 m toward the eastern end of the section (Fig. 2a). The contact is marked by an area of high strain associated with folding and shearing where the phyllite has been juxtaposed against the meta-siltstone. The light-green coloured phyllite consists of fine- to medium-grained micas and quartz, mineralogically differentiated to form intercalated chlorite-muscovite and muscovite-rich bands averaging 3 to 10 mm in width.

A sharp contact defines the boundary between the meta-siltstone and that of a lower dolomitic unit containing silt-dominated layers (meta-silty dolomite). The meta-silty dolomite is crudely layered with vague original laminations 10-30 mm in thickness. Along weathering surfaces, oxidation within the more dolomitic layers has produced a deep, earthy red colour, while the more silty layers remain dark to light grey.

## BRECCIA BODIES

The lithological units of Slab Creek are host to two discordant breccia bodies that together cover a 50-m area. The breccias form the core of the Slab Creek exposure. Type 2a breccia is the most prominent feature of the study area, outcropping to a height of over 40 m and contacting sharply with that of the surrounding country rock. A later phase of breccia, termed Type 2b breccia, is observed to extensively finger into the earlier breccia body and meta-sedimentary rocks.

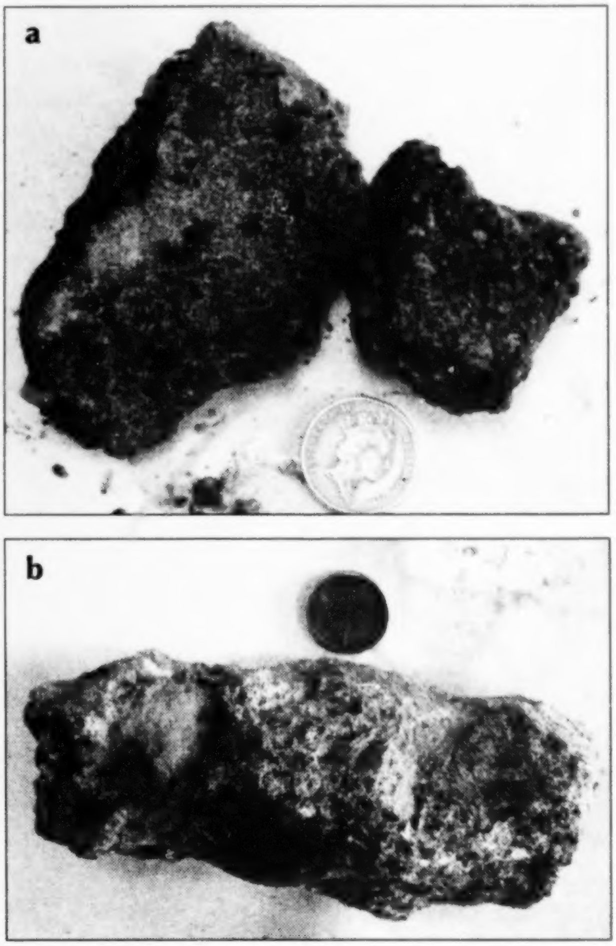

*Figure 4. (a) Type 2a breccia containing monotonous grey clasts set in a similar matrix of microbreccia and hydrothermal infill. (b) Type 2b breccia containing multi-coloured clasts within a similar matrix of microbreccia and hydrothermal infill.*

Type 2a breccia consists of monotonous grey clasts of mainly meta-siltstone and meta-silty dolomite set in a well-cemented, similarly coloured, porous matrix of microbreccia and hydrothermal precipitate (Fig. 4a). Having been invariably metasomatized, clast colour rarely reflects that of the parent lithology, and compositional layering, in most cases, is not discernable. The clasts and matrix are mostly quartzo-feldspathic, typically sub-angular to well-rounded and, on average, range in size from 1 to 10 cm.

Faulting took place prior to emplacement of the later Type 2b breccia (Fig. 4b). Faulting along the Type 2a breccia and meta-silty dolomite contact is evident by the presence of fault gouge. Type 2b breccia fingers into these faulted margins, and elsewhere intrudes along lithological contacts such as that of the earlier, Type 2a, breccia-host rock contacts (Fig. 3b). Type 2b breccia contains altered clasts of meta-siltstone, meta-silty dolomite and phyllite. Clasts are various colours, including pink, green, yellow and grey and are surrounded by a porous matrix composed of similar micro-rock fragments and hydrothermal infill. Clasts are sub- to well-rounded and range in size from less than 1 cm to 7 cm, and locally are well over 1 m. One such megaclast occurs as a 3 x 5 m block of crackle-brecciated meta-silty dolomite. Clasts of altered, laminated meta-siltstone commonly contain veins of, and disseminated, chalcopyrite.

# ALTERATION ZONATION, VEINING AND MINERALIZATION

The Slab Creek breccia bodies form a locus for alteration, veining and mineralization, with breccia bodies themselves intensely altered. Three alteration zones were recognized within Slab Creek, an inner feldspar-rich alteration zone surrounded by a quartz-chlorite-carbonate zone, with an outer zone of localized sericite-chlorite alteration amongst relatively unaltered meta-sedimentary rocks. Previous work carried out by Laznicka and Edwards (1979), and Laznicka and Gaboury (1988) on similar alteration types indicate that feldspathic alteration is predominantly albite, however further work is required to define this in the Slab Creek area. Vein distribution and mineralogy also varies between the different alteration zones, and vein paragenesis has been established, based on field relationships, for each alteration zone (Figs. 5, 6, 7). The degree of veining and mineralization (copper, gold, iron oxide ± cobalt ± uranium; based on preliminary, unpublished geochemical analyses) increases markedly toward the feldspar-rich core where chalcopyrite, magnetite, hematite, minor Au, Co and U minerals are disseminated and occur as fracture fillings.

## SERICITE ± CHLORITE ALTERATION ZONE

Sericite alteration occurs as discrete lenses within the meta-siltstone at the far-western section of the study area, as well as pervasively throughout finely laminated meta-siltstone, adjacent to phyllite located toward the eastern end of the study area. The pale sericitic bands overprint relict compositional layering and chloritiod porphyroblasts, and are concordant with the relatively unaltered to chloritic meta-siltstone. Bands are commonly 1 m to 1.5 m in length and 1 m to 5 cm wide, and alteration intensity within these bands decreases outward from their centres. Sericitic alteration overprints earlier chlorite and minor hematite alteration in the more silty horizons of the meta-siltstone. Distally, chlorite-dominated alteration of phyllite has produced intercalated bands of chlorite and muscovite in which the chlorite-rich bands contain regularly distributed, aligned magnetite crystals up to 3 mm in length.

There are five stages of veining within the sericite ± chlorite alteration zone (Fig. 5). Minor veining in Stage SC1 overprints sericite ± chlorite alteration and occurs as veinlets of vuggy textured quartz (<6 mm wide) surrounded by a thin chlorite selvage. These veinlets are crosscut by abundant (one vein approximately every metre) carbonate-hematite-chlorite ± magnetite ± quartz veins averaging 3 cm to 4 cm wide (Stage SC2). These veins are kinked (or exploit this fabric) within the more pervasively sericite-chlorite altered meta-sedimentary rocks (Fig. 8a). Stage SC3 veins, containing chlorite-hematite-quartz infill, crosscut SC2 veins and are locally kinked. SC3 veins have a similar abundance to SC2 veins. SC4 veins crosscut this kinking fabric and contain abundant quartz-magnetite with minor chlorite-chalcopyrite-malachite-muscovite. Unlike earlier veins,

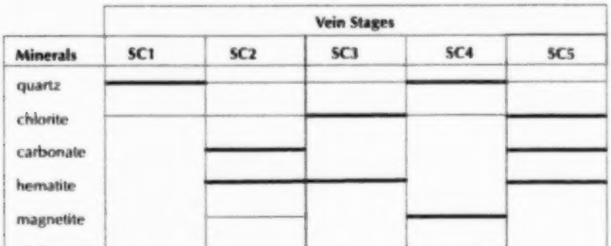

**Figure 5.** *Sericite ± chlorite alteration zone - preliminary vein paragenesis.*

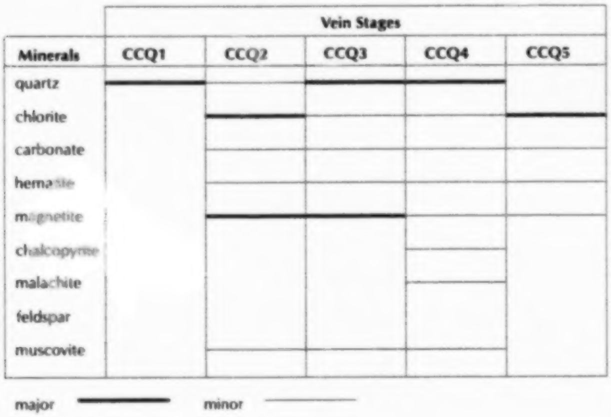

**Figure 6.** *Chlorite-carbonate-quartz alteration zone – preliminary vein paragenesis.*

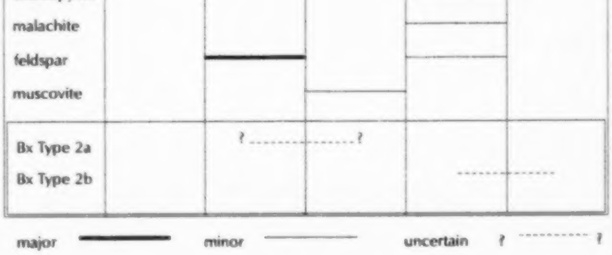

**Figure 7.** *Feldspar alteration zone – preliminary vein paragenesis and inferred timing of Type 2a and Type 2b breccia emplacement. Bx = breccia.*

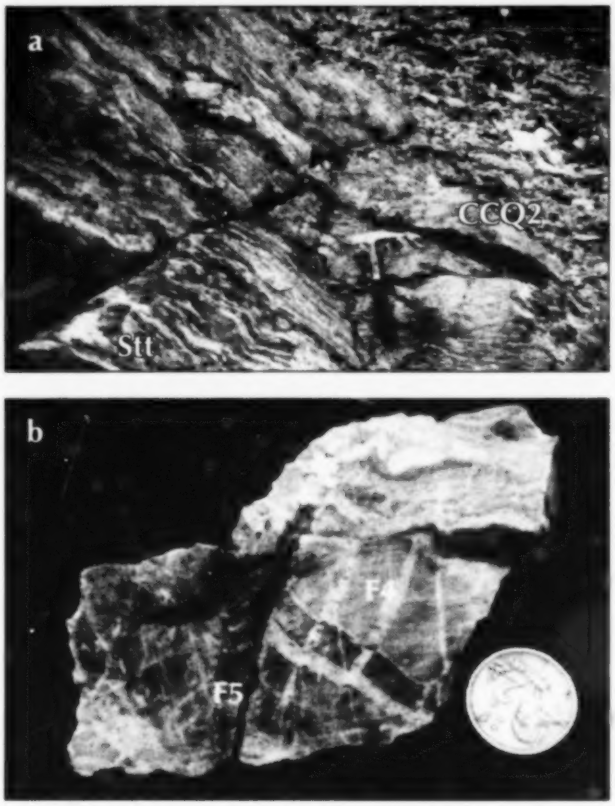

***Figure 8.** (a) Chlorite-carbonate-quartz altered meta-siltstone containing a kinked stage CCQ2 vein of carbonate-hematite-magnetite-chlorite ± quartz. (b) Meta-siltstone of the feldspar alteration zone containing crosscutting Stage F4 veins of quartz-magnetite-chalcopyrite ± carbonate ± feldspar overprinted by F5 stage veins of carbonate-chlorite-quartz.*

Stage SC4 veins occur less frequently and are commonly less than 2 cm wide. There is an obvious exception to this, given that one of these veins (although lacking in any observable mineralization) is 20 cm wide and spans a third of the length of the Slab Creek outcrop (Fig. 2b). Stage SC5 veins of chlorite-carbonate-hematite ± quartz crosscut all other stages (Fig. 8b). Veins are typically 3 cm to 4 cm wide, although one SC5 vein of similar width and length to that of the large SC4 vein is easily recognized (Fig. 2b). The smaller SC5 veins are more common, occurring at a frequency of one vein to every 5 m.

## CHLORITE-CARBONATE-QUARTZ ALTERATION ZONE

Chlorite-carbonate-quartz alteration is proximal to the feldspar alteration centre associated with the breccia bodies. The alteration occurs in meta-siltstone as preferential replacement of specific horizons with carbonate-quartz recrystallization of more carbonate-rich layers and chloritization of the more silty layers. In places, hematite forms specularite pods within patchy chloritic alteration. Toward the contact between the feldspar alteration zone and the chlorite-carbonate-quartz alteration zone, clasts and matrix of the Type 2b breccia are locally chlorite-carbonate-quartz altered and in places, contain perfectly formed rhombs of rare pyrite up to 1 cm in diameter. The more dolomitic horizons of the meta-silty dolomite are dominated by pervasive ferrous carbonatization with disseminated magnetite and quartz. Chlorite is present along cleavage planes and fracture surfaces.

Veins occur in five stages (Fig. 6). Early quartz veins (Stage CCQ1), commonly less than 1 cm wide and averaging four to every metre, are crosscut by chlorite-magnetite-carbonate-hematite ± quartz veins (CCQ2) of similar abundance, averaging 3 cm to 4 cm in width. A thin envelope of muscovite alteration rims these veins. In kinked host lithology, these veins contain a similar kinking fabric. Discordant veins of Stage CCQ3 are dominated by quartz-magnetite, are commonly rimmed by muscovite, and locally contain small (<2 cm) chloritized clasts of wall rock. Both Stage 2 and 3 veins are the most abundant in the chlorite-carbonate-quartz alteration zone. Less common are the chalcopyrite-bearing veins of Stage CCQ4 containing quartz-chlorite-magnetite-chalcopyrite-malachite and minor hematite-muscovite. Chalcopyrite mineralization is sparse, but when apparent, forms relatively well-defined crystals. This minor mineralization is followed by a final stage of chlorite-carbonate-hematite-magnetite ± quartz veins (CCQ5) similar to that of SC5 stage veining in the sericite-chlorite alteration zone.

## FELDSPAR ALTERATION ZONE

Although not extensive, feldspar-rich alteration is one of the more conspicuous alterations of Slab Creek. This alteration zone is particularly prominent at the contact between breccia and meta-siltstone, where the latter is intensely bleached. Relict compositional layering is discernable in the meta-siltstone, however chloritoid porphyroblasts are no longer visible. Copper mineralization is the most dominant feature of this alteration zone, with the oxidized sulphide minerals discolouring weathering surfaces to rusty brown. Feldspathic alteration occurs pervasively throughout the Type 2a breccia and adjacent meta-siltstone, and as feldspar infill within the intensely fractured meta-siltstone.

Five stages of veining can be recognized within the feldspar alteration zone (Fig. 7). Quartz veins up to 5 cm in diameter (Stage F1) are common at the very centre of the alteration zone. Their size and number decrease dramatically outward within the space of 2 m to 3 m. The larger quartz veins (<5 cm) average four veins every 1 m and grade outward to smaller veins (<1 cm) and veinlets of less than one vein per metre. Crosscutting these veins are prominent vein sets of feldspar ± quartz infill (Stage F2). These veins (<3 cm wide) are similarly oriented with an average strike trending north-northwest and occurring at an average abundance of two veins to every 1 m. Stage F3 veins contain vuggy quartz with carbonate infill and crosscut feldspar veining. Iron oxide-copper mineralization occurs concurrently with carbonate-quartz ± feldspar veining (Stage F4). Stage F4 veins contain disseminated to massive chalcopyrite and magnetite. This is the first stage of veining observed to crosscut the Type 2a breccia. Late chlorite-carbonate-quartz veinlets (Stage F5) overprint all other vein stages, and are similarly seen to crosscut both Type 2a and Type 2b breccias.

## DISCUSSION

Field observations indicate that the breccia bodies in Slab Creek play a significant role in the development of alteration zonation, associated veining and mineralization. The breccia bodies, hosted by meta-sedimentary rocks, form an alteration and mineralization locus about which three distinct alteration zones can be recognized: an inner feldspar zone, surrounded by a chlorite-carbonate-quartz zone, grading outward into a sericite-chlorite zone. Alteration zones are host to numerous crosscutting veins of which their relative timing, mineralogy and distribution varies between each zone. The most intense fracturing, vein infill and pervasive mineralization occurs within the feldspar alteration zone, coinciding with the extensive breccia bodies.

Several stages of veining took place prior to brecciation, including SC1, CCQ1 and F1 stage quartz veining, and SC2 and CCQ2 stage chlorite-carbonate-hematite ± magnetite ± quartz veining. These veins often appear kinked. The kinking event is inferred by Brideau et al. (this volume) to be related to late stages of Racklan orogenesis that took place prior to breccia emplacement. Type 2a breccia locally contains clasts with chlorite-carbonate-hematite ± magnetite ± quartz veins, which suggests the breccia postdates F1, SC1, CCQ1, SC2 and CCQ2 stage veins. The exact timing of Stage F2, feldspar ± quartz veins and feldspar alteration, and F3, quartz-carbonate veins relative to brecciation (Type 2a) remains unclear (Fig. 7). Further petrographic work is required to evaluate this relationship. Chalcopyrite mineralization dominates Stage F4 carbonate-quartz-magnetite- ± feldspar vein infill and clearly crosscuts Type 2a breccia. Furthermore, this mineralization stage is most abundant in the feldspar-altered meta-siltstone where in contact with Type 2a breccia, which suggests that the breccia may have been utilized as a channel for mineralizing hydrothermal fluids. Structural controls such as faults along the breccia-host rock boundaries may have also contributed to localizing mineralization. It is certainly evident that the Type 2b breccia also exploited these structures. The final stage of chlorite-dominated veining is clearly seen to overprint both breccias and all three alteration zones.

Field observations have helped constrain the relationship between breccia bodies and hydrothermal fluids involved in alteration, veining and mineralization. Petrographic and geochemical data are currently being evaluated to better define these relationships, and will be reported in April of 2002 in the form of a fourth year Honours thesis, being completed by the first author at James Cook University, Australia.

## ACKNOWLEDGEMENTS

Many thanks to Grant Abbott of the Yukon Geology Program for suggesting this project, and to Newmont Mining Corp., and Derek Thorkelson, John Laughton, Marc-Andre Brideau and Grant Redfern for their insight and assistance in the field.

## REFERENCES

Archer, A.R. and Schmidt, U., 1978. Mineralised breccias of Early Proterozoic age, Bonnet Plume River district, Yukon Territory. C.I.M. Bulletin, vol. 71, p. 53-58.

Brideau, M-A., Thorkelson, D.J., Godin, L. and Laughton, J.R., 2002 (this volume). Paleoproterozoic deformation of the Racklan Orogeny, Slats Creek (106D/16) and Fairchild Lake (106C/13) map areas, Wernecke Mountains, Yukon. *In:* Yukon Exploration and Geology 2001, D.S. Emond, L.H. Weston and L.L. Lewis (eds.), Exploration and Geological Services Division, Yukon Region, Indian and Northern Affairs Canada, p. 65-72.

Delaney, G.D., 1981. The mid-Proterozoic Wernecke Supergroup, Wernecke Mountains, Yukon Territory. Geological Survey of Canada, Paper 81-10, p. 1-23.

Grabrielse, H., 1967. Tectonic evolution of the northern Canadian Cordillera. Canadian Journal of Earth Sciences. vol. 4, p. 271-298.

Hoffman, P., 1989. Precambrian geology and tectonic history of North America. *In:* The Geology of North America - An Overview, A.W. Bally and A.R. Palmer (eds.), Geological Society of America, Geology of North America, vol. A., p. 447-512.

Hunt, J., Laughton, J., Brideau, M-A., Thorkelson, D.J., Brookes, M.L. and Baker, T. 2002 (this volume). New mapping in the Slab Mountain area of the Wernecke Mountains (parts of NTS 106C/13, 106D/16, 106E/1 and 106F/4): Breccia and iron oxide-copper-gold mineralization. *In:* Yukon Exploration and Geology 2001, D.S. Emond, L.H. Weston and L.L. Lewis (eds.), Exploration and Geological Services Division, Yukon Region, Indian and Northern Affairs Canada, p. 125-138.

Laznicka, P. and Edwards, R.J., 1979. Dolores Creek, Yukon - Disseminated copper mineralization in sodic metasomatites. Economic Geology, vol. 74, p. 1352-1370.

Laznicka, P. and Gaboury, D., 1988. Wernecke Breccias and Fe, Cu, U mineralization: Quartet Mountain-Igor area (NTS 106E). *In:* Yukon Geology Volume 2, J.G. Abbott (ed.), Exploration and Geological Services Division, Yukon Region, Indian and Northern Affairs Canada, p. 42-50.

Thorkelson, D.J., 2000. Geology and mineral occurrences of the Slats Creek, Fairchild Lake and "Dolores Creek" areas, Wernecke Mountains, Yukon Territory (106D/16, 106C/13, 106C/14). Exploration and Geological Services Division, Yukon Region, Indian and Northern Affairs Canada, Bulletin 10, 73 p.

Thorkelson, D.J., Mortensen, J.K., Abbott, J.G., Creaser, R.A. and Davidson, G.J., 2000. Epicontinental rifting of western Laurentia. *In:* Abstracts Volume (compact disc), 31st International Geological Congress, August, 2000, Rio de Janeiro.

Thorkelson, D.J., Mortensen, J.K., Creaser, R.A., Davidson, G.J. and Abbott, J.G., 2001. Early Proterozoic magmatism in Yukon, Canada: Constraints on the evolution of northwestern Laurentia. Canadian Journal of Earth Science, vol. 38, p. 1479-1494.

Yukon MINFILE, 2001. Nash Creek – 106D. Exploration and Geological Services Division, Yukon Region, Indian and Northern Affairs Canada.

# Ray Gulch tungsten skarn, Dublin Gulch, central Yukon: Gold-tungsten relationships in intrusion-related ore systems and implications for gold exploration

***V.S. Brown, T. Baker[1] and J.R. Stephens***
*James Cook University[1]*

Brown, V.S., Baker, T. and Stephens, J.R., 2002. Ray Gulch tungsten skarn, Dublin Gulch, central Yukon: Gold-tungsten relationships in intrusion-related ore systems and implications for gold exploration. *In:* Yukon Exploration and Geology 2001, D.S. Emond, L.H. Weston and L.L. Lewis (eds.), Exploration and Geological Services Division, Yukon Region, Indian and Northern Affairs Canada, p. 259-268.

## ABSTRACT

The Ray Gulch tungsten skarn and the Eagle Zone intrusion-related gold deposit are associated with the Dublin Gulch intrusion, which forms part of the mid-Cretaceous Tombstone Plutonic Suite. Tungsten mineralization occurs in a roof pendant of hornfelsed Neoproterozoic to Early Cambrian Hyland Group metasedimentary rocks. Five main paragenetic stages include Stage I wollastonite-quartz skarn and later Stage II pyroxene-garnet-scheelite skarn that forms the main tungsten mineralization. Stages III (quartz-scheelite-clinopyroxene), IV (quartz-amphibole-calcite) and V (quartz-K-feldspar-pyrrhotite-molybdenite-arsenopyrite-pyrite-chalcopyrite) are vein related and are volumetrically insignificant (<10 vol. %). Geochemical analysis of the skarn and veins indicates that the deposit lacks gold and bismuth. The earliest veins in the Eagle Zone are similar to Stage V veins at Ray Gulch. Gold at the Eagle Zone occurs in a later sericite-carbonate-bismuth-sulphide vein stage; this stage is critically absent from the skarn. Thus, although tungsten is commonly associated with intrusion-related gold mineralization, it predates gold-bismuth and may occur spatially separate from it.

## RÉSUMÉ

Le gisement de skarn tungsténifère Ray Gulch et le gisement d'or Eagle Zone sont associés à l'intrusion de Dublin Gulch, qui constitue une partie de la suite plutonique de Tombstone du Crétacé moyen. La minéralisation en tungstène se trouve dans un enclave de roches métasédimentaires du Groupe de Hyland, d'âge Néoprotérozoïque à Cambrien précoce, qui ont été transformées en cornéennes. La paragenèse comprend cinq associations principales : l'association I (skarn à wollastonite-quartz) et, ultérieurement, l'association II (skarn à pyroxène-grenat-scheelite), qui constitue le principal corps minéralisé en tungstène; l'association III (quartz-scheelite-clinopyroxène), l'association IV (quartz-amphibole-calcite) et l'association V (quartz-feldspath potassique-pyrrhotine-molybdénite-arsénopyrite-pyrite-chalcopyrite) sont associées à des filons et présentent un volume peu important (<10 %). L'analyse géochimique des skarns et des filons indique que le gisement ne renferme ni or ni bismuth. Les filons précoces du gisement Eagle Zone sont similaires aux filons de l'association V du gisement Ray Gulch. L'or du gisement Eagle Zone se trouve dans des veines plus récentes renfermant l'association de séricite-carbonates-bismuth-sulfures; il est très important de noter que le skarn ne renferme pas cette association. Bien que le tungstène est couramment associé à une minéralisation en or reliée à une intrusion, celui-ci s'est formé avant l'or et le bismuth et peut donc se trouver à d'autres endroits.

---

[1] *Economic Geology Research Unit, School of Earth Sciences, James Cook University, Townsville, Queensland, Australia, tim.baker@jcu.edu.au*

## INTRODUCTION

The Ray Gulch tungsten skarn deposit is located within the Dublin Gulch property in central Yukon. The deposit consists of several tungsten-bearing skarn units containing drill-indicated and inferred reserves of 5.4 Mt at 0.82% $WO_3$ (Lennan, 1983). Adjacent to the Ray Gulch deposit is the Dublin Gulch - Eagle Zone gold resource, a granite-hosted, sheeted-vein deposit with an inferred and potential resource of 50.3 Mt at 0.93 g/t Au (Maloof et al., 2001).

Even though these two deposits were studied separately in the past (Lennan, 1983; Hitchins and Orssich, 1995; Maloof et al., 2001), previous reports did not discuss possible genetic links or timing of mineralization between the two deposits. Recent work focused on relogging and sampling a number of drill holes with emphasis on paragenetic relationships, as well as costean mapping and infill mapping within and around the deposit outskirts. The aims of this paper are to discuss the paragenetic and mineralization history of the skarn deposit, and to re-evaluate the skarn deposit in light of new data from the Eagle Zone (Maloof et al., 2001). This comparison enables consideration of the spatial and temporal relationships between tungsten and gold-bismuth in intrusion-related ore systems, which may be useful when exploring for gold in regions of known tungsten occurrences.

## LOCAL GEOLOGY

The Dublin Gulch property is located in central Yukon Territory, approximately 70 km by road northeast of the town of Mayo (Fig. 1). The tungsten deposit is situated on a plateau at an elevation of approximately 1370 m and is surrounded by gently rolling hills and peaks of the Selwyn Ranges. The Eagle Zone is approximately 2.5 km southwest of Ray Gulch and occupies an area roughly 400 m by 600 m on the steep southwestern slopes of the Dublin Gulch intrusion (Maloof et al., 2001). Access onto the deposit sites is possible by four-wheel drive vehicle (a four-wheel quad bike is advisable), via a network of old, unmaintained drill roads.

The Dublin Gulch property is located within the Selwyn fold belt and is hosted by Neoproterozoic to Early Cambrian metasedimentary rocks of the Hyland Group. These units have been thrust over younger Mississippian Keno Hill Quartzite and intruded by mid-Cretaceous

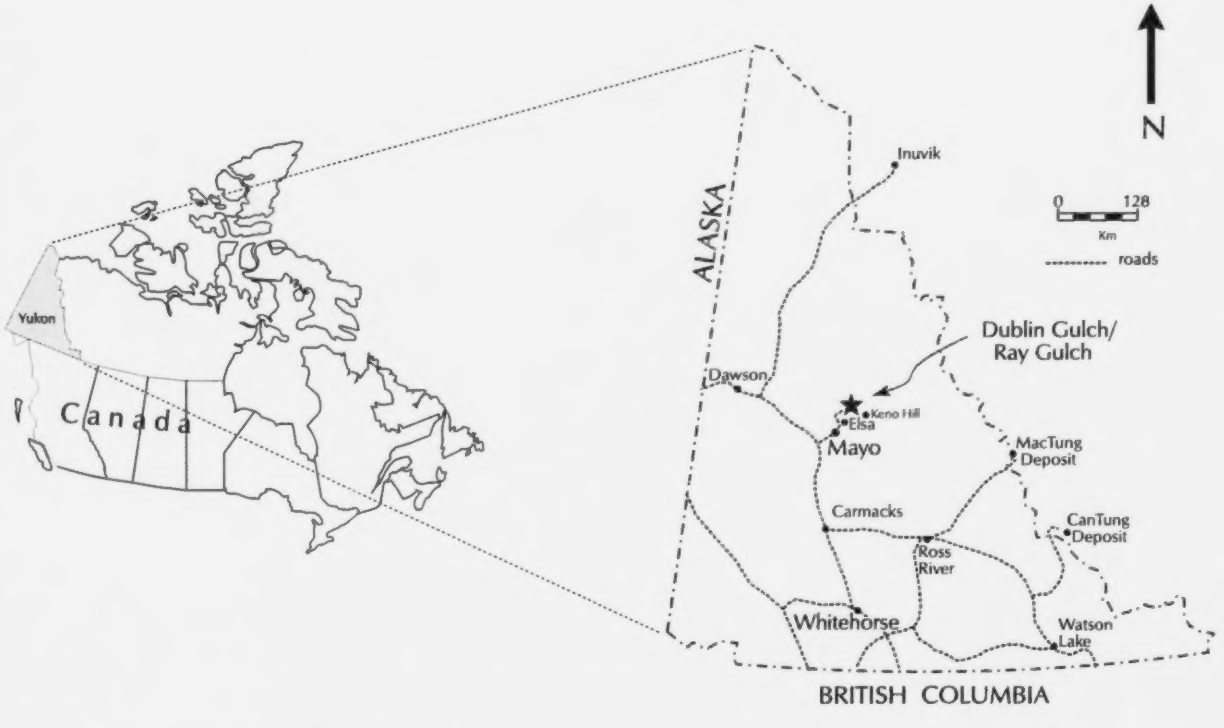

***Figure 1.*** *Location map of the Ray Gulch tungsten skarn deposit.*

granitoid plutons of the Tombstone Plutonic Suite (Hitchins and Orssich, 1995). The Hyland Group in this area has been subdivided into four main lithological units: the Lower Schist, the Central Quartzite, the Upper Schist and the Grit Unit (Fig. 2; Lennan, 1983). The Ray Gulch deposit is hosted within the Grit Unit rocks and consists of interbedded gritty and micaceous quartzite, massive white quartzite, limestone and phyllite (Lennan, 1983). Several deformation events affected the rocks and metamorphism reached greenschist facies. Later contact metamorphism associated with the Dublin Gulch intrusion produced fine-grained quartz and biotite hornfels, with disseminated pyrrhotite and andalusite, and skarn within the limestone units.

Four phases of intrusive rocks have been identified in outcrop and/or drill core within the Dublin Gulch area. They are, from youngest to oldest: leucocratic granite and aplite, quartz monzonite, quartz diorite and granodiorite (Lennan, 1983). The main intrusive feature is the Dublin Gulch granodiorite stock, an elongate body that strikes 070° and dips shallowly to steeply to the north on the northern side of the intrusion, and steeply to the north on the southern margin. The surface dimensions of the intrusion are approximately 6 km by 2 km, with a hornfels aureole extending up to 2 km from the contact (Maloof et al., 2001).

## MINERAL OCCURRENCES

Mineral occurrences within the property that are spatially related to the granodiorite stock include the Ray Gulch tungsten skarn deposit (Yukon MINFILE, 2001, 106D 027) and an array of gold-bearing sheeted-vein deposits (the Eagle, Olive, Shamrock and Steiner zones; Yukon MINFILE, 2001, 106D 025) within the east-central and northern contact zones (Maloof et al., 2001). Quartz-sulphide

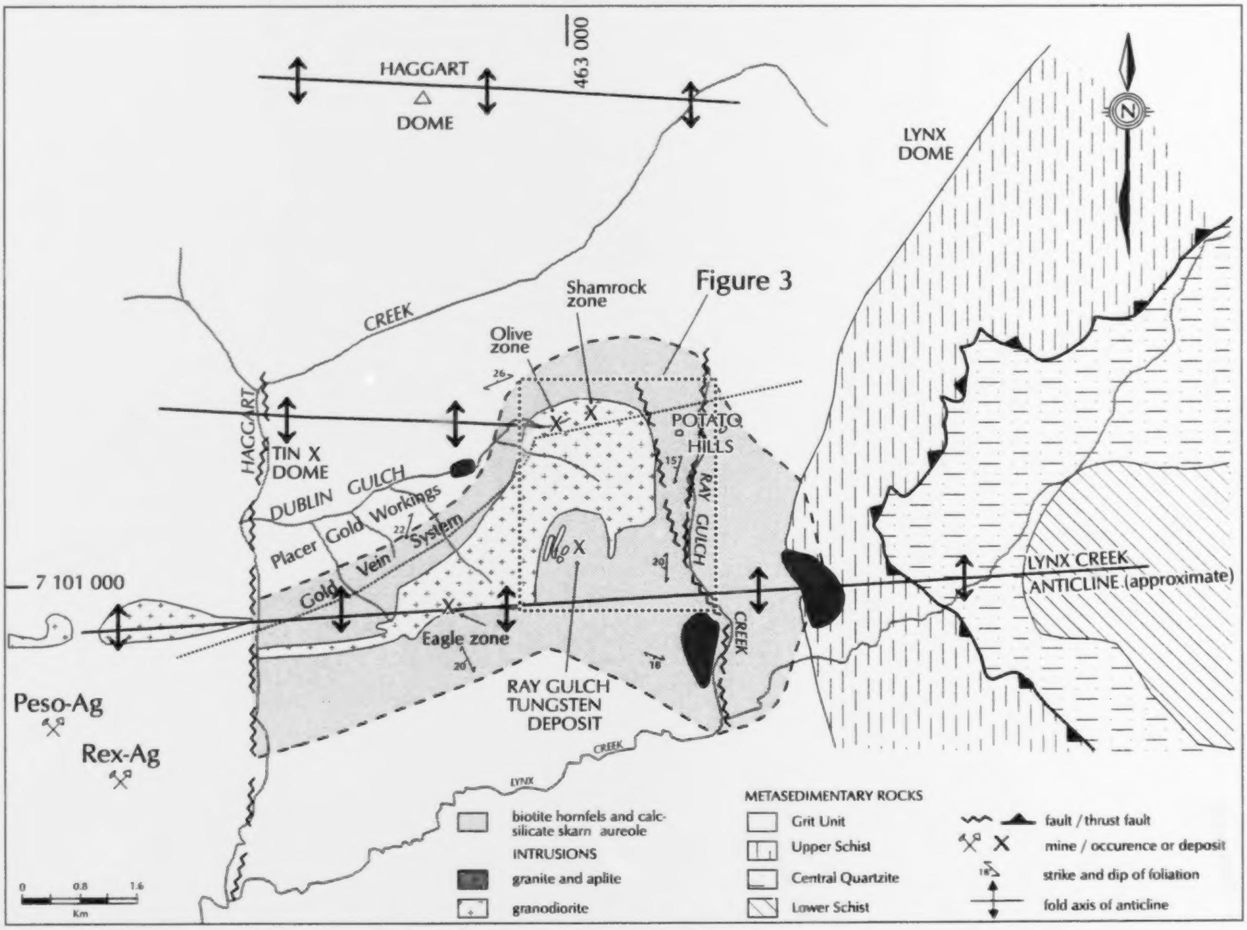
463 000
HAGGART DOME
LYNX DOME
N
Figure 3
Shamrock zone
Olive zone
CREEK
HAGGART
TIN DOME
DUBLIN GULCH
Placer Gold Workings
Gold Vein System
POTATO HILLS
RAY GULCH
CREEK
7 101 000
Eagle zone
RAY GULCH TUNGSTEN DEPOSIT
LYNX CREEK ANTICLINE (approximate)
Peso-Ag
Rex-Ag
LYNX
CREEK
26
22
15
20
20
18
0
0.8
1.6
Km
biotite hornfels and calc-silicate skarn aureole
INTRUSIONS
granite and aplite
granodiorite
METASEDIMENTARY ROCKS
Grit Unit
Upper Schist
Central Quartzite
Lower Schist
fault / thrust fault
mine / occurence or deposit
strike and dip of foliation
fold axis of anticline

***Figure 2.*** *Geological map of the Dublin Gulch area and surrounding prospects (after Lennan, 1983).*

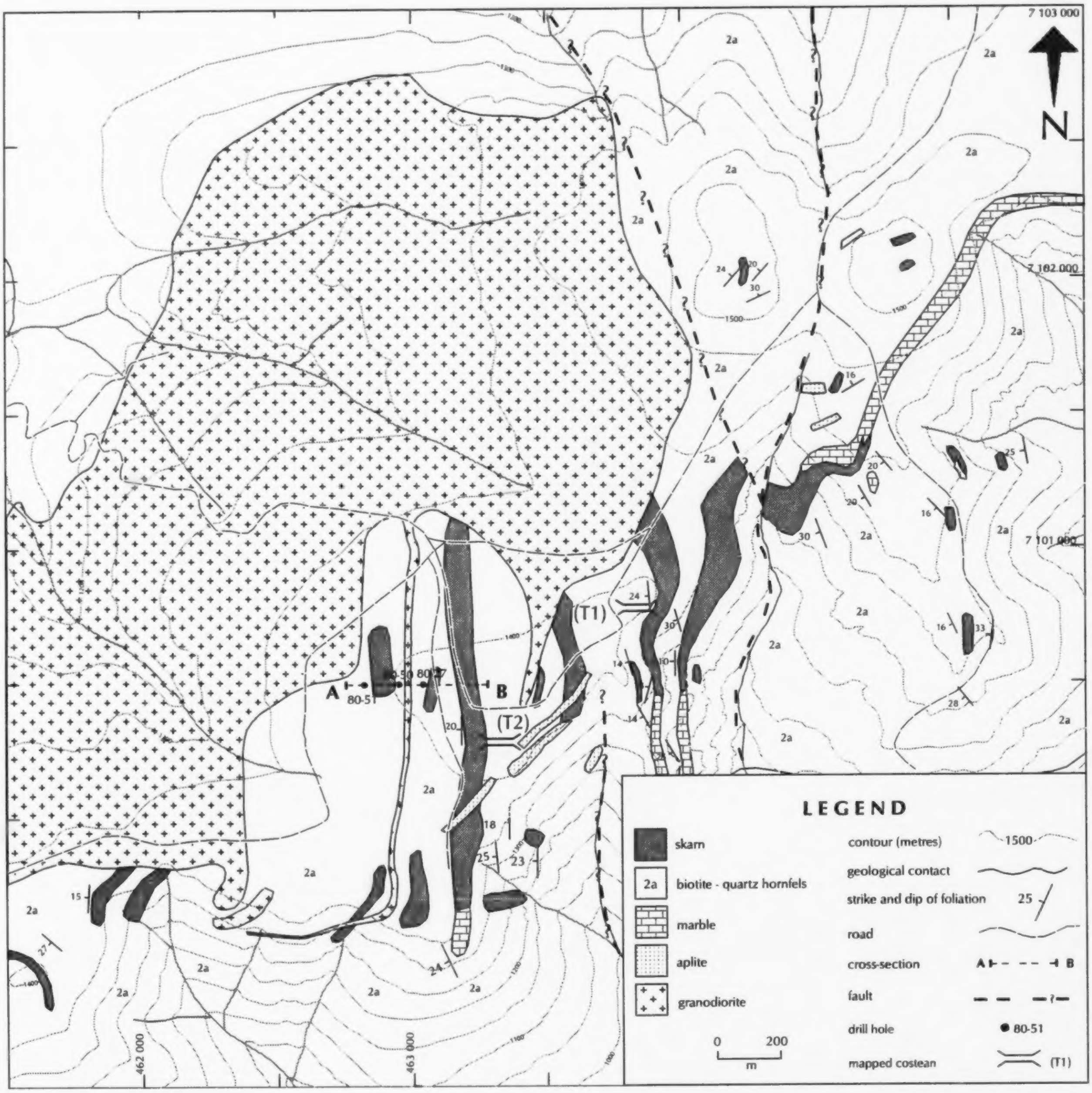
7 103 000
N
7 102 000
7 101 000
462 000
463 000
2a
(T1)
(T2)
A
B
80-51
80-50
80-27
LEGEND
skarn
2a biotite - quartz hornfels
marble
aplite
granodiorite
contour (metres) 1500
geological contact
strike and dip of foliation 25
road
cross-section A B
fault ?
drill hole ● 80-51
mapped costean (T1)
0 200
m

***Figure 3.*** *Simplified geological map of the Ray Gulch tungsten skarn deposit. Diamond holes 80-27, 80-50 and 80-51 were logged and sampled along with 2 costeans (T1 and T2). This map was compiled using maps from Lennan (1983) and data collected from field observations.*

mineral fissure veins occur between Haggart Creek and Potato Hills, and cassiterite-bearing breccias of Tin Dome can be found to the south of the stock (Fig. 2; Hitchins and Orssich, 1995; Yukon MINFILE, 2001, 106D 024). Deposits outside of the Dublin Gulch intrusion zone include the Len and Tag gold showings, the Shanghai and Skate silver showings, and the Rex and Peso quartz-sulphide mineral fissure veins (139 000 tonnes at 719 g/t Ag and 3.7% Pb) located to the west of Haggart Creek (Fig. 2; Yukon MINFILE 2001, 106D 018, 019, 020, 021).

## DEPOSIT GEOLOGY AND CONFIGURATION

The tungsten deposit is hosted within a hornfelsed roof pendant and occupies the crest and northern limb of the westerly plunging Lynx Creek antiform (Fig. 2; Lennan, 1983). Foliation in the local rock units changes from a northerly strike and 25° westerly dip in the central portion of the deposit, to a strike of 15° and dip of 25° west-northwest in the northern portion of the deposit (Fig. 3; Lennan, 1983). The Dublin Gulch granodiorite stock crops out along the northern, eastern and western margins of the deposit and plunges south and west under the metasedimentary rocks that host the deposit (Lennan, 1983). Dark green pyroxene-rich skarn lenses host the majority of the scheelite found in the deposit. Minor scheelite is also found in later crosscutting veins.

The deposit consists of six main mineralized zones that have a northerly strike and a westerly dip of approximately 25° (Fig. 4; Lennan, 1983). Zone 1 has the highest elevation and Zone 6 has the lowest elevation, with each zone comprising several skarn horizons of varying thickness. The skarn horizons are laterally continuous, massive and generally coarse grained. Tungsten grade increases proportionally with pyroxene content, and with increasing depth toward the granodiorite contact. The grade of the zones are as

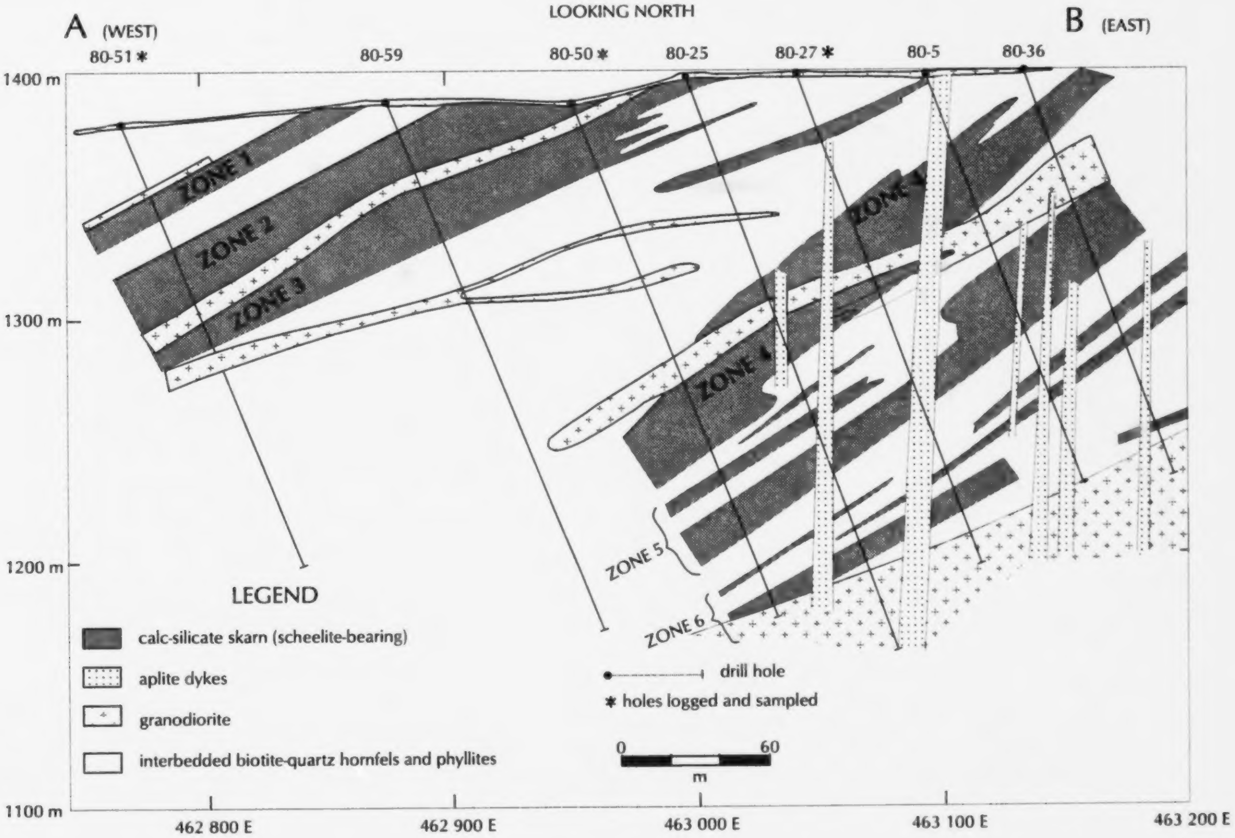
LOOKING NORTH
A (WEST)
B (EAST)
80-51 *
80-59
80-50 *
80-25
80-27 *
80-5
80-36
1400 m
1300 m
1200 m
1100 m
ZONE 1
ZONE 2
ZONE 3
ZONE 4
ZONE 4
ZONE 5
ZONE 6
LEGEND
calc-silicate skarn (scheelite-bearing)
aplite dykes
granodiorite
interbedded biotite-quartz hornfels and phyllites
drill hole
* holes logged and sampled
0
60
m
462 800 E
462 900 E
463 000 E
463 100 E
463 200 E

***Figure 4.*** *Geological cross-section of the Ray Gulch tungsten skarn (modified after Lennan, 1983). Refer to Figure 3 for cross-section location.*

mineral fissure veins occur between Haggart Creek and Potato Hills, and cassiterite-bearing breccias of Tin Dome can be found to the south of the stock (Fig. 2; Hitchins and Orssich, 1995; Yukon MINFILE, 2001, 106D 024). Deposits outside of the Dublin Gulch intrusion zone include the Len and Tag gold showings, the Shanghai and Skate silver showings, and the Rex and Peso quartz-sulphide mineral fissure veins (139 000 tonnes at 719 g/t Ag and 3.7% Pb) located to the west of Haggart Creek (Fig. 2; Yukon MINFILE 2001, 106D 018, 019, 020, 021).

## DEPOSIT GEOLOGY AND CONFIGURATION

The tungsten deposit is hosted within a hornfelsed roof pendant and occupies the crest and northern limb of the westerly plunging Lynx Creek antiform (Fig. 2; Lennan, 1983). Foliation in the local rock units changes from a northerly strike and 25° westerly dip in the central portion of the deposit, to a strike of 15° and dip of 25° west-northwest in the northern portion of the deposit (Fig. 3; Lennan, 1983). The Dublin Gulch granodiorite stock crops out along the northern, eastern and western margins of the deposit and plunges south and west under the metasedimentary rocks that host the deposit (Lennan, 1983). Dark green pyroxene-rich skarn lenses host the majority of the scheelite found in the deposit. Minor scheelite is also found in later crosscutting veins.

The deposit consists of six main mineralized zones that have a northerly strike and a westerly dip of approximately 25° (Fig. 4; Lennan, 1983). Zone 1 has the highest elevation and Zone 6 has the lowest elevation, with each zone comprising several skarn horizons of varying thickness. The skarn horizons are laterally continuous, massive and generally coarse grained. Tungsten grade increases proportionally with pyroxene content, and with increasing depth toward the granodiorite contact. The grade of the zones are as

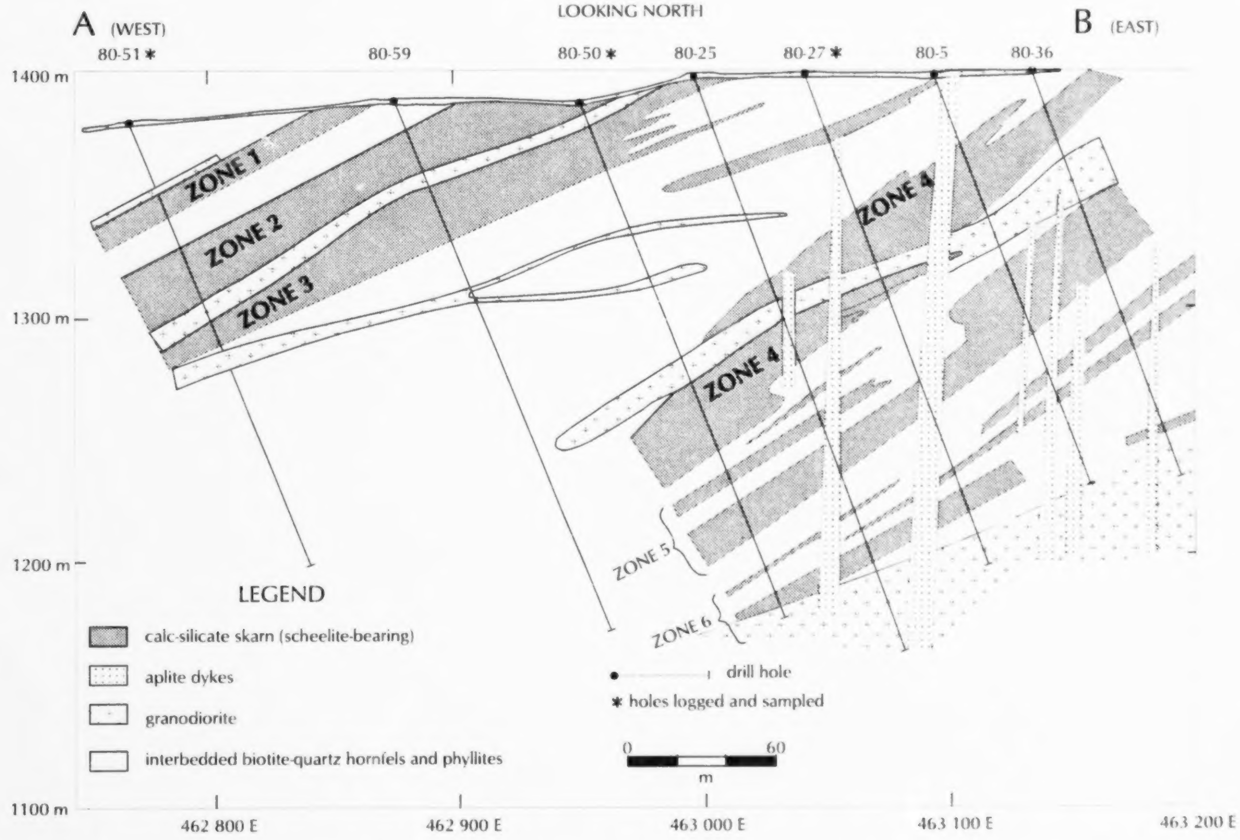
LOOKING NORTH
A (WEST)
B (EAST)
80-51 ✱
80-59
80-50 ✱
80-25
80-27 ✱
80-5
80-36
1400 m
1300 m
1200 m
1100 m
ZONE 1
ZONE 2
ZONE 3
ZONE 4
ZONE 4
ZONE 5
ZONE 6
LEGEND
calc-silicate skarn (scheelite-bearing)
aplite dykes
granodiorite
interbedded biotite-quartz hornfels and phyllites
drill hole
✱ holes logged and sampled
0
60
m
462 800 E
462 900 E
463 000 E
463 100 E
463 200 E

***Figure 4.*** *Geological cross-section of the Ray Gulch tungsten skarn (modified after Lennan, 1983). Refer to Figure 3 for cross-section location.*

follows: Zone 1 - 0.40% $WO_3$, Zone 2 - 0.51% $WO_3$, Zone 3 - 0.55% $WO_3$, Zone 4 - 0.65% $WO_3$, Zone 5 - 0.75% $WO_3$, Zone 6 - 1.03% $WO_3$ (Lennan, 1983).

## MINERALOGY AND PARAGENESIS

The deposit consists of two mineralogically different skarn types: an early scheelite-barren wollastonite-quartz skarn (Stage I), and the scheelite-rich pyroxene skarn (Stage II; Fig. 5). The principal minerals found within these skarn types are clinopyroxene, wollastonite, plagioclase, quartz, calcite, amphibole, scheelite and garnet, with accessory amounts of sphene, apatite, vesuvianite, clintonite and allanite (Lennan, 1983). Wollastonite-quartz skarn is a fine-grained, siliceous rock, white to pale light green with banding defined by alternating lenses of wollastonite, quartz, calcite, K-feldspar, pyroxene and relic bedding (Fig. 6a). This rock unit makes up approximately 5% of the total rock mass in the deposit. The wollastonite-quartz skarn was subsequently overprinted by the Stage II scheelite-bearing pyroxene skarn (Fig. 6b). The amount of wollastonite-quartz skarn within pyroxene skarn horizons decreases as pyroxene alteration intensifies with depth. The pyroxene skarn is a medium- to coarse-grained dark green rock composed of clinopyroxene, plagioclase, quartz, grossular garnet, disseminated 0.2 to 5 mm scheelite grains and calcite (Fig. 6c), with minor amphibole that is typically the product of retrograde alteration of pyroxene. Locally, scheelite also occurs as large subhedral grains in later veins. On average, pyroxene skarn consists of up to 70% clinopyroxene, 10% quartz, 10% feldspar, 5-10% grossular garnet, 5-15% amphibole, 5% calcite and variable amounts of scheelite (up to 3%).

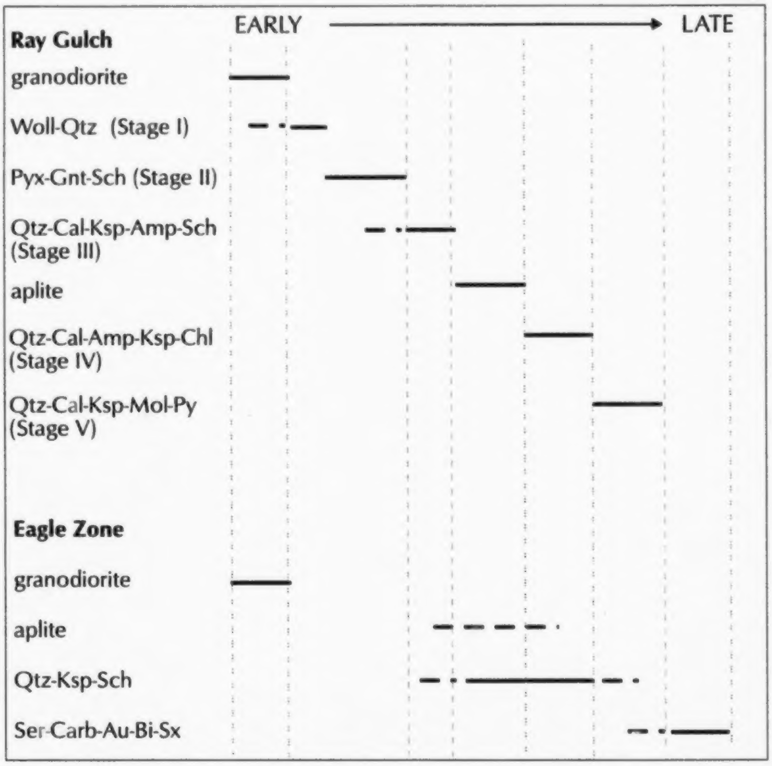

***Figure 5.*** *Comparison of the paragenesis at Ray Gulch and Eagle Zone. The gold mineralization occurs in a distinct event postdating scheelite. Abbreviations: Woll = wollastonite; Qtz = quartz; Pyx = pyroxene; Gnt = garnet; Sch = scheelite; Cal = calcite; Amp = amphibole; Ksp = K-feldspar; Chl = chlorite; Mol = molybdenite; py = pyrite; Ser = sericite; Sx = sulphide minerals.*

Microprobe analysis of clinopyroxene revealed considerable compositional variation within each skarn type. There is an evolutionary trend toward iron enrichment from pyroxene in the wollastonite-quartz skarn to the pyroxene found in the scheelite-bearing skarn. This tendency toward iron-enriched pyroxenes in the later stages of prograde growth of calcic tungsten-bearing skarn is a common worldwide phenomenon (Einaudi et al., 1981). Stage I wollastonite skarn consists of ferrosalite pyroxene, a calcium-iron pyroxene with a magnesium content of approximately 20 mol% to 30 mol%. The average composition of these pyroxenes is $Hd_{60}Di_{38}Jo_2$. Stage II pyroxene skarn contains abundant hedenbergite, with a slight variation from $Hd_{92}Di_5Jo_3$ to $Hd_{81}Di_{17}Jo_2$. The manganese component (johannsenite) of these pyroxenes is low, below 5 mol%. The presence of abundant hedenbergite pyroxene and grossular garnet suggests formation occurred in a reduced environment, since oxidized skarns typically produce magnesium-rich pyroxenes and garnets (Kwak, 1994). Scheelite analysis revealed a very low powellite composition, below 1 wt.% molybdenum, further suggesting a reduced environment.

Three main stages of vein paragenesis were recognized and postdate skarn formation. Stage III veins consist of quartz-scheelite-clinopyroxene ± K-feldspar ± calcite ± sphene ± biotite. The veins are typically only a centimetre wide and contribute less than 10% of the total veining in the skarn deposit. They contain coarse-grained, subhedral scheelite, and lack amphibole and visible alteration selvages (Fig. 6c). These veins are commonly found within pyroxene skarn units, and the intergrown nature of pyroxene and scheelite in some of these veins suggests they may have been part of the main pyroxene skarn formation. These veins crosscut granodiorite intrusive

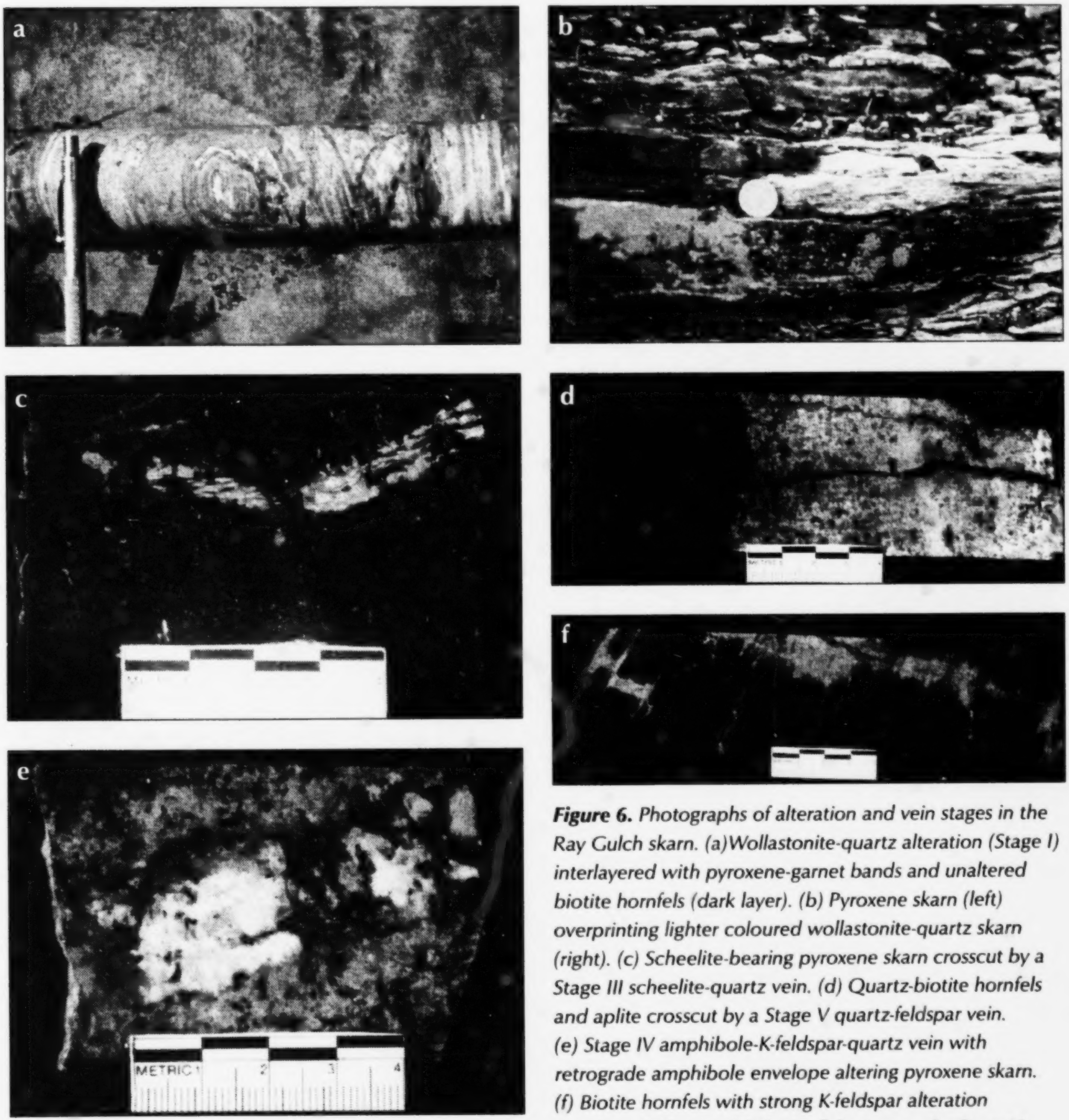

**Figure 6.** *Photographs of alteration and vein stages in the Ray Gulch skarn. (a)Wollastonite-quartz alteration (Stage I) interlayered with pyroxene-garnet bands and unaltered biotite hornfels (dark layer). (b) Pyroxene skarn (left) overprinting lighter coloured wollastonite-quartz skarn (right). (c) Scheelite-bearing pyroxene skarn crosscut by a Stage III scheelite-quartz vein. (d) Quartz-biotite hornfels and aplite crosscut by a Stage V quartz-feldspar vein. (e) Stage IV amphibole-K-feldspar-quartz vein with retrograde amphibole envelope altering pyroxene skarn. (f) Biotite hornfels with strong K-feldspar alteration envelope (± fine molybdenite flakes) around a Stage V quartz-feldspar vein.*

units, but not the aplitic dyke units. Aplitic dykes distinctly crosscut the pyroxene skarn stages and do not show any alteration equivalent to endoskarn in the granodiorite. The emplacement of these aplitic dykes was followed by late stage (Stage IV and Stage V) veining events (Fig. 6d).

Stage IV consists of quartz-amphibole (hornblende, actinolite, and ferrohastingsite)-calcite ± plagioclase ± K-feldspar ± biotite ± sphene ± epidote ± chlorite ± minor molybdenite ± pyrrhotite (Fig. 6e). The most common appearance of this vein type is as sheeted veinlets cutting both pyroxene skarn and wollastonite skarn, and more rarely granodiorite and aplite. They have a strong amphibole alteration selvage that locally extends for more than a few millimetres into the host rock. Although there is scant recorded large-scale retrograde alteration, this stage represents the majority of the hydrous minerals found in the skarn. Abundant actinolite crystals occur in veins, while ferrohastingsite and hornblende are associated with the alteration of clinopyroxene grains around the crosscutting veins. This vein style contributes approximately 20 to 30% of total vein types in the deposit.

Stage V consists of quartz-K-feldspar ± calcite ± epidote ± chlorite ± sphene ± pyrrhotite ± molybdenite ± arsenopyrite ± pyrite ± chalcopyrite. The majority of Stage V veins are entirely composed of quartz-feldspar. Molybdenite is common in quartz-calcite veins that have a strong feldspathic alteration selvage (Fig. 6f). This stage of veining is the most predominant in the skarn deposit, making up approximately 60 to 70% of veins found in the skarn. The veins range in width from a few millimetres up to 5 cm. The veins crosscut all units within the deposit, but are most abundant in the intrusive units. Although strong feldspar alteration selvages typically accompany these veins, only minor sericite alteration occurs where veins crosscut granodiorite and aplite units. The quartz-feldspar-rich veins that cut hornfels units display the most intense selvage development, commonly replacing biotite-rich lenses up to 2 cm away from the vein. Sulphide minerals are rare and confined to vein assemblages, with the exception of pyrrhotite, which is found in biotite-rich lenses in hornfels and as minor infill in veins. The overall sulphide content of the skarn is in the order of 1% to 2%.

## GEOCHEMISTRY

Geochemical analysis was undertaken to assess the overall metal composition, especially gold and bismuth contents of the various units (Table 1). Unaltered host rocks displayed very low metal content, gold was below detection, and tungsten no greater than 3 ppm. This is substantiated by a lithogeochemical study of the area by Gleeson and Boyle (1977) that reported the average tungsten content of the area as approximately 2 ppm, similar to host units found at MacTung (1-3 ppm) and Scheelite Dome (2 ppm). Igneous rock samples returned metal values generally below 100 ppm. Unaltered granodiorite samples from within Ray Gulch were typically barren of any tungsten mineralization. However, analysis of granodiorite from the Eagle Zone displayed an apparent enrichment of tungsten (average 160 ppm from nine samples). Both the wollastonite-quartz skarn and pyroxene skarn had low to below-detection results for most metals. In the past, only selected samples of core from Ray Gulch had been analysed for gold, with preliminary results indicating that the skarn contained no significant amounts of gold mineralization. Lennan (1983) mentions scattered quartz-arsenopyrite veins in core and outcrop that assayed between 2 and 30 g/t Au, which are perhaps genetically related to the sheeted vein complex found at the Eagle Zone. Recent analysis confirms the low gold results; the highest was 148 ppb Au from a quartz vein in a sample of pyroxene skarn that also returned a value of 400 ppm W. Pyroxene skarn returned values between 9.7 ppb and 38.1 ppb Au; other units were below detection. Gold deposits within the Tombstone gold belt (British Columbia and Yukon Chamber of Mines, 2000) have been found to have a strong correlation with bismuth. Gold in the Eagle Zone occurs as free grains with molybdenite, lead-bismuth sulphosalts, galena and bismuthinite (Maloof et al. 2001). Bismuth was very low in all samples analysed from the Ray Gulch skarn, consistent with the low to below-detection gold values.

## DISCUSSION

The Ray Gulch tungsten deposit is one of many tungsten skarns in the Yukon Territory associated with mid-Cretaceous intrusions. The Ray Gulch deposit likely formed early in the magmatic-metasomatic history of the Dublin Gulch area (Fig. 5). The abundance of veins in the skarn is minor when compared to that in the Eagle Zone. Veins in the skarn deposit comprise less than 10% of total units observed in drill core and are rarely more than 1 cm thick.

***Table 1.*** *Lithogeochemical data (by Neutron Activation Analysis) for a variety of samples collected around the Ray Gulch tungsten skarn.*

| Sample description | Ag | As | Au (ppb) | Ba | Ca (%) | Co | Cr | Fe (%) | La | Mo | Sb | Sn | Te | Th | W | Zn | Zr | Bi |
|---|---|---|---|---|---|---|---|---|---|---|---|---|---|---|---|---|---|---|
| wollastonite skarn | -5 | 5.21 | -5 | 706 | 14.2 | 9.71 | 171 | 2.91 | 36.4 | -5 | 0.54 | -500 | -5 | 17.8 | -2 | 117 | -500 | 0.9 |
| granodiorite with quartz vein | -5 | 5 | -5 | 688 | 3.22 | 2.74 | 214 | 1.14 | 32.1 | -5 | 0.68 | -500 | -5 | 19.8 | -2 | -100 | -500 | 0.97 |
| quartz-amphibole-feldspar vein | -5 | -5 | 148 | -800 | 3.42 | 3.57 | 362 | 2.43 | 20.3 | -20 | 1.3 | -1000 | -10 | 1.95 | 21,400 | -100 | 910 | 1.03 |
| aplite with quartz vein | -5 | -1 | -5 | 604 | 2.94 | -1 | 208 | 0.32 | 23.1 | -5 | 0.57 | -500 | -5 | 13.4 | 3.89 | -100 | -500 | 1.09 |
| granodiorite | -5 | 3.01 | -5 | -100 | 8.03 | 3.37 | 156 | 2.1 | 50 | -10 | 0.86 | -500 | -5 | 20.4 | -2 | -100 | -500 | 1.03 |
| aplite with quartz vein | -5 | 2.84 | -5 | -100 | 2.96 | -1 | 245 | 0.33 | 4.37 | -10 | 4.64 | -500 | -5 | 24.3 | 2.49 | -100 | -500 | 1.09 |
| quartz-pyroxene-feldspar vein | -5 | -15 | -50 | -2000 | 11 | -1 | 79.5 | 4.29 | 25.7 | -40 | -5 | -2000 | -20 | -2 | 100,000 | -100 | -3000 | 1.08 |
| quartz vein in pyroxene skarn | -5 | -1 | -5 | 185 | -1 | 1.93 | 750 | 0.76 | 0.66 | -10 | -0.2 | -500 | -5 | -0.5 | 1130 | -100 | -500 | 1.02 |
| quartz-pyroxene vein in granodiorite | -5 | 2.99 | -5 | -100 | 1.27 | 1.34 | 478 | 0.57 | 5.89 | -5 | 0.79 | -500 | -5 | 1.94 | 62 | -100 | -500 | 1.03 |
| granodiorite with quartz vein | -5 | 4 | -5 | 1720 | 4.62 | 7.34 | 168 | 2.81 | 58.1 | -10 | 0.8 | -500 | -5 | 24.3 | 4.84 | 133 | -500 | 1.05 |
| biotite hornfels | -5 | 1.71 | -5 | 708 | 1.46 | 6.61 | 192 | 2.19 | 37.2 | -5 | 0.65 | -500 | -5 | 17 | -2 | -100 | -500 | 1.09 |
| quartz vein in hornfels | -5 | 3.03 | -5 | 105 | 1.58 | 1.69 | 521 | 0.7 | 9.15 | 5.9 | 0.42 | -500 | -5 | 4.68 | 92.6 | -100 | -500 | 1.09 |
| endoskarn with quartz vein | -5 | 4.71 | -5 | 138 | 14.8 | 21.1 | 111 | 9.43 | 43.7 | -10 | 0.85 | -500 | -5 | 30.7 | 16.2 | 171 | -500 | 1.05 |
| biotite hornfels | -5 | 4.3 | -5 | 880 | 1.49 | 10.5 | 224 | 3.19 | 55.4 | -5 | 0.35 | -500 | -5 | 20.4 | 11.5 | 116 | -500 | 0.96 |
| biotite hornfels with quartz vein | -5 | 14.4 | -5 | 974 | 1.02 | 12.2 | 193 | 3.77 | 63.5 | 6 | 0.47 | -500 | -5 | 23.4 | -2 | -100 | -500 | 0.99 |
| pyroxene skarn with quartz vein | -5 | -10 | -20 | -1000 | 10.9 | 20.8 | 65.2 | 9.48 | 23.5 | 86.4 | 3.1 | -1500 | -15 | -2 | 48,100 | -100 | 2350 | 1.04 |
| pyroxene skarn | -5 | -10 | -20 | -1000 | 10.1 | 25.1 | 83.7 | 10.7 | 47.1 | 60.4 | 4.41 | -1500 | -15 | 2.56 | 46,300 | -100 | 1640 | 1.02 |
| pyroxene skarn | -5 | -5 | -15 | -500 | 9.35 | 7.43 | 132 | 3.84 | 87.6 | 27.6 | 1.65 | -500 | -10 | 8.49 | 13,200 | -100 | 586 | 1.09 |
| pyroxene skarn with amphibole veins | -5 | 3.28 | -5 | -200 | 18.4 | 33.1 | 54.2 | 17.7 | 17.2 | 8.3 | 0.69 | -500 | -5 | 7.15 | 816 | 225 | -500 | 0.96 |
| pyroxene skarn with amphibole veins | -5 | 2.11 | -10 | -500 | 12.6 | 18.2 | 75.1 | 9.35 | 39.5 | 20 | 0.54 | -500 | -5 | 12.2 | 2550 | -100 | 520 | – |
| pyroxene skarn | -5 | 2.63 | 12.6 | 316 | 12.5 | 37.5 | 38.2 | 8.84 | 41.9 | -5 | 0.56 | -500 | -5 | 13.8 | 214 | 105 | -500 | – |
| limestone | -5 | 1.52 | -5 | 174 | 37.2 | 2.9 | 9.1 | 0.29 | 5.48 | -5 | 0.27 | -500 | -5 | 2.32 | 26.5 | -100 | -500 | – |
| limestone | -5 | 1.84 | -5 | 160 | 34.8 | 6.12 | 7.5 | 0.54 | 6.82 | -5 | -0.2 | -500 | -5 | 2.07 | 61.9 | -100 | -500 | – |
| wollastonite skarn | -5 | 1.4 | -5 | 426 | 9.3 | 24.8 | 26.3 | 0.95 | 15.5 | 6.2 | 0.29 | -500 | -5 | 6.4 | 334 | -100 | -500 | – |
| pyroxene skarn | -5 | -1 | -5 | 475 | 12.8 | 50.1 | -5 | 16.2 | 0.58 | 68.6 | -0.2 | -500 | -5 | -0.5 | 3450 | 126 | -1000 | – |
| pyroxene skarn | -5 | -2 | 38.1 | 3130 | 10.3 | 29 | -10 | 10.8 | 35.7 | 171 | 4.86 | -1000 | -10 | -2 | 24,400 | -100 | -5000 | – |
| pyroxene skarn | -5 | 3.53 | -5 | 716 | 11.6 | 33.7 | 62.8 | 8.52 | 41.8 | 24.2 | 0.47 | -500 | -5 | 13.5 | 1300 | 115 | -500 | – |
| pyroxene skarn | -5 | 1.65 | -5 | 370 | 15.8 | 40 | 17.3 | 16.6 | 17.7 | 40.3 | 0.48 | -500 | -5 | 2.58 | 2010 | 107 | -500 | – |
| pyroxene skarn | -5 | 3.82 | -5 | 237 | 14.3 | 42.7 | 65.1 | 9.68 | 49.2 | -5 | 0.78 | -500 | -5 | 17.4 | 258 | 307 | -500 | – |
| pyroxene skarn | -5 | 1.37 | 9.7 | -100 | 15.1 | 33.8 | 37.4 | 15.1 | 28.3 | 11.9 | 0.45 | -500 | -5 | 9.15 | 665 | 194 | -500 | – |

**Notes**

- Au is ppb, Fe and Ca are in wt %; all other results are in ppm.
- Negative number indicates values below detection limits.

In the Eagle Zone, veins are 0.5 to 10 cm wide and vein densities range from <1 to >20 per metre with an average of 5 per metre. The veins, which developed along sheeted east-trending fracture zones, comprise early quartz-K-feldspar-scheelite with later calcite-muscovite ± molybdenite ± galena ± sphalerite ± Pb-Bi-Sb-sulphosalts ± gold ± bismuthinite (Maloof, et al., 2001). Significantly, the gold-bearing veins in the Eagle Zone that cut early quartz-feldspar-scheelite veins are lacking in the Ray Gulch skarn. This explains the low gold and bismuth content in the latter.

This study has established that the tungsten mineralization was temporally and spatially separate from, and occurred earlier than gold-bismuth mineralization in this system, even though it is likely that the mineralizing fluids evolved from a similar magmatic source. Other gold-tungsten occurrences need to be carefully evaluated in light of this data with a special emphasis on the timing and spatial distribution of gold and tungsten, and controls on fluid pathways and precipitation sites.

## ACKNOWLEDGEMENTS

The authors would like to thank James Cook University, Mineral Deposit Research Unit and Yukon Geology Program for financial and logistical help for this project. Ted Takacs, the placer miner at Dublin Gulch, provided much welcomed accommodation and greatly appreciated hospitality during field work.

## REFERENCES

British Columbia and Yukon Chamber of Mines, 2000. The Tintina Gold Belt: Concepts, Exploration, and Discoveries. Cordilleran Roundup, January, 2000, T.L. Tucker and M.T. Smith (session chairs), Special Volume 2, 225 p.

Einaudi, M.T., Meinert, L.D. and Newberry, R.J., 1981. Skarn deposits. Economic Geology 75th Anniversary Volume, Society of Economic Geologists, p. 317-391.

Gleeson, C.F. and Boyle, R.W., 1977. The lithogeochemistry of the Keno Hill District, Yukon Territory. Geological Survey of Canada, Paper 77-31, 38 p.

Hitchins, A.C. and Orssich C.N., 1995. The Eagle Zone gold-tungsten sheeted vein porphyry deposit and related mineralization, Dublin Gulch, Yukon Territory. *In:* Porphyry Deposits of the Northwestern Cordillera of North America, T.G. Schroeter (ed.), Canadian Institute of Mining and Metallurgy and Petroleum, Special Volume 46, p. 803-810.

Kwak, T.A.P., 1994. Hydrothermal alteration in carbonate-replacement deposits. Geological Association of Canada, Short Course Notes, vol. 11, p. 381-402.

Lennan, W.B., 1983. Ray Gulch tungsten skarn deposit Dublin Gulch area, central Yukon. *In:* Mineral Deposits of Northern Cordillera, J.A. Morin (ed.), The Canadian Institute of Mining and Metallurgy, Special Volume 37, p. 245-254.

Maloof, T.L., Baker, T. and Thompson, J.F.H., 2001. The Dublin Gulch intrusion-hosted gold deposit, Tombstone Plutonic Suite, central Yukon. Mineralium Deposita, p. 583-593.

Yukon MINFILE, 2001. Nash Creek – 106 D. Exploration and Geological Services Division, Yukon Region, Indian and Northern Affairs Canada.

# Geology, mineralization and sampling results from the Kalzas tungsten property, central Yukon

**Gerald G. Carlson**
*Copper Ridge Explorations Inc.*[1]

Carlson, G.G., 2002 Geology, mineralization and sampling results from the Kalzas tungsten property, central Yukon. *In:* Yukon Exploration and Geology 2001, D.S. Emond, L.H. Weston and L.L. Lewis (eds.), Exploration and Geological Services Division, Yukon Region, Indian and Northern Affairs Canada, p. 269-278.

## ABSTRACT

Kalzas, in central Yukon, is a porphyry-style stockwork and sheeted-vein wolframite deposit. Alteration includes a potassic core, a quartz-tourmaline-sericite zone and an outer quartz-sericite-pyrite zone, the latter in excess of 2 km in diameter. Wolframite is confined to the inner two zones, in an oval area 1500 m by 800 m. The wolframite is disseminated within the quartz-tourmaline stockwork and also occurs as coarse crystals in sheeted veins. Mineralization occurs within Neoproterozoic to Early Cambrian Hyland Group quartzites and phyllites, which are likely intruded at depth by a pluton, possibly of the Cretaceous Tombstone Suite.

From 1981 to 1984, Union Carbide carried out mapping, soil and rock geochemistry, an airborne magnetometer survey, road building, trenching and drilling of two diamond drill holes. Results from Copper Ridge's 2001 sample program range from 0.3% $WO_3$ to 0.5% $WO_3$ over widths up to 70 m. They demonstrate the potential to define a significant resource of surface-mineable tungsten mineralization at a grade of 0.4% $WO_3$ or better. Drilling is required to confirm grade continuity at depth and along strike.

## RÉSUMÉ

Le gisement Kalzas, dans la partie centrale du Yukon, est un stockwerk de type porphyrique constitué de filons feuilletés de wolframite. L'altération comprend un noyau potassique, une zone de quartz-tourmaline-séricite et une zone externe de quartz-séricite-pyrite qui mesure plus de 2 km de diamètre. Seules les deux zones internes renferment de la wolframite, dans une région ovale de 1500 m sur 800 m. La wolframite est disséminée dans le stockwerk de quartz-tourmaline; on en trouve également sous forme de cristaux grossiers dans les filons feuilletés. La minéralisation se trouve dans des quartzites et des phyllades du Groupe de Hyland datant du Néoprotérozoïque au Cambrien précoce, sans doute pénétrés en profondeur par un pluton qui pourrait faire partie de la Suite de Tombstone (Crétacé).

Entre 1981 et 1984, la société Union Carbide a dressé des cartes, fait des analyses géochimiques du sol et de la roche, effectué un levé aéromagnétique, construit des routes, creusé des tranchées et exécuté deux forages au diamant. Les résultats obtenus en 2001 dans le cadre du programme d'échantillonnage de Copper Ridge indiquent de 0,3 % à 0,5 % de $WO_3$ sur des largeurs atteignant 70 mètres. Ces résultats démontrent qu'il est possible de délimiter une importante minéralisation en tungstène qui est exploitable depuis la surface et présente une teneur en $WO_3$ de 0,4 % ou plus. Il est nécessaire de forer pour s'assurer que la teneur est la même en profondeur et dans l'axe de la minéralisation.

---

[1] *500-625 Howe St., Vancouver, British Columbia, Canada V6C 2T6; gcarlson@copper-ridge.com*

# INTRODUCTION

Kalzas is a world class tungsten deposit consisting of wolframite mineralization in sheeted veins and stockwork. Similar deposits are known particularly in China, Bolivia and Portugal. Kalzas is located south of the Stewart River, 70 km southeast of Mayo (Fig. 1) and 290 km north of Whitehorse. The claims are located in the Mayo Mining District on NTS sheet 105M/7, centred at 63°16'N, and 134°42'W, and are described in Yukon MINFILE (2001, 105M 066). Access is by helicopter from Mayo. A serviceable airstrip exists on the property, accommodating up to a Twin Otter aircraft. Union Carbide developed a 75 km winter road from Mayo in 1983, but it is impossible to discern in many places. The main showing areas of the property are easily reached from the intact bulldozer trails, and these extend to the former campsite and airstrip (1350 m elevation). Most of these are on the north and western flank of the western Kalzas Twin (1936 m elevation). Big Kalzas Lake, 4 km to the south, has an elevation of 780 m. Most of the property is alpine and covered by talus, with some grass and moss on stable slopes. Outcrop is limited to ridge crests and less commonly near the base of talus slopes. Sparse bush and alpine spruce occur below 1400 m. All of the key mineralization discovered to date is above tree line.

The Kalzas property lies within the Selwyn tungsten belt (Cathro, 1969), one of the world's largest tungsten districts (Fig. 1). The belt includes Mactung (32 Mt at 0.92% $WO_3$ reserves - Dawson, 1995), one of the top three of the world's known tungsten deposits, and Cantung (9 Mt at 1.42% $WO_3$ production plus reserves – Dawson, 1995), Canada's largest historical tungsten producer. Numerous other known deposits and showings include skarns such as Ray Gulch, Clea and Lened, and an intrusive-related stockwork W-Mo deposit known as Logtung. Coincidentally, this belt partially overlaps the Tintina gold belt (British Columbia and Yukon Chamber of Mines, 2000). Both the gold and the tungsten appear to be genetically related to the mid-Cretaceous Tombstone Plutonic Suite.

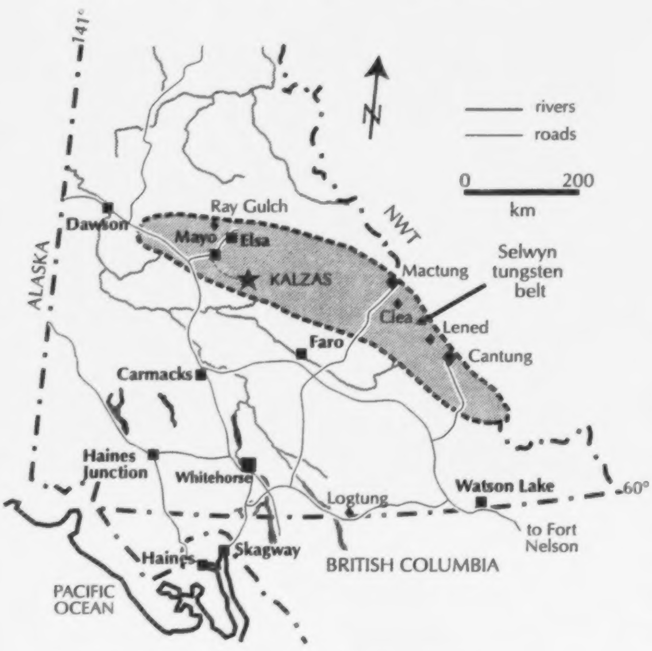

***Figure 1.** Kalzas property in central Yukon.*

# HISTORY

The property was discovered and staked in 1978 by prospector J.D. Randolph, who was initially investigating high-grade silver showings. In 1980, the property was optioned to Union Carbide Corporation. Union Carbide carried out prospecting, geological mapping, soil sampling, rock and talus sampling and flew an aeromagnetic survey in 1981 and 1982. In 1983, a winter road was constructed from Mayo. Road building and bulldozer trenching exposed outcrop for sampling on the upper slopes of the mountain. An 840-m airstrip was constructed near the camp on the north side of the mountain (Fig. 2). Late in the season, two core drill holes were completed for a total of 668 m.

The initial work by Union Carbide defined a strong (+1000 ppm) tungsten anomaly in soils and talus fines (Fig. 2). The anomaly trends northwest and measures 1500 m long by 300 m to 900 m wide (Fig. 2), and is surrounded and partially overlapped by anomalous values of silver and tin. Sampling of the talus material was carried out in detail on some of the grid lines with 20 kg bulk samples along 20-m and 25-m intervals. On line 43N, a 150-m length averaged 1.04% $WO_3$ in the quartz vein material and 0.21% $WO_3$ in country rock. On line 40N, a 175-m interval averaged 0.32% $WO_3$ (including both quartz veins and country rock).

Union Carbide's work showed the potential for in excess of 100 million tonnes of low-grade (0.1% to 0.2% $WO_3$) tungsten. Re-sampling by Copper Ridge Explorations Inc. in 2001 confirmed higher-grade zones with widths up to 70 m and grades in the 0.3% to plus 0.5% $WO_3$ range, and suggested the earlier Union Carbide analyses had understated the tungsten grade.

The property geology was described in internal reports to Union Carbide by Forster in 1981 and 1984. Lynch (1985a,b, 1989) described the mineralization and alteration, and Roots (1997) mapped the bedrock at 1:250 000 scale.

# GEOLOGY AND MINERALIZATION

## REGIONAL GEOLOGY

The Kalzas property is underlain by the Yusezyu Formation belonging to the Neoproterozoic to Early Cambrian Hyland Group. It consists of metasandstone with grit, quartzite and phyllite, a distinctive black slate member, and minor limestone and conglomerate. Regionally, these rocks form the basal unit of the Selwyn Basin, deposited on the continental margin of ancient North America. These sedimentary rocks were subsequently deformed between Upper Jurassic and Lower Cretaceous time and intruded by mid-Cretaceous 'S'-type granitic rocks.

In the Kalzas region, deformation consisted of imbricate faulting, folding and transposition on slaty cleavage. The layering in most outcrops is tectonic, rather than depositional, and few primary bedding features are preserved (Roots, 1997).

The nearest exposed intrusions are granite, located about 10 km north of the Kalzas property. Kalzas is slightly south of a southeasterly trend of small plugs spaced about 40 km apart between Scheelite Dome (Mair et al., 2000) and the Russell Range. These are part of the 90 Ma to 95 Ma Tombstone Plutonic Suite and many have associated gold and/or tungsten mineralization. A buried intrusion likely underlies the property, as suggested by a large concentrically zoned alteration halo at Kalzas (Lynch, 1985a,b) combined with a complex, annular aeromagnetic anomaly. However, no granitic rocks have been found in outcrop at Kalzas.

## GEOLOGY OF THE KALZAS PROPERTY

Unaltered host rock at Kalzas consists of interbedded chloritic phyllite and feldspathic quartzite, with lesser amounts of siltstone, dark shale and quartz-feldspar pebble conglomerate. The phyllite is composed of chlorite, sericite and quartz and commonly grades into siltstone. It sometimes displays rusty weathering due to minor pyrite content.

The quartzite consists of 80% to 90% quartz as coarse sand-sized grains, with the remainder of the rock consisting of feldspar with trace zircon and magnetite. Individual quartzite layers are up to 3 m thick and contacts with phyllite are typically sharp. There are at least two conglomerate layers within the wolframite zone, with rounded quartz clasts and up to 10% feldspar clasts. Bedding strikes northwesterly and has steep to vertical dips. Tight folding has been observed, and bedding attitudes suggest a property-scale southeasterly plunging antiform.

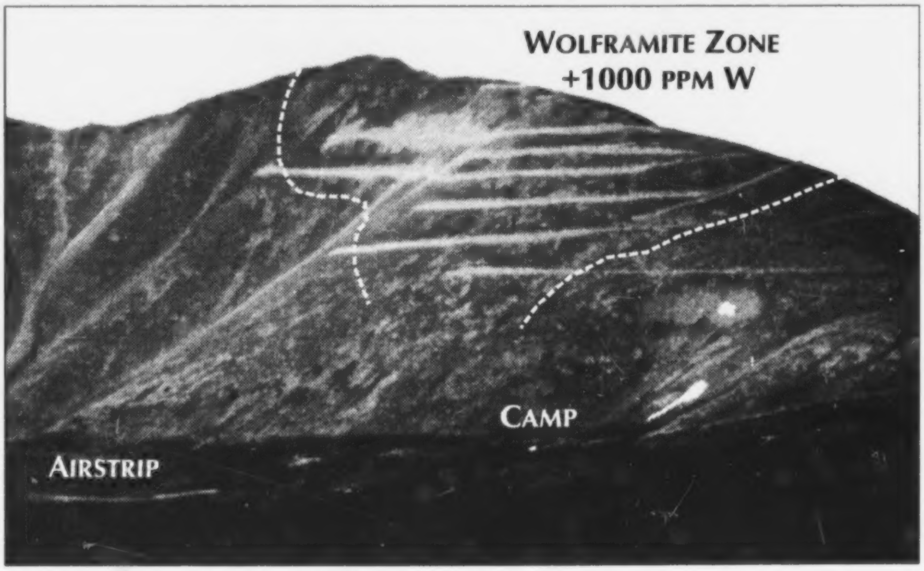

***Figure 2.*** *Southeast view of the tungsten zone on west Kalzas Twin (photo by C. Roots).*

## INTRODUCTION

Kalzas is a world class tungsten deposit consisting of wolframite mineralization in sheeted veins and stockwork. Similar deposits are known particularly in China, Bolivia and Portugal. Kalzas is located south of the Stewart River, 70 km southeast of Mayo (Fig. 1) and 290 km north of Whitehorse. The claims are located in the Mayo Mining District on NTS sheet 105M/7, centred at 63°16'N, and 134°42'W, and are described in Yukon MINFILE (2001, 105M 066). Access is by helicopter from Mayo. A serviceable airstrip exists on the property, accommodating up to a Twin Otter aircraft. Union Carbide developed a 75 km winter road from Mayo in 1983, but it is impossible to discern in many places. The main showing areas of the property are easily reached from the intact bulldozer trails, and these extend to the former campsite and airstrip (1350 m elevation). Most of these are on the north and western flank of the western Kalzas Twin (1936 m elevation). Big Kalzas Lake, 4 km to the south, has an elevation of 780 m. Most of the property is alpine and covered by talus, with some grass and moss on stable slopes. Outcrop is limited to ridge crests and less commonly near the base of talus slopes. Sparse bush and alpine spruce occur below 1400 m. All of the key mineralization discovered to date is above tree line.

The Kalzas property lies within the Selwyn tungsten belt (Cathro, 1969), one of the world's largest tungsten districts (Fig. 1). The belt includes Mactung (32 Mt at 0.92% $WO_3$ reserves - Dawson, 1995), one of the top three of the world's known tungsten deposits, and Cantung (9 Mt at 1.42% $WO_3$ production plus reserves – Dawson, 1995), Canada's largest historical tungsten producer. Numerous other known deposits and showings include skarns such as Ray Gulch, Clea and Lened, and an intrusive-related stockwork W-Mo deposit known as Logtung. Coincidentally, this belt partially overlaps the Tintina gold belt (British Columbia and Yukon Chamber of Mines, 2000). Both the gold and the tungsten appear to be genetically related to the mid-Cretaceous Tombstone Plutonic Suite.

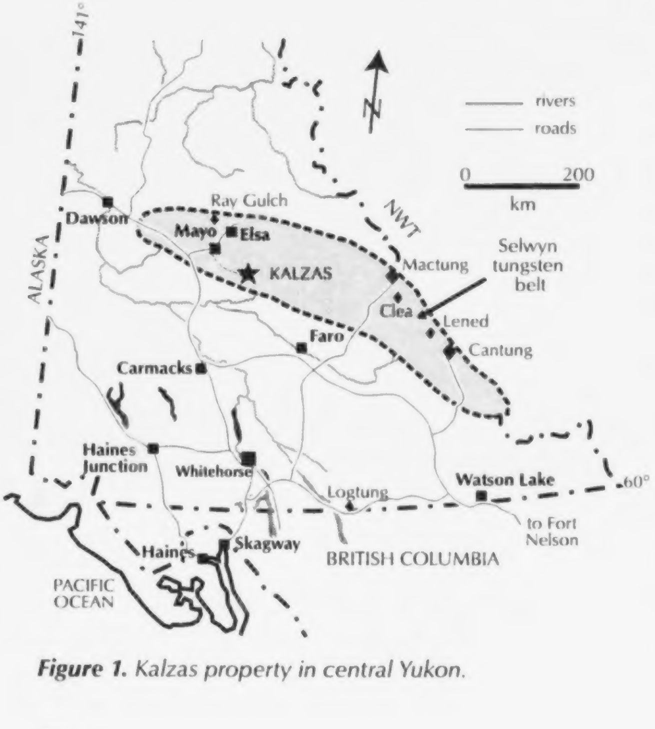

***Figure 1.** Kalzas property in central Yukon.*

## HISTORY

The property was discovered and staked in 1978 by prospector J.D. Randolph, who was initially investigating high-grade silver showings. In 1980, the property was optioned to Union Carbide Corporation. Union Carbide carried out prospecting, geological mapping, soil sampling, rock and talus sampling and flew an aeromagnetic survey in 1981 and 1982. In 1983, a winter road was constructed from Mayo. Road building and bulldozer trenching exposed outcrop for sampling on the upper slopes of the mountain. An 840-m airstrip was constructed near the camp on the north side of the mountain (Fig. 2). Late in the season, two core drill holes were completed for a total of 668 m.

The initial work by Union Carbide defined a strong (+1000 ppm) tungsten anomaly in soils and talus fines (Fig. 2). The anomaly trends northwest and measures 1500 m long by 300 m to 900 m wide (Fig. 2), and is surrounded and partially overlapped by anomalous values of silver and tin. Sampling of the talus material was carried out in detail on some of the grid lines with 20 kg bulk samples along 20-m and 25-m intervals. On line 43N, a 150-m length averaged 1.04% $WO_3$ in the quartz vein material and 0.21% $WO_3$ in country rock. On line 40N, a 175-m interval averaged 0.32% $WO_3$ (including both quartz veins and country rock).

Union Carbide's work showed the potential for in excess of 100 million tonnes of low-grade (0.1% to 0.2% $WO_3$) tungsten. Re-sampling by Copper Ridge Explorations Inc. in 2001 confirmed higher-grade zones with widths up to 70 m and grades in the 0.3% to plus 0.5% $WO_3$ range, and suggested the earlier Union Carbide analyses had understated the tungsten grade.

The property geology was described in internal reports to Union Carbide by Forster in 1981 and 1984. Lynch (1985a,b, 1989) described the mineralization and alteration, and Roots (1997) mapped the bedrock at 1:250 000 scale.

## GEOLOGY AND MINERALIZATION

### REGIONAL GEOLOGY

The Kalzas property is underlain by the Yusezyu Formation belonging to the Neoproterozoic to Early Cambrian Hyland Group. It consists of metasandstone with grit, quartzite and phyllite, a distinctive black slate member, and minor limestone and conglomerate. Regionally, these rocks form the basal unit of the Selwyn Basin, deposited on the continental margin of ancient North America. These sedimentary rocks were subsequently deformed between Upper Jurassic and Lower Cretaceous time and intruded by mid-Cretaceous 'S'-type granitic rocks.

In the Kalzas region, deformation consisted of imbricate faulting, folding and transposition on slaty cleavage. The layering in most outcrops is tectonic, rather than depositional, and few primary bedding features are preserved (Roots, 1997).

The nearest exposed intrusions are granite, located about 10 km north of the Kalzas property. Kalzas is slightly south of a southeasterly trend of small plugs spaced about 40 km apart between Scheelite Dome (Mair et al., 2000) and the Russell Range. These are part of the 90 Ma to 95 Ma Tombstone Plutonic Suite and many have associated gold and/or tungsten mineralization. A buried intrusion likely underlies the property, as suggested by a large concentrically zoned alteration halo at Kalzas (Lynch, 1985a,b) combined with a complex, annular aeromagnetic anomaly. However, no granitic rocks have been found in outcrop at Kalzas.

### GEOLOGY OF THE KALZAS PROPERTY

Unaltered host rock at Kalzas consists of interbedded chloritic phyllite and feldspathic quartzite, with lesser amounts of siltstone, dark shale and quartz-feldspar pebble conglomerate. The phyllite is composed of chlorite, sericite and quartz and commonly grades into siltstone. It sometimes displays rusty weathering due to minor pyrite content.

The quartzite consists of 80% to 90% quartz as coarse sand-sized grains, with the remainder of the rock consisting of feldspar with trace zircon and magnetite. Individual quartzite layers are up to 3 m thick and contacts with phyllite are typically sharp. There are at least two conglomerate layers within the wolframite zone, with rounded quartz clasts and up to 10% feldspar clasts. Bedding strikes northwesterly and has steep to vertical dips. Tight folding has been observed, and bedding attitudes suggest a property-scale southeasterly plunging antiform.

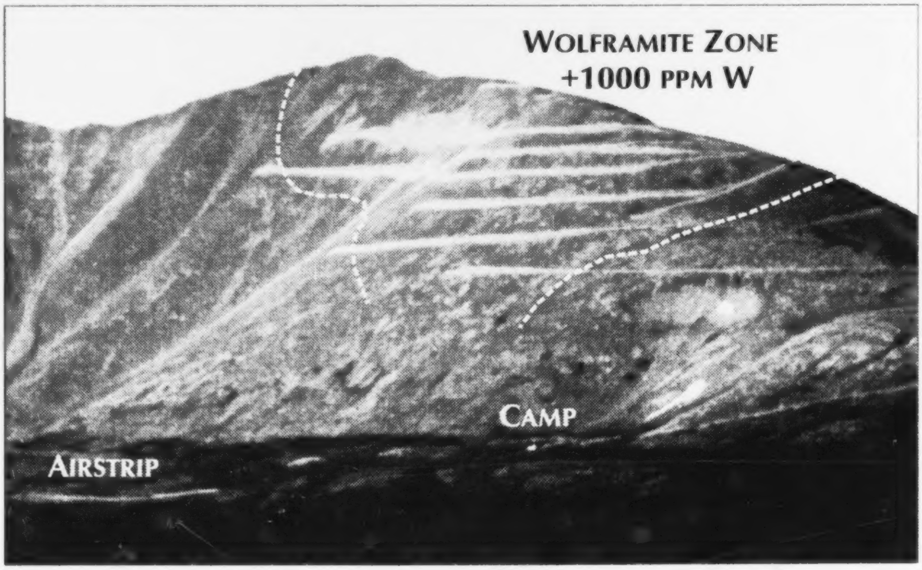

***Figure 2.*** *Southeast view of the tungsten zone on west Kalzas Twin (photo by C. Roots).*

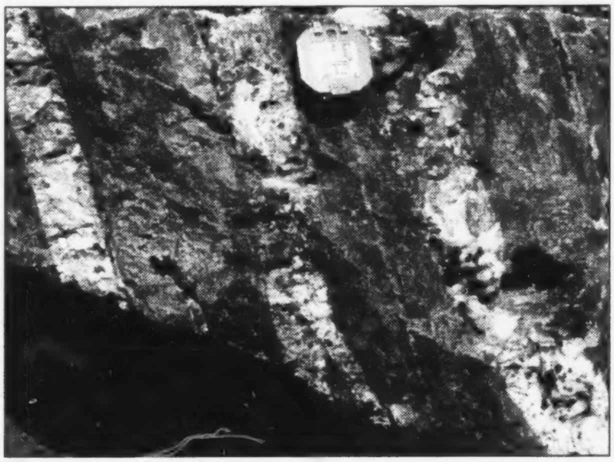

*Figure 3.* Vuggy sheeted veins, containing bladed wolframite crystals, cutting tourmalinized quartzite.

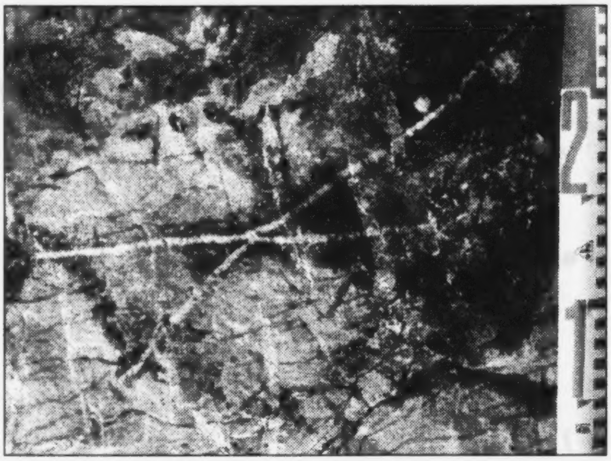

*Figure 4.* Quartz stockwork with tourmalinization (dark patches) along selvage and along fractures. The sericitized-quartzite host rock is pale in colour. Scale divisions are in centimetres.

## SHEETED VEINS AND STOCKWORK

Mineralization and alteration at Kalzas are related to a broad zone of sheeted veins and stockwork that comprise an oval, northwesterly elongated, porphyry style hydrothermal system. Sheeted veins (Fig. 3) range from 5 cm to as much as 60 cm thick, averaging about 20 cm. They are typically tabular, occur in sets and have been traced up to 50 m along strike. Although the larger sheeted veins have a variety of orientations, most strike approximately 070° and dip 35° to the northwest, roughly perpendicular to the southeast plunging fold axis.

Stockwork veinlets typically range from 0.1 to 1 cm thick, forming a complex boxwork. The veinlets are vuggy and contain euhedral to subhedral quartz, wolframite and tourmaline, with a complete gradation from pure tourmaline to pure quartz. Lynch (1985a,b) recognized up to six different ages of veinlets. Open fractures that appear to be younger than the stockwork mineralization are typically dark rusty-weathering and are commonly coated with a black, glassy, limonitic stain. Some fractures are lined with cassiterite crystals.

## ALTERATION

Three roughly concentric alteration phases form a northwest-trending oval, approximately 2.5 km long. The core is a K-feldspar zone, followed by a quartz-tourmaline-sericite zone and the outermost quartz-sericite-pyrite zone (Lynch, 1985a,b).

The quartz-sericite-pyrite zone has a distinct whitish colour with rusty patches due to pyrite weathering. Weak and relatively minor stockwork and sheeted veins occur in this zone, whereas sericitization is pervasive. There is typically less than 5% disseminated pyrite, as 1-2 mm cubes.

The quartz-tourmaline-sericite zone is characterized by tourmaline in sheeted veins, stockwork, vein halos, and as pervasive alteration of the host rocks. Halos to these veinlets typically consist of several millimetres of tourmaline, grading to sericite. Where stockwork is less intense, the rock tends to be pervasively altered, with sericite dominating in the quartzitic units and tourmaline in the phyllite (Fig. 4).

The core zone is characterized by K-feldspar and minor sulphide minerals in sheeted veins, and biotite in the wallrock. Biotite occurs preferentially in the quartzite, replacing chlorite. Biotite also occurs in sinuous micro-veinlets. Sulphide minerals include pyrite, pyrrhotite, chalcopyrite, molybdenite, bismuthinite, galena and arsenopyrite. Other accessory minerals include apatite and rutile.

## MINERALIZATION

Tungsten mineralization at Kalzas consists mainly of wolframite, with up to 10% of the tungsten values occurring as scheelite, in sheeted veins and stockwork. The zone of tungsten mineralization overlaps the core potassic zone and most of the quartz-tourmaline-sericite zone.

Wolframite occurs as coarse-grained bladed crystals up to 20 cm long within the sheeted veins and quartz stockwork. It is also disseminated within the quartz-tourmaline-altered host rock (Fig. 4). Scheelite occurs as encrustations on wolframite and sometimes as large, euhedral crystals in quartz veins. Tin occurs as cassiterite in tabular crystals and amorphous masses irregularly on fracture surfaces around the periphery of the wolframite zone.

Higher-grade sections occur in areas dominated by quartzite and conglomerate units. Phyllitic bands may be present in higher-grade sections. Generally, the greater the proportion of phyllite, the lower the tungsten grade. Many of the fractures and stockwork zones that appear to correlate with the higher-grade mineralized zones are sub-parallel to the bedding direction. Bedding throughout the mineralized zone is typically steeply dipping and strikes northwest, parallel to the long axis of the mineralized system (Fig. 5).

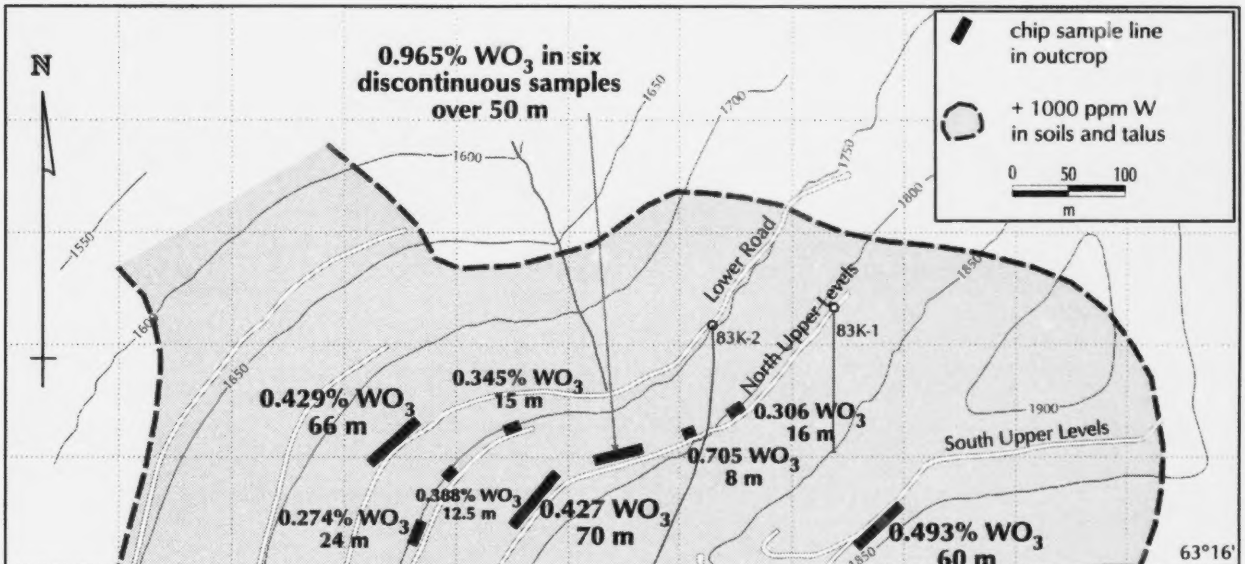
N
0.965% $WO_3$ in six discontinuous samples over 50 m
chip sample line in outcrop
+ 1000 ppm W in soils and talus
0 50 100
m
0.429% $WO_3$ 66 m
0.345% $WO_3$ 15 m
0.306 $WO_3$ 16 m
0.705 $WO_3$ 8 m
0.388% $WO_3$ 12.5 m
0.274% $WO_3$ 24 m
0.427 $WO_3$ 70 m
0.493% $WO_3$ 60 m
Lower Road
North Upper Levels
South Upper Levels
Middle Road
83K-2
83K-1
1500
1550
1600
1650
1700
1750
1800
1850
1900
63°16'
134°42'

*Figure 5. Location sketch showing results of tungsten chip samples in trenches at the Kalzas property.*

The structural control of mineralization is probably related to the regional structures that controlled emplacement of the underlying pluton. In addition to the dominant northwest-, and regional east- and northeast-trending structures, interpretation of Union Carbide's airborne magnetics survey indicates a local radial fracture pattern that was noted by C. Forster (pers. comm., 1984) and could be related to intrusion of the pluton.

It appears from the structural observations noted above and the pattern of higher-grade tungsten zones in bedrock as shown in Figure 5, that the west-northwest orientation (305°), roughly parallel to the fold axis and to bedding, is important in controlling these high-grade zones.

## 2001 ACTIVITY

After acquiring an option on the Kalzas property, Copper Ridge completed a one-week program of resampling core and trenches in August, 2001.

### ANALYTICAL METHODS

Table 1 shows analytical results from this study. Initially, the 127 trench samples were analysed at Acme Analytical Laboratories for whole rock trace elements by inductively coupled plasma-mass spectometry (ICP-MS) using a lithium borate fusion. Subsequently, 22 samples were sent to Activation Laboratories, Inc. for confirmation of tantalum analysis using neutron activation ('INAA'). Both the tantalum and the tungsten concentrations by INAA were lower than those by ICP-MS; the tungsten averaged 20% lower than the original whole rock results.

Subsequently, 29 samples of mostly higher-grade tungsten intervals were selected for assay at Acme. The assay values averaged approximately 7% higher than the equivalent whole rock analysis, with considerable variability, particularly for low to medium tungsten values. A further check on these samples by assay at Bondar Clegg gave results that confirmed the Acme assays, typically within a few percent.

### RESULTS

The results from the Copper Ridge trench sampling show a significant increase in tungsten values over those reported by Union Carbide. However, exact comparisons cannot be made because the locations of Union Carbide samples are not precisely known, and individual assay results are not available. Table 2 shows averages from the Copper Ridge sampling over the higher grade sections.

***Table 1.*** *Comparison of whole-rock geochemistry and assays by Acme and Bondar Clegg.*

| Sample Number | Acme Whole Rock W% | Acme Assay W% | Bondar Clegg Assay W% |
|---|---|---|---|
| C 115009 | 0.84 | 0.73 | 0.73 |
| C 115010 | 0.77 | 0.61 | 0.60 |
| C 115011 | 0.27 | 0.21 | 0.21 |
| C 115012 | 0.12 | 0.09 | 0.10 |
| C 115013 | 0.83 | 0.91 | 0.83 |
| C 115014 | 1.46 | 1.52 | 1.38 |
| C 115025 | 0.11 | 0.09 | 0.10 |
| C 115026 | 0.99 | 0.89 | 1.06 |
| C 115027 | 0.11 | 0.09 | 0.10 |
| C 115028 | 0.91 | 1.04 | 0.96 |
| C 115029 | 0.10 | 0.06 | 0.09 |
| C 115030 | 0.02 | 0.01 | 0.02 |
| C 115031 | 0.06 | 0.06 | 0.06 |
| C 115032 | 0.16 | 0.14 | 0.15 |
| C 115033 | 0.05 | 0.05 | 0.06 |
| C 115046 | 1.79 | 2.06 | 1.99 |
| C 115083 | 3.47 | 4.10 | 4.23 |
| C 115142 | 0.19 | 0.22 | 0.20 |
| C 115143 | 0.71 | 0.80 | 0.92 |
| C 115144 | 0.45 | 0.37 | 0.44 |
| C 115145 | 0.09 | 0.07 | 0.09 |
| C 115146 | 0.10 | 0.10 | 0.10 |
| C 115147 | 1.46 | 1.72 | 1.78 |
| C 115148 | 0.11 | 0.10 | 0.10 |
| C 115149 | 0.07 | 0.07 | 0.07 |
| C 115150 | 1.24 | 1.49 | 1.53 |
| C 115153 | 0.18 | 0.20 | 0.18 |
| C 115154 | 0.03 | 0.03 | 0.03 |
| C 115155 | 0.19 | 0.22 | 0.19 |
| **Averages** | **0.58** | **0.62** | **0.63** |

***Table 2.*** *Tungsten geochemistry (by ICP-MS) of trenched areas on west Kalzas Twin (see Figure 5 for location).*

| Trench | Width (m) | Grade (% $WO_3$) |
|---|---|---|
| South Upper Road | 60 | 0.493% |
| North Upper Road (east end) | 16 | 0.306% |
| North Upper Road (middle) | 8 | 0.705% |
| North Upper Road (west end) | 70 | 0.427% |
| North Middle Road | 20 | 0.268% |
| North Lower Road | 64 | 0.442% |

Results from individual samples within these intervals are listed in Appendix A.

Some of the highest results come from the middle of the North Upper Road in an area of discontinuous outcrop of intense stockwork mineralization within a quartzite unit. Here, 26.5 m of sampled outcrop within the 50-m interval along the road averaged 0.965% $WO_3$.

A strongly mineralized zone along the South Upper Road averages 0.493% $WO_3$ over 60 m. Characteristic of this section, and most of the other trench intervals that assayed high tungsten values, the host rock is sericitized quartzite ranging from pale grey to greenish yellow with a dark brown, rusty weathering on many of the exposed outcrop surfaces. This section contains few larger or sheeted veins. Most of the tungsten appears to be related to stockwork veins and possibly also to disseminated or fracture-controlled mineralization.

### COPPER RIDGE VS. UNION CARBIDE TRENCH ASSAY RESULTS

Although exact comparisons cannot be made because of lack of detailed descriptions of the Union Carbide sampling program, Copper Ridge results are on the order of 30% to over 50% higher than those of Union Carbide. In his 1984 internal company report, Forster described the on-site analytical procedure. Samples were crushed to -1/4 in., split, pulverized to -100 mesh, and analysed on an Asoma 8010 XRF field analyser in camp to determine the percent $WO_3$. Forster noted that laboratory checks done by Bondar-Clegg in Whitehorse tended to be lower for results less than 0.35% $WO_3$ but 30% higher than the field XRF results for higher values.

Potential errors could be introduced at a number of stages in this field analytical procedure. During sample preparation, particularly during sample splitting, tungsten could be lost to the final sample because of the high density of the tungsten minerals (wolframite and scheelite). Field portable XRF technology was crude in 1983, and results were not as reliable as could be achieved in a laboratory. For example, because of low power output, the unit would have scanned only the surface of any powdered sample, rather than the entire sample (B. Smee, pers. comm., 2001). Even lab results of that era, probably using an acid digestion followed by atomic absorption, might have understated tungsten values had the digestion of the sample not been complete or had the instrument flame not been hot enough.

Most of the Copper Ridge sampling was on the north and western slope of the western Kalzas Twin peak. The sheeted veins typically dip to the northwest at 30° to 35°. As a result, very few sheeted veins outcrop on this slope. The majority of the mineralization sampled by Copper Ridge appeared to be stockwork or disseminated in nature, with relatively little visible wolframite. Sample to sample results from the Copper Ridge sampling program do show variability (see Appendix A), but not the extreme fluctuations that would be expected if a nugget effect was significantly influencing the results.

## DISCUSSION

Union Carbide's exploration program showed the size potential of Kalzas to be in the hundreds of millions of tonnes, or a smaller tonnage at higher grades. However, the estimation of average grade proved to be a difficult issue for Union Carbide because of the perceived nugget effect created by the coarse wolframite mineralization in the sheeted veins. In contrast, the evaluation by Copper Ridge described here suggests that the grade estimation problem may have related more to sample handling procedures and analytical technique.

Average grades reported by Union Carbide are in the range of 0.2% $WO_3$ to 0.3% $WO_3$, typically over widths of 50 m to 75 m. It appears that the Union Carbide work was focused on defining a resource of greater than 100 million tonnes.

Sampling by Copper Ridge during the current program was directed at confirming the tungsten values and assessing the potential for commercial tantalum mineralization. No tantalum minerals were identified and subsequent analysis both by wet chemical methods and by neutron activation failed to detect economic values of tantalum. Typical tantalum values at Kalzas are in the range of 1-2 ppm, with a high of 8.7 ppm.

Copper Ridge's tungsten sampling, however, demonstrated a significant increase over the Union Carbide results. The Copper Ridge averages are in the range of 0.3% $WO_3$ to 0.5% $WO_3$ over widths up to 70 m. The results of the Copper Ridge sampling suggest that the nugget effect issue may not be so great a concern. Very little of the Copper Ridge sampling was actually in sheeted veins, but more in stockwork and disseminated mineralization. The results of this sampling are reasonably consistent from one sample to the next, with less variability than would be expected with a nugget effect problem.

The Copper Ridge results are based on chip channel samples averaging 5 m in length over exposures limited by the Union Carbide trenching. No firm conclusions can be drawn regarding actual grades, widths and continuity of zones without further detailed sampling, including both large diameter core drilling and bulk samples.

## ECONOMIC POTENTIAL

Union Carbide identified the broad, sheeted vein and stockwork tungsten complex over 1000 m in length and over 500 m in width. The potential within this zone is to develop a deposit in the hundreds of millions of tonnes of mineralization. Sampling suggests the grade of such a deposit could be in excess of 0.1% $WO_3$. In terms of size, this would rank Kalzas as one of the top three or four tungsten deposits in the world.

The sampling and evaluation by Copper Ridge indicates the possibility of defining a resource on the order of several tens of millions of tonnes of surface-mineable tungsten mineralization at a grade of 0.4% $WO_3$ or better. This mineralization occurs in higher-grade zones on the order of 50 m wide, in excess of 500 m in length and trending west-northwest, parallel to the bedding and the main structural grain of the deposit. Drilling will be required to demonstrate grade continuity within these higher-grade zones both at depth and along strike from sampled surface exposures.

A preliminary economic analysis carried out by Copper Ridge suggests that open pit mining at a rate of 5000 tonnes per day on a resource of 20 to 30 million tonnes grading about 0.5% $WO_3$ has the potential to provide an attractive rate of return. However, because of the very large size of the Kalzas mineralized system and the grade variability within it, both higher and lower throughputs will be examined based upon future exploration work and pre-feasibility studies.

## ACKNOWLEDGEMENTS

Many of the geological descriptions in this paper are based on a solid base of fieldwork during the period 1981 to 1984 by Union Carbide Corporation, under the direction of Charlie Forster, and M.Sc. thesis fieldwork by Greg Lynch at Washington State University. The current sampling program was carried out by Aurum Geological Consultants under the able guidance of Al Doherty. Yukon Geology Program geologists Craig Hart and Mike Burke visited the project during the sampling program and provided useful discussion and ideas. Diane Emond and Charlie Roots provided helpful and constructive reviews of the paper.

## REFERENCES

British Columbia and Yukon Chamber of Mines, 2000. The Tintina Gold Belt: Concepts, Exploration, and Discoveries. Cordilleran Roundup, January, 2000, T.L. Tucker and M.T. Smith (session chairs), Special Volume 2, 225 p.

Cathro, R.J., 1969. Tungsten in Yukon. Paper presented at the Third Northern Resource Conference, Whitehorse, Yukon, April 10, 1969, 8 p.

Dawson, K.M., 1995. Skarn tungsten. *In:* Geology of Canadian Mineral Deposit Types, O.R. Eckstrand, W.D. Sinclair and R.I. Thorpe (eds.), Geological Survey of Canada, Geology of Canada, no. 8, p. 495-502.

Lynch, G., 1985a. Alteration and zonation in the Kalzas W-Sn-Mo porphyry-vein deposit, 105M/7, Yukon. *In:* Yukon Exploration and Geology 1983, Exploration and Geological Services, Yukon Region, Indian and Northern Affairs Canada, p. 79-87.

Lynch, J.V.G., 1985b. Mineralization and alteration zonation of the Kalzas wolframite vein deposit, Yukon Territory, Canada. Unpublished M.Sc. thesis, Washington State University, 123 p.

Lynch, J.V.G., 1989. Hydrothermal alteration, veining, and fluid-inclusion characteristics of the Kalzas wolframite deposit, Yukon. Canadian Journal of Earth Sciences, vol. 26, p. 2106-2115.

Mair, J.L., Hart, C.J.R., Goldfarb, R.J., O'Dea, M. and Harris, S., 2000. Geology and metallogenic signature of gold occurrences at Scheelite Dome, Tombstone gold belt, Yukon. *In:* Yukon Exploration and Geology 1999, D.S. Emond and L.H. Weston (eds.), Exploration and Geological Services Division, Yukon Region, Indian and Northern Affairs Canada, p. 165-176.

Roots, C.F., 1997. Geology of the Mayo map area, Yukon Territory (105M). Exploration and Geological Services Division, Yukon Region, Indian and Northern Affairs Canada, Bulletin 7, 81 p.

Yukon MINFILE, 2001. Mayo area - 105M. Exploration and Geological Services Division, Yukon Region, Indian and Northern Affairs Canada.

## APPENDIX A. SUMMARY OF TUNGSTEN VALUES (BY ICP-MS), TRENCH RESULTS

Kalzas Project: Tungsten values and averages, chip channel and core samples, August 1-6, 2001.

| | Sample | Abbreviated UTM coordinates | | Width | | Averages | |
|---|---|---|---|---|---|---|---|
| **Location** | **No.** | **East** | **North** | **(m)** | **WO$_3$(%)** | **Width (m)** | **WO$_3$(%)** |
| Upper Levels | 115001 | 4951 | 5130 | 5.0 | 0.379 | 16.0 | 0.306 |
| Upper Levels | 115002 | 4946 | 5128 | 5.0 | 0.345 | | |
| Upper Levels | 115003 | 4944 | 5124 | 6.0 | 0.214 | | |
| Upper Levels | 115005 | 4922 | 5107 | 4.0 | 0.312 | 8.0 | 0.705 |
| Upper Levels | 115006 | 4916 | 5107 | 4.0 | 1.097 | | |
| Upper Levels | 115009 | 4874 | 5095 | 8.0 | 1.053 | 26.5 | 0.965 |
| Upper Levels | 115010 | 4856 | 5099 | 2.8 | 0.971 | | |
| Upper Levels | 115011 | 4850 | 5088 | 2.8 | 0.347 | 26.5 m of discontinuous outcrop exposure over approximately 50 m | |
| Upper Levels | 115012 | 4850 | 5085 | 4.0 | 0.155 | | |
| Upper Levels | 115013 | 4846 | 5081 | 4.5 | 1.050 | | |
| Upper Levels | 115014 | 4837 | 5079 | 4.4 | 1.847 | | |
| Upper Levels | 115025 | 4786 | 5060 | 5.0 | 0.139 | 70.0 | 0.427 |
| Upper Levels | 115026 | 4781 | 5056 | 10.0 | 1.247 | | |
| Upper Levels | 115027 | 4772 | 5050 | 10.0 | 0.143 | | |
| Upper Levels | 115028 | 4767 | 5040 | 10.0 | 1.147 | | |
| Upper Levels | 115029 | 4762 | 5036 | 5.0 | 0.123 | | |
| Upper Levels | 115030 | 4757 | 5032 | 5.0 | 0.027 | | |
| Upper Levels | 115031 | 4753 | 5027 | 5.0 | 0.076 | | |
| Upper Levels | 115032 | 4747 | 5022 | 10.0 | 0.198 | | |
| Upper Levels | 115033 | 4740 | 5013 | 10.0 | 0.068 | | |
| Middle Road | 115044 | 4753 | 5115 | 5.0 | 0.059 | 15.0 | 0.345 |
| Middle Road | 115045 | 4750 | 5114 | 3.0 | 0.011 | 20.0 | 0.268 |
| Middle Road | 115046 | 4747 | 5114 | 2.0 | 2.261 | | |
| Middle Road | 115047 | 4741 | 5114 | 5.0 | 0.065 | | |
| Middle Road | 115049 | 4704 | 5082 | 5.0 | 0.140 | 12.5 | 0.388 |
| Middle Road | 115050 | 4699 | 5071 | 5.0 | 0.794 | | |
| Middle Road | 115051 | 4699 | 5067 | 2.5 | 0.074 | | |
| Middle Road | 115058 | 4681 | 5027 | 5.0 | 0.183 | 24.0 | 0.274 |
| Middle Road | 115059 | 4681 | 5028 | 5.0 | 0.886 | | |
| Middle Road | 115060 | 4683 | 5013 | 5.0 | 0.034 | | |
| Middle Road | 115061 | 4683 | 5001 | 5.0 | 0.077 | | |
| Middle Road | 115062 | 4682 | 5008 | 4.0 | 0.172 | | |
| Middle Road | 115063 | 4673 | 5005 | 5.0 | 0.135 | 11.0 | 0.178 |
| Middle Road | 115064 | 4673 | 5000 | 3.0 | 0.396 | | |
| Middle Road | 115065 | 4673 | 4999 | 3.0 | 0.032 | | |
| South Slope | 115075 | 5085 | 5052 | 4.3 | 0.221 | 7.3 | 0.164 |
| South Slope | 115076 | | | 3.0 | 0.082 | | |
| Lower Road | 115080 | 4698 | 5151 | 10.0 | 0.109 | 66.0 | 0.429 |
| Lower Road | 115081 | 4689 | 5146 | 10.0 | 0.047 | | |
| Lower Road | 115082 | 4682 | 5135 | 5.0 | 0.007 | | |
| Lower Road | 115083 | 4679 | 5128 | 5.0 | 4.375 | 41.0 | 0.652 |

## APPENDIX A. (continued)

| Location | Sample No. | Abbreviated UTM coordinates East | North | Width (m) | $WO_3$(%) | Averages Width (m) | $WO_3$ (%) |
|---|---|---|---|---|---|---|---|
| Lower Road | 115084 | 4674 | 5124 | 5.0 | 0.101 | | |
| Lower Road | 115085 | 4670 | 5119 | 5.0 | 0.150 | | |
| Lower Road | 115086 | 4664 | 5123 | 3.0 | 0.025 | | |
| Lower Road | 115087 | 4664 | 5118 | 4.5 | 0.153 | | |
| Lower Road | 115088 | 4657 | 5119 | 5.0 | 0.127 | | |
| Lower Road | 115089 | 4653 | 5109 | 5.0 | 0.289 | | |
| Lower Road | 115090 | 4649 | 5108 | 4.5 | 0.085 | | |
| Lower Road | 115091 | 4650 | 5104 | 2.0 | 0.179 | | |
| South U. Levels | 115142 | 5039 | 5023 | 5.0 | 0.238 | 60.0 | 0.493 |
| South U. Levels | 115143 | 5045 | 5024 | 5.0 | 0.891 | | |
| South U. Levels | 115144 | 5047 | 5029 | 5.0 | 0.563 | | |
| South U. Levels | 115145 | 5050 | 5033 | 5.0 | 0.119 | | |
| South U. Levels | 115146 | 5054 | 5033 | 5.0 | 0.127 | | |
| South U. Levels | 115147 | 5056 | 5039 | 5.0 | 1.836 | | |
| South U. Levels | 115148 | 5059 | 5044 | 5.0 | 0.143 | | |
| South U. Levels | 115149 | 5064 | 5046 | 5.0 | 0.094 | | |
| South U. Levels | 115150 | 5068 | 5052 | 5.0 | 1.566 | | |
| South U. Levels | 115175 | 5069 | 5055 | 5.0 | 0.205 | | |
| South U. Levels | 115176 | 5074 | 5057 | 5.0 | 0.070 | | |
| South U. Levels | 115177 | 5078 | 5062 | 5.0 | 0.067 | | |